Green Chemistry and Sustainable Technology

Konstantin P. Bryliakov *Editor*

Frontiers of Green Catalytic Selective Oxidations

Springer

Green Chemistry and Sustainable Technology

Aims and Scope

The series Green Chemistry and Sustainable Technology aims to present cutting-edge research and important advances in green chemistry, green chemical engineering and sustainable industrial technology. The scope of coverage includes (but is not limited to):

- Environmentally benign chemical synthesis and processes (green catalysis, green solvents and reagents, atom-economy synthetic methods etc.)
- Green chemicals and energy produced from renewable resources (biomass, carbon dioxide etc.)
- Novel materials and technologies for energy production and storage (bio-fuels and bioenergies, hydrogen, fuel cells, solar cells, lithium-ion batteries etc.)
- Green chemical engineering processes (process integration, materials diversity, energy saving, waste minimization, efficient separation processes etc.)
- Green technologies for environmental sustainability (carbon dioxide capture, waste and harmful chemicals treatment, pollution prevention, environmental redemption etc.)

The series Green Chemistry and Sustainable Technology is intended to provide an accessible reference resource for postgraduate students, academic researchers and industrial professionals who are interested in green chemistry and technologies for sustainable development.

More information about this series at http://www.springer.com/series/11661

Konstantin P. Bryliakov
Editor

Frontiers of Green Catalytic Selective Oxidations

Springer

Editor
Konstantin P. Bryliakov
Russian Academy of Sciences
Boreskov Institute of Catalysis
Novosibirsk, Russia

ISSN 2196-6982 ISSN 2196-6990 (electronic)
Green Chemistry and Sustainable Technology
ISBN 978-981-32-9750-0 ISBN 978-981-32-9751-7 (eBook)
https://doi.org/10.1007/978-981-32-9751-7

This Springer imprint is published by the registered company Springer Nature Singapore Pte Ltd.
The registered company address is: 152 Beach Road, #21-01/04 Gateway East, Singapore 189721, Singapore

Preface

Catalyzed processes of selective oxidation of hydrocarbons, as well as of complex organic substrates, have had a long and illustrious track record, nowadays constituting one of the foundation stones of modern synthetic chemistry. Nevertheless, new developments in the field, mostly focused on enhancing the oxidation selectivity and improving their environmental sustainability, but also launching previously unachieved catalytic reactivity, have continued apace to this day, thus suggesting that the field is far from its maturity.

This book embodies contributions of recognized experts who have surveyed recent developments at the forefront of the environmentally sustainable catalytic oxidations, ranging from the well-established chemo- and stereoselective oxidations of olefins, sulfides, alcohols, as well as the much less developed C–H oxidations of aromatic and aliphatic substrates, including methane. In all cases, most catalyst systems relying on the environmentally benign oxidants H_2O_2 and O_2 are discussed. "Green" aspects of those oxidations, such as the process atom economy, the nature of reaction solvents, are considered.

We hope that this collection can serve as a reference book for professionals, as well as a guide and inspiration for students and young researchers at the beginning of their career. The topics of the chapters have been selected in a more or less voluntaristic fashion, in agreement with our current vision of the most challenging research directions in the field, holding the promise of significantly enriching, perhaps even revolutionizing the chemical industry in a one-generation time horizon. At the same time, we would like to stress that current selective oxidation catalysis is not limited to the topics considered here and provides enough alternative opportunities for investing research efforts that can appear highly rewarding.

Novosibirsk, Russia Konstantin P. Bryliakov

Contents

Contributors

Nishtha Agarwal Cardiff Catalysis Institute, Cardiff, UK

Konstantin P. Bryliakov Novosibirsk State University, Novosibirsk, Russian Federation;
Boreskov Institute of Catalysis, Novosibirsk, Russian Federation

Miquel Costas Departament de Química i Institut de Química Computacional i Catàlisi, Facultat de Ciències, Girona, Catalonia, Spain

Graham J. Hutchings Cardiff Catalysis Institute, Cardiff, UK

Oxana A. Kholdeeva Boreskov Institute of Catalysis, Siberian Branch of the Russian Academy of Sciences, Novosibirsk, Russia;
Novosibirsk State University, Novosibirsk, Russia

Alessandra Lattanzi Dipartimento di Chimica e Biologia, Università di Salerno, Fisciano, Italy

Oleg Y. Lyakin Boreskov Institute of Catalysis, Novosibirsk, Russia;
Novosibirsk State University, Novosibirsk, Russia

Roman V. Ottenbacher Novosibirsk State University, Novosibirsk, Russia;
Boreskov Institute of Catalysis, Novosibirsk, Russia

Hélène Pellissier Aix-Marseille Université, CNRS, Marseille, France

Georgiy B. Shul'pin Department of Dynamics of Chemical and Biological Processes, Semenov Institute of Chemical Physics, Russian Academy of Sciences, Ulitsa Kosygina, Moscow, Russia;
People's Friendship University of Russia, Moscow, Russia

Evgenii P. Talsi Boreskov Institute of Catalysis, Novosibirsk, Russia;
Novosibirsk State University, Novosibirsk, Russia

Stuart H. Taylor Cardiff Catalysis Institute, Cardiff, UK

Andrei N. Vedernikov Department of Chemistry and Biochemistry, University of Maryland, College Park, MD, USA

Laia Vicens Departament de Química i Institut de Química Computacional i Catàlisi, Facultat de Ciències, Girona, Catalonia, Spain

Konstantin Volcho Novosibirsk Institute of Organic Chemistry, Novosibirsk, Russia

Chapter 1
Metal-Catalyzed Oxidation of C–H Compounds with Peroxides in Unconventional Solvents

Georgiy B. Shul'pin

Abstract This chapter describes some examples of oxidation of C–H compounds (saturated and aromatic hydrocarbons and alcohols) with peroxides catalyzed by various metal compounds (mainly coordination complexes). The nature of the solvent plays a very important role in these reactions: the yield of products and selectivity can be dramatically changed when one solvent is replaced by another one. Adding certain cocatalysts to the reaction solution we can also significantly modify the yield and selectivity. Especially, interesting and attractive are oxidations in "green" solvents, first of all in water. The focus is made on the author's own works.

Keywords Saturated hydrocarbons · Aromatic hydrocarbons · Alcohols · Hydrogen peroxide *tert*-Butyl hydroperoxide · Carbonylation · Acetonitrile · Aqueous solutions · Acids as solvents · Ionic liquids · Hydroxyl radicals · Alkyl hydroperoxides · Regio-selectivity · Stereoselectivity

1.1 Introduction "Green Chemistry"

In recent decades, interest in "green" methods of oxidation of various compounds including C–H derivatives (alkanes, aromatics, and alcohols) has grown from the point of view of both academic and applied science [1–9]. "Green chemistry efficiently utilises (preferably renewable) raw materials, eliminates waste and avoids the use of toxic and/or hazardous reagents and solvents in the manufacture and application of chemical products" [10]. The following 12 principles of Green Chemistry [11] have been formulated: 1. Waste prevention instead of remediation; 2. Atom efficiency; 3. Less hazardous/toxic chemicals; 4. Safer products by design; 5. Innocuous solvents

G. B. Shul'pin (✉)
Department of Dynamics of Chemical and Biological Processes, Semenov Institute of Chemical Physics, Russian Academy of Sciences, Ulitsa Kosygina, ulitsa Kosygina, Dom 4, Moscow 119991, Russia
e-mail: shulpin@chph.ras.ru

People's Friendship University of Russia, ulitsa Miklukho-Maklaya, Dom 6, Moscow 117198, Russia

K. P. Bryliakov (ed.), *Frontiers of Green Catalytic Selective Oxidations*,
Green Chemistry and Sustainable Technology,
https://doi.org/10.1007/978-981-32-9751-7_1

and auxiliaries; 6. Energy efficient by design; 7. Preferably renewable raw materials; 8. Shorter syntheses (avoid derivatization); 9. Catalytic rather than stoichiometric reagents; 10. Design products for degradation; 11. Analytical methodologies for pollution prevention; and 12. Inherently safer processes. "Sustainable chemistry can be defined as the development of an even safer and more environmentally-friendly chemistry but bone which also equally integrates the priorities of economic competitiveness and societal concerns" [12, 13].

Metrics to "green chemistry" were proposed [14, 15]. Hudlicky proposed a metric known as effective mass yield that is defined "as the percentage of the mass of desired product relative to the mass of all non-benign materials used in its synthesis":

$$\text{Effective mass yield (\%)} = \frac{\text{Mass of products} \times 100}{\text{Mass of non} - \text{benign reagents}}$$

A second metric, E-factor, was proposed by Sheldon and is defined as follows:

$$\text{E Factor} = \frac{\text{Total waste (kg)}}{\text{kg product}}$$

The nature of a solvent as well as the method of stimulating a reaction plays a very important role in chemical transformations [16–19]. Very recently, Luzyanin, Kukushkin, and coworkers unexpectedly found that solubility of organometallics is noticeably improved in diiodomethane when compared to other haloalkane solvents. Better solvation properties of CH_2I_2 are due to a dramatic growth of the sigma-hole donating ability of this solvent which results in the formation of the uniquely strong solvent-(metal complex) halogen bonding [20].

In the beginning of 80th we discovered a method for preparation of sigma-aryl platinum(IV) complexes [21, 22]. The reaction of $PtCl_6^{2-}$ anion with an aromatic compound in aqueous trifluoroacetic acid afforded octahedral Pt(IV) complex [23–25]:

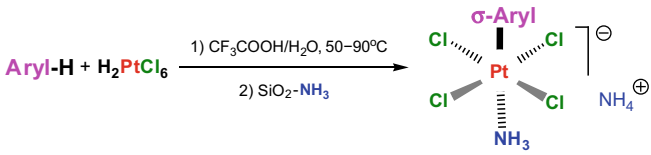

The process of formation of platinated toluene in the thermal reaction in aqueous trifluoroacetic acid is accompanied by its *para*⇆*meta* isomerization. The activation energies of the formation and the *para*⇆*meta* isomerization are approximately 100 kJ mol^{-1}. The acidity of the solvent affects the reaction rates of both the formation and the *para*⇆*meta* isomerization of the sigma-tolyl complex, the increase being approximately five times on going from the solvent CH_3COOH/H_2O to the CF_3COOH/H_2O. The relative rates of the thermal reaction with mono-substituted benzenes C_6H_5X decrease in the following sequence of X: OH > OCH_3 > CH_3 > C_2H_5 > OC_6H_5 > $CH(CH_3)_2$ > H > C_6H_5 > F > $COCH_3$ > COOH > Cl > NO_2.

Surprisingly, the reaction of $PtCl_6^{2-}$ anion with aromatics can be carried out at room temperature under light or γ-irradiation. The relative rates of the photoinduced reaction with C_6H_5X decrease in the following sequence: OH > OC_2H_5 > OCH_3 > OC_6H_5 > CH_3. It is important to emphasize that no *para*⇆*meta* isomerization was observed in the photoinduced (as well as γ-induced) reaction in the CF_3COOH/H_2O solution at room temperature. Only *para*-platinated compounds were produced. The observed activation energy for the photochemical reaction of anisole in CH_3COOH was 21 kJ mol^{-1} [23–25]. One more remarkable peculiarity of the photochemical reaction is the independence of the reaction rate on the acidity of the medium. Moreover, the reaction can be carried out in methylene chloride as a solvent. Thus, irradiation of a solution of $(^nBu_4N)_2PtCl_6 \cdot 6H_2O$ and an aromatic compound with full light of a medium-pressure mercury lamp afforded sigma-aryl complexes of Pt(IV) in 10–87% yield [26]. It should be also noted that for the aerobic oxidation of cyclohexane photocatalyzed by H_2PtCl_6, acetonitrile was used as a solvent [27]. Various solvents were used in alkane aerobic oxidation photocatalyzed by transition metal complexes [28–34].

1.2 New Catalysts

1.2.1 Complexes of Transition and Non-transition Metals

Various complexes of transition metals have been used as catalysts for efficient oxidation of saturated and aromatic hydrocarbons, alcohols as well as some other organic compounds containing C–H bonds. The main complexes described in the literature are briefly listed below [35]. Usually, acetonitrile was employed as a solvent in these works [36–38]. Graphene [39] and enzymes [40–42] have been applied in oxidations. For example, it has been shown that an iron-sulfur protein, AlkG, can efficiently transfer electrons toward the nonheme iron monooxygenase, AlkB, for the subsequent conversion of medium-chain length *n*-alkanes to primary alcohols. Immobilized AlkG on SPCE can interact with the AlkB-enriched membrane to form a complex for efficient conversion of C5−C12 *n*-alkanes to primary alcohols with the specific activity in TOF of 250–1000 min^{-1} (Fig. 1.1) [43]. There were no particular relationship between the specific activity and the chain length of alkanes. This phenomenon was explained by the assumption that the recombinant AlkB is heterogeneously expressed on the membrane of *E. coli* and may cause the promiscuity in the selection of substrates. Small alkanes including propane and *n*-butane can be accommodated in the hydrophobic pocket of AlkB for C–H bond activation.

Iron derivatives were used very often as catalysts (for examples, see [44–51]). Complexes of osmium [52–56], (examples of extremely efficient in alkane oxidation catalysts are presented in Fig. 1.2) copper, manganese, and vanadium also showed high activity in C–H oxidation in acetonitrile. Oxidations in acetonitrile, catalyzed with derivatives of titanium, rhenium, ruthenium, cobalt, rhodium and iridium, nickel,

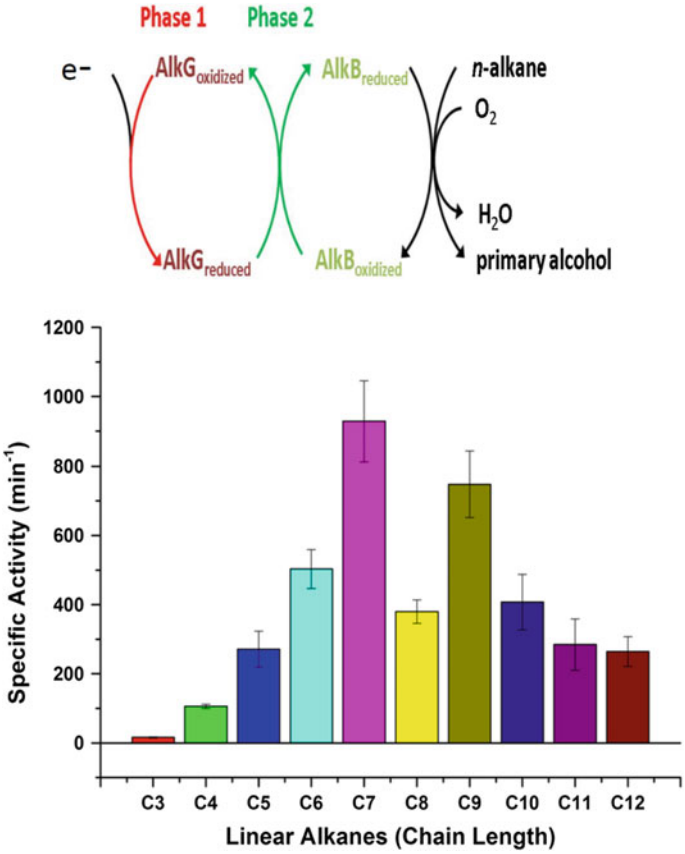

Fig. 1.1 Top: The catalytic oxidation of medium-chain length *n*-alkane mediated by the membrane-bound alkane hydroxylase (AlkB) from *Pseudomonas putida* GPo1 AlkB with electrons supplied from a soluble rubredoxin-2 (AlkG). Bottom: Specific activity in turnover frequency (TOF) for the electrochemical conversion of medium-chain length *n*-alkanes (C3–C12) to primary alcohols Adapted from ref. [43]

palladium and platinum, silver and gold, chromium, molybdenum and tungsten, have been described in the literature. A few publications have been devoted to the alkane oxidations catalyzed by non-transition metal complexes (aluminum, gallium, beryllium, and others [57–60]. Thus, the catalytic activity of aquacomplexes of the Group III metals $[M(H_2O)_n]^{3+}$ (M = Ga, In, Sc, $n = 6$; M = Y, $n = 8$; M = La, $n = 9$) toward the oxidation of hydrocarbons with H_2O_2 was investigated by DFT methods [61] (Fig. 1.3). The reaction occurs via two competitive reaction channels which are realized concurrently, i.e., (*a*) hydroperoxidation of the allylic C atom(s) via a radical Fenton-like mechanism involving HO· radicals and leading to alkyl hydroperoxides ROOH and (*b*) epoxidation of the C=C bond through a one-step mechanism involving oxygen transfer from the hydroperoxo ligand in an active catalytic form

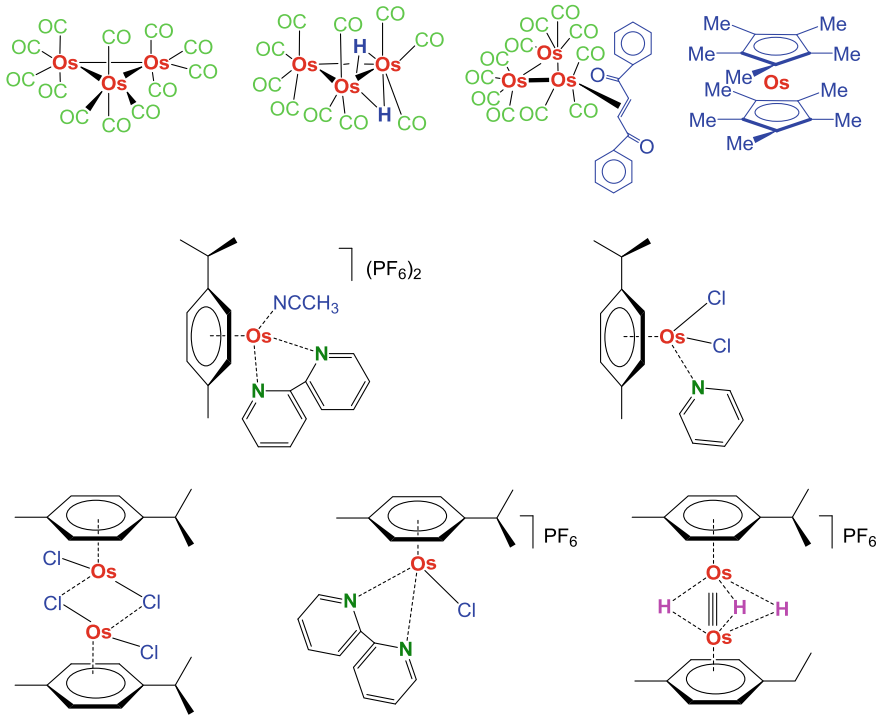

Fig. 1.2 Osmium complexes used as catalysts in the hydrocarbon oxidation with H_2O_2

$[M(H_2O)_{n-k}(OOH)]^{2+}$ (M = Ga, In, Y, La, $k = 2$; M = Sc, $k = 1$) to olefin molecule, leading to epoxides and/or *trans*-diols.

The catalytic system $Bi(NO_3)_3/H_2O_2/HNO_3/CH_3CN + H_2O$ was also used (Fig. 1.3) [62]. Dissolution of bismuth nitrate in water in the presence of strong acid results in the formation of aquacomplexes $[Bi(H_2O)_n]^{3+}$. The coordination number of Bi^{3+} in such solutions is highly variable, the formation of octa ($n = 8$) or/and ennea ($n = 9$) hydrates is proposed. These complexes formed from the simple soluble salts in aqueous media efficiently catalyze the hydrocarbon oxidation. The selectivity parameters and kinetic data as well as theoretical DFT calculations indicate that the reaction occurs *via* a mechanism involving the formation of the hydroxyl radicals which directly react with alkane molecules. The mechanism of the HO· generation (which is the rate-limiting step of the whole process) includes the substitution of a water ligand for H_2O_2 in the initial aqua complex $[Bi(H_2O)_8]^{3+}$, hydrolysis of the coordinated H_2O_2, second H_2O-for-H_2O_2 substitution, and the homolytic HO–OH bond cleavage in complex $[Bi(H_2O)_4(H_2O_2)(OOH)]^{2+}$. This mechanism does not require a change of the metal oxidation state. Instead, the OOH^- co-ligand in intermediate $[M(H_2O)_{n-m}(H_2O_2)(OOH)]^{(k-1)+}$ plays the same role as the transition metal does in the classical Fenton or Fenton-like processes. The OOH^- ligand is easily

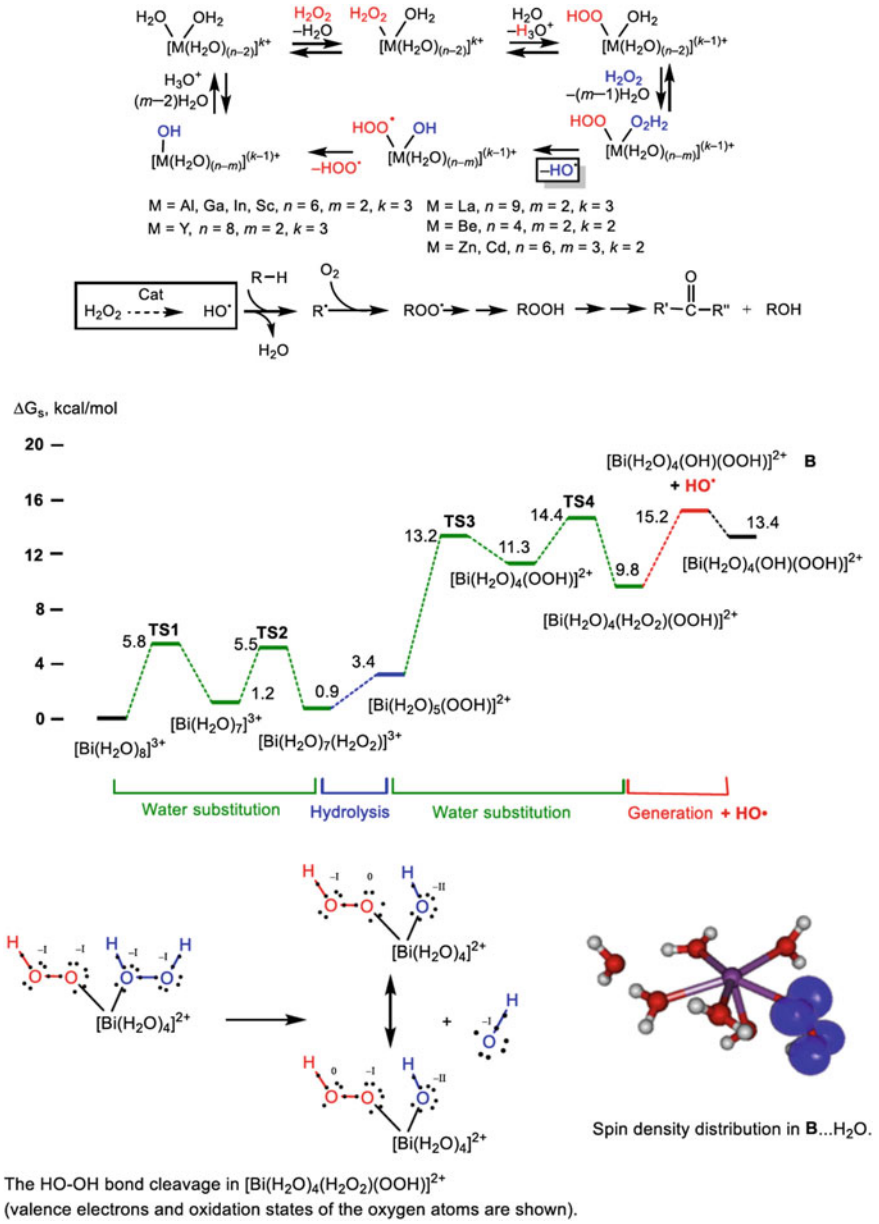

Fig. 1.3 Top: Mechanism of hydroperoxidation of alkanes with the systems $[M(H_2O)_n]^{k+}/H_2O_2$ (M = Al, Ga, In, Sc, Y, La, Be, Zn, Cd) *via* the formation of hydroxyl radical (the rate-limiting step of the whole process is boxed). Bottom: Energy profile for the proposed mechanism of the HO· generation (numbers indicate the relative energies) Adapted from Refs. [59–62]

oxidized by one electron upon the homolytic HO–OH bond cleavage leading to the stable complex $[M(H_2O)_{n-m}(OH)(\cdot OOH)]^{(k-1)+}$.

1.2.2 New Ligands

It is known that using certain ligands or adding to the reaction solutions some compounds that are able to coordinate as ligands to the metal complex catalysts, we can dramatically enhance both activity and selectivity of the oxidation [63–66]. Recently, to traditional species coordinated to metal ions, new "exotic" ligands were added, to produce catalysts based on MOFs [67], polymetallates [68–84], zeolites [85–87], and scorpionates [88–90].

Redox-active ligands at transition metal ions look very promising for oxidations. Thus, for example, vanadate anion and "simple" vanadium(V) and vanadium(IV) derivatives do not catalyze generation of hydroxyl radicals from hydrogen peroxide. Figure 1.4 shows the formation of oxygenates (after the reduction with PPh_3, the concentrations of cyclohexanol (-ol) and cyclohexanone (-one) were measured by GC) in vanadate anion catalyzed oxidation of cyclohexane with H_2O_2 in the presence (system **1**) or in the absence of pyrazinecarboxylic acid (PCA) [91].

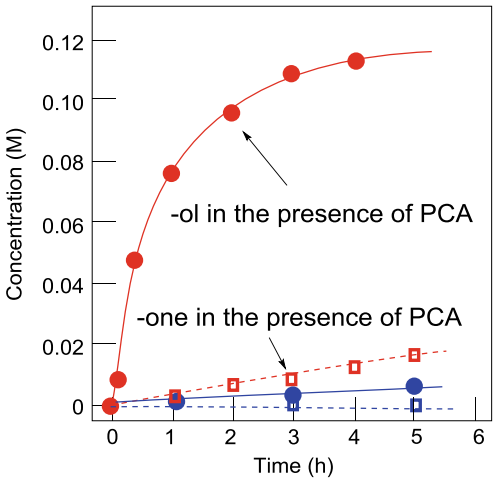

Fig. 1.4 Accumulation of cyclohexanol (-ol) or cyclohexanone (-one) in the oxidation of cyclohexane with H_2O_2 in the presence (red symbols) or in the absence (blue symbols) of PCA; the concentrations were measured after reduction of the reaction sample with PPh_3. Conditions: catalyst **1** $[n\text{-}Bu_4NVO_3]_0 = 1.0 \times 10^{-4}$ M, $[PCA]_0 = 4.0 \times 10^{-4}$ M; $[H_2O_2]_0 = 2.0$ M (50% aqueous), $[\text{cyclohexane}]_0 = 0.46$ M; MeCN up to total 5 mL volume; 50 °C Adapted from Ref. [91]

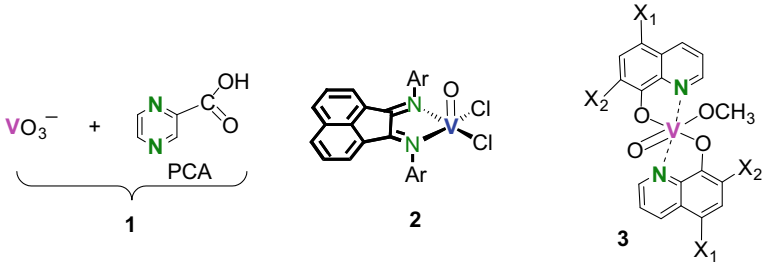

Introduced into the oxidovanadium (IV) complex [$VOCl_2$ (dpp-bian)] (**2**) the redox-active acenaphthene-1,2-diimine ligand gave a catalyst which is active in alkane oxidation with hydrogen peroxide (Fig. 1.5). It is interesting that addition of PCA to the reaction mixture leads to the enhanced activity) [91]. In contrast to complex **2**, other vanadium derivatives, namely, monomeric oxovanadium(V) complexes [VO(OMe)(N∩O)$_2$] with the nitro or halogen substituted quinolin-8-olate ligands (complex **3**) catalyze the decomposition of hydrogen peroxide, and the reaction does not require adding PCA [92]. The activation of H_2O_2 toward homolysis occurs upon simple coordination of hydrogen peroxide to the metal center of the catalyst molecule and does not require the change of the metal oxidation state and formation of the HOO radical. This activation is associated with the redox active nature of the quinolin-8-olate ligands. One of the key points of the successful use of complex **2** in the catalytic oxidation of alkanes is the phenomenon of "activating complexation" in the BIAN-V(O)Cl_2 system. Such effect is known for complexes of flavins and quinones. Effects of metal ions on thermal and photoinduced electron transfer reactions from electron donors, D, to electron acceptors, A, have been reviewed [93, 94]

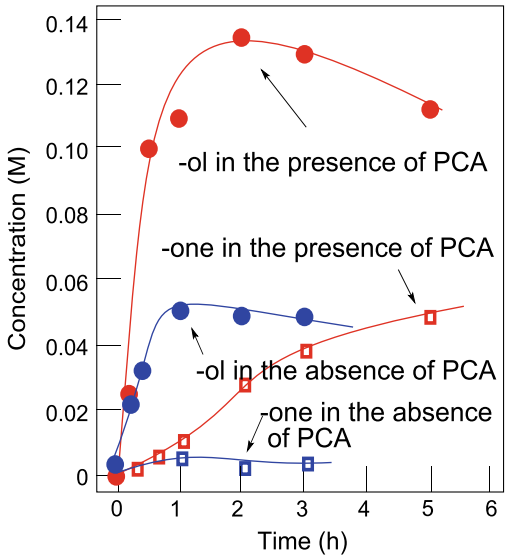

Fig. 1.5 Accumulation of cyclohexanol (-ol) or cyclohexanone (-one) is catalyzed by complex **2** oxidation of cyclohexane with H_2O_2 in the presence or in the absence of PCA; the concentrations were measured after reduction of the reaction sample with PPh_3. Conditions: [catalyst **2**]$_0$ = 5.0 × 10^{-4} M, [PCA]$_0$ = 2.0 × 10^{-3} M; [H_2O_2]$_0$ = 2.0 M (50% aqueous), [cyclohexane]$_0$ = 0.46 M; MeCN up to total 5 mL volume; 50 °C Adapted from Ref. [91]

in terms of metal ion-coupled electron transfer (MCET) versus metal ion-decoupled electron transfer (MDET).

1.3 New Methods of Reaction Stimulation

1.3.1 Oxidants

The most common and simultaneously "green" oxidants are undoubtedly molecular oxygen [95] O_2 (or air) [96] and hydrogen peroxide [97]. In addition, other peroxides are used in oxidations of organic compounds. These oxidants are peroxy acids (for example, peroxyacetic acid, [98–101] peroxybenzoic acids [102]), alkyl hydroperoxides [103–106], peroxydisulfate, [107, 108], and oxone [109].

1.3.2 The Participation of Radicals in Oxidations

Many reactions between hydrocarbons and hydrogen peroxide are proceed with the intermediate formation of hydroxyl radicals. We earlier proposed a few new methods in order to get insight into the mechanism of the oxygenation. These methods have been added to known tests demonstrating the generation of hydroxyl radicals [110].

A Comparison of Chromatograms of Oxygenated Products Obtained Before and After Reduction with PPh_3

The samples obtained in the alkane oxidation in acetonitrile should be analyzed twice both before and after their treatment with PPh_3 by GC. This method (the comparison of chromatograms of the same sample obtained before and after addition of PPh_3) [25, 64, 65, 110–112] allows us to estimate the real concentration of an alkyl hydroperoxide, ketone (aldehyde), and alcohol present in the reaction solution. Addition of solid PPh_3 to the aliquot taken from the reaction mixture immediately quenches the reaction. The formation of alkyl hydroperoxide detected by use of this (so-called Shul'pin test) method indicates that in the oxidation reaction an alkane, RH, is transformed into the corresponding alkyl radical, R·, which rapidly captures molecular oxygen. Peroxyl radical ROO·, thus formed, can further be reduced to alkyl hydroperoxide, ROOH. Garcia-Bosch and Siegler studied the cyclohexane oxidation with H_2O_2 in MeCN catalyzed various copper complexes. "GC analysis of the crude product mixture by the method described by Shul'pin confirmed the formation of cyclohexyl hydroperoxide as the main product: when the crude product mixture was injected directly, a 1:1 mixture of cyclohexanol and cyclohexanone was observed; treatment of the crude reaction mixture with excess PPh_3 prior to GC analysis led to the observation of cyclohexanol as the main product, indicative of the presence

of cyclohexyl hydroperoxide in solution" [113]. Sutradhar *et al*. studied the cyclohexane oxidation with H_2O_2 catalyzed by a copper(II) tetramer with arylhydrazone of barbituric acid [114]. "The formation of cyclohexyl hydroperoxide as a primary product was confirmed by following Shul'pin method. The duplicate GC analyses of the reaction mixture, before and after addition of PPh_3, has shown that the amount of alcohol detected by GC increased after addition of PPh_3 as a result of the reduction of CyOOH to cyclohexanol, with a concomitant decrease of the amount of cyclohexanone, allowing us to assume the CyOOH as the primary product of this reaction". Thus, if the yields of -ol and -one before the reduction with phosphine were 8.5 and 9.4%, respectively, the reduction gave the yields of 21.7 and 1.3% [114].

It is necessary to emphasize that only *comparison* of chromatograms obtained before and after the reduction can give information on the presence of alkyl hydroperoxide and allow the chemists to estimate its concentration. Indeed, alcohol can be produced in high concentration not after the reduction but in the oxidation reaction and alkyl hydroperoxide is not formed in this case at all. Determination of concentrations of alcohol and ketone only without reduction with PPh_3 (as in Refs. [39, 52]) and only after reduction with PPh_3 (for examples, see: Ref. [86] and "The oxidation reactions were monitored by withdrawing small aliquots after different periods of time; these were treated with PPh_3 for the reduction of remaining H_2O_2 and cycloalkyl hydroperoxides" [52] and "excess solid triphenylphosphine was added in order to capture alkyl hydroperoxides (if present)" [115]) does not give a valuable information on the real content of peroxide, alcohol, and ketone in the reaction solution. Only in the case when we have chromatograms obtained *before and after* the reduction and we can compare these chromatograms we will obtain information on the presence or absence of alkyl hydroperoxide in the reaction mixture.

1.3.3 A Competition of RH and MeCN for Hydroxyl Radical

Oxidation of cyclohexane with H_2O_2 catalyzed by vanadium complex **2** in combination with PCA is presented [91] in Fig. 1.6 (Graph A). Similar dependence has been found in the cyclohexane oxidation catalyzed by another vanadium complex **3** [92]. It can be seen that at relatively high concentrations of cyclohexane the rate W_0 is approaching a plateau. This dependence reflects the competition between cyclohexane and acetonitrile. For treatment of the data shown in Fig. 1.6, we applied the following kinetic scheme:

$$\mathrm{H_2O_2} + \text{ complex } \mathbf{3} \xrightarrow{k_i} \mathrm{HO}\cdot \tag{1.i}$$

$$\mathrm{HO}\cdot + \mathrm{RH} \xrightarrow{k_{\mathrm{RH}}} \mathrm{ROOH} \tag{1.1}$$

$$\mathrm{HO}\cdot + \mathrm{MeCN} \xrightarrow{k_{\mathrm{MeCN}}} \text{products} \tag{1.2}$$

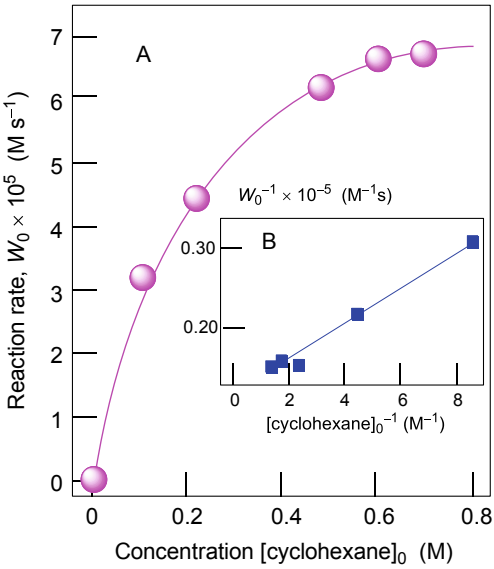

Fig. 1.6 Dependence of the initial oxidation rate W_0 on initial concentration of cyclohexane in the cyclohexane oxidation in acetonitrile (Graph A). Conditions: [complex **2**]$_0$ = 5.0×10^{-4} M; [PCA]$_0$ = 2×10^{-3} M; [H_2O_2]$_0$ = 2 M (50% aqueous), 50 °C. Concentrations of oxygenates (sum of cyclohexanol and cyclohexanone) were measured after reduction with PPh_3. Linear anamorphosis of the curve shown in Graph A is presented in Graph B in the coordinates W_0^{-1} vs. [cyclohexane]$_0^{-1}$

Here (i) is the reaction of hydroxyl radical generation; (1) is the process of RH transformation into ROOH with a bimolecular interaction between HO· and RH as the rate-limiting step; (2) is the process of acetonitrile oxidation with the participation of hydroxyl radicals (a bimolecular interaction between HO· and CH_3CN as the rate-limiting step). The analysis of experimental data given in Fig. 1.6, Graph A led to a straight line corresponding to the linear dependence of W_0^{-1} on [CyH]$_0^{-1}$ (Fig. 1.6, Graph B). Taking into account that [MeCN] ≈ 17 M we can obtain the ratio $k_{MeCN}/k_{CyH} \approx 8.3 \cdot \times 10^{-3}$. The value of this parameter is in agreement with the assumption about the participation of hydroxyl radicals (Table 1.1 [53, 116, 117]).

1.3.4 An Effect of Added Benzene

As shown in Fig. 1.7, addition of benzene (0.23 M) to the solution of cyclohexane (0.23 M) very slightly decreases the initial oxidation rate. It has been found that the systems operate with the generation of hydroxyl radicals. It has been demonstrated that reactions of hydroxyl radical with benzene were faster in water than in acetonitrile, by a significant factor of 65 (Ref. [118]). It is interesting that the catalytic activity can be significantly improved by adding water to acetonitrile solvent [119]. These data can explain a weak effect of added benzene in the cyclohexane oxidation in acetonitrile catalyzed by complex **2**.

Table 1.1 Kinetic parameters for the competitive oxidation of cyclohexane and acetonitrile with various systems based on H_2O_2

Entry	System	$k_{MeCN}[CH_3CN]/k_{CyH}$ (M)	k_{MeCN}/k_{CyH}
1	$H_2O_2/O_2/(n\text{-}Bu_4N)VO_3$/PCA	0.14	0.008
2	H_2O_2/O_2/"**Cu_4**"/CF_3COOH	0.20	0.012
3	H_2O_2/O_2/"**Cu_4**"/HCl	0.10	0.006
4	$H_2O_2/O_2/[Co_4Fe_2OSae_8]/HNO_3$	0.14	0.008
5	$H_2O_2/O_2/Cp^*{}_2Os$/py	0.09 ÷ 0.19	0.0055 ÷ 0.011
6	$H_2O_2/O_2/Cp_2Fe$/Py/PCA	0.19	0.011
7	H_2O_2/O_2/"Fe_2(TACN)"/PCA	0.19	0.011

Conditions. Concentration $[CH_3CN]_0$ was assumed to be 17 M. *Abbreviations*. PCA is pyrazine-2-carboxylic acid. "**Cu_4**" is tetracopper(II) triethanolaminate complex $[O{\subset}Cu_4\{N(CH_2CH_2O)_3\}_4(BOH)_4][BF_4]_2$. Complex $[Co_4Fe_2OSae_8] \cdot 4DMF \cdot H_2O$, where H_2Sae = salicylidene-2-ethanolamine. Cp $*_2Os$ is decamethylosmocene. Cp_2Fe is ferrocene. "Fe_2(TACN)" is an iron(III) complex with 1,4,7-triazacyclononane

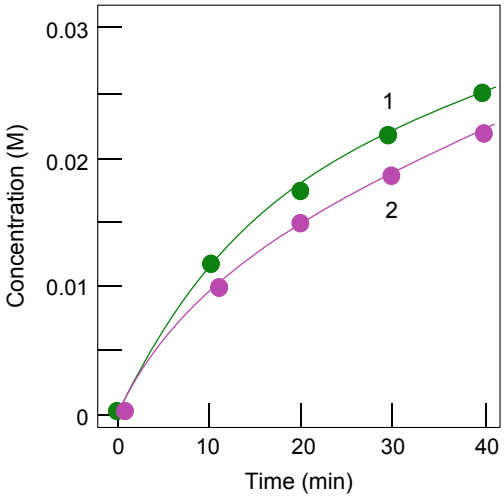

Fig. 1.7 Accumulation of cyclohexanol and cyclohexanol (a sum) in the initial period after treating with PPh_3 in the cyclohexane oxidation in acetonitrile in the absence of benzene (curve 1) and in the presence of benzene (curve 2). Conditions: [complex **2**]$_0$ = 5.0×10^{-4} M; $[H_2O_2]_0$ = 2 M (50% aqueous), [cyclohexane]$_0$ = 0.23 M, [benzene]$_0$ = 0.23 M (for curve 2 only), 40 °C. Concentrations of oxygenates (sum of cyclohexanol and cyclohexanone) were measured after reduction with PPh_3 Adapted from ref. [91]

1.3.5 Recently Proposed Methods of Reaction Stimulation

In recent decades, new methods of catalytic oxidation stimulation have been added to traditional methods (such as heating, light irradiation). Thus, copper complexes with an arylhydrazone of methyl 2-cyanoacetate catalyzed the oxidation of cyclohexane with TBHP in MeCN, using low power microwave (MW) irradiation [120]. Copper(I) and copper(II) metallacycles catalyze microwave-assisted selective oxidation of cyclohexane via the formation of cyclohexyl hydroperoxide (CyOOH) as the primary product [121].

Another method is presented by sonochemistry [122, 123]. Degradation of selected groups of organic compounds by cavitation [124] as well as a method of treatment of industrial effluents under acoustic cavitation have been recently described [125].

1.4 Non-conventional Media and Solvents

1.4.1 Acetonitrile and Other Traditional Solvents

As it has been mentioned above, very many oxidations of alkanes are carried out in acetonitrile as solvent. This is possible because the reactivity of alkanes is even higher than that of cyclohexane and usual hydrocarbons (see, for example, above Table 1.1). Ethane and especially methane are much less reactive in the reaction with hydroxyl radicals. Acetone, dimethylsulfoxide, and some other organic liquids are more rarely used in alkane oxidations with peroxides. However, it is hard to say that acetonitrile and organic liquids are green solvents for alkane oxidations.

1.4.2 Solvent-Free Oxidations

Some hydrocarbons and, more frequently, alcohols have been functionalized under the action of oxidants without participation of any solvent [126]. Thus, scorpionate complexes of vanadium [127] and the $Al_{60}Cu_5Co_{35}$ alloy [128] induce the oxidation of cyclohexane with dioxygen; a bis(μ-chlorido) bridged cobalt(II) complex $[Co_2(mu–Cl)_2(HL_2)_4][CoCl_4]$, where HL_2 is a silyl-containing Schiff base, was found to act as an effective homogeneous (pre)catalyst in the microwave-assisted net oxidation of cyclohexane with aqueous TBHP [129].

1.4.3 Oxidation in Aqueous Solutions

Water is the most attractive solvent [130–132] for green oxidations. A few examples are described in this Section. As hydrocarbons are sparingly soluble in water, the reactions are often carried out in emulsions [133].

Oxidation of Alcohols

Alcohols can be easily oxidized by peroxides (H_2O_2) in water. Such a reaction was catalyzed by a water-soluble copper(II) complex bearing 4-bromobenzoate/2,2′-dipyridylamine ligands. This complex was active also in the oxidation of alkenes with TBHP in aqueous solution [134].

Glycerol, containing hydroxyl groups, is a by-product of biodiesel manufacturing [135–137]. Oxidative transformations of glycerol [138] are especially important from the practical point of view (Scheme 1.1). Glycerol can be easily dehydrated to α-hydroxyacetone (acetol) which can also be oxidized, potentially leading to the formation of products of industrial interest (Scheme 1.2). The oxidation of acetol by cheap and green homogeneous catalytic system $FeCl_3/H_2O_2$ has been recently described [139]. Acetic acid and formic acid, as well as carbon dioxide, were the main products. The experiments in the atmosphere of $^{16}O_2$ and $^{16}O_2 + {}^{18}O_2$ led to the conclusion that molecular oxygen from atmosphere takes part in the reaction and these atoms are incorporated into the products. It should be emphasized that the yield of acetic acid is higher and reaches ca. 70% if water is used as solvent and 50% in acetonitrile solution (Fig. 1.8).

In the oxidation of acetone with H_2O_2, catalyzed by the cationic dinuclear manganese(IV) derivative $[Mn_2L_2O_3]^{2+}$ (complex **4**, where L = 1,4,7-trimethyl-1,4,7-triazacyclononane), the substrate played also the role of the solvent [140]. This reaction at 40 °C in the presence of oxalic acid gave rise to the formation of acetic acid as a sole product (a kinetic curve is shown in Fig. 1.9). The initial rate of acetic acid accumulation and its yield after 3 h linearly depend on the concentration of catalyst **4** (Fig. 1.9). It is interesting that the initial rate of acetic acid accumulation only slightly depends on temperature in the interval of 10–50 °C.

Oxidation of Hydrocarbons

Ruthenium(0) nanospecies, with small sizes of approximately 1.75 nm, proved to be active, selective, and retrievable nanocatalysts for the room temperature oxidation of various cycloalkanes in neat water, using TBHP as an oxidant [141]. Alvarez and Sorokin [142] found that in oxidation by H_2O_2, catalyzed with supported μ-nitrido diiron phthalocyanines, the reactivities of C–H bonds in methane, ethane, and propane were very similar when the reaction was performed in water. Contrastingly, in diluted acidic solution, the μ-nitrido diiron phthalocyanine-H_2O_2 system exhibited five times higher activity oxidation of the methane C–H bond compared to the ethane C–H bond.

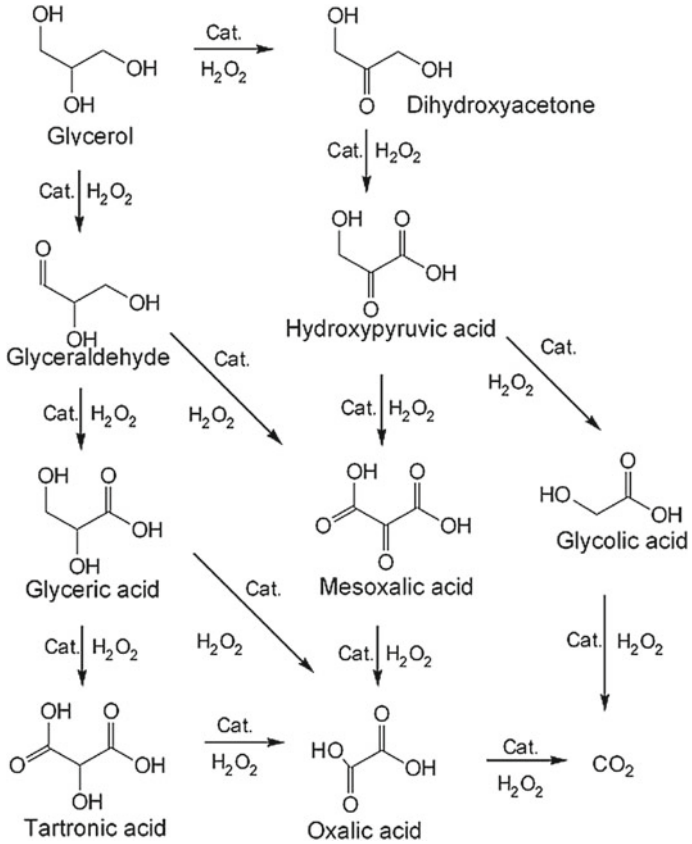

Scheme 1.1 Oxidative transformations of glycerol

The oxidation of alkanes with hydrogen peroxide in water solution at 10–50 °C is efficiently catalyzed by the cationic dinuclear manganese(IV) derivative **4**, if oxalic acid is present as a cocatalyst [143]. Methane was transformed into methanol and formaldehyde (after reduction of the reaction mixture with ascorbic acid). Cyclohexane was oxidized to produce cyclohexyl hydroperoxide, cyclohexanone, and cyclohexanol (the ketone was the main product, although at room temperature almost pure alkyl hydroperoxide was formed). The oxidation of *n*-heptane by this system gave (after the reduction of the ether extract with PPh_3) a mixture of all possible isomeric alcohols and ketones (aldehyde), witnessing that hydrogens at position 3 and especially at position 4 are much more reactive than hydrogen atoms in position 2. Similar profiles have been obtained for the selectivities in oxidations of *n*-hexane and *n*-pentane. This picture is in a striking contrast with the corresponding profiles for the oxidation in acetonitrile (see Fig. 1.10). It was assumed that hydrocarbon chains exist in aqueous solution in the folded conformation and in this case position 4 of *n*-heptane is more accessible for the attack than position 2.

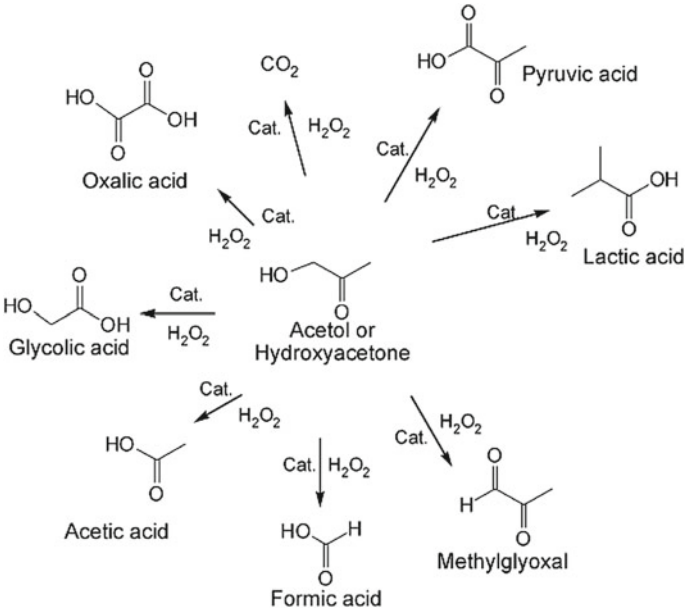

Scheme 1.2 Oxidation of acetol with H_2O_2

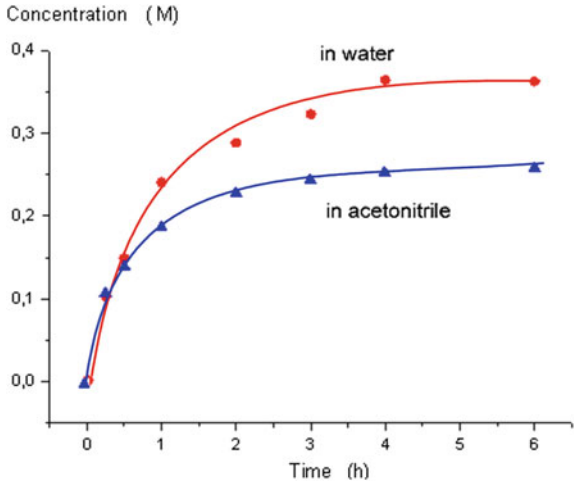

Fig. 1.8 Acetic acid concentration versus time for the $FeCl_3$-catalyzed oxidation of acetol in water or acetonitrile. Conditions: acetol, 0.5 M; $FeCl_3$, 1×10^{-3} M; H_2O_2, 0.5 M; solvent up to 5 mL; 60 °C Adapted from ref. [139]

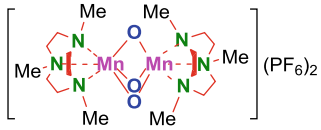

Complex **4**

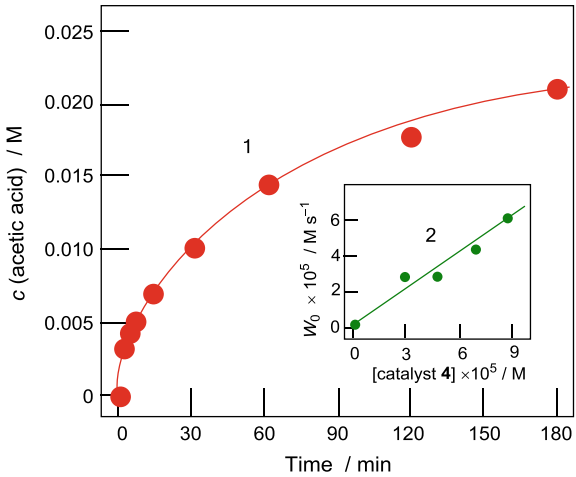

Fig. 1.9 Oxidation of acetone with hydrogen peroxide (0.54 M) catalyzed by complex **4** (5×10^{-5} M) and oxalic acid (0.125 M) at 40 °C. Solvent: acetone containing MeCN (1 mL). Total volume of the reaction solution was 5 mL. Accumulation of acetic acid with time (curve 1) and dependence of the initial rate of formation of acetic acid W_0 (curve 2) on the initial concentration of catalyst **4** are shown Adapted from Ref. [140]

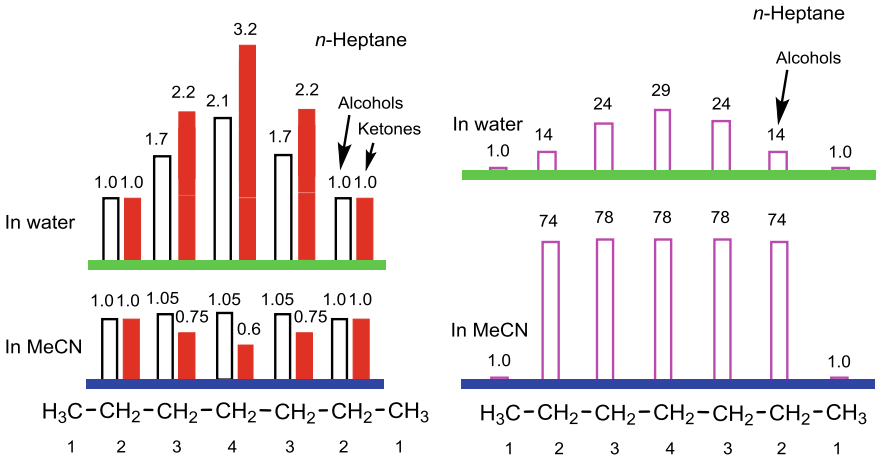

Fig. 1.10 Selectivity parameters C(2): C(3): C(4) which are normalized (i.e., calculated taking into account the number of hydrogen atoms at each position) relative reactivities of hydrogen atoms at positions 2, 3, and 4 of the hydrocarbon chain, respectively, calculated for both obtained alcohols and ketones (the reactivity of the CH_2 hydrogens at position 2 is accepted to be equal 1.0 and C(1): C(2): C(3): C(4) for the oxidation of *n*-heptane by the **4**–oxalic acid–H_2O_2 system in water and acetonitrile Adapted from Ref. [143]

When an emulsion of cyclohexane and an aqueous solution of $Fe(ClO_4)_3$ in air was light irradiated, cyclohexanone was produced. No cyclohexanol was detected [144]. The reaction occurs *via* the formation of cyclohexyl hydroperoxide, which in water was highly selectively decomposed to afford cyclohexanone. A copper-based metal-organic framework (Fig. 1.11), synthesized from imidazole carboxylate ligands 5-(1H-imidazol-1-yl)isophthalic acid and copper(II) ions induced hydroxylation of benzene to phenol with a benzene conversion of 29% as well as a high phenol selectivity above 95% at 60 °C in water [145]. The catalytic mechanism follows a Fenton-type route (Fig. 1.11). Other solvents, such as ethanol, methanol, dichloromethane, and N, N-dimethylformamide were not appropriate for the benzene transformation into phenol. A low benzene conversion along with an excellent phenol selectivity was obtained in pure acetonitrile or water. Mixed solvents acetonitrile-water had a better effect because the benzene hydroxylation occurred in the aqueous phase, and acetonitrile extracted phenol from water, avoiding over-oxidation.

Recently, Hollman and coworkers [146] demonstrated that visible-light-driven, catalytic water oxidation can be used for in situ generation of H_2O_2 from water, rendering the peroxygenase catalytically active. In this way, the stereoselective oxy-functionalization of ethylbenzene can be achieved by using the catalytic system,

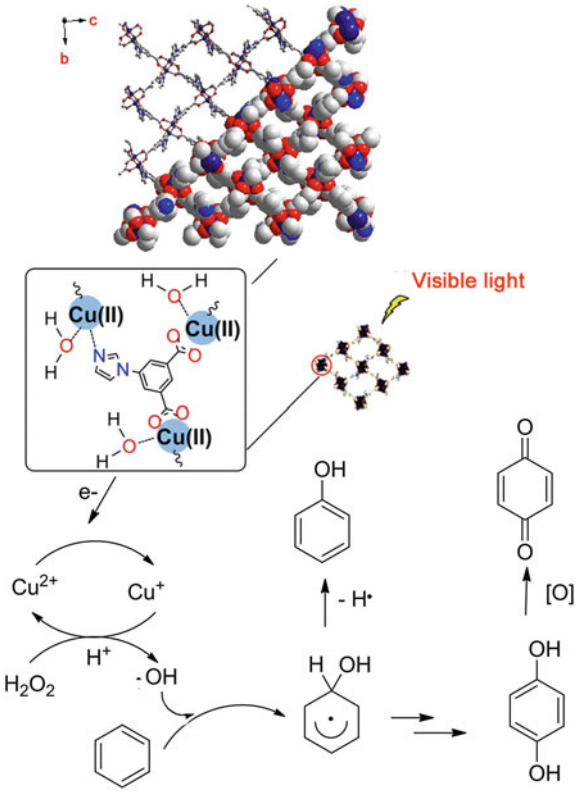

Fig. 1.11 Proposed mechanism of the hydroxylation of benzene to phenol with the copper-based MOF Adapted from Ref. [145]

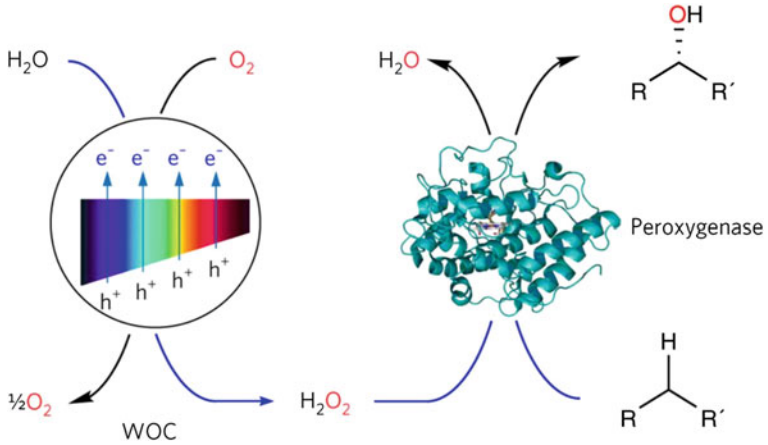

Fig. 1.12 Photochemical water oxidation generating H_2O_2 to promote peroxygenase-catalyzed hydroxylations of ethylbenzene. Reproduced from Ref. [146] with permission of Springer Nature

water, and visible light as shown in Fig. 1.12. The photochemical oxidation of water under the action of a water oxidation catalyst (WOC) delivers the liberated reducing equivalents to molecular oxygen to produce H_2O_2. The system oxidizes ethylbenzene in > 99% *ee*.

Propane was oxidized to acetone, isopropanol, propanal, and propionic acid by the H_2O_2–$NaVO_3$–H_2SO_4 system in water [147]. The oxidation of methane with the reagent "hydrogen peroxide–vanadate anion–pyrazine-2-carboxylic acid (PCA)" in an aqueous solution to afford largely formic acid is accompanied by the intense parallel degradation of the cocatalyst. Additives of strong acids (sulfuric, trifluoroacetic, or perchloric) increase the yield of the products [148].

In 1969, Shilov and coworkers discovered the H/D exchange in alkanes, RH, under the action of a simple platinum(II) salt, Na_2PtCl_4 in solution of D-containing water or acetic acid (see reviews [24, 149]).

$$RH + D_2O \xrightarrow{Na_2PtCl_4} RD + HOD$$

Later, the same authors described the oxidation of alkanes with H_2PtCl_6 in the presence of a catalytic amount of Na_2PtCl_4. In this case, alkane was transformed into the corresponding alcohol and alkyl chloride.

$$RH + H_2PtCl_6 \xrightarrow{Na_2PtCl_4} RCl + ROH + H_2PtCl_4$$

It is important to emphasize that simple platinum salts in water or aqueous acetic acid under relatively mild conditions could induce such challenging reactions. The Shilov reactions present the first example of "genuine, organometallic" (that is occurring with the formation of carbon–metal bonds) activation of C–H bonds in alkanes by

metal complexes. A combined investigation of rate constants k_{ex} and k_{ox} of the H/D exchange and oxidation, respectively, under conditions when only species $Pt^{II}Cl_3^-$ are active, was carried out [24]. When concentration [Pt(IV)] rises and $[D^+]$ decreases, the value k_{ex} for exchange decreases and the constant for oxidation k_{ox} increases. However, the sum of constants for both processes is maintained constant and equal to the activation rate constant $k_{ex} + k_{ox} = k_{act}$. This testifies that both processes occur with the participation of common intermediates. It was found that the rate constant for interaction of RPt^{II} with Pt^{IV} is 10^4 times higher than the constant for reaction of RPt^{II} with D^+. A qualitative model which takes into account these data has been proposed [24] This mechanism includes as a first step the equilibrium pre-activation of Pt(II) complex leading to the generation of coordination vacancy. A very active $(Pt^{II})^*$ complex containing a coordination vacancy forms then an adduct with the alkane RH. In the subsequent step, all accessible C–H bonds of RH are split with almost equal rate. Interestingly, a striking similarity of kinetic parameters for Shilov reaction and that for the reaction of alkanes with hydroxyl radicals in water has been documented [24].

1.4.4 Strong Acids as Solvents

Periana and coworkers proposed (2,2′-bipyrimidyl)platinum(II)dichloride as catalyst for the "Periana System"; see recent reviews [150–152]. Fuming sulfuric acid is the oxidant in this case. A scheme of the catalytic cycle is shown in Fig. 1.13. The authors postulated that there could be three distinct classes of catalyst/oxidant/solvent systems. The established electrophilic class combines electron-poor catalysts in acidic solvents. The nucleophilic class matches electron-rich catalysts with basic solvents. The third class involves ambiphilic catalysts that can conceptually react with both the HOMO and LUMO of the CH bond and would typically involve neutral reaction solvents. The "Periana System" was capable of the selective, high-yield functionalization of methane to ~1 M methanol in H_2SO_4. Its stability was the result of oxidative dissolution of Pt^0 by H_2SO_4 facilitated by the bipyrimidine (bpym) ligand.

In 1973, Rudakov and coworkers discovered the alkane oxidation in sulfuric acid by palladium(II) ions as analogs of Pt(II), and later by Hg^{II}, Pt^{III}, sulfuric acid itself, and other reagents (see reviews [24, 153]). Shilov reaction astoundingly differs from the alkane reaction with palladium(II) ions. The latter process occurs only in strongly acidic media (>70% H_2SO_4).

Strassner [154] found that palladium(II) complexes of bridged bis(N-heterocyclic carbenes) (NHC) catalyze the direct conversion of methane in trifluoroacetic acid with a much higher activity than palladium acetate. The palladium-catalyzed oxidation of methane was divided into three steps: CH activation, oxidation, and reductive elimination. The reaction did not work in acetic acid. The authors calculated the corresponding rate-determining transition state (Fig. 1.14). The formation of the cationic sigma-complex is significantly higher in energy at 25.0 kcal mol^{-1}, in comparison to 16.1 kcal mol^{-1} for the trifluoroacetate complex. The energy differences between

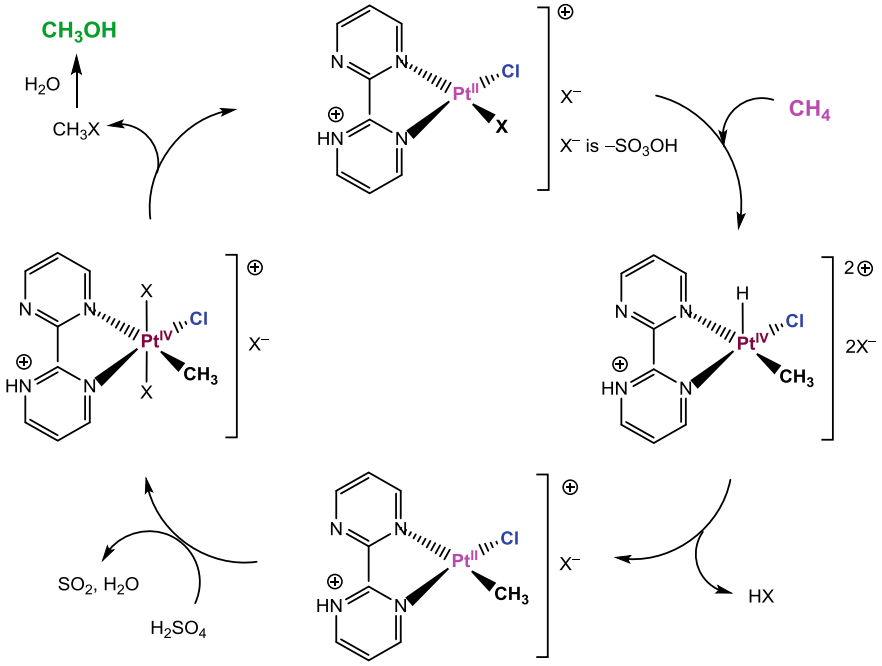

Fig. 1.13 The catalytic cycle for the methane oxidation by the Periana system Adapted from Ref. [151]

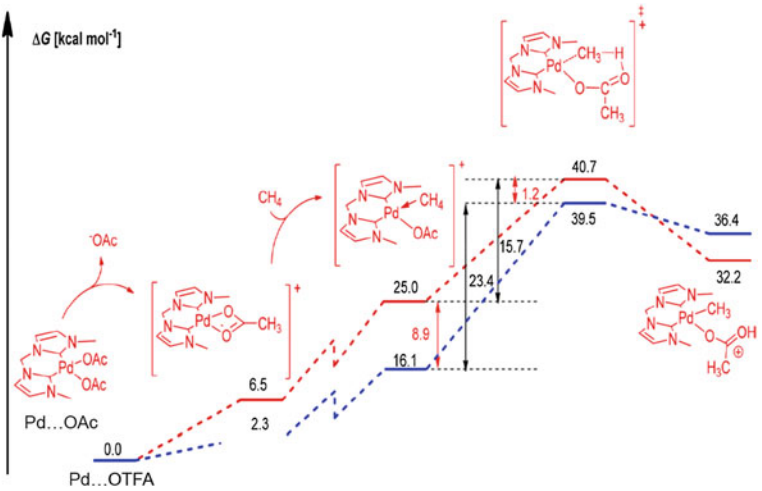

Fig. 1.14 Comparison of the overall reaction barriers for trifluoroacetic acid (HOTFA, in blue) and acetic acid (HOAc, in red) Adapted from Ref. [154]

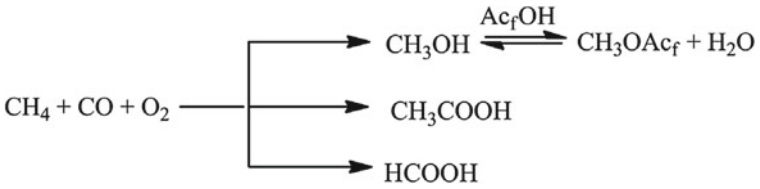

Scheme 1.3 Oxidation and carbonylation of methane in Ac_fOH/H_2O medium in the presence of Rh–I–Cl, Rh–Cu–Cl, and Rh–Fe–Cl catalytic systems Adapted from Ref. [158]

the transition states and the corresponding sigma-complexes are 23.4 kcal mol^{-1} for the trifluoroacetate transition state and 15.7 kcal mol^{-1} for the corresponding acetate transition state. Overall, the reaction barrier is 1.2 kcal mol^{-1} higher in energy for the acetate transition state, which is in agreement with the experimental data.

$$CH_4 + 2H_2SO_4 \xrightarrow[H_2SO_4, 220\ ^\circ C]{PtCl_2(bpym)} CH_3OSO_3H + 2H_2O + SO_2$$

Sen demonstrated [155] that carbon monoxide can efficiently trap alkyl radicals generated in the reaction of methane or ethane with $SO_4^{-}\cdot$ radical (generated from $S_2O_8^{2-}$ in aqueous medium, at 105–115 °C. The resultant acyl radicals were ultimately converted into the homologous carboxylic acids. Later, Fujiwara and coworkers reported on a system for the conversion of CH_4, CO, and O_2 (or $K_2S_2O_8$) to acetic acid in the presence of Pd^{II} catalysts in trifluoroacetic acid as solvent [156]. Pombeiro and coworkers reported carbonylation of alkanes with CO and $K_2S_2O_8$ in trifluoroacetic acid at 80 °C, catalyzed by vanadium complexes [157]. Chepaikin [158] and coworkers demonstrated that catalytic systems $RhCl_3$–KI–NaCl and $RhCl_3$–$Cu(OAc_f)_2$–NaCl in aqueous perfluorinated carboxylic acids(CF_3COOH, C_3F_7COOH) are effective in coupled oxidation of alkanes and carbon monoxide with dioxygen (Scheme 1.3). The process occurs partially by the inner-sphere mechanism involving Rh–alkyl intermediates. This mechanism is supported by the formation of alkyl chlorides, synthesis of acetic acid in conversion of methane, and positional selectivity in oxidation of propane.

1.4.5 Supercritical Liquids

Supercritical fluids are considered as promising solvents for chemical reactions [159]. One of the most extensively used supercritical liquids is supercritical carbon dioxide ($scCO_2$) which is nontoxic and nonflammable compound, completely miscible with water and with molecular oxygen, and can be easily separated from the reaction mixtures. For example, recently the cis-dioxidomolybdenum(VI) complexes $[MoO_2(L^1)]$, $[MoO_2(L^2)]$ and $[MoO_2(L^3)]$, where H_2L^1 = 2,3-dihydroxybenzylidene-2-hydroxybenzohydrazide,

H_3L^2 = 2,3-dihydroxybenzylidene-benzohydrazide and H_2L^3= (3,5-di-*tert*-butyl-2-hydroxybenzylidene)-2-hydroxybenzohydrazide, were employed in oxidation of cyclohexane with TBHP in CH_3CN, ionic liquid (1-butyl-3-methylimidazolium hexafluorophosphate, [bmim][PF_6]), supercritical carbon dioxide (sc–CO_2), and sc–CO_2/[bmim][PF_6] mixed solvent [160].

1.4.6 Ionic Liquids

Many metal catalysts and substrates either do not dissolve in water or rapidly decompose in aqueous solutions. "Ionic liquids, fluorous solvents and supercritical fluids may offer a solution in avoiding" some of such problems [161–163]. Thus, the efficiency of Pt/C–heteropoly acid catalyst in a liquid-phase oxidation of cyclohexane using an O_2–H_2 mixture the catalytic effect of the Pt/C–$H_3PMo_{12}O_{40}$–CH_3CN system at 35 °C is significantly improved, by slowing the rate of side reactions resulting in water formation, increasing the rate of oxygenate formation, and inhibiting their secondary oxidation reactions by small additives of ionic liquid (BMImBr, Bu_4NBr, or Bu_4NHSO_4) [164].

The first example of alkane hydrocarboxylation in an ionic liquid medium was reported. Compound **A** (Fig. 1.15) can effectively catalyze the hydrocarboxylation of cyclohexane not only in aqueous MeCN but also in an aqueous ionic liquid medium, water/ionic liquid [BMPyr][NTf_2], BMPyr = 1-butyl-1-methylpyrrolidinium; NTf_2 = bis(trifluoromethanesulfonyl)imide, producing the corresponding cyclohexanecarboxylic acid as the main product [165]. The reaction proceeds mainly *via* a radical mechanism (Fig. 1.15).

1.5 Perspectives

Traditional organic solvents are widely employed in catalytic organic synthesis. These solvents are acetic acid, acetonitrile, alcohols, dimethylformamide, dichloromethane, dimethylsulfoxide, etc. The material described in this chapter demonstrates that oxidations of C–H compounds in nontraditional solvents (particularly, in supercritical fluids, for example, sc–CO_2, ionic liquids, strong acids, such as sulfuric and trifluoroacetic acids) have an advantage relative to traditional organic solvents. Water, which is the most abundant molecule on Earth, is simultaneously the most attractive and perspective solvent. It is the cheapest and environmentally benign solvent. "Due to hydrophobic effects, using water as a solvent not only accelerates reaction rates but also enhances reaction selectivities, even when the reactants are sparingly soluble or insoluble in this medium. Furthermore, the low solubility of oxygen gas in water, an important property in the early development of life in an anaerobic environment, can facilitate air-sensitive transition-metal catalysis in open air" [131]. "It is often recognized that the use of water as a solvent has tremendous

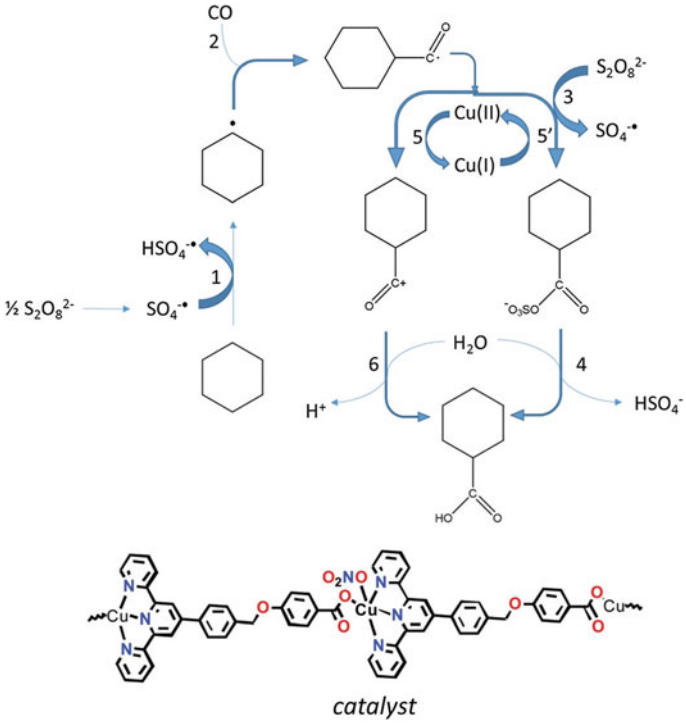

Fig. 1.15 Proposed mechanism for the hydrocarboxylation of cyclohexane Adapted from Ref. [165]

benefits as a green chemistry solvent. Certainly, it is obvious that water is nontoxic, nonflammable, cheap, and available. When compared to the typically used organic solvents based on petroleum feed-stocks, one would argue that water is the pinnacle of the green solvents" [166]. However, water as solvent has some serious limitations: one of them is the problem of product separation. Nevertheless, chemists can assume that water as a solvent will be used more and more widely in catalytic organic synthesis.

References

1. Matienko LI, Mosolova LA, Zaikov GE (2010) Selective catalaytic hydrocarbons oxidation. In: New perspectives. Nova Science Publ. Inc., New York, USA
2. Lancaster M (2002) Green chem: an introductory text. RSC, Cambridge
3. Lange J-P (2002) Sustainable development: efficiency and recycling in chemicals manufacturing. Green Chem 4:546–550. https://doi.org/10.1039/b207546f
4. Sheldon RA, Arends IWCE, Hanefeld U (2007) Green Chem and Catal. WILEY-VCH Verlag GmbH & Co. KGaA, Weinheim. 1–433. https://doi.org/10.1002/9783527611003
5. Sheldon RA (2008) E Factors, green chemistry and catalysis: an odyssey. Chem Commun 29:3352–3365. https://doi.org/10.1039/b803584a
6. Editors: Ameta SC Ameta R (2013) Green chemistry. Fundamentals and applications. CRC Press, Boca Raton. ISBN 9781926895437 - CAT# N10733
7. Sheldon RA (2012) Fundamentals of green chemistry: efficiency in reaction design. Chem Soc Rev 4:1437–1451. https://doi.org/10.1039/c1cs15219j
8. Caballero A, Pérez PJ (2013) Methane as raw material in synthetic chemistry: the final frontier. Chem Soc Rev 42:8809–8820. https://doi.org/10.1039/c3cs60120j
9. Liu W-C, Baek J, Somorjai GA (2018) The methanol economy: methane and carbon dioxide conversion. Top Catal 61:530–541. https://doi.org/10.1007/s11244-018-0907-4
10. Sheldon RA (2005) Green solvents for sustainable organic synthesis: state of the art. Green Chem 7:267–278. https://doi.org/10.1039/b418069k
11. Anastas PT, Heine LG, Williamson TC (Eds.) (2000) Green chemical syntheses and processes. Am Chem Soc (Washington DC). https://doi.org/10.1021/bk-2000-0767.ch001
12. Marion P, Bernela B, Piccirilli A, Estrine B, Patouillard N, Guilbot JJF (2017) Sustainable chemistry: how to produce better and more from less? Green Chem 19:4973–4989. https://doi.org/10.1039/c7gc02006f
13. Deyris P-A, Griso C (2018) Ecology and chemistry: an unusual combination for a new green catalysis, ecocatalysis. current opinion in green and sustainable chemistry. Nature 10:6–10. https://doi.org/10.1016/j.cogsc.2018.02.002
14. Constable DJC, Curzons AD, Cunningham VL (2002) Metrics to 'green' chemistry—which are the best? Green Chem 4:521–527. https://doi.org/10.1039/b206169b
15. Sheldon RA (2017) The E factor 25 years on: the rise of green chemistry and sustainability. Green Chem 19:18–43. https://doi.org/10.1039/c6gc02157c
16. Zaikov GE, Maizus ZK (1968) Effect of solvents on rates and routes of oxidation reactions. Oxidation of organic compounds. Mayo F Adv Chem Am Chem Soc (Washington, DC) 12:150–164. https://doi.org/10.1021/ba-1968-0075
17. Lee DG, Keith CB, Karaman H (1986) Oxidation of hydrocarbons. 17. Solvent and substituent effects on the oxidation of styrene derivatives by quaternary ammonium permanganates. Can J Chem 64:1054–1059. https://doi.org/10.1139/v86-177
18. Nelson WM (2003) Green solvents for chemistry: perspectives and practice. Oxford University Press, ISBN-10:0195157362
19. Adams DJ, Dyson PJ, Tavener SJ (2003) Chemistry in alternative reaction media. Wiley, ISBN:0-471-49849-1
20. Kinzhalov MA, Kashina MV, Mozheeva EA, Mikherdov AS, Ivanov DM, Novikov AS, Smirnov AS, Kryukova MA, Ivanov AY, Smirnov SN, Kukushkin VY, Luzyanin KV (2018) Solubility of halide-containing organometallics is dramatically enhanced in diiodomethane: can the solvent complex halogen bonding be held responsible? Angew Chem Int Ed 57(39):12785–12789. https://doi.org/10.1002/anie.201807642
21. Shul'pin GB, Shilov AE, Kitaigorodskii AN, Zeile Krevor JV (1980) The reaction of H_2PtCl_6 with aromatic compounds affording the sigma-aryl complexes of Pt(IV). II. The synthesis of Pt(IV) complexes of benzene, alkylbenzenes and chlorinated benzenes. J Organomet Chem 201:319–325. https://doi.org/10.1021/cr9411886?src=recsys

22. Shul'pin GB (1981) Reaction of aromatic compounds with H_2PtCl_6 in $CF_3COOH–H_2O$ system leading to the preparation of anionic sigma-aryl complexes of Pt(IV). J Gen Chem USSR 51(9, Part 2):1808–1818
23. Shul'pin GB, Nizova GV, Nikitaev AT (1984) The reaction of $PtCl_6^{2-}$ with aromatic compounds to afford anionic sigma-aryl complexes of Pt(IV). VIII. Kinetics and mechanisms of thermal, photochemical and gamma-induced reactions with arenes and arylmercury compounds (electrophilic substitution involving electron transfer). J Organomet Chem 276(1):115–153. https://doi.org/10.1016/0022-328x(84)80609-9
24. Rudakov ES, Shul'pin GB (2015) Stable organoplatinum complexes as intermediates and models in hydrocarbon functionalization (review). J Organomet Chem 793:4–16. https://doi.org/10.1016/j.jorganchem.2015.01.032
25. Shul'pin GB (2016) new trends in oxidative functionalization of carbon–hydrogen bonds: a review. Catalysts 6(4):paper No. 50. https://doi.org/10.3390/catal6040050
26. Nizova GV, Shul'pin GB (1990) The formation of sigma-aryl Pt(IV) complexes in the photochemical reaction of $PtCl_6^{2-}$ ion with arenes in CH_2Cl_2 (photoelectrophilic substitution). Metalloorgan. Khimiya 3(2):463–464 (in Russian)
27. [27] Lederer P, Nizova GV, Kats MM, Shul'pin GB (1992) Photooxygenation of cyclohexane by dioxygen in the presence of metal chlorides in acetonitrile <Part XIX in the series "Photoinduced Reactions of Organic Compounds with Transition Metal Complexes">. Coll Czech Chem Commun 57:107–112
28. Druzhinina AN, Shul'pina LS, Shul'pin GB (1991) Photochemical oxidation of hydrocarbons by atmospheric oxygen in acetonitrile catalyzed by cyclopentadienyliron complexes. Bull Acad Sci USSR Div Chem Sci 40(7, Part 2):1492–1494
29. Nizova GV, Losenkova GV, Shul'pin GB (1991) Unusual selectivity in photooxygenation of alkanes by air in CH_3CN solutions catalyzed by $CrCl_3–C_6H_5CH_2N(C_2H_5)_3Cl$. React Kinet Catal Lett 45(1):27–34. https://doi.org/10.1007/bf02078604
30. Shul'pin GB, Nizova GV (1991) Contribution of air oxygen to photooxidation of alkanes by V(V) and Cr(VI) oxocomplexes. React Kinet Catal Lett 45(1):7–14. https://doi.org/10.1007/bf02078602
31. Nizova GV, Muzart J, Shul'pin GB (1991) Cyclohexane photooxygenation by air oxygen in CH_2Cl_2 in the presence of chromium oxocomplex–iodosylbenzene system. React Kinet Catal Lett 45(2):173–178. https://doi.org/10.1007/bf02070424
32. Shul'pin GB, Druzhinina AN (1992) Iron(III) chloride catalysed photooxygenation of alcohol solutions of alkanes by atmospheric oxygen. Mendeleev Commun 1:36–37. https://doi.org/10.1070/mc1992v002n01abeh000116
33. Muzart J, Druzhinina AN, Shul'pin GB (1993) Photooxygenation of cyclohexane with air oxygen in methylene chloride catalyzed by an oxo complex of chromium(IV) <Report XXVI from series "Photoinitiated reactions of organic compounds with metal complexes">. Petrol Chem (Russia) 33(20):113–115
34. Shul'pin GB, Bochkova MM, Nizova GV (1995) Aerobic oxidation of saturated hydrocarbons into alkyl hydroperoxides induced by visible light and catalysed by a "quinone – copper acetate" system <Part 30 of the series "Photoinduced Reactions of Organic Compounds with Transition Metal Complexes". J Chem Soc, Perkin Trans 2 (7):1465–1469. https://doi.org/10.1039/P29950001465 29950001465
35. Gichumbi JM, Friedrich HB (2018) Half-sandwich complexes of platinum group metals (Ir, Rh, Ru and Os) and some recent biological and catalytic applications. J Organomet Chem 866:123–143. https://doi.org/10.1016/j.jorganchem.2018.04.021
36. Alshaheri AA, Tahir MIM, Rahman MBA, Beguma T, Saleh TA (2017) Synthesis, characterisation and catalytic activity of dithiocarbazate Schiff base complexes in oxidation of cyclohexane. J Mol Liq 240:486–496. https://doi.org/10.1016/j.molliq.2017.05.081
37. Nakazawa J, Doi Y, Hikichi S (2017) Alkane oxidation reactivity of homogeneous and heterogeneous metal complex catalysts with mesoporous silica-immobilized (2-pyridylmethyl)amine type ligands. Mol Cat 443:14–24. https://doi.org/10.1016/j.mcat.2017.09.027

38. Boekfa B, Treesukol P, Injongkol Y, Maihom T, Maitarad P, Limtrakul J (2018) The activation of methane on Ru, Rh, and Pd decorated carbon nanotube and boron nitride nanotube: A DFT study. Catalysts 18(8):190. https://doi.org/10.3390/catal8050190.]
39. Sun W, Gao L, Feng X, Sun X, Zheng G (2018) High-efficiency catalytic oxidation of inert $C(sp^3)-H$ bond functionalization with oxygen by synergetic Cu NPs/N-Doped graphene. Eur J Org Chem 2018(9):1121–1129. https://doi.org/10.1002/ejoc.201701286
40. Jimenez-Halla JOC, Nazemi A, Cundari TR (2018) DFT study of substituent effects in the hydroxylation of methane and toluene mediated by an ethylbenzene dehydrogenase active site model. J Organomet Chem 864:44–49. https://doi.org/10.1016/j.jorganchem.2018.01.007
41. Romero-Guido C, Baez A, Torres E (2018) Dioxygen activation by laccases: green chemistry for fine chemical synthesis. Catalysts 8:223. https://doi.org/10.3390/catal8060223
42. Chapman J, Ismail AE, Dinu CZ (2018) Industrial applications of enzymes: recent advances, techniques, and outlooks. Catalysts 8:238. https://doi.org/10.3390/catal8060238
43. Tsai Yi-F, Luo W-I, Chang J-L, Chang C-W, Chuang H-C, Ramu R, Wei G-T, Zen J-M, Yu SS-F (2017) Electrochemical Hydroxylation of C3–C12 *n*-Alkanes by Recombinant Alkane Hydroxylase (AlkB) and Rubredoxin-2 (AlkG) from Pseudomonas putida GPo1. Scientific Reports 7, Article number:8369. https://doi.org/10.1038/s41598-017-08610-w
44. Kudrik EV, Sorokin AB (2017) Oxidation of aliphatic and aromatic CH bonds by *t*-BuOOH catalyzed by mu-nitrido diiron phthalocyanine. J Mol Cat A: Chem 426:499–505. https://doi.org/10.1016/j.molcata.2016.08.013
45. Mitra M, Nimir H, Hrovat DA, Shteinman AA, Richmond MG, Costas M, Nordlander E (2017) Catalytic C–H oxidations by nonheme mononuclear Fe(II) complexes of two pentadentate ligands: evidence for an Fe(IV) oxo intermediate. J Mol Cat A: Chemical 426:350–356. https://doi.org/10.1016/j.molcata.2016.10.010
46. Bryliakov KP, Talsi EP (2014) Active sites and mechanisms of bioinspired oxidation with H_2O_2, catalyzed by non-heme Fe and related Mn complexes. Coord Chem Rev 276:73–96. https://doi.org/10.1016/j.ccr.2014.06.009
47. Canta M, Font D, Gomez L, Ribas X, Costas M (2014) The Iron(II) complex $[Fe(CF_3SO_3)_2(mcp)]$ as a convenient, readily available catalyst for the selective oxidation of methylenic sites in alkanes. Adv Synth Cat 356:818–830. https://doi.org/10.1002/adsc.201300923
48. Bauer EB (2017) Recent advances in iron catalyzed oxidation reactions of organic compounds. Isr J Chem 57:1131–1150. https://doi.org/10.1002/ijch.201700050
49. Gómez L, Canta M, Font D, Prat I, Ribas X, Costas M (2013) Regioselective oxidation of nonactivated alkyl C–H groups using highly structured non-heme iron catalysts. J Org Chem 78:1421–1433. https://doi.org/10.1021/jo302196q
50. Collins TJ, Ryabov AD (2017) Targeting of high-valent iron-TAML activators at hydrocarbons and beyond. Chem Rev 117:9140–9162. https://doi.org/10.1021/acs.chemrev.7b00034
51. Olivo G, Cussy O, Borrell M, Costas M (2017) Oxidation of alkane and alkene moieties with biologically inspired nonheme iron catalysts and hydrogen peroxide: from free radicals to stereoselective transformations. J Biol Inorg Chem 22(2–3):425–452. https://doi.org/10.1007/s00775-016-1434-z
52. Shul'pin GB, Kozlov YN, Shul'pina LS, Kudinov AR, Mandelli D (2009) Extremely efficient alkane oxidation by a new catalytic reagent $H_2O_2/Os_3(CO)_{12}$/pyridine. Inorg Chem 48(22):10480–10482. https://doi.org/10.1021/ic901576r
53. Shul'pin GB, Vinogradov MM, Shul'pina LS (2018) Oxidative functionalization of C–H compounds induced by extremely efficient osmium catalysts (A review). Catal Sci Technol. https://doi.org/10.1039/c8cy00659h
54. Vinogradov MM, Kozlov YN, Nesterov DS, Shul'pina LS, Pombeiro AJL, Shul'pin GB (2014) Oxidation of hydrocarbons with H_2O_2/O_2 catalyzed by osmium complexes containing *p*-cymene ligands in acetonitrile. Catal Sci Technol 4:3214–3226. https://doi.org/10.1039/c4cy00492b

55. Shul'pin GB, Kozlov YN, Shul'pina LS, Carvalho W, Mandelli D (2013) Oxidation reactions catalyzed by osmium compounds. Part 4. Highly efficient oxidation of hydrocarbons and alcohols including glycerol by the $H_2O_2/Os_3(CO)_{12}$/pyridine reagent. RSC Ad 3(35):15065–15074. https://doi.org/10.1039/c3ra41997e
56. Vinogradov MM, Shul'pina LS, Kozlov Y.N, Kudinov AR, Ikonnikov NS, Shul'pin GB (2015) Oxidation of hydrocarbons and alcohols with peroxides catalyzed by new pi-cymene osmium complexes. J Organomet Chem 784:52–61. https://doi.org/10.1016/j.jorganchem.2014.07.026
57. Goldsmith CR (2018) Aluminum and gallium complexes as homogeneous catalysts for reduction/oxidation reactions. Coord Chem Rev 377:209–224. https://doi.org/10.1016/j.ccr.2018.08.025
58. Kuznetsov ML, Kozlov YN, Mandelli D, Pombeiro AJL, Shul'pin GB (2011) Mechanism of Al^{3+}-Catalyzed Oxidations of Hydrocarbons: Dramatic Activation of H_2O_2 toward O–O Homolysis in Complex $[Al(H_2O)_4(OOH)(H_2O_2)]^{2+}$ Explains the Formation of HO· Radicals. Inorg Chem 50:3996–4005. https://doi.org/10.1021/ic102476x
59. Novikov AS, Kuznetsov ML, Pombeiro AJL, Bokach NA, Shul'pin GB (2013) Generation of HO radical from hydrogen peroxide catalyzed by aqua complexes of the group III metals $[M(H_2O)n]^{3+}$ (M = Ga, In, Sc, Y, or La): a theoretical study. ACS Catal 3(6):1195–1208. https://doi.org/10.1021/cs400155q
60. Kuznetsov ML, Teixeira FA, Bokach NA, Pombeiro AJL, Shul'pin GB (2014) Radical decomposition of hydrogen peroxide catalyzed by aqua complexes $[M(H_2O)n]^{2+}$ (M = Be, Zn, Cd). J Catal 313:135–148. https://doi.org/10.1016/j.jcat.2014.03.010
61. Novikov AS, Kuznetsov ML, Rocha BGM, Pombeiro AJL, Shul'pin GB (2016) Oxidation of olefins with H_2O_2 catalysed by salts of group III metals (Ga, In, Sc, Y and La): epoxidation versus hydroperoxidation. Catal Sci Technol 6:1343–1356. https://doi.org/10.1039/c5cy01367d
62. Rocha BGM, Kuznetsov ML, Kozlov YN, Pombeiro AJL, Shul'pin GB (2015) Simple soluble Bi(III) salts as efficient catalysts for the oxidation of alkanes with H_2O_2. Catal Sci Technol 5:2174–2187. https://doi.org/10.1039/c4cy01651c
63. Shul'pin GB (2013) Selectivity in C–H functionalizations. Reedijk J, Poeppelmeier K, Casella L (eds) Comprehensive inorganic chemistry II, 2nd edn, vol 6, Chapter 6.04. Elsevier, pp 79–104. http://www.sciencedirect.com/science/referenceworks/9780080965291
64. Shul'pin GB (2002) Metal-catalysed hydrocarbon oxygenations in solutions: the dramatic role of additives: a review. J Mol Catal A: Chem 189(1):39–66. https://doi.org/10.1016/s1381-1169(02)00196-6
65. Shul'pin GB (2010) Selectivity enhancement in functionalization of C–H bonds: A review. Org Biomol Chem 8:4217–4228. https://doi.org/10.1039/c004223d
66. Shul'pin GB (2013) C–H functionalization: thoroughly tuning ligands at a metal ion, a chemist can greatly enhance catalyst's activity and selectivity, perspective. Dalton Trans 42(36):12794–12818. https://doi.org/10.1039/c3dt51004b
67. Metal-Organic Frameworks. Academic editor Shobha Waghmode. Savitribai Phule Pune University, India. ISBN: 978-953-51-6857-7
68. Levitsky MM, Bilyachenko AN, Shul'pin GB (2017) Oxidation of C–H compounds with peroxides catalyzed by polynuclear transition metal complexes in Si- or Ge-sesquioxane frameworks: a review. J Organomet Chem 849–850:201–218. https://doi.org/10.1016/j.jorganchem.2017.05.007
69. Bilyachenko AN, Dronova MS, Yalymov AI, Korlyukov AA, Shul'pina, LS, Arkhipov DE, Shubina ES, Levitsky MM, Kirilin AD, Shul'pin GB (2013) New binuclear cage-like copper(II) silsesquioxane ("cooling tower"); its high catalytic activity in oxidation of benzene and alcohols. Eur J Inorg Chem 30:5240–5246. https://doi.org/10.1002/ejic.201300878
70. Dronova MS, Bilyachenko AN, Yalymov AI, Kozlov YN, Shul'pina LS, Korlyukov AA, Arkhipov DE, Levitsky MM, Shubina ES, Shul'pin GB (2014) Solvent-controlled synthesis of tetranuclear cage-like copper(II) silsesquioxanes. Remarkable features of the cage structures and their high catalytic activity in oxidation with peroxides. Dalton Trans 43(2):872–88. https://doi.org/10.1039/C3DT52508B

71. Bilyachenko AN, Dronova MS, Yalymov AI, Lamaty F, Bantreil X, Martinez J, Bizet C, Shul'pina LS, Korlyukov AA, Arkhipov DE, Levitsky MM, Shubina ES, Kirillov AM, Shul'pin GB (2015) Cage-like Copper(II) Silsesquioxanes: Transmetalation Reactions, Structural, Quantum Chemical and Catalytic Studies. Chem Eur J 21 (28):8758–8770. https://doi.org/10.1002/chem.201500791
72. Bilyachenko AN, Yalymov AI, Shul'pina LS, Mandelli D, Korlyukov AA, Vologzhanina AV, Es'kova MA, Shubina ES, Levitsky MM, Shul'pin GB (2016) Novel cage-like hexanuclear Nickel(II) silsesquioxane. Synthesis, structure, and catalytic activity in oxidations with peroxides. Molecules 21(665). https://doi.org/10.3390/molecules21050665
73. Bilyachenko AN, Levitsky, MM, Yalymov AI, Korlyukov AA, Vologzhanina AV, Kozlov YN, Shul'pina LS, Nesterov DS, Pombeiro AJL, Lamaty F, Bantreil X, Fetre A, Liu D, Martinez J, Long J, Larionova J, Guari Y, Trigub AL, Zubavichus YV, Golub IE, Filippov OA, Shubina ES, Shul'pin GB (2016) A heterometallic (Fe_6Na_8) cage-like silsesquioxane: synthesis, structure, spin glass behavior and high catalytic activity. RSC Adv (6):48165–48180. https://doi.org/10.1039/c6ra07081g
74. Bilyachenko AN, Yalymov AI, Levitsky MM, Korlyukov AA, Es'kova MA, Long J, Larionova J, Guari Y, Shul'pina LS, Ikonnikov NS, Trigub AL, Zubavichus YV, Golub IE, Shubina ES, Shul'pin GB (2016) First cage-like pentanuclear Co(II)-silsesquioxane. Dalton Trans 45:13663–13666. https://doi.org/10.1039/c6dt02026g
75. Bilyachenko AN, Levitsky MM, Yalymov AI, Korlyukov AA, Khrustalev VN, Vologzhanina AV, Shul'pina LS, Ikonnikov NS, Trigub AE, Dorovatovsky PV, Bantreil X, Lamaty F. Long J, Larionova J, Golub IE, Shubina ES, Shul'pin GB (2016) Cage-like Fe,Na-Germsesquioxanes: Structure, Magnetism, and Catalytic Activity. Angew Chem Int Ed 55(49):15360–15363. https://doi.org/10.1002/anie.201607189
76. Yalymov AI, Bilyachenko AN, Levitsky MM, Korlyukov AA, Khrustalev VN, Shul'pina LS, Dorovatovskii PV, Es'kova MA, Lamaty F, Bantreil X, Villemejeanne B, Martinez J, Shubina E S, Kozlov YN, Shul'pin GB (2017) High catalytic activity of heterometallic (Fe_6Na_7 and Fe_6Na_6) cage silsesquioxanes in oxidations with peroxides. Catalysts 7(4):101 (18 pages). https://doi.org/10.3390/catal7040101
77. Bilyachenko AN, Kulakova AN, Levitsky MM, Petrov AA, Korlyukov AA, Shul'pina LS, Khrustalev VN, Dorovatovskii PVVologzhanina, AV, Tsareva US, Golub IE, Gulyaeva ES, Shubina ES, Shul'pin GB (2017) Unusual Tri-, Hexa- and nonanuclear organosilicon copper clusters: synthesis, structures and catalytic activity in oxidations with peroxides. Inorg Chem 56(7):4093–4103. https://doi.org/10.1021/acs.inorgchem.7b00061
78. Bilyachenko AN, Kulakova AN, Levitsky, MM, Korlyukov, AA, Khrustalev VN, Vologzhanina, AV, Titov AA, Dorovatovskii PV, Shul'pina LS, Lamaty F, Bantreil X, Villemejeanne B, Ruiz C, Martinez J, Shubina ES, Shul'pin GB (2017) Ionic complexes of Tetra- and Nonanuclear Cage Copper(II) phenylsilsesquioxanes: synthesis and high activity in oxidative catalysis. ChemCatChem 9(23):4437–4447. https://doi.org/10.1002/cctc.201701063
79. Kulakova AN, Bilyachenko AN, Levitsky MM, Khrustalev VN, Korlyukov AA, Zubavichus Y V, Dorovatovskii PV, Lamaty F, Bantreil X, Villemejeanne B, Martinez J, Shul'pina LS, Shubina ES, Gutsul EI, Mikhailov IA, Ikonnikov NS, Tsareva US, Shul'pin GB (2017) $Si_{10}Cu_6N_4$ cage hexacoppersilsesquioxanes containing n-ligands: synthesis, structure, and high catalytic activity in peroxide oxidations. Inorg Chem 56(24):15026–15040. https://doi.org/10.1021/acs.inorgchem.7b02320
80. Bilyachenko AN, Khrustalev VN, Zubavichus YV, Shul'pina LS, Kulakova AN, Bantreil X, Lamaty F, Levitsky MM, Gutsul EI, Shubina ES, Shul'pin GB (2018) Heptanuclear Fe_5Cu_2-Phenylgermsesquioxane containing 2,2'-Bipyridine: synthesis, structure, and catalytic activity in oxidation of C–H compounds. Inorg Chem 57(1):528–534. https://doi.org/10.1021/acs.inorgchem.7b02881
81. Bilyachenko AN, Levitsky MM, Khrustalev VN, Zubavichus YV, Shul'pina LS, Shubina ES, Shul'pin GB (2018) Mild and regioselective hydroxylation of methyl group in neocuproine: approach to an N,O-Ligated Cu6 cage phenylsilsesquioxane. Organometallics 37(2):168–171. https://doi.org/10.1021/acs.organomet.7b00845

82. Bilyachenko AN, Kulakova AN, Shul'pina LS, Levitsky MM, Korlyukov AA, Khrustalev VN, Zubavichus YV, Dorovatovskii PV, Tsareva US, Shubina ES, Petrov AA, Vorontsov NV, Shul'pin GB (2018) Family of penta- and hexanuclear metallasilsesquioxanes: synthesis, structure and catalytic properties in oxidations. J Organomet Chem 867:133–141. https://doi.org/10.1016/j.jorganchem.2017.10.033
83. Bilyachenko AN, Levitsky MM, Korlyukov AA, Khrustalev VN, Zubavichus YV, Shul'pina LS, Shubina ES, Vologzhanina AV, Shul'pin GB (2018) Heptanuclear cage Cu(II)-Silsesquioxanes. features of synthesis, structure and catalytic activity. Eur J Inorg Chem 22:2505–2511. https://doi.org/10.1002/ejic.201701340
84. Astakhov GS, Bilyachenko AN, Korlyukov AA, Levitsky MM, Shul'pina LS, Bantreil X, Lamaty F, Vologzhanina AV, Shubina ES, Dorovatovskii PV, Nesterov DS, Pombeiro AJL, Shul'pin GB (2018) High cluster (Cu_9) cage silsesquioxanes. Synthesis, structure and catalytic activity. Inorg Chem 57(18):11524–11529. https://doi.org/10.1021/acs.inorgchem.8b01496
85. Kholdeeva OA (2014) Recent developments in liquid-phase selective oxidation using environmentally benign oxidants and mesoporous metal-silicates. Catal Sci Technol 4:1869–1889. https://doi.org/10.1039/c4cy00087k
86. Yamaguchi S, Miyake Y, Takiguchi K, Ihara D, Yahiro H (2018) Oxidation of cyclic hydrocarbons with hydrogen peroxide over iron complexes encapsulated in cation-exchanged zeolite. Catal Today 303:249–255. https://doi.org/10.1016/j.cattod.2017.10.047
87. Dyballa M, Pappas DK, Borfecchia E, Beato P, Olsbye U, Lillerud KP, Arstad B, Svelle S (2018) Tuning the material and catalytic properties of SUZ-4 zeolites for the conversion of methanol or methane. Microporous Mesoporous Mater 265:112–122. https://doi.org/10.1016/j.micromeso.2018.02.004
88. Otero A, Fernandez-Baeza J, Lara-Sanchez A, Sanchez-Barb LF (2013) Metal complexes with heteroscorpionate ligands based on the bis(pyrazol-1-yl)methane moiety: catalytic chemistry. Coord Chem Rev 257:1806–1868. https://doi.org/10.1016/j.ccr.2013.01.027
89. Ribeiro APC, Martins LMDRS, Carabineiro SAC, Buijnsters JG, Figueiredo JL, Pombeiro AJL (2018) Heterogenized C-Scorpionate Iron (II) complex on nanostructured carbon materials as recyclable catalysts for microwave-assisted oxidation reactions. ChemCatChem 10:1821–1828. doi:https://doi.org/10.1002/cctc.201702031
90. Ribeiro APC, Matias IAS, Alegria ECBA, Ferraria AM, Botelho do Rego AM, Pombeiro AJL, Martins LMDRS (2018) New trendy magnetic C-scorpionate iron catalyst and its performance towards cyclohexane oxidation. Catalysts 8:69. https://doi.org/10.3390/catal8020069
91. Fomenko YS, Gushchin AL, Shul'pina LS, Ikonnikov NS, Abramov PA, Romashev NF, Poryvaev AS, Sheveleva AM, Bogomyakov AS, Shmelev NY, Fedin MV, Shul'pin GB, Sokolov MN (2018) New oxidovanadium (IV) complex with redox-active acenaphthene-1,2-diimine ligand: synthesis, structure, redox properties and catalytic activity in alkane oxidations with hydrogen peroxide. New J Chem New J. Chem. 42:16200–16210. http://dx.doi.org/10.1039/C8NJ03358G
92. Gryca I, Czerwińska K, Machura B, Chrobok A, Shul'pina LS, Kuznetsov ML, Nesterov DS, Kozlov YN, Pombeiro AJL, Varyan IA, Shul'pin GB (2018) High catalytic activity of vanadium complexes in alkane oxidations with hydrogen peroxide: an effect of 8-hydroxyquinoline derivatives as noninnocent ligands. Inorg Chem 57(4):1824–1839. https://doi.org/10.1021/acs.inorgchem.7b02684
93. Fukuzumi S, Ohkubo K (2010) Metal ion-coupled and decoupled electron transfer. Coord Chem Rev 254:372–385. https://doi.org/10.1016/j.ccr.2009.10.020
94. Abakumov GA, Cherkasov VK, Piskunov AV, Trofimova OYu, Romanenko GV (2010) activating complex formation in the diazabutadiene-zinc halide system. Dokl Chem 434:237–240. https://doi.org/10.1134/s0012500810090077
95. Ottenbacher RV, Talsi EP and Bryliakov KP (2018) Catalytic asymmetric oxidations using molecular oxygen. Russ Chem Rev 87(9):821–830. https://doi.org/10.1070/RCR4825
96. Denisov ET, Afanas'ev IB (2005) Oxidation and antioxidants in organic chemistry and biology. Taylor & Francis, Boca Raton

97. USP Technologies. http://www.h2o2.com/products-and-services/us-peroxide-technologies.aspx?pid=112&name=Hydrogen-Peroxide, Accesses 27 Nov 2018
98. Barkanova SV, Kaliya OL (1999) Naphthalene oxidation by peracetic acid catalysed by Mn(III) porphine-like complexes: nature of intermediates. J Porphyrins and Phthalocyanines 3(3):180–187. https://doi.org/10.1002/(sici)1099-1409(199903)3:3%3c180:aid-jpp121%3e3.0.co;2-0
99. Gonzalez Cuervo L, Kozlov YN, Süss-Fink G, Shul'pin GB (2004) Oxidation of saturated hydrocarbons with peroxyacetic acid catalyzed by vanadium complexes. J Mol Catal A: Chem 218(2):171–177. https://doi.org/10.1016/j.molcata.2004.04.025
100. Klenk H, Götz PH, Siegmeier R, Mayr W (2005) Peroxy compounds, organic. Ullmann's encyclopedia of industrial chemistry, Weinheim: Wiley-VCH. https://doi.org/10.1002/14356007.a19_199
101. Lyakin OY, Zima AM, Tkachenko NV, Bryliakov KP, Talsi EP (2018) Direct Evaluation of the reactivity of nonheme iron (V)-oxo intermediates toward arenes. ACS Catal 8:5255–5260. https://doi.org/10.1021/acscatal.8b00661
102. Shul'pin GB, Loginov DA, Shul'pina LS, Ikonnikov NS, Idrisov VO, Vinogradov MM, Osipov SN, Nelyubina YV, Tyubaeva PM, stereoselective alkane oxidation with *meta*-Chloroperoxybenzoic acid (MCPBA) catalyzed by organometallic cobalt complexes. Molecules 21(11):E1593. https://doi.org/10.3390/molecules21111593
103. Shul'pin GB, Gradinaru J, Kozlov YN (2003) Alkane hydroperoxidation with hydroperoxides catalysed by copper complexes. Org Biomol Chem 1(20):3611–3617. https://doi.org/10.1039/b306382h
104. Shul'pin GB, Kozlov YN (2003) Kinetics and mechanism of alkane hydroperoxidation with *tert*-butyl hydroperoxide catalyzed by a vanadate ion. Org Biomol Chem 1(13):2303–2306. https://doi.org/10.1039/b302228e
105.] Kozlov YN, Nizova GV, Shul'pin GB (2008) Alkane oxidation by the system '*tert*-butyl hydroperoxide–$[Mn_2L_2O_3][PF_6]_2$ (L = 1,4,7-trimethyl-1,4,7-triazacyclononane)–carboxylic acid'. J Phys Org Chem 21:119–126. https://doi.org/10.1002/poc.1295
106. Kirillova MV, Kirillov AM, Mandelli D, Carvalho WA, Pombeiro AJL, Shul'pin GB (2010) Mild homogeneous oxidation of alkanes and alcohols including glycerol with *tert*-butyl hydroperoxide catalyzed by a tetracopper(II) complex. J Catal 272:9–17. https://doi.org/10.1016/j.jcat.2010.03.017
107. Kirillov AM, Karabach YY, Kirillova MV, Haukka M, Pombeiro AJL (2012) Topologically unique 2D heterometallic Cu^{II}/Mg coordination polymer: synthesis, structural features, and catalytic use in alkane hydrocarboxylation. Cryst Growth Des 12:1069–1074. https://doi.org/10.1021/cg201459k
108. da Costa Ribeiro AP, Ribeiro Dias, de Sousa Martins LM, Correia Carabineiro SA, Figueiredo JL, Pombeiro AJL (2017) Gold nanoparticles deposited on surface modifiedcarbon xerogels as reusable catalysts for cyclohexane C–H activation in the presence of CO and water. Molecules 22:603. https://doi.org/10.3390/molecules22040603
109. Shul'pin GB, Kozlov YN, Shul'pina LS, Pombeiro, AJL (2012) Hydrocarbon oxygenation with Oxone catalyzed by complex $[Mn_2L_2O_3]^{2+}$ (L = 1,4,7-trimethyl-1,4,7-triazacyclononane) and oxalic acid. Tetrahedron 68:8589–8599. https://doi.org/10.1016/j.tet.2012.07.098
110. Olivo G, Lanzalunga O, Di Stefano S (2016) Non-heme imine-based iron complexes as catalysts for oxidative processes. Adv Synth Catal 358:843–863. https://doi.org/10.1002/adsc.201500967
111. Shulpin GB, Druzhinina AN (1992) Hydroperoxidation of alkanes by atmospheric oxygen in the presence of hydroquinone or quinone catalyzed by copper(II) acetate under visible light irradiation. React Kinet Catal Lett 47(2):207–211. https://doi.org/10.1007/bf02137651
112. See review [64]
113. Shul'pin GB (2003) Metal-catalyzed hydrocarbon oxidations. Comptes Rendus Chim 6(2):163–178. https://doi.org/10.1016/s1631-0748(03)00021-3

114. Shul'pin GB, Kozlov YN, Shul'pina LS, Petrovskiy PV (2010) Oxidation of alkanes and alcohols with hydrogen peroxide catalyzed by complex $Os_3(CO)_{10}$(mu–H)$_2$ Appl Organomet Chem 24(6):464–472. https://doi.org/10.1002/aoc.1641
115. Shul'pin GB (2009) Hydrocarbon oxygenations with peroxides catalyzed by metal compounds. Mini Rev Org Chem 6:95–104. https://doi.org/10.2174/157019309788167738
116. Shul'pin GB, Nesterov DS, Shul'pina LS, Pombeiro AJL (2017) A hydroperoxo-rebound mechanism of alkane oxidation with hydrogen peroxide catalyzed by binuclear manganese (IV) complex in the presence of an acid with involvement of atmospheric dioxygen. Inorg Chim Acta 455 (P2):666–676. https://doi.org/10.1016/j.ica.2016.04.035
117. Nesterov DS, Chygorin EN, Kokozay VN, Bon VV, Boča R, Kozlov YN, Shul'pina LS, Jezierska J, Ozarowski A, Pombeiro AJL, Shul'pin GB (2012) Heterometallic $Co_4^{III}Fe_2^{III}$ schiff base complex: structure, electron paramagnetic resonance, and alkane oxidation catalytic activity. Inorg Chem 51(16):9110–9122. https://doi.org/10.1021/ic301460q
118. DeMatteo MP, Poole JS, Shi X, Sachdeva R, Hatcher PG. Hadad CM, Platz MS (2005) On the electrophilicity of hydroxyl radical: a laser flash photolysis and computational study. J Am Chem Soc 127(19):7094–7109. https://doi.org/10.1021/ja043692q
119. Yamaguchi S, Ohnishi T, Miyake Y, Yahiro H (2015) Effect of water added into acetonitrile solvent on oxidation of benzene with hydrogen peroxide over iron complexes encapsulated in zeolite. Chem Let 44(10):1287–1288. https://doi.org/10.1246/cl.150479
120. Jlassi R, Ribeiro APC, Alegria ECBA, Naïli H, Tiago GAO, Rüffer T, Lang H, Zubkov FI, Pombeiro AJL, Rekik W (2018) Copper(II) complexes with an arylhydrazone of methyl 2-cyanoacetate as effective catalysts in the microwave-assisted oxidation of cyclohexane. Inorg Chim Acta 471:658–663. https://doi.org/10.1016/j.ica.2017.12.001
121. Galassi R, Simon OC, Burini A, Tosi G, Conti C, Graiff C, Martins NMR, M. Guedes da Silva, FC, Pombeiro AJL, Martins LMDRS (2017) copper(I) and copper(II) metallacycles as catalysts for microwave assisted selective oxidation of cyclohexane. Polyhedron 134:143–152. https://doi.org/10.1016/j.poly.2017.06.020
122. Cintas P, Luche J-L (1999) Green chemistry. The sonochemical approach. Green Chemistry. 1:115–125. https://doi.org/10.1039/a900593e
123. Ribeiro APC, Alegria ECBA, Kopylovich MN, Ferraria AM, Botelho do Rego AM, Pombeiro AJL (2018) Comparison of microwave and mechanochemical energy inputs in the catalytic oxidation of cyclohexane. Dalton Trans 47(25):8193–8198. https://doi.org/10.1039/c8dt00866c
124. Gągola M, Przyjazny A, Boczkaj G (2018) Highly effective degradation of selected groups of organic compounds by cavitation based AOPs under basic pH conditions. Ultrason Sonochemistry 45:257–266. https://doi.org/10.1016/j.ultsonch.2018.03.013
125. Gągola M, Przyjazny A, Boczkaj G (2018) Effective method of treatment of industrial effluents under basic pH conditions using acoustic cavitation—A comprehensive comparison with hydrodynamic cavitation processes. Chem Eng Process 128:103–113. https://doi.org/10.1016/j.cep.2018.04.010
126. Tanaka K (2009) Solvent-free organic synthesis. Wiley-VCH
127. Mishra GS, Silva Telma FS, Martins LMDRS, Pombeiro AJL (2009) Scorpionate complexes of vanadium (III or IV) as catalyst precursors for solvent-free cyclohexane oxidation with dioxygen. Pure Appl Chem 81(7):1217–1227. https://doi.org/10.1351/pac-con-08-10-08
128. Song X, Hao J, Bai Y, Han L, Yan G, Lian X, Liu J (2017) Solvent-free oxidation of cyclohexane by oxygen over Al–Cu–Co alloys: influence of the phase structure and electrical conductivity on catalytic activity. New J Chem 41(10):4031–4039. https://doi.org/10.1039/c7nj00238f
129. Zaltariov M, Vieru V, Zalibera M, Cazacu M, Martins NMR (2017) Martins LMDRS, Rapta P, Novitchi G, Shova S, Pombeiro AJL, Arion VB (2017) A new bis (μ-chlorido) bridged cobalt (II) complex with silyl-containing schiff-base as catalyst precursor in solvent-free oxidation of cyclohexane. Eur J Inorg Chem 37:4324–4332. https://doi.org/10.1002/ejic.201700875
130. Organic Reactions in Water (2007) Principles, strategies and applications. Lindström UM (ed). Wiley-Blackwell, ISBN: 9781405138901, 9780470988817

131. Li C-J, Chen L (2006) Organic chemistry in water. Chem Soc Rev 35:68–82. https://doi.org/10.1039/b507207g
132. Gonsalvi L (2018) Homogeneous catalysis and mechanisms in water and biphasic media. Catalysts 8:543. https://doi.org/10.3390/catal8110543
133. Hapiot F, Monflier E (2017) Unconventional approaches involving cyclodextrin-based, self-assembly-driven processes for the conversion of organic substrates in aqueous biphasic catalysis. Catalysts 7:173. https://doi.org/10.3390/catal7060173
134. Ünver H, Kani I (2018) Homogeneous oxidation of alcohol and alkene with copper(II) complex in water. J Chem Sci 130:33. https://doi.org/10.1007/s12039-018-1439-y
135. da Silva CRB, Gonçalves VLC, Lachter ER, Mota CJA (2009) Etherification of glycerol with benzyl alcohol catalyzed by solid acids. J Braz Chem Soc 20(2):201–204. https://doi.org/10.1590/s0103-50532009000200002
136. de Rezende SM, de Castro Reis M, Reid MG, Silva PL, Coutinho Jr., FMB, da S.S. Gil RA, Lachter ER (2008) Transesterification of vegetable oils promoted by poly(styrene-divinylbenzene) and poly (divinylbenzene). Appl. Catal. A: Gen 349(1–2):198–203. https://doi.org/10.1016/j.apcata.2008.07.030
137. Sels B, D'Hondt E, Jacobs P (2007) Catalytic Transformation of Glycerol". In: Centi G, van Santen RA (eds) Catalysis for renewables. Wiley-VCH Verlag, Weinheim
138. Mandelli D, Shul'pina LS, Kirillova MV, Kirillov AM, Carvalho WA, Pombeiro AJL, Shul'pin GB (2014) Chapter 19 oxidation of glycerol with hydrogen peroxide catalyzed by metal complexes. In: Advances in organometallic chemistry and catalysis pombeiro, pp. 247–258. Wiley, ISBN 978-1-118-51014-8
139. de Araújo ML, Mandelli D, Kozlov YN, Carvalho WA, Shul'pin GB (2016) Oxidation of hydroxyacetone (acetol) with hydrogen peroxide in acetonitrile solution catalyzed by iron (III) chloride. J Mol Catal A: Chem 422:103–114. https://doi.org/10.1016/j.molcata.2016.02.011
140. Shul'pin GB, Matthes MG, Romakh VB, Barbosa MIF, Aoyagi JLT, Mandelli D (2008) Oxidations by the system 'hydrogen peroxide–$[Mn_2L_2O_3][PF_6]_2$ (L = 1,4,7-trimethyl-1,4,7-triazacyclononane)–carboxylic acid'. Part 10: Co-catalytic effect of different carboxylic acids in the oxidation of cyclohexane, cyclohexanol, and acetone. Tetrahedron 64:2143–2152. https://doi.org/10.1016/j.tet.2007.12.033
141. Denicourt-Nowicki A, Lebedeva A, Bellini C, Roucoux A (2016) Highly selective cycloalkane oxidation in water with ruthenium nanoparticles. ChemCatChem 8:357–362. https://doi.org/10.1002/cctc.201500805
142. Alvarez LX, Sorokin AB (2015) Mild oxidation of ethane to acetic acid by H_2O_2 catalyzed by supported mu-nitrido diiron phthalocyanines. J Organomet Chem 793:139–144. https://doi.org/10.1016/j.jorganchem.2015.02.045
143. Shul'pin GB, Nizova GV, Kozlov YN, Arutyunov VS, dos Santos ACM, Ferreira ACT, Mandelli D (2005) Oxidations by the system "hydrogen peroxide–$[Mn_2L_2O_3][PF_6]_2$ (L = 1,4,7-trimethyl-1,4,7-triazacyclononane)–oxalic acid". Part 6. Oxidation of methane and other alkanes and olefins in water. J Organometal Chem 690(20):4498–4504. https://doi.org/10.1016/j.jorganchem.2005.01.065
144. Shul'pin GB, Nizova GV (1995) Selective photochemical ketonization of cyclohexane by air in aqueous emulsion in the presence of iron ions. Mendeleev Comm 5(4):143–145. https://doi.org/10.1070/mc1995v005n04abeh000498
145. Li Zhang, Qiu S, Jiang G, Jiang G, Tang R (2018) A CuII-based metal-organic framework as an efficient photocatalyst for direct hydroxylation of benzene to phenol in aqueous solution. Asian J Org Chem 7(1):165–170. https://doi.org/10.1002/ajoc.201700501
146. Zhang W, Fernández-Fueyo E, Ni Y, van Schie M, Gacs J, Renirie R, Wever R, Mutti FG, Rother D, Alcalde and Hollmann F (2018) Selective aerobic oxidation reactions using a combination of photocatalytic water oxidation and enzymatic oxyfunctionalizations. Nature Catalysis 1:55–62. https://doi.org/10.1038/s41929-017-0001-5
147. Shul'pina LS, Kirillova MV, Pombeiro AJL, Shul'pin GB (2009) Alkane oxidation by the H_2O_2–$NaVO_3$–H_2SO_4 system in acetonitrile and water. Tetrahedron 65:2424–2429. https://doi.org/10.1016/j.tet.2009.01.088

148. Romakh VB, Süss-Fink G, Shul'pin GB (2008) Vanadate ion-catalyzed oxidation of methane with hydrogen peroxide in an aqueous solution. Petrol Chem 48(6):440–443. https://doi.org/10.1134/s0965544108060066
149. Shilov AE, Shul'pin GB (2000) Activation and catalytic reactions of saturated hydrocarbons in the presence of metal complexes, 548 pp, Kluwer Academic Publishers: New York, Boston, Dordrecht, London, Moscow, 2002. ISBN 978-0-306-46945-9
150. Gunsalus NJ, Konnick MM, Hashiguchi BG, Periana RA (2014) Discrete molecular catalysts for methane functionalization. Isr J Chem 54:1467–1480. https://doi.org/10.1002/ijch.201300130
151. Hashiguchi BG, Bischof SM, Konnick MM, Periana RA (2012) Designing catalysts for functionalization of unactivated C–H bonds based on the CH activation reaction. Acc Chem Res 45:885–898. https://doi.org/10.1021/ar200250r
152. Gunsalus NJ, Koppaka A, Park SH, Bischof SM, Hashiguchi BG, Periana RA (2017) Homogeneous functionalization of methane. Chem Rev 117:8521–8573. https://doi.org/10.1021/acs.chemrev.6b00739154
153. Rudakov ES (2017) Mechanisms of alkane CH-activation: the 5/6 effect, single-factor compensation effect, strongest reactant and earliest transition state.A puzzle of Shilov reaction. J Mol Catal A: Chemical 426:465–473. https://doi.org/10.1016/j.molcata.2016.07.034
154. Munz D, Meyer D, Strassner T (2013) Methane CH activation by palladium complexes with chelating bis (NHC) ligands: a DFT study. Organometallics 32(12):3469–3480. https://doi.org/10.1021/om400232u
155. Lin M, Sen A (1992) Oxidation and oxidative carbonylation of methane and ethane by hexaoxo-mu-peroxodisulfate(2-) ion in aqueous medium. A model for alkane oxidation through the hydrogen-atom abstraction pathway. J Chem Soc Chem Commun 892–893. http://dx.doi.org/10.1039/C39920000892
156. Nakata K, Yamaoka Y, Miyata T, Taniguchi Y, Takaki K, Fujiwara Y (1994) Palladium(II) and/or copper(II)-catalyzed carboxylation of small alkanes such as methane and ethane with carbon monoxide. J Organomet Chem 473:329–334. https://doi.org/10.1016/0022-328x(94)80134-7
157. da Silva JAL, da Silva JJR, Pombeiro AJL (2011) Oxovanadium complexes in catalytic oxidations. Coord Chem Rev 255(19):2232–2248. https://doi.org/10.1016/j.ccr.2011.05.009
158. Chepaikin EG, Bezruchenko AP, Menchikova GN, Gekhman AE (2017) Homogeneous oxidation of alkanes: role of rhodium–alkyl complexes. J Mol Cat A: Chemical 426:389–392. https://doi.org/10.1016/j.molcata.2016.07.026
159. Jessop PG (2006) Homogeneous catalysis using supercritical fluids: recent trends and systems studied. J Supercrit Fluids 211–231
160. Sutradhar M, Ribeiro APC, Guedes da Silva MFC, Palavra AMF, Pombeiro AJL (2017) Application of molybdenum complexes for the oxidation of cyclohexane in acetonitrile, ionic liquid and supercritical CO_2 media, a comparative study. Mol Catal. http://dx.doi.org/10.1016/j.mcat.2017.10.026
161. Dai C, Zhang J, Huang C, Lei Z (2017) Ionic liquids in selective oxidation: catalysts and solvents. Chem Rev 117:6929–6983. https://doi.org/10.1021/acs.chemrev.7b00030
162. Dyson PJ, Geldbach TJ (2005) Metal catalysed reactions in ionic liquids. Springer, ISBN:1-4020-3914-X
163. Zhu L, Hu C (2013) Ionic liquids: "Green" solvent for catalytic oxidations with hydrogen peroxide. In: Ionic liquids: "Green" Solvent for catalytic oxidations. https://doi.org/10.5772/51936.]
164. Kuznetsova LI, Kuznetsova NI (2017) Cyclohexane oxidation with an O_2–H_2 mixture in the presence of a two-component Pt/C–heteropoly acid catalyst and ionic liquids. Kinet Catal 58(5):522–532. https://doi.org/10.1134/s0023158417050147

165. Paul A, Ribeiro APC, Karmakar Guedes, da Silva MFC, Pombeiro AJL (2016) A Cu(II) OF with a flexible bifunctionalised terpyridine as an efficient catalyst for the single-pot hydrocarboxylation of cyclohexane to carboxylic acid in water/ionic liquid medium. Dalton Trans 45:12779–12789. https://doi.org/10.1039/c6dt01852a
166. Anastas PT (2007) Organic reactions in water: principles, strategies and applications. Edited by Lindström UM, p XVI. Wiley-Blackwell

Chapter 2
Low-Temperature Catalytic Selective Oxidation of Methane to Methanol

Nishtha Agarwal, Stuart H. Taylor and Graham J. Hutchings

Abstract The selective oxidation of methane, which is the primary component of natural gas, is one of the most important challenges in catalysis. While the search for catalysts capable of converting methane directly to higher value commodity chemicals and liquid fuels, such as methanol, has been ongoing for over a century, an industrially viable process has not yet been developed. In nature, this process is selectively demonstrated by methane monooxygenase using dioxygen at room temperature, but such a process has not been commercialised. Currently, large scale upgrading of natural gas proceeds indirectly by employing high-temperature conversion to syngas which is then processed to synthesis fuels and chemicals. Other routes for methane activation include gas-phase oxidative and non-oxidative coupling to form higher hydrocarbons and aromatic compounds, and liquid-phase oxidation to methanol, formaldehyde and acetic acid. Low-temperature selective oxidation of methane to methanol has also been widely studied and remains an open challenge for catalysis in the twenty-first century.

Keywords Methane Oxidation · Zeolites · Gold–palladium catalysis · Low temperature · Hydrogen peroxide · Electrophilic activation · Liquid-phase oxidation · Methane to methanol

2.1 Methane and Natural Gas

Natural gas is a mixture of components, comprised primarily of gaseous hydrocarbons, such as methane, ethane and higher hydrocarbons in various concentrations. In addition, contaminants like sulphur and nitrogen are also present in the crude mixture. In 2016, natural gas production was estimated to be about 3,613 billion cubic metres and continues to rise annually. It is considered as a versatile fuel and supplies 22% of worldwide energy demand, and demand is expected to grow faster than both oil and coal [1]. It also plays a crucial role as a chemical feedstock for

N. Agarwal · S. H. Taylor · G. J. Hutchings (✉)
Cardiff Catalysis Institute, Cardiff, UK
e-mail: Hutch@cardiff.ac.uk

K. P. Bryliakov (ed.), *Frontiers of Green Catalytic Selective Oxidations*,
Green Chemistry and Sustainable Technology,
https://doi.org/10.1007/978-981-32-9751-7_2

industry, especially for methanol production, and has environmental benefits compared to other fossil fuels, since it increases air quality by decreasing greenhouse and volatile organic compound (VOC) emissions [2]. With the recent advancements in the liquefaction and transportation of natural gas, usage as a feedstock has increased drastically over recent years. However, it still remains a widely underutilised feedstock, primarily due to high costs and significant safety concerns associated with its transportation. About 4% of global production of natural gas is still being flared at oilfield wellheads, because of their inconvenient locations, which results in a lack of other feasible long-term options [3].

Therefore, while natural gas is currently used as an energy source, its valorisation to energy-dense liquid derivatives (such as methanol or mid-range hydrocarbons) is highly desirable to increase its utilisation. The composition is primarily methane (up to 0.99 molar fraction), along with higher hydrocarbons such as ethane as shown in Table 2.1 [4]. Methane is also a significant by-product of oil refining and chemical processing. Since methane is one of the main components of natural gas, many approaches are being employed to convert methane into a product (chemical or fuel) that could be easily transported. Since methane has the potential to be a source of carbon for the synthesis of chemical commodities, its transformation is of utmost importance and direct activation of methane has been named as one of the *grand challenges* for chemists [5].

Current approaches of methane transformation (Fig. 2.1) include conversion of methane to methanol or formic acid (either directly or indirectly) via synthesis gas ($CO + H_2$), oxidative coupling to higher hydrocarbons and non-oxidative conversion of methane to aromatics, such as benzene [6]. The methane to methanol (MTM)

Table 2.1 Typical composition range of natural gas

Compound	Molar fraction
Hydrocarbons	
Methane	0.75–0.99
Ethane	0.01–0.15
Propane	0.01–0.10
n-Butane	0.00–0.02
Isobutane	0.00–0.01
n-Pentane	0.00–0.01
Isopentane	0.00–0.01
Hexane	0.00–0.01
Heptane plus higher hydrocarbons	0.00–0.001
Nonhydrocarbons	
Nitrogen	0.00–0.15
Carbon Dioxide	0.00–0.30
Hydrogen sulphide	0.00–0.30
Helium	0.00–0.05

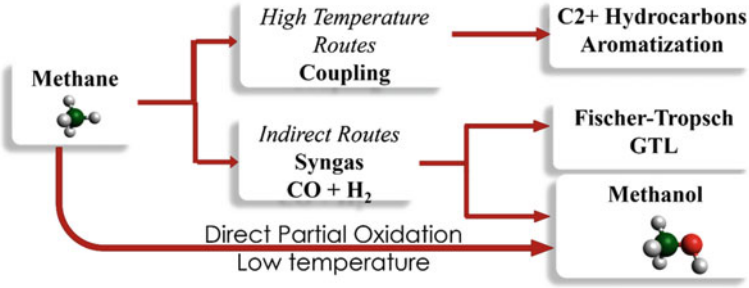

Fig. 2.1 Overview of different routes for the valorisation of methane

process is by far the most attractive among these, since methanol is not only a more energy-dense liquid derivative, which aids transportation costs, but it is also a highly desirable precursor to a number of commodity chemicals and useful products such as ethylene, dimethyl ether and methyl methacrylate [7]. In addition, it is also used as a solvent in chemical processing, used itself for production of higher hydrocarbons and gasoline by industrial processes and has also been proposed as a candidate for a cleaner and greener fuel [6, 8, 9]. For instance, methanol is used in the methanol to gasoline (MTG) process that yields a mixture of aromatics and was developed by Mobil, the Lurgi methanol to propylene process (MTP), and the Syn Energy Technology Co.'s dimethyl ether/methanol to olefin process (DMTO) and Hydro/UOP MTO process that primarily produces ethene and propene for polymerisation feedstock.

Thus, while activation and direct oxidation of methane to methanol are highly desirable, the selective oxidation reaction has proved very difficult to achieve (Eq. 2.1).

$$CH_4 + \frac{1}{2}O_2 \longrightarrow CH_3OH \tag{2.1}$$

Methane is the least reactive of all hydrocarbons, due to a very high C–H bond strength of 439 kJ/mol [10]. Hence, the oxidation processes are either limited to lower conversion or to lower selectivity with energy-intensive conditions. Deeper oxygenated species (COx) become the major product because the conditions used for methane oxidation also have the undesirable effect of activating the target products, given that C–H bond strength in these species is much lower than methane (373 kJ/mol in the case of methanol [11]). Selective oxidation of methane to value-added products requires design of a highly efficient catalytic system and its process development has been an area of research and development for many years [9].

2.2 Routes for Methane Upgrading

As mentioned earlier, there are several approaches that have been used and studied over many years for methane activation and upgrading. This section explores different processes that are being used industrially, and academic studies for direct activation and oxidation, both at high temperature in the gas phase and low temperature in the liquid phase. Liquid-phase activation typically uses mild conditions to increase selectivity, but the catalytic cycle is usually not closed in most of these cases.

2.2.1 Industrial Methane Processing

As a consequence of the difficulty of directly oxidising methane, industrial utilisation of methane into useful products is performed at large scale by first producing synthesis gas (a mixture of carbon monoxide and hydrogen). It can be further transformed to methanol, or to higher hydrocarbons via Fischer–Tropsch synthesis [8]. Different ratios of CO and H_2 can be achieved based on methane reforming (steam or dry) or partial oxidation reactions.

Methane reforming reactions

$$CH_4 + H_2O \longrightarrow CO + 3H_2 \tag{2.2}$$

$$CH_4 + CO_2 \longrightarrow 2CO + 2H_2 \tag{2.3}$$

are endothermic whereas partial oxidation

$$CH_4 + \frac{1}{2}O_2 \longrightarrow CO + 2H_2 \tag{2.4}$$

is slightly exothermic, but requires oxygen which adds the hazards of handling large quantities of undiluted oxygen as well as O_2/CH_4 mixtures. Partial oxidation (Eq. 2.4) can be seen as a combination of total combustion and reforming which are separated in a process known as auto-thermal reforming [12]. Steam reforming with H_2O (Eq. 2.2) is a commonly used technique and dry reforming with CO_2 (Eq. 2.3) is another potential technology, but it has not yet reached the efficiency needed to be used industrially. However, it continues to be a very attractive option because it utilises two of the major greenhouse gases.

Nickel-based catalysts used for methane reforming are operated under energy-intensive conditions with high temperatures (850 °C) and moderate pressures (40 bar). This puts limitations on the size of reactors due to problems related to heat transfer. The catalyst itself is also prone to deposition of graphitic carbon that leads to catalyst deactivation.

Following the manufacture of synthesis gas ($CO + H_2$) and some CO_2 that is present due to reforming reactions, methanol synthesis is performed by the following two methods:

$$CO + 2H_2 \longrightarrow CH_3OH \tag{2.5}$$

$$CO_2 + 3H_2 \longrightarrow CH_3OH + H_2O \tag{2.6}$$

Methanol yield is maximised at temperatures around 250 °C, pressure of 5–10 bar and by adjusting concentrations of CO and CO_2 over a Cu–ZnO–Al_2O_3 catalyst with numerous dopants added [11]. As a result of process optimisation over decades, high yields and selectivity towards methanol are achieved, but it is clear that this indirect process of methane to methanol process is highly energy intensive due to the very high temperatures and pressures and with high operational costs. Given these disadvantages, direct partial oxidation of methane to methanol at mild conditions is highly desirable and is being researched extensively.

2.3 Methane Oxidation

Conversion of methane to value-added products is difficult due to inherent stability and low reactivity of methane. This is further complicated by overoxidation of products to COx. There is a need to design and develop a catalytic system and process which activates methane and avoids product overoxidation. Due to these difficulties, catalytic conversion of methane to partial oxygenates has been called the *holy-grail* of catalysis and has been studied by employing various approaches, which are broadly classified into gas phase (usually at high temperatures) and low-temperature liquid-phase reactions. Despite the difficulties in a highly selective and active process to oxidise methane to methanol at low temperature in an aqueous solution, such a method exists in nature.

2.3.1 Biological Methane Oxidation

Methanotropic micro-organisms have an enzyme called methane monooxygenase (MMO), which catalyses methane oxidation as an initial step in their respiration process (Eq. 2.7).

$$CH_4 + NADH + H^+ + O_2 \longrightarrow CH_3OH + NAD^+ + H_2O \tag{2.7}$$

The two major forms are membrane-bound particulate (pMMO) and soluble (sMMO), the former being more common. Due to difficulties in isolation and purifi-

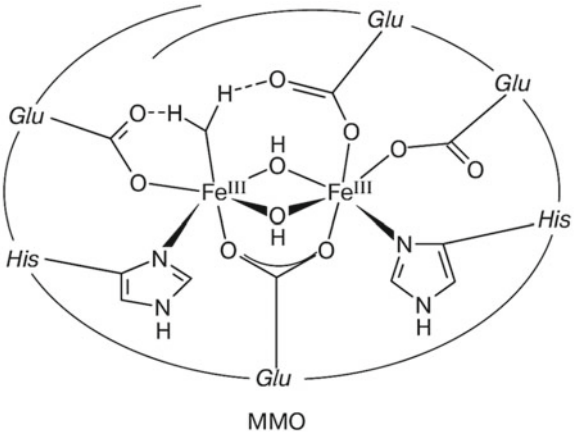

Fig. 2.2 Active centre containing a di-iron μ-oxo sites in methane monooxygenase enzyme. Reproduced by permission from Springer Nature: Ref. [15]. Copyright 2001

cation, sMMO variations from *Methylococcus capsulates* (Bath) have been well characterised and studied [13]. Studies have also demonstrated the non-specificity of the MMO enzyme, which efficiently oxidises a wide range of aliphatic and aromatic hydrocarbons. It is also an efficient catalyst for methane to methanol oxidation selectively, without forming formic acid or other overoxidation products [14]. The productivity of sMMO for methane oxidation with molecular oxygen was found to be 5.05 $\text{moles}_{\text{methanol}}\ \text{kg}^{-1}_{\text{protein}}\ \text{h}^{-1}$.

Primary active sites have been identified as a binuclear iron μ-oxo species as shown in Fig. 2.2 [15]. These binuclear Fe sites are responsible for the reductive activation of O_2 with an NADH cofactor, and during the redox cycle, it is considered that each Fe centre varies between +2 and +4 oxidation states, leading to the formation of high-valent ferryl ion ($[FeO]^{2+}$) [15]. It is also believed that this provides the driving force towards the hydroxylation of non-activated C–H bond.

Methyl monooxygenase enzymes with active sites other than Fe metal have also been studied recently. Although not completely understood, the active site in pMMO is considered to contain copper as opposed to sMMO [13]. These biological systems are unlikely to be used industrially due to high costs associated with isolation and purification of these enzymes. Additionally, enzymatic systems are also prone to deactivation by fluctuations of temperature, pressure and concentration, and hence have a limited working range. However, these enzymes have provided new insight into development of synthetic catalysts.

2.3.2 Gas-Phase Oxidative Routes

Typical gas-phase oxidation reactions are carried out with air, molecular oxygen and nitrous oxide as oxidants at high temperatures. High-temperature oxidation systems generally involve complex radical pathways, which also leads to side coupling

products and overoxidation products limiting selectivity and yield of primary products [16]. By varying reaction parameters and reactor design, moderate selectivity to methanol can be achieved at higher temperatures (450–600 °C) and moderate pressures (30–60 bar) [17]. By tuning the methane partial pressure, radical concentration can be tuned to reduce competition with coupling reactions; but generally formaldehyde is the major gas-phase oxygenate produced rather than methanol [18]. O_2 is used as the oxidant in these cases, which oxidises the methoxy radical ($CH_3O\cdot$) species before protonation to produce CH_3OH. However, the high temperatures lead to overoxidation to CO_2 resulting in lower oxygenate selectivity.

In order to mimic the methane monooxygenase enzymatic systems, heterogeneous catalysts have been developed based on zeolite systems. Zeolites are microporous, crystalline aluminosilicates which can accommodate a wide variety of cations. They are composed of SiO_4 and AlO_4^- tetrahedral, which are connected by bridging oxygen atoms. The extra-framework cations balance the negative charge of the AlO_4^- tetrahedra and are exchangeable, which gives rise to a diverse chemistry associated with zeolites. Some examples of zeolites used for methane oxidation are MFI type zeolites such as Fe–Cu–ZSM–5, TS-1, chabazite and mordenite. The composition of zeolites can be manipulated to modify the levels of Brönsted acidity, with H^+ as the counter-cation, and Lewis acidity, through dealumination of the zeolite framework. This gives a huge advantage in tuning the activity and selectivity of zeolite-based catalysts. Zeolites have a 3-dimensional system of pores and cavities, with dimensions varying from 3 to 14 Å. This pore specificity for different zeolites makes them highly shape-selective catalysts capable of tuning substrate and product selectivity. These porous cavities also demonstrate a confinement effect, changing the contact time between different substrates and active sites.

Cyclic gas-phase oxidation of CH_4 with metal-exchanged zeolite catalysts with O_2, N_2O, or H_2O has been studied at high temperatures (150–500 °C) to activate the oxidant and desorb the CH_3OH produced. Panov et al. showed that methane could be oxidised with Fe-ZSM-5 to methanol using N_2O as oxidant [19]. N_2O decomposition creates an anion-radical species, which is an active species for oxidation of methane. A limitation of the system is a lack of a complete catalytic cycle, because an additional step to extract the methanol is required, typically by steaming or washing the zeolite. Addition of water into the feed-stream showed an increase in methanol selectivity from 1.9 to 16% [20, 21]. The same Fe-ZSM-5 system with molecular O_2 led to total combustion products [22]. Fe and Cu modified ZSM-5 catalyst was also found to be effective for this reaction using H_2O_2 under continuous flow conditions [23]. A methanol selectivity of 92% was observed at 0.5% conversion (0.46% yield). Oxidants like H_2O_2 or N_2O led to higher conversion compared to O_2. Instead of Fe, Cu containing ZSM-5 and mordenite (MOR) have also been studied, with their use inspired by sMMO systems [24].

Recently, an isothermal catalytic cycle was reported to convert methane to methanol over Cu-mordenite (CuMOR) at 200 °C with molecular O_2 [25]. In this process, the catalyst was first activated with O_2 followed by reaction with methane, and methanol was extracted using steam (Fig. 2.3). Microscopy of CuMOR activated at 200 °C showed intact zeolite structure with small copper oxide particles.

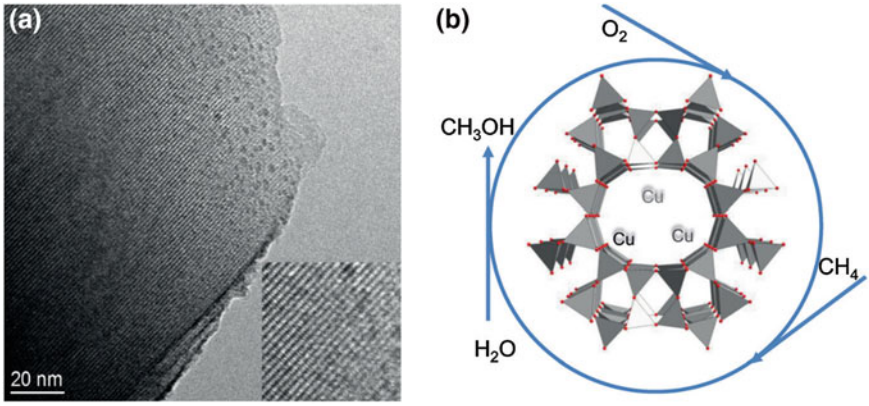

Fig. 2.3 Schematic representation of methane oxidation using CuMOR. Reproduced by permission from Ref. [25]. Copyright 2016 John Wiley and Sons

The active site was then re-activated for further oxidation cycles. A methanol yield of 56.2 μmol g^{-1} was observed after 13 h of O_2 activation followed by reaction at a methane pressure of 37 bar. Instead of a sequential process, continuous production of methanol from methane, oxygen and water was achieved with Cu modified zeolites by tuning the process conditions [26]. In this case, 1.81 μmol $h^{-1}g_{cat}^{-1}$ of methanol was obtained with 0.981 bar of CH_4. The catalyst was pretreated with O_2 at 550 °C for 5 h. Cu containing mordenite zeolites were also utilised for methane conversion to methanol using water.

Sushkevich et al. recently reported anaerobic direct oxidation by using water, both as a solvent and an oxidant, with a high methanol selectivity of 97% [27]. Water molecules acted as a cheap and abundant source of oxygen, but also regenerated the active sites. It also facilitated desorption of the product and stabilisation of the reaction intermediates.

The activation of the catalyst was performed at 400 °C, which was followed by the reaction with 7 bar of methane and then water at 200 °C. Consistent production of 0.2 mol of CH_3OH per mol of copper was observed. A mechanism involving reduction of dicopper sites of mordenite providing two electrons to oxidise methane to methanol was presented. Subsequent reduction of water, with concurrent formation of hydrogen, returns the two electrons to regenerate the mono (μ-oxo) dicopper active species.

Gas phase and high-temperature processes have limited methanol yield, due to lower methanol stability and hence decreased selectivity at higher conversion. Compared to previously discussed gas-phase oxidation, liquid-phase approaches use milder conditions to avoid overoxidation of methanol to COx. A lot of catalyst developments in these low-temperature approaches were inspired by nature.

2.3.3 Liquid-Phase Electrophilic Oxidation

Earlier methane oxidation approaches were based on work pioneered by Shilov and co-workers on electrophilic activation by oxidation-tolerant complexes [28]. They showed that both methanol (and methyl chloride) can be obtained as shown in Eq. 2.8 in a Cl^- containing aqueous medium at 120 °C with a Pt catalytic system using water as the source of oxygen [28–30].

$$R - H + [PtCl_6]^{2-} \xrightarrow[{[H_2O/120°]}]{cat\cdot[PtCl_4]^{2-}} R - OH + R - Cl + [PtCl_4]^{2-} + 2HCl \qquad (2.8)$$

The reaction (Eq. 2.8) is catalytic in Pt(II) but requires Pt(IV) in stoichiometric amounts, which makes it unfeasible on any large scale, but it does demonstrate the possibility of catalytic oxidation of methane via activation of C–H bond with late transition metals with the general scheme as shown in Fig. 2.4.

The first step in the Shilov-type catalytic system is the activation of methane by formation of methyl-Pt complex. Subsequently, $[PtCl_6]^{2-}$ oxidises the complex by electron donation, making it susceptible to nucleophilic attack by water (or chlorine) at the C–Pt bond, liberating CH_3OH (or CH_3Cl) and HCl [29]. Along with the stoichiometric use of $[PtCl_6]^{2-}$, the catalytic species are not particularly stable in solution due to formation of metallic platinum, since the redox potential for Pt(II)–Pt(0) couple is very close to the redox potential for Pt(IV)–Pt(II) couple. Understanding the proposed Shilov mechanism (Fig. 2.4) was crucial in understanding electrophilic activation of methane and led to the development of various liquid-phase catalysts. Later Periana et al. showed that $[PtCl_6]^{2-}$ can be replaced by conc. H_2SO_4 as an oxidant, i.e. using S in +6 oxidation state as highly oxidising species [32]. A homogeneous Hg(II)-based catalyst was also employed. The reaction was carried out at 180 °C and produced methyl bisulphate (CH_3OSO_3H) from methane and water, and sulphur dioxide from H_2SO_4 [32].

$$CH_4 + 2H_2SO_4 \longrightarrow CH_3OSO_3H + SO_2 + 2H_2O \qquad (2.9)$$

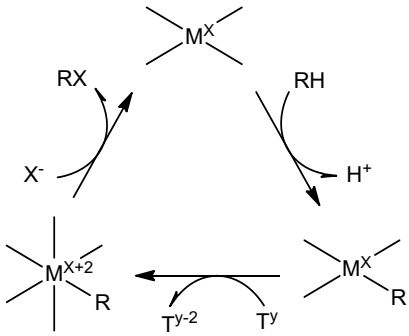

Fig. 2.4 Reaction cycle for electrophilic activation of C–H bond as seen in Shilov systems [31]

At 50% conversion, 85% selectivity to CH_3OSO_3H was achieved (Eq. 2.10), this product had to be separately hydrolysed to generate methanol as shown in giving a total yield of 43%.

$$CH_3OSO_3H + H_2O \longrightarrow CH_3OH + H_2SO_4 \tag{2.10}$$

An advantage of forming the bisulphate moiety as a product is protection from overoxidation. Due to the electron withdrawing nature of this group, there is a decrease in electron density on the primary carbon making it two orders of magnitude less susceptible to overoxidation [32]. As shown in Eq. 2.11, the process is also limited by re-oxidation of SO_2 which limits its application industrially.

$$SO_2 + \frac{1}{2}O_2 + H_2O \longrightarrow H_2SO_4 \tag{2.11}$$

As the reaction is not fully efficient, dilute H_2SO_4 is produced and a fully closed catalytic cycle is not achieved. This remains a limitation for liquid-phase oxidation even if there is site separation between methane oxidation and oxidant regeneration [6]. The overall equation represented in Eq. 2.2 shows a partial methane oxidation to methanol using O_2, but the oxidant used is concentrated H_2SO_4.

$$\textit{Net}:\ CH_4 + \frac{1}{2}O_2 \longrightarrow CH_3OH \tag{2.12}$$

This process was later improved upon by the same researchers, who substituted the mercuric catalyst by bipyramidal bis(2,2′-bipirimidine)Pt(II)Cl_2 complex, as shown in Fig. 2.5a [33]. This turned out to be a better system with 90% conversion of methane at selectivity of 81% to methyl bisulphate, and is used as a benchmark to compare catalyst efficiency. Similar to the mechanism proposed by Shilov, the electrophilic Pt(II)–CH_3 intermediate was proposed as shown in Fig. 2.5b. Similarly, thallium, palladium and the cations of gold were also used to oxidise methane to methanol.

Pd(II) was shown to activate methane in a similar manner, but the yield was limited due to the formation of Pd(0) [34, 35]. This limitation was overcome by Kalucki and co-workers by using metallic palladium in fuming sulphuric acid. Fuming sulphuric acid contains free sulphur trioxide, which is a stronger oxidant, and as a result of

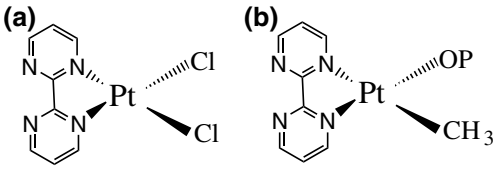

Fig. 2.5 Pt-based Periana catalyst. **a** Structure of the bipyramidal catalyst and **b** Pt(II)–CH_3 intermediate where OP is the oxidising ligand, in this case Cl or HSO_4 [33]

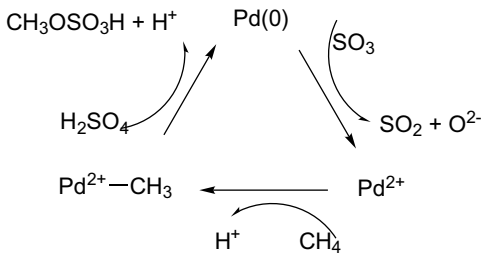

Fig. 2.6 Catalytic cycle using metallic palladium [36]

which, Pd(0) was oxidised to Pd(II) and was used to activate methane as shown in Fig. 2.6 [36]. The metal itself could be recovered and reused for multiple reactions and showed higher activity with higher SO_3 content.

Similarly, Jones et al. used cationic gold as an efficient electrophilic catalyst, but even in strongly acidic media such as triflic or sulphuric acid, there was irreversible formation of metallic gold after only one cycle, which led to only stoichiometric reaction and a turnover of <1% [37]. Au(III) species were found to be essential for the reaction, as metallic Au showed no activity. Selenic acid with Se(VI) was used as the oxidising agent since it is stronger than S(VI). It is almost as acidic as sulphuric acid and could stabilise the Au(III) cationic species. The reaction was then catalytic with turnover numbers of up to 30 [37].

In addition to concentrated H_2SO_4 and oleum, and stronger acids such as SO_3 and $HSeO_4$, Pd-based catalysts along with other transition metals have also been studied in trifluoroacetic acid systems to activate methane. Sen and co-workers showed that peroxytrifluoroacetic acid, which was generated from hydrogen peroxide and trifluoroacetic acid anhydride, can oxidise methane to methyl trifluoroacetate (CF_3COOCH_3) with the reaction catalysed by Pd(II) [38]. Park et al. reported the oxidation of methane to a mixture of CF_3COOCH_3 and CH_3OOH over a C-supported Pd heterogeneous catalyst in the presence of $Cu(CH_3COO)_2$ additive [39, 40]. In these cases, trifluoroacetic acid acts as the solvent and as a protecting group for methanol, H_2O_2 could also be synthesised in situ through the reaction between H_2 and O_2 [39]. Vargaftik et al. also proposed methane activation using Co(III)-based catalyst in trifluoroacetic acid at 180 °C, which produced methyl trifluoroacetate [41]. The reaction was stoichiometric due to conversion to Co(II). The reaction was catalytic in the presence of O_2, which regenerated the catalytic Co(III) species. H_2O_2 is favoured as an oxidant because of its high oxygen content and benign nature of its water by-product, but the low yield and high cost of H_2O_2 limits industrial viability.

Despite the efficacy of the C–H activation approach discussed above and the high selectivity observed for methanol derivatives with H_2SO_4 and CF_3COOH, these processes have limited applicability due to the corrosive solvent and the nature of oxidants are required to achieve a catalytic cycle. There are significant environmental, safety and process engineering concerns using these solvent systems. Moreover, most of the above mentioned are homogeneous catalytic systems and have disadvantages for an industrial process based around downstream processing and product separation. To overcome this, the Periana Pt-based catalyst was heterogenized by Palkovitz

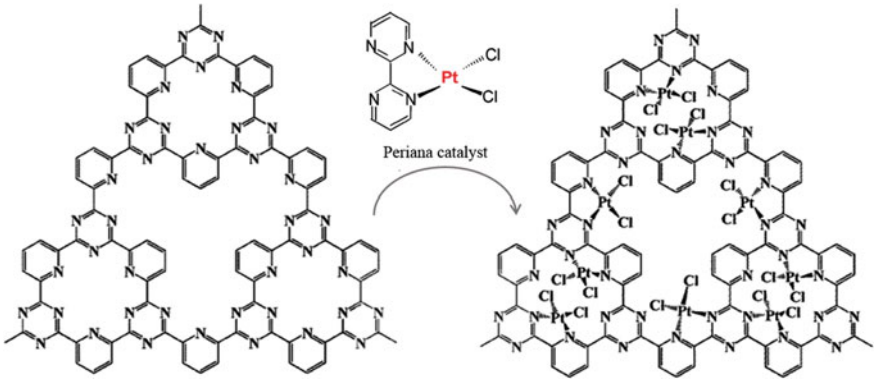

Fig. 2.7 CTF-moiety based heterogeneous system for Periana Pt-based catalyst. Reproduced by permission from Ref. [42]. Copyright 2009 John Wiley and Sons

et al. by using a polymer framework based on a covalent triazine (CTF) [42] as shown in Fig. 2.7. This CTF moiety was connected to the bipyramidal Pt species and it required concentrated sulfuric acid according to the conditions described by Periana et al. [33, 43].

The next development in a catalytic system was driven by the need to replace strong protic solvents and oxidants with more benign ones. Methane activation was observed in acetonitrile solution in the presence of $[NBu_4]VO_3$-pyrazine-2-carboxylic acid and H_2O_2 as the promoter in the presence of air by Shulpin and co-workers [44]. Different Fe(III) complexes were also investigated for methane oxidation by the same group [45]. Pyrazine-2-carboxylic acid was shown to have a positive effect on the catalytic activity, which was attributed to the formation of ferryl ion [45]. In contrast to the previous Shilov-type electrophilic activation, formation of hydroxyl and hydroperoxy radical species were considered as the mechanism for these processes, and they were formed due to the interaction with H_2O_2. An aqueous-phase approach was reported by Yuan et al., in which a number of transition metal chloride catalysts, like $OsCl_3$ and $HAuCl_4$, were studied for selective oxidation of methane and ethane, which again showed radical-based mechanisms of conversion [46].

2.3.4 Zeolites for Liquid-Phase Oxidation

Several catalysts have been developed on biomimetic approaches focusing on iron-based active sites at low temperature using milder conditions, such as aqueous solvents and benign oxidants. One of the notable examples was demonstrated by the use of metal-phthalocyanine complexes of Fe and Cu encapsulated within zeolites [47]. Raja and Ratnasamy successfully catalysed methane oxidation to a mixture of methanol and formaldehyde at ambient and sub-ambient (0 °C) temperatures in the liquid phase with O_2/TBHP (tert-butyl hydroperoxide) oxidant mixtures [47].

Although they obtained very low overoxidation to CO_2, a maximum 2% was obtained within 12 h with Fe-phthalocyanine encapsulated within zeolite-X in acetonitrile. Significant activity was only obtained in chemically reactive organic solvents, while a much lower activity of the same catalyst was obtained when it was employed in water.

Further research was carried out by Sorokin et al. with SiO_2 supported metal-phthalocyanine complexes [48, 49]. H_2O_2 was used as the oxidant and the reaction was carried out at ambient temperature forming methanol, formaldehyde and formic acid. A μ-nitrido iron phthalocyanine complex grafted onto silica was also investigated for methane oxidation with H_2O_2 in water and was found to be unstable under reaction conditions [50]. Un-modified silica support was also found to be active, and Fe/SiO_2 was found to have similar activity as Fe-phthalocyanine grafted on silica with high selectivities and much higher stability suggesting a Fenton type chemistry was involved.

Other catalysts containing iron and copper have also been investigated for methane oxidation inspired by the monooxygenase enzyme. Most notably, zeolites have gained a lot of attention in this field. As discussed earlier, zeolites have been employed in gas-phase methane oxidation with N_2O and O_2. Gas-phase methane oxidation leads to lower selectivities due to more facile overoxidation. Liquid-phase methane oxidation with zeolites have also been studied extensively. The most notable example of this is ZSM-5-based catalysts [23, 51]. H-ZSM-5 ($SiO_2/Al_2O_3 = 30$), which has been calcined at high temperatures (550 °C), was found to be active for methane oxidation with H_2O_2, achieving a conversion of 0.3% with a selectivity of 95% to oxygenated products.

Elemental analysis carried out on the samples showed a trace amount of iron present in the framework. With the addition of extra-framework iron, there was an increase in the catalytic activity, which resulted in a methane conversion of 0.7%, still maintaining a high selectivity of methanol and limited selectivity to deep oxidation products. Spectroscopy studies suggested iron to be present as a diiron complex containing antiferromagnetically coupled high-spin octahedral Fe^{3+} centres. A proposed catalytic cycle on these binuclear Fe species is shown in Fig. 2.8. The overall charge in each case is formally +2 as the species acts as an extra-framework cation.

Methyl hydroperoxide is proposed to be the primary reaction product, which can undergo selective conversion to methanol or non-selective conversion to formic acid. Formic acid and carbon dioxide are consecutive overoxidation products from methanol. With 2.5% Fe loading on Fe/ZSM-5 (30) catalyst, the major products were formic acid (72%), methanol (10%), methyl hydroperoxide (1%) and CO_2 (17%) [52].

With the addition of extra-framework or homogeneous Cu^{+2}, in addition to iron, a major change of selectivity was noted, as methanol became the major product (85%), this was achieved by stopping methanol oxidation to formic acid (Fig. 2.9). EPR studies showed Cu^{+2} was acting as a scavenger of hydroxyl radicals, which was shown to play a role in the overoxidation of methanol to formic acid and CO_2 [52]. Although, the Fe–Cu/ZSM–5 catalyst showed similarity to iron and copper-based

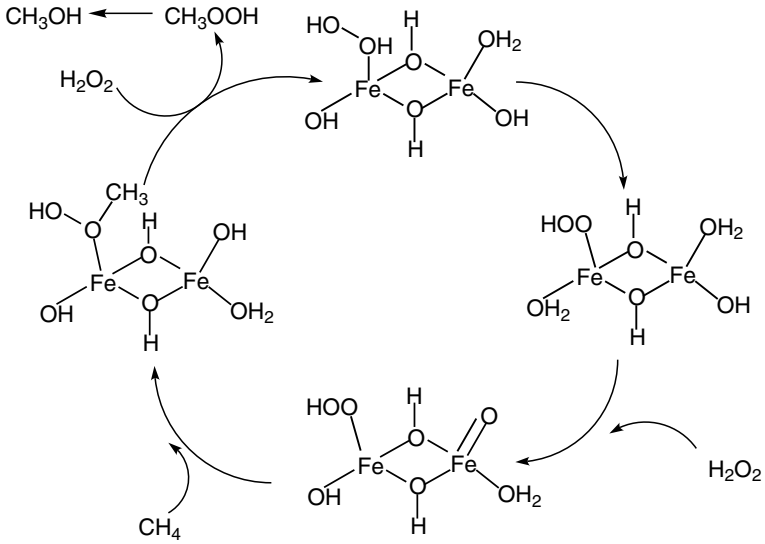

Fig. 2.8 Proposed catalytic cycle for the oxidation of methane catalysed by a binuclear Fe species in ZSM-5. Reproduced by permission from Ref. [52]. Copyright 2012 John Wiley and Sons

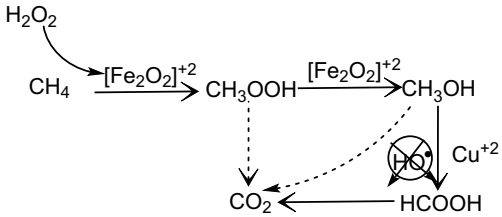

Fig. 2.9 Proposed reaction scheme for selective oxidation of methane with H_2O_2. Reproduced by permission from Ref. [52]. Copyright 2012 John Wiley and Sons

methane monooxygenase enzymatic catalysts, it showed no catalytic activity with molecular oxygen, limiting its commercial significance.

Recently, mononuclear rhodium (Rh) species anchored on ZSM-5 catalyst was reported to catalyse the direct conversion of methane to methanol and acetic acid, using oxygen and carbon monoxide under mild conditions [53]. The acidity of the zeolite has been reported to promote the selectivity of Cu–ZSM–5 catalysts for acetic acid and a high methanol selectivity was achieved using Na–ZSM–5. The reaction was carried out in a batch reactor with catalysts suspended in water. Methane pressure of 20 bar and CO pressure of 5 bar was used. O_2 pressure was varied to vary the product selectivity. Upon optimisation of the reaction, a yield of 22,000 μmoles of acetic acid per gram of catalyst or 230 μmoles of methanol per gram of catalyst was formed after 3 h, with selectivity of 60% and 100%, respectively, at 150 °C, as shown in Fig. 2.10 [53]. It was hypothesised that isolated Rh^+ cations facilitated activation of methane with O_2 to form Rh–CH_3 species. Rh–OCH_3 species were then observed in the presence of CO, suggesting the role of CO was as a co-catalyst.

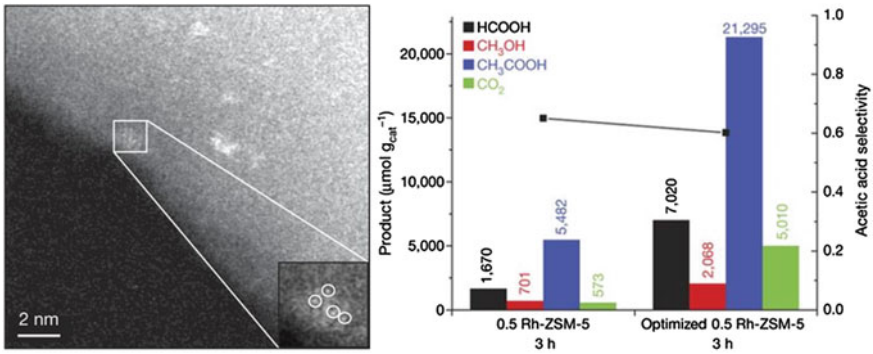

Fig. 2.10 Single site Rh/ZSM-5 catalyst for methane transformation into CH_3COOH using CO and O_2. Reproduced by permission from Springer Nature: Ref. [53]. Copyright 2017

It was also involved in regeneration of the Rh–ZSM–5 catalyst. A similar catalytic transformation was also demonstrated with Rh_1O_5/ZSM–5, and an isotope labelled experiments using $^{13}CH_4$ and ^{13}CO showed that the CH_3 of CH_3COOH forms from the activation of CH_4 and C=O from the insertion of CO to Rh–OH [54]. Single-atom Rh/ZrO_2 catalysts were also recently investigated for methane oxidation to methanol under mild aqueous conditions at 70 °C in the liquid phase and to ethane with O_2 in the gas phase at 300 °C [55].

Zeolites have proved to be an important class of heterogeneous catalysts and are being studied extensively for methane oxidation. They have been found to be active for methane oxidation under mild conditions using environmentally favourable oxidants like H_2O_2 and benign solvents like water. However, the use of H_2O_2 is not economically viable and industrially favourable since the cost of H_2O_2 is greater when compared to the value of the product, methanol. The use of molecular oxygen, which is not only environmentally benign but also readily available and inexpensive, is required and its use has not been reported in many cases. The ability of gold and palladium-based catalysts to efficiently synthesise H_2O_2 using molecular O_2 and H_2 has led to the investigation of methane oxidation efficacy of these bimetallic catalysts.

2.3.5 Gold–Palladium-Based Methane Oxidation Catalysts

For many years gold was regarded as a poor catalyst due to its inert nature in bulk form, but catalysis by gold has gained a lot of attention in the past few decades since Haruta's discovery of gold being an excellent catalyst for CO oxidation in 1985 [56] and Hutchings' prediction of gold being an excellent catalyst for acetylene hydrochlorination [57]. The latter has also led to commercialisation of gold supported on activated carbon, as an active catalyst for acetylene hydrochlorination to synthesise

vinyl chloride monomer [58]. Subsequently, there has been a rapid increase in use and study of different gold-based catalysts for various reactions.

Productivity of gold catalysed reaction has been modified in certain reactions by adding a second metal, or sometimes even a third metal, to synthesise bimetallic or trimetallic catalysts. In such cases, palladium has been found to have an enhancing effect on the activity of gold nanoparticles, since gold and palladium show a synergistic effect towards many substrates [59]. Palladium itself has been used in oxidation chemistry for many relevant industrial reactions, such as the Wacker process for the oxidation of ethylene to acetaldehyde [60]. Hutchings and co-workers have previously shown that supported Au–Pd nanoparticles are highly effective catalysts for the direct synthesis of H_2O_2 [61], the oxidation of alcohols like benzyl alcohol [62] and the oxidation of primary C–H bonds in toluene [63].

The aforementioned reactions are considered to be linked by the hydroperoxy intermediate, which could be formed by oxidants like H_2O_2 and tert-butyl hydroperoxide (TBHP). Since hydroperoxy intermediate formation was also found in methane oxidation in previous studies [33, 52], such supported Au–Pd nanoparticles were tested for methane oxidation using H_2O_2 as the oxidant. 5 wt% Au–Pd/TiO_2 catalysts prepared by impregnation were found to be active for methane oxidation at low temperatures of 50 °C with H_2O_2 as the oxidant in aqueous conditions to produce high oxygenate selectivity (90%), although with low productivity (0.28 $mol_{(products)}kg^{-1}_{(cat)}h^{-1}$) [64]. Reactions were also performed with only O_2 as the oxidant, but no oxygenated products were obtained. methyl hydroperoxide was found to be the primary product following the reaction scheme shown in Fig. 2.11, and it can be converted to methanol. Oxidation of both methyl hydroperoxide and methanol led to formic acid and CO_2 was also detected as the total oxidation product.

Since Au–Pd nanoparticles were shown to be active for direct synthesis of H_2O_2, it was proposed that hydroperoxy species could be formed in situ from gaseous H_2 and O_2 to oxidise methane. Thus, methane oxidation was carried out under a mixture of CH_4, H_2 and O_2 diluted with N_2 to avoid flammable mixtures. Similar productivity, with a higher methanol selectivity (68% compared to 49% in the earlier case), was

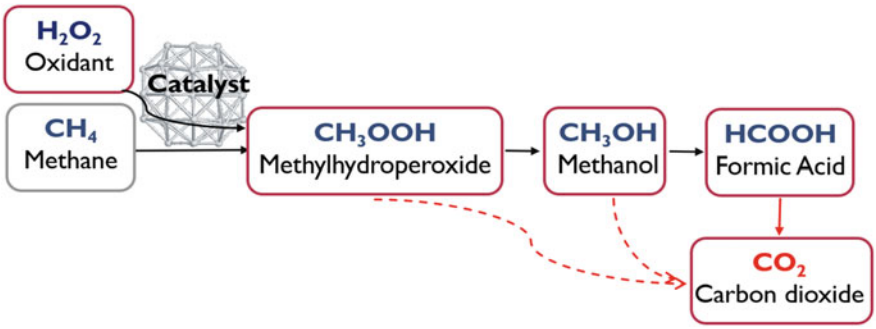

Fig. 2.11 Proposed reaction scheme for selective oxidation of methane over Au–Pd/TiO_{-2} supported catalysts with H_2O_2

observed when using in situ generated H_2O_2 [64]. Reactions were also carried out by modifying the support to CeO_2, C, SiO_2 and Al_2O_3, but narrow variation in productivities, ranging between 0.1 and 0.3 $mol_{(products)}kg^{-1}_{(cat)}h^{-1}$, was observed. Stabiliser-free sol-immobilisation Au–Pd/TiO_2 catalysts were also investigated, to try to understand and improve upon the *as-prepared* catalysts, which show low catalytic activity along with higher H_2O_2 consumption rates [65]. Heat treatments by high-temperature calcination to modify nanoparticle sizes and rutile-anatase TiO_2 supports were studied to maximise the efficiency and performance of the resulting catalysts. After high-temperature calcination of the TiO_2 support at 800 °C for 3 h, followed by catalyst calcination at 800 °C for 3 h, productivity of 0.677 $mol_{(products)}kg^{-1}_{(cat)}h^{-1}$ was achieved and 1785 μmol of H_2O_2 were consumed in the process.

Following on from the methane oxidation activity of bimetallic Au–Pd catalysts, trimetallic Au–Pd–Cu catalysts supported on TiO_2 were investigated for low-temperature selective oxidation of methane with H_2O_2 at 50 °C [66]. The rate of methane oxidation for these Au–Pd–Cu/TiO_2 catalysts was found to be enhanced by a factor of 5, with high oxygenate selectivity of more than 95%. In all these cases supported nanoparticles were found to be inefficient with respect to H_2O_2 consumption, and much lower amounts of products were observed per mole of H_2O_2 consumed. Thus, an investigation was carried out to understand the intrinsic activity of Au–Pd nanoparticles, focusing on the difference between supported and unsupported catalysts. Unsupported Au–Pd nanoparticles stabilised using polyvinylpyrrolidone polymer have been demonstrated to be highly active and selective catalysts for methane oxidation under mild conditions, i.e. aqueous solvents and low temperatures such as 50 °C [67]. The colloidal catalyst was found to be stable under reaction conditions since negligible agglomeration or leaching of metal ions was observed from characterisation by microscopy (Fig. 2.12).

Using isotopically labelled oxygen ($^{18}O_2$) as an oxidant in the presence of H_2O_2, high incorporation of gas-phase O_2 into the methanol product was demonstrated, confirming the efficacy of molecular oxygen as the oxidant. By tuning the amount of H_2O_2, high productivities and selectivity were observed. More oxygenated products were formed than the amount of H_2O_2 consumed, suggesting that the controlled breakdown of H_2O_2 activates methane, which subsequently incorporates molecular oxygen through a radical process as shown in Fig. 2.13.

Although these colloidal catalysts were found to be stable and reusable, industrially heterogeneous catalysts have been preferred given the ease of re-usability of the catalysts. Also, these catalysts still require addition of H_2O_2, which has a relatively high associated cost. Commercial viability will depend on the use of no or catalytic amounts of H_2O_2 and using air or O_2 as the oxidant.

2.4 Conclusions and Future Outlook

Methane activation is one of the *grand challenges* that the catalysis community faces. Methane is the main component of natural gas and also a significant by-product of oil

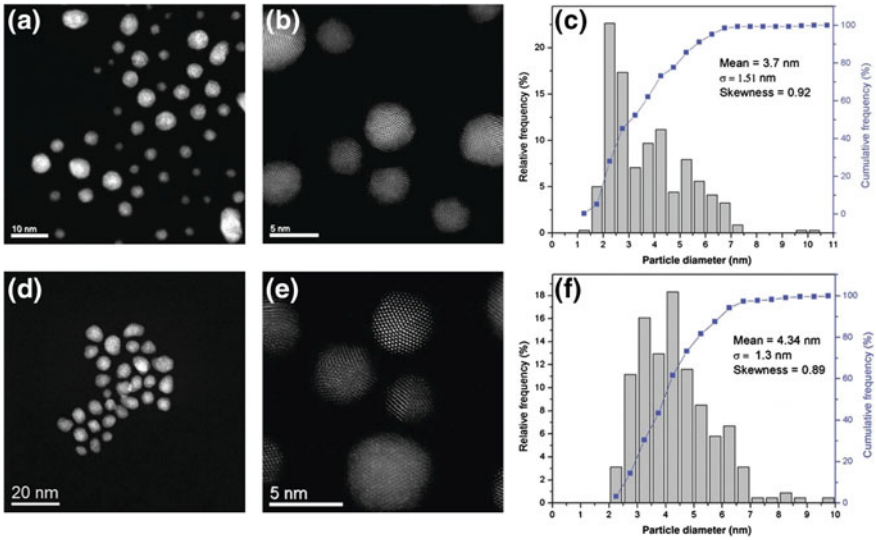

Fig. 2.12 Representative HAADF images and particle size distribution in fresh (A–C) and used (D–F) Au–Pd–PVP colloids. From [67]. Reprinted with permission from AAAS

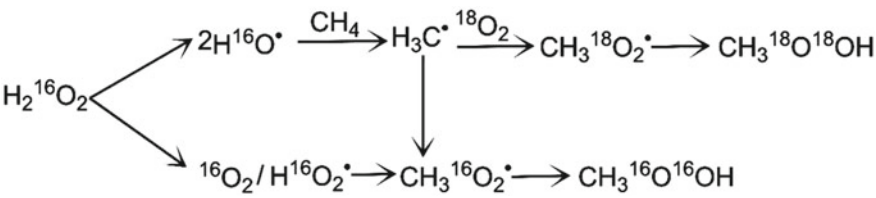

Fig. 2.13 Proposed reaction scheme for methane oxidation using Au–Pd–PVP colloids in the presence of H_2O_2 and O_2. From [67]. Reprinted with permission from AAAS

refining and chemical processing. Thus, methane valorisation to energy-dense liquid derivatives, like methanol, is highly desirable. Present approaches for direct conversion include high-temperature routes, which are characterised by poor oxygenate selectivity, and low-temperature routes, which can be limited due to low conversion and non-closed catalytic cycles. Although higher methane conversion is observed over homogeneous catalysts such as electrophilic activation in Pt-based systems [33, 68], or radical-based approaches in gold–palladium systems [67], their heterogeneous counterparts also show some promising results. Zeolites, and specially doped zeolites with Cu, Rh and other such systems, are exciting and novel catalytic formulations which may be applied on an industrial scale as well [52, 53]. But the use of expensive and potentially corrosive solvents and oxidants, limit or in many cases, are detrimental for industrial operation. In some cases, use of H_2O_2 as the oxidant can potentially be eliminated by coupling processes which could generate similar radical

species, for example photochemical [69, 70] or electrochemical [71, 72] approaches, but more industrial engineering and chemical understanding needs to be performed to validate such processes. The other concern is overoxidation to CO_2. The catalyst needs to be active for methane oxidation to methanol but avoid methanol oxidation to CO_2, especially on increasing temperature or residence time to increase methane conversion.

In contrast to methane oxidation to methanol, some positive developments are being made to generate acetic acid from methane. Such systems employ gases like CO and CH_4 which potentially can be used alongside present syngas technologies. The anticipated performance of such catalytic systems was achieved using either expensive solvents or oxidising agents in batch reactors. For any industrial operation, further studies need to be performed to assess production feasibility and costs.

Considering the above scrutiny, the future development and industrial applicability depend on the overall process feasibility and profitability. This in turn not only depends on the value add of the products which can be derived from methane, but also on the costs and availability of the co-reactants, energy for the reaction and costs of product separation. Large scale operation would potentially be performed in a continuous flow type reactor with preferably a heterogeneous catalyst. Several kinetic and thermodynamic limitations need to be taken into consideration while developing the process to maximise oxygenate selectivity and reduce overoxidation to CO_2. The studies performed with homogeneous catalysts are highly important as well because they not only provide fundamental building blocks for tailoring design of more industrially applicable heterogeneous catalysts but also help in understanding the mechanistic relationship between the desired reaction and undesired side products.

In addition to designing heterogeneous counterparts for homogeneous systems, further research is also required for catalytic development of existing heterogeneous systems, namely, zeolites. Methane oxidation in zeolites is seen as a multistep process, consisting of site separation between activation of methane, oxidant of active species and oxidant regeneration. Some studies have demonstrated that both activation and reaction can proceed under isothermal conditions simultaneously [27], but more research is required to further understand the process and design the process and reactor accordingly.

Acknowledgements The authors would like to acknowledge Cardiff University for financial support as part of the MAXNET Energy Consortium.

References

1. International Energy Agency Natural Gas Information (2017). www.iea.org/statistics/topics/naturalgas/. Accessed 1 Jan 2017
2. BP (2017) BP Energy Outlook Energy 2017. BP Stat Rev World Energy 52. https://doi.org/10.1017/cbo9781107415324.004
3. International Energy Agency (2013) Resources to reserves 2013—Oil, gas and coal technologies for the energy markets of the future

4. Hammer G, Lübcke T, Kettner R et al (2006) Natural gas. In: Ullmann's encyclopedia of industrial chemistry. Wiley-VCH Verlag GmbH & Co. KGaA, Weinheim, Germany
5. Bergman RG (2007) Organometallic chemistry: C–H activation. Nature 446:391–394. https://doi.org/10.1038/446391a
6. Olivos-Suarez AI, Szécsényi À, Hensen EJM et al (2016) Strategies for the direct catalytic valorization of methane using heterogeneous catalysis: challenges and opportunities. ACS Catal 6:2965–2981. https://doi.org/10.1021/acscatal.6b00428
7. Olah GA, Goeppert A, Prakash GKS (2009) The "methanol economy": general aspects. Beyond oil and gas: the methanol economy. Wiley-VCH Verlag GmbH & Co. KGaA, Weinheim, Germany, pp 179–184
8. Wilhelm D, Simbeck D, Karp A, Dickenson R (2001) Syngas production for gas-to-liquids applications: technologies, issues and outlook. Fuel Process Technol 71:139–148. https://doi.org/10.1016/S0378-3820(01)00140-0
9. Sheldon D (2017) Methanol production—A technical history. Johnson Matthey Technol Rev 61:172–182. https://doi.org/10.1595/205651317X695622
10. Blanksby SJ, Ellison GB (2003) Bond dissociation energies of organic molecules. Acc Chem Res 36:255–263. https://doi.org/10.1021/AR020230D
11. Ott J, Gronemann V, Pontzen F et al (2012) Methanol. In: Ullmann's encyclopedia of industrial chemistry
12. da Silva MJ (2016) Synthesis of methanol from methane: Challenges and advances on the multi-step (syngas) and one-step routes (DMTM). Fuel Process Technol 145:42–61. https://doi.org/10.1016/J.FUPROC.2016.01.023
13. Balasubramanian R, Smith SM, Rawat S et al (2010) Oxidation of methane by a biological dicopper centre. Nature 465:115–119. https://doi.org/10.1038/nature08992
14. Colby J, Stirling DI, Dalton H (1977) The soluble methane mono-oxygenase of methylococcus capsulatus (Bath). Biochem J 165:395–402
15. Shteinman AA (2001) The role of metal-oxygen intermediates in biological and chemical monooxygenation of alkanes. Russ Chem Bull 50:1795–1810. https://doi.org/10.1023/A:1014321827168
16. Otsuka K, Wang Y (2001) Direct conversion of methane into oxygenates. Appl Catal Gen 222:145–161. https://doi.org/10.1016/S0926-860X(01)00837-7
17. Gesser HD, Hunter NR, Prakash CB (1985) The direct conversion of methane to methanol by controlled oxidation. Chem Rev 85:235–244. https://doi.org/10.1021/cr00068a001
18. Walker GS, Lapszewicz JA, Foulds GA (1994) Partial oxidation of methane to methanol-comparison of heterogeneous catalyst and homogeneous gas phase reactions. Catal Today 21:519–526. https://doi.org/10.1016/0920-5861(94)80175-4
19. Sobolev VI, Dubkov KA, Panna OV, Panov GI (1995) Selective oxidation of methane to methanol on a FeZSM-5 surface. Catal Today 24:251–252. https://doi.org/10.1016/0920-5861(95)00035-E
20. Chow YK, Dummer NF, Carter JH et al (2018) A kinetic study of methane partial oxidation over Fe–ZSM–5 Using N_2O as an oxidant. ChemPhysChem 19:402–411. https://doi.org/10.1002/cphc.201701202
21. Parfenov MV, Starokon EV, Pirutko LV, Panov GI (2014) Quasicatalytic and catalytic oxidation of methane to methanol by nitrous oxide over FeZSM–5 zeolite. J Catal 318:14–21. https://doi.org/10.1016/J.JCAT.2014.07.009
22. Starokon EV, Parfenov MV, Arzumanov SS et al (2013) Oxidation of methane to methanol on the surface of FeZSM-5 zeolite. J Catal 300:47–54. https://doi.org/10.1016/j.jcat.2012.12.030
23. Xu J, Armstrong RD, Shaw G et al (2016) Continuous selective oxidation of methane to methanol over Cu- and Fe-modified ZSM-5 catalysts in a flow reactor. Catal Today 270:93–100. https://doi.org/10.1016/J.CATTOD.2015.09.011
24. Groothaert MH, Smeets PJ, Sels BF et al (2005) Selective oxidation of methane by the bis (u-oxo) dicopper core stabilized on ZSM-5 and mordenite zeolites. J Am Chem Soc 127:1394–1395. https://doi.org/10.1021/ja047158u

25. Tomkins P, Mansouri A, Bozbag SE et al (2016) Isothermal cyclic conversion of methane into methanol over copper-exchanged zeolite at low temperature. Angew Chem Int Ed 55:5467–5471. https://doi.org/10.1002/anie.201511065
26. Narsimhan K, Iyoki K, Dinh K, Román-Leshkov Y (2016) Catalytic oxidation of methane into methanol over copper-exchanged zeolites with oxygen at low temperature. ACS Cent Sci 2:424–429. https://doi.org/10.1021/acscentsci.6b00139
27. Sushkevich VL, Palagin D, Ranocchiari M, Bokhoven JA van (2017) Selective anaerobic oxidation of methane enables direct synthesis of methanol. Science 356(80):523–527. https://doi.org/10.1016/s0166-9834(00)80103-7
28. Shilov AE, Shulpin GB (1987) Activation and catalytic reactions of alkanes in solutions of metal complexes complexes. Russ Chem Rev 56:442–464. https://doi.org/10.1070/RC1987v056n05ABEH003282
29. Labinger JA, Bercaw JE (2002) Understanding and exploiting C–H bond activation. Nature 417:507–514. https://doi.org/10.1038/417507a
30. Lin M, Shen C, Garcia-zayas EA et al (2001) Catalytic Shilov chemistry: platinum chloride-catalyzed oxidation of terminal methyl groups by dioxygen. J Am Chem Soc 6:1000–1001. https://doi.org/10.1021/ja001926+
31. Webb JR, Bolaño T, Gunnoe TB (2011) Catalytic oxy-functionalization of methane and other hydrocarbons: fundamental advancements and new strategies. ChemSusChem 4:37–49. https://doi.org/10.1002/cssc.201000319
32. Periana RA, Taube DJ, Evitt ER et al (1993) A mercury-catalyzed, high-yield system for the oxidation of methane to methanol. Science 259:340–343. https://doi.org/10.1126/science.259.5093.340
33. Periana RA, Taube DJ, Gamble S et al (1998) Methanol derivative platinum catalysts for the high-yield oxidation of methane to a methanol derivative. Science 280:560–564. https://doi.org/10.1126/science.280.5363.560
34. Gretz E, Oliver TF, Sen A (1987) Carbon-hydrogen bond activation by electrophilic transition-metal compounds. Palladium (II)-mediated oxidation of arenes and alkanes including methane. J Am Chem Soc 109:8109–8111. https://doi.org/10.1021/ja00260a040
35. Sen A, Benvenuto MA, Lin M et al (1994) Activation of methane and ethane and their selective oxidation to the alcohols in protic media. J Am Chem Soc 116:998–1003. https://doi.org/10.1021/ja00082a022
36. Michalkiewicz B, Kałucki K, Sośnicki JG (2003) Catalytic system containing metallic palladium in the process of methane partial oxidation. J Catal 215:14–19. https://doi.org/10.1016/S0021-9517(02)00088-X
37. Jones CJ, Taube D, Ziatdinov VR et al (2004) Selective oxidation of methane to methanol catalyzed, with C–H activation, by homogeneous, cationic gold. Angew Chem Int Ed 43:4626–4629. https://doi.org/10.1002/anie.200461055
38. Kao LC, Hutson AC, Sen A (1991) Low-temperature, palladium (II)-catalyzed, solution-phase oxidation of methane to a methanol derivative. J Am Chem Soc 113:700–701. https://doi.org/10.1021/ja00002a063
39. Park ED, Hwang Y-S, Lee CW, Lee JS (2003) Copper- and vanadium-catalyzed methane oxidation into oxygenates with in situ generated H_2O_2 over Pd/C. Appl Catal Gen 247:269–281. https://doi.org/10.1016/S0926-860X(03)00125-X
40. Lin M, Sen A (1992) A highly catalytic system for the direct oxidation of lower alkanes by dioxygen in aqueous medium. A formal heterogeneous analog of alkane monooxygenases. J Am Chem Soc 114:7307–7308. https://doi.org/10.1021/ja00044a059
41. Vargaftik MN, Stolarov IP, Moiseev II (1990) Highly selective partial oxidation of methane to methyl trifluoroacetate. J Chem Soc Chem Commun 0:1049–1050. https://doi.org/10.1039/c39900001049
42. Palkovits R, Antonietti M, Kuhn P et al (2009) Solid catalysts for the selective low-temperature oxidation of methane to methanol. Angew Chem Int Ed 48:6909–6912. https://doi.org/10.1002/anie.200902009

43. Kamiya K, Kamai R, Hashimoto K, Nakanishi S (2014) Platinum-modified covalent triazine frameworks hybridized with carbon nanoparticles as methanol-tolerant oxygen reduction electrocatalysts. Nat Commun 5:5040. https://doi.org/10.1038/ncomms6040
44. Nizova G V., Süss-Fink G, Shul'pin GB (1997) Catalytic oxidation of methane to methyl hydroperoxide and other oxygenates under mild conditions. Chem Commun 0:397–398. https://doi.org/10.1039/a607765j
45. Shul'pin GB, Nizova GV, Kozlov YN et al (2004) Hydrogen peroxide oxygenation of alkanes including methane and ethane catalyzed by iron complexes in acetonitrile. Adv Synth Catal 346:317–332. https://doi.org/10.1002/adsc.200303147
46. Yuan Q, Deng W, Zhang Q, Wang Y (2007) Osmium-catalyzed selective oxidations of methane and ethane with hydrogen peroxide in aqueous medium. Adv Synth Catal 349:1199–1209. https://doi.org/10.1002/adsc.200600438
47. Raja R, Ratnasamy P (1997) Direct conversion of methane to methanol. Appl Catal Gen 158:L7–L15. https://doi.org/10.1016/S0926-860X(97)00105-1
48. Sorokin AB, Kudrik EV, Alvarez LX et al (2010) Oxidation of methane and ethylene in water at ambient conditions. Catal Today 157:149–154. https://doi.org/10.1016/J.CATTOD.2010.02.007
49. Sorokin AB, Kudrik EV, Bouchu D (2008) Bio-inspired oxidation of methane in water catalyzed by N-bridged diiron phthalocyanine complex. Chem Commun 0:2562–2563. https://doi.org/10.1039/b804405h
50. Forde MM, Grazia BC, Armstrong R et al (2012) Methane oxidation using silica-supported N-bridged di-iron phthalocyanine catalyst. J Catal 290:177–185. https://doi.org/10.1016/J.JCAT.2012.03.013
51. Hammond C, Conrad S, Hermans I (2012) Oxidative methane upgrading. ChemSusChem 5:1668–1686. https://doi.org/10.1002/cssc.201200299
52. Hammond C, Forde MM, Ab Rahim MH et al (2012) Direct catalytic conversion of methane to methanol in an aqueous medium by using copper-promoted Fe–ZSM–5. Angew Chem Int Ed 51:5129–5133. https://doi.org/10.1002/anie.201108706
53. Shan J, Li M, Allard LF et al (2017) Mild oxidation of methane to methanol or acetic acid on supported isolated rhodium catalysts. Nature 551:605–608. https://doi.org/10.1038/nature24640
54. Tang Y, Li Y, Fung V et al (2018) Single rhodium atoms anchored in micropores for efficient transformation of methane under mild conditions. Nat Commun 9:1231. https://doi.org/10.1038/s41467-018-03235-7
55. Kwon Y, Kim TY, Kwon G et al (2017) Selective activation of methane on single-atom catalyst of rhodium dispersed on zirconia for direct conversion. J Am Chem Soc 139:17694–17699. https://doi.org/10.1021/jacs.7b11010
56. Haruta M, Kobayashi T, Sano H, Yamada N (1987) Novel gold catalysts for the oxidation of carbon monoxide at a temperature far below 0 and C. Chem Lett 16:405–408. https://doi.org/10.1246/cl.1987.405
57. Hutchings GJ (1985) Vapor phase hydrochlorination of acetylene: Correlation of catalytic activity of supported metal chloride catalysts. J Catal 96:292–295. https://doi.org/10.1016/0021-9517(85)90383-5
58. Hutchings GJ, Haruta M (2005) A golden age of catalysis: a perspective. Appl Catal Gen 291:2–5. https://doi.org/10.1016/J.APCATA.2005.05.044
59. Landon P, Collier PJ, Papworth AJ et al (2002) Direct formation of hydrogen peroxide from H2/O2 using a gold catalyst. Chem Commun 0:2058–2059. https://doi.org/10.1039/b205248m
60. Jira R (2009) Acetaldehyde from ethylene-a retrospective on the discovery of the wacker process. Angew Chem Int Ed 48:9034–9037. https://doi.org/10.1002/anie.200903992
61. Edwards JK, Freakley SJ, Carley AF et al (2013) Strategies for designing supported gold-palladium bimetallic catalysts for the direct synthesis of hydrogen peroxide. Acc Chem Res 47:845–854. https://doi.org/10.1021/ar400177c
62. Pritchard J, Piccinini M, Tiruvalam R et al (2013) Effect of heat treatment on Au–Pd catalysts synthesized by sol immobilisation for the direct synthesis of hydrogen peroxide and benzyl alcoholoxidation. Catal Sci Technol 3:308–317. https://doi.org/10.1039/C2CY20234D

63. Kesavan L, Tiruvalam R, Hasbi M et al (2011) Solvent-free oxidation of primary carbon-hydrogen bonds in toluene using Au–Pd alloy nanoparticles. Science 331(80):195–199. https://doi.org/10.1126/science.1198458
64. AbRahim MH, Forde MM, Jenkins RL et al (2013) Oxidation of methane to methanol with hydrogen peroxide using supported gold-palladium alloy nanoparticles. Angew Chem 125:1318–1322. https://doi.org/10.1002/ange.201207717
65. Williams C, Carter JH, Dummer NF et al (2018) Selective oxidation of methane to methanol using supported AuPd catalysts prepared by stabilizer-free sol-immobilization. ACS Catal 8:2567–2576. https://doi.org/10.1021/acscatal.7b04417
66. Ab Rahim MH, Armstrong RD, Hammond C et al (2016) Low temperature selective oxidation of methane to methanol using titania supported gold palladium copper catalysts. Catal Sci Technol 6:3410–3418. https://doi.org/10.1039/C5CY01586C
67. Agarwal N, Freakley SJ, McVicker RU et al (2017) Aqueous Au–Pd colloids catalyze selective CH_4 oxidation to CH_3OH with O_2 under mild conditions. Science 358(80):223–227. https://doi.org/10.1126/science.aan6515
68. Periana RA, Bhalla G, Tenn WJ et al (2004) Perspectives on some challenges and approaches for developing the next generation of selective, low temperature, oxidation catalysts for alkane hydroxylation based on the CH activation reaction. J Mol Catal: Chem 220:7–25. https://doi.org/10.1016/j.molcata.2004.05.036
69. Gondal MA, Hameed A, Suwaiyan A (2003) Photo-catalytic conversion of methane into methanol using visible laser methanol using visible laser. Appl Catal Gen 243:165–174. https://doi.org/10.1016/S0926-860X(02)00562-8
70. Noceti RP, Taylor CE, D'Este JR (1997) Photocatalytic conversion of methane. Catal Today 33:199–204. https://doi.org/10.1039/b710575b
71. Tomita A, Nakajima J, Hibino T (2008) Direct oxidation of methane to methanol at low temperature and pressure in an electrochemical fuel cell. Angew Chem Int Ed 47:1462–1464. https://doi.org/10.1002/anie.200703928
72. Frese K (1991) Partial electrochemical oxidation of methane under mild conditions. Langmuir 7:13–15. https://doi.org/10.1021/la00049a004

Chapter 3
Recent Progress in Selective Oxidations with Hydrogen Peroxide Catalyzed by Polyoxometalates

Oxana A. Kholdeeva

Abstract In this chapter, we summarize recent progress achieved in the liquid-phase selective oxidation of organic compounds using hydrogen peroxide as the green oxidant and anionic transition-metal oxide nano-sized clusters or polyoxometalates (POMs) as catalysts. POMs possess a unique combination of properties, including inorganic nature, metal oxide-like structure, thermal stability, thermodynamic stability to oxidation and hydrolysis over a wide pH range, tunable solubility, acid, and redox properties. In recent years, POMs have received significant attention as homogeneous molecular catalysts and building blocks for the construction of heterogeneous catalysts for green selective oxidations. Therefore, both homogeneous and heterogeneous POM-based catalyst systems will be covered in their relevance to the environmentally benign production of vital oxygen-containing compounds and oxidative decontamination of toxic compounds. The chapter starts with a description of some novel highly selective POM catalysts capable of heterolytic activation of H_2O_2. Then new approaches to biphasic catalysis with POMs are discussed in terms of their compliance with the principles of green chemistry. Finally, recent achievements in POM immobilization techniques, such as irreversible adsorption on carbon nanomaterials, encapsulation within supramolecular complexes covalently anchored to silica, and incorporation within metal–organic frameworks, are surveyed with special attention given to catalyst stability and reusability.

Keywords Polyoxometalates · Selective oxidation · Liquid phase · Homogeneous catalysis · Heterogeneous catalysis · Green oxidants · Hydrogen peroxide

O. A. Kholdeeva (✉)
Boreskov Institute of Catalysis, Siberian Branch of the Russian Academy of Sciences, Lavrentieva ave., 5, Novosibirsk 630090, Russia
e-mail: khold@catalysis.ru

Novosibirsk State University, Pirogova Str. 2, Novosibirsk 630090, Russia

K. P. Bryliakov (ed.), *Frontiers of Green Catalytic Selective Oxidations*, Green Chemistry and Sustainable Technology,
https://doi.org/10.1007/978-981-32-9751-7_3

3.1 Introduction

Liquid-phase selective oxidation finds numerous applications in the modern chemical industry since it is the most economical and ecological way for the production of a variety of chemicals ranging from the commodities to fine chemicals [1–4]. While the bulk chemicals industry widely employs both homogeneous and heterogeneous catalysts, most manufactures of fine chemicals still use classical stoichiometric methodologies with risky oxidants such as permanganate, manganese dioxide, chromium(VI) reagents, periodate, nitric acid, peroxy acids, and some others, which produce lots of waste. In the twenty-first century, the development and implementation of highly selective and atom-efficient processes that avoid the use of hazardous reactants and diminish generation of wastes have become a demanding task permanently stimulated by increasing environmental concerns. There is undoubtedly an urgent need for green catalytic technologies employing clean primary oxidants, such as molecular oxygen or hydrogen peroxide, which produce water as the sole by-product [5, 6].

Although O_2 remains the oxidant of choice from the economic viewpoint, aqueous H_2O_2 is the second sought-after oxidant in terms of environmental sustainability [7–10]. Hydrogen peroxide contains 47% of active oxygen, it is relatively cheap (550–600 €/metric ton), easy to handle, and rather safe (<60% in water, <20% in organic solvent). In the fine chemicals industry, hydrogen peroxide can be preferable to molecular oxygen because H_2O_2-based processes do not require high-pressure—high-temperature conditions and can be readily implemented in standard batch equipment [6, 11, 12].

Like dioxygen, hydrogen peroxide is inert toward most organic substrates and its use in oxidation reactions requires catalysts. Redox transition metals readily perform homolytic activation of H_2O_2 and realize Fenton-type chemistry [13, 14]. However, in this case, unproductive decomposition of H_2O_2 leading to molecular oxygen and water strongly competes with the target oxidation of organic substrate, which results in a very low oxidant utilization efficiency. Moreover, generation of free radicals (HO, HO_2) is most often detrimental to oxidation selectivity. Therefore, a great challenge of oxidation catalysis is the development of efficient catalysts capable of heterolytic activation of the oxidant, i.e., oxygen atom transfer from H_2O_2 to an organic substrate without the formation of free radicals.

One of the main problems of existing selective oxidation catalysts is their low productivity because of the destruction of active sites under turnover conditions [4]. While transition-metal (TM) complexes with organic and organometallic ligands are prone to oxidative degradation, most of the inorganic solid catalysts, such as TM-containing zeolites and zeotypes, suffer from hydrolytic instability, especially in the presence of aqueous H_2O_2. A rare exception is the famous heterogeneous catalyst titanium–silicalite TS-1 developed by the ENI researchers in the 1980s [15, 16], which is currently employed in three large-scale H_2O_2-based industrial processes [17–19]. The development of TS-1 was a major breakthrough in liquid-phase oxidation catalysis with aqueous H_2O_2, but its scope is limited to relatively small organic

substrates, which are able to penetrate into the micropores (0.53 × 0.56 nm) of the catalyst. The development of a hydrolytically stable mesoporous catalyst capable of heterolytic activation of H_2O_2 still remains a challenging goal of the fine chemicals industry that deals with the transformation of bulky organic molecules [20, 21]. Recent progress in this direction is currently related to the elaboration of mesoporous niobium-silicates [22–24]. However, the search for alternative types of catalysts that address most if not all the principles of green chemistry remains an important task.

Early TM oxygen-anion clusters or polyoxometalates (POMs) possess totally inorganic, metal oxide-like structure and are, therefore, thermodynamically stable to oxidation, which provides advantages of POMs over conventional TM complexes while operating in oxidative media. In general, POMs possess hydrolytic stability in a wide range of pH and have fairly good thermal stability (350–450 °C in the presence of O_2). Redox and acid–base properties of POMs can be controlled by varying the chemical composition and/or structure while their solubility can be tuned by choosing a proper counter cation.

The composition of POMs can be described by a general formula $[X_xM_mO_y]^{q-}$ ($x \leq m$), where X is a heteroatom (a transition-metal or main-group element) and M are addenda atoms (most often Mo^{VI} or W^{VI}) [25, 26]. Some structural types of POMs that will be mentioned in this chapter in relation to their use in oxidation catalysis are shown in Fig. 3.1.

Compounds comprising heterometal center(s) strongly bound to a multidentate POM ligand provide wide opportunities for the activation of green oxidants, such as molecular oxygen and aqueous hydrogen peroxide [27–33]. All these allow one to consider POMs as promising homogeneous catalysts and active components of heterogeneous catalysts for green selective oxidations and energy-related conversions. Moreover, since POMs can be comprehensively characterized at the atomic/molecular level using experimental and computational techniques, they are successfully employed as soluble molecular models for studying structure–activity–selectivity relationships and mechanisms of heterogeneous oxidation catalysis [34–39].

An extensive review literature, including several special issues [40–42], covers different aspects of POM chemistry, in particular, their application in catalysis [27–33, 43–52]. Maldotti and coworkers reviewed on heterogeneous photocatalysis for selective oxidations with molecular oxygen and POMs [51]. Carraro et al. surveyed on the use of POMs in sustainable oxidations and energy applications [48]. Recent review

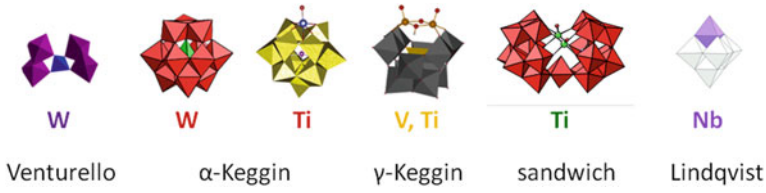

Fig. 3.1 Representative structures of POMs with an indication of the catalytically active metal

paper of Hill and coworkers provided an up-to-date assessment of polyoxometalate-based water oxidation/reduction catalysts as well as immobilized species for the production of solar fuel [53]. A book chapter of Hill and Kholdeeva covered a considerable part of the literature until 2012 related to POM immobilization and use in environmentally benign selective oxidations [46]. However, this field has rapidly expanded in recent years, and the aim of this chapter is to reflect some new trends and achievements in the selective oxidation catalysis with POMs, focusing on the catalysts systems that employ green oxidants. Given that a very recent review of Weinstock and coworkers [33] covered practically all aspects of dioxygen activation with POMs, including selective oxidations with O_2, we discuss here mostly POM catalyst systems which employ the second green oxidant—H_2O_2.

3.2 Homogeneous Selective Oxidations with POMs and H_2O_2

3.2.1 Ti-POM Catalyzed Oxidations

The tremendous success of TS-1 in H_2O_2-based oxidations has stimulated the research work directed at the synthesis of Ti-containing POMs and evaluation of their catalytic performance. Early studies demonstrated that phosphotungstates of the Keggin structure comprising isolated 6-coordinated Ti(IV) atoms (see Fig. 3.1 for the structure) are fairly good catalysts for one-electron oxidation processes, such as oxidation of phenols [54, 55] and allylic oxidation of alkenes [56]. However, similar to mesoporous Ti, Si-catalysts, such Ti-POMs are not able to accomplish selectively two-electron oxidations using H_2O_2, in particular, they are poor catalysts for epoxidation of alkenes with highly reactive allylic H atoms, such as cyclohexene (CyH) [34–36]. Subsequent experimental and theoretical studies revealed that protonation of Ti-POMs is a useful tool which allows selectivity of epoxidation to be increased through reducing the oxygen transfer barrier [57, 58]. Figure 3.2 demonstrates how the addition of protons to the Ti-monosubstituted Keggin POM changes

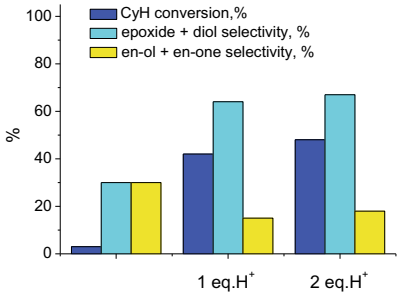

Fig. 3.2 Effect of protons on product distribution in CyH oxidation over $TBA_4[PTi(OH)W_{11}O_{39}]$ (hereinafter, TBA stands for tetrabutyl ammonium cations)

the product distribution in CyH oxidation in favor of epoxide and *trans*-diol (heterolytic oxidation products) at the expense of allylic (homolytic) oxidation products.

Another way to enhance selectivity of epoxidation with Ti-POMs is to change the coordination geometry of Ti(IV) sites. In 2006, the Mizuno group reported the synthesis of a silicatungstate $TBA_8[\{\gamma\text{-}SiTi_2W_{10}O_{36}(OH)_2\}_2(\mu\text{-}O)_2]$ of the γ-Keggin structure comprising a tetranuclear Ti core and demonstrated its ability to catalyze mono-oxygenation reactions [59]. By changing the central heteroatom from Si^{4+} to P^{5+}, the negative charge of the POM anion decreases, and thus the catalytic activity for electrophilic oxidation can be further improved. Indeed, the same group prepared a P-containing tetra-Ti-POM, $TBA_6[\{\gamma\text{-}PTi_2W_{10}O_{36}(OH)_2\}_2(\mu\text{-}O)_2]$, that turned out more active and selective than its Si analog in a range of selective oxidations with H_2O_2 [60].

In 2007, the Kortz team synthesized a unique sandwich-type POM, $[Ti_2(OH)_2As_2W_{19}O_{67}(H_2O)]^{8-}$, containing two unprecedented 5-coordinated Ti atoms with square-pyramidal geometry in the belt (see Fig. 3.1 for the structure) [61]. This POM is stable under turnover conditions and mimics well the catalytic performance of TS-1: it is able to oxidize selectively alkenes to epoxides, thioethers to sulfoxides, alcohols to ketones, and diols to ketols and dicarboxylic acids [62, 63]. In particular, it is an excellent catalyst for epoxidation of the "difficult" alkene substrate cyclohexene: 81-94% selectivity toward epoxide at 74-80% alkene conversion can be attained with only 1 equiv of H_2O_2, which implies fairly good oxidant utilization efficiency. The unique catalytic performance of the sandwich Ti-POM in alkene epoxidation is related to its ability to perform β-oxygen transfer from a hydroperoxo species $[Ti(OOH)As_2W_{19}O_{67}]^{8-}$ to C=C bond with a low energy barrier [64] and high energy costs of homolytic O–O bond breaking in the hydroperoxo intermediate [65].

Recently, the Proust group reported on the synthesis of a hybrid Ti-POM with unprecedented (for POM) tetrahedrally coordinated Ti(IV), $[SbW_9O_{33}(^tBuSiO)_3Ti(OiPr)]^{3-}$ [38]. In this compound, hydrophobicity provided by tetrahexyl ammonium cations and *t*-butyl groups and rigidity of the POM framework disfavor the increase of the Ti(IV) coordination number and prevent hydrolysis. UV-vis and Raman studies implicated the formation of a titanium η^1-hydroperoxo species upon interaction with H_2O_2 capable of epoxidizing allylic alcohols but inert toward unfunctionalized alkenes [38].

Table 3.1 briefly summarizes on the oxidation of representative unsaturated compounds with H_2O_2 in the presence of various Ti-POMs.

3.2.2 V-POM Catalyzed Oxidations with H_2O_2

Research work published over the past decades has established the significant potential of V-POMs as homogeneous oxidation catalysts. Depending on the composition and structure, V-POMs can be employed in combination with either molecular oxygen or hydrogen peroxide. The capability of the mixed addenda Keggin POMs of

Table 3.1 Summary on selective oxidations with H_2O_2 catalyzed by Ti-POMs in MeCN

Ti-POM	Substrate	Conv. (%)	H_2O_2, equiv.	Main products/selectivity[a]	References
$TBA_8[(PTiW_{11}O_{39})_2O]$		24	1	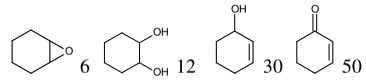 6, 12, 30, 50	[36]
$TBA_{5.5}Na_{1.5}K_{0.5}H_{0.5}[Ti_2(OH)_2As_2W_{19}O_{67}\ H_2O)]$		80	1	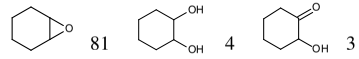 81, 4, 3	[63]
$TBA_{5.5}K_{0.5}H_2[Ti_2(OH)_2As_2W_{19}O_{67}(H_2O)]$		70	1	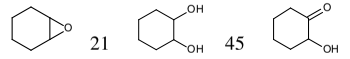 21, 45, 17	[63]
		50	4	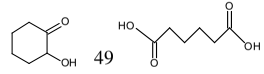 49, 43	[63]
		70	4	 98	[63]
$TBA_8[\{\gamma\text{-}SiTi_2(OH)_2W_{10}O_{36}\}_2(\mu\text{-}O)_2]$			0.2[b]	 64 (*syn*/*anti* = 19/81)	[59]
$TBA_6[\{\gamma\text{-}PTi_2W_{10}O_{36}(OH)_2\}_2(\mu\text{-}O)_2]$			0.2[b]	 80 (*syn*/*anti* = 23/77)	[60]
$THA_3[SbW_9O_{33}(^tBuSiO)_3Ti(OiPr)]$	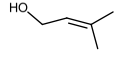	57	1	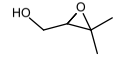 80	[38]

[a]Yield based on the substrate consumed. [b]Yield was calculated based on initial H_2O_2

the general formula $[PV_nMo_{12-n}O_{40}]^{(3+n)-}$ (HPA-n; n = 2–6) to oxidize organic substrates and then to restore the initial state through reoxidation of V^{IV} to V^{V} with molecular oxygen was discovered by Matveev in the late 1970s [66] and afterward it has been widely explored by many research groups all over the world. The numerous literature in this area has been thoroughly analyzed in the review papers of Neumann and Khenkin [30, 44] and then in the more recent comprehensive review of Weinstock and coworkers [33].

Absolutely different type of chemistry has been realized using H_2O_2 as oxidant and divanadium-substituted polyoxotungstates of the γ-Keggin structure, $[\gamma\text{-}XW_{10}O_{38}V_2(\mu\text{-}O)(\mu\text{-}OH)]^{n-}$ (X = P or Si, n = 4 or 5). Mizuno and coworkers first revealed that the di-V-POMs interact with H_2O_2 to produce highly reactive peroxo species, which makes possible selective oxidation of a wide range of organic substrates [31, 67–71]. The reactions usually require the presence of acid cocatalyst. The nature of central atom in this POM is crucial for the catalytic performance: while the di-V-POM with Si is an effective catalyst for epoxidation of electron-rich alkenes [67], its P analog (hereinafter $\gamma\text{-}PV_2W_{10}$) is also able to perform epoxidation of electron-deficient alkenes [69] and oxidation of alkanes [68]. Moreover, $\gamma\text{-}PV_2W_{10}$ turned out a unique POM that enables highly selective aromatic hydroxylation of alkylbenzenes [72, 73]. The aromatic oxidations proceed with unusual regioselectivity, indicating that steric factors control the oxygen transfer process. For example, pseudocumene (PC) in the presence of $\gamma\text{-}PV_2W_{10}$ and H_2O_2 gives a mixture of 2,4,5- and 2,3,5-trimethylphenols (TMP) with the ratio of ca. 7:1, whereas oxidation of 2-methylnaphthalene (2-MN) affords predominantly 6-methyl-1,4-naphthoquinone (6-MNQ) rather than the most common isomer 2-MNQ (Fig. 3.3) [73].

The high selectivity of aromatic oxidation of alkylbenezenes and unusual regioselectivity of these reactions have been rationalized in terms of an electrophilic oxygen transfer mechanism from a sterically hindered peroxo species, $[\gamma\text{-}PW_{10}O_{38}V_2(\mu\text{-}O)_2]^{3-}$ [72, 74].

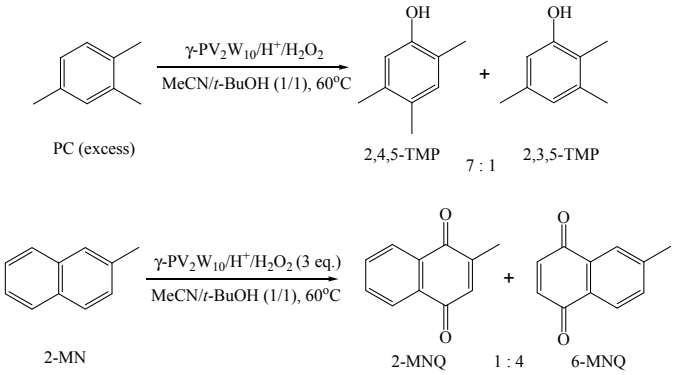

Fig. 3.3 Unusual regioselectivity in H_2O_2-based aromatic oxidations with $\gamma\text{-}PV_2W_{10}$

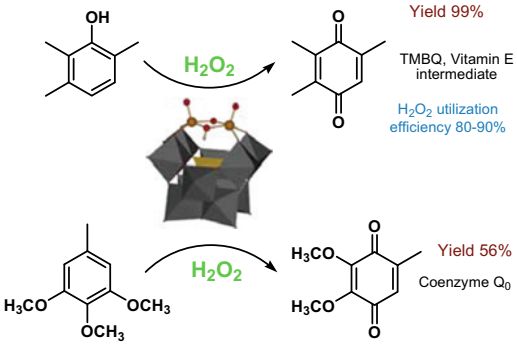

Fig. 3.4 Quinone production using H_2O_2 and γ-PV_2W_{10}

The capability of γ-PV_2W_{10} to catalyze oxidations with H_2O_2 was further realized in the selective transformation of alkylphenols/naphtholes [75] and methoxyarenes [76] to the corresponding *p*-benzoquinones (Fig. 3.4). The industrially relevant oxidation of TMP afforded trimethyl-*p*-benzoquinone (TMBQ, Vitamin E precursor) with a nearly quantitative yield, high oxidant utilization efficiency (80–90%), and unprecedentedly high turnover frequency (TOF 500–1000 h^{-1}) and space-time yield (450 g L^{-1} h^{-1}) [75, 77]. In contrast to other γ-PV_2W_{10}-catalyzed oxidations, the oxidation of phenols does not require the use of acid cocatalyst. Another practically important example is oxidation of 3,4,5-trimethoxytoluene (TMT) to 2,3-dimethoxy-5-methyl-1,4-benzoquinone (ubiquinone 0 or coenzyme Q_0), which is the key intermediate for the synthesis of coenzyme Q_{10} and other vital biologically active compounds (Fig. 3.4). The γ-PV_2W_{10} catalyst retains its structure under the turnover conditions and can be recycled and reused without significant loss of activity and selectivity.

3.2.3 Nb-POM Catalyzed Oxidations

Although a large number of Nb-containing POMs have been reported in the literature, especially in relation to their antitumor and antiviral activity [78, 79], their potential for selective oxidation catalysis was underestimated until recently. Indeed, early works on the use of Nb-POM in H_2O_2-based oxidations were not too encouraging: $TBA_5H_2[(NbO_2)_3SiW_9O_{37}]$ [80] and $TBA_4H_2[(NbO_2)_3PW_9O_{37}]$ [81] could accomplish epoxidation of allylic alcohols but were inert toward unfunctionalized alkenes. Later on, the Mizuno group reported the synthesis of a di-Nb-substituted POM, $TBA_5[\gamma\text{-}HSiW_{10}O_{38}Nb_2(\eta^2\text{-}O_2)_2]$, and its catalytic performance in the oxidation of a few organic substrates with H_2O_2 [82]. Two equivalents of additional protons were required for H_2O_2 activation over this POM.

Meanwhile, recent reports on high catalytic activity and selectivity of mesoporous niobium-silicates in alkene epoxidation with H_2O_2 [22–24] have stimulated a new round of research interest in oxidation catalysis by Nb-POMs. Surprisingly, Nb-

monosubstituted tungstates of the Lindqvist structure, $TBA_3[Nb(O)W_5O_{18}]$ (see Fig. 3.1 for the structure) and $TBA_4[(NbW_5O_{18})_2O]$, turned out to be a highly efficient catalyst for H_2O_2-based epoxidation of alkenes (Table 3.2) [39]. The oxidation of cyclohexene, which is very prone to allylic oxidation, produced heterolytic oxidation products (epoxide, diol, and ketol) with total selectivity as high as 92–93%. The oxidant utilization efficiency was incredibly high and reached 98%. Product, kinetic, and spectroscopic studies revealed that the presence of a source of protons (Nb–OH or, alternatively, $Nb{=}O{+}H^+$) is critical for the oxidation catalysis because protons participate in the formation of an active peroxo niobium species, $TBA_2[HNb(O_2)W_5O_{18}]$ ("$HNb(O_2)$"), where peroxo ligand is attached to Nb(V) in a η^2-coordination mode while proton is located at Nb–O–W bridging oxygen. However, DFT calculations revealed that peroxo species "$HNb(O_2)$" is present in equilibrium with a hydroperoxo one, "$Nb(\eta^2\text{–}OOH)$", and the latter is the real epoxidizing species in CH_3CN solution since it has a lower activation barrier for the oxygen atom transfer to C = C bond of alkene [39]. Subsequent studies by experimental and computational tools suggested that the superior activity and selectivity of the Nb catalysts in alkene epoxidation are due to (1) lower energy barrier of the heterolytic pathway leading to epoxida-

Table 3.2 Alkene epoxidation with H_2O_2 catalyzed by Lindqvist Nb-POM (adapted from [39])

Substrate	Catalyst	Time (h)	Substrate conversion (%)	Epoxide selectivity (%)
	$TBA_3[Nb(O)W_5O_{18}]$	5	55	53[a]
	$TBA_3[Nb(O)W_5O_{18}]$	6	54	98
	$TBA_4[(NbW_5O_{18})_2O]$	3	55	100
	$TBA_3[Nb(O)W_5O_{18}]$	6	47	47[b]
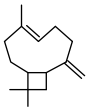	$TBA_3[Nb(O)W_5O_{18}]$	5	50[c]	>99
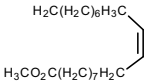	$TBA_3[Nb(O)W_5O_{18}]$	6	45	94[d]
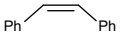	$TBA_4[(NbW_5O_{18})_2O]$	2	38	45[e]

Reaction conditions: 0.2 M alkene, 0.2 M H_2O_2, 0.004 M **2** or 0.002 M **1**, 50 °C, 1 mL CH_3CN
[a]Other products: *trans*-cyclohexane-1,2-diol (25%), 2-hydroxycyclohexanone (14%), and allylic oxidation products (7% all). [b]Other products: benzaldehyde (41%), benzoic acid (7%), and 1-phenyl-1,2-ethanediol (2%). [c]70 °C. [d]Methyl *cis*-9,10-epoxyoctadecanoate; main by-product: methyl 9,10-dihydroxyoctadecanoate (6%). [e]*Cis*-epoxide; other products: benzaldehyde (20% yield) and *trans*-stilbene (8% yield)

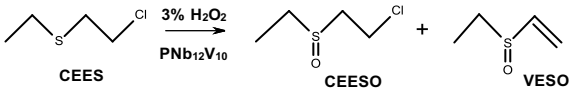

Fig. 3.5 Selective oxidation of 2-chloroethyl ethylsulfide with H_2O_2 catalyzed by $PNb_{12}V_{10}$

tion and (2) higher energy cost of homolytic O–O bond breaking in "Nb(η^2–OOH)" intermediate [39].

Polyoxoniobates possess a basic nature in aqueous media [83], and this feature has been exploited in base catalysis reactions [84–86]. A combination of basic and oxidizing properties was nicely realized in a structurally novel double-anion complex, $H_{13}[(CH_3)_4N]_{12}[PNb_{12}O_{40}(V^VO)_2(V^{IV}{}_4O_{12})_2]$ ($PNb_{12}V_{10}$), based on bicapped polyoxoniobate and tetranuclear polyoxovanadate [87]. This POM revealed unprecedented activity and selectivity in both hydrolysis and H_2O_2-based oxidation reactions. In particular, it transformed sulfur mustard simulant, 2-chloroethyl ethylsulfide (CEES) to nontoxic 2-chloroethyl ethyl sulfoxide (CEESO) and vinyl ethyl sulfoxide (VESO) without formation of the highly toxic sulfone using a quasi-stoichiometric amount of 3% H_2O_2 with a turnover frequency (TOF) of 16 000 h^{-1} (Fig. 3.5).

3.3 New Approaches to Biphasic Catalysis with POMs

The development of well-adapted tools for catalyst recovery and recycling constitutes a challenging goal of green chemistry [5, 6]. The use of two-phase water/organic (w/o) systems enables recycling of a homogeneous catalyst by phase separation. Since the pioneer works of Venturello [88] and Ishii [89] in the 1980s, biphasic oxidation catalysis with POMs has been widely employed for the production of oxygenated compounds using phase transfer, micellar, (micro)emulsion, and some other approaches to enhance mass transfer and facilitate catalyst separation [90]. The majority of research works in this filed was devoted to exploring the possibilities of the Venturello complex $\{PO_4[WO(O_2)_2]_4\}^{3-}$ [88] that can be easily generated in situ from commercially available reactants, e.g., $H_3PW_{12}O_{40}$ heteropolyacid [89] or tungstates in the presence of phosphoric acid and hydrogen peroxide [91 and references cited therein].

Xi and coworkers managed to combine the advantages of both homogeneous and heterogeneous catalysts in one system through reaction-controlled phase transfer of the catalyst composed of quaternary ammonium heteropolyoxotungstates of the general formula $[\pi\text{-}C_5H_5N(CH_2)_{15}CH_3]_3[PW_4O_{16}]$ [92]. The catalyst itself was insoluble in the reaction medium, but under the action of H_2O_2, it formed soluble active species (low-nuclearity oxoperoxotungstates) that selectively transferred oxygen to organics substrates. At the end of the reaction (after complete H_2O_2 consumption), the catalyst returned to its original state and precipitated from the reaction medium, providing an easy separation and reuse. When coupled with the 2-ethylanthraquinone

(EAQ)/2-ethylanthrahydroquinone redox process for H_2O_2 production, O_2 could be employed for the epoxidation of propylene to propylene oxide with 85% yield based on EAQ without any coproducts.

Through combining POM anions with various surfactants to form the so-called surfactant-type catalysts (STC) and tuning the hydrophile–lipophile balance, amphiphilic catalysts can be designed and adapted to different oxidation reactions. To increase the interface area, Li et al. have studied emulsification properties of various $Q_3[PW_{12}O_{40}]$ (Q = quaternary ammonium cations) salts and developed the catalytic oxidation of S-compounds and alcohols with H_2O_2 in emulsion systems [93]. The catalyst $[(C_{18}H_{37})_2N(CH_3)_2]_3[PW_{12}O_{40}]$ demonstrated 96% efficiency of the oxidant utilization and nearly 100% selectivity to sulfones for real diesel. The catalyst is distributed in the interface of two immiscible liquids and forms stable emulsion droplets, which behave as a homogeneous catalyst (Fig. 3.6). The catalyst could be separated and recycled by reversible demulsification and re-emulsification. The same group found that another amphiphilic catalyst, $[C_{18}H_{37}N(CH_3)_3]_4[H_2NaPW_{10}O_{36}]$, assembled in emulsion exhibits high catalytic activity in the oxidation of benzothiophene and its derivatives under mild conditions [94]. The sulfur level in a prehydrotreated diesel could be reduced from 500 to 0.1 ppm while that of a straight-run diesel could be lowered from 6000 to 30 ppm after the oxidative desulfurization process.

Liu and coworkers reported a new approach to form functional emulsions using POM–organic hybrid amphiphilic molecules, viz. hexavanadates covalently functionalized with long alkyl tails, and used these systems to perform oxidative desulfurization [95]. The rate of thiophene oxidation was considerably increased due to improved contact between the catalyst and the reactants at the w/o interface. Song and coworkers suggested an efficient oxidative desulfurization system based on an amphiphilic lanthanide-containing polyoxometalate $DDA_9LaW_{10}/[omim]PF_6$ (DDA = dimethyldioctadecylammonium, omim = 1-octyl-3-methyl-imidazolium)

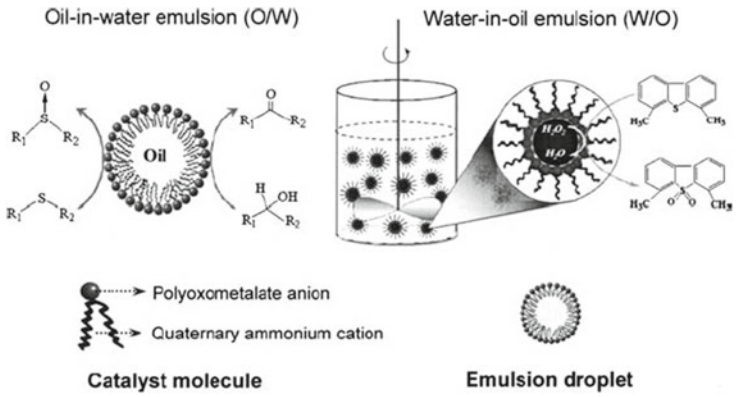

Fig. 3.6 Selective oxidations with H_2O_2 catalyzed by $Q_3[PW_{12}O_{40}]$ in emulsion droplets. Reproduced from ref. [93] with permission of Springer, Copyright 2005

and aqueous H_2O_2 [96]. This system enabled deep desulfurization to be achieved in only 14 min with 100% conversion of dibenzothiophene (DBT) under mild conditions.

Another important application of POM-based STC is the production of (di)carboxylic acids, which serve as intermediates in many large-scale industrial processes of organic synthesis [97]. Zu et al. used surfactant-type peroxotungstates for the oxidation of cyclohexene and 1,2-cyclohexanediol to produce adipic acid in excellent yields with hydrogen peroxide and without any organic solvents and cocatalysts [98].

Use of renewable resources in organic synthesis is one of the important tasks in green chemistry. Oils and fats of vegetable and animal origin have recently attracted growing interest as renewable raw materials in oleochemical industries [99]. During the past decade, a great piece of research work was devoted to the development of environmentally benign approaches to epoxidation and oxidative cleavage of unsaturated fatty acids/esters (UFAs) that would replace the currently employed processes based on peroxy acids and ozone, respectively, which are associated with hazardous reactants. A range of selective oxidations of UFAs was accomplished under solvent-free conditions using peroxopolyoxotungstates and various phase-transfer agents [100–103]. Godard et al. compared four phase-transfer agents, including cetylpyridinium chloride (CPC), methyltrioctylammonium chloride (Aliquat® 336), tetrabutylammonium chloride, and tetraoctylammonium chloride, in the oxidative cleavage of the most widely distributed and abundant UFA oleic acid with $Q_3\{PO_4[WO(O_2)_2]_4\}$ [102]. The best result was achieved with CPC that enabled the production of azelaic and pelargonic acid with 81 and 86% yields, respectively, in an organic solvent-free system (Fig. 3.7).

Neumann and coworkers suggested an interesting approach to aqueous biphasic oxidation catalysis in the absence of organic solvent that involved electrostatic attachment of catalytically active POMs to quaternary ammonium sites of the alkylated polyethylenimine [104]. These catalysts possessed hydrophobic regions enabling the solubilization or binding of hydrophobic substrates, thereby accelerating the selective oxidation of such substrates in water. In the oxidation of methyl oleate, such system showed high selectivity toward nonanal (97% yield). Another interesting approach to phase separation suggested by the same group employed polyfluorinated quaternary ammonium to encapsulate a sandwich POM, $[WZnM_2(H_2O)_2(ZnW_9O_{34})_2]^{12-}$ (M = Mn(II), Zn(II)) known as a highly efficient catalyst for selec-

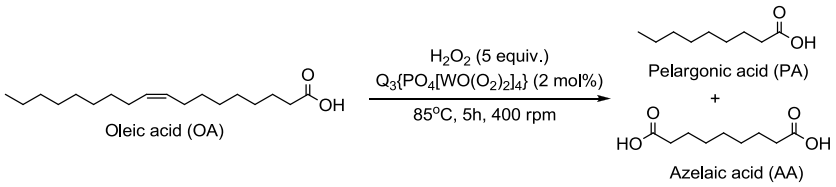

Fig. 3.7 Oxidative cleavage of oleic acid with H_2O_2 catalyzed by $Q_3\{PO_4[WO(O_2)_2]_4\}$

tive oxidations with aqueous H_2O_2 [105]. The catalyst became soluble in organic medium upon heating but could be easily separated upon cooling.

Surfactant-encapsulated POM (SEP) catalysts have been prepared with dendritic cationic surfactants and employed in a range of selective oxidations [106, 107]. Structurally well-defined enantiopure structures composed of chiral dendritic amines and PW_4 have been designed and used to catalyze asymmetric thioether oxidation with aqueous H_2O_2 in two-phase systems [108, 109]. Although very modest *ee* values (maximum 14%) were attained, the authors demonstrated chirality transfer to the POM unit in an asymmetric transformation. Some of these catalysts could be recovered and reused without significant loss of the catalytic properties.

Since the use of synthetic surfactants and organic solvents increases the environmental impact, the development and implementation of surfactant-free and solvent-free biphasic catalyst systems have become a challenging goal of green chemistry. Some novel trends in the field of biphasic catalysis have recently been reviewed by Pera-Titus and coworkers [110]. In particular, they considered interfacial catalysis in Pickering emulsions, which are surfactant-free dispersions of two immiscible fluids kinetically stabilized by colloidal particles, as a novel methodology with promising green permits. Nardello-Rataj and coworkers prepared w/o Pickering emulsions stabilized by catalytic POM nanoparticles incorporating alkylammonium chains and used them to perform epoxidation of alkenes with an easy product and catalyst separation [111]. Zhang and coworkers suggested a composite catalyst on the basis of $[Bmim]_3[PW_{12}O_{40}]$ (Bmim = 1-butyl-3-methylimidazolium) supported on SiO_2 for oxidative desulfurization with H_2O_2 [112]. The catalyst exhibited superior activity in DBT oxidation owing to the formation of Pickering emulsions [110] and could be easily separated by filtration and reused without reduction in activity [112].

Reversible assembly/disassembly between POM and specific light-sensitive azobenzene-terminated surfactants was elegantly used to modulate catalytic performance [113, 114], in particular, to control phase-transfer oxidation catalysis. After catalytic reaction in a solvent of low polarity, a SEP complex of $[WZn_3(H_2O)_2(ZnW_9O_{34})_2]^{12-}$ with a weakly polar *trans*-azobenzene periphery was separated from the reaction mixture and transferred into a polar aqueous phase due to *trans*- to *cis*-isomerization of the azo-moiety upon 365 nm light irradiation (*cis*-conformation has a higher polarity than the *trans*-one). After removal of the product and addition of a fresh portion of substrate, the photosensitive catalyst could be returned back to the organic phase using visible-light (450 nm) irradiation [114]. A comprehensive review on organically encapsulated POM catalysts can be found in a recent book chapter of Wu [115].

3.4 Selective Oxidations with Immobilized POMs

Heterogeneous catalysts have clear advantages of easy separation and recycling and amenability to continuous processing and thus perfectly meet the requirements of green chemistry, provided that they are stable toward metal leaching in the liquid phase [4]. Various approaches to the preparation of POM-based heterogeneous cat-

alysts have been proposed [45, 46, 116–122]. Traditional methodologies involve the elaboration of insoluble POM salts using Cs^+, Ag^+, K^+, NH_4^+, and specific organic polycations [107, 123–125], entrapment within silica by means of sol–gel synthesis [56, 118, 126–128], electrostatic attachment accomplished by anion exchange with layered double hydroxides [129–131] or silica modified by cationic functional groups [132–136], anchoring through the formation of dative bonds between POM and surface ligands [137, 138], and finally, covalent binding of organo-functionalized POMs [48, 117, 119, 121, 139, 140]. In the last decade, some novel approaches that involve combinations of various types of interactions, including supramolecular ones, between POM and surface have been developed and successfully used for the preparation of stable POM-based selective oxidation catalysts. Some of them will be described in the following sections.

3.4.1 N-Doped Carbon Nanomaterials as Smart Supports for Immobilization of POMs

Active carbons have long been used as supports of catalytically active POMs [141]. Van Bekkum et al. demonstrated that the surface structure and origin of the carbon, along with the mode of its activation, strongly affect the strength and amount of adsorption of heteropolyacids [142]. A survey of the early literature on this topic has been done by Hill and Kholdeeva [46].

The synthetic mesoporous carbon Sibunit turned out one of the best carbon supports that enabled strong irreversible adsorption of catalytically active POMs with retention of their structure and catalytic performance [118, 143]. However, the main problem of the POM/Sibunit catalysts is their poor reusability: they lose activity after the first use because of strong adsorption of oxidation products, which cannot be removed by extraction or evacuation [118, 143] (calcination cannot be employed for this type of catalysts).

In recent years, carbon nanomaterials (CNMs) have received great attention for the preparation of hybrid inorganic materials for electronics, energy conversion and storage, molecular sensors, and catalysis [144]. Composites based on POMs and CNMs have been widely used as electrocatalysts for redox reactions in fuel cells and splitting of water [145–150]. Song and coworkers, in their recent review paper [150], identified two main pathways for the preparation of POM/nanocarbon composites, viz. non-covalent and covalent functionalization. Non-covalent approaches involve liquid-phase adsorption of POM onto the surface of CNMs [147, 149, 151] or its impregnation with a POM solution [152, 153], as well as more sophisticated methodologies, e.g., post-modification of carbon surface by cationic functional groups followed by electrostatic attachment of polyanions [145]. A typical covalent approach employs POMs functionalized with a pendant amine which is then linked to oxidized nanocarbons through the formation of amides [154].

So far, only a few reports have been devoted to the application of POM/CNT composites as catalysts for oxidations with H_2O_2 [152, 153]. A catalyst prepared by deposition of $Cs_{2.5}H_{0.5}PW_{12}O_{40}$ on CNTs was used for the oxidative removal of dibenzothiophene, with a desulfurization efficiency of up to 100% [153]. Unfortunately, hot filtration tests [155] were not reported to prove unambiguously heterogeneous nature of the observed catalysis.

On the other hand, doping of carbon nanomaterials with nitrogen in the process of their synthesis results in the formation of different types of surface N species, e.g., pyridine-like, pyrrole-like, and quaternary ones, which provide additional opportunities for immobilization of catalytically active species and, moreover, may affect hydrophilic and electronic properties of the supported catalysts [156, 157]. N-CNMs have been employed as supports for metal [157–161] and metal oxide [162] nanoparticles.

In 2018, Evtushok et al. first reported the use of N-CNMs for immobilization of POM [143]. The di-V-substituted γ-Keggin phosphotungstate $[\gamma\text{-}PW_{10}O_{38}V_2(\mu\text{-}O)(\mu\text{-}OH)]^{4-}$ was irreversibly adsorbed from a MeCN solution on N-doped carbon nanotubes (N-CNTs) with bamboo-like morphology [143] and nanofibers (N-CNFs) having herring-bone packing of graphite layers [163]. The presence of nitrogen in the CNMs was crucial for molecular dispersion of $\gamma\text{-}PV_2W_{10}$ on the carbon surface and catalyst stability toward leaching in polar media. The interplay of various non-covalent interactions, such as electrostatic forces and hydrogen bonding, seems to ensure the irreversible immobilization with retention of the POM structure.

Previous attempts of immobilization of $\gamma\text{-}PV_2W_{10}$ (in combination with $\alpha\text{-}SiW_{12}$) onto commercially available Fe_2O_3 led to catalysts that were stable in a 1:1 mixture of EtOAc/*t*-BuOH but lost POMs in MeCN [164]. Use of N-CNTs as supports has led to the elaboration of highly efficient catalysts for selective oxidation of alkylphenols to corresponding alkyl-*p*-benzoquinones with aqueous H_2O_2 in MeCN [143]. By applying the optimal catalyst $\gamma\text{-}PV_2W_{10}$/N-CNTs enclosing 15 wt% of $\gamma\text{-}PV_2W_{10}$ and 1.8 at.% of N, TMBQ could be obtained with a nearly quantitative yield and 80% oxidant utilization efficiency (Fig. 3.8). The same parameters were achieved with homogeneous $\gamma\text{-}PV_2W_{10}$ [75]. Immobilization using other approaches, such as embedding into silica, electrostatic attachment to amine-modified SiO_2 or metal–organic framework MIL-101, and adsorption on Sibunit resulted in a significant loss of catalytic activity and selectivity of $\gamma\text{-}PV_2W_{10}$ (Fig. 3.9) [143].

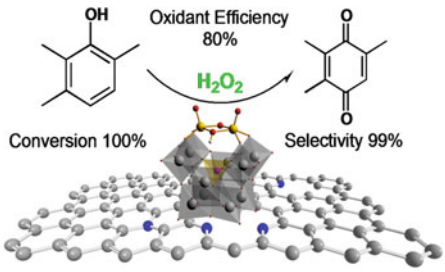

Fig. 3.8 TMP oxidation to TMBQ with H_2O_2 over $\gamma\text{-}PV_2W_{10}$ immobilized on N-CNTs. Reprinted from ref. [143], with permission of American Chemical Society, copyright 2018

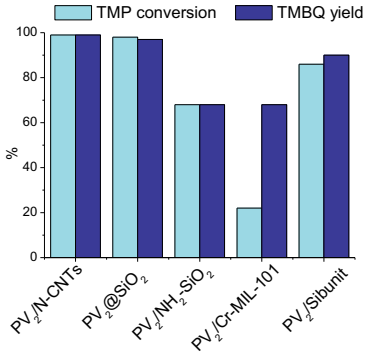

Fig. 3.9 Comparison of different approaches to immobilization of γ-PV_2W_{10}

The catalyst γ-PV_2W_{10}/N-CNTs demonstrated truly heterogeneous nature of the catalysis and unprecedentedly high turnover frequencies (500 h^{-1}) and space-time yield (450 g L^{-1} h^{-1}), did not suffer from metal leaching and, in sharp contrast to the Sibunit-supported POM, could be used repeatedly without loss of the catalytic performance. At least, 360 TON (turnover number) could be achieved after six recycles with γ-PV_2W_{10} supported on N-CNTs. FT-IR and XPS spectroscopy confirmed the stability of γ-PV_2W_{10} and N-CNT support under the turnover conditions. Comparison of the catalytic performance of γ-PV_2W_{10}/N-CNTs with that of mesoporous titanium-silicates (the most effective heterogeneous catalysts reported so far for TMBQ production) [165, 166] demonstrates clear benefits of the former in terms of H_2O_2 utilization efficiency, activity (TOF), space-time yield (STY), and volume yield (Fig. 3.10).

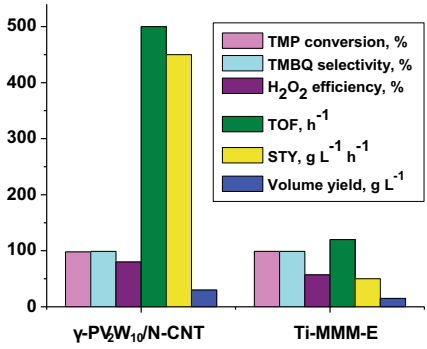

Fig. 3.10 Comparison of catalytic performances of γ-PV_2W_{10}/N-CNTs and mesoporous titanium-silicate Ti-MMM-E [165] in TMP oxidation with H_2O_2. Adapted from ref. [143], with permission of American Chemical Society, Copyright 2018

3.4.2 Encapsulation Within Covalently Anchored Supramolecular Complexes

Although encapsulation of POMs within silica by the sol–gel technique may lead to highly active and recyclable oxidation catalysts [56, 128], the size of pores in the resulting composites is critical for catalyst stability with regards to POM leaching [143]. Moreover, this approach is hardly applicable to POMs which are not soluble in alcoholic media [143]. Therefore, one might anticipate that a combination of the sol–gel approach with a covalent one would significantly contribute to the catalyst stability.

Wu and coworkers have developed a novel methodology for the preparation of heterogeneous POM catalysts that involves both covalent and non-covalent interactions [115, 167, 168]. Through electrostatic interactions, the counterions of a POM can be replaced by a hydroxy-terminated surfactant, such as di(11-hydroxyundecyl)dimethylammonium (DOHDA), and then sol–gel co-condensation of the surfactant-encapsulated POM complexes with tetraethyl orthosilicate (TEOS) results in covalent anchoring of the SEP to the silica matrix (Fig. 3.11). This procedure is not solvent-dependent and is amenable to different POMs. Supramolecular interactions are not only crucial to the formation of the hybrid catalyst but also play a significant role in promoting catalytic activity since the hydrophobic environment around POM clusters facilitates catalyst ability to adsorb organic substrates of low polarity and desorbing more polar oxidation products, thereby maximizing the catalyst efficiency. Phosphotungstate PW_{12} immobilized using such approach revealed superior catalytic performance in the selective oxidation of alkenes, alcohols, and thioethers [167]. The catalyst could be easily recovered by simple filtration and maintained the catalytic activity for at least five recycles.

Following the same methodology, Wu and coworkers introduced a chiral cationic head into a surfactant-encapsulated sandwich $[WZn_3(H_2O)_2(ZnW_9O_{34})_2]^{12-}$ [169]. The supramolecular chirality around the POM made possible kinetic resolution of racemic alcohols via catalytic oxidation with H_2O_2.

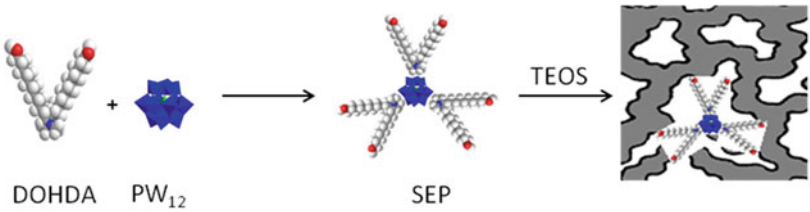

Fig. 3.11 Schematic representation of the synthesis of supramolecular hybrid catalyst with SEP covalently bound to silica

3.4.3 Incorporation Within Metal–Organic Frameworks

In recent years, the incorporation of POMs into the structural nodes or cages of metal–organic frameworks (MOFs) has attracted significant attention [170–172]. Férey and coworkers first demonstrated that a large cage of the mesoporous chromium terephthalate MIL-101 can accommodate up to five POMs of the Keggin structure [173]. Maksimchuk et al. accomplished immobilization of a range of catalytically active POMs using MIL-101 as an anion exchanger [174–176]. They also found that only one POM anion per the MOF cage is strongly attached to the MOF by electrostatic forces (Fig. 3.12) while the other four easily leach into solution. Studies by XRD, FT-IR, and ^{31}P NMR MAS spectroscopy confirmed maintenance of the structure of both POM and MIL-101 in the resulting hybrid materials [173–176].

The combination of MIL-101 and a POM capable of activating H_2O_2 made possible use of hydrogen peroxide as an oxidant in a range of selective oxidations [174, 175]. The POM/MIL-101 hybrid materials (POM = $[PW_{11}TiO_{40}]^{5-}$) catalyzed the epoxidation of the natural terpene caryophellene with H_2O_2 and demonstrated a significant improvement of epoxidation selectivity and alkene conversion compared to MIL-101 and the POM taken separately [174]. Moreover, both epoxide selectivity and substrate conversion increased with enlarging concentration of the oxidant, in spite of increasing water concentration in the system (H_2O_2 was taken as a 30% solution in water) [174].

A similar phenomenon was observed for PW_{12}/MIL-101 hybrid catalysts, which demonstrated superior activity and selectivity in the epoxidation of various alkenes with H_2O_2 [175]. Importantly, the opposite trend was found in the presence of homogeneous PW_{12} (Fig. 3.13), which is more common, because the increasing concentration of H_2O_2/H_2O usually facilitates epoxide ring opening and enhances overoxidation. The extraordinary behavior of the hybrid POM/MIL-101 catalysts in alkene epoxidation with aqueous H_2O_2 was explained by the specific sorption properties of MIL-101 [172]: the hydrophobic part of the terephthalate linkers favors adsorption of nonpolar hydrocarbons and H_2O_2 and, oppositely, hinders adsorption of water.

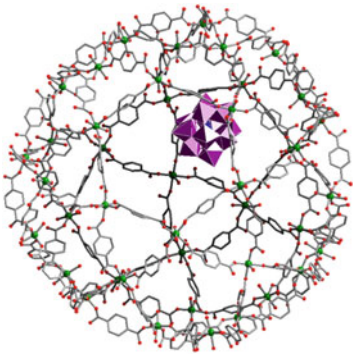

Fig. 3.12 Keggin-type POM within a large cage of MIL-101. Reproduced from ref. [172], with permission of Elsevier, copyright 2016

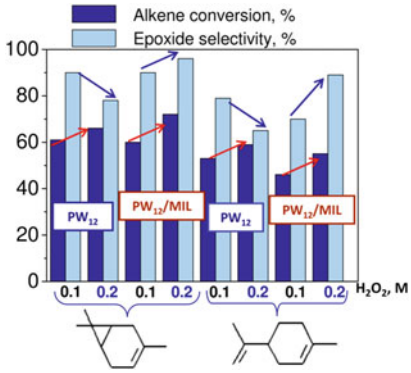

Fig. 3.13 Cyclohexene conversion and epoxide selectivity versus concentration of H_2O_2 in the reactions catalyzed by heterogeneous PW_{12}/MIL-101 catalyst and homogeneous PW_{12}. Reproduced from ref. [172], with permission of Elsevier, copyright 2016

Immobilization of POM within MIL-101 improved the thermal stability of the MOF [173] and also increased the solvolytic stability of POM [175]. The overall TON attained without degradation of PW_{12} was 770 and 155 for PW_{12}/MIL-101 and homogeneous PW_{12}, respectively [175]. In general, the stability of the hybrid POM/MIL-101 catalysts toward POM leaching depends on the reaction conditions employed [176].

Using the same approach, Balula et al. inserted a sandwich-type polyoxometalate $\{(TBA)_7H_3[Co_4(H_2O)_2(PW_9O_{34})_2]\}$ within MIL-101(Cr) [177]. They also prepared a composite material through immobilization of the trivacant Keggin-type polyoxometalate ($[A\text{-}PW_9O_{34}]^{9-}$, PW_9) in the cavities of MIL-101(Cr) and used this composite for the oxidation of monoterpenes and S-compounds with H_2O_2 [178]. Geraniol was converted to 2,3-epoxygeraniol within 30 min at room temperature, while the total desulfurization of the model oil containing 1707 ppm of sulfur was achieved after 2 h. In the oxidative desulfurization, the catalyst could be recycled without a significant loss of activity. The catalyst stability and heterogeneous nature of the catalysis were confirmed by several techniques and leaching tests.

Lin et al. synthesized water-stable MOFs with tunable window diameters, MOF-808X, and used them as supports for immobilization of PW_{12} [179]. The catalyst with 42% of PW_{12} could completely remove DBT in a model fuel with an initial sulfur content of 1000 ppm within 30 min and could be reused in, at least, five operation cycles without loss of activity. The high catalytic activity was attributed to a cooperative effect of metal clusters in the host MOF and the guest PW_{12} molecules.

Recently, PW_{12} was encapsulated within the highly stable Zr-based metal–organic framework UiO-66 by a direct hydrothermal reaction of $ZrCl_4$, terephthalic acid, and $H_3PW_{12}O_{40}$ in DMF [180]. The hybrid material was very active in the selective oxidation of cyclopentene to glutaraldehyde (GA) with hydrogen peroxide as the oxidant. A 95% substrate conversion and 78% yield of GA were attained with a 35 wt% PW_{12}@UiO-66 catalyst, which did not suffer metal leaching and could be used repeatedly.

Inclusion of POM moieties directly into MOF single-crystal materials was accomplished using various approaches, including: d/f-blockmetal ion-modified POM units

directly connected with organic ligands, POM anions residing within the cages of MOFs as templates, and porous inorganic–organic materials with POM anions as pillars [47, 170, 181, 182]. However, few of these materials have been employed as selective oxidation catalysts. Hill and coworkers succeeded in combining the catalytically active POM $[CuPW_{11}O_{39}]^{5-}$ with MOF-199 (HKUST-1) [183]. The close matching of POM diameter and MOF pore size in the POM–MOF material, $[Cu_3(C_9H_3O_6)_2]_4[\{(CH_3)_4N\}_4CuPW_{11}O_{39}H]$ resulted in a synergistic stabilization of both the MOF and the POM and a dramatic increase in the catalytic activity of the POM for aerobic oxidation of S-compounds. Zou et al. reported the synthesis of a layered POM–Mn^{III}–metalloporphyrin-based hybrid framework that demonstrated a remarkable capability of scavenging of dyes and selective oxidation of alkylbenzenes with the environmentally benign oxidant—*tert*-butyl hydroperoxide [184]. Duan and coworkers incorporated $[BW_{12}O_{40}]^{5-}$ polyanion, Ni(II) cations, and an asymmetric organocatalytic group L- or D-pyrrolidin-2-ylimidazole within one single MOF [185]. The resulting MOF served as a heterogeneous catalyst to accomplish the asymmetric dihydroxylation of olefins, where enantiomeric excess (ee) values could reach >95% at appreciable substrate conversions.

3.5 Conclusion and Outlook

Polyoxometalates undoubtedly have enormous potential as catalysts for the liquid-phase selective oxidation of organic compounds using green oxidants, in particular, aqueous hydrogen peroxide. During the past two decades, several new highly selective POM catalysts have been discovered and various strategies have been suggested with regard to POM-based catalyst systems to better meet the demands of green chemistry. The most developed and widely used methodologies that enable an easy catalyst separation and recycling involve biphasic (liquid–liquid) catalysis and immobilization of POMs on the surface of solid supports by means of different types of chemical bonding and supramolecular interactions. These efforts certainly have opened up new opportunities for environmentally friendly production of oxygenated compounds and decontamination of toxic compounds using highly selective POM catalysts. However, the practical application of POM-based catalyst systems will depend on the progress made in overcoming the operation and economic obstacles, such as cost of catalyst relative to the cost of products, catalyst lifetime, and possibility of regeneration. The elaboration of new phase separation techniques and new synthetic approaches to the preparation of leaching-tolerant porous solids is indispensable to ensure the required purity of the target products. As usual, synthetic POM chemists certainly outnumber researchers engaged in studying catalysis, and many new POMs and POM-based materials still wait for the evaluation of their catalytic potential for green and sustainable chemical processes.

Acknowledgements The author thanks all coauthors of the joint papers published on selective oxidation catalysis by polyoxometalates.

References

1. Cavani F, Centi G, Perathoner S, Trifiro F (eds) (2009) Sustainable industrial processes. Wiley-VCH, Weinheim
2. Duprez D, Cavani F (eds) (2014) Handbook of advanced methods and processes in oxidation catalysis. Imperial College Press, London
3. Catal. Sci. Technol. 1 (2011) Special issue on heterogeneous catalysis for fine chemicals. Pagliaro M, Hutchings G (guest eds)
4. Clerici MG, Kholdeeva OA (eds) (2013) Liquid phase oxidation via heterogeneous catalysis: organic synthesis and industrial applications. Wiley, Hoboken, New Jersey
5. Anastas PT, Warner JC (1998) Green chemistry: theory and practice. Oxford University Press, New York
6. Sheldon R, Arends IWCE, Hanefeld U (2007) Green chemistry and catalysis. Wiley-VCH, Weinheim
7. Strukul G (ed) (1992) Catalytic oxidations with hydrogen peroxide as oxidant. Kluwer Academic Publishers, Dordrecht, Boston
8. Jones CW (1999) Application of hydrogen peroxide and derivatives. Royal Society of Chemistry, Cambridge
9. Strukul G, Scarso A (2013) Environmentally benign oxidants. In: Clerici MG, Kholdeeva OA (eds) Liquid phase oxidation via heterogeneous catalysis: organic synthesis and industrial applications. Wiley, Hoboken, New Jersey, pp 1 – 20. https://doi.org/10.1002/9781118356760.ch1
10. Catalysts (2019) Special issue on direct synthesis of hydrogen peroxide, Strukul G, Menegazzo F (guest eds), https://www.mdpi.com/si/catalysts/hydrogen_peroxide
11. Sheldon RA, van Bekkum H (eds) (2001) Fine chemicals through heterogeneous catalysis. Wiley-VCH, Weinheim
12. Hook BD (2013) Engineering aspects of liquid phase oxidations. In: Clerici MG, Kholdeeva OA (eds) Liquid phase oxidation via heterogeneous catalysis: organic synthesis and industrial applications. Wiley, Hoboken, New Jersey, pp 496 – 506. https://doi.org/10.1002/9781118356760.ch10
13. Sheldon RA, Kochi JK (1981) Metal-catalyzed oxidations of organic compounds. Academic Press, New York
14. Masarwa A, Rachmilovich-Calis S, Meyerstein N, Meyerstein D (2005) Oxidation of organic substrates in aerated aqueous solutions by the Fenton reagent. Coord Chem Rev 249:1937–1943. https://doi.org/10.1016/j.ccr.2005.01.003
15. Taramasso M, Perego G, Notari B (1983) Preparation of porous crystalline synthetic material comprised of silicon and titanium oxides. US Patent application 4 410 501
16. For recent review see: Clerici MG, Domine ME (2013) Oxidation reactions catalyzed by transitions metal–substituted zeolites. In: Clerici MG, Kholdeeva OA (eds) Liquid phase oxidation via heterogeneous catalysis: organic synthesis and industrial applications. Wiley, Hoboken, New Jersey, pp 21 – 93. https://doi.org/10.1002/9781118356760.ch2
17. Romano U, Ricci M (2013) The hydroxylation of phenol to hydroquinone and catechol, In: Clerici MG, Kholdeeva OA (eds) Liquid phase oxidation via heterogeneous catalysis: organic synthesis and industrial applications. Wiley, Hoboken, New Jersey, pp 451 – 462. https://doi.org/10.1002/9781118356760.ch10
18. Rivetti F, Buzzoni R (2013) The greening of nylon: the ammoximation process. In: Clerici MG, Kholdeeva OA (eds) Liquid phase oxidation via heterogeneous catalysis: organic synthesis and industrial applications. Wiley, Hoboken, New Jersey, pp 462 – 474. https://doi.org/10.1002/9781118356760.ch10
19. Forlin A, Bergamo M, Lindner J (2013) Production of propylene oxide. In: Clerici MG, Kholdeeva OA (eds) Liquid phase oxidation via heterogeneous catalysis: organic synthesis and industrial applications. Wiley, Hoboken, New Jersey, pp 474 – 496. https://doi.org/10.1002/9781118356760.ch10

20. Kholdeeva OA (2013) Selective oxidations catalyzed by mesoporous metal silicates. In: Clerici MG, Kholdeeva OA (eds) Liquid phase oxidation via heterogeneous catalysis: organic synthesis and industrial applications. Wiley, Hoboken, New Jersey, pp 127 – 219. https://doi.org/10.1002/9781118356760.ch4
21. Kholdeeva OA (2014) Recent developments in liquid-phase selective oxidation using environmentally benign oxidants and mesoporous metal silicates. Catal Sci Technol 4:1869–1889. https://doi.org/10.1039/C4CY00087K
22. Gallo A, Tiozzo C, Psaro R, Carniato F, Guidotti M (2013) Niobium metallocenes deposited onto mesoporous silica via dry impregnation as catalysts for selective epoxidation of alkenes. J Catal 298:77–83. https://doi.org/10.1016/j.jcat.2012.11.015
23. Ivanchikova ID, Maksimchuk NV, Skobelev IY, Kaichev VV, Kholdeeva OA (2015) Mesoporous niobium-silicates prepared by evaporation-induced self-assembly as catalysts for selective oxidations with aqueous H_2O_2. J Catal 332:138–148. https://doi.org/10.1016/j.jcat.2015.10.003
24. Kholdeeva OA, Ivanchikova ID, Maksimchuk NV, Skobelev IY, H_2O_2-based selective oxidations: Nb(V) versus Ti(IV). Catal Today, https://doi.org/10.1016/j.cattod.2018.04.002
25. Pope MT (1983) Heteropoly and isopoly oxometalates. Springer-Verlag, Berlin
26. Pope MT (2004) Polyoxo anions: synthesis and structure. In: Wedd AG (ed) Comprehensive coordination chemistry II, vol. 4. Elsevier Science, New York, pp 635–678. https://doi.org/10.1002/chin.200440229
27. Hill CL, Prosser-McCartha CM (1995) Catalysis by transition metal oxygen anion clusters. Coord Chem Rev 143:407–455. https://doi.org/10.1016/0010-8545(95)01141-B
28. Neumann R (2004) Polyoxometalates as catalysts for oxidation with hydrogen peroxide and molecular oxygen. In: Beller M, Bolm C (eds) Transition metals for organic synthesis, 2nd ed, vol. 2, Wiley-VCH, Weinheim; pp. 415–426. https://doi.org/10.1002/9783527619405.ch5k
29. Hill CL (2004) Polyoxometalates: reactivity. In: Wedd AG (ed) Comprehensive coordination chemistry II, vol. 4. Elsevier Science, New York, pp 679–759. https://doi.org/10.1002/chin.200440228
30. Neumann R (2010) Activation of molecular oxygen, polyoxometalates, and liquid-phase catalytic oxidation. Inorg Chem 49:3594–3601. https://doi.org/10.1021/ic9015383
31. Mizuno N, Kamata K (2011) Catalytic oxidation of hydrocarbons with hydrogen peroxide by vanadium-based polyoxometalates. Coord Chem Rev 255:2358–2370. https://doi.org/10.1016/j.ccr.2011.01.041
32. Wang S-S, Yang G-Y (2015) Recent advances in polyoxometalate-catalyzed reactions. Chem Rev 115:4893–4962. https://doi.org/10.1021/cr500390v
33. Weinstock IA, Schreiber RE, Neumann R (2018) Dioxygen in polyoxometalate mediated reactions. Chem Rev 118:2680–2717. https://doi.org/10.1021/acs.chemrev.7b00444
34. Kholdeeva OA (2006) Titanium-monosubstituted polyoxometalates: relation between homogeneous and heterogeneous Ti–single–site–based catalysis. Top Catal 40:229–243. https://doi.org/10.1007/s11244-006-0124-4
35. Kholdeeva OA, Maksimovskaya RI (2007) Titanium–and zirconium-monosubstituted polyoxometalates as molecular models for studying mechanisms of oxidation catalysis. J Mol Catal A: Chem 262:7–24. https://doi.org/10.1016/j.molcata.2006.08.023
36. Kholdeeva OA (2013) Hydrogen peroxide activation over TiIV: what have we learned from studies on Ti-containing polyoxometalates? Eur J Inorg Chem 2013:1595–1605. https://doi.org/10.1002/ejic.201201396
37. Guillemot G, Matricardi E, Chamoreau L-M, Thouvenot R, Proust A (2015) Oxidovanadium (V) anchored to silanol-functionalized polyoxotungstates: molecular models for single-site silica–supported vanadium catalysts. ACS Catal 5:7415–7423. https://doi.org/10.1021/acscatal.5b01878
38. Zhang T, Mazaud L, Chamoreau L-M, Paris C, Guillemot G, Proust A (2018) Unveiling the active surface sites in heterogeneous titanium-based silicalite epoxidation catalysts: input of silanol-functionalized polyoxotungstates as soluble analogues. ACS Catal 8:2330–2342. https://doi.org/10.1021/acscatal.8b00256

39. Maksimchuk NV, Maksimov GM, Evtushok VYu, Ivanchikova ID, Chesalov YuA, Maksimovskaya RI, Kholdeeva OA, Solé-Daura A, Poblet JM, Carbó JJ (2018) Relevance of protons in heterolytic activation of H_2O_2 over Nb(V): insights from model studies on nb-substituted polyoxometalates. ACS Catal 8:9722–9737. https://doi.org/10.1021/acscatal.8b02761
40. Thematic issue on polyoxometalates (1998) Hill CL (guest ed) Chem Rev 98:1–390
41. Thematic issue frontiers in metal oxide cluster science (2011) Weinstock IA (guest ed) Israel J Chem 51:169–302
42. Themed collection polyoxometalate cluster science (2012) Cronin L, Müller A (guest eds) Chem Soc Rev 41:7325–7648
43. Kozhevnikov IV (2002) Catalysis by polyoxometalates. In: Roberts SN, Kozhevnikov IV, Derouane E (eds) Catalysts for fine chemical synthesis, vol 2. Wiley, Chichester
44. Neumann R, Khenkin AM (2006) Molecular oxygen and oxidation catalysis by phosphovanadomolybdates. Chem Commun 2529–2538. https://doi.org/10.1039/b600711m
45. Mizuno N, Kamata K, Uchida S, Yamaguchi K (2009) Liquid-phase oxidations with hydrogen peroxide and molecular oxygen catalyzed by polyoxometalate-based compounds. In: Mizuno N (ed) Modern heterogeneous oxidation catalysis: design, reactions and characterization. Wiley–VCH, Weinheim, pp 185–217. https://doi.org/10.1002/9783527627547.ch6
46. Hill CL, Kholdeeva OA (2013) Selective liquid phase oxidations in the presence of supported polyoxometalates. In: Clerici MG, Kholdeeva OA (eds) Liquid phase oxidation via heterogeneous catalysis: organic synthesis and industrial applications. Wiley, Hoboken, New Jersey, pp 263–319. https://doi.org/10.1002/9781118356760.ch6
47. Du D-Y, Yan L-K, Su Z-M, Li S-L, Lan Y-Q, Wang E-B (2013) Chiral polyoxometalate-based materials: from design syntheses to functional applications. Coord Chem Rev 257:702–717. https://doi.org/10.1016/j.ccr.2012.10.004
48. Carraro M, Fiorani G, Sartorel A, Bonchio M (2014) Polyoxometalates catalysts for sustainable oxidations and energy applications, In: Duprez D, Cavani F (eds) Handbook of advanced methods and processes in oxidation catalysis. Imperial College Press, London, pp 586 − 630. https://doi.org/10.1142/9781848167513_0021
49. Sun M, Zhang J, Putaj P, Caps V, Lefebvre F, Pelletier J, Basset J-M (2014) Catalytic oxidation of light alkanes (C_1–C_4) by heteropoly compounds. Chem Rev 114:981–1019. https://doi.org/10.1021/cr300302b
50. Kamata K (2015) Design of highly functionalized polyoxometalate-based catalysts. Bull Chem Soc Jpn 88:1017–1028. https://doi.org/10.1246/bcsj.20150154
51. Maldotti A, Amadelli R, Molinari A (2013) Heterogeneous photocatalysis for selective oxidations with molecular oxygen. In: Clerici MG, Kholdeeva OA (eds) Liquid phase oxidation via heterogeneous catalysis: organic synthesis and industrial applications. Wiley, Hoboken, New Jersey, pp 411–450. https://doi.org/10.1002/9781118356760.ch9
52. Sullivan KP, Yin Q, Collins-Wildman DL, Tao M, Geletii YV, Musaev DG, Lian T, Hill CL (2018) In: Debbie C (ed) Frontiers in chemistry 6. https://doi.org/10.3389/fchem.2018.00365
53. Lauinger SM, Yin Q, Geletii YV, Hill CL (2017) Adv Inorg Chem 69:117–154. https://doi.org/10.1016/bs.adioch.2016.12.002
54. Kholdeeva OA, Maksimov GM, Maksimovskaya RI, Kovaleva LA, Fedotov MA, Grigoriev VA, Hill CL (2000) Dimeric titanium-containing polyoxometalate. Synthesis, characterization, and catalysis of H_2O_2–based thioether oxidation. Inorg Chem 39:3828–3837. https://doi.org/10.1021/ic0000653
55. Kholdeeva OA, Trubitsina TA, Maksimov GM, Golovin AV, Maksimovskaya RI (2005) Synthesis, characterization, and reactivity of Ti(IV)–monosubstituted Keggin polyoxometalates. Inorg Chem 44:1635–1642. https://doi.org/10.1021/ic0490829
56. Maksimchuk NV, Melgunov MS, Mrowiec-Białoń J, Jarzębski AB, Kholdeeva OA (2005) H_2O_2-based allylic oxidation of α-pinene over different single site catalysts. J Catal 235:175–183. https://doi.org/10.1016/j.jcat.2005.08.001
57. Kholdeeva OA, Trubitsina TA, Timofeeva MN, Maksimov GM, Maksimovskaya RI, Rogov VA (2005) The role of protons in cyclohexene oxidation with H_2O_2 catalysed by Ti(IV)-monosubstituted Keggin polyoxometalate. J Mol Catal A: Chemical 232:173–178. https://doi.org/10.1016/j.molcata.2005.01.036

58. Jiménez-Lozano P, Ivanchikova ID, Kholdeeva OA, Poblet JM, Carbó JJ (2012) Alkene oxidation by Ti-containing polyoxometalates. Unambiguous characterization of the role of protonation state. Chem Commun 48:9266–9268. https://doi.org/10.1039/c2cc34577c
59. Goto Y, Kamata K, Yamaguchi K, Uehara K, Hikichi S, Mizuno N (2006) Synthesis, structural characterization, and catalytic performance of dititanium-substituted γ-Keggin silicotungstate. Inorg Chem 45:2347–2356. https://doi.org/10.1021/ic052179q
60. Takahashi E, Kamata K, Kikukawa Y, Sato S, Suzuki K, Yamaguchi K, Mizuno N (2015) Synthesis and oxidation catalysis of a Ti-substituted phosphotungstate, and identification of the active oxygen species. Catal Sci Tecnol 5:4778–4789. https://doi.org/10.1039/C5CY01031D
61. Hussain F, Bassil BS, Kortz U, Kholdeeva OA, Timofeeva MN, de Oliveira P, Keita B, Nadjo L (2007) Dititanium-containing 19-tungstodiarsenate(III) [Ti2(OH)2As2W19O67(H2O)]8−: synthesis, structure, electrochemistry, and oxidation catalysis. Chem Eur J 13:4733–4742. https://doi.org/10.1002/chem.200700043
62. Kholdeeva OA, Donoeva BG, Trubitsina TA, Al-Kadamany G, Kortz U (2009) Unique catalytic performance of the polyoxometalate $[Ti_2(OH)_2As_2W_{19}O_{67}(H_2O)]^{8-}$: the role of 5-coordinated titanium in H_2O_2 activation. Eur J Inorg Chem 2009:5134–5141. https://doi.org/10.1002/ejic.200900608
63. Donoeva BG, Trubitsina TA, Antonova NS, Carbó JJ, Poblet JM, Al Kadamany G, Kortz U, Kholdeeva OA (2010) Epoxidation of alkenes with H_2O_2 catalyzed by di-titanium-containing 19-tungstodiarsenate(III): experimental and theoretical studies. Eur J Inorg Chem 2010:5312–5317. https://doi.org/10.1002/ejic.201000615
64. Jiménez-Lozano P, Skobelev IY, Kholdeeva OA, Poblet JM, Carbó JJ (2016) Alkene epoxidation catalyzed by Ti-containing polyoxometalates: unprecedented β-oxygen transfer mechanism. Inorg Chem 55:6080–6084. https://doi.org/10.1021/acs.inorgchem.6b00621
65. Antonova NS, Carbó JJ, Kortz U, Kholdeeva O, Poblet JM (2010) Mechanistic insights into alkene epoxidation with H_2O_2 by Ti- and other TM-containing polyoxometalates: role of the metal nature and coordination environment. J Am Chem Soc 132:7488–7497. https://doi.org/10.1021/ja1023157
66. Matveev KI (1977) Development of new homogeneous catalysts for oxidation of ethylene to acetaldehyde. Kinet Katal 18:716–728
67. Nakagawa Y, Kamata K, Kotani M, Yamaguchi K, Mizuno N (2005) Polyoxovanadometalate-catalyzed selective epoxidation of alkenes with hydrogen peroxide. Angew Chem Int Ed 44:5136–5141. https://doi.org/10.1002/ange.200500491
68. Kamata K, Yonehara K, Nakagawa Y, Uehara K, Mizuno N (2010) Efficient stereo- and regioselective hydroxylation of alkanes catalysed by a bulky polyoxometalate. Nat Chem 2:478–483. https://doi.org/10.1038/nchem.648
69. Kamata K, Sugahara K, Yonehara K, Ishimoto R, Mizuno N (2011) Efficient epoxidation of electron-deficient alkenes with hydrogen peroxide catalyzed by [γ-PW10O38V2(μ-OH)2]3−. Chem Eur J 17:7549–7559. https://doi.org/10.1002/chem.201101001
70. Yamaura T, Kamata K, Yamaguchi K, Mizuno N (2013) Efficient sulfoxidation with hydrogen peroxide catalyzed by a divanadium-substituted phosphotungstate. Catal Today 203:76–80. https://doi.org/10.1016/j.cattod.2012.01.026
71. Yonehara K, Kamata K, Yamaguchi K, Mizuno N (2011) An efficient H_2O_2-based oxidative bromination of alkenes, alkynes, and aromatics by a divanadium-substituted phosphotungstate. Chem Commun 47:1692–1694. https://doi.org/10.1039/C0CC04889E
72. Kamata K, Yamaura T, Mizuno N (2012) Chemo- and regioselective direct hydroxylation of arenes with hydrogen peroxide catalyzed by a divanadium-substituted phosphotungstate. Angew Chem Int Ed 51:7275–7278. https://doi.org/10.1002/anie.201201605
73. Zalomaeva OV, Evtushok VY, Maksimov GM, Kholdeeva OA (2015) Selective oxidation of pseudocumene and 2-methylnaphthalene with aqueous hydrogen peroxide catalyzed by γ-Keggin divanadium-substituted polyoxotungstate. J Organomet Chem 793:210–216. https://doi.org/10.1016/j.jorganchem.2015.04.020

74. Skobelev IY, Evtushok VYu, Kholdeeva OA, Maksimchuk NV, Maksimovskaya RI, Ricart JM, Poblet JM, Carbó JJ (2017) Understanding the regioselectivity of aromatic hydroxylation over divanadium-substituted γ-Keggin polyoxotungstate. ACS Catal 7:8514–8523. https://doi.org/10.1021/acscatal.7b02694
75. Ivanchikova ID, Maksimchuk NV, Maksimovskaya RI, Maksimov GM, Kholdeeva OA (2014) Highly selective oxidation of alkylphenols to *p*-benzoquinones with aqueous hydrogen peroxide catalyzed by divanadium-substituted polyoxotungstates. ACS Catal 4:2706–2713. https://doi.org/10.1021/cs500738e
76. Zalomaeva OV, Evtushok VY, Maksimov GM, Maksimovskaya RI, Kholdeeva OA (2017) Synthesis of coenzyme Q_0 through divanadium-catalyzed oxidation of 3,4,5-trimethoxytoluene with hydrogen peroxide. Dalton Trans 46:5202–5209. https://doi.org/10.1039/C7DT00552K
77. Kholdeeva OA, Zalomaeva OV (2016) Recent advances in transition-metal-catalyzed selective oxidation of substituted phenols and methoxyarenes with environmentally benign oxidants. Coord Chem Rev 306:302–330. https://doi.org/10.1016/j.ccr.2015.07.019
78. Zhang D, Liang Z, Xie S, Ma P, Zhang C, Wang J, Niu J (2014) A new Nb_{28} cluster based on tungstophosphate, $[\{Nb_4O_6(OH)_4\}\{Nb_6P_2W_{12}O_{61}\}_4]^{36-}$. Inorg Chem 53:9917–9922. https://doi.org/10.1021/ic501575x
79. Rhule JT, Hill CL, Judd DA, Schinazi RF (1998) Polyoxometalates in medicine. Chem Rev 98:327–357. https://doi.org/10.1021/cr960396q
80. Droege MW, Finke RG (1991) a novel triperoxyniobium-containing polyoxoanion, SiW9(NbO2)3O377−: synthesis, characterization, catalytic allylic epoxidations with H_2O_2 and preliminary kinetic studies. J Mol Catal 69:323–338. https://doi.org/10.1016/0304-5102(91)80113-H
81. Harrup MK, Kim GS, Zeng H, Johnson RP, VanDerveer D, Hill CL (1998) Triniobium polytungstophosphates. syntheses, structures, clarification of isomerism and reactivity in the presence of H_2O_2. Inorg Chem 37:5550–5556. https://doi.org/10.1021/ic980467z
82. Satake N, Hirano T, Kamata K, Suzuki K, Yamaguchi K, Mizuno N (2015) Synthesis, structural characterization, and oxidation catalysis of a diniobium-substituted silicodecatungstate. Chem Lett 44:899–901. https://doi.org/10.1246/cl.150213
83. Nyman M (2011) Polyoxoniobate chemistry in the 21st century. Dalton Trans 40:8049–8058. https://doi.org/10.1039/C1DT10435G
84. Kinnan MK, Creasy WR, Fullmer LB, Schreuder-Gibson HL, Nyman M (2014) Nerve agent degradation with polyoxoniobates. Eur J Inorg Chem 2014:2361–2367. https://doi.org/10.1002/ejic.201400016
85. Ge W, Wang X, Zhang L, Du L, Zhou Y, Wang J (2016) Fully-occupied Keggin type polyoxometalate as solid base for catalyzing CO_2 cycloaddition and Knoevenagel condensation. Catal Sci Technol 6:460–467. https://doi.org/10.1039/C5CY01038A
86. Guo W, Lv H, Sullivan KP, Gordon WO, Balboa A, Wagner GW, Musaev DG, Bacsa J, Hill CL (2016) Broad-spectrum liquid- and gas-phase decontamination of chemical warfare agents by one-dimensional heteropolyniobates. Angew Chem Int Ed 55:7403–7407. https://doi.org/10.1002/anie.201601620
87. Dong J, Hu J, Chi Y, Lin Z, Zou B, Yang S, Hill CL, Hu C (2017) A polyoxoniobate-polyoxovanadate double-anion catalyst for simultaneous oxidative and hydrolytic decontamination of chemical warfare agent simulants. Angew Chem Int Ed 56:4473–4477. https://doi.org/10.1002/anie.201700159
88. Venturello C, Alneri E, Ricci M (1983) A new, effective catalytic system for epoxidation of olefins by hydrogen peroxide under phase-transfer conditions. J Org Chem 48:3831–3833. https://doi.org/10.1021/jo00169a052
89. Ishii Y, Yamawaki K, Ura T, Yamada H, Yoshiba T, Ogawa M (1988) Hydrogen peroxide oxidation catalyzed by heteropoly acids combined with cetylpiridinium chloride: epoxidation of olefins and allylic alcohols, ketonization of alcohols and diols, and oxidative cleavage of 1,2-diols and olefins. J Org Chem 53:3587–3593. https://doi.org/10.1021/jo00250a032

90. Zhou Y, Guo ZJ, Hou W, Wang Q, Wang J (2015) Polyoxometalate-based phase transfer catalysis for liquid–solid organic reactions: a review. Catal Sci Technol 5:4324–4335. https://doi.org/10.1021/jo00250a032
91. Duncan DC, Chambers RC, Hecht E, Hill CL (1995) Mechanism and dynamics in the $H_3[PW_{12}O_{40}]$-catalyzed selective epoxidation of terminal olefins by H_2O_2. Formation, reactivity, and stability of $\{PO_4[WO(O_2)_2]_4\}^{3-}$. J Am Chem Soc 117:681–691. https://doi.org/10.1021/ja00107a012
92. Xi Z, Zhou N, Sun Y, Li K (2001) Reaction-controlled phase-transfer catalysis for propylene epoxidation to propylene oxide. Science 292:1139–1141. https://doi.org/10.1126/science.292.5519.1139
93. Li C, Gao J, Jiang Z, Wang S, Lu H, Yang Y, Jing F (2005) Selective oxidations on recoverable catalysts assembled in emulsions. Top Catal 35:169–175. https://doi.org/10.1007/s11244-005-3821-5
94. Lu H, Gao J, Jiang Z, Jing F, Yang Y, Wang G, Li C (2006) Ultra-deep desulfurization of diesel by selective oxidation with $[C_{18}H_{37}N(CH_3)_3]_4[H_2NaPW_{10}O_{36}]$ catalyst assembled in emulsion droplets. J Catal 239:369–375. https://doi.org/10.1016/j.jcat.2006.01.025
95. Yin P, Wang J, Xiao Z, Wu P, Wei Y, Liu T (2012) Polyoxometalate-organic hybrid molecules as amphiphilic emulsion catalysts for deep desulfurization. Chem Eur J 18:9174–9178. https://doi.org/10.1002/chem.201201551
96. Xu J, Zhao S, Ji Y, Song Y-F (2013) Deep desulfurization by amphiphilic lanthanide-containing polyoxometalates in ionic-liquid emulsion systems under mild conditions. Chem Eur J 19:709–715. https://doi.org/10.1002/chem.201202595
97. Cavani F, Alini S (2009) In: Cavani F, Centi G, Perathoner S, Trifiro F (eds) Sustainable industrial processes. Wiley-VCH, pp 331–391
98. Zhu W, Li H, He X, Zhang Q, Shu H, Yan Y (2008) Synthesis of adipic acid catalyzed by surfactant-type peroxotungstates and peroxomolybdates. Catal Commun 9:551–555. https://doi.org/10.1016/j.catcom.2007.07.038
99. Kerenkan AE, Beland F, Do TO (2016) Chemically catalyzed oxidative cleavage of unsaturated fatty acids and their derivatives into valuable products for industrial applications: a review and perspective. Catal Sci Technol 6:971–987. https://doi.org/10.1039/c5cy01118c
100. Santacesaria E, Sorrentino A, Rainone F, Di Serio M, Speranza F (2000) Oxidative cleavage of the double bond of monoenic fatty chains in two steps: a new promising route to azelaic acid and other industrial products. Ind Eng Chem Res 39:2766–2771. https://doi.org/10.1021/ie990920u
101. Poli E, Clacens JM, Barrault J, Pouilloux Y (2009) Solvent-free selective epoxidation of fatty esters over a tungsten-based catalyst. Catal Today 140:19–22. https://doi.org/10.1016/j.cattod.2008.07.004
102. Godard A, De Caro P, Thiebaud-Roux S, Vedrenne E, Mouloungui Z (2013) New environmentally friendly oxidative scission of oleic acid into azelaic acid and pelargonic acid. J Am Oil Chem Soc 90:133–140. https://doi.org/10.1007/s11746-012-2134-7
103. Kadyrov R, Hackenberger D (2014) Oxidative cleavage of long chain olefins to carboxylic acids with hydrogen peroxide. Top Catal 57:1366–1371. https://doi.org/10.1007/s11244-014-0304-6
104. Haimov A, Cohen H, Neumann R (2004) Alkylated polyethyleneimine/polyoxometalate synzymes as catalysts for the oxidation of hydrophobic substrates in water with hydrogen peroxide. J Am Chem Soc 126:11762–11763. https://doi.org/10.1021/ja046349u
105. Maayan G, Fish RH, Neumann R (2003) Polyfluorinated quaternary ammonium salts of polyoxometalate anions: fluorous biphasic oxidation catalysis with and without fluorous solvents. Org Lett 5:3547–3550. https://doi.org/10.1021/ol0348598
106. Zeng H, Newkome GR, Hill CL (2000) Poly(polyoxometalate) dendrimers: molecular prototypes of new catalytic materials. Angew Chem Int Ed 39:1772–1774. https://doi.org/10.1002/(SICI)1521-3773(20000515)39:10%3c1771:AID-ANIE1771%3e3.0.CO;2-D

107. Plault L, Hauseler A, Nlate S, Astruc D, Ruiz J, Gatard S, Neumann R (2004) Synthesis of dendritic polyoxometalate complexes assembled by ionic bonding and their function as recoverable and reusable oxidation catalysts. Angew Chem Int Ed 43:2924–2928. https://doi.org/10.1002/anie.200453870
108. Jahier C, Cantuel M, McClenaghan ND, Buffeteau T, Cavagnat D, Agbossou F, Carraro M, Nlate S (2009) Enantiopure dendritic polyoxometalates: chirality transfer from dendritic wedges to a POM cluster for asymmetric sulfide oxidation. Chem Eur J 15:8703–8708. https://doi.org/10.1002/chem.200901512
109. Jahier C, Coustou MF, Cantuel M, McClenaghan ND, Buffeteau T, Cavagnat D, Carraro M, Nlate S (2011) Optically active tripodal dendritic polyoxometalates: synthesis, characterization and their use in asymmetric sulfide oxidation with hydrogen peroxide. Eur J Inorg Chem 2011:727–738. https://doi.org/10.1002/ejic.201001111
110. Pera-Titus M, Leclercq L, Clacens JM, De Campo F, Nardello-Rataj V (2014) Pickering interfacial catalysis for biphasic systems: from emulsion design to green reactions. Angew Chem Int Ed 53:2–18. https://doi.org/10.1002/anie.201402069
111. Leclercq L, Mouret A, Proust A, Schmitt V, Bauduin P, Aubry JM, Nardello-Rataj V (2012) Pickering emulsion stabilized by catalytic polyoxometalate nanoparticles: a new effective medium for oxidation reactions. Chem Eur J 18:14352–14358. https://doi.org/10.1002/chem.201201799
112. Zhang J, Wang A, Wang Y, Wang H, Gui J (2014) Heterogeneous oxidative desulfurization of diesel oil by hydrogen peroxide: catalysis of an amphipathic hybrid material supported on SiO_2. Chem Eng J 245:65–70. https://doi.org/10.1016/j.cej.2014.01.103
113. Yang Y, Yue L, Li HL, Maher E, Li YG, Wang YZ, Wu LX, Yam VWW (2012) Photoresponsive self-assembly of an azobenzene-ended surfactant-encapsulated polyoxometalate complex for modulating catalytic reactions. Small 8:3105–3110. https://doi.org/10.1002/smll.201200768
114. Yang Y, Zhang B, Wang YZ, Yue L, Li W, Wu LX (2013) A photo-driven polyoxometalate complex shuttle and its homogeneous catalysis and heterogeneous separation. J Am Chem Soc 135:14500–14503. https://doi.org/10.1021/ja405788
115. Wu L (2017) Organically encapsulated polyoxometalate catalysts: supramolecular composition and synergistic catalysis. In: Encapsulated catalysts. Elsevier, pp 1 − 33 http://dx.doi.org/10.1016/B978-0-12-803836-9.00001-8
116. Vazylyev M, Sloboda-Rozner D, Haimov A, Maayan G, Neumann R (2005) Strategies for oxidation catalyzed by polyoxometalates at the interface of homogeneous and heterogeneous catalysis. Topics Catal 34:93–99. https://doi.org/10.1007/s11244-005-3793-5
117. Proust A, Thouvenot R, Gouzerh P, Functionalization of polyoxometalates: towards advanced applications in catalysis and materials science. Chem Commun 2008:1837–1852. https://doi.org/10.1039/b715502f
118. Kholdeeva OA, Maksimchuk NV, Maksimov GM (2010) Polyoxometalate-based heterogeneous catalysts for liquid phase selective oxidations: Comparison of different strategies. Catal Today 157:107–113. https://doi.org/10.1016/j.cattod.2009.12.016
119. Dolbecq A, Dumas E, Mayer CR, Mialane P (2010) Hybrid organic−inorganic polyoxometalate compounds: from structural diversity to applications. Chem Rev 110:6009–6048. https://doi.org/10.1021/cr1000578
120. Song YF, Tsunashima R (2012) Recent advances on polyoxometalate-based molecular and composite materials. Chem Soc Rev 41:7384–7402. https://doi.org/10.1039/C2CS35143A
121. Proust A, Matt B, Villanneau R, Guillemot G, Gouzerh P, Izzet G (2012) Functionalization and post-functionalization: a step towards polyoxometalate-based materials. Chem Soc Rev 41:7605–7622. https://doi.org/10.1039/C2CS35119F
122. Zhou Y, Chen G, Long Z, Wang J (2014) Recent advances in polyoxometalate-based heterogeneous catalytic materials for liquid-phase organic transformations. RSC Adv 4:42092–42113. https://doi.org/10.1039/C4RA05175K
123. Rhule JT, Neiwert WA, Hardcastle KI, Do BT, Hill CL (2001) $Ag_5PV_2Mo_{10}O_{40}$, a heterogeneous catalyst for air-based selective oxidation at ambient temperature. J Am Chem Soc 123:12101–12102. https://doi.org/10.1021/ja015812p

124. Mizuno N, Kamata K, Yamaguchi K (2006) Liquid-phase oxidations catalyzed by polyoxometalates. In: Richards R (ed) Surface and nanomolecular catalysis. CRC Press LLC, Boca Raton, Fla, pp 463–492
125. Mizuno N, Uchida S, Kamata K, Ishimoto R, Nojima S, Yonehara K, Sumida Y (2010) A flexible nonporous heterogeneous catalyst for size-selective oxidation through a bottom-up approach. Angew Chem Int Ed 49:9972–9976. https://doi.org/10.1002/anie.201005275
126. Izumi Y (1998) Recent advances in immobilization of heteropolyacids. Res Chem Intermed 24:461–471. https://doi.org/10.1163/156856798X00500
127. Okuhara T (2002) Water-tolerant solid acid catalysts. Chem Rev 102:3641–3666. https://doi.org/10.1021/cr0103569
128. Kholdeeva OA, Vanina MP, Timofeeva MN, Maksimovskaya RI, Trubitsina TA, Melgunov MS, Burgina EB, Mrowiec-Bialon J, Jarzebski AB, Hill CL (2004) Co-containing polyoxometalate-based heterogeneous catalysts for the selective aerobic oxidation of aldehydes under ambient conditions. J Catal 226:363–371. https://doi.org/10.1016/j.jcat.2004.05.032
129. Yun SK, Pinnavaia TJ (1996) Layered double hydroxides intercalated by polyoxometalate anions with Keggin (α-$H_2W_{12}O_{40}^{6-}$), Dawson (α-$P_2W_{18}O_{62}^{6-}$), and Finke ($(Co_4(H_2O)_2(PW_9O_{34})_2^{10-}$) structures. Inorg Chem 35:6853–6860. https://doi.org/10.1021/ic960287u
130. Jana SK, Kubota Y, Tatsumi T (2008) Cobalt-substituted polyoxometalate pillared hydrotalcite: synthesis and catalysis in liquid-phase oxidation of cyclohexanol with molecular oxygen. J Catal 255:40–47. https://doi.org/10.1016/j.jcat.2008.01.022
131. Omwoma S, Chen W, Tsunashima R, Song YF (2014) Recent advances on polyoxometalates intercalated layered double hydroxides: from synthetic approaches to functional material applications. Coord Chem Rev 258–259:58–71. https://doi.org/10.1016/j.ccr.2013.08.039
132. Neumann R, Miller HJ (1995) Alkene oxidation in water using hydrophobic silica particles derivatized with polyoxometalates as catalysts. J Chem Soc Chem Commun 2277 – 2278. https://doi.org/10.1039/c39950002277
133. Okun NM, Anderson TM, Hill CL (2003) $[(Fe^{III}(OH_2)_2)_3(A\text{-}\alpha\text{-}PW_9O_{34})_2]^{9-}$ on cationic silica nanoparticles, a new type of material and efficient heterogeneous catalyst for aerobic oxidations. J Am Chem Soc 125:3194–3195. https://doi.org/10.1021/ja0267223
134. Bordoloi A, Lefebvre F, Halligudi SB (2007) Selective oxidation of anthracene using inorganic–organic hybrid materials based on molybdovanadophosphoric acids. J Catal 247:166–175. https://doi.org/10.1016/j.jcat.2007.01.020
135. Yamaguchi K, Yoshida C, Uchida S, Mizuno N (2005) Peroxotungstate immobilized on ionic liquid-modified silica as a heterogeneous epoxidation catalyst with hydrogen peroxide. J Am Chem Soc 127:530–531. https://doi.org/10.1021/ja043688e
136. Maksimchuk NV, Melgunov MS, Chesalov YuA, Mrowiec-Białoń J, Jarzębski AB, Kholdeeva OA (2007) Aerobic oxidations of α-pinene over cobalt-substituted polyoxometalate supported on amino-modified mesoporous silicates. J Catal 246:241–248. https://doi.org/10.1016/j.jcat.2006.11.026
137. Neumann R, Cohen M (1997) Solvent-anchored supported liquid phase catalysis: polyoxometalate-catalyzed oxidations. Angew Chem Int Ed 36:1738–1740. https://doi.org/10.1002/anie.199717381
138. Johnson BJS, Stein A (2001) Surface modification of mesoporous, macroporous, and amorphous silica with catalytically active polyoxometalate clusters. Inorg Chem 40:801–808. https://doi.org/10.1021/ic991440y
139. Liu Y, Murata K, Inaba M (2004) Epoxidation of propylene with molecular oxygen in methanol over a peroxo-heteropoly compound immobilized on palladium exchanged HMS. Green Chem 6:510–515. https://doi.org/10.1039/B407290C
140. Carraro M, Sandei L, Sartorel A, Scorrano G, Bonchio M (2006) Hybrid polyoxotungstates as second-generation POM-based catalysts for microwave-assisted H_2O_2 activation. Org Lett 8:3671–3674. https://doi.org/10.1021/ol061197o

141. Izumi Y, Urabe K (1981) Catalysis of heteropoly acids entrapped in activated carbon. Chem Lett 663–66 https://doi.org/10.1246/cl.1981.6634
142. Schwegler MA, Vinke P, van der Eijk M, van Bekkum H (1992) Activated carbon as a support for heteropolyanion catalysts. Appl Catal 80:41–57. https://doi.org/10.1016/0926-860X(92)85107-M
143. Evtushok VYu, Suboch AN, Podyacheva OYu, Stonkus OA, Zaikovskii VI, Chesalov YuA, Kibis LS, Kholdeeva OA (2018) Highly efficient catalysts based on divanadium-substituted polyoxometalate and N-doped carbon nanotubes for selective oxidation of alkylphenols. ACS Catal 8:1297–1307. https://doi.org/10.1021/acscatal.7b03933
144. Eder D (2010) Carbon nanotube−inorganic hybrids. Chem Rev 110:1348–1385. https://doi.org/10.1021/cr800433k
145. Toma FM, Sartorel A, Iurlo M, Carraro M, Parisse P, Maccato C, Rapino S, Gonzalez BR, Amenitsch H, Da Ros T, Casalis L, Goldoni A, Marcaccio M, Scorrano G, Scoles G, Paolucci F, Prato M, Bonchio M (2010) Nat Chem 2:826–831. https://doi.org/10.1038/NCHEM.761
146. Guo SX, Liu Y, Lee CY, Bond A, Zhang MJ, Geletii YV, Hill CL (2013) Graphene-supported $[\{Ru_4O_4(OH)_2(H_2O)_4\}(\gamma\text{-}SiW_{10}O_{36})_2]^{10-}$ for highly efficient electrocatalytic water oxidation. Energy Environ Sci 6:2654–2663. https://doi.org/10.1039/c3ee41892h
147. Pan D, Chen J, Tao W, Nie L, Yao S (2006) Polyoxometalate-modified carbon nanotubes: new catalyst support for methanol electro-oxidation. Langmuir 22:5872–5876. https://doi.org/10.1021/la053171w
148. Cui Z, Li CM, Jiang SP (2011) PtRu catalysts supported on heteropolyacid and chitosan functionalized carbon nanotubes for methanol oxidation reaction of fuel cells. Phys Chem Chem Phys 13:16349–16357. https://doi.org/10.1039/C1CP21271K
149. Kawasaki N, Wang H, Nakanishi R, Hamanaka S, Kitaura R, Shinohara H, Yokoyama T, Yoshikawa H, Awaga K (2011) Nanohybridization of polyoxometalate clusters and single-wall carbon nanotubes: applications in molecular cluster batteries. Angew Chem Int Ed 50:3471–3474. https://doi.org/10.1002/ange.201007264
150. Ji Y, Huang L, Hu J, Streb C, Song YF (2015) Polyoxometalate-functionalized nanocarbon materials for energy conversion, energy storage and sensor systems. Energy Environ Sci 8:776–789. https://doi.org/10.1039/C4EE03749A
151. Giusti A, Charron G, Mazerat S, Compain JD, Mialane P, Dolbecq A, Riviere E, Wernsdorfer W, Biboum RN, Keita B, Nadjo L, Filoramo A, Bourgoin JP, Mallah T (2009) Magnetic bistability of individual single-molecule magnets grafted on single-wall carbon nanotubes. Angew Chem Int Ed 48:4949–4952. https://doi.org/10.1002/ange.200901806
152. Salavati H, Tangestaninejad S, Moghadam M, Mirkhani V, Mohammadpoor-Baltork I (2010) Sonocatalytic epoxidation of alkenes by vanadium-containing polyphosphomolybdate immobilized on multi-wall carbon nanotubes. Ultrason Sonochemistry 17:453–459. https://doi.org/10.1016/j.ultsonch.2009.09.011
153. Wang R, Yu F, Zhang G, Zhao H (2010) Performance evaluation of the carbon nanotubes supported $Cs_{2.5}H_{0.5}PW_{12}O_{40}$ as efficient and recoverable catalyst for the oxidative removal of dibenzothiophene. Catal Today 150:37–41. https://doi.org/10.1016/j.cattod.2009.10.001
154. Chen W, Huang L, Hu J, Li T, Jia F, Song YF (2014) Connecting carbon nanotubes to polyoxometalate clusters for engineering high-performance anode materials. Phys Chem Chem Phys 16:19668–19673. https://doi.org/10.1039/C4CP03202K
155. Sheldon RA, Wallau M, Arends IWCE, Schuchardt U (1998) Heterogeneous catalysts for liquid-phase oxidations: philosophers' stones or Trojan horses? Acc Chem Res 31:485–493. https://doi.org/10.1021/ar9700163
156. Podyacheva OYu, Ismagilov ZR (2015) Nitrogen-doped carbon nanomaterials: to the mechanism of growth, electrical conductivity and application in catalysis. Catal Today 249:12–22. https://doi.org/10.1016/j.cattod.2014.10.033
157. Arrigo R, Schuster ME, Xie Z, Yi Y, Wowsnick G, Sun LL, Hermann KE, Friedrich M, Kast P, Hävecker M, Knop-Gericke A, Schlögl R (2015) Nature of the N-Pd interaction in nitrogen-doped carbon nanotube catalysts. ACS Catal 5:2740–2753. https://doi.org/10.1021/acscatal.5b00094

158. Xia W (2016) Interactions between metal species and nitrogen-functionalized carbon nanotubes. Catal Sci Technol 6:630–644. https://doi.org/10.1039/C5CY01694K
159. Li M, Xu F, Li H, Wang Y (2016) Nitrogen-doped porous carbon materials: promising catalysts or catalyst supports for heterogeneous hydrogenation and oxidation. Catal Sci Technol 6:3670–3693. https://doi.org/10.1039/C6CY00544F
160. Cao Y, Mao S, Li M, Chen Y, Wang Y (2017) Metal/porous carbon composites for heterogeneous catalysis: old catalysts with improved performance promoted by N-doping. ACS Catal 7:8090–8112. https://doi.org/10.1021/acscatal.7b02335
161. Bulushev DA, Zacharska M, Shlyakhova EV, Chuvilin AL, Guo Y, Beloshapkin S, Okotrub AV, Bulusheva LG (2016) Single isolated Pd^{2+} cations supported on N-doped carbon as active sites for hydrogen production from formic acid decomposition. ACS Catal 6:681–691. https://doi.org/10.1021/acscatal.5b02381
162. Podyacheva OY, Lisitsyn AS, Kibis LS, Stadnichenko AI, Boronin AI, Slavinskaya EM, Stonkus OA, Yashnik SA, Ismagilov ZR (2018) Influence of the nitrogen-doped carbon nanofibers on the catalytic properties of supported metal and oxide nanoparticles. Catal Today 301:125–133. https://doi.org/10.1016/j.cattod.2017.01.004
163. Evtushok VY, Podyacheva OY, Suboch AN, Maksimchuk NV, Stonkus OA, Kibis LS, Kholdeeva OA H_2O_2-based selective oxidation by divanadium-substituted polyoxotungstate supported on nitrogen-doped carbon nanomaterials. Catal. Today, submitted. https://doi.org/10.1016/j.cattod.2019.03.060
164. Wang Y, Kamata K, Ishimoto R, Ogasawara Y, Suzuki K, Yamaguchi K, Mizuno N (2015) Composites of $[\gamma\text{-}H_2PV_2W_{10}O_{40}]^{3-}$ and $[\alpha\text{-}SiW_{12}O_{40}]^{4-}$ supported on Fe_2O_3 as heterogeneous catalysts for selective oxidation with aqueous hydrogen peroxide. Catal Sci Technol 5:2602–2611. https://doi.org/10.1039/c4cy01693a
165. Kholdeeva OA, Ivanchikova ID, Guidotti M, Ravasio N (2007) Highly efficient production of 2,3,5-trimethyl-1,4-benzoquinone using aqueous H_2O_2 and grafted Ti(IV)/SiO_2 catalyst. Green Chem 9:731–733. https://doi.org/10.1039/B617162A
166. Ivanchikova ID, Kovalev MK, Mel'gunov MS, Shmakov AN, Kholdeeva OA (2014) User-friendly synthesis of highly selective and recyclable mesostructured titanium-silicate catalysts for the production of bulky benzoquinones. Catal Sci Technol 4:200–207. https://doi.org/10.1039/C3CY00615H
167. Qi W, Wang Y, Li W, Wu L (2010) Surfactant-encapsulated polyoxometalates as immobilized supramolecular catalysts for highly efficient and selective oxidation reactions. Chem Eur J 16:1068–1078. https://doi.org/10.1002/chem.200902261
168. Yan Y, Wu L (2011) Polyoxometalate-incorporated supramolecular self assemblies: structures and functional properties. Isr J Chem 51:181–190. https://doi.org/10.1002/ijch.201000077
169. Shi L, Wang YZ, Li B, Wu LX (2014) Polyoxometalate complexes for oxidative kinetic resolution of secondary alcohols: unique effects of chiral environment, immobilization and aggregation. Dalton Trans 43:9177–9188. https://doi.org/10.1039/C4DT00742E
170. Hwang YK, Férey G, Lee UH, Chang JS Liquid phase oxidation of organic compounds by metal-organic frameworks. In: Clerici MG, Kholdeeva OA (eds) Liquid phase oxidation via heterogeneous catalysis: organic synthesis and industrial applications. Wiley, Hoboken, New Jersey, pp 371–409. https://doi.org/10.1002/9781118356760.ch8
171. Du DY, Qin JS, Li SL, Su ZM, Lan YQ (2014) Recent advances in porous polyoxometalate based metal–organic framework materials. Chem Soc Rev 43:4615–4632. https://doi.org/10.1016/j.ccr.2012.10.004
172. Kholdeeva OA (2016) Liquid-phase selective oxidation catalysis with metal-organic frameworks. Catal Today 278:22–29. https://doi.org/10.1016/j.cattod.2016.06.010
173. Férey G, Mellot-Draznieks C, Serre C, Millange F, Dutour J, Surblé S, Margiolaki I (2005) A chromium terephthalate-based solid with unusually large pore volumes and surface area. Science 309:2040–2042. https://doi.org/10.1126/science.1116275
174. Maksimchuk NV, Timofeeva MN, Melgunov MS, Shmakov AN, Chesalov YuA, Dybtsev DN, Fedin VP, Kholdeeva OA (2008) Heterogeneous selective oxidation catalysts based on coordination polymer MIL-101 and transition metal substituted polyoxometalates. J Catal 257:315–323. https://doi.org/10.1016/j.jcat.2008.05.014

175. Maksimchuk NV, Kovalenko KA, Arzumanov SS, Chesalov YuA, Stepanov AG, Fedin VP, Kholdeeva OA (2010) Hybrid polyoxotungstate/MIL-101 materials: synthesis, characterization, and catalysis of H_2O_2-based alkene epoxidation. Inorg Chem 49:2920–2930. https://doi.org/10.1021/ic902459f
176. Maksimchuk NV, Kholdeeva OA, Kovalenko KA, Fedin VP (2011) MIL-101 supported polyoxometalates: synthesis, characterization and catalytic applications in selective liquid-phase oxidation. Israel J Chem 2:281–289. https://doi.org/10.1002/ijch.201000082
177. Balula SS, Granadeiro CM, Barbosa ADS, Santos ICMS, Cunha-Silva L (2013) Multifunctional catalyst based on sandwich-type polyoxotungstate and MIL-101 for liquid phase oxidations. Catal Today 210:142–148. https://doi.org/10.1016/j.cattod.2012.12.003
178. Granadeiro CM, Barbosa ADS, Ribeiro S, Santos ICMS, de Castro B, Cunha − Silva L, Balula SS (2014) Oxidative catalytic versatility of a trivacantpolyoxotungstate incorporated into MIL-101(Cr). Catal Sci Technol 4:1416–1425. https://doi.org/10.1039/c3cy00853c
179. Lin ZJ, Zheng HQ, Chen J, Zhuang WE, Lin YX, Su JW, Huang YB, Cao R (2018) Encapsulation of phosphotungstic acid into metal—organic frameworks with tunable window sizes: screening of PTA@MOF Catalysts for efficient oxidative desulfurization. Inorg Chem 57:13009–13019. https://doi.org/10.1021/acs.inorgchem.8b02272
180. Yang X-L, Qiao L-M, Dai W-L (2015) Phosphotungstic acid encapsulated in metal-organic framework UiO-66: an effective catalyst for the selective oxidation of cyclopentene to glutaraldehyde. Microporous Mesoporous Mater 211:73–81. https://doi.org/10.1016/j.micromeso.2015.02.035
181. Cao R, Han JW, Anderson TM, Hillesheim DA, Hardcastle KI, Slonkina E, Hedman B, Hodgson KO, Kirk ML, Musaev DG, Morokuma K, Geletii YV, Hill CL (2008) Late transition metal-oxo compounds and open-framework materials that catalyze aerobic oxidations. Adv Inorg Chem 60:245–272. https://books.google.ru/books?isbn=0123739772
182. Yu R, Kuang XF, Wu XY, Lu CZ, Donahue JP (2009) Stabilization and immobilization of polyoxometalates in porous coordination polymers through host–guest interactions. Coord Chem Rev 253:2872–2890. https://doi.org/10.1016/j.ccr.2009.07.003
183. Song J, Luo Z, Britt DK, Furukawa H, Yaghi OM, Hardcastle KI, Hill CL (2011) A multiunit catalyst with synergistic stability and reactivity: a polyoxometalatemetal organic framework for aerobic decontamination. J Am Chem Soc 133:6839–16846. https://doi.org/10.1021/ja203695h
184. Zou C, Zhang Z, Xu X, Gong Q, Li J, Wu C-D (2012) A multifunctional organic–inorganic hybrid structure based on Mn^{III}−porphyrin and polyoxometalate as a highly effective dye scavenger and heterogenous catalyst. J Am Chem Soc 134:87–90. https://doi.org/10.1021/ja209196t
185. Han Q, He C, Zhao M, Qi B, Niu J, Duan C (2013) Engineering chiral polyoxometalate hybrid metal−organic frameworks for asymmetric dihydroxylation of olefins. J Am Chem Soc 135:10186–10189. https://doi.org/10.1021/ja401758c

Chapter 4
Recent Developments in the Catalytic Asymmetric Sulfoxidation Reactions

Konstantin Volcho

Abstract Chiral sulfoxides constitute an important class of organic compounds. The progress in the asymmetric oxidation of prochiral sulfides to sulfoxides over the last decade, from 2009 to 2018, is reviewed. Titanium- and vanadium-containing complexes are most frequently used as catalysts for sulfoxidation reactions. Considerable attention is paid to the asymmetric synthesis of chiral sulfoxides using complexes with other metals, including manganese, iron, molybdenum, copper, tungsten, and aluminum, as well as to organocatalysts.

Keywords Oxidation · Sulfide · Sulfoxide · Hydrogen peroxide · Oxygen · Catalysis

4.1 Introduction

Sulfoxides with different R^1 and R^2 substituents (Fig. 4.1) are chiral compounds; the other two substituents inducing asymmetry are an oxygen atom and a lone pair of electrons. Chiral sulfoxides are broadly used in asymmetric synthesis [1–3].

The high efficiency of using sulfoxides in asymmetric transformations is largely due to high configurational stability of the sulfoxide group and significant steric and electronic differences among the lone electron pair, oxygen, and aliphatic or aromatic substituents [4, 5]. Considerable interest in chiral sulfoxides is also associated with isolation of natural compounds containing an asymmetric sulfoxide group [6] as well as the discovery of biologically active sulfoxides with a definite configuration [7–9], including highly effective anti-ulcer drugs, e.g., esomeprazole [10].

The main approaches to production of chiral sulfoxides with high enantiomeric purity include resolution of racemates of chiral sulfoxides, asymmetric synthesis based on the addition of a sulfoxide group into an optically active compound, followed, if necessary, by separation of diastereomers, and asymmetric oxidation of sulfides [11]. The last approach is most atom-efficient and thus preferable from the

K. Volcho (✉)
Novosibirsk Institute of Organic Chemistry, Lavrentjev av. 9, Novosibirsk 630090, Russia
e-mail: volcho@nioch.nsc.ru

K. P. Bryliakov (ed.), *Frontiers of Green Catalytic Selective Oxidations*,
Green Chemistry and Sustainable Technology,
https://doi.org/10.1007/978-981-32-9751-7_4

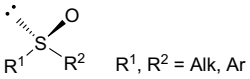

Fig. 4.1 Structure of chiral sulfoxides

green chemistry perspective. In this review, we discuss modern approaches to the asymmetric oxidation of sulfides to chiral sulfoxides using "green" oxidants, such as hydrogen peroxide [12] or oxygen, which have been reported over the last decade, from 2009 to 2018. These reactions are usually conducted in the presence of metal complex catalysts. The review is structured in accordance with the used metals; however, the applicability of organocatalysts is also discussed.

4.2 Oxidation of Sulfides to Chiral Sulfoxides Using Aqueous Hydrogen Peroxide as an Oxidant

4.2.1 Asymmetric Synthesis of Chiral Sulfoxides Using Titanium Complexes

The first catalyst systems for asymmetric oxidation of sulfides to sulfoxides using metal complexes were proposed independently by Kagan [13] and Modena groups [14] in 1984. Both systems were based on the Sharpless epoxidation reagent that had been developed for asymmetric oxidation of allyl alcohols and included equimolar titanium isopropylate ($Ti(O\mathit{i}Pr)_4$) and optically active diethyl tartrate as well as tert-butyl hydroperoxide as an oxidizing agent [15]. While direct application of the Sharpless system led to the formation of racemic sulfoxides only, the addition of one equivalent of water (Kagan system [13]) or the use of a fourfold excess of diethyl tartrate with respect to $Ti(O\mathit{i}Pr)_4$ (Modena system [14]) allowed for the production of sulfoxides with high enantiomeric purity from aryl alkyl sulfides.

Strict limitations placed on these systems for water content during the reaction, which are associated with instability of titanium isopropylate in the presence of moisture, complicated the reaction and interfered with application of one of the most environmentally friendly oxidants, aqueous hydrogen peroxide.

However, anion exchange intercalation of the titanium tartrate complex into the interlayer of layered double hydroxides enabled the use of H_2O_2 as an oxidant instead of previously used organic peroxides [16, 17]. The oxidation of thioanisole **1** to sulfoxide **2** (Scheme 4.1) occurred much slower than in the case of a non-immobilized complex, but with significantly greater enantiomeric excess amounting to 48% *ee*. Somewhat greater enantioselectivity (up to 58% *ee*) was achieved using L-tartrate anions pre-immobilized into the interlayer of layered double hydroxides, followed by the inclusion of Ti (IV) centers [18].

Scheme 4.1 Oxidation of thioanisole **1** to sulfoxide **2**

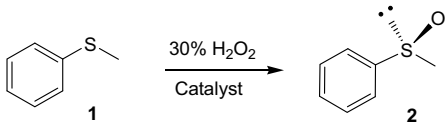

Replacement of diethyl tartrate by salicylaldehydimine **3** (Fig. 4.2) in Ti(O*i*Pr)$_4$-catalyzed oxidation of thioanisole **1** led to the formation of the target sulfoxide **2** with good yield (up to 89%) and moderate enantioselectivity of 73% *ee* [19]. The use of titanium and salicylaldehydimine **4** complexes (Fig. 4.2) was more effective and yielded methylsulfinylbenzene **2** with up to 84% *ee* and with high conversion and chemoselectivity [20].

Moderate enantioselectivity (51% *ee*) was observed in the oxidation of methyl phenyl sulfide **1** in the presence of titanium-salan catalyst **5** (Fig. 4.3) [21]. Enantioselective sulfide **1** oxidation was accompanied by kinetic resolution of the resulting sulfoxide **2** (preferential oxidation of one of the enantiomeric sulfoxides to sulfone), which enhanced the enantiomeric excess, but led to a decrease in the sulfoxide yield. Replacement of a solvent CH_2Cl_2 by ionic liquids led to a sharp decrease in the reaction enantioselectivity.

The use of dimeric titanium-salan catalyst **6a** (Fig. 4.3) for the oxidation of aryl alkyl sulfides (Scheme 4.2) provided corresponding sulfoxides with an enantiomeric

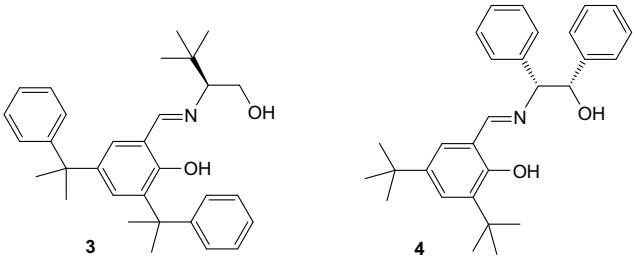

Fig. 4.2 Structures of ligands **3** and **4**

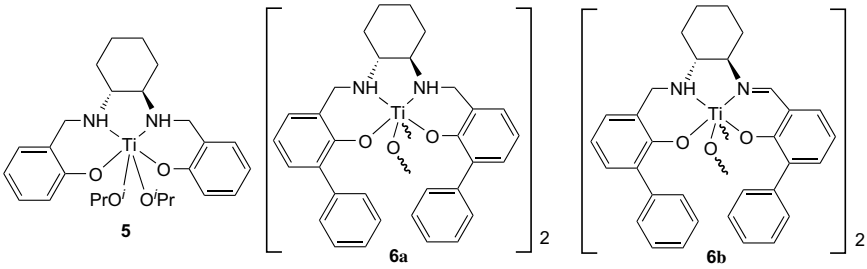

Fig. 4.3 Structures of complexes **5** and **6a, b**

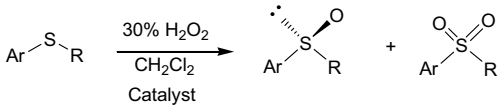

Scheme 4.2 Oxidation of aryl alkyl sulfides to corresponding sulfoxides and sulfones

excess of up to 98.5% *ee* and good yields [22, 23]. The combination of asymmetric sulfoxidation and kinetic resolution was critical for achieving high enantioselectivity. The best results were obtained with a bulky benzyl substituent R.

Titanium-salan complex **6a** (Fig. 4.3) and its analogs, substituted in aromatic rings, were also used for the asymmetric synthesis of practically important compounds, including anti-ulcer drugs, (*S*)-Omeprazole (Esomeprazole) and (*R*)-Lansoprazole (Dexlansoprazole) (Scheme 4.3), which were obtained with up to 95% yields and 94% *ee* [24]. Interestingly, the temperature dependence of enantioselectivity in the presence of complex **1** is non-monotonic, demonstrating an isoinversion behavior as the temperature is decreased. It should be noted that Ti-catalyzed approaches commonly used for the synthesis of esomeprazole are based on the use of organic peroxides as oxidants [25, 26]. The use of titanium-salalen complex **6b** (Fig. 4.3) for (*R*)-Omeprazole and (*R*)-Lansoprazole synthesis was even more effective, providing the sulfoxides with up to 96% yield at 96% *ee* [27].

New complexes **7** (Fig. 4.4) enabling effective oxidation of both bulky aryl benzyl sulfides and small alkyl phenyl sulfides with high enantioselectivity (62–93% *ee*) were created by removing bulky substituents at positions 3 and 3′ of the aromatic rings and addition of halogen atoms into positions 5 and 5′ in complexes **6** (Fig. 4.3) [28].

Considerable attention has been paid to the development of immobilized Ti-salen-based catalysts that would enable asymmetric oxidation with water as a solvent and could also be easily recovered from reaction mixtures for repeated use.

Metallomicelles containing Ti-salen complex **8** (Fig. 4.4) and azobenzene moieties were successfully used for the UV-responsive asymmetric hydrogen peroxide-based oxidation of aryl methyl sulfides to sulfoxides with excellent yield and enan-

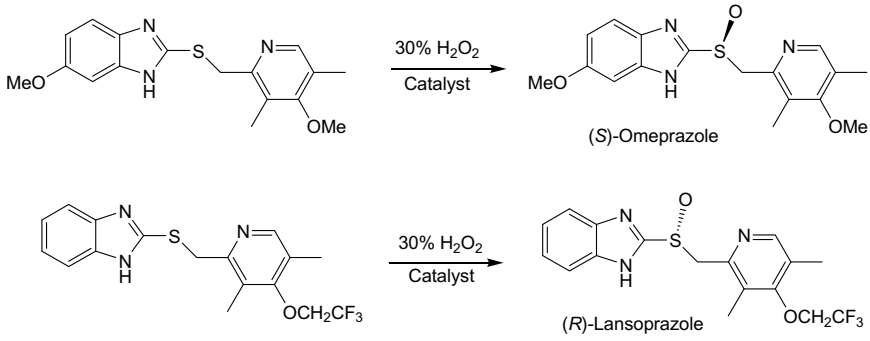

Scheme 4.3 Synthesis of (*S*)-Omeprazole and (*R*)-Lansoprazole

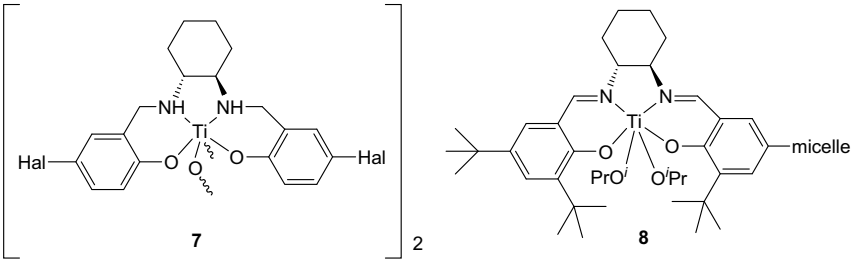

Fig. 4.4 Structures of catalysts **7** and **8**

tioselectivity (both up to 99%) [29]. An important advantage of this system is the opportunity of using water as a solvent. Similar results were obtained with micelles synthesized on the basis of thermo-responsive amphiphilic copolymers of poly(*N*-isopropylacrylamide-co-*N*,*N*-dimethyl acrylamide) [30]. The use of catalytic complex **5** (Fig. 4.3) attached to ionic liquid-functionalized graphene oxide was slightly less effective [31]. Deionized water was used as a solvent; the yield of aryl methyl sulfoxides ranged from 76 to 98%, with the conversion being 80% and higher, and the enantioselectivity ranging from 56 to 98% *ee*. Regardless of the substrate, the graphene-containing complex was more active and provided higher enantioselectivity than the neat complex. Another approach to immobilization of Ti-salen systems was their use in metal–organic frameworks (MOFs). The use of new chiral MOFs prepared using unsymmetrical Ti-containing complex as a building block enabled oxidation of aryl alkyl sulfides to corresponding sulfoxides with an enantiomeric excess of up to 62% [32]. Dendritic chiral complexes obtained by attachment of a salen Ti(IV) catalyst to a polyamidoamine dendrimer through a flexible ionic liquid linker turned out to be good catalysts for the asymmetric sulfoxidation of methyl aryl sulfides, with an enantiomeric excess reaching 85% *ee* at high conversion and selectivity [33].

The use of dimeric salen complexes **9** (Fig. 4.5) with various polyethylene glycol-based dicationic ionic liquid linkers [34] was also effective. Asymmetric oxidation of methyl aryl sulfides in water resulted in sulfoxides with yields of 74–90% and enantiomeric excess of up to 91% *ee*. Another type of artificial metalloenzyme **10** (Fig. 4.5) was produced using polymer-attached oxazole ligands [35]. Asymmetric sulfoxidation of aryl alkyl sulfides using these catalysts led to the formation of the corresponding sulfoxides with excellent yields and enantioselectivity (both up to 99%). Water was used as a solvent.

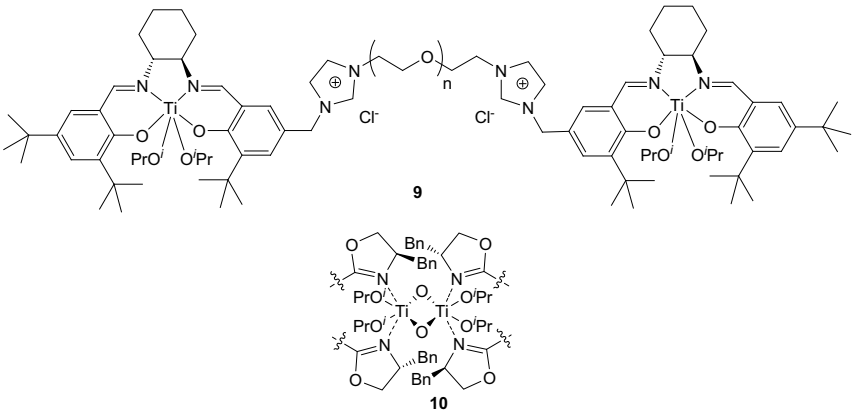

Fig. 4.5 Structures of catalysts **9** and **10**

4.2.2 Asymmetric Synthesis of Chiral Sulfoxides Using Vanadium Complexes

A broadly used alternative to titanium-containing systems is vanadium ion complexes [36, 37]. In 1995, Bolm's group demonstrated that vanadium complexes with ligands **11** and **12** (Fig. 4.6), synthesized from the corresponding salicylic aldehydes and optically active β-amino alcohols, enabled production of sulfoxides from aryl alkyl sulfides with good yields (up to 94%) and moderate enantioselectivity (usually 50–70% *ee*) [38]. Aqueous hydrogen peroxide was used as an oxidant, and chiral complexes produced in situ via the interaction between $VO(acac)_2$ and ligands were used in catalytic amounts (0.01–1 mol%).

An important advantage of vanadium-based oxidative systems is their tolerance to other functional groups. For example, selective oxidation of the sulfide group in the presence of an olefinic double bond in compounds **13** to sulfoxides **14** (Fig. 4.6) was carried out using catalyst **15** containing a ligand structurally similar to compounds

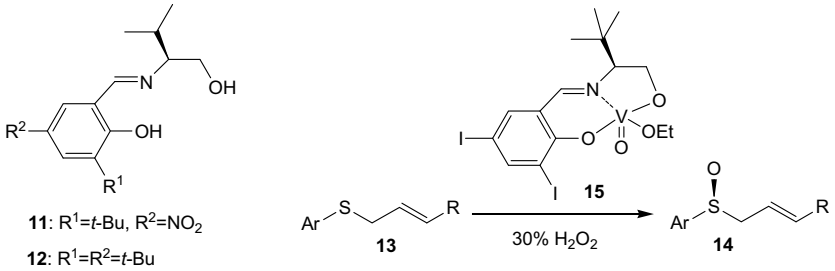

Fig. 4.6 Structures of ligands **11** and **12** and catalyst **15**, and oxidation of sulfide **13**

11 and **12** [39]. Products **14** were formed with high enantioselectivity (up to 97% *ee*) but only with moderate yields (43–57%).

The excellent enantioselectivity (up to 99% *ee*) and a satisfactory yield (55–65%) were achieved in the oxidation of thioanisole **1** with naphthalene-based ligand **16** (Fig. 4.7) [40]. The use of another type of chiral ligand containing a naphthol moiety, compound **17**, on the contrary, provided a good yield (81%), but only moderate stereoselectivity (50% *ee*) [41]. Ligand **18** with a tetrahydroquinoline core (Fig. 4.7) was proposed in ref. [42]. Oxidation of thioanisole **1** with aqueous hydrogen peroxide in acetone at 0 °C was optimal; the yield of sulfoxide **2** reached 89% with 71% *ee*.

An excellent enantiomeric excess of up to 99% *ee* (the yield of sulfoxide **2** was 81%) was achieved in the vanadium-catalyzed oxidation of thioanisole **1** using ligand **19** (Fig. 4.7) comprising two centers of chirality [43]. However, oxidation of 2-phenyl-1,3-dithiane **21** (Scheme 4.4) to sulfoxide **22**, which resulted in the emergence of two asymmetric centers, was most effective (up to 96% *ee* and a yield of 94%) in the presence of ligand **20** (Fig. 4.7) with a different structure of substituents [44], indicating that these ligands may be finely tuned for each specific sulfide.

Another ligand with two chiral centers, compound **23** (Fig. 4.8), was derived from benzothiophene [45]. The use of ligand **23** in the vanadium-catalyzed asymmetric

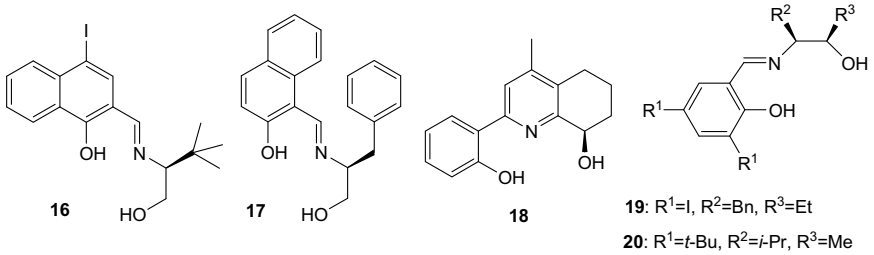

Fig. 4.7 Structures of ligands **16–20**

Scheme 4.4 Oxidation of 1,3-dithiane **21**

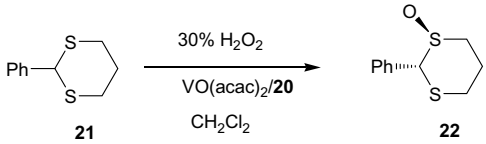

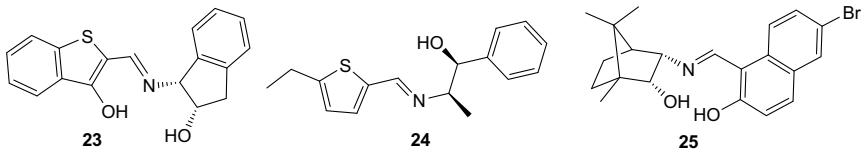

Fig. 4.8 Structures of ligands **23–25**

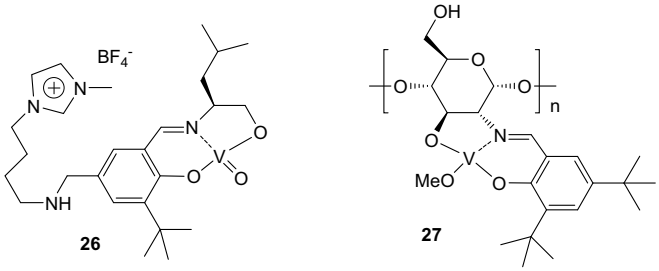

Fig. 4.9 Structures of catalysts **26** and **27**

oxidation of aryl alkyl sulfides resulted in yields and enantioselectivities comparable to those for classical ligand **12**. Using thiophene-based ligand **24** in the oxidation of thioanisole **1** provided sulfoxide **2** with an optical purity of up to 96% *ee* and 90% yield [46].

Despite abundance in nature and high optical purity, monoterpenoids have been rarely considered as sources of chirality for vanadium-catalyzed oxidation of sulfides, and enantiomeric excesses achieved in these studies are usually not large [47–49]. However, the use of camphor-derived Schiff base **25** (Fig. 4.8) enabled successful asymmetric oxidation of various aryl alkyl sulfides with acceptable yields (60–74%) and optical purities of the resulting sulfoxides up to 97% *ee* [50].

Of course, an attractive idea is to modify or immobilize the catalytic complex, which would provide facile regeneration and reuse of the catalyst. A conjugate of the catalytic complex with the Schiff base in ionic liquid was prepared (**26**, Fig. 4.9). The conjugate could be easily recovered from the reaction mixture after sulfoxidation and reused without reducing the yield and enantioselectivity; however, oxidation of aryl methyl sulfides using catalyst **26** resulted in a moderate enantiomeric excess (38–43% *ee*) [51]. Immobilization of various chiral vanadium-containing complexes using mesoporous SBA-15 [52] and microcapillaries [53] also resulted in sulfoxides with low *ee* (up to 33%). An example of successful immobilization is the attachment of vanadium complex **27** (Fig. 4.9) to chitosan placed, in turn, on SiO_2 [54]. The use of this catalytic complex enabled oxidation of both model aryl alkyl sulfides (up to 67% *ee*) and, most importantly, production of (*S*)-Omeprazole (Scheme 4.3) with a yield of 92% and 68% *ee*.

4.2.3 Asymmetric Synthesis of Chiral Sulfoxides Using Other Metals

4.2.3.1 Manganese

A complex of ligand **28** (Fig. 4.10) with manganese, the source of which was $Mn(OTf)_2$, was successfully used to oxidize a large set of structurally different sulfides to the corresponding sulfoxides (up to 90% yield and up to 99% *ee*) using

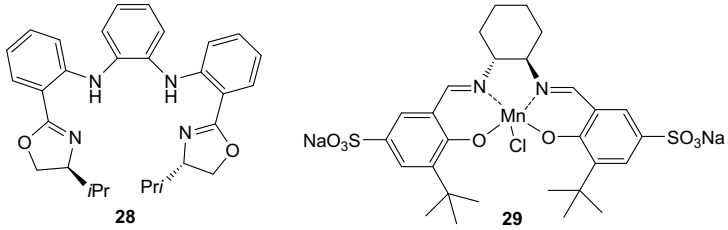

Fig. 4.10 Structures of ligand **28**, complex **29**

aqueous hydrogen peroxide as an oxidant. The reactions were conducted in the presence of organic acids, either acetic acid [55] or 1-adamantanecarboxylic acid [56]. The same catalytic system was used for the synthesis of chiral sulfoxides in a continuous-flow microreactor [57].

Chiral salen complex **29** (Fig. 4.10) was triply immobilized using polysiloxane, then axially coordinated by 3-aminopropyl functionalized SiO_2, and dispersed into ionic liquid [58]. The use of this catalyst enabled oxidation of thioanisole **1** to sulfoxide **2** with enantioselectivity of up to 92% *ee*. The catalyst can be repeatedly used, but there is a significant decrease in enantioselectivity. Another approach providing a heterogeneous Mn-containing catalyst for asymmetric reactions was based on the production of a new phosphonate metal–organic framework (MOF) platform [59]. This catalyst was used for the oxidation of sulfides; in the oxidation of thioanisole **1**, the enantiomeric excess and yield were 92% *ee* and 93%, respectively.

4.2.3.2 Iron

A complex of salen ligand **30** (Fig. 4.11) with $FeCl_3$ was used for the asymmetric synthesis of sulfoxides **2**; however, both the yield and the enantiomeric excess were moderate (about 50%) [60]. Significantly higher enantioselectivity (up to 81% *ee*) was achieved with the use of disalen ligand **31**; in this case, $Fe(acac)_3$ was used as a source of iron [61]. Adding 2 mol% of *para*-$MeOC_6H_4COOH$ to the reaction mixture

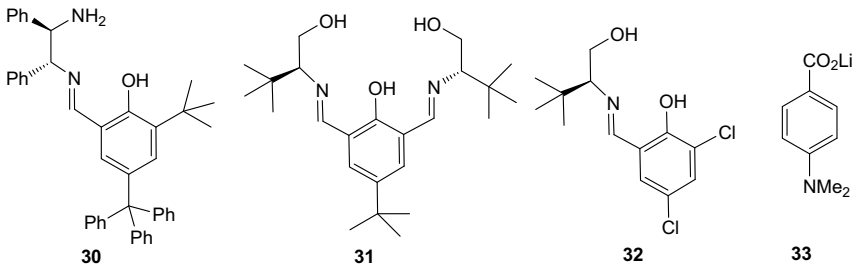

Fig. 4.11 Structures of ligands **30**–**32**, additive **33**

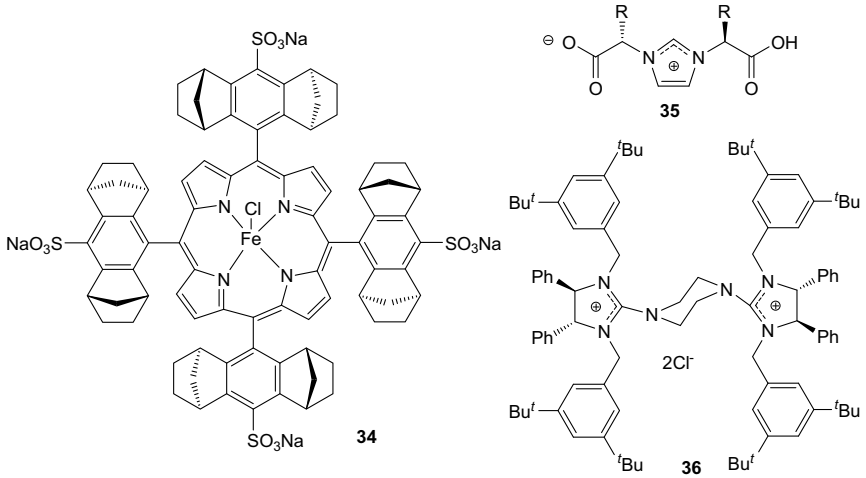

Fig. 4.12 Structures of complex **34** and imidazolium-based ligands **35** and **36**

provided a further increase in the enantiomeric excess. Ligand **32** and additive **33** were most effective in iron-catalyzed synthesis of (*S*)-Omeprazole (Scheme 4.3) (up to 99% *ee*) [62].

Chiral iron-porphyrin **34** (Fig. 4.12) was successfully used for asymmetric oxidation of aryl methyl sulfides; an enantiomeric excess of sulfoxides reached 87% [63, 64]. Although the reaction could be performed in water, the best results were obtained with methanol as a solvent.

4.2.3.3 Molybdenum

The use of a complex produced by mixing β-cyclodextrin bearing an ethylenediamine moiety with Na_2MoO_4 enabled the oxidation of thioanisole in aqueous medium [65]. The optical purity of sulfoxide **2** reached 53% *ee*, with yield being 89%. Moderate enantioselectivity (up to 47% *ee*) was also observed for the catalytic complex formed by $[Mo(O)(O_2)_2(H_2O)_n]$, $[PPh_4]Br$, and chiral imidazolium-based dicarboxylate ligand **35** (Fig. 4.12) [66, 67].

The use of another imidazolium-based charged ligand **36** for asymmetric oxidation of thioesters **37** (Scheme 4.5) was highly effective; enantiomeric excess in sulfoxides **38** reached 94% with high chemical yields [68].

Scheme 4.5 Oxidation of thioesters **37**

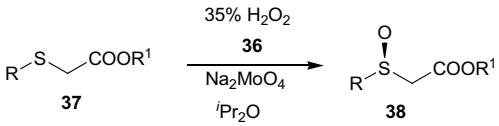

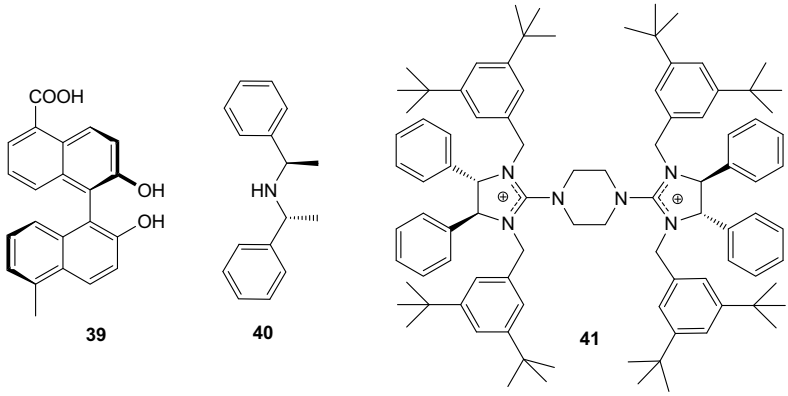

Fig. 4.13 Structures of ligands **39–41**

4.2.3.4 Copper

Salicylaldimine **32** (Fig. 4.11) and its analogs, in which chlorine atoms were replaced by other halogens, were used as ligands in the copper-catalyzed asymmetric oxidation of aryl benzyl sulfides to corresponding sulfoxides with 97% *ee* [69, 70]. A chiral copper MOF was synthesized using binaphthol **39** as a building block (Fig. 4.13) [71]. The use of this MOF for the asymmetric oxidation of methyl benzyl sulfide led to the formation of the corresponding sulfoxides with *ee* of up to 82% [72]. The heterogeneous catalyst may be filtered off and reused, but the enantioselectivity significantly decreased in this case.

4.2.3.5 Tungsten

A rare example of tungsten-containing catalytic systems used to synthesize chiral sulfoxides is polyoxometalate $Na_{12}[WZn_3(H_2O)_2(ZnW_9O_{34})_2]$ that forms spherical supramolecular assemblies in the presence of chiral amine hydrochloride **40** (Fig. 4.13) [73]. It should be noted that very moderate enantiomeric excess was achieved in the presence of this catalyst rather through kinetic resolution of the resulting racemic sulfoxide than through asymmetric sulfoxidation.

At the same time, the use of an Ag_2WO_4 complex with ligand **41** (Fig. 4.13) in the presence of dihydrogen phosphates for the oxidation of heterocyclic sulfides enabled the production of the target sulfoxides with high yields and enantioselectivities [74]. In particular, an anti-ulcer drug (*S*)-Lansoprazole (Scheme 4.3) was obtained with 81% yield and 90% *ee*.

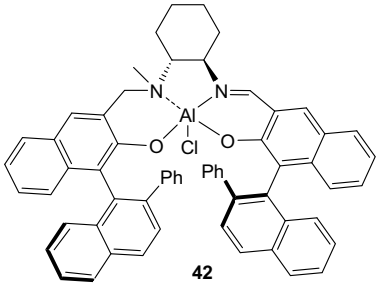

Fig. 4.14 Structure of complex **42**

4.2.3.6 Aluminum

It was found earlier that aluminum (salalen) chiral complex **42** (Fig. 4.14) can be used for highly enantioselective oxidation of aryl methyl sulfides with aqueous hydrogen peroxide [75]. The complex was applied later [76] for the asymmetric oxidation of dithioacetal **21** (Scheme 4.4) in the presence of pH 7.4 phosphate buffer which was important for increasing the synthesis reproducibility. Among the solvents studied, ethyl acetate was selected as the most effective one with respect to the reaction rate. The yield of *trans*-sulfoxide **22** was up to 94% with excellent 99% *ee*.

4.2.4 Asymmetric Synthesis of Chiral Sulfoxides Using Organocatalysts

Over recent years, particular attention has been paid to the development of organocatalytic methodologies [77].

A large group of effective organocatalysts for asymmetric sulfoxidations consists of BINOL-derived chiral phosphoric acids. For example, oxidation of thioanisole **1** with 50% H_2O_2 in the presence of acid **43** (Fig. 4.15) led to the formation of sulfoxide **2** with moderate yield and enantioselectivity (up to 78% *ee*) [78]. The use of imidodiphosphoric Brønsted acid **44** comprising two BINOL moieties increased the enantiomeric excess of sulfoxide **2** to 98% [79, 80]. The same chiral catalyst was successfully used for the synthesis of (*R*)-Sulindac (Scheme 4.6) [81].

Another planar-chiral catalyst, flavinium salt **45** (Fig. 4.15), was also able to catalyze the asymmetric oxidation of aryl alkyl sulfides to sulfoxides, but only with a moderate enantiomeric excess (up to 54% *ee*) [82]. The use of its analog **46** increased the enantioselectivity up to 61% *ee* [83]. Finally, the use of flavin–β-cyclodextrin conjugate **47** was the most effective, enabling the formation of aryl alkyl sulfoxides with up to 80% *ee* [84]. The use of a physical mixture of β-cyclodextrin and flavin led to the formation of racemic sulfoxides.

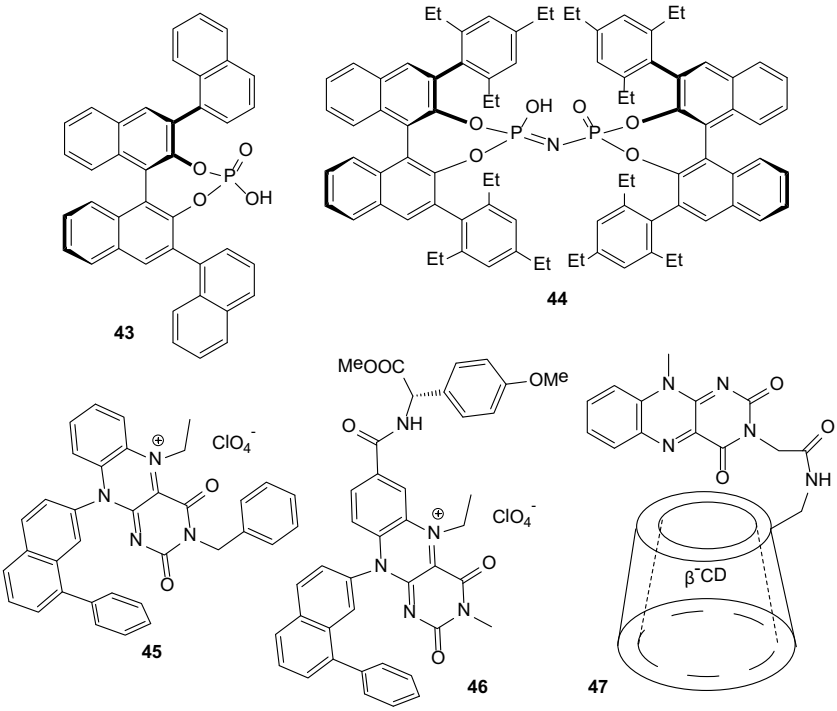

Fig. 4.15 Structures of organocatalysts **43**–**47**

Scheme 4.6 Synthesis of (*R*)-Sulindac

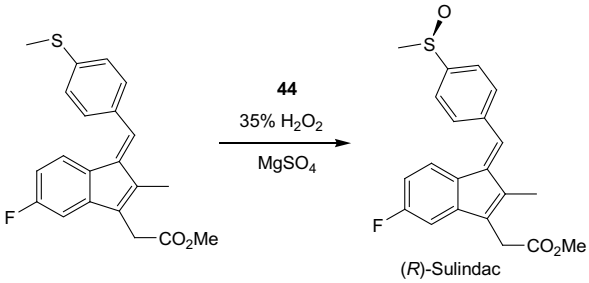

4.3 Oxidation of Sulfides to Chiral Sulfoxides Using Oxygen as an Oxidant

Obviously, oxygen is the most "green" oxidant. However, asymmetric sulfoxidation using oxygen is still a challenging target. One of the very few examples of successful asymmetric oxidation of sulfides by air is associated with complex **48** (Fig. 4.16) [85, 86]. The reaction was carried out in AcOEt at atmospheric pressure and room temperature under visible light irradiation with a halogen lamp. The irra-

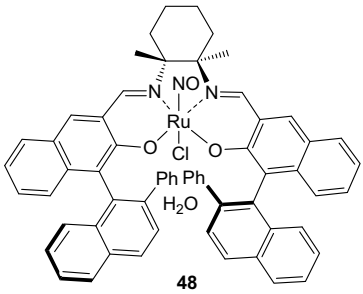

Fig. 4.16 Structures of complex **48**

diation promotes the dissociation the bond between Ru and the NO ligand, affording the catalytically active species [87]. The yields of sulfoxides upon oxidation of aryl methyl sulfides ranged from 61% to 86%, with *ee* amounting to 96%. The use of 2-phenyl-1,3-dithiane **21** (Scheme 4.4) as a substrate resulted in a 98% enantiomeric excess of sulfoxide **22** [85].

4.4 Conclusions

In the last decade, considerable progress has been made in the asymmetric sulfoxidations using "green" oxidants, primarily aqueous hydrogen peroxide. Although titanium- and vanadium-containing complexes remain the most frequently used catalysts, considerable attention has been paid to asymmetric synthesis of chiral sulfoxides using other metals, such as manganese, iron, molybdenum, and copper. Although some of the catalyst systems discussed have demonstrated high synthetic potential, so far there have not been published reports on their industrial applications.

Application of organocatalysts fundamentally solves the problem of oxidation product contamination with traces of heavy metals that are components of metal complex catalysts, but examples of successful studies in this direction are not numerous.

To date, a number of catalytic systems have exhibited good performance in the oxidation of various aryl alkyl sulfides, mostly usually model compounds, to the corresponding sulfoxides, ensuring high sulfoxide yields and enantioselectivities up to 99% *ee*. Importantly, some catalysts have been demonstrated to be suitable for the production of practically important, biologically active sulfoxides, such as approved drugs (*S*)-Omeprazole and (*R*)-Sulindac. Despite the lack of truly universal approaches to oxidation of structurally different sulfides, now there is the opportunity of choosing an appropriate catalytic system (or its modification) for the oxidation of sulfides of different types.

In the last decade, the only reported example of aerobic asymmetric oxidation of sulfides has been the Katsuki's catalyst system, relying on the use of the "second-

generation" ruthenium salen complexes. So, the catalyst systems capable of utilizing dioxygen in asymmetric sulfoxidations continue to be a challenge.

Also, different approaches to the synthesis of reusable, in particular, heterogeneous catalysts have been proposed. The results achieved so far have shown good promise for the future, and further research in this area may be potentially highly rewarding.

References

1. O'Mahony GE, Ford A, Maguire AR (2013) Asymmetric oxidation of sulfides. J Sulfur Chem 34:301–341. https://doi.org/10.1080/17415993.2012.725247
2. Han J, Soloshonok VA, Klika KD, Drabowicz J, Wzorek A (2018) Chiral sulfoxides: advances in asymmetric synthesis and problems with the accurate determination of the stereochemical outcome. Chem Soc Rev 47:1307–1350. https://doi.org/10.1039/c6cs00703a
3. Otocka S, Kwiatkowska M, Madalińska L, Kiełbasiński P (2017) Chiral organosulfur ligands/catalysts with a stereogenic sulfur atom: applications in asymmetric synthesis. Chem Rev 117:4147–4181. https://doi.org/10.1021/acs.chemrev.6b00517
4. O'Mahony GE, Kelly P, Lawrence SE, Maguire AR (2011) Synthesis of enantioenriched sulfoxides. Arkivoc 2011:1–110. https://doi.org/10.3998/ark.5550190.0012.101
5. Volcho KP, Salakhutdinov NF, Tolstikov AG (2003) Metal complexes in asymmetric oxidation of sulfides. Russ J Org Chem 39:1537–1552
6. Takaishi Y, Murakami Y, Uda M, Ohashi T, Hamamura N, Kido M, Kadota S (1997) Hydroxyphenylazoformamide derivatives from Calvatia craniformis. Phytochemistry 45:997–1001. https://doi.org/10.1016/S0031-9422(97)00066-6
7. Ding HX, Leverett CA, Kyne RE, Liu KKC, Fink SJ, Flick AC, O'Donnell CJ (2015) Synthetic approaches to the 2013 new drugs. Bioorganic Med Chem 23:1895–1922. https://doi.org/10.1016/j.bmc.2015.02.056
8. Volcho KP, Salakhutdinov NF (2009) Asymmetric oxidation of sulfides catalyzed by titanium and vanadium complexes in the synthesis of biologically active sulfoxides. Russ Chem Rev 78. https://doi.org/10.1070/rc2009v078n05abeh004023
9. Bühler S, Goettert M, Schollmeyer D, Albrecht W, Laufer SA (2011) Chiral sulfoxides as metabolites of 2-thioimidazole-based p38α mitogen-activated protein kinase inhibitors: enantioselective synthesis and biological evaluation. J Med Chem 54:3283–3297. https://doi.org/10.1021/jm101623p
10. Laine L, Fennerty MB, Osato M, Sugg MSJ, Suchower L, Probst P, Levine JG (2000) Esomeprazole-based Helicobacter pylori eradication therapy and the effect of antibiotic resistance: results of three US multicenter, double-blind trials. Am J Gastroenterol 95:3393–3398. https://doi.org/10.1111/j.1572-0241.2000.03349.x
11. Wojaczyńska E, Wojaczyński J (2010) Enantioselective synthesis of sulfoxides: 2000–2009. Chem Rev 110:4303–4356. https://doi.org/10.1021/cr900147h
12. Srour H, Le Maux P, Chevance S, Simonneaux G (2013) Metal-catalyzed asymmetric sulfoxidation, epoxidation and hydroxylation by hydrogen peroxide. Coord Chem Rev 257:3030–3050. https://doi.org/10.1016/j.ccr.2013.05.010
13. Pitchen P, Dunach E, Deshmukh MN, Kagan HB (1984) An efficient asymmetric oxidation of sulfides to sulfoxides. J Am Chem Soc 106:8188–8193. https://doi.org/10.1021/ja00338a030
14. Di Furia F, Modena G, Seraglia R (1984) Synthesis of chiral sulfoxides by metal-catalyzed oxidation with t-butyl hydroperoxide. Synthesis (Stuttg) 1984:325–326. https://doi.org/10.1055/s-1984-30829

15. Katsuki T, Sharpless KB (1980) 5974 Table. J Am Chem Soc 102:5976–5978. https://doi.org/10.1021/ja00538a077
16. Shi H, Yu C, He J (2010) Constraining titanium tartrate in the interlayer space of layered double hydroxides induces enantioselectivity. J Catal 271:79–87. https://doi.org/10.1016/j.jcat.2010.02.006
17. Shi H, Yu C, He J (2010) On the structure of layered double hydroxides intercalated with titanium tartrate complex for catalytic asymmetric sulfoxidation. J Phys Chem C 114:17819–17828. https://doi.org/10.1021/jp106931g
18. Shi H, He J (2011) Orientated intercalation of tartrate as chiral ligand to impact asymmetric catalysis. J Catal 279:155–162. https://doi.org/10.1016/j.jcat.2011.01.012
19. Wang Y, Wang M, Wang L, Wang Y, Wang X, Sun L (2011) Asymmetric oxidation of sulfides with H2O2catalyzed by titanium complexes of Schiff bases bearing a dicumenyl salicylidenyl unit. Appl Organomet Chem 25:325–330. https://doi.org/10.1002/aoc.1762
20. Bera PK, Ghosh D, Abdi SHR, Khan NUH, Kureshy RI, Bajaj HC (2012) Titanium complexes of chiral amino alcohol derived Schiff bases as efficient catalysts in asymmetric oxidation of prochiral sulfides with hydrogen peroxide as an oxidant. J Mol Catal A: Chem 361–362:36–44. https://doi.org/10.1016/j.molcata.2012.04.014
21. Adão P, Avecilla F, Bonchio M, Carraro M, Costa Pessoa J, Correia I (2010) Titanium(IV)-salan catalysts for asymmetric sulfoxidation with hydrogen peroxide. Eur J Inorg Chem 5568–5578. https://doi.org/10.1002/ejic.201000792
22. Bryliakov KP, Talsi EP (2008) Titanium-salan-catalyzed asymmetric oxidation of sulfides and kinetic resolution of sulfoxides with H_2O_2 as the oxidant. Eur J Org Chem 3369–3376. https://doi.org/10.1002/ejoc.200800277
23. Bryliakov KP, Talsi EP (2011) Catalytic enantioselective oxidation of bulky alkyl aryl thioethers with H_2O_2 over titanium-salan catalysts. Eur J Org Chem 4693–4698. https://doi.org/10.1002/ejoc.201100557
24. Talsi EP, Bryliakov KP (2017) Ti-Salan catalyzed asymmetric sulfoxidation of pyridylmethylthiobenzimidazoles to optically pure proton pump inhibitors. Catal Today 279:84–89. https://doi.org/10.1016/j.cattod.2016.03.006
25. Cotton H, Elebring T, Larsson M, Li L, Sörensen H, Von Unge S (2000) Asymmetric synthesis of esomeprazole. Tetrahedron Asymmetry 11:3819–3825. https://doi.org/10.1016/S0957-4166(00)00352-9
26. Khomenko TM, Volcho KP, Komarova NI, Salakhutdinov NF (2008) An efficient procedure for the synthesis of Esomeprazole using a titanium complex with two chiral ligands. Russ J Org Chem 44:124–127. https://doi.org/10.1007/s11178-008-1016-9
27. Talsi EP, Rybalova TV, Bryliakov KP (2015) Isoinversion behavior in the enantioselective oxidations of pyridylmethylthiobenzimidazoles to chiral proton pump inhibitors on titanium salalen complexes. ACS Catal 5:4673–4679. https://doi.org/10.1021/acscatal.5b01212
28. Talsi EP, Bryliakov KP (2013) Titanium-salan-catalyzed asymmetric sulfoxidations with H_2O_2: design of more versatile catalysts. Appl Organomet Chem 27:239–244. https://doi.org/10.1002/aoc.2968
29. Gao M, Tan R, Hao P, Zhang Y, Deng J, Yin D (2017) Ultraviolet-responsive self-assembled metallomicelles for photocontrollable catalysis of asymmetric sulfoxidation in water. RSC Adv 7:54570–54580. https://doi.org/10.1039/c7ra11022g
30. Zhang Y, Tan R, Zhao G, Luo X, Xing C, Yin D (2016) Thermo-responsive self-assembled metallomicelles accelerate asymmetric sulfoxidation in water. J Catal 335:62–71. https://doi.org/10.1016/j.jcat.2015.12.012
31. Xing C, Deng J, Tan R, Gao M, Hao P, Yin D, Yin D (2017) Cooperative chiral salen TiIVcatalyst supported on ionic liquid-functionalized graphene oxide accelerates asymmetric sulfoxidation in water. Catal Sci Technol 7:5944–5952. https://doi.org/10.1039/c7cy01511a

32. Zhu C, Chen X, Yang Z, Du X, Liu Y, Cui Y (2013) Chiral microporous Ti(salan)-based metal-organic frameworks for asymmetric sulfoxidation. Chem Commun 49:7120–7122. https://doi.org/10.1039/c3cc43225d
33. Chen Y, Tan R, Zhang Y, Zhao G, Yin D (2015) Dendritic chiral salen titanium(IV) catalysts enforce the cooperative catalysis of asymmetric sulfoxidation. ChemCatChem 7:4066–4075. https://doi.org/10.1002/cctc.201500900
34. Zhao G, Tan R, Zhang Y, Luo X, Xing C, Yin D (2016) Cooperative chiral salen Ti IV catalysts with built-in phase-transfer capability accelerate asymmetric sulfoxidation in water. RSC Adv 6:24704–24711. https://doi.org/10.1039/c6ra01130f
35. Zhang Y, Wang W, Fu W, Zhang M, Tang Z, Tan R, Yin D (2018) Titanium (iv)-folded single-chain polymeric nanoparticles as artificial metalloenzyme for asymmetric sulfoxidation in water. Chem Commun 54:9430–9433. https://doi.org/10.1039/c8cc05590d
36. da Silva JAL, da Silva JJRF, Pombeiro AJL (2011) Oxovanadium complexes in catalytic oxidations. Coord Chem Rev 255:2232–2248. https://doi.org/10.1016/j.ccr.2011.05.009
37. Pellissier H (2015) Recent advances in enantioselective vanadium-catalyzed transformations. Coord Chem Rev 284:93–110. https://doi.org/10.1016/j.ccr.2014.09.014
38. Bolm C (2003) Vanadium-catalyzed asymmetric oxidations. Coord Chem Rev 237:245–256. https://doi.org/10.1016/S0010-8545(02)00249-7
39. Zeng Q, Gao Y, Dong J, Weng W, Zhao Y (2011) Vanadium-catalyzed enantioselective oxidation of allyl sulfides. Tetrahedron Asymmetry 22:717–721. https://doi.org/10.1016/j.tetasy.2011.04.023
40. Wang Y, Wang M, Wang Y, Wang X, Wang L, Sun L (2010) Highly enantioselective sulfoxidation with vanadium catalysts of Schiff bases derived from bromo- and iodo-functionalized hydroxynaphthaldehydes. J Catal 273:177–181. https://doi.org/10.1016/j.jcat.2010.05.013
41. Adão P, Kuznetsov ML, Barroso S, Martins AM, Avecilla F, Pessoa JC (2012) Amino alcohol-derived reduced Schiff base VIVO and VV compounds as catalysts for asymmetric sulfoxidation of thioanisole with hydrogen peroxide. Inorg Chem 51:11430–11449. https://doi.org/10.1021/ic301153p
42. Liu H, Wang M, Wang Y, Wang Y, Sun H, Sun L (2009) Asymmetric oxidation of sulfides with hydrogen peroxide catalyzed by a vanadium complex of a new chiral NOO-ligand. Catal Commun 11:294–297. https://doi.org/10.1016/j.catcom.2009.10.017
43. Wu Y, Liu J, Li X, Chan ASC (2009) Vanadium-catalyzed asymmetric oxidation of sulfides using Schiff base ligands derived from ß-amino alcohols with two stereogenic centers. European J Org Chem 2:2607–2610. https://doi.org/10.1002/ejoc.200900289
44. Wu Y, Mao F, Meng F, Li X (2011) Enantioselective vanadium-catalyzed oxidation of 1,3-dithianes from aldehydes and ketones using β-amino alcohol derived schiff base ligands. Adv Synth Catal 353:1707–1712. https://doi.org/10.1002/adsc.201000803
45. Jeong YC, Ahn DJ, Lee WS, Lee SH, Ahn KH (2011) Synthesis of new chiral ligands based on thiophene derivatives for use in catalytic asymmetric oxidation of sulfides. Bull Korean Chem Soc 32:1063–1066. https://doi.org/10.5012/bkcs.2011.32.3.1063
46. Aydin AE (2013) Synthesis of novel β-amino alcohols and their application in the catalytic asymmetric sulfoxidation of sulfides. Tetrahedron Asymmetry 24:444–448. https://doi.org/10.1016/j.tetasy.2013.03.011
47. Khomenko TM, Salomatina OV, Kurbakova SY, Il'ina IV, Volcho KP, Komarova NI, Korchagina DV, Salakhutdinov NF, Tolstikov AG (2006) New chiral ligands from myrtenal and caryophyllene for asymmetric oxydation of sulfides catalyzed by metal complexes. Russ J Org Chem 42. https://doi.org/10.1134/s1070428006110091
48. Kuchin AV, Ashikhmina EV, Rubtsova SA, Dvornikova IA (2010) Terpene ligands as the basis of catalytic systems for the asymmetric oxidation of phenylphenacyl sulfide. Russ J Bioorganic Chem 36:877–883. https://doi.org/10.1134/S1068162010070150
49. Koneva EA, Volcho KP, Korchagina DV, Komarova NI, Kochnev AI, Salakhutdinov NF, Tolstikov AG (2008) New chiral Schiff bases derived from (+)- and (−)-α-pinenes in the metal complex catalyzed asymmetric oxidation of sulfides. Russ Chem Bull 57:108–117. https://doi.org/10.1007/s11172-008-0017-8

50. Chuo TH, Boobalan R, Chen C (2016) Camphor-based schiff base of 3-endo-aminoborneol (SBAB): novel ligand for vanadium-catalyzed asymmetric sulfoxidation and subsequent kinetic resolution. ChemistrySelect 1:2174–2180. https://doi.org/10.1002/slct.201600379
51. Yin D, Tan R, Li C, Peng Z, Yin D (2011) Preparation of chiral oxovanadium (IV) Schiff base complex functionalized by ionic liquid for enantioselective oxidation of methyl aryl sulfides. Catal Commun 12:1488–1491. https://doi.org/10.1016/j.catcom.2011.06.006
52. Lazar A, Sharma P, Singh AP (2013) Chiral VIVO-Sal-Indanol complex over modified SBA-15: an efficient, reusable enantioselective catalyst for asymmetric sulfoxidation reaction. Microporous Mesoporous Mater 170:331–339. https://doi.org/10.1016/j.micromeso.2012.12.014
53. Sandel S, Weber SK, Trapp O (2012) Oxidations with bonded salen-catalysts in microcapillaries. Chem Eng Sci 83:171–179. https://doi.org/10.1016/j.ces.2011.10.034
54. Shen C, Qiao J, Zhao L, Zheng K, Jin J, Zhang P (2017) An efficient silica supported Chitosan@vanadium catalyst for asymmetric sulfoxidation and its application in the synthesis of esomeprazole. Catal Commun 92:114–118. https://doi.org/10.1016/j.catcom.2017.01.018
55. Dai W, Li J, Chen B, Li G, Lv Y, Wang L, Gao S (2013) Asymmetric oxidation catalysis by a porphyrin-inspired manganese complex: highly enantioselective sulfoxidation with a wide substrate scope. Org Lett 15:5658–5661. https://doi.org/10.1021/ol402612x
56. Dai W, Shang S, Lv Y, Li G, Li C, Gao S (2017) Highly chemoselective and enantioselective catalytic oxidation of heteroaromatic sulfides via high-valent manganese(IV)-oxo cation radical oxidizing intermediates. ACS Catal 7:4890–4895. https://doi.org/10.1021/acscatal.7b00968
57. Dai W, Mi Y, Lv Y, Chen B, Li G, Chen G, Gao S (2016) Development of a continuous-flow microreactor for asymmetric sulfoxidation using a biomimetic manganese catalyst. Adv Synth Catal 358:667–671. https://doi.org/10.1002/adsc.201501023
58. Zhang Z, Guan F, Huang X, Wang Y, Sun Y (2012) New ternary immobilization of chiral sulfonato-(salen)manganese(III) complex for aqueous asymmetric oxidation reactions. J Mol Catal A: Chem 363–364:343–353. https://doi.org/10.1016/j.molcata.2012.07.010
59. Chen X, Peng Y, Han X, Liu Y, Lin X, Cui Y (2017) Sixteen isostructural phosphonate metal-organic frameworks with controlled Lewis acidity and chemical stability for asymmetric catalysis. Nat Commun 8:1–9. https://doi.org/10.1038/s41467-017-02335-0
60. Stingl KA, Weiß KM, Tsogoeva SB (2012) Asymmetric vanadium- and iron-catalyzed oxidations: new mild (R)-modafinil synthesis and formation of epoxides using aqueous H_2O_2 as a terminal oxidant. Tetrahedron 68:8493–8501. https://doi.org/10.1016/j.tet.2012.07.052
61. Bera PK, Kumari P, Abdi SHR, Khan NUH, Kureshy RI, Subramanian PS, Bajaj HC (2014) In situ-generated chiral iron complex as efficient catalyst for enantioselective sulfoxidation using aqueous H_2O_2 as oxidant. RSC Adv 4:61550–61556. https://doi.org/10.1039/c4ra09237f
62. Nishiguchi S, Izumi T, Kouno T, Sukegawa J, Ilies L, Nakamura E (2018) Synthesis of esomeprazole and related proton pump inhibitors through iron-catalyzed enantioselective sulfoxidation. ACS Catal 9738–9743. https://doi.org/10.1021/acscatal.8b02610
63. Le Maux P, Simonneaux G (2011) First enantioselective iron-porphyrin-catalyzed sulfide oxidation with aqueous hydrogen peroxide. Chem Commun 47:6957–6959. https://doi.org/10.1039/c1cc11675d
64. Srour H, Jalkh J, Le Maux P, Chevance S, Kobeissi M, Simonneaux G (2013) Asymmetric oxidation of sulfides by hydrogen peroxide catalyzed by chiral manganese porphyrins in water/methanol solution. J Mol Catal A: Chem 370:75–79. https://doi.org/10.1016/j.molcata.2012.12.016
65. Shen HM, Ji HB (2012) Amino alcohol-modified β-cyclodextrin inducing biomimetic asymmetric oxidation of thioanisole in water. Carbohydr Res 354:49–58. https://doi.org/10.1016/j.carres.2012.03.034
66. Carrasco CJ, Montilla F, Galindo A (2016) Molybdenum-catalyzed asymmetric sulfoxidation with hydrogen peroxide and subsequent kinetic resolution, using an imidazolium-based dicarboxylate compound as chiral inductor. Catal Commun 84:134–136. https://doi.org/10.1016/j.catcom.2016.06.021

67. Carrasco CJ, Montilla F, Galindo A (2018) Molybdenum-catalyzed enantioselective sulfoxidation controlled by a nonclassical hydrogen bond between coordinated chiral imidazolium-based dicarboxylate and peroxido ligands. Molecules 23:1595. https://doi.org/10.3390/molecules23071595
68. Zong L, Wang C, Moeljadi AMP, Ye X, Ganguly R, Li Y, Hirao H, Tan CH (2016) Bisguanidinium dinuclear oxodiperoxomolybdosulfate ion pair-catalyzed enantioselective sulfoxidation. Nat Commun 7:1–7. https://doi.org/10.1038/ncomms13455
69. O'Mahony GE, Ford A, Maguire AR (2012) Copper-catalyzed asymmetric oxidation of sulfides. J Org Chem 77:3288–3296. https://doi.org/10.1021/jo2026178
70. O'Mahony GE, Eccles KS, Morrison RE, Ford A, Lawrence SE, Maguire AR (2013) Investigation of steric and electronic effects in the copper-catalysed asymmetric oxidation of sulfides. Tetrahedron 69:10168–10184. https://doi.org/10.1016/j.tet.2013.08.063
71. Tanaka K, Oda S, Shiro M (2008) A novel chiral porous metal-organic framework: asymmetric ring opening reaction of epoxide with amine in the chiral open space. Chem Commun 820–822. https://doi.org/10.1039/b714083e
72. Tanaka K, Kubo K, Iida K, Otani KI, Murase T, Yanamoto D, Shiro M (2013) Asymmetric catalytic sulfoxidation with H_2O_2 using chiral copper metal-organic framework crystals. Asian J Org Chem 2:1055–1060. https://doi.org/10.1002/ajoc.201300140
73. Wang Y, Li H, Qi W, Yang Y, Yan Y, Li B, Wu L (2012) Supramolecular assembly of chiral polyoxometalate complexes for asymmetric catalytic oxidation of thioethers. J Mater Chem 22:9181–9188. https://doi.org/10.1039/c2jm16398e
74. Ye X, Moeljadi AMP, Chin KF, Hirao H, Zong L, Tan CH (2016) Enantioselective sulfoxidation catalyzed by a bisguanidinium diphosphatobisperoxotungstate ion pair. Angew Chemie—Int Ed 55:7101–7105. https://doi.org/10.1002/anie.201601574
75. Yamaguchi T, Matsumoto K, Saito B, Katsuki T (2007) Asymmetric oxidation catalysis by a chiral Al (salalen) complex: highly enantioselective oxidation of sulfides with aqueous hydrogen peroxide. Angew Chemie—Int Ed 46:4729–4731. https://doi.org/10.1002/anie.200700792
76. Fujisaki J, Matsumoto K, Matsumoto K, Katsuki T (2011) Catalytic asymmetric oxidation of cyclic dithioacetals: Highly diastereo- and enantioselective synthesis of the S-oxides by a chiral aluminum(salalen) complex. J Am Chem Soc 133:56–61. https://doi.org/10.1021/ja106877x
77. Stingl KA, Tsogoeva SB (2010) Recent advances in sulfoxidation reactions: a metal-free approach. Tetrahedron Asymmetry 21:1055–1074. https://doi.org/10.1016/j.tetasy.2010.05.020
78. Liu ZM, Zhao H, Li MQ, Lan YB, Yao QB, Tao JC, Wang XW (2012) Chiral phosphoric acid-catalyzed asymmetric oxidation of aryl alkyl sulfides and aldehyde-derived 1,3-dithianes: using aqueous hydrogen peroxide as the terminal oxidant. Adv Synth Catal 354:1012–1022. https://doi.org/10.1002/adsc.201100810
79. Jindal G, Sunoj RB (2014) Axially chiral imidodiphosphoric acid catalyst for asymmetric sulfoxidation reaction: insights on asymmetric induction. Angew Chemie—Int Ed 53:4432–4436. https://doi.org/10.1002/anie.201309532
80. Sunoj RB (2016) Transition state models for understanding the origin of chiral induction in asymmetric catalysis. Acc Chem Res 49:1019–1028. https://doi.org/10.1021/acs.accounts.6b00053
81. Liao S, Čorić I, Wang Q, List B (2012) Activation of H_2O_2 by chiral confined Brønsted acids: a highly enantioselective catalytic sulfoxidation. J Am Chem Soc 134:10765–10768. https://doi.org/10.1021/ja3035637
82. Jurok R, Cibulka R, Dvořáková H, Hampl F, Hodačová J (2010) Planar chiral flavinium salts—prospective catalysts for enantioselective sulfoxidation reactions. Eur J Org Chem 5217–5224. https://doi.org/10.1002/ejoc.201000592
83. Jurok R, Hodačová J, Eigner V, Dvořáková H, Setnička V, Cibulka R (2013) Planar chiral flavinium salts: synthesis and evaluation of the effect of substituents on the catalytic efficiency in enantioselective sulfoxidation reactions. Eur J Org Chem 7724–7738. https://doi.org/10.1002/ejoc.201300847

84. Mojr V, Herzig V, Budíšnský M, Cibulka R, Kraus T (2010) Flavin-cyclodextrin conjugates as catalysts of enantioselective sulfoxidations with hydrogen peroxide in aqueous media. Chem Commun 46:7599–7601. https://doi.org/10.1039/c0cc02562c
85. Tanaka H, Nishikawa H, Uchida T, Katsuki T (2010) Photopromoted Ru-catalyzed asymmetric aerobic sulfide oxidation and epoxidation using water as a proton transfer mediator. J Am Chem Soc 132:12034–12041. https://doi.org/10.1021/ja104184r
86. Uchida T, Katsuki T (2013) Green asymmetric oxidation using air as oxidant. J Synth Org Chem Jpn 71:1126–1135. https://doi.org/10.5059/yukigoseikyokaishi.71.1126
87. Koya S, Nishioka Y, Mizoguchi H, Uchida T, Katsuki T (2012) Asymmetric epoxidation of conjugated olefins with dioxygen. Angew Chemie—Int Ed 51:8243–8246. https://doi.org/10.1002/anie.201201848

Chapter 5
Non-covalent Organocatalytic Approach in the Asymmetric Epoxidation of Electron-Poor Alkenes: Recent Developments

Alessandra Lattanzi

Abstract Chiral non-racemic epoxides are often endowed with important biological activities, but most of all, they are fundamental building blocks, frequently involved in the synthesis of natural and non-natural products, drugs and agrochemicals. Indeed, a great variety of functionalizations are achievable via ring-opening reactions of epoxides, where two contiguous stereocenters are fixed with predictable regio- and stereochemistry. It is not surprising that over the years synthetic chemists focused their interest in the development of new methodologies based on the asymmetric epoxidation of alkenes, as the most straightforward and convenient route to obtain epoxides. Unsurprisingly, this area has matured, gradually increasing the attention to environmental concerns, availability of the catalysts to use under homogeneous and heterogenous versions, suitable for recycling. This chapter collects the developments in asymmetric epoxidation of electron-poor alkenes, mediated by small organic molecules able to activate the reagents via non-covalent interactions, reported since 2010. Epoxidation reactions mediated by peptides have been recently reviewed and will be not included. The chapter has been divided into two sections, according to the nature of the organocatalysts used to promote the epoxidation. The sections deal successively with stereoselective epoxidation reactions promoted by phase-transfer catalysts and bifunctional/multifunctional organocatalysts.

Keywords Asymmetric epoxidation · Stereoselective organocatalysis · Bifunctional organocatalysts · Phase-transfer catalysis · Electron-poor alkenes

Abbreviations

CHP	Cumene hydroperoxide
DFT	Density functional theory

A. Lattanzi (✉)
Dipartimento di Chimica e Biologia, Università di Salerno, Via Giovanni Paolo II, 132, 84084 Fisciano, Italy
e-mail: lattanzi@unisa.it

K. P. Bryliakov (ed.), *Frontiers of Green Catalytic Selective Oxidations*, Green Chemistry and Sustainable Technology,
https://doi.org/10.1007/978-981-32-9751-7_5

NMR Nuclear magnetic resonance
PTC Phase-transfer catalysis
TBHP *tert*-Butyl hydroperoxide
TEMPO 2,2,6,6-Tetramethyl-1-piperidinyloxy, free radical
TON Turnover numbers

5.1 Introduction

A consistent part of asymmetric transformations applied in organic synthesis [1] relies on metal and more recently organocatalysed epoxidations, which have the advantage to use readily available feedstocks, including the oxygen sources such as hydrogen peroxide, molecular oxygen and *tert*-butyl hydroperoxide (TBHP) [2–5]. The application of enzymatic catalysis is also a useful tool to achieve this goal, although the efficiency and the level of enantioselectivity show a substrate-dependence, thus limiting the successful application to specific cases [6, 7].

Among the variety of oxidation reactions, the preparation of chiral non-racemic epoxides represents a milestone in organic synthesis. Epoxides are among the most important heterocycles, being reactive key intermediates in several total syntheses of natural and non-natural compounds, pharmaceuticals, agrochemicals and small highly functionalized compounds [8, 9]. Optically active epoxides are also endowed with different biological activities, which are often the result of inhibition of enzymes, due to the formation of a covalent bond via ring-opening reactions of the oxirane with nucleophilic groups present in the active site. As an example, (−)-depudecin, featuring a bis-epoxy alcohol fragment, first isolated by a fungus, showed to have selective inhibition of histone deacetylases I and II, thus gaining notable interest as an antitumor agent (Scheme 5.1) [10].

Other well known examples of active drugs against breast, lung and prostate cancers, featuring at least an optically active epoxide structural unit, are epothilones and ovalicin [11].

The beginning of popularity and importance of chiral non-racemic oxiranes can be dated back to 1980, when the first breakthrough was reported by Katsuki and Sharpless [12]. The asymmetric titanium-tartrate based epoxidation of allylic alco-

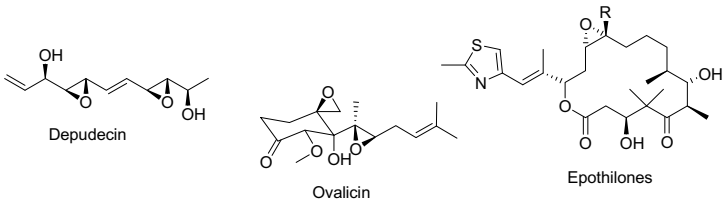

Scheme 5.1 Representative bioactive epoxides

hols provides a practical, convenient and general methodology extensively applied, with reliable stereochemical confidence, in both academia and industry [13]. Other fundamental metal-based systems were developed thereafter by Katsuki [14], Jacobsen [15], Yamamoto [16] and Shibasaki [17] for the asymmetric epoxidation of a great variety of alkenes, comprising challenging *cis*-alkenes with high efficiency and level of enantioselectivity. General organocatalytic systems for the stereoselective epoxidation of alkenes have been developed by Shi, via sugar-derived dioxiranes, which can be applied with success to *E*-di, *Z*-di-, tri-, tetrasubstituted and terminal alkenes [18].

The area of asymmetric epoxidation of alkenes [19] can be roughly divided into two sections: (i) nucleophilic systems for the epoxidation of electron-poor alkenes, (ii) electrophilic systems for the epoxidation of alkenes. The asymmetric organocatalytic epoxidation of electron-poor alkenes received a lot of attention over the last decades as a convenient tool to prepare functionalized epoxides, which serve as valuable intermediates for further manipulations either at the epoxide and the electron-withdrawing groups [20, 21]. The organocatalytic epoxidation is additionally partitioned in (i) covalent activation of the alkene, via formation of an intermediate iminium ion with the secondary or primary amine catalyst; (ii) non-covalent activation of the alkene and the oxygen source via ion-pairing/hydrogen-bonding interactions. The covalent activation of reagents has been significantly explored since 2005, achieving great advances in the stereoselective synthesis of epoxides starting from readily available α,β-unsaturated aldehydes and ketones. These developments have been recently reviewed and will not be included [19, 22].

In this chapter, advances in the asymmetric epoxidation of electron-poor alkenes will be described, where ion-pairing/hydrogen-bonding interactions is the key-activation strategy exploited in the oxidation. Examples, collected from the literature since 2010, will be illustrated.

5.2 Phase-Transfer Catalysis

In the area of organocatalytic methods for the asymmetric epoxidation of electron-poor alkenes, a central role is played by phase-transfer catalysis (PTC) [19, 23]. The epoxidation reactions are generally performed under mild conditions, using catalytic loadings of readily available or commercially available quaternary ammonium salts, often derived from natural sources. Moreover, hydrogen peroxide is often the most effective and cheap oxidant, being not particularly aggressive, with good atom-efficiency, providing harmless side-products. All these features make the PTC, a welcome tool also for industrial applications.

In 1976, Wynberg reported the asymmetric epoxidation of enones, promoted by quinine and quinidine-derived quaternary ammonium salts, hydrogen peroxide as the oxidant under biphasic conditions (NaOH/toluene) [24]. This first example of PTC, useful to prepare enantioenriched epoxides, showcased the great potential of ammonium salts in the area of asymmetric epoxidation to prompt significant interest

and efforts in improving the stereocontrol and expanding the substrate scope [25, 26]. Over the years, structurally different ammonium salts were synthesized to develop highly enantioselective epoxidation protocols of *trans*-enones, which represented the focus of investigations, essentially aimed at checking the performance of newly designed organocatalysts (Scheme 5.2). Dimers of original *Cinchona*-derived quaternary ammonium salts were active at as low as 1 mol% loading and in the presence of surfactant [27]. PT catalysts bearing axial chirality, such as the well known Maruoka catalysts, provided the epoxides with excellent level of enantioselectivity [28].

Mixed ammonium salt/crown ethers or sugar-derived crown ethers could be also employed, providing direct transfer of the inorganic salt into the organic phase [29, 30]. More recently, besides the design of new PT catalysts, the attention has been also paid to expand the applicability of PTC to different classes of electron-poor alkenes.

In 2013, Shibata and co-authors illustrated an interesting process for the asymmetric epoxidation of the β,β-disubstituted enones bearing a β-trifluoromethyl group (Scheme 5.3) [31]. Readily available *Cinchona* alkaloids derived quaternary ammonium salt **1** was used at 5 mol% in the presence of methylhydrazine, an inorganic base and molecular oxygen as the terminal oxidant. Under these mild and convenient conditions, the corresponding challenging epoxides, bearing a quaternary stereocenter, were isolated in excellent yields, diastereo- and enantioselectivity (up to >99% ee). This reaction represents a first practical approach to optically pure CF_3-substituted epoxides, which can be important intermediates for the pharmaceutical industry.

Mechanistically, a single electron-transfer radical pathway has been suggested, where methylhydrazine is oxidized by molecular oxygen, affording H_2O_2 as the real in situ generated oxidant and producing methyl radicals (Scheme 5.4). When using isotopically labelled $^{18}O_2$, the incorporation of ^{18}O in the epoxides was almost quantitatively observed. Moreover, the epoxidation performed with 50% H_2O_2 as

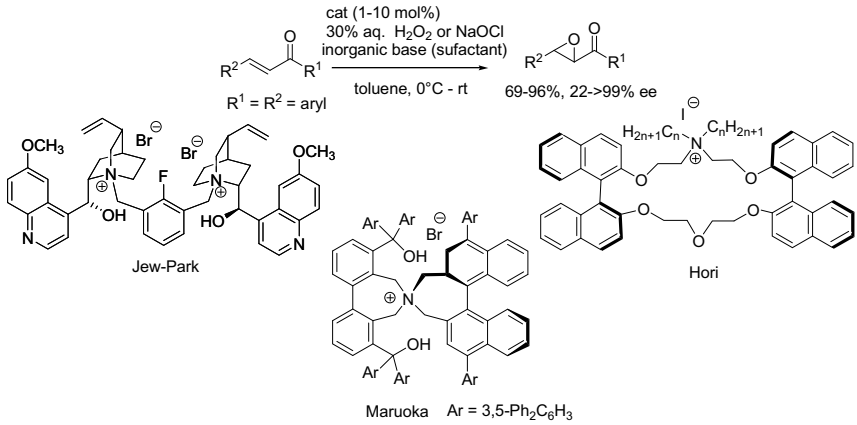

Scheme 5.2 Most effective PT catalysts used in the asymmetric epoxidation of *trans*-enones

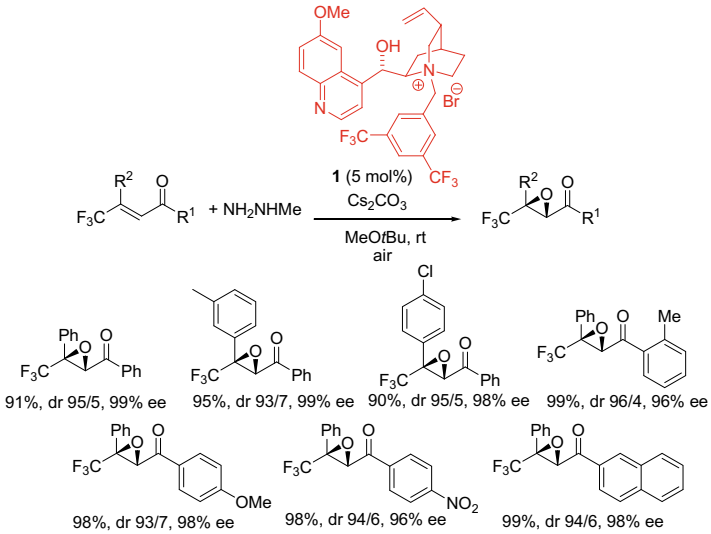

Scheme 5.3 PT catalysed asymmetric epoxidation of β,β-disubstituted enones under air

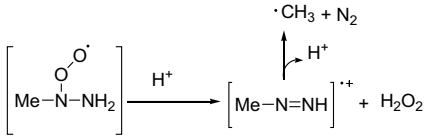

Scheme 5.4 Principal radical intermediates proposed to be involved in the process

the oxidant afforded the product with the same level of enantioselectivity, although in lower yield.

When the radical scavenger TEMPO was added, the *O*-methylated TEMPO was detected, confirming the involvement of methyl radical species in the reaction mixture.

Concurrently, the group of Chen disclosed a similar system for the asymmetric epoxidation of β-trifluoromethyl-β,β-disubstituted unsaturated ketones, by using 30% H_2O_2 as the oxidant and 50% KOH as base in the presence of 3 mol% loading of a pentafluorine-substituted *Cinchona* alkaloids derived quaternary ammonium salt **2** (Scheme 5.5) [32]. The epoxides were obtained in good to high yields, excellent diastereoselectivity and ee values. Aliphatic groups at the β-position of the enones were tolerated, although the level of enantioselectivity achieved was up to 82% ee. Gram-scale application demonstrated to be a feasible process, with the epoxide being obtained with the same stereocontrol. Interestingly, the epoxidation carried out on model Z-enone afforded the epoxide in stereospecific manner and 99% ee. Moreover, functionalized trifluoromethylated alcohols could be obtained by reductive ring-opening reaction with maintained ee values.

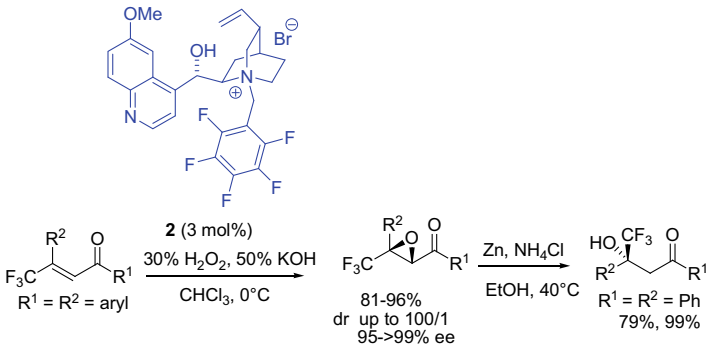

Scheme 5.5 Alternative system for the PT catalysed asymmetric epoxidation of β,β-disubstituted enones

These ketoalcohols are valuable building blocks to prepare biologically active compounds. Concerning the activation of reagents, a crucial role of the free OH group in the organocatalyst was attested by the inactivity demonstrated in the epoxidation by the *O*-benzylated analogues. π–π Interactions were also invoked to be active in the stereocontrol.

More recently, a supported version of catalyst **1** has been prepared by Liu et al. through a thiol-ene click reaction with mesostructured silica and employed in a one-pot procedure to ketoalcohols [33]. Conditions reported in Scheme 5.3 were applied to a variety of β-trifluoromethyl-β,β-disubstituted unsaturated ketones to prepare epoxides, followed by the addition of Zn/NH_4Cl and EtOH in a one-pot fashion. A straightforward synthesis of highly enantiomerically enriched ketoalcohols was thus developed. The heterogeneous catalyst could be readily recovered by centrifugation and recycled for up to eight reactions with a good performance in terms of yield and stereoselectivity (91% yield, 95% ee for the last run).

Jeong and Park applied a similar *O*-allyl protected *Cinchona* alkaloids derived quaternary ammonium salt **3** at 5 mol% loading in the highly enantioselective asymmetric epoxidation of *trans*-chalcones, using an aqueous solution of NaOCl in toluene at 0 °C (Scheme 5.6) [34]. The *trans*-epoxides were recovered in good to high yields

Scheme 5.6 PT catalysed asymmetric epoxidation of *trans*-chalcones by *O*-protected *Cinchona* alkaloids derived ammonium salt

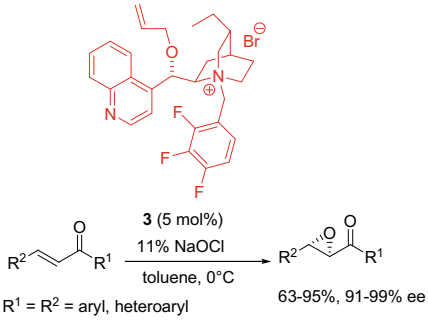

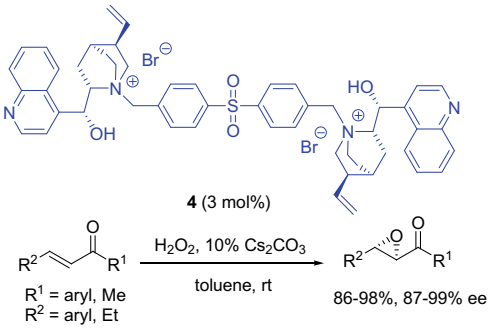

Scheme 5.7 PT catalysed asymmetric epoxidation of *trans*-chalcones by dimeric *Cinchona* alkaloids derived ammonium salt

and excellent ee values. It is interesting to note that the presence of fluorine atoms in the benzyl moiety on nitrogen appears to be important to achieve good results.

The same process was demonstrated to be efficiently catalysed by a dimeric quaternary ammonium salt **4** with hydrogen peroxide as the oxidant and aqueous Cs_2CO_3 at room temperature (Scheme 5.7) [35]. Under mild reaction conditions, the epoxides were recovered with high yields and enantioselectivity.

From all the data concerning the *Cinchona* alkaloids derived ammonium salts mediated epoxidation reactions, it comes out that when the C9 free OH group is present in the catalyst, the highest ee values are achieved using hydrogen peroxide as the oxidant, whereas in the presence of the corresponding *O*-protected ammonium salt, bleach is the best oxygen source.

A useful recent one-pot application of the asymmetric epoxidation of *trans*-chalcones catalysed by the Lygo-Corey system [36, 37], has been illustrated for the preparation of enantioenriched γ-butenolides [38], important subunits present in natural products and bioactive compounds [39].

A first example of an asymmetric catalytic epoxidation of nitroalkenes to nitroepoxides has been recently reported by González and co-authors, using the *Cinchona* alkaloids derived PT catalyst **5** and bleach as the oxidant, working at low temperature in toluene (Scheme 5.8) [40].

The epoxidation of nitroalkenes to chiral non-racemic nitroepoxides has always been a challenging goal, due to the high reactivity of nitroalkenes as Michael acceptors and their propensity to undergo polymerization as side reaction. Nitroepoxides are interesting intermediates, amenable of further ring-opening and elaboration reactions to α-functionalized carbonyl compounds [41], 1,2-diamines [42], heterocycles [43]. The mild reaction conditions enabled the preparation of mostly α-methyl β-aryl-substituted nitroepoxides in good to high yields and good to high ee values. The protocol is not effective with β-alkyl-substituted nitroalkenes, which reacted sluggishly and with poor enantiocontrol. A DFT study of the process suggested that the antracenyl portion of the catalyst would be important to establish π–π-interactions with the aryl group of the nitroalkene, whereas the free OH group of the organocatalyst would be involved in H-bonding interaction with the ClO^- anion, directing the

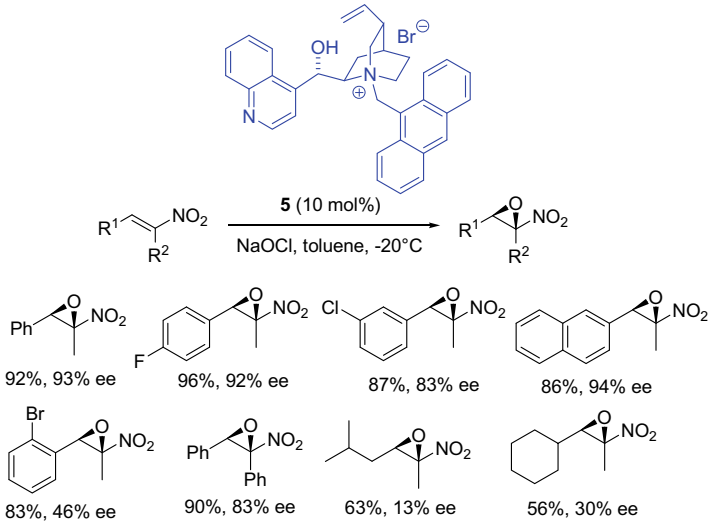

Scheme 5.8 PT catalysed asymmetric epoxidation of nitroalkenes

face-selectivity. Within this framework, the lack of enantiocontrol observed when a β-alkyl group was present in the nitroalkene, would be rationalized.

5.3 Bifunctional/Multifunctional Organocatalysts

5.3.1 L-*Diaryl Prolinols as Organocatalysts*

Commercially or readily available L-diaryl prolinols, are small bifunctional organic molecules, embedding a β-aminoalcohol portion, in analogy to popular *Cinchona* alkaloids, where a tertiary amine is present instead of a secondary amine group. Highly popular Hayashi–Jørgensen catalyst, the L-diphenyl prolinol bearing the trimethylsilyl protected OH group, has been extensively used in covalent activation of aldehydes via formation of enamine/iminium intermediates [44]. L-diphenyl prolinol **6a** and other aryl-substituted derivatives were found to be able to provide general acid–base activation of reagents, in analogy to the well known behaviour displayed by *Cinchona* alkaloids [45]. This additional catalytic ability has been usefully applied in organocatalysis for the stereoselective carbon–carbon and carbon-heteroatom bonds formation [46].

In 2005, the L-diphenyl prolinol **6a**/*tert*-butyl hydroperoxide (TBHP) system was disclosed by Lattanzi for the asymmetric epoxidation of *trans*-enones in hexane as the solvent [47]. This simple protocol was successively improved in terms of efficiency and investigated by the same and other groups in the epoxidation of electron-poor

alkenes [45, 46]. The non-covalent general acid–base activation of the reactive partners was supported by experimental and DFT studies [48]. This and related systems proved to be of wider applicability in the asymmetric epoxidation of uncommon and less-investigated trisubstituted electron-poor alkenes (Scheme 5.9). L-prolinols **6b** or **6c**/TBHP or CHP system turned out to be useful for the enantioselective epoxidation of 2-arylidene-1,3-diketones, achieving good ee values for the epoxides, improved to >90% ee by a single crystallization [49]. Optically enriched spiroepoxides, derived

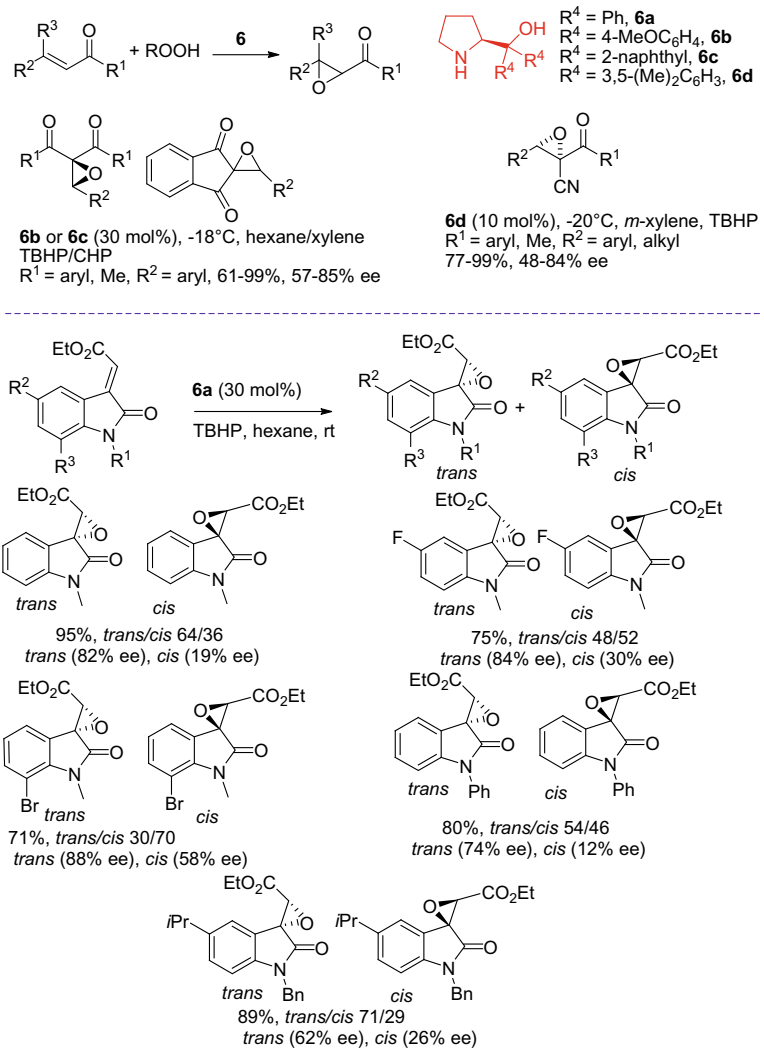

Scheme 5.9 Asymmetric epoxidation of trisubstituted electron-poor alkenes with the diaryl prolinols/TBHP system

from alkyliden-1,3-indandiones, were used as the synthetic precursors of a potent inhibitors series of the human papillomavirus HPV11 E1-E2 protein-protein interaction [50].

The epoxidation of *trans*-2-aroyl-3-substituted acrylonitriles was investigated by the same group, using catalyst **6d** at 10 mol% loading in *m*-xylene at −20 °C (Scheme 5.9) [51]. The epoxides, bearing contiguous tertiary and quaternary stereocenters, were isolated in high yields, complete *trans*-diastereoselectivity and good enantioselectivity, easily improved to excellent level by crystallization. A controlled reduction of the enantioenriched epoxides to *anti*-allylic alcohols was demonstrated to be an alternative route to the direct Sharpless asymmetric epoxidation of poorly reactive 2-cyano allylic alcohols mediated by the Ti/tartrate/TBHP system [52].

Finally, the asymmetric epoxidation of α-ylideneoxindoles esters was studied by Gasperi and co-workers, using the **6a**/TBHP system in hexane to give functionalized spirocyclic oxiranes in good yields as a mixture of *trans*- and *cis*-isomers (Scheme 5.9) [53]. Modest to good enantiocontrol was observed for the *trans*-epoxides, whereas only modest ee values were achieved for the *cis*-epoxides. The presence of *cis*-diastereoisomer can be justified according to the stepwise Weitz–Scheffer mechanism of the nucleophilic epoxidation (Scheme 5.10).

After the first oxa-Michael addition step, the peroxy enolate intermediate would give ring closure at significantly lower rate, to compete with the carbon–carbon bond rotation, to justify the presence of the *cis*-epoxide. Moreover, the presence of halogen substituents on the aromatic ring would compete for H-bonding interactions with the organocatalyst, significantly affecting the *trans*/*cis* ratio.

An unusual oxidative approach to optically enriched α,β-epoxy ketones has been reported by Siva and co-authors, reacting terminal alkenes, aryl aldehydes and TBHP in the presence of a catalytic loading of a bifunctional C_3-symmetric catalyst **7**, derived from L-proline (Scheme 5.11) [54]. The epoxide formation is the result of a C–H functionalisation and C–C/C–O bond formation cascade process.

Different styrenes and aromatic aldehydes were converted at room temperature to the corresponding α,β-epoxyketones in good to high yields and enantioselectivity. The reaction performed on an aliphatic aldehyde was much less productive, showing a modest conversion as well as ee value for the final epoxide. The authors suggested a radical mechanism for the epoxidation, where *tert*-butoxy radicals, formed by a non-catalytic bond homolysis, would be involved to produce acyl radicals of aldehydes, which then would couple with styrenes to give benzyl-type radicals (Scheme 5.12). The following coupling with *tert*-butylperoxy radicals produces mixed peroxides. At this stage, the organocatalyst should abstract the α-proton and the carbon radical

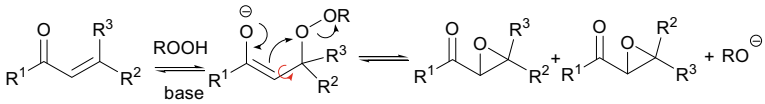

Scheme 5.10 Weitz–Scheffer mechanism for the epoxidation of electron-poor alkenes

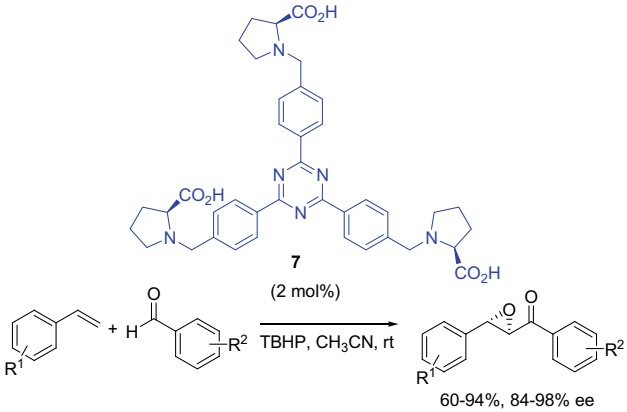

Scheme 5.11 Asymmetric cascade oxidative coupling to α,β-epoxy ketones catalysed by a C_3-symmetric proline-derived organocatalyst

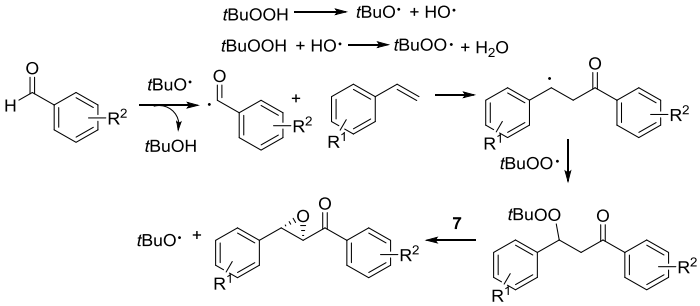

Scheme 5.12 Radical oxidative mechanism of the epoxidation

would proceed, in a chiral environment, to ring closure with elimination of the *tert*-butoxy radical and formation of the optically active epoxy ketone.

Although the role of the organocatalyst remains unclear, this process appears to be a simple and alternative approach to obtain epoxyketones, starting from readily available styrenes and aryl aldehydes.

5.3.2 Thiourea-Amines as Organocatalysts

Bifunctional thiourea-amines and simple thioureas have been introduced in organocatalysis back in 2003 by the groups of Takemoto [55] and Schreiner [56]. Thereafter, an incredible number of examples of stereoselective methods have been

developed for the formation of carbon–carbon and carbon-heteroatom bonds, including cascade processes leading to a convenient synthesis of highly functionalized carbo- and heterocycles [57, 58]. The thiourea moiety in the organocatalyst was suggested to behave like a Lewis acid, complexing the electrophile, generally carbonyl compounds or nitroalkenes, via a double H-bonding interaction. The amine group serves as a useful hand for general base catalysis, involved in the activation of a variety of pronucleophiles. The bifunctionality of thiourea-amines opened the door to effective catalysis of several simple and more sophisticated reactions in organic chemistry.

In the area of oxidation reactions, the first concern for their employment was to check the stability under oxidative conditions of thioureas. A first idea came from the use of bis-3,5-trifluoromethyl phenyl thiourea (Schreiner's catalyst) in sulphides catalysed oxidation to sulfoxides at 1 mol% loading at room temperature with TBHP as the oxidant [59]. The performance was found to be comparable in TON (turnover numbers), to that of well known metal-catalysts used for this process and catalyst's degradation found to be a negligible side reaction. The area of asymmetric organocatalysed epoxidation of electron-poor alkenes, exploiting a non-covalent activation of the reagents was soon after investigated, showing the applicability of thiourea-amines in asymmetric oxidation reactions.

Terminal epoxides are likely the most useful intermediates in synthetic applications, thanks to the high regioselectivity achievable in ring-opening reactions with different nucleophiles. The most commonly used and available *Cinchona* alkaloids derived thioureas were reported by Lattanzi and co-authors to be competent organocatalysts in the first enantioselective epoxidation of α-aroyl acrylamides with TBHP (Scheme 5.13) [60]. The reaction proceeded at room temperature in toluene with 5 mol% of catalyst **8**, affording the epoxides, bearing a quaternary stereocen-

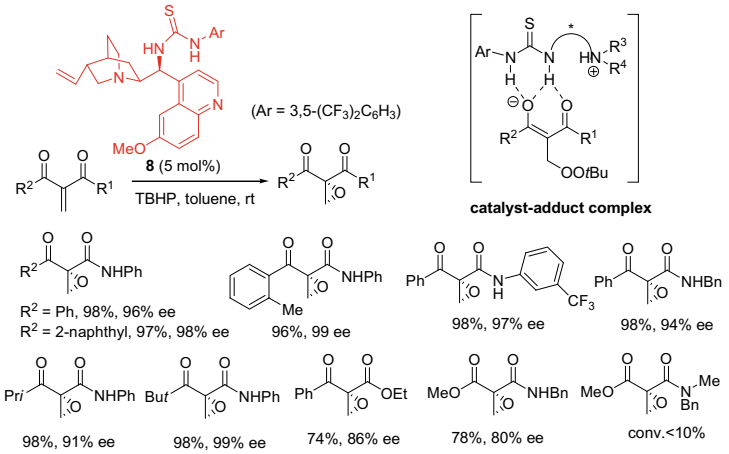

Scheme 5.13 *Cinchona* alkaloids derived thiourea catalysed enantioselective epoxidation of α-aroyl acrylamides and acrylates

ter in excellent yield and high to excellent enantioselectivity. The presence of the secondary amide in the alkene was important for fast conversion to the product, as it would contribute to organize the catalyst-reagent complex, associated through H-bonding interactions. Indeed, when a tertiary amide group was inserted in the alkene, a complete lack of reactivity was observed.

In contrast to typical nucleophilic epoxidation reactions, the stereogenic centre was formed in the second step of the Weitz–Scheffer mechanism (Scheme 5.10), where the ring closure would occur preferentially in a catalyst adduct-complex to give the enantioenriched epoxide. The formation of the peroxy adduct was detected by NMR spectroscopy. The highly regioselective ring-opening of the optically active epoxides with thiol and azide nucleophiles to prepare functionalized derivatives was demonstrated.

Natural spiroepoxides, including fumagillin [61], luminacin D [62] and FR901464, [63] show potent antibiotic, antiangiogenic and anticancer activities. Catalytic methods to optically active spiroepoxides, based on the epoxidation of alkenes, are quite limited and essentially restricted to spiro-epoxyoxindoles [53, 64]. 4-Spiro-5-pyrazolones are heterocycles of interest as agrochemicals and in medicinal chemistry [65].

The first asymmetric synthesis of spiropyrazolone epoxides has been based on the organocatalytic epoxidation of unsaturated pyrazolones as reported by Lattanzi and co-workers (Scheme 5.14) [66]. The easily available thiourea-amine **9**/TBHP system afforded a variety of *trans*-spiroepoxides with good diastereoselectivity and high ee

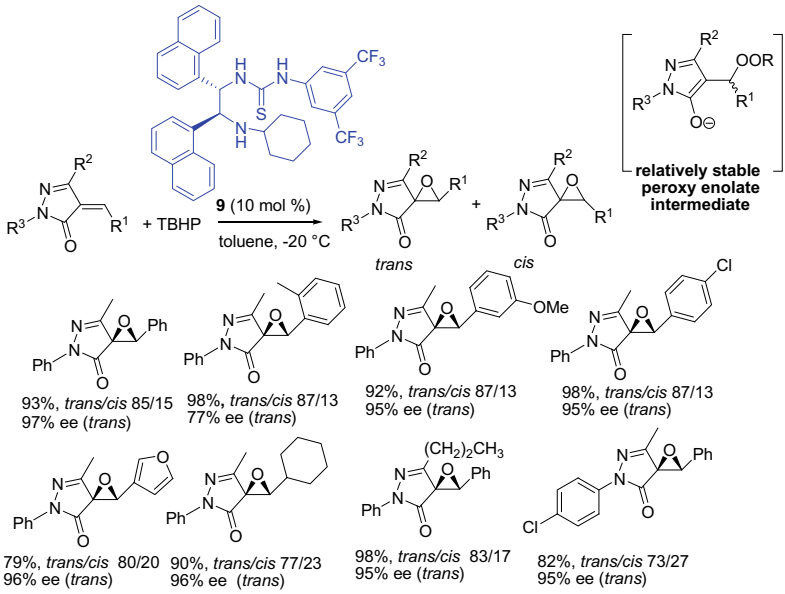

Scheme 5.14 1,2-dinaphthyl-1,2-diamine derived thiourea catalysed enantioselective epoxidation of unsaturated pyrazolones

values. Interestingly, a quinidine-derived thiourea was the most effective catalyst to produce the *cis*-spiroepoxides when working in trifluoromethyl benzene at room temperature achieving higher diastereocontrol and excellent level of enantioselectivity (96–99% ee). This work illustrated, for the first time, that when relatively stable peroxy enolate intermediates are involved in a nucleophilic epoxidation, a diastereodivergent process, leading to both diastereoisomeric epoxides in an enantioselective manner, can be developed by proper choice of the organocatalyst.

Alkylidene malononitriles are quite reactive Michael acceptors, but in contrast to carbonyl or nitro groups, the cyano moiety only moderately engages with H-bonding donors, thus restricting their application as reagents in stereoselective organocatalytic application.

Dicyanoepoxides are synthetic equivalents of dication ketenes and when are treated with binucleophilic diamines, bioactive heterocycles such as 3-substituted piperazin-2-ones are obtained [67].

Asymmetric epoxidation of these alkenes has been set-up by the same group, using multifunctional thiourea-amines derived from *Cinchona* alkaloids able to engage in larger network of hydrogen-bonding interactions with the alkene and the oxidant (Scheme 5.15) [68].

Quinine-derived thiourea **10**, bearing additional stereocenters and the OH donor group, was the most efficient organocatalyst in the presence of cumyl hydroperoxide (CHP) as the oxidant, providing the aryl-substituted epoxides in good yields and moderate to satisfactory level of enantioselectivity. Lower efficiency has been observed when reacting alkyl-substituted dicyanoalkenes. A one-pot procedure was also developed to directly obtain valuable enantioenriched 3-substituted piperazin-2-ones from alkylidenemalononitriles, adding diamines after the formation of the epoxides. Hence, a simple protocol to access substituted piperazin-2-ones, important

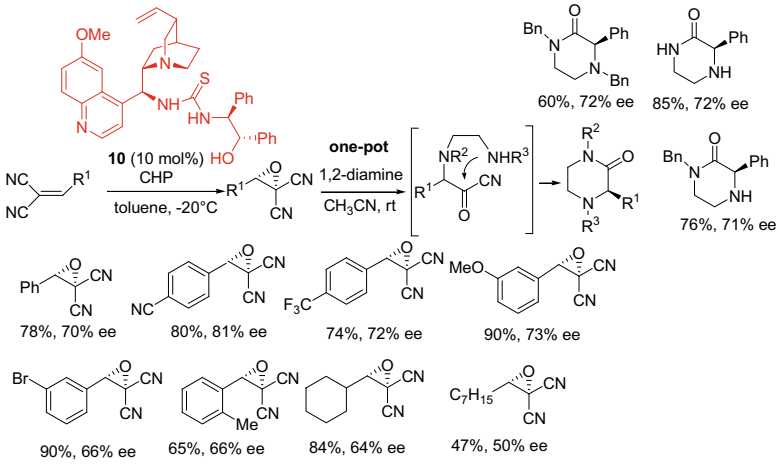

Scheme 5.15 *Cinchona* alkaloids derived multifunctional thiourea catalysed enantioselective epoxidation of alkylidenemalononitriles

pharmacophores, has been established. A one-pot procedure, starting from alkylidenemalononitriles, followed by the addition of diamines after the formation of the epoxides, furnished the heterocyclic compounds in good yields and maintained ee values.

The epoxidation would proceed through a ternary complex, where the alkene is H-bonded with thiourea and the OH groups, whereas the oxidant is strongly engaged in H-bonding interaction with the basic quinuclidine nitrogen (Scheme 5.16).

A similar *epi*-quinidine/dinaphthyl ethylenediamine derived thiourea **11**/TBHP system has been developed by the same group for the asymmetric epoxidation of *trans*-α-cyano-α,β-unsaturated esters (Scheme 5.17) [69]. The reaction proceeded

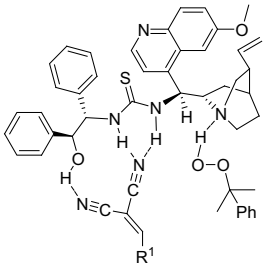

Scheme 5.16 Hypothetical pre-transition state for the asymmetric epoxidation of alkylidenemalononitriles

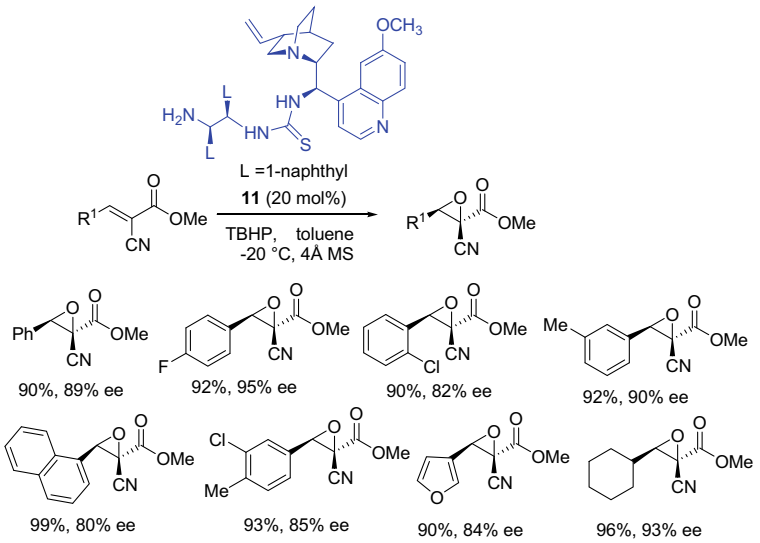

Scheme 5.17 *Cinchona* alkaloids derived multifunctional thiourea catalysed enantioselective epoxidation of *trans*-α-cyano-α,β-unsaturated esters

at −20 °C with 20 mol% loading of catalyst in toluene to give the aryl and alkyl-substituted glycidic esters in excellent yields and high enantioselectivity.

The role of the NH_2 group and well established thiourea groups in tuning the stereocontrol in the epoxidation might be justified with the involvement of additional H-bonding engagement with the cyano and ester groups of the alkene. This work highlights the utility of uncommon moieties such as primary amine groups as helpful donor–acceptor H-bonding sites to exploit in non-covalent organocatalysis. Indeed, their classical role is recognized in covalent activation of aldehydes and ketones, via formation of iminium/enamine intermediates.

Optically active cyanoglycidic esters showed to be of synthetic interest as illustrated by chemo- and regioselective elaborations to prepare small molecules, hard to access by alternative methods (Scheme 5.18).

Reduction with $NaBH_4$ chemoselectively yielded the model enantioenriched cyano epoxy alcohol, difficult to prepare via Sharpless Ti/tartrate mediated asymmetric epoxidation of cyano allylic alcohol. Hydrolysis of the cyano group and hydrogenation of the epoxide led to α,β-dihydroxy amide or ester, bearing a quaternary carbon stereocenter in good yield. Tosylation of the diol, followed by ring closure, afforded challenging epoxy methyl ester maintaining the initial ee value (89% ee). This terminal epoxide is a useful building block for the synthesis of a new class of HIV-1 protease inhibitors [70] and Bicalutamide-like molecules, active against prostate cancer cell lines [71].

Quinones are *cis*-alkenes, whose asymmetric epoxidation failed to achieve high stereocontrol, likely due to their rigid and symmetric shape, which makes the two faces of the olefin almost equivalent towards the attack of a chiral oxidative system [19]. Enantioselective protocols for the epoxidation of 1,4-naphthoquinones are highly desirable reactions to obtain optically active 1,4-naphthoquinone epoxides, which are useful intermediates for the synthesis of bioactive compounds. Literature

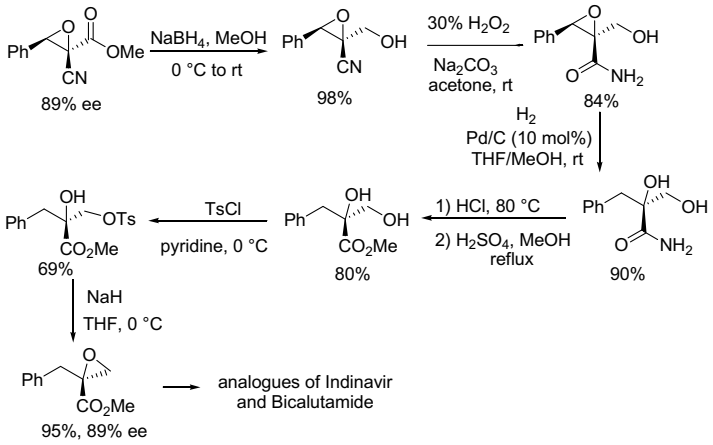

Scheme 5.18 Synthetic transformations of model glycidic methyl ester

precedents showed that PT catalysis could serve to prepare epoxide of vitamin K_3 (2-methyl-1,4-naphthoquinone) with up to 86% ee [72].

Recently, Nagasawa et al. reported a C_2-symmetric guanidine-bisurea organocatalyst **12**, active at 5 mol% loading in methyl *tert*-butyl ether/H_2O at 0 °C in the presence of TBHP as the oxidant and KOH as the inorganic base (Scheme 5.19) [73].

The same group previously showed that a similar organocatalyst was very effective for the asymmetric epoxidation of *trans*-chalcones [74]. Interestingly, the bifunctional hybrid catalyst **12** can activate the reagents via ionic interactions, typical of PT catalysis and hydrogen-bonding, displayed by thioureas and ureas. A variety of epoxides, bearing different alkyl moieties and electron-donating or withdrawing groups in the 1,4-naphthoquinone scaffold, were isolated in good yields and good to high ee values.

DFT study showed that halogen substituents in the urea groups are involved in the control of the enantioselectivity, being engaged in intramolecular H-bonding interactions, helpful for the stabilization of the transition state of the oxa-Michael step. In the oxa-Michael addition, the quinone is H-bonded with one urea group and partially by the guanidinium moiety. The peroxy anion is coordinated by the other urea group, directing the attack to the quinone (Scheme 5.20).

The ring closure of the peroxyenolate H-bonded with the catalyst was found to be the rate and stereoselectivity determining-step.

This protocol represents the most efficient system reported up to now for the enantioselective epoxidation of 1,4-naphthoquinone.

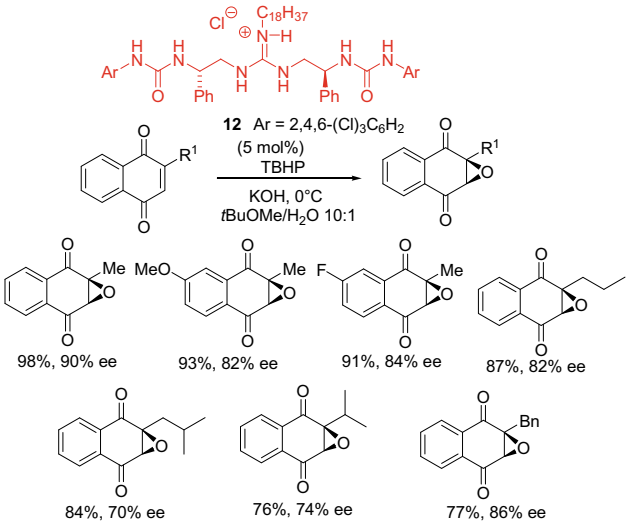

Scheme 5.19 Guanidine–bisurea catalysed enantioselective epoxidation of 1,4-naphthoquinones

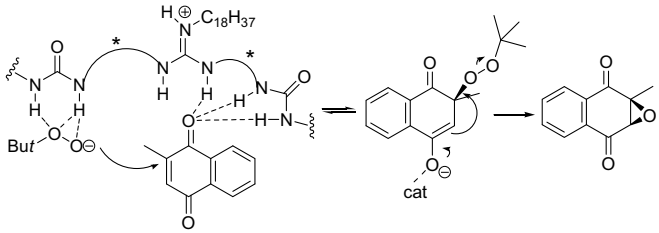

Scheme 5.20 Postulated mechanism for the asymmetric epoxidation of 1,4-naphthoquinones

5.4 Summary and Outlook

In the last years, significant advances in the area of non-covalent organocatalytic asymmetric epoxidation of electron-poor alkenes have been reported. The most relevant achievements concerned the application of *Cinchona* alkaloids derived PT catalysts for the stereoselective preparation of new classes of functionalized epoxides, bearing quaternary and tertiary stereocenters, amenable of further elaboration for the synthesis of pharmaceuticals and bioactive compounds. The reaction conditions respect, in most cases, the basic principles of green chemistry and perspective for large-scale application or recycling of the catalyst has been explored.

Besides the substrate scope enlargement of the known commercially available diaryl prolinol/TBHP system, ready available amine-thioureas appeared in the catalysis arena, as new useful organic catalysts. These bifunctional or multifunctional promoters demonstrated to be stable for their employment, under oxidative conditions, in the asymmetric epoxidation of challenging classes of alkenes, including terminal olefins. Mixed urea-PT catalysts proved to be suitable promoters in the highly enantioselective epoxidation of difficult targets, such as 1,4-naphthoquinones. Non-covalent organocatalytic epoxidation reactions deserve an important place in the area of asymmetric epoxidation of alkenes. However, improvements in terms of catalytic efficiency and operational parameters are still necessary, to consider them a practical and sustainable choice for industrial applications. Moreover, the design of new organocatalysts is necessary to succeed in the asymmetric epoxidation of α,β-unsaturated esters [75], and amides [76], whose epoxides are valuable synthetic intermediates, but still hard to prepare due to their scarce reactivity.

Acknowledgements Funding from MIUR, University of Salerno, POR Regione Campania FESR 2007–2013-O.O. 2.1 (FarmaBioNet) and the European COST Action CM0905-Organocatalysis (ORCA) is gratefully acknowledged.

References

1. Blaser HU, Schmidt E (eds) (2004) Asymmetric catalysis on industrial scale, challenges, approaches and solutions. Wiley-VCH, Weinheim
2. Bryliakov KP (2017) Catalytic asymmetric oxygenations with the environmentally benign oxidants H_2O_2 and O_2. Chem Rev 117:11406–11459. https://doi.org/10.1021/acs.chemrev.7b00167
3. Wang C, Yamamoto H (2015) Asymmetric epoxidation using hydrogen peroxide as oxidant. Chem Asian J 10:2056–2068. https://doi.org/10.1002/asia.201500293
4. Russo A, De Fusco C, Lattanzi A (2012) Organocatalytic asymmetric oxidations with hydrogen peroxide and molecular oxygen. ChemCatChem 4:901–916. https://doi.org/10.1002/cctc.201200139
5. De Faveri G, Ilyashenko G, Watkinson M (2011) Recent advances in catalytic asymmetric epoxidation using the environmentally benign oxidant hydrogen peroxide and its derivatives. Chem Soc Rev 40:1722–1760. https://doi.org/10.1039/c0cs00077a
6. Urlacher VB, Eiben S (2006) Cytochrome P450 monooxygenases: perspectives for synthetic application. Trends Biotechnol 24:324–330. https://doi.org/10.1016/j.tibtech.2006.05.002
7. Wang L, Wei S, Pan X, Liu P, Du X, Zhang C, Pu L, Wang Q (2018) Enhanced turnover for the P450 119 peroxygenase-catalyzed asymmetric epoxidation of styrenes by random mutagenesis. Chem Eur J 24:2741–2749. https://doi.org/10.1002/chem.201705460
8. Marco-Contelles J, Molina MT, Anjum S (2004) Naturally occurring cyclohexane epoxides: sources, biological activities, and synthesis. Chem Rev 104:2857–2900. https://doi.org/10.1021/cr980013j
9. Miyashita K, Imanishi T (2005) Syntheses of natural products having an epoxyquinone structure. Chem Rev 105:4515–4536. https://doi.org/10.1021/cr040613k
10. Cheng-Sánchez I, Garcнa-Ruiz C, Guerrero-Vásquez GA, Sarabia F (2017) An olefin cross-metathesis approach to depudecin and stereoisomeric analogues. J Org Chem 82:4744–4757. https://doi.org/10.1021/acs.joc.7b00424
11. Turk BE, Griffith EC, Wolf S, Biemann K, Chang Y-H, Liu JO (1999) Selective inhibition of amino-terminal methionine processing by TNP-470 and ovalicin in endothelial cells. Chem Biol 6(11):823–833. https://doi.org/10.1016/s1074-5521(99)80129-x
12. Katsuki T, Sharpless KB (1980) The first practical method for asymmetric epoxidation. J Am Chem Soc 102:5974–5976. https://doi.org/10.1021/ja00538a077
13. Heravi MM, Lashaki TB, Poorahmad N (2015) Applications of Sharpless asymmetric epoxidation in total synthesis. Tetrahedron Asymmetry 26:405–495. https://doi.org/10.1016/j.tetasy.2015.03.006
14. Irie R, Noda K, Ito Y, Matsumoto N, Katsuki T (1990) Catalytic asymmetric epoxidation of unfunctionalized olefins. Tetrahedron Lett 31:7345–7348. https://doi.org/10.1016/s0040-4039(00)88562-7
15. Zhang W, Loebach JL, Wilson SR, Jacobsen EN (1990) Enantioselective epoxidation of unfunctionalized olefins catalyzed by salen manganese complexes. J Am Chem Soc 112:2801–2803. https://doi.org/10.1021/ja00163a052
16. Makita N, Hoshino Y, Yamamoto H (2003) Asymmetric epoxidation of homoallylic alcohols and application in a concise total synthesis of (−)-α-bisabolol and (−)-8-epi-α-bisabolol. Angew Chem Int Ed 42:941–943. https://doi.org/10.1002/anie.200390250
17. Bougauchi M, Watanabe S, Arai T, Sasai H, Shibasaki M (1997) Catalytic asymmetric epoxidation of α, β-unsaturated ketones promoted by lanthanoid complexes. J Am Chem Soc 119:2329–2330. https://doi.org/10.1021/ja964037o
18. Zhu Y, Wang Q, Cornwall R, Shi Y (2014) Organocatalytic asymmetric epoxidation and aziridination of olefins and their synthetic application. Chem Rev 114:8199–8256. https://doi.org/10.1021/cr500064w
19. Pellissier H, Lattanzi A, Dalpozzo R (eds) (2017) Asymmetric synthesis of three-membered rings. Wiley-VCH, Weinheim

20. Smith JG (1984) Synthetically useful reactions of epoxides. Synthesis 10:629–656. https://doi.org/10.1055/s-1984-30921
21. Lauret C (2001) Epoxy ketones as versatile building blocks in organic synthesis. Tetrahedron Asymmetry 12:2359–2383. https://doi.org/10.1016/s0957-4166(01)00412-8
22. Davis RL, Stiller J, Naicker T, Jiang H, Jørgensen KA (2014) Asymmetric organocatalytic epoxidations: reactions, scope, mechanisms, and applications. Angew Chem Int Ed 53:7406–7426. https://doi.org/10.1002/anie.201400241
23. Lattanzi A (2008) Advances in asymmetric epoxidation of α, β-unsaturated carbonyl compounds: the organocatalytic approach. Curr Org Synth 5:117–133. https://doi.org/10.2174/157017908784221594
24. Helder R, Hummelen JC, Laane RWPM, Wiering JS, Wynberg H (1976) Catalytic asymmetric induction in oxidation reactions. The synthesis of optically active epoxides. Tetrahedron Lett 17:1831–1834. https://doi.org/10.1016/s0040-4039(00)93796-1
25. Albanese DCM, Foschi F, Penso M (2016) Sustainable oxidations under phase-transfer catalysis conditions. Org Process Res Dev 20:129–139. https://doi.org/10.1021/acs.oprd.5b00385
26. Shirakawa S, Maruoka K (2013) Recent developments in asymmetric phase-transfer reactions. Angew Chem Int Ed 52:4312–4348. https://doi.org/10.1002/anie.201206835
27. Jew S-s, Lee J-H, Jeong B-S, Yoo M-S, Kim M-J, Lee Y-J, Lee J, Choi S-h, Lee K, Lah M-S, Park H-g (2005) Highly enantioselective epoxidation of 2,4-diarylenones by using dimeric Cinchona phase-transfer catalysts: enhancement of enantioselectivity by surfactants. Angew Chem Int Ed 44:1383–1385. https://doi.org/10.1002/anie.200462254
28. Ooi T, Ohara D, Tamura M, Maruoka K (2004) Design of new chiral phase-transfer Catalysts with dual functions for highly enantioselective epoxidation of α, β-unsaturated ketones. J Am Chem Soc 126:6844–6845. https://doi.org/10.1021/ja048600b
29. Hori K, Tamura M, Tani K, Nishiwaki N, Ariga M, Tohda Y (2006) Asymmetric epoxidation catalyzed by novel azacrown ether-type chiral quaternary ammonium salts under phase-transfer catalytic conditions. Tetrahedron Lett 47:3115–3118. https://doi.org/10.1016/j.tetlet.2006.02.142
30. Bakó P, Bakó T, Mészáros A, Keglevich G, Szöllösy À, Bodor S, Makó A, Töke L (2004) Phase transfer catalysed asymmetric epoxidation of chalcones using chiral crown ethers derived from *d*-glucose and *d*-mannose. Synlett 643–646. https://doi.org/10.1055/s-2004-817751
31. Kawai H, Okusu S, Yuan Z, Tokunaga E, Yamano A, Shiro M, Shibata N (2013) Enantioselective synthesis of epoxides having a tetrasubstituted trifluoromethylated carbon center: methylhydrazine-induced aerobic epoxidation of β, β-Disubstituted Enones. Angew Chem Int Ed 52:2221–2225. https://doi.org/10.1002/anie.201209355
32. Wu S, Pan D, Cao C, Wang Q, Chen F-X (2013) Diastereoselective and enantioselective epoxidation of acyclic β-trifluoromethyl-β, β-disubstituted enones by hydrogen peroxide with a pentafluorinated quinidine-derived phase-transfer catalyst. Adv Synth Catal 355:1917–1923. https://doi.org/10.1002/adsc.201300249
33. Li C, Shu X, Li L, Zhang G, Jin R, Cheng T, Liu G (2016) A Cinchona alkaloid-functionalized mesostructured silica for construction of enriched chiral β-trifluoromethyl-β-hydroxy ketones over an epoxidation-relay reduction process. Chem Asian J 11:2072–2077. https://doi.org/10.1002/asia.201600640
34. Yoo M-S, Kim D-G, Ha MW, Jew S-s, Park H-g, Jeong B-S (2010) Synthesis of (αR, βS)-epoxyketones by asymmetric epoxidation of chalcones with Cinchona phase-transfer catalysts. Tetrahedron Lett 51:5601–5603. https://doi.org/10.1016/j.tetlet.2010.08.056
35. Ashokkumar V, Balasaravanan R, Sadhasivam V, Jenofar SM, Siva A (2015) A new class of bifunctional chiral phase transfer catalysts for highly enantioselective asymmetric epoxidation of α, β-unsaturated ketones at ambient temperature. J Mol Catal A Chem 409:127–136. https://doi.org/10.1016/j.molcata.2015.08.016
36. Corey EJ, Zhang F-Y (1999) Mechanism and conditions for highly enantioselective epoxidation of α, β-enones using charge-accelerated catalysis by a rigid quaternary ammonium salt. Org Lett 1:1287–1290. https://doi.org/10.1021/ol990964z

37. Lygo B, Wainwright PG (1999) Phase-transfer catalysed asymmetric epoxidation of enones using N-anthracenylmethyl-substituted *Cinchona* alkaloids. Tetrahedron 55:6289–6300. https://doi.org/10.1016/s0040-4020(99)00205-7
38. Vieira LCC, Matsuo BT, Martelli LSR, Gall M, Paixão MW, Corrêa AG (2017) Asymmetric synthesis of new γ-butenolides via organocatalyzed epoxidation of chalcones. Org Biomol Chem 15:6098–6103. https://doi.org/10.1039/c7ob00165g
39. Yan L, Wu XH, Liu HJ, Xie LY, Jiang ZY (2013) Catalytic asymmetric synthesis of γ-butenolides by direct vinylogous reactions. Mini Rev Med Chem 13:845–853. https://doi.org/10.2174/1389557511313060007
40. Vidal-Albalat A, Świderek K, Izquierdo J, Rodríguez S, Moliner V, González FV (2016) Catalytic enantioselective epoxidation of nitroalkenes. Chem Commun 52:10060–10063. https://doi.org/10.1039/c6cc03539f
41. Vankar YD, Shah K, Bawa A, Singh SP (1991) Chemistry of α-nitroepoxides: synthesis of useful intermediates via nucleophilic ring-opening of α-nitroepoxides. Tetrahedron 47(42):8883–8906. https://doi.org/10.1016/s0040-4020(01)81002-4
42. Agut J, Vidal A, Rodríguez S, González FV (2013) Dynamic kinetic asymmetric ring-opening/reductive amination sequence of racemic nitroepoxides with chiral amines: enantioselective synthesis of chiral vicinal diamines. J Org Chem 78:5717–5722. https://doi.org/10.1021/jo400501k
43. Newman H, Angier RB (1970) The preparation and chemistry of α-nitroepoxides. Tetrahedron 26:825–836. https://doi.org/10.1016/s0040-4020(01)97880-9
44. Donslund BS, Johansen TK, Poulsen PH, Halskov KS, Jørgensen KA (2015) The diarylprolinol silyl ethers: ten years after. Angew Chem Int Ed 54:13860–13874. https://doi.org/10.1002/anie.201503920
45. Lattanzi A (2009) α,α-Diarylprolinols: bifunctional organocatalysts for asymmetric synthesis. Chem Commun 1452–1463. https://doi.org/10.1039/b900098d
46. Meninno S, Lattanzi A (2013) Asymmetric organocatalysis mediated by α, α-L-diaryl prolinols: recent advances. Chem Commun 49:3821–3832. https://doi.org/10.1039/c3cc36928e
47. Lattanzi A (2005) Enantioselective epoxidation of α, β-enones promoted by α, α-diphenyl-L-prolinol as bifunctional organocatalyst. Org Lett 7(13):2579–2582. https://doi.org/10.1021/ol050694m
48. Capobianco A, Russo A, Lattanzi A, Peluso A (2012) On the mechanism of asymmetric epoxidation of enones catalyzed by α,α-L-diaryl prolinols: a theoretical insight. Adv Synth Catal 354:2789–2796. https://doi.org/10.1002/adsc.201200415
49. Russo A, Lattanzi A (2010) Asymmetric epoxidation of 2-arylidene-1,3-diketones: facile access to synthetically useful epoxides. Org Biomol Chem 8:2633–2638. https://doi.org/10.1039/c002587a
50. Yoakim C, Ogilvie WW, Goudreau N, Naud J, Haché B, O'Meara JA, Cordingley MG, Archambault J, White PW (2003) Discovery of the first series of inhibitors of human papillomavirus type 11: inhibition of the assembly of the E1–E2–Origin DNA complex. Bioorg Med Chem Lett 13:2539–2541. https://doi.org/10.1016/s0960-894x(03)00510-9
51. De Fusco C, Tedesco C, Lattanzi A (2011) Organocatalytic stereoselective epoxidation of trisubstituted acrylonitriles. J Org Chem 76:676–679. https://doi.org/10.1021/jo102020a
52. Aiai M, Robert A, Baudy-Floc'h M, Le Grel P (1995) First sharpless epoxidation of electrophilic 2-cyanoallylic alcohols. Tetrahedron Asymmetry 6:2249–2252. https://doi.org/10.1016/0957-4166(95)00300-e
53. Palumbo C, Mazzeo G, Mazziotta A, Gambacorta A, Loreto MA, Migliorini A, Superchi S, Tofani D, Gasperi T (2011) Noncovalent organocatalysis: a powerful tool for the nucleophilic epoxidation of α-ylideneoxindoles. Org Lett 13(23):6248–6251. https://doi.org/10.1021/ol202646w
54. Ashokkumar V, Siva A (2017) One-pot synthesis of α, β-epoxy ketones through domino reaction between alkenes and aldehydes catalyzed by proline based chiral organocatalysts. Org Biomol Chem 15:2551–2561. https://doi.org/10.1039/c7ob00031f

55. Okino T, Hoashi Y, Takemoto Y (2003) Enantioselective Michael reaction of malonates to nitroolefins catalyzed by bifunctional organocatalysts. J Am Chem Soc 125:12672–12673. https://doi.org/10.1021/ja036972z
56. Wittkopp A, Schreiner PR (2003) Metal-free, noncovalent catalysis of Diels-Alder reactions by neutral hydrogen bond donors in organic solvents and in water. Chem Eur J 9:407–414. https://doi.org/10.1002/chem.200390042
57. Tsakos M, Kokotos CG (2013) Primary and secondary amine-(thio)ureas and squaramides and their applications in asymmetric organocatalysis. Tetrahedron 69:10199–10222. https://doi.org/10.1016/j.tet.2013.09.080
58. Fang X, Wang C-J (2015) Recent advances in asymmetric organocatalysis mediated by bifunctional amine–thioureas bearing multiple hydrogen-bonding donors. Chem Commun 51:1185–1197. https://doi.org/10.1039/c4cc07909d
59. Russo A, Lattanzi A (2010) Hydrogen-bonding catalysis: mild and highly chemoselective oxidation of sulfides. Adv Synth Catal 351:521–524. https://doi.org/10.1002/adsc.200900020
60. Russo A, Galdi G, Croce G, Lattanzi A (2012) Highly enantioselective epoxidation catalyzed by Cinchona thioureas: synthesis of functionalized terminal epoxides bearing a quaternary stereogenic center. Chem Eur J 18:6152. https://doi.org/10.1002/chem.201200500
61. Yamaguchi J, Toyoshima M, Shoji M, Kakeya H, Osada H, Hayashi Y (2006) Concise enantio- and diastereoselective total syntheses of Fumagillol, RK-805, FR65814, Ovalicin, and 5-Demethylovalicin. Angew Chem Int Ed 45:789–793. https://doi.org/10.1002/anie.200502826
62. Shotwell JB, Krygowski ES, Hines J, Koh B, Huntsman EWD, Choi HW, Schneekloth JS, Wood JL, Crews CM (2002) Total synthesis of luminacin D. Org Lett 4:3087–3089. https://doi.org/10.1021/ol026382q
63. Thompson CF, Jamison TF, Jacobsen EN (2001) FR901464: total synthesis, proof of structure, and evaluation of synthetic analogues. J Am Chem Soc 123:9974–9983. https://doi.org/10.1021/ja016615t
64. Mukaiyama T, Ogata K, Ono T, Hayashi Y (2015) Asymmetric organocatalyzed epoxidation of 2-oxoindoline-3-ylidene acetaldehydes. ChemCatChem 7:155–159. https://doi.org/10.1002/cctc.201402811
65. Chauhan P, Mahajan S, Enders D (2015) Asymmetric synthesis of pyrazoles and pyrazolones employing the reactivity of pyrazolin-5-one derivatives. Chem Commun 51:12890–12907. https://doi.org/10.1039/c5cc04930j
66. Meninno S, Roselli A, Capobianco A, Overgaard J, Lattanzi A (2017) Diastereodivergent and enantioselective access to spiroepoxides via organocatalytic epoxidation of unsaturated pyrazolones. Org Lett 19:5030–5033. https://doi.org/10.1021/acs.orglett.7b02189
67. Hurtaud D, Baudy-Floc'h M, Robert A, Le Grel P (1994) Chemoselective nucleophilic attack of α, α-dicyano epoxides: a simple synthesis of α-amino amides, epoxy amidines and their cyclic analogs. J Org Chem 59:4701–4703. https://doi.org/10.1021/jo00095a059
68. Meninno S, Vidal-Albalat A, Lattanzi A (2015) Asymmetric epoxidation of alkylidene-malononitriles: key step for one-pot approach to enantioenriched 3-substituted piperazin-2-ones. Org Lett 17:4348–4351. https://doi.org/10.1021/acs.orglett.5b02186
69. Meninno S, Zullo L, Overgaard J, Lattanzi A (2017) Tunable Cinchona-based thioureas-catalysed asymmetric epoxidation to synthetically important glycidic ester derivatives. Adv Synth Catal 359:913–918. https://doi.org/10.1002/adsc.201700146
70. Ekegren JK, Unge T, Safa MZ, Wallberg H, Samuelsson B, Hallberg A (2005) A new class of HIV-1 protease inhibitors containing a tertiary alcohol in the transition-state mimicking scaffold. J Med Chem 48:8098–8102. https://doi.org/10.1021/jm050790t
71. Guerrini A, Tesei A, Ferroni C, Paganelli G, Zamagni A, Carloni S, Di Donato M, Castoria G, Leonetti C, Porru M, De Cesare M, Zaffaroni N, Beretta GL, Del Rio A, Varchi G (2014) A new avenue toward androgen receptor pan-antagonists: C2 sterically hindereds of hydroxypropanamides. J Med Chem 57:7263–7279. https://doi.org/10.1021/jm5005122
72. Berkessel A, Guixa M, Schmidt F, Neudorfl JM, Lex J (2007) Highly enantioselective epoxidation of 2-methylnaphthoquinone (vitamin K_3) mediated by new Cinchona alkaloid phase-transfer catalysts. Chem Eur J 13:4483–4498. https://doi.org/10.1002/chem.200600993

73. Kawaguchi M, Nakano K, Hosoya K, Orihara T, Yamanaka M, Odagi M, Nagasawa K (2018) Asymmetric epoxidation of 1,4-naphthoquinones catalyzed by guanidine-urea bifunctional organocatalyst. Org Lett 20:2811–2815. https://doi.org/10.1021/acs.orglett.8b00641
74. Tanaka S, Nagasawa K (2009) Guanidine-urea bifunctional organocatalyst for asymmetric epoxidation of 1,3-diarylenones with hydrogen peroxide. Synlett 667–670. https://doi.org/10.1055/s-0028-1087811
75. Kakei H, Tsuji R, Ohshima T, Shibasaki M (2005) Catalytic asymmetric epoxidation of α, β-unsaturated esters using an yttrium-biphenyldiol complex. J Am Chem Soc 127:8962–8963. https://doi.org/10.1021/ja052466t
76. Nemoto T, Kakei H, Gnanadesikan V, Tosaki S, Ohshima T, Shibasaki M (2002) Catalytic asymmetric epoxidation of α, β-unsaturated amides: efficient synthesis of β-aryl α-hydroxy amides using a one-pot tandem catalytic asymmetric epoxidation—Pd-catalyzed epoxide opening process. J Am Chem Soc 124:14544–14545. https://doi.org/10.1021/ja028454e

Chapter 6
Green Oxidative Kinetic Resolutions of Secondary Alcohols

Hélène Pellissier

Abstract This chapter updates the field of nonenzymatic oxidative kinetic resolutions of secondary alcohols, covering the literature since 2004. These practical methodologies provide a simple access to chiral alcohols that are key intermediates in asymmetric synthesis. The chapter is divided into seven sections, dealing successively with palladium-catalyzed reactions, vanadium-catalyzed reactions, ruthenium-catalyzed reactions, manganese-catalyzed reactions, iron-catalyzed reactions, reactions catalyzed by other metals and organocatalyzed reactions.

Keywords Oxidative kinetic resolution · Secondary alcohols · Metal catalysis · Organocatalysis · Nonenzymatic kinetic resolution · Chirality · Asymmetric catalysis

6.1 Introduction

Along with asymmetric synthesis, kinetic resolutions [1–9] represent very simple, direct, and practical methodologies to prepare chiral compounds [9–19]. In addition to enzymatic kinetic resolutions, metal-catalyzed and more recently developed organocatalyzed kinetic resolutions have encountered much progress with the discovery of novel types of catalysts since the publication of the first catalytic nonenzymatic kinetic resolution by Fajans and Bredig in 1908 using chiral alkaloid catalysts [20]. Later in 1981, Sharpless reported the kinetic resolution of allylic alcohols using tartrate ligands [21], which still knows wide success [22, 23]. Among highly efficient kinetic resolutions [24–27] are oxidative kinetic resolution of alcohols [28–31].

This chapter collects the developments in nonenzymatic oxidative kinetic resolution of secondary alcohols reported since 2004. It is divided into seven sections dealing successively with palladium-catalyzed reactions, vanadium-catalyzed reactions, ruthenium-catalyzed reactions, manganese-catalyzed reactions, iron-catalyzed

H. Pellissier (✉)
Aix-Marseille Université, CNRS, Centrale Marseille, iSm2, Marseille, France
e-mail: h.pellissier@univ-amu.fr

K. P. Bryliakov (ed.), *Frontiers of Green Catalytic Selective Oxidations*,
Green Chemistry and Sustainable Technology,
https://doi.org/10.1007/978-981-32-9751-7_6

reactions, reactions catalyzed by other metals, and organocatalyzed reactions. It must be noted that special kinetic resolutions, including stoichiometric kinetic resolutions [32], parallel kinetic resolutions [33, 34], and dynamic kinetic resolutions [35–43] are not included in this chapter.

6.2 Palladium-Catalyzed Reactions

The groups of Stoltz and Sigman have independently developed palladium-catalyzed aerobic oxidative kinetic resolutions of a wide range of allylic, benzylic, and cyclopropyl secondary alcohols in the presence of (−)-sparteine as ligand [44–53]. These methodologies performed under oxygen atmosphere have allowed high selectivity factors of up to 122 to be achieved by using, for example, catalyst **13** (Scheme 6.1, first equation) [54–61]. Furthermore, this methodology was applied to the syntheses of several alkaloids, such as (+)-amurensinine, (−)-aurantioclavine, (−)-lobeline, and (−)- and (+)-sedamine [62, 63]. In the same area, another chiral palladium catalyst in situ generated from $Pd(nbd)Cl_2$ and (−)-sparteine was applied by Stoltz et al. to the oxidative kinetic resolution of a functionalized secondary alcohol (Scheme 6.1, second equation) [64]. The reaction was performed at 80 °C in toluene, affording the (3*R*,5*S*)-alcohol with a high enantioselectivity (>95% ee) and a good selectivity factor ($s = 23$) while the corresponding (3*S*)-ketone was obtained in 57% conversion. This chiral alcohol was employed as intermediate in the synthesis of the natural anticancer agent bielschowskysin.

Along with expensive sparteine, structurally modified only with difficulty, another chiral diamine derived from (−)-cystine was employed in 2008 by O'Brien et al. for the oxidative aerobic kinetic resolution of indan-1-ol [65]. The process led to indanone and recovered (*R*)-indan-1-ol in high enantioselectivity (92% ee) and a selectivity factor of 8. It must be noted that the stereocontrol was lower than that obtained by using sparteine to afford the corresponding (*S*)-product (98% ee) [66]. On the other hand, moderate enantioselectivities (≤42% ee) and selectivity factors (≤4.6) were described by Sacchetti et al. by using sparteine analogs, such as novel chiral 9-keto-bispidines, in the kinetic resolution of 1-phenylethanol [67]. In 2009, Breuning et al. investigated the kinetic resolution of 1-(4-methoxyphenyl)ethanol performed under oxygen atmosphere by using 9-oxabispidine ligand **14** [68]. The reaction provided an excellent enantioselectivity (>99% ee) combined with a selectivity factor of 19 (Scheme 6.2).

Novel chiral *N*-heterocyclic carbene ligands derived from BINAM and H_8-BINAM were developed by Shi et al. to be investigated in the palladium-catalyzed aerobic oxidative kinetic resolution of cyclic arylalkanols [69–71]. As shown in Scheme 6.3, moderate to good selectivity factors (≤49) were obtained with moderate to high enantioselectivities (≤99% ee) when the reaction was promoted by catalyst **15** under oxygen atmosphere.

The kinetic resolution of unprotected diols is still undeveloped related to the difficult control of its regioselectivity [27]. In 2016, Hua et al. reported the aerobic oxida-

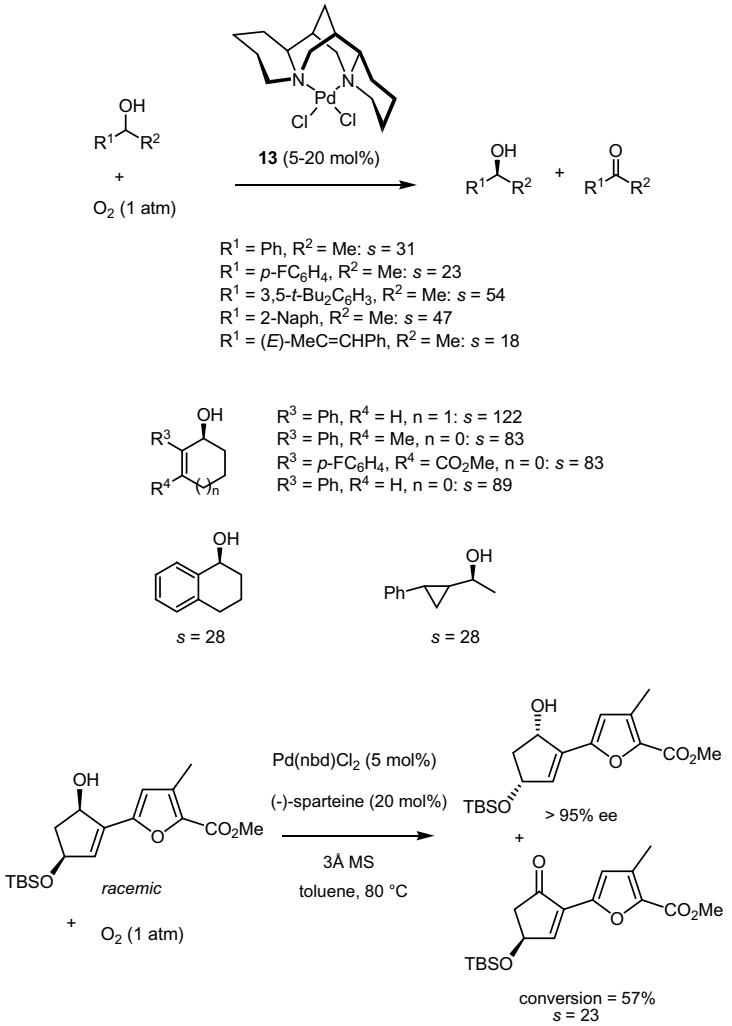

Scheme 6.1 Aerobic oxidative kinetic resolutions of secondary alcohols catalyzed with sparteine-derived palladium complexes

Scheme 6.2 Aerobic oxidative kinetic resolution of benzylic alcohols catalyzed with a 9-oxabispidine-derived palladium complex

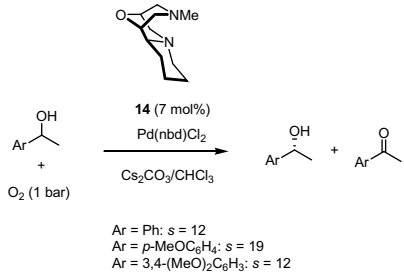

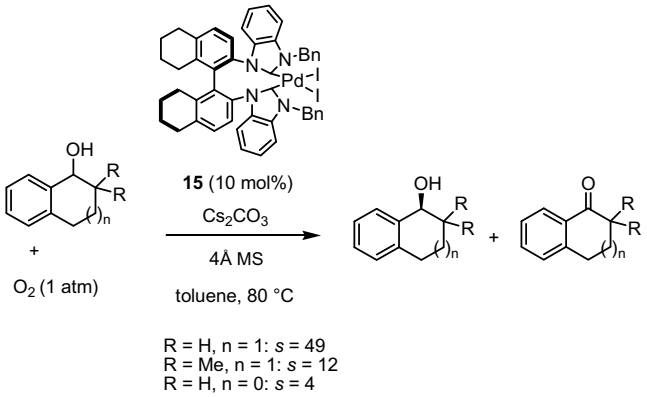

Scheme 6.3 Aerobic oxidative kinetic resolution of cyclic arylalkanols catalyzed with an *N*-heterocyclic carbene-derived palladium complex

tive kinetic resolution of *trans*-1,3- and *trans*-1,2-cycloalkanediols by using novel chiral-substituted poly-*N*-vinylpyrrolidinones as ligands of a bimetallic (Pd/Au) nanocluster derived from polymeric chiral pyrrolidinone **16** [72]. The kinetic resolution of *trans*-1,3-cycloalkanediols performed in water in the presence of only 0.15 mol% of catalyst loading led to the corresponding (*S*)-ketones in high enantioselectivities (83–99% ee) and good yields (46–49%) along with (*R,R*)-*trans*-1,3-cycloalkanediols in high enantioselectivities (79–92% ee) and good yields (50–53%), as shown in Scheme 6.4. When applied to the kinetic resolution of *trans*-1,2-cycloalkanediols, the process afforded the corresponding enantiopure (*S*)- ketones (99% ee) in good yields (45–47%) along with (*R,R*)-*trans*-1,2-cycloalkanediols with high enantioselectivities (87–88% ee) and good yields (50–54%).

6.3 Vanadium-Catalyzed Reactions

Chiral vanadium complexes are also compatible catalysts for oxidative kinetic resolutions of secondary alcohols. For example, a chiral catalyst in situ generated from $VO(O\textit{i}\text{-}Pr)_3$ and Schiff base ligand **17** was applied in 2005 by Toste et al. to promote the oxidation of a series of α-hydroxy esters under oxygen atmosphere with high selectivity factors (≤50) [73]. In 2010, this catalyst system was also employed by Li et al. in the kinetic resolution of methyl *o*-chloromandelate, a key intermediate in the synthesis of the antiplatelet agent (*S*)-clopidogrel, which was achieved with an excellent enantioselectivity (99% ee) [74]. The scope of this methodology was extended to the kinetic resolution of other α-hydroxy esters with selectivity factors of up to 88 (Scheme 6.5). It was shown that the steric hindrance of the *tert*-butyl groups of the ligand had a great influence on the enantioselectivity of the process. Furthermore, these reaction conditions were also applied by Toste et al. to the total

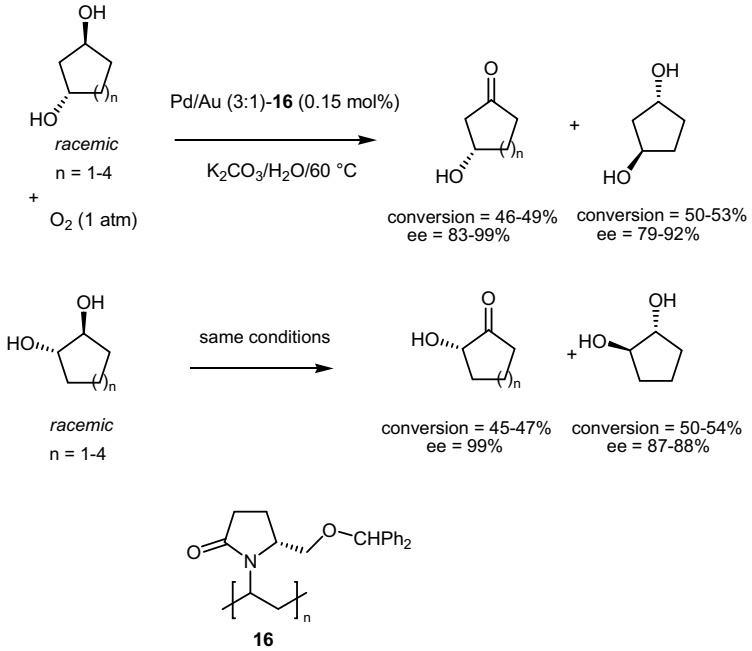

Scheme 6.4 Aerobic oxidative kinetic resolution of *trans*-1,3- and *trans*-1,2-cycloalkanediols catalyzed with a Pd/Au (3:1) nanocluster derived from a chiral-substituted poly-*N*-vinylpyrrolidinone

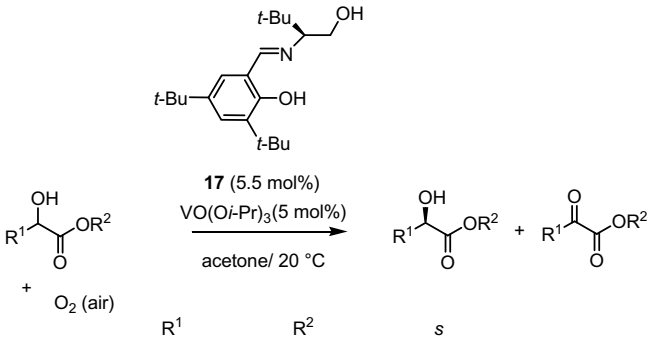

R^1	R^2	*s*
Ph	Et	> 50
p-$CF_3C_6H_4$	Me	29
i-Bu	*i*-Pr	30
$TBSO(CH_2)_2$	Me	42
$PhC(=CH_2)-CH_2$	Et	34
o-ClC_6H_4	Me	16
p-ClC_6H_4	Et	88
2,4,6-(*t*-Bu)$_3C_6H_2$	Et	69

Scheme 6.5 Aerobic oxidative kinetic resolution of α-hydroxy esters catalyzed with a chiral Schiff base-derived vanadium complex

syntheses of natural products, such as (−)octalactin A [75] and (−)-pantofuranoid E [76].

A closely related chiral vanadium catalyst **18** was employed by Chen et al. in 2006 in the oxidative kinetic resolution of α-hydroxy phosphonates, providing high selectivity factors (≤100), as shown in Scheme 6.6 [77, 78]. The best results were achieved in the reaction of various α-aryl- and α-heteroaryl-α-hydroxy phosphonates. In contrast, lower enantioselectivities were observed by using related catalyst **19** derived from a ligand bearing more hindered *tert*-butyl groups in these reactions. On the other hand, remarkable selectivity factors of up to 1057 were obtained with this catalyst **19** in the kinetic resolution of α-hydroxy esters and α-hydroxy amides. Moreover, the kinetic resolution of other α-hydroxy acid derivatives including α-hydroxy thioesters was performed in the presence of the same catalyst with high selectivity factors of up

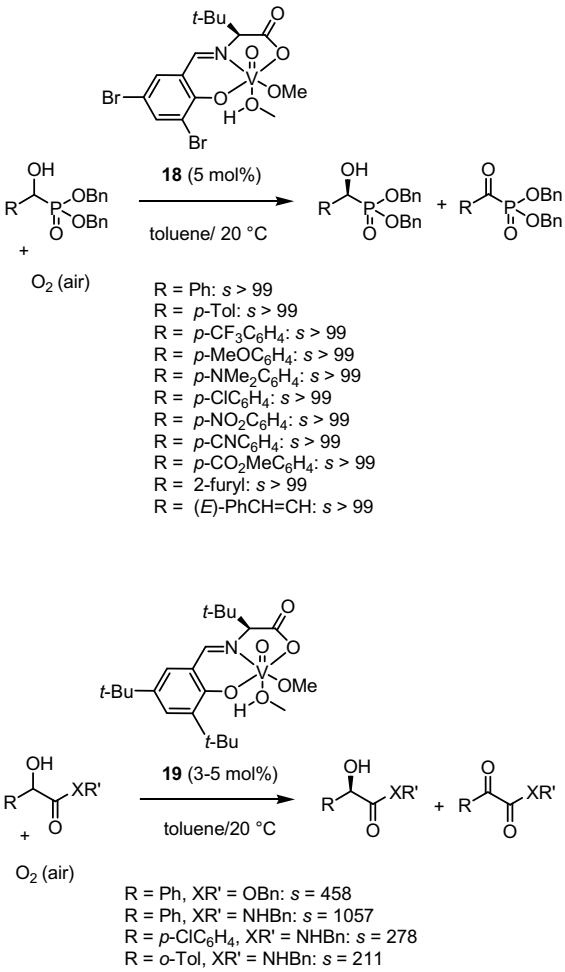

Scheme 6.6 Aerobic oxidative kinetic resolutions of α-hydroxy phosphonates, α-hydroxy esters, and α-hydroxy amides catalyzed with *N*-salicylidene vanadyl(V) carboxylate catalysts

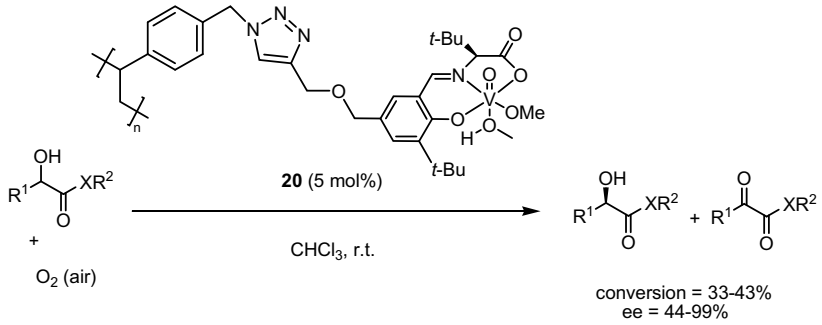

R^1 = Ph, *p*-Tol, *p*-ClC_6H_4, *p*-$F_3CC_6H_4$, *o*-Tol, *o*-ClC_6H_4, 1-Naph, 2-thiophenyl, (*E*)-PhCH=CH, *c*-Pr, *i*-Pr
R^2 = OBn, OMe, OEt, O*i*-Pr, SBn, NHBn, $NHCH(Ph)_2$, NH*i*-Pr

Scheme 6.7 Aerobic oxidative kinetic resolution of α-hydroxy (thio)esters and α-hydroxy amides catalyzed with a polystyrene-supported *N*-salicylidene vanadyl(V) carboxylate catalyst

to 500 [79]. These results show that this is through a judicious selection of the C3- and C5-substituents in the *N*-salicylidene moiety of the catalyst that high enantioselectivities could be achieved. For example, 3,5-di-*tert*-butyl-*N*-salicylidene-based vanadyl complex **19** was selected as optimal catalyst for the kinetic resolution of α-hydroxy esters, amides, and thioesters, whereas 3,5-dibromo-*N*-salicylidene-based vanadyl complex **18** was the optimal catalyst for the kinetic resolution of α-hydroxy phosphonates.

In 2011, a polystyrene-supported vanadium catalyst **20** was developed by the same authors and further applied to promote the kinetic resolution of a wide range of α-hydroxy (thio)esters and α-hydroxy amides under oxygen atmosphere with high enantioselectivities of up to 99% ee and moderate yields (33–43%), as shown in Scheme 6.7 [80]. Especially, uniformly high enantioselectivities (87–96% ee) were obtained for mandelates and a α-hydroxy (thio)ester. High enantioselectivities (80–99% ee) were also achieved in the kinetic resolution of various benzyl α-hydroxy amides (XR^2 = NHBn) bearing different α-aryl and alkyl groups (R^1). However, a lower enantioselectivity (44% ee) was exceptionally observed in the reaction of a substrate exhibiting a α-isopropyl group (R^1 = *i*-Pr). Notably, the catalyst could be recovered by filtration and reused four times.

6.4 Ruthenium-Catalyzed Reactions

In 2005, Chan et al. reported the synthesis of chiral arsinooxazoline–ruthenium(II) complexes, such as **21**, which were further investigated to promote the oxidative kinetic resolution of substituted 1-arylalkanols [81]. As shown in Scheme 6.8, remarkable enantioselectivities (>99% ee) and good conversions (>50%) were

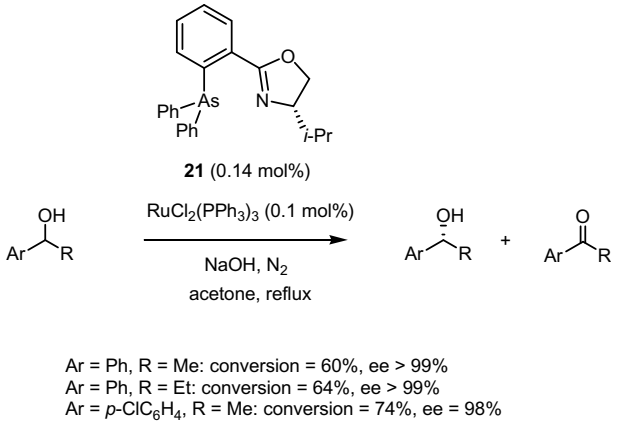

Scheme 6.8 Oxidative kinetic resolution of benzylic alcohols catalyzed with an arsinooxazoline–ruthenium(II) complex

obtained at room temperature in alkaline acetone as oxidant in the reaction of unhindered aryl alcohols, such as 1-phenylethanol.

In 2007, enantioselectivities of up to 99% ee were described by Katsuki et al. by using salen ruthenium complexes, such as **22**, in the kinetic resolution of simple secondary alcohols with air as hydrogen acceptor (Scheme 6.9) [82]. Selectivity factors of up to 30 were achieved by using at room temperature under photoirradiation in the presence of an additive, such as 1,3-bis(*p*-bromophenyl)propane-1,3-dione.

Scheme 6.9 Aerobic photochemical oxidative kinetic resolution of secondary alcohols catalyzed with a salen ruthenium complex

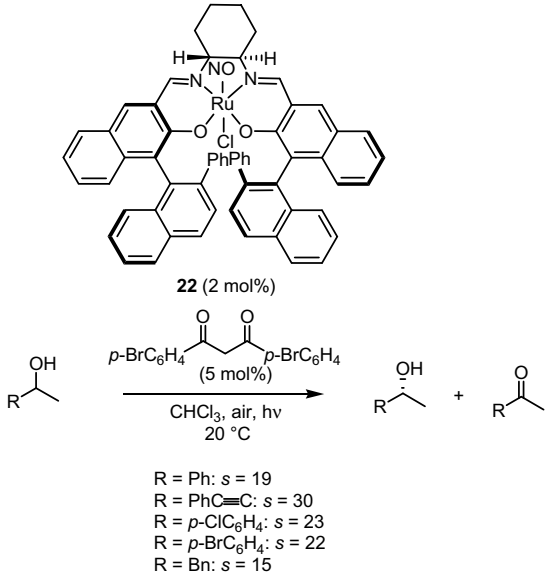

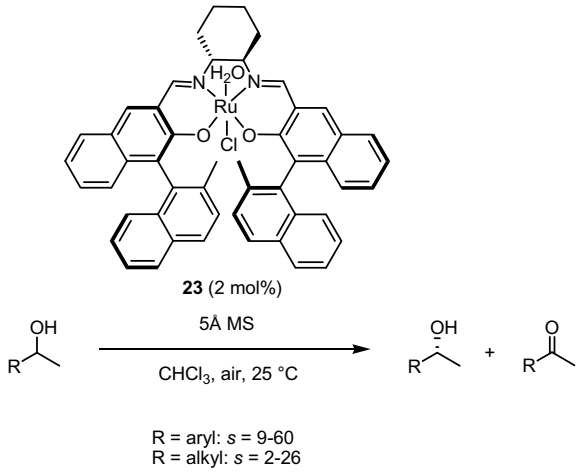

Scheme 6.10 Aerobic oxidative kinetic resolution of aromatic/aliphatic alcohols catalyzed with an aqua salen ruthenium complex

In 2014, these reactions were also performed by the same authors without irradiation when catalyzed by a chiral aqua salen ruthenium complex **23** in air [83]. Enantioselectivities of up to >98% ee were obtained in the reaction of many aromatic and aliphatic alcohols (Scheme 6.10). Especially, the best results (selectivity factors of up to 60) were achieved in the kinetic resolution of activated alcohols, such as benzylic ones bearing a substituent at the *para*-, *meta*- or *ortho*-position, while lower selectivity factors (2–26) were obtained for more challenging aliphatic alcohols.

6.5 Manganese-Catalyzed Reactions

While expensive $PhI(OAc)_2$ has been often employed as oxidant in the presence of chiral salen manganese catalysts [84–96] in kinetic resolutions of secondary alcohols, greener oxidants, such as H_2O_2 [97], also provided good results in such reactions. For example, Bryliakov et al. described in 2017 oxidative kinetic resolutions of secondary benzylic alcohols with H_2O_2 catalyzed by a tetradentate aminopyridine manganese complex **12** (Scheme 6.11) [98]. This catalyst was employed at only 0.06–0.1 mol% of catalyst loading in acetonitrile at −10 °C without any additive. Under these conditions, a series of *para*-substituted 1-phenylethanols provided the corresponding chiral alcohols with good conversions (64–68%) and low to excellent enantioselectivities (22–95% ee). The reaction of unsubstituted (*S*)-1-phenylethanol gave comparable results (69% conversion, 92% ee).

Soon after, Sun et al. reinvestigated these green reactions in the presence of 0.2 mol% of a closely related chiral tetradentate aminopyridine manganese complex **11** [99]. In this case, the reaction was performed at 0 °C in the presence of H_2SO_4 as additive. In this context, various secondary benzylic alcohols afforded the

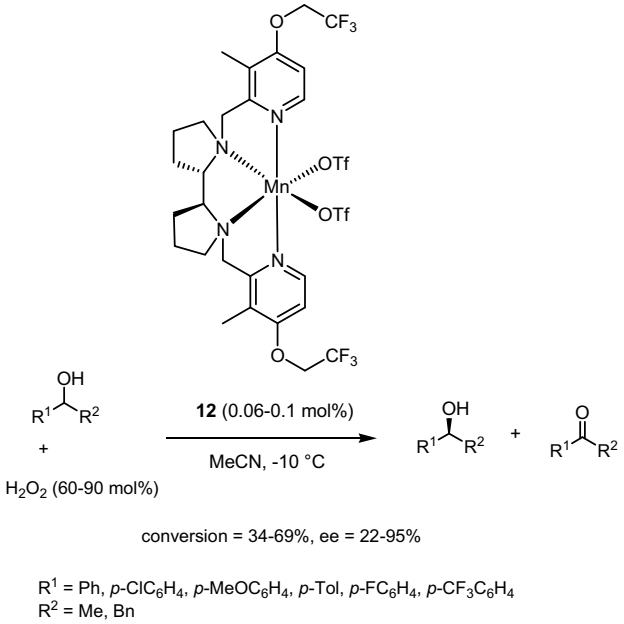

Scheme 6.11 Oxidative kinetic resolution of secondary benzylic alcohols catalyzed with another tetradentate aminopyridine manganese complex and using H_2O_2 as oxidant

corresponding chiral alcohols with excellent enantioselectivities (90–96% ee) and good conversions (60–74%), as shown in Scheme 6.12.

Scheme 6.12 Oxidative kinetic resolution of secondary benzylic alcohols catalyzed by a manganese complex derived from a tetradentate aminopyridine ligand and using H_2O_2 as oxidant

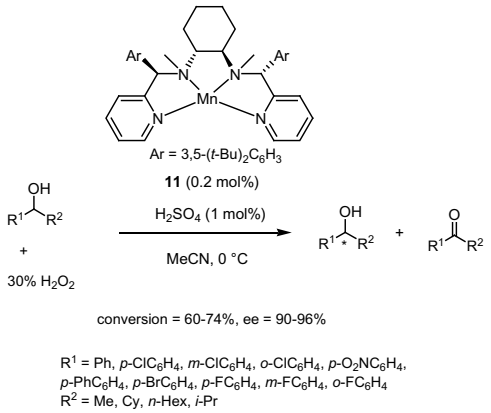

6.6 Iron-Catalyzed Reactions

In 2009, an inexpensive and environmentally benign metal, such as an in situ generated (*R*)-BINAM-derived iron catalyst **24**, was applied by Sekar et al. to promote the oxidative kinetic resolution of benzoins [100]. The reaction was performed at 60 °C in hexanes in the presence of TEMPO and molecular oxygen as oxidant. In these environmentally friendly conditions, selectivity factors of up to 10.6 were obtained, as shown in Scheme 6.13. It must be noted that this study represented the first use of a chiral iron catalyst in oxidative kinetic resolution of secondary alcohols.

Actually, the first general methodology for iron-catalyzed aerobic oxidative kinetic resolution of secondary alcohols was reported in 2011 by Katsuki et al. [101]. It was based on the use of 3 mol% of salen iron chiral complex **25** in toluene at 50 °C in the presence of 1-naphthol as an additive (Scheme 6.14). A wide range of chiral alcohols was achieved with good conversions (52–62%) and moderate to excellent enantioselectivities (67–99% ee). Especially very good results (90–97% ee) were obtained in the reaction of secondary benzylic alcohols regardless of the electronic nature of the aryl substituents. 1-(2-Naphthyl)ethanol was also compatible with 94% ee. However, a lower enantioselectivity (73% ee) was obtained in the kinetic resolution of 1-phenylethanol. Cyclic carbinols were also tolerated, although the observed enantioselectivities (67–88% ee) were found dependent on the ring size of the substrates. The reaction of alkenyl carbinols was also highly enantioselective (90% ee) as well as that of nonactivated dialkyl alcohols (86–99% ee).

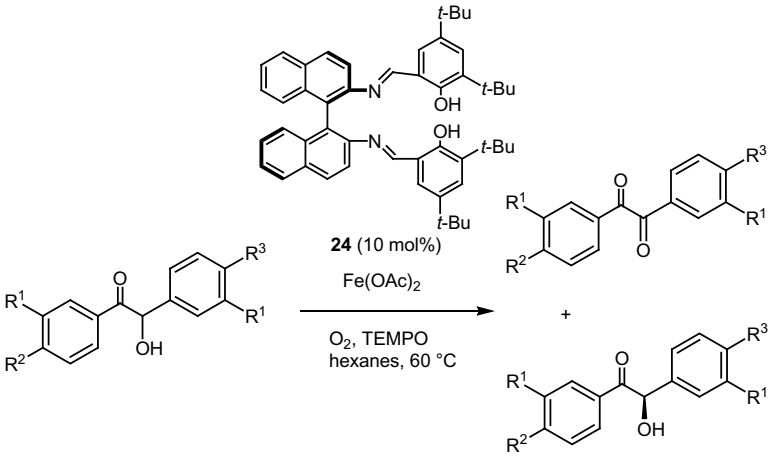

$R^1 = R^2 = R^3 = H$: conversion = 21%, ee = 98%, s = 7.2
$R^1 = H$, $R^2 = R^3 = Me$: conversion = 32%, ee = 90%, s = 7.7
$R^1 = R^2 = H$, $R^3 = Cl$: conversion = 31%, ee = 97%, s = 8.8
$R^1 = Me$, $R^2 = R^3 = H$: conversion = 33%, ee = 96%, s = 10.6

Scheme 6.13 Iron-catalyzed aerobic oxidative kinetic resolution of benzoins

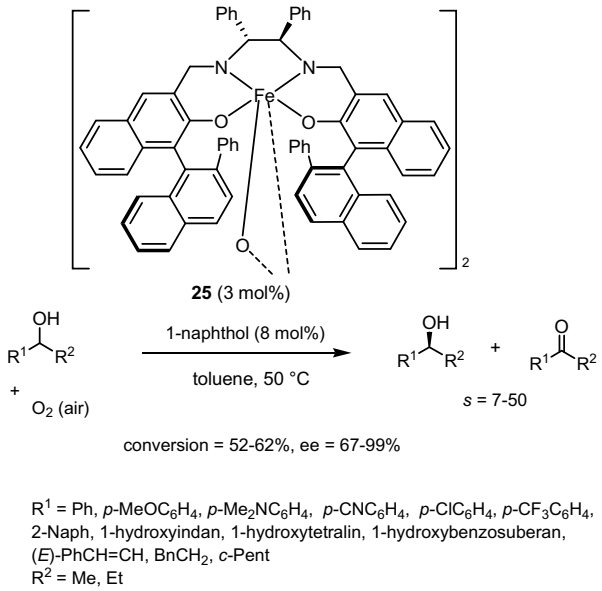

Scheme 6.14 Iron-catalyzed aerobic oxidative kinetic resolution of secondary alcohols

6.7 Reactions Catalyzed with Other Metals

In 2006, Gao et al. reported that an iridium(I) complex derived from chiral diaminodiphosphine **26** promoted the oxidative kinetic resolution of secondary arylalkanols with excellent enantioselectivities (≤98% ee) [102]. The reaction was performed in acetone as green oxidant and solvent in the presence of a base such as KOH, providing selectivity factors of up to 34 (Scheme 6.15, first equation). Excellent selectivity factors (≤100) were also reported by Ikariya et al. by using chiral iridium complex **27** bearing an *N*-sulfonylated diamine ligand in the aerobic kinetic resolution of secondary arylalkanols [Scheme 6.15 (second equation)] [103, 104].

Since many metals are expensive, the copper-catalyzed oxidative kinetic resolution of alcohols represents an economic challenge. The first copper-catalyzed oxidative kinetic resolution of secondary alcohols was reported in 2009 by Sekar et al. (Scheme 6.16) [105, 106]. High enantioselectivities of up to 98% ee were achieved by using a catalyst in situ generated from $Cu(OTf)_2$ and (*R*)-BINAM as ligand. In particular, secondary biaryl alcohols, such as benzoins and amino alcohols, were resolved in the presence of TEMPO under molecular oxygen as oxidant.

Moreover, cobalt-catalyzed oxidative kinetic resolutions of secondary alcohols using simple molecular oxygen have been developed. As an example, a chiral ketoiminatocobalt(II) complex **28** was applied in 2009 by Yamada et al. to promote the aerobic kinetic resolution of various secondary benzylic alcohols with good to high enantioselectivities (≤96% ee), as shown in Scheme 6.17 [107], whereas the use of

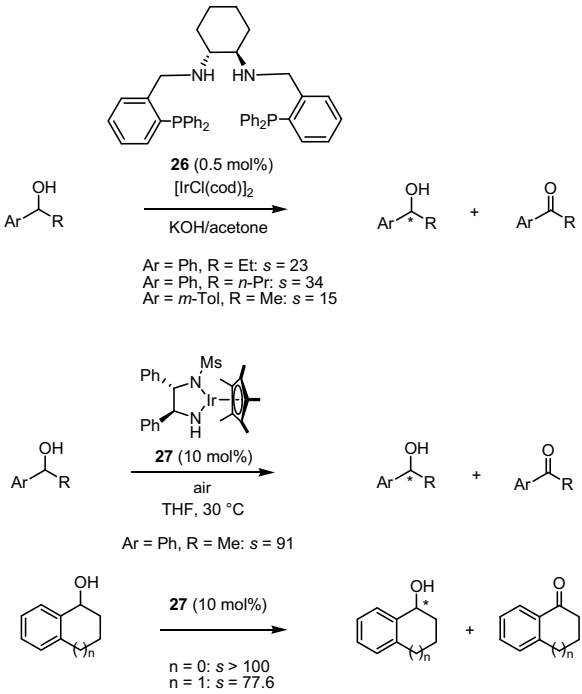

Scheme 6.15 Iridium-catalyzed oxidative kinetic resolutions of secondary arylalkanols

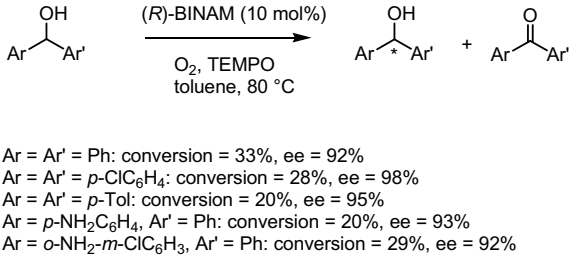

Scheme 6.16 Copper-catalyzed aerobic oxidative kinetic resolution of secondary biaryl alcohols

another cobalt complex bearing the Schiff base ligand **29** was applied to promote the kinetic resolution of α-hydroxy ketones and α-hydroxy esters with high selectivity factors of up to 47 and 31.9, respectively [108, 109].

In another context, Shibasaki et al. demonstrated that mixed BINOL/biphenol La/Li heterobimetallic complexes could be used to promote the oxidative kinetic resolution of tertiary α-nitroalcohols with high enantioselectivities (≤97% ee) combined with moderate to good conversions (30–47%) [110, 111]. Selectivity factors of up to 58.2 were observed by using a 2:1 mixture of La-Li_3(binaphthoxide)$_3$ complex and La-Li_3(biphenoxide)$_3$ complex **30** in THF at −20 °C, as shown in Scheme 6.18.

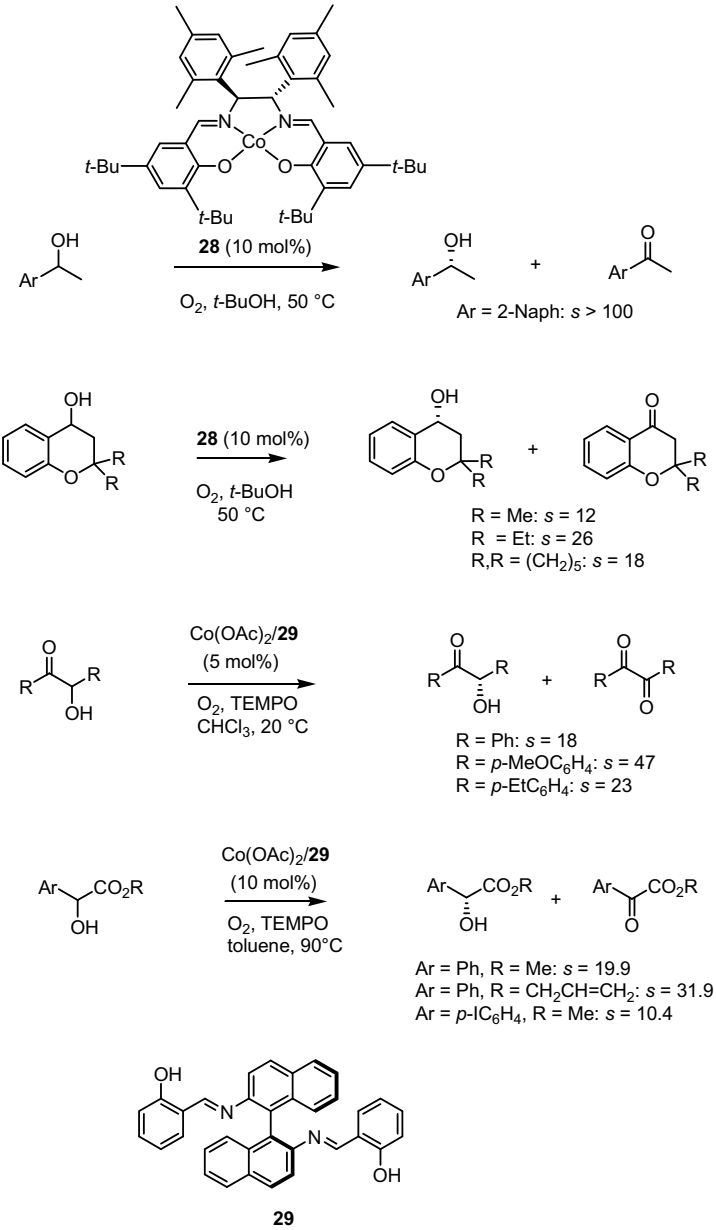

Scheme 6.17 Cobalt-catalyzed aerobic oxidative kinetic resolutions of secondary benzylic alcohols

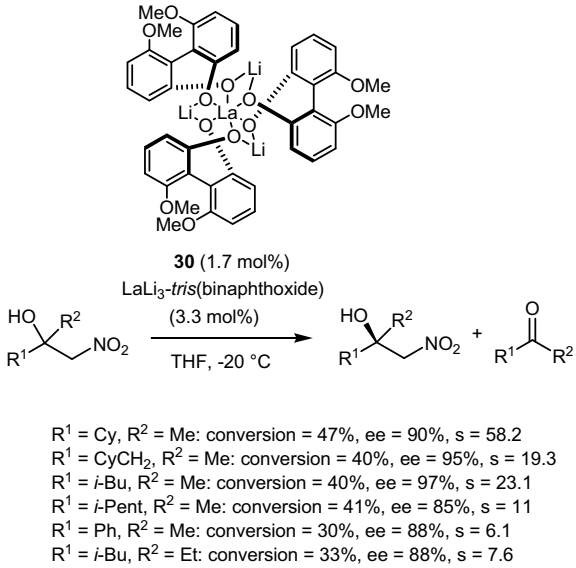

Scheme 6.18 Oxidative kinetic resolution of secondary alcohols catalyzed by mixed La/Li heterobimetallic complexes

The synthesis of chiral surfactants bearing two long alkyl chains with hydroxyl groups at their terminals was reported in 2014 by Wu et al. [112]. The latter was employed to encapsulate a polyoxometalate through electrostatic interaction. These thus formed chiral surfactant-encapsulated polyoxometalate complexes were further covalently immobilized on silica. The formed chiral supramolecular hybrid catalyst was found capable to promote the oxidative kinetic resolution of 1-phenylethanol with high enantioselectivity (89% ee).

6.8 Organocatalyzed Reactions

It is only recently that the first examples of enantioselective organocatalytic oxidative kinetic resolution of secondary alcohols were reported [113–115]. As an example, organocatalyzed oxidative kinetic resolutions of aldol products were developed in 2010 by Cheng et al. (Scheme 6.19) [116]. The process was catalyzed by chiral primary–tertiary amine organocatalyst **32** in acetone as green oxidant and solvent, providing selectivity factors of up to 115. It must be noted that the diastereoselectivity of the reaction remained unchanged.

Another type of chiral 1,2-diamines, such as (*R*,*R*)-1,2-di(1-naphthyl)-1,2-ethanediamine (NEDA), was shown by Repo et al. to be an efficient catalyst for the oxidative kinetic resolution of secondary benzyl alcohols by using TBHP as oxidant [117]. As shown in Scheme 6.20, the reaction was performed at room temperature in dichloromethane as solvent, leading to the corresponding chiral alcohols with moderate to high enantioselectivities (52–98% ee) and good conversions (39–55%).

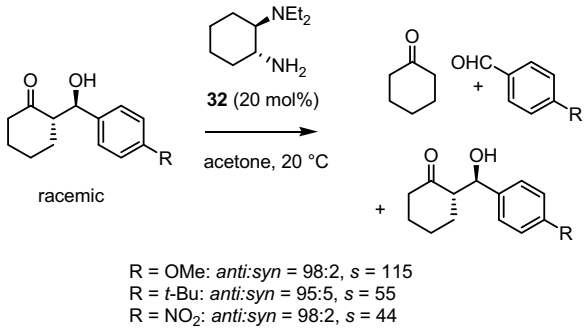

Scheme 6.19 Organocatalyzed oxidative kinetic resolution of aldol products

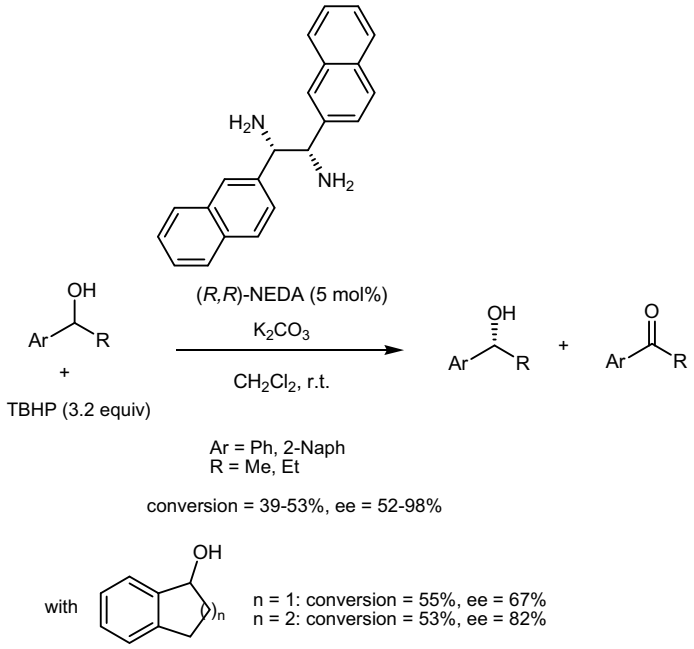

Scheme 6.20 Organocatalyzed oxidative kinetic resolution of benzylic secondary alcohols

Notably, even hindered cyclic carbinols, such as 1-tetranol and 1-indanol, were tolerated with moderate to good enantioselectivities (67–82% ee).

Another type of organocatalysts, such as quinine-derived urea organocatalyst **33**, was employed by Zhao et al. in 2013 to promote the oxidative kinetic resolution of *cis*-1,2-diols [118]. This process involved *N*-bromophthalimide as oxidant in chloroform as solvent. The scope of the methodology was extended to a *cis*-1,2-diol that was resolved with a low enantioselectivity (13% ee) whereas the corresponding α-hydroxyketone was obtained with 70% ee (Scheme 6.21).

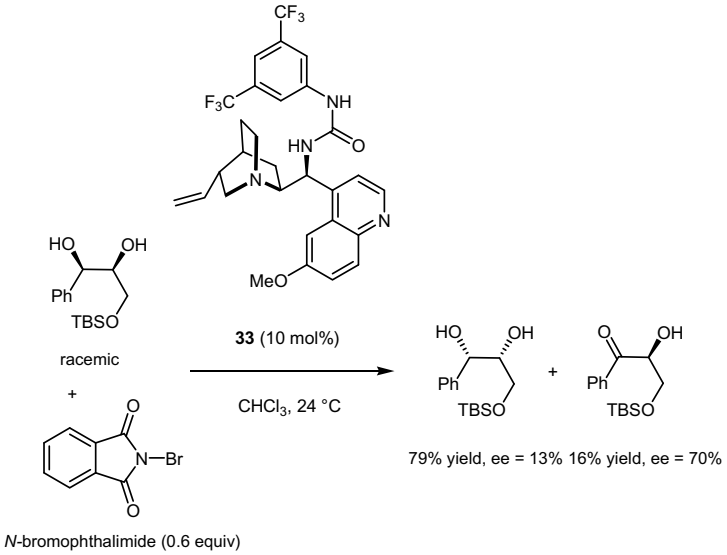

Scheme 6.21 Organocatalyzed oxidative kinetic resolution of a *cis*-1,2-diol

In addition, a kinetic oxidation of secondary aromatic alcohols through electrochemical oxidation was reported by Onomura et al. in 2008 [119]. These reactions were promoted by chiral azabicyclo-*N*-oxyls derived from L-hydroxyproline, such as **35**, providing moderate enantioselectivities (39–76% ee) and selectivity factors (5.3–21), as shown in Scheme 6.22.

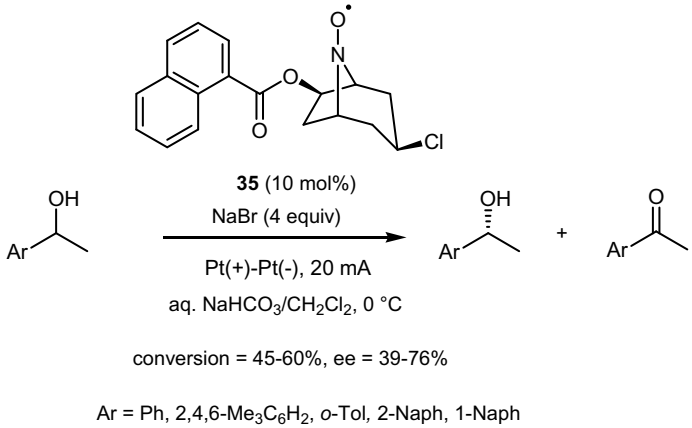

Scheme 6.22 Electrochemical oxidative kinetic resolution of secondary benzylic alcohols using an L-hydroxyproline-derived azabicyclo-*N*-oxyl organocatalyst

6.9 Conclusions

In the last decade, significant advances have been reported in the field of oxidative kinetic resolution of secondary racemic alcohols by using chiral palladium, vanadium, ruthenium, manganese, iridium, and cobalt complexes and more environmentally benign and inexpensive copper and iron chiral complexes, in addition to organocatalysts more recently developed. Among these versatile procedures, many provided chiral alcohols with very high enantioselectivities and good conversions by using these very different chiral catalysts and green oxidants, such as simple oxygen atmosphere or environmentally benign H_2O_2. Furthermore, it is only in the last 9 years that the first organocatalyzed oxidative kinetic resolutions have been developed. Further progress is expected in the future with the discovery of novel green chiral catalysts to be used with oxygen from air as simple and green oxidant.

References

1. Hoveyda AH, Didiuk MT (1998) Metal-catalyzed kinetic resolution processes. Curr Org Chem 2:489–526
2. Cook GR (2000) Transition metal-mediated kinetic resolution. Curr Org Chem 4:869–885. https://doi.org/10.2174/1385272810004080869
3. Keith M, Larrow JF, Jacobsen EN (2001) Practical considerations in kinetic resolution reactions. Adv Synth Catal 343:5–26. https://doi.org/10.1002/1615-4169
4. Robinson DEJE, Bull SD (2003) Kinetic resolution strategies using nonenzymatic catalysts. Tetrahedron Asymmetry 14:1407–1446. https://doi.org/10.1016/s0957-4166/2803/2900209-x
5. Breuer M, Ditrich K, Habicher T, Hauer B, Keβeler M, Stürmer R, Zelinski T (2004) Enantiomerically pure intermediates. Angew Chem Int Ed 43:788–824. https://doi.org/10.1002/anie.200300599
6. Vedejs E, Jure M (2005) Efficiency in nonenzymatic kinetic resolution. Angew Chem Int Ed 44:3974–4001. https://doi.org/10.1002/anie.200460842
7. Fogassy E, Nogradi M, Kozma K, Egri G, Palovics E, Kiss V (2006) Optical resolution methods. Org Biomol Chem 4:3011–3030. https://doi.org/10.1039/B603058K
8. Wurz RP (2007) Chiral dialkylaminopyridine catalysts in asymmetric synthesis. Chem Rev 107:5570–5595. https://doi.org/10.1021/cr068370e
9. Kagan HB, Fiaud, JC (1988) Kinetic resolution. In: Eliel EL, Wilen SH (eds) Top stereochem, vol 18. Wiley, Weinheim, pp 249–330
10. Collins AN, Sheldrake GN, Crosby J (eds) (1992) Chirality in industry. Wiley, Chichester
11. Koskinen A (ed) (1993) Asymmetric synthesis of natural products. Wiley, New York
12. Nogradi M (ed) (1995) Stereoselective synthesis. Wiley-VCH, Weinheim
13. Atkinson SC (ed) (1995) Stereoselective synthesis. Wiley, New York
14. Gadamasetti KG (ed) (1999) Process chemistry in the pharmaceutical industry. Marcel Dekker, New York
15. Blaser HU, Spindler F, Studer M (2001) Enantioselective catalysis in fine chemicals production. Appl Catal A 221:119–143. https://doi.org/10.1016/S0926-860X(01)00801-8
16. Noyori R (2003) Asymmetric catalysis: science and opportunities (nobel lecture 2001). Adv Synth Catal 345:15–32. https://doi.org/10.1002/adsc.200390002
17. Blaser HU, Schmidt E (eds) (2004) Asymmetric catalysis on industrial scale, challenges, approaches and solutions. Wiley-VCH, Weinheim

18. Farina V, Reeves JT, Senanayake CH, Song JJ (2006) Asymmetric synthesis of active pharmaceutical ingredients. Chem Rev 106:2734–2793. https://doi.org/10.1021/cr040700c
19. Wu G, Huang M (2006) Organolithium reagents in pharmaceutical asymmetric processes. Chem Rev 106:2596–2616. https://doi.org/10.1021/cr040694k
20. Bredig G, Fajans K (1908) Zur Stereochemie der Katalyse. Ber Dtsc Chem Ges 41:752–763. https://doi.org/10.1002/cber.190804101138
21. Martin VS, Woodard SS, Katsuki T, Yamada Y, Ikeda M, Sharpless KB (1981) Kinetic resolution of racemic allylic alcohols by enantioselective epoxidation. A route to substances of absolute enantiomeric purity? J Am Chem Soc 103:6237–6240. https://doi.org/10.1021/ja00410a053
22. Sharpless KB, Verhoeven TR (1979) Metal-catalyzed, highly selective oxygenations of olefins and acetylenes with tert-butyl hydroperoxide. Practical considerations and mechanisms. Aldrichimica Acta 12:63–74. https://doi.org/10.1021/ol027190y
23. Reetz MT (2001) Combinatorial and evolution-based methods in the creation of enantioselective catalysts. Angew Chem Int Ed 40:284–310. https://doi.org/10.1002/1521-3773
24. Pellissier H (2011) Catalytic nonenzymatic kinetic resolution. Adv Synth Catal 353:1613–1666. https://doi.org/10.1002/adsc.201100111
25. Pellissier H (2014) Catalytic kinetic resolution. In: Todd M (ed) Separation of enantiomers, synthetic methods. Wiley-VCH, Weinheim, pp 75–122
26. Petersen KS (2016) Chiral Brønsted acid catalyzed kinetic resolutions. Asian J Org Chem 5:308–320. https://doi.org/10.1002/ajoc.201600021
27. Yang H, Zheng WH (2018) Recent advances on nonenzymatic catalytic kinetic resolution of diols. Tetrahedron Lett 59:583–591. https://doi.org/10.1016/j.tetlet.2017.12.080
28. Jacobsen EN, Pfaltz A, Yamamoto H (eds) (2004) Comprehensive asymmetric catalysis, Suppl. 1. Springer, Heidelberg
29. Wills M (2008) Asymmetric catalysis using air: clean kinetic resolution of secondary alcohols. Angew Chem Int Ed 47:4264–4267. https://doi.org/10.1002/anie.200801152
30. Nicholas KM, Ferreira EM, Stoltz BM, Jensen DR, Pugsley JS, Sigman MS (2001) Palladium-catalyzed oxidative kinetic resolution of secondary alcohols. Chemtracts 14:654–658
31. Patel RN (2013) Biocatalytic synthesis of chiral alcohols and amino acids for development of pharmaceuticals. Biomolecules 3:741–777. https://doi.org/10.3390/biom3040741
32. Bull SD, Davies SG, Garner AC, Mujtaba N (2001) The asymmetric synthesis of (2R,3R)- and (2R,3S)-3-methyl-aspartates via an enantiodiscrimination strategy. Synlett 781–784. https://doi.org/10.1055/s-2001-14596
33. Dehli JR, Gotor V (2002) Parallel kinetic resolution of racemic mixtures: a new strategy for the preparation of enantiopure compounds? Chem Soc Rev 31:365–370. https://doi.org/10.1039/B205280F
34. Eames J (2003) In: Schmalz HG, Wirth T (eds) Organic synthesis highlights V. Wiley-VCH, Weinheim, pp 151–164
35. Noyori R, Tokunaga M, Kitamura M (1995) Stereoselective organic synthesis via dynamic kinetic resolution. Bull Chem Soc Jpn 68:36–55. https://doi.org/10.1246/bcsj.68.36
36. Huerta FF, Minidis ABE, Bäckvall J-E (2001) Racemisation in asymmetric synthesis. Dynamic kinetic resolution and related processes in enzyme and metal catalysis. Chem Soc Rev 321–331. https://doi.org/10.1039/b105464n
37. Stecher H, Faber K (1997) Biocatalytic deracemization techniques: dynamic resolutions and stereoinversions. Synthesis 1–16. https://doi.org/10.1055/s-1997-1515
38. Pellissier H (2003) Dynamic kinetic resolution. Tetrahedron 59:8291–8327. https://doi.org/10.1016/S0040-4020/2803/2901022-6
39. Pellissier H (2008) Recent developments in dynamic kinetic resolution. Tetrahedron 64:1563–1601. https://doi.org/10.1016/j.tet.2007.10.080
40. Pellissier H (2011) Recent developments in dynamic kinetic resolution. Tetrahedron 67:3769–3802. https://doi.org/10.1016/j.tet.2011.04.001
41. Pellissier H (ed) (2011) Chirality from dynamic kinetic resolution. The Royal Society of Chemistry, Cambridge

42. Pellissier H (2011) Catalytic nonenzymatic kinetic resolution. Adv Synth Catal 353:659–676. https://doi.org/10.1002/adsc.201000751
43. Pellissier H (2016) Recent developments in dynamic kinetic resolution. Tetrahedron 72:3133–3150. https://doi.org/10.1016/j.tet.2016.04.053
44. Ferreira EM, Stoltz BM (2001) The palladium-catalyzed oxidative kinetic resolution of secondary alcohols with molecular oxygen. J Am Chem Soc 123:7725–7726. https://doi.org/10.1021/ja015791z
45. Trend RM, Stolz BM (2004) An experimentally derived model for stereoselectivity in the aerobic oxidative kinetic resolution of secondary alcohols by (sparteine)$PdCl_2$. J Am Chem Soc 126:4482–4483. https://doi.org/10.1021/ja039551q
46. Jensen DR, Pugsley JS, Sigman MS (2001) Palladium-catalyzed enantioselective oxidations of alcohols using molecular oxygen. J Am Chem Soc 123:7475–7576. https://doi.org/10.1021/ja015827n
47. Mueller JA, Sigman MS (2003) Mechanistic investigations of the palladium-catalyzed aerobic oxidative kinetic resolution of secondary alcohols using (−)-sparteine. J Am Chem Soc 125:7005–7013. https://doi.org/10.1021/ja034262n
48. Jensen DR, Sigman MS (2003) Palladium catalysts for aerobic oxidative kinetic resolution of secondary alcohols based on mechanistic insight. Org Lett 5:63–65. https://doi.org/10.1021/ol027190y
49. Mandal SK, Jensen KR, Pugsley JS, Sigman MS (2003) Scope of enantioselective palladium(II)-catalyzed aerobic alcohol oxidations with (−)-sparteine. J Org Chem 68:4600–4603. https://doi.org/10.1021/jo0269161
50. Mandal SK, Sigman MS (2003) Palladium-catalyzed aerobic oxidative kinetic resolution of alcohols with an achiral exogenous base. J Org Chem 68:7535–7537. https://doi.org/10.1021/jo034717r
51. Bagdanoff JT, Ferreira EM, Stoltz BM (2003) Palladium-catalyzed enantioselective oxidation of alcohols: a dramatic rate acceleration by Cs_2CO_3/t-BuOH. Org Lett 5:835–837. https://doi.org/10.1021/ol027463p
52. Stoltz BM (2004) Palladium catalyzed aerobic dehydrogenation: from alcohols to indoles and asymmetric catalysis. Chem Lett 33:362–367. https://doi.org/10.1246/cl.2004.362
53. Sigman MS, Jensen DR (2006) Ligand-modulated palladium-catalyzed aerobic alcohol oxidations. Acc Chem Res 39:221–229. https://doi.org/10.1021/ar040243m
54. Bagdanoff JT, Stoltz BM (2004) Palladium-catalyzed oxidative kinetic resolution with ambient air as the stoichiometric oxidation gas. Angew Chem Int Ed 43:353–357. https://doi.org/10.1002/anie.200352444
55. Caspi DD, Ebner DC, Bagdanoff JT, Stoltz BM (2004) The resolution of important pharmaceutical building blocks by palladium-catalyzed aerobic oxidation of secondary alcohols. Adv Synth Catal 346:185–189. https://doi.org/10.1002/adsc.200303188
56. Mueller JA, Cowell A, Chandler BD, Sigman MS (2005) Origin of enantioselection in chiral alcohol oxidation catalyzed by Pd[(−)-sparteine]Cl_2. J Am Chem Soc 127:14817–14824. https://doi.org/10.1021/ja053195p
57. Ebner DC, Novak Z, Stoltz BM (2006) Oxidative kinetic resolution-Claisen rearrangement sequence to enantio-enriched aryl cycloalkenes. Synlett 20:3533–3539. https://doi.org/10.1055/s-2006-958415
58. Trend RM, Stoltz BM (2008) Structural features and reactivity of (sparteine)$PdCl_2$: a model for selectivity in the oxidative kinetic resolution of secondary alcohols. J Am Chem Soc 130:15957–15966. https://doi.org/10.1021/ja804955e
59. Ebner DC, Trend RM, Genet C, McGrath MJ, O'Brien P, Stoltz BM (2008) Palladium-catalyzed enantioselective oxidation of chiral secondary alcohols: access to both enantiomeric series. Angew Chem Int Ed 47:6367–6370. https://doi.org/10.1002/anie.200801865
60. Ebner DC, Bagdanoff JT, Ferreira EM, McFadden RM, Caspi DD, Trend RM, Stoltz BM (2009) The palladium-catalyzed aerobic kinetic resolution of secondary alcohols: reaction development, scope, and applications. Chem Eur J 15:12978–12992. https://doi.org/10.1002/chem.200902172

61. Thakur VV, Sudalai A, Indian (2005) Enantioselective synthesis of (S)-α-arylpropionic acids via Pd-catalyzed kinetic resolution of benzylic alcohols. Indian J Chem B 44B:557–562
62. Tambar UK, Ebner DC, Stoltz BM (2006) A convergent and enantioselective synthesis of (+)-amurensinine via selective C-H and C-C bond insertion reactions. J Am Chem Soc 128:11752–11753. https://doi.org/10.1021/ja0651815
63. Krishnan S, Bagdanoff JT, Ebner DC, Ramtohul YK, Tambar UK, Stoltz BM (2008) Pd-catalyzed enantioselective aerobic oxidation of secondary alcohols: applications to the total synthesis of alkaloids. J Am Chem Soc 130:13745–13754. https://doi.org/10.1021/ja804738b
64. Meyer ME, Phillips JH, Ferreira EM, Stoltz BM (2013) Use of a palladium(II)-catalyzed oxidative kinetic resolution in synthetic efforts toward bielschowskysin. Tetrahedron 69:7627–7635. https://doi.org/10.1016/j.tet.2013.02.034
65. Brien PO (2008) Basic instinct: design, synthesis and evaluation of (+)-sparteine surrogates for asymmetric synthesis. Chem Commun 655–667. https://doi.org/10.1039/b711420f
66. Dearden MJ, McGrath MJ, Brien PO (2004) Evaluation of (+)-sparteine-like diamines for asymmetric synthesis. J Org Chem 69:5789–5792. https://doi.org/10.1021/jo049182w
67. Lesma G, Pilati T, Sacchetti A, Silvani A (2008) New chiral diamino ligands as sparteine analogues. Application to the palladium-catalyzed kinetic oxidative resolution of 1-phenyl ethanol. Tetrahedron Asymmetry 19:1363–1366. https://doi.org/10.1016/j.tetasy.2008.05.006
68. Breuning M, Steiner M, Mehler C, Paasche A, Hein D (2009) A flexible route to chiral 2-endo-substituted 9-oxabispidines and their application in the enantioselective oxidation of secondary alcohols. J Org Chem 74:1407–1410. https://doi.org/10.1021/jo802409x
69. Chen T, Jiang J-J, Xu Q, Shi M (2007) Axially chiral NHC-Pd(II) complexes in the oxidative kinetic resolution of secondary alcohols using molecular oxygen as a terminal oxidant. Org Lett 9:865–868. https://doi.org/10.1021/ol063061w
70. Lj Liu, Wang F, Shi M (2009) Synthesis of chiral bis(N-heterocyclic carbene) palladium and rhodium complexes with 1,1'-biphenyl scaffold and their application in asymmetric catalysis. Organometallics 28:4416–4420. https://doi.org/10.1021/om900320c
71. Liu SJ, Liu L-j, Shi M (2009) Preparation of novel axially chiral NHC-Pd(II) complexes and their application in oxidative kinetic resolution of secondary alcohols. Appl Organometal Chem 23:183–190. https://doi.org/10.1002/aoc.1491
72. Hao B, Gunaratna MJ, Zhang M, Weerasekara S, Seiwald SN, Nguyen VT, Meier A, Hua DH (2016) Chiral-substituted poly-N-vinylpyrrolidinones and bimetallic nanoclusters in catalytic asymmetric oxidation reactions. J Am Chem Soc 138:16839–16848. https://doi.org/10.1021/jacs.6b12113
73. Radosevich AT, Misich C, Toste FD (2005) Vanadium-catalyzed asymmetric oxidation of α-hydroxy esters using molecular oxygen as stoichiometric oxidant. J Am Chem Soc 127:1090–1091. https://doi.org/10.1021/ja0433424
74. Yin L, Jia X, Li XS, Chan ASC (2010) Simply air: vanadium-catalyzed oxidative kinetic resolution of methyl o-chloromandelate by ambient air. Chin Chem Lett 21:774–777. https://doi.org/10.1016/j.cclet.2010.03.002
75. Radosevich AT, Chan VS, Shih H-W, Toste FD (2008) Synthesis of (−)-octalactin A by a strategic vanadium-catalyzed oxidative kinetic resolution. Angew Chem Int Ed 47:3755–3758. https://doi.org/10.1002/anie.200800554
76. Blanc A, Toste FD (2006) Enantioselective synthesis of cyclic ethers through a vanadium-catalyzed resolution/oxidative cyclization. Angew Chem Int Ed 45:2096–2099. https://doi.org/10.1002/anie.200503852
77. Weng S-S, Shen M-W, Kao J-Q, Munot YS, Chen C-T (2006) Chiral N-salicylidene vanadyl carboxylate-catalyzed enantioselective aerobic oxidation of α-hydroxy esters and amides. Proc Natl Acad Sci U S A 103:3522–3527. https://doi.org/10.1073/pnas.0511021103
78. Pawar VD, Bettigeri S, Weng S-S, Kao J-Q, Chen C-T (2006) Highly enantioselective aerobic oxidation of α-hydroxyphosphonates catalyzed by chiral vanadyl(V) methoxides bearing N-salicylidene-α-aminocarboxylates. J Am Chem Soc 128:6308–6309. https://doi.org/10.1021/ja060639o

79. Chen C-T, Bettigeri S, Weng S-S, Pawar VD, Lin Y-H, Liu C-Y, Lee W-Z (2007) Asymmetric aerobic oxidation of α-hydroxy acid derivatives by C4-symmetric, vanadate-centered, tetrakisvanadyl(V) clusters derived from N-salicylidene-α-aminocarboxylates. J Org Chem 72:8175–8185. https://doi.org/10.1021/jo070575f
80. Salunke SB, Babu NS, Chen C-T (2011) Asymmetric aerobic oxidation of α-hydroxy acid derivatives catalyzed by reusable, polystyrene-supported chiral N-salicylidene oxidovanadium tert-leucinates. Adv Synth Catal 353:1234–1240. https://doi.org/10.1002/adsc.201100062
81. Tan DM, Chan KS (2005) Asymmetric transfer hydrogenation of ketones in 2-propanol catalyzed by arsinooxazoline-ruthenium(II) complex. Tetrahedron Lett 46:503–505. https://doi.org/10.1016/j.tetlet.2004.11.097
82. Nakamura Y, Egami H, Matsumoto K, Uchida T, Katsuki T (2007) Aerobic oxidative kinetic resolution of racemic alcohols with bidentate ligand-binding Ru(salen) complex as catalyst. Tetrahedron 63:6383–6387. https://doi.org/10.1016/j.tet.2007.03.105
83. Mizoguchi H, Uchida T, Katsuki T (2014) Ruthenium-catalyzed oxidative kinetic resolution of unactivated and activated secondary alcohols with air as the hydrogen acceptor at room temperature. Angew Chem Int Ed 53:3178–3182. https://doi.org/10.1002/anie.201310426
84. Sun W, Wang H, Xia C, Li J, Zhao P (2003) Chiral-Mn(salen)-complex-catalyzed kinetic resolution of secondary alcohols in water. Angew Chem Int Ed 42:1042–1044. https://doi.org/10.1002/anie.200390268
85. Li Z, Tang ZH, Hu XX, Xia CG (2005) Insight into the mechanism of oxidative kinetic resolution of racemic secondary alcohols by using manganese(III)(salen) complexes as catalysts. Chem Eur J 11:1210–1216. https://doi.org/10.1002/chem.200400818
86. Cheng Q, Deng F, Xia C, Sun W (2008) The Mn(salen)-catalyzed oxidative kinetic resolution of secondary alcohols: reaction development and scope. Tetrahedron Asymmetry 19:2359–2362. https://doi.org/10.1016/j.tetasy.2008.10.008
87. Pathak K, Ahmad I, Abdi SHR (2007) Oxidative kinetic resolution of racemic secondary alcohols catalyzed by recyclable chiral dimeric Mn(III) salen catalysts. J Mol Catal A 274:120–126. https://doi.org/10.1016/j.molcata.2007.04.036
88. Kureshy RI, Ahmad I, Pathak K, Khan N-UH, Abdi SHR, Prathap JK, Jasra RV (2007) Easily recyclable chiral polymeric Mn(III) salen complexes for oxidative kinetic resolution of racemic secondary alcohols. Chirality 19:352–357. https://doi.org/10.1002/chir.20387
89. Sun W, Wu X, Xia C (2007) Enantioselective oxidation of secondary alcohols catalyzed by soluble chiral polymeric [N′, N′-Bis(salicylidene)ethane-1,2-diaminato(2−)]manganese(III) (Mn^{III}(salen)) type complexes in a biphasic system. Helv Chim Acta 90:623–626. https://doi.org/10.1002/hlca.200790064
90. Bera PK, Maity NC, Abdi SHR, Khan N-UH, Kureshy RI, Bajaj HC (2013) Macrocyclic Mn(III) salen complexes as recyclable catalyst for oxidative kinetic resolution of secondary alcohols. Appl Catal A 467:542–551. https://doi.org/10.1016/j.apcata.2013.07.055
91. Li C, Zhao J, Tan R, Peng Z, Luo R, Peng M, Yin D (2011) Recyclable ionic liquid-bridged chiral dimeric salen Mn(III) complexes for oxidative kinetic resolution of racemic secondary alcohols. Catal Commun 15:27–31. https://doi.org/10.1016/j.catcom.2011.08.009
92. Tan R, Dong Y, Peng M, Zheng W, Yin D (2013) Thermoresponsive chiral salen Mn(III) complexes as efficient and reusable catalysts for the oxidative kinetic resolution of secondary alcohols in water. Appl Catal A 458:1–10. https://doi.org/10.1016/j.apcata.2013.03.015
93. Tan C, Jiao J, Li Z, Liu Y, Han X, Cui YL (2018) Design and assembly of a chiral metallosalen-based octahedral coordination cage for supramolecular asymmetric catalysis. Angew Chem Int Ed 57:2085–2090. https://doi.org/10.1002/anie.201711310
94. Kantam ML, Ramani T, Chakrapani L, Choudary BM (2007) Oxidative kinetic resolution of racemic secondary alcohols catalyzed by resin supported sulfonato-Mn(salen) complex in water. J Mol Catal A 274:11–15. https://doi.org/10.1016/j.molcata.2007.04.020
95. Sahoo S, Kumar P, Lefebvre F, Halligudi SB (2009) Oxidative kinetic resolution of alcohols using chiral Mn–salen complex immobilized onto ionic liquid modified silica. Appl Catal A 354:17–25. https://doi.org/10.1016/j.apcata.2008.10.039

96. Sahoo S, Kumar P, Lefebvre F, Halligudi SB (2008) A chiral Mn(III) salen complex immobilized onto ionic liquid modified mesoporous silica for oxidative kinetic resolution of secondary alcohols. Tetrahedron Lett 49:4865–4868. https://doi.org/10.1016/j.tetlet.2008.06.014
97. Ren L, Li L, Li Y, Zhang G, Huang B, Imam Z, Zheng A, Sun Y (2016) Mesoporous helical silica immobilizing manganese(III)-salen complex for oxidative kinetic resolution of secondary alcohols. J Porous Mater 23:19–33. https://doi.org/10.1007/s10934-015-0052-4
98. Talsi TS, Samsonenko DG, Bryliakov KP (2017) Asymmetric autoamplification in the oxidative kinetic resolution of secondary benzylic alcohols catalyzed by manganese complexes. ChemCatChem 9:2599–2607. https://doi.org/10.1002/cctc.201700438
99. Miao C, Li X-X, Lee Y-M, Xia C, Wang Y, Nam W, Sun W (2017) Manganese complex-catalyzed oxidation and oxidative kinetic resolution of secondary alcohols by hydrogen peroxide. Chem Sci 8:7476–7482. https://doi.org/10.1039/c7sc00891k
100. Muthupandi P, Alamsetti SK, Sekar G (2009) Chiral iron complex catalyzed enantioselective oxidation of racemic benzoins. Chem Commun 3288–3290. https://doi.org/10.1039/b904021h
101. Kunisu T, Oguma T, Katsuki T (2011) Aerobic oxidative kinetic resolution of secondary alcohols with naphthoxide-bound iron(salan) complex. J Am Chem Soc 133:12937–12939. https://doi.org/10.1021/ja204426s
102. Li YY, Zhang X-Q, Dong Z-R, Shen W-Y, Chen G, Gao J-X (2006) Kinetic resolution of racemic secondary alcohols catalyzed by chiral diaminodiphosphine-Ir(I) complexes. Org Lett 8:5565–5567. https://doi.org/10.1021/ol062244f
103. Arita S, Koike T, Kayaki Y, Ikariya Y (2008) Aerobic oxidative kinetic resolution of racemic secondary alcohols with chiral bifunctional amido complexes. Angew Chem Int Ed 47:2447–2449. https://doi.org/10.1002/anie.200705875
104. Ikariya T, Kuwata S, Kayaki Y (2010) Aerobic oxidation with bifunctional molecular catalysts. Pure Appl Chem 82:1471–1483. https://doi.org/10.1351/PAC-CON-09-09-08
105. Alamsetti SK, Mannam S, Mutupandi P, Sekar G (2009) Galactose oxidase model: biomimetic enantiomer-differentiating oxidation of alcohols by a chiral copper complex. Chem Eur J 15:1086–1090. https://doi.org/10.1002/chem.200802064
106. Mannam S, Sekar G (2009) An enantiopure galactose oxidase model: synthesis of chiral amino alcohols through oxidative kinetic resolution catalyzed by a chiral copper complex. Tetrahedron Asymmetry 20:497–502. https://doi.org/10.1016/j.tetasy.2009.02.013
107. Yamada T, Higano S, Yano T, Yamashita Y (2009) Cobalt-catalyzed oxidative kinetic resolution of secondary benzylic alcohols with molecular oxygen. Chem Lett 38:40–41. https://doi.org/10.1246/cl.2009.40
108. Alamsetti SK, Muthupandi P, Sekar G (2009) Chiral cobalt-catalyzed enantiomer-differentiating oxidation of racemic benzoins by using molecular oxygen as stoichiometric oxidant. Chem Eur J 15:5424–5427. https://doi.org/10.1002/chem.200900387
109. Alamsetti SK, Sekar G (2010) Chiral cobalt-catalyzed enantioselective aerobic oxidation of α-hydroxy esters. Chem Commun 46:7235–7237. https://doi.org/10.1039/C0CC01917H
110. Sy Tosaki, Hara K, Gnanadesikan V, Morimoto H, Harada S, Sugita M, Tamagiwa N, Matsunaga S, Shibasaki M (2006) Mixed La–Li heterobimetallic complexes for tertiary nitroaldol resolution. J Am Chem Soc 128:11776–11777. https://doi.org/10.1021/ja0648581
111. Hara K, Sy Tosaki, Gnanadesikan V, Morimoto H, Harada S, Sugita M, Yamagiwa N, Matsunaga S, Shibasaki M (2009) Mixed La-Li heterobimetallic complexes for tertiary nitroaldol resolution. Tetrahedron 65:5030–5036. https://doi.org/10.1016/j.tet.2009.02.031
112. Shi L, Wang Y, Li B, Wu L (2014) Polyoxometalate complexes for oxidative kinetic resolution of secondary alcohols: unique effects of chiral environment, immobilization and aggregation. Dalton Trans 43:9177–9188. https://doi.org/10.1039/C4DT00742E
113. Tomizawa M, Shibuya M, Iwabuchi Y (2009) Highly enantioselective organocatalytic oxidative kinetic resolution of secondary alcohols using chirally modified AZADOs. Org Lett 11:1829–1831. https://doi.org/10.1021/ol900441f
114. Tomizawa M, Shibuya M, Iwabuchi Y (2014) Correction to highly enantioselective organocatalytic oxidative kinetic resolution of secondary alcohols using chirally modified AZADOs. Org Lett 16:4968. https://doi.org/10.1021/ol502543r

115. Murakami K, Sasano Y, Tomizawa M, Shibuya M, Kwon E, Iwabuchi Y (2014) Highly enantioselective organocatalytic oxidative kinetic resolution of secondary alcohols using chiral alkoxyamines as precatalysts: catalyst structure, active species, and substrate scope. J Am Chem Soc 136:17591–17600. https://doi.org/10.1021/ja509766f
116. Luo S, Zhou P, Li J, Cheng JP (2010) Asymmetric retro- and transfer-aldol reactions catalyzed by a simple chiral primary amine. Chem Eur J 16:4457–4461. https://doi.org/10.1002/chem.201000181
117. Al-Hunaiti A, Räisänen M, Pihko P, Leskelä M, Repo T (2014) Organocatalytic oxidation of secondary alcohols using 1,2-Di(1-naphthyl)-1,2-ethanediamine (NEDA). Eur J Org Chem 6141–6144. https://doi.org/10.1002/ejoc.201402991
118. Rong ZQ, Pan HJ, Yan HL, Zhao Y (2014) Enantioselective oxidation of 1,2-diols with quinine-derived urea organocatalyst. Org Lett 16:208–211. https://doi.org/10.1021/ol4032045
119. Shiigi H, Mori H, Tanaka T, Demizu Y, Onomura O (2008) Chiral azabicyclo-*N*-oxyls mediated enantioselective electrooxidation of sec-alcohols. Tetrahedron Lett 49:5247–5251. https://doi.org/10.1016/j.tetlet.2008.06.112

Chapter 7
Asymmetric Epoxidation Catalyzed by Biologically Inspired Non-heme Iron Catalysts and Hydrogen Peroxide

Laia Vicens and Miquel Costas

Abstract Asymmetric epoxidation is a very interesting reaction in organic synthesis because it allows the transformation of highly abundant hydrocarbons in chiral oxygenated products that can be further used in the preparation of more complex chiral compounds. Different catalysts that perform this transformation with high efficiency and with high levels of selectivity have been developed in the last years. However, those based on the combination of iron and hydrogen peroxide as oxidant are especially attractive. It is proposed that these catalysts worked through the formation of high-valent species bearing metal-oxo moieties. Herein, we describe the most relevant examples of bioinspired non-heme iron catalysts that have been reported in the literature for asymmetric epoxidations using H_2O_2, and also provide some considerations about the mechanism of this transformation.

Keywords Asymmetric epoxidation · Hydrogen peroxide · Iron · Bioinspired catalysis · Catalyst design · Reaction mechanisms · Non-heme

7.1 Introduction

7.1.1 Iron-Catalyzed Epoxidation in Nature

Asymmetric epoxidation is a very useful reaction in organic synthesis. Olefins are readily available feedstocks and epoxides have well-established rich chemistry [1]. Chiral epoxides are currently used as intermediates in the synthesis of more elaborated chiral products with applications in the pharmaceutical and chemical industries [2]. For example, one of the synthetic pathways to synthesize the HIV protease inhibitor Crixivan® involves the asymmetric epoxidation of indene [3], and diastereoselective epoxidation is employed in the preparation of the proteasome inhibitor Carfilzomib (Scheme 7.1), approved for the treatment of multiple myeloma

L. Vicens · M. Costas (✉)
Departament de Química i Institut de Química Computacional i Catàlisi, Facultat de Ciències, Campus de Montilivi, 17071 Girona, Catalonia, Spain
e-mail: miquel.costas@udg.edu

K. P. Bryliakov (ed.), *Frontiers of Green Catalytic Selective Oxidations*,
Green Chemistry and Sustainable Technology,
https://doi.org/10.1007/978-981-32-9751-7_7

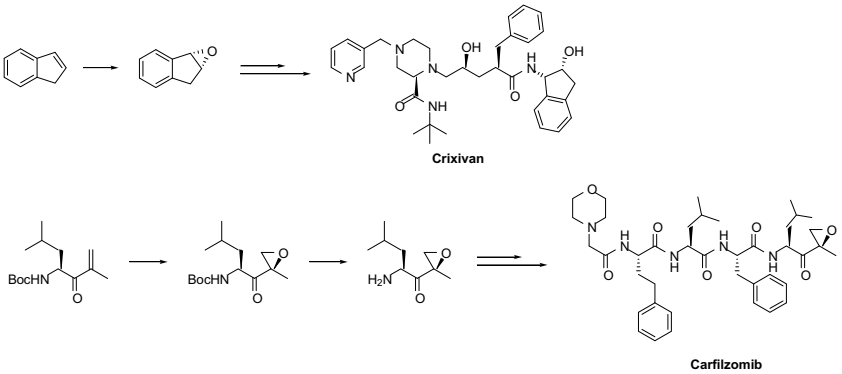

Scheme 7.1 Schematic synthesis of Crixivan and Carfilzomib

(marketed as Kaprolis®) [4]. Owing to their enormous potential, catalytic asymmetric epoxidation reactions have been actively explored over the last two decades. Metal-catalyzed reactions and organocatalysis have contributed in providing methods that permit epoxidation of a wide variety of olefins with high levels of enantioselectivity [5, 6]. Arguably, the major reagent versatility provided by organocatalysis has contributed in a more extensive manner to extend the substrate scope of the reaction [7–9]. However, the common limitation of organocatalysts, namely the large catalyst loadings and long reaction times usually required makes metal catalysis a competitive or preferable alternative in a number of cases.

Base metals constitute the most attractive option for metal catalyst development because of their availability and cost [10–12]. Among them, iron represents the optimum case [13–19]. Besides being the most abundant transition metal in the earth crust, it is readily accessible and it has minimum, if any, environmental impact. Iron indeed is a crucial element for life and plays a key role in red–ox processes taking place in living organisms. Notoriously, iron is prevalent in a number of enzymes that catalyze the oxidation of organic molecules. Epoxidation is also a notable reaction in the reactivity portfolio of oxygenases. For example, P450 catalyzes the epoxidation of arachidonic acid [20, 21], and non-heme iron-dependent epoxidases have been reported in various biosynthetic pathways, for example Hyoscyamine 6β-hydroxylase (H6H) in scopolamine [22], DdaC in N_{β}-epoxysuccinamoyl-DAP-Val [23], PntD in pentalenolactone [24], and the recently discovered AsqJ in quinolone alkaloid biosynthesis (Scheme 7.2) [25].

The ability of heme and non-heme enzymes to catalyze stereoselective epoxidations has promoted the development of synthetic iron complexes as chiral epoxidation catalysts [16, 26–29]. Historically, iron-catalyzed asymmetric epoxidations were first based in iron porphyrins [30–39]. Non-heme complexes capable of engaging in enantioselective epoxidation did not appear until more recently but have gained very rapid interest because of their improved performance with regard to hemes [19, 27, 28]. The structural versatility of non-heme catalysts also suggests that their potential applications and substrate scope are far superior to porphyrins.

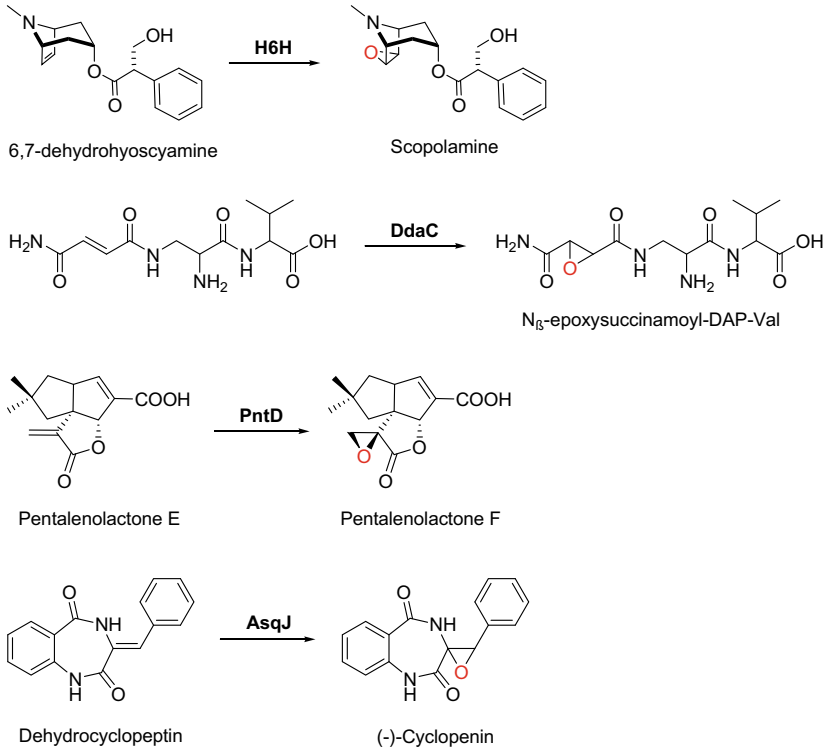

Scheme 7.2 Examples of epoxidations catalyzed by non-heme iron-dependent epoxidases

Among the oxidants employed, hydrogen peroxide and dioxygen stand up as particularly interesting from the point of view of atom economy, cost, and minimization of residues [11, 29, 40]. Hydrogen peroxide is particularly convenient. It is readily available and easy to handle in the form of aqueous solutions, and its byproduct is only water [41]. The use of metal catalysts effectively activates this molecule and oxidations can be performed without the need of elevated temperatures, as otherwise is often required when O_2 is employed as oxidant. This makes hydrogen peroxide a more convenient oxidant in terms of safety. Finally, hydrogen peroxide is a 2e-oxidant, and because of that its chemistry is simple to accommodate to 2e-oxidation reactions such as epoxidations. Instead, dioxygen is a 4e-oxidant and their use in epoxidation requires a cosubstrate or other 2e-source.

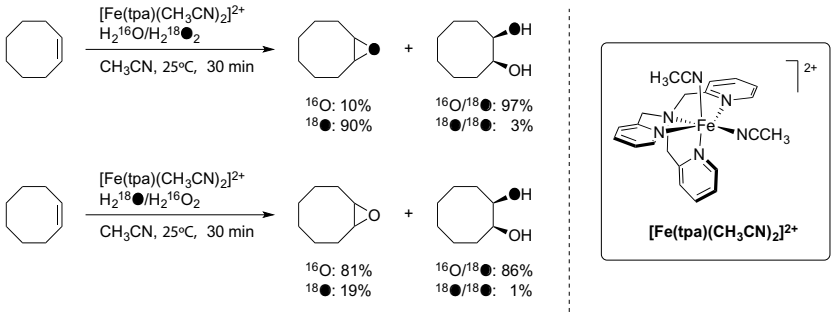

Scheme 7.3 Isotopic labeling experiments performed by Que and coworkers in the oxidation of cyclooctene using $[Fe(tpa)(CH_3CN)_2]^{2+}$ and H_2O_2

7.1.2 Non-heme Oxygenases as Models for Epoxidation Catalysts Development

The last decade has seen a very important advance in our knowledge of the number, structural, and chemical versatility of non-heme iron-dependent oxygenases [42–45]. These studies have shown that iron centers ligated to imidazole and carboxylic acid-containing protein residues can generate high-valent iron-oxo species competent for selective oxygen atom transfer to organic substrates [46], such as epoxidation. In parallel, synthetic bioinorganic chemistry has provided solid evidence that selected non-heme iron complexes, upon reaction with hydrogen peroxide, generate high-valent iron-oxo species and not hydroxyl radicals [18, 19, 47, 48]. A landmark study in this regard was described by Que and coworkers, who showed that the complex $[Fe(tpa)(CH_3CN)_2]^{2+}$ (Scheme 7.3) upon reaction with hydrogen peroxide, oxidizes cyclooctene to a mixture of cyclooctene-epoxide and cyclooctane-1,2-*syn*-diol [49]. Most remarkably, the formation of the two products proceed with stereoretention, and ^{18}O-isotopic labeling studies showed that hydrogen peroxide and water were the origin of the oxygen atoms incorporated into products, while atmospheric O_2 was not incorporated.

These reactions were performed with low substrate conversion conditions (<5%), and had no synthetic relevance. However, they revealed that these complexes have the potential to become selective olefin oxidation catalysts.

7.2 Iron Catalysts for Asymmetric Epoxidation Using H_2O_2

7.2.1 Early Examples with In Situ Generated Catalysts

One of the first described examples of a non-heme iron asymmetric epoxidation was reported by Jacobsen and Francis in 1999 [50]. The authors used a combinatorial

approach in which they combined a large set of chiral peptides with different metal salts. The resulting library of 5760 metal–ligand complexes was tested in the asymmetric epoxidation of *trans*-*β*-methylstyrene. The best results were obtained with the iron complexes (up to 78% yield when $FeCl_2$ was used in combination with **2**, Scheme 7.4), although only low enantioselectivities of up to 20% were achieved, probably due to the small control over the first coordination sphere around the metal, which was not identified. However, close inspection of the series of peptides **1**–**3** reveals common structural features; the three contain a pyridine or quinoline heterocycle, and a meridional $O_{carbonyl}$-$N_{H/imine}$-$N_{py/quin}$ donor set can be identified, along with a hydroxyl moiety, from a threonine residue.

In 2007, Beller and coworkers developed a practical methodology for the asymmetric epoxidation of olefins [51]. It consists, in the *in situ* generation, of iron catalyst by mixing $FeCl_3 \cdot 6H_2O$, pyridine-2,6-dicarboxylic acid, and a chiral diamine (**4**). This system is applied in the epoxidation of *trans*-stilbene derivatives, obtaining moderate to excellent yields and enantioselectivities (up to 92% yield and 97% ee). It was also tested in the epoxidation of styrene derivatives, but only moderate enantioselectivities were achieved (up to 53% ee) [52]. Despite its simplicity, the limited substrate scope of this system constitutes its most obvious limitation (Scheme 7.5).

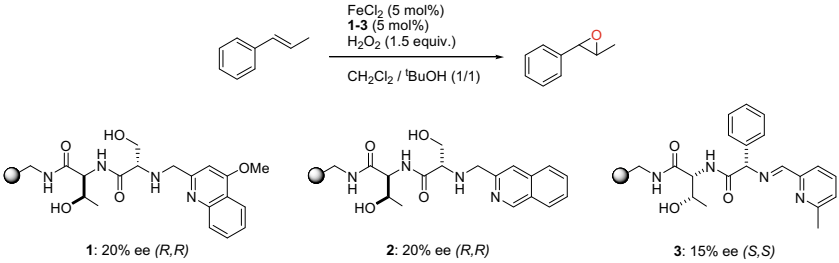

Scheme 7.4 Asymmetric epoxidation using $FeCl_2$ and peptide ligands (**1**–**3**) evolved from a combinatorial library

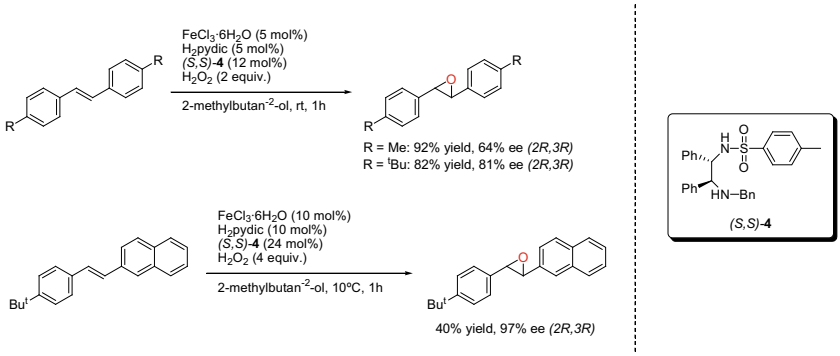

Scheme 7.5 Asymmetric epoxidation of olefins with $FeCl_3$, H_2pydic, and a chiral diamine (**4**)

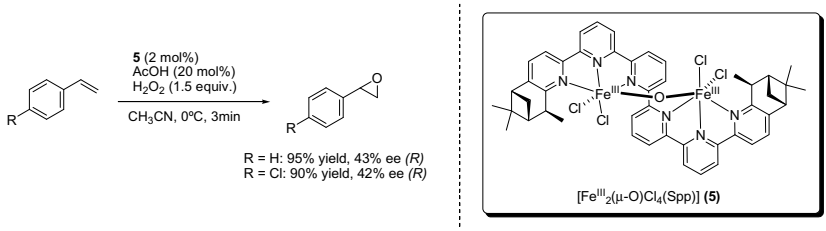

Scheme 7.6 Asymmetric epoxidation of styrene derivatives catalyzed by the Fe-hexapyridine complex (**5**)

7.2.2 Early Examples with Well-Defined Coordination Complexes as Catalysts

A more elaborated catalyst from the point of view of the ligand and the coordination structure of the iron center was reported 1 year later by Kwong and coworkers [53]. The catalyst was based on a hexapyridine ligand containing a pinene group attached at two of the pyridine rings. When the ligand is combined with two equivalents of $FeCl_2$, an oxo-bridged dimer is generated, which is able to epoxidize styrenes using H_2O_2 in the presence of acetic acid in very short reaction times, obtaining high yields of the epoxide (50–100%), but only moderate levels of enantioselectivity (up to 43% ee) (Scheme 7.6).

7.2.3 Catalysts Based on Nitrogen-Based Tetradentate Ligands

Arguably, the most successful family of non-heme iron catalysts developed for asymmetric epoxidation are those based on tetradentate ligands with a linear *bis*-amine-*bis*-pyridine (or related heterocycle) structure [54]. These catalysts bear structural similarities to the early described Fe(tpa) catalyst; in first place, they have an N-donating tetradentate ligand combining pyridine and aliphatic amine donors; in second place, the ligand leaves two labile binding sites in the octahedral coordination sphere of the iron center, readily available for peroxide binding and activation. Finally, these can be seen as strong field ligands that favor low-spin states. Furthermore, when these ligands are bonded to the metal, they form three five-membered chelate cycles, which provides high stability to the complexes. In an octahedral complex, linear *bis*-amine-*bis*-pyridine ligands can be bound to the metal center *via* three different topologies: *cis*-α, *cis*-β, or *trans* (Fig. 7.1, left) [55–57]. So far, *cis*-α complexes have been most commonly and successfully explored in asymmetric epoxidation catalysis. In this topology, the two pyridines are *trans* to each other, and the two aliphatic diamines are in *cis*. These leave two *cis*-labile coordination sites, which will be used to activate H_2O_2. Moreover, the aliphatic diamine of the ligand defines the chirality

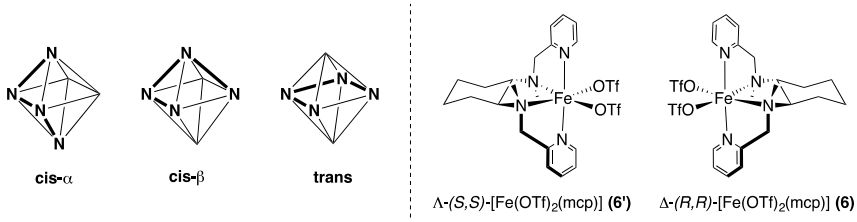

Fig. 7.1 Topologies for octahedral iron complexes with linear tetradentate ligands (left) and enantiomeric forms of $[Fe(OTf)_2(mcp)]$, OTf = trifluoromethanesulfonate anion, depending on the chirality of the diamine backbone (right)

at the metal (Λ or Δ) [56, 58, 59]. Therefore, although the chiral diamine is not at the same site of the complex where the peroxide is activated, its chirality is effectively translated toward the chirality at the metal, and the latter effectively impacts the enantioselectivity of the reactions (Fig. 7.1, right).

The epoxidation activity of this class of complexes was first described by Que and Jacobsen. The latter described their ability to catalyze alkene epoxidation on preparative scales. Jacobsen used $[Fe^{II}(men)(CH_3CN)_2](SbF_6)_2$ **(22)**, a complex based on a non-chiral linear ligand that combines two pyridines and a dimethylethylenediamine unit [60]. Using acetic acid as an additive, high yields were obtained (61–90%) in the epoxidation of a series of aliphatic alkenes (Scheme 7.7). Although this complex does not produce chiral epoxides, its discovery as a particularly effective epoxidation catalyst and the straightforward possibility of designing related chiral versions was recognized by different authors in the field as the basis for the preparation of chiral epoxidizing iron complexes (Fig. 7.2). The main strategy pursued is based on changing the aliphatic diamine of the catalyst and installing readily available chiral diamines [28].

In parallel, Que and coworkers studied the asymmetric epoxidation ability of (R,R)-$[Fe^{II}(OTf)_2(mcp)]$ **(6)**, in which the mcp ligand contains a chiral 1,2-cyclohexanediamine as the backbone. In this case, only low enantioselectivity (up to 12% ee) was obtained in the epoxidation of *trans*-2-heptene [61]. However, in 2011, Sun and coworkers reexamined the use of the same complex in the epoxidation of other families of substrates (i.e., *trans*-chalcones), obtaining remarkably improved

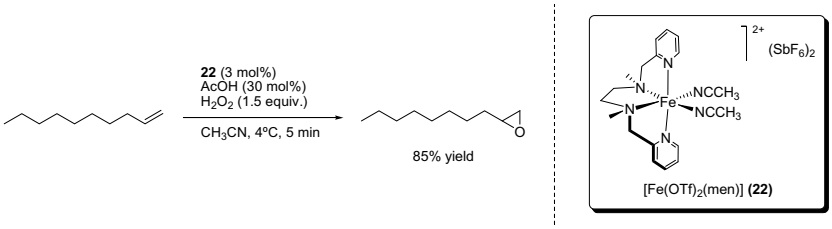

Scheme 7.7 Epoxidation of olefins with $[Fe^{II}(men)(CH_3CN)_2](SbF_6)_2$ **(22)** and H_2O_2

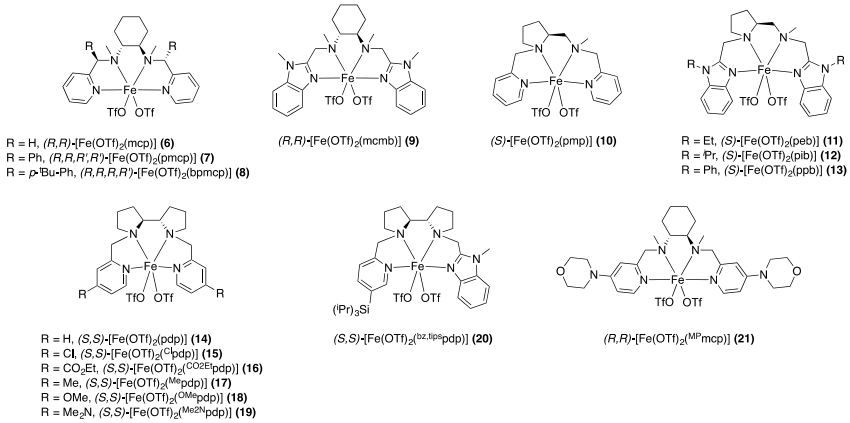

Fig. 7.2 Examples of iron complexes used in the asymmetric epoxidation of olefins

enantioselectivities up to 54% ee when acetic acid was used as additive [62]. The authors also reported a structurally more elaborated catalyst in which aromatic groups were introduced in the pseudo-benzylic positions **(7–8)**, achieving up to 78% ee in the epoxidation of substituted *trans*-chalcones using **8**. A few years later, **6** was further modified by the same authors by replacing the pyridines of the ligand by benzylimidazoles **(9)**, and it was successfully applied in the asymmetric epoxidation of chalcone derivatives, improving the enantioselectivity up to 95% [63]. Probably the main limitation of this system is that high enantioselectivities have so far only been described in the epoxidation of aromatic *trans*-α,β-enones (Scheme 7.8; Table 7.1).

Shortly afterward, the same group reported a new catalyst in which the ligand diamine backbone was based on proline **(10)** [64]. This complex is significantly

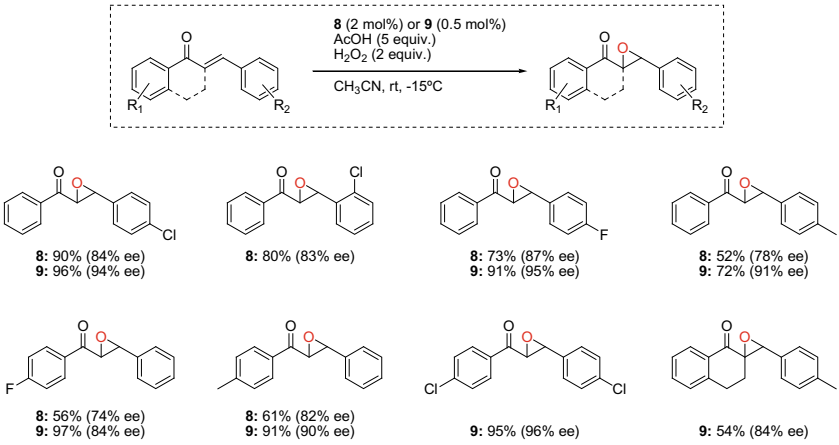

Scheme 7.8 Representative substrate scope of catalysts **8** and **9**

Table 7.1 Asymmetric epoxidation of chalcone with the series of catalysts **6–9** and H_2O_2, showing the progressive improvement in enantioselectivity

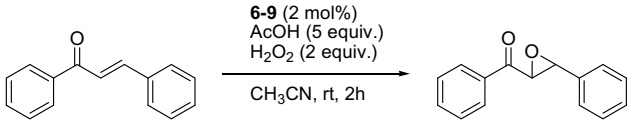

Entry	Catalyst	Yield (%)	ee (%)	Ref.
1	**6**	47	54	[62]
2	**7**	45	71	[62]
3	**8**	47	72	[62]
4[a]	**8**	52	78	[62]
5[b]	**9**	94	90	[63]

[a]T = −30 °C
[b]0.5 mol% **9**, T = −20 °C

different from the previously described examples because this diamine provides C_1 symmetry to the catalyst. This catalyst was applied in the asymmetric epoxidation of *trans*-chalcone obtaining moderate yields and enantioselectivities (up to 68% yield and 56% ee). However, these results were substantially improved when the pyridines of the catalyst were substituted by benzylimidazoles **(11–13)**, where up to 99% yield and 98% ee were obtained in the epoxidation of the same kind of substrates (Scheme 7.9; Table 7.2).

In parallel, Talsi, Bryliakov, and coworkers explored the use of (*S,S*)-[Fe(OTf)$_2$(pdp)] **(14)** in the asymmetric epoxidation of aromatic enones [65]. This complex had been previously reported by Que and coworkers [66] replacing the acetonitrile ligands present in the original catalyst described by White and Chen [67], by triflate anions. The White-Chen catalyst was originally used in C–H oxidation

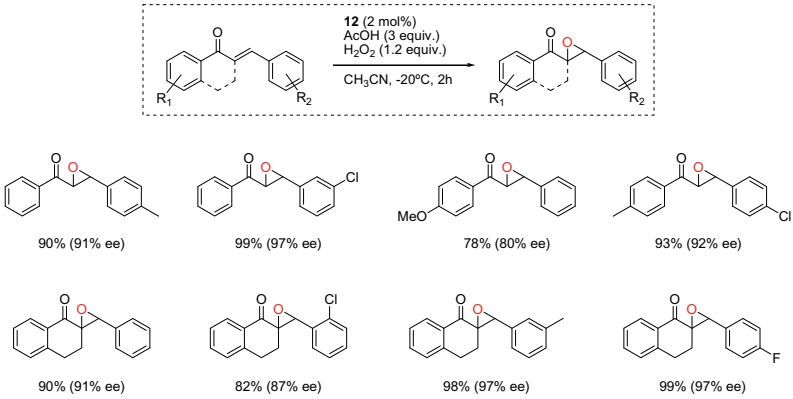

Scheme 7.9 Representative substrate scope exhibited by C_1-symmetric catalyst **12**

Table 7.2 Asymmetric epoxidation of chalcone with the series of catalysts **10–13** and H_2O_2 [64]

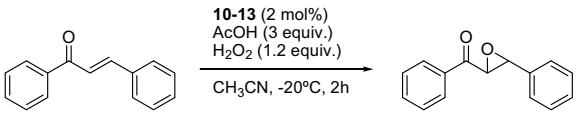

Entry	Catalyst	Yield (%)	ee (%)
1	**10**	68	56
2	**11**	89	92
3	**12**	90	88
4	**13**	83	86

reactions under similar conditions to those employed in the epoxidations. This work demonstrated that the replacement of the cyclohexyldiamine by a *bis*-pyrrolidine backbone results in a catalyst that provides better enantioselectivities (up to 71% ee). Moreover, in this work, the authors demonstrated that different carboxylic acids could be used instead of acetic acid, having a high influence in the yield and the enantiomeric excess of the final epoxide (Table 7.3). Also, this catalyst was applied to other substrates distinct from chalcones, such as styrene derivatives, but only moderate enantioselectivities were then obtained (Scheme 7.10).

Closer in time, Cussó et al. modified the family of *bis*-pyrrolidine-based complexes by introducing different groups in position 4 of the pyridines in the ligand, with the final goal to study the impact of tuning the electronic properties of these tetradentate ligands on the catalytic properties of the corresponding iron complexes $[Fe^{II}(OTf)_2(^{x}pdp)]$ **(15–19)** [68]. This set of catalysts was tested in the asymmetric epoxidation of *cis-ß*-methylstyrene and it was observed that the yield and the stereos-

Table 7.3 Asymmetric epoxidation of chalcone with catalyst **4**, H_2O_2, and different carboxylic acids [65]

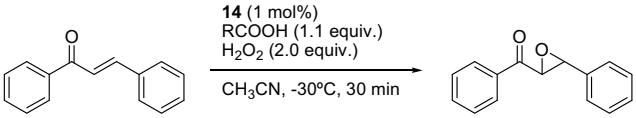

Entry	RCOOH	Conv (%)	Yield (%)	ee (%)
1	AcOH	92	92	71
2	FA	10	10	65
3	BuA	97	91	72
4	^{i}BuA	97	97	78
5	2-eha	100	98	86

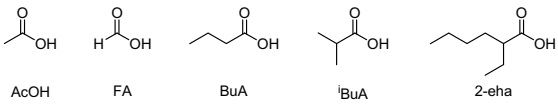

Scheme 7.10 Substrate scope of catalyst **14** beyond chalcones

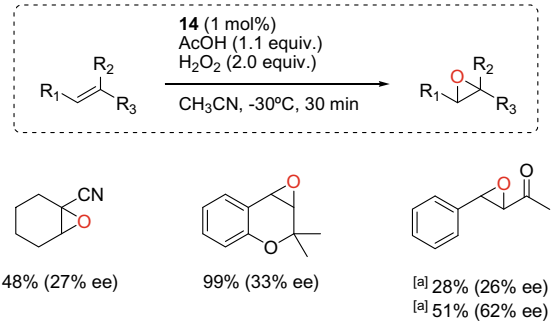

[a] *2-eha was used instead of AcOH*

electivity of the product were systematically dependent on the electronic properties of the ligand: the more electron donating was the ligand the higher was the yield and the enantioselectivity of the resulting epoxide (the yield improved from 13 to 87% and the enantioselectivity from 16 to 62% ee) (Table 7.4). Moreover, using the complex bearing the most electron-donating ligand **(19)**, the chemoselectivity and the enantioselectivity of the epoxidation remained unaltered when only catalytic amounts of acetic acid were used. This behavior was not observed with the less electron-rich catalysts as a decrease of the yields was observed when the amounts of acetic acid were reduced (Table 7.4). Using the best catalyst of the series, $[Fe^{II}(OTf_2)(^{Me2N}pdp)]$ **(19)**, different carboxylic acids were tested, finding that (*S*)-ibuprofen and 2-ethylhexanoic acid provided the best enantioselectivities in the epoxidation of a large scope of substrates (Scheme 7.11).

Table 7.4 Impact of the electronic properties of the complexes in the efficiency and enantioselectivity of the series of catalysts **14–19** [68]

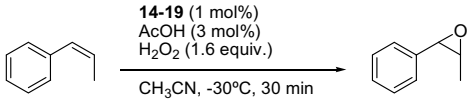

Entry	Catalyst	Conv (%)	Yield (%)	ee (%)
1	**15**	57	33	15
2	**16**	44	22	19
3	**14**	61	38	21
4	**17**	44	27	31
5	**18**	64	37	39
6	**19**	100	82	60
7[a]	**19**	100	87	62
8[a]	**15**	32	15	16

[a]3 mol% AcOH

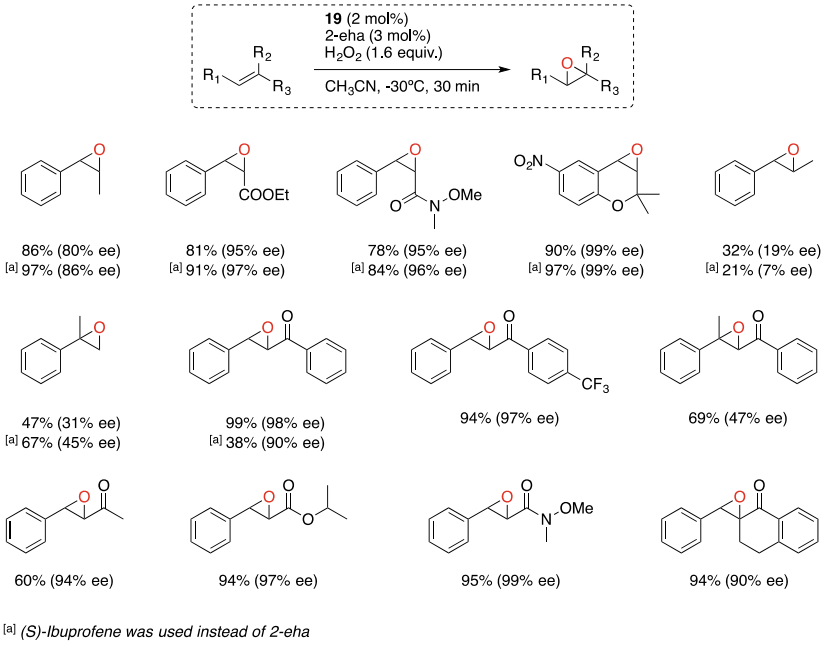

[a] *(S)-Ibuprofene was used instead of 2-eha*

Scheme 7.11 Representative substrate scope of the catalyst **19**

Building in these precedents, the authors explored the combination of catalyst **19** with *N*-protected amino acids as co-ligands instead of aliphatic carboxylic acids [69]. A different series of amino acids were tested in the asymmetric epoxidation of *cis-β*-methylstyrene. Since amino acids are chiral, possible match–mismatch effects resulting from the combination of the chirality of the catalyst and the amino acid were investigated. The best results were obtained using (*R,R*)**-19** in combination with *N*-Npha-Ile-OH **(23)**. Under the optimal conditions, the reaction was explored against styrene substrates with a different type of substitutions at the olefinic site (Fig. 7.3). Interestingly, α-methylstyrene, a substrate particularly difficult for current epoxidation methods, was epoxidized in good yield and enantioselectivity.

Exploration of the substrate scope of the system against a series of 1,1-disubstituted styrenes showed that the enantioselectivity improves systematically as the alkyl substituent changes from methyl to isopropyl and *t*-butyl, obtaining up to 90% yield and 97% ee (Scheme 7.12).

The same complex was then tested in combination with peptides containing a terminal free carboxylic acid as co-ligands (Scheme 7.13) [70]. In this approach, the peptide is envisioned to shape a second coordination sphere around the metal, resulting in a more elaborated system. Different peptides, some of them previously used in organocatalytic asymmetric reactions [71, 72], were tested taking into account the two possible enantiomeric forms of the catalyst, in order to investigate possible match–mismatch effects with the chirality of the peptide (Scheme 7.13).

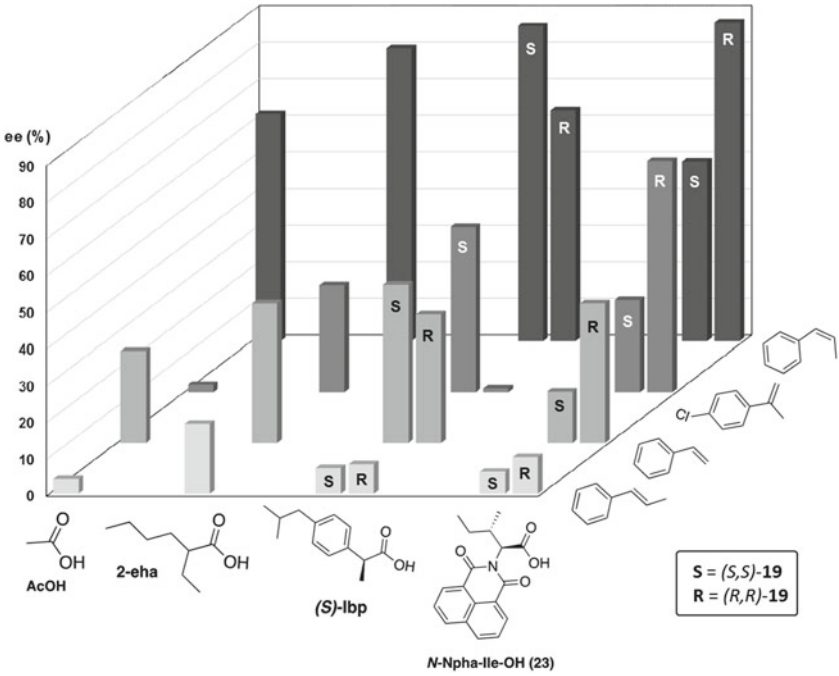

Fig. 7.3 Representation of the stereoselectivity on the epoxidation of structurally different styrenes with (*R,R*) and (*S,S*) forms of catalyst **19**. The bars containing "R" represent the enantiomeric excess obtained when (*R,R*)-**19** is used and the ones containing "S" represent the ee obtained when (*S,S*)-**19** was used. When chirality is not specified, (*S,S*)-**19** was used

Optimum results were obtained with peptide **28** and (*S,S*)-**19**, for which up to 82% yield and 92% ee was observed in the epoxidation of α-alkyl styrenes, including *ortho*-substituted ones (Scheme 7.14). Control experiments demonstrated that the combination of the peptide and the catalyst is necessary for good catalytic activity (Table 7.5), and remarkably, replacement of **24** by peptide **24-OMe**, where the carboxylic acid moiety has been esterified, resulted in a very poor catalytic system. Therefore, the carboxylic acid at the peptide effectively acts in combination with the catalyst in the activation of H_2O_2.

As both amino acids and peptides constitute natural ligands in non-heme iron-dependent oxygenases, these two last examples can be considered a significant advance toward the design of biologically inspired oxidation catalysts.

More recently, Cussó et al. reported a new family of C_1-symmetric catalysts $[Fe^{II}(OTf)_2(^{x,y}pdp)]$ that consists in a chiral *bis*-pyrrolidine combined with two different pyridines or related heterocycles, and applied it to the epoxidation of cyclic enones [73]. The best results in the asymmetric epoxidation of 2-cyclohexenone were obtained using the complex that combines a bulky pyridine substituted in position 5 with a bulky *tris*-isopropylsilyl group and a benzylimidazole, $[Fe^{II}(OTf_2)(^{bz,tips}pdp)]$ **(20)**. This system was the first example of iron catalysts competent to epox-

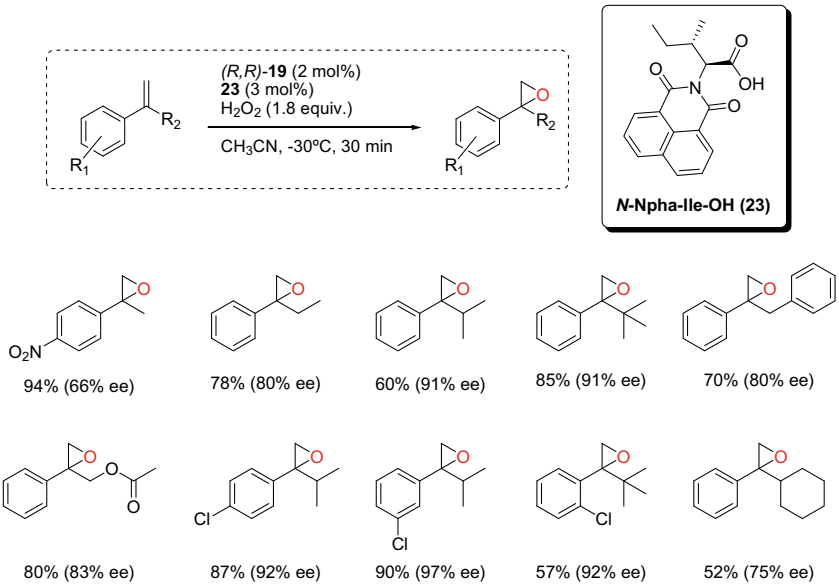

Scheme 7.12 Representative substrate scope of catalyst **19** in combination with *N*-Npha-Ile-OH (**23**)

idize cyclic aliphatic enones in high yields and excellent enantioselectivities (up to 95% ee) (Scheme 7.15).

It is remarkable to note that for cyclopentenone, a notoriously difficult substrate [74, 75], the epoxide was obtained in a 75% isolated yield and in 90% ee. These excellent results were also obtained with cyclohexenone, but a slight decrease in enantioselectivity was observed when the cycle was enlarged up to seven- and eight-membered rings (84% and 81% ee respectively). Important effects were also observed when alkyl substituents were introduced in the two sites of the olefin of the cyclic enones. In general, substitutions at the olefinic sites (α and β) produced an erosion of the ee and yields of the products, probably due to steric reasons. In an opposite manner, when the substituents were located in the other positions of the ring (α', β', or γ), the enantioselectivities tend to improve. This is an important observation since α and α' substituted enones are not suitable substrates for most organocatalytic methods, which rely on the covalent interaction between the catalyst and the carbonyl moiety. Cyclohexene-1-ketones, substrates that also lack suitable direct epoxidation alternatives [76, 77], could be also epoxidized with good yields and excellent enantioselectivities. Different results were obtained depending on the nature of the alkyl chains, observing a decrease in enantioselectivity when branched groups are present, such as *tert*-butyl and cyclopropyl.

Interestingly, this catalyst is able to epoxidize, in a regioselective manner, dienones, obtaining only the product resulting from the epoxidation at the more electron-rich site with excellent yields and stereoselectivities (Scheme 7.16). There-

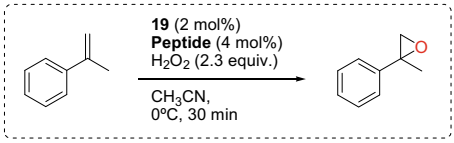

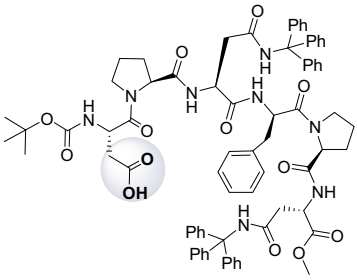

24

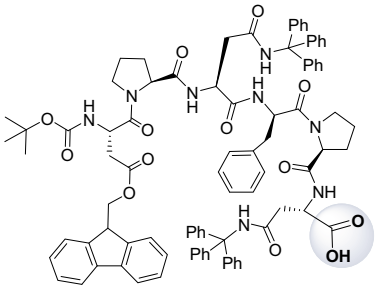

25

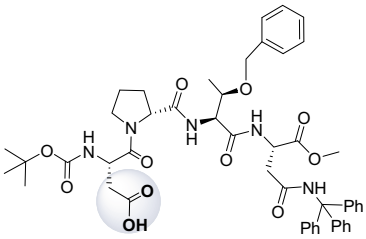

26

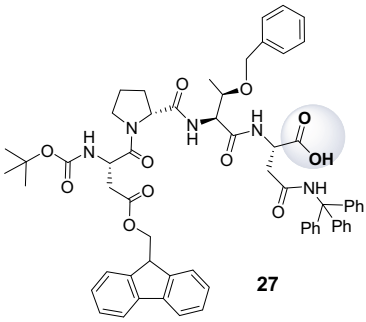

27

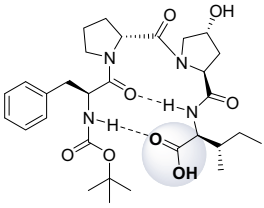

28

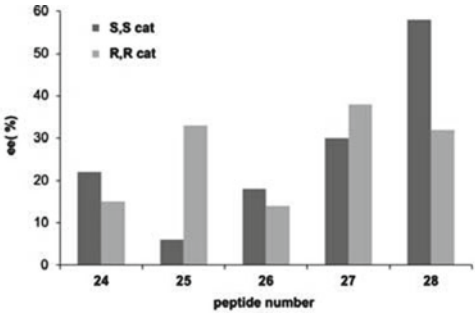

Scheme 7.13 Structure of representative peptides studied in the asymmetric epoxidation of a-methylstyrene catalyzed by **19** and graphical representation of the enantioselectivities obtained. For each peptide, the dark bar corresponds to the ee obtained with (*S,S*)-**19** while the light bar corresponds to the ee obtained with (*R,R*)-**19**

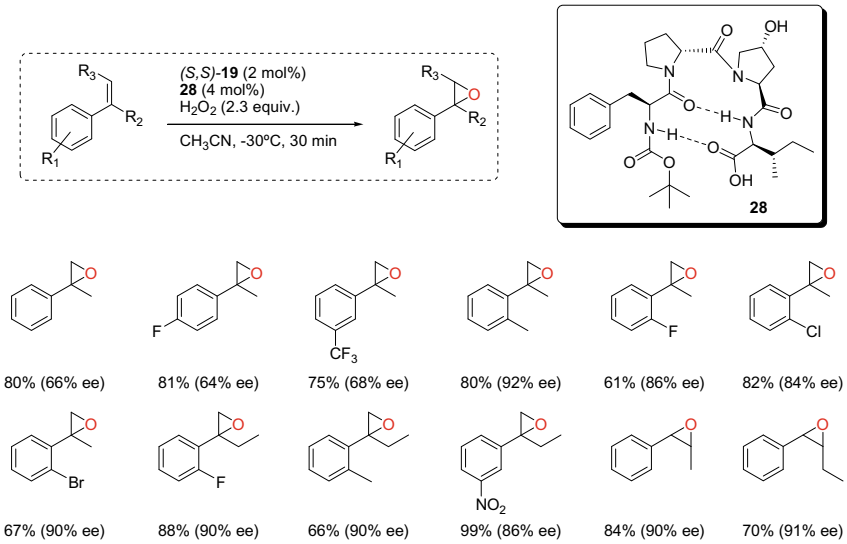

Scheme 7.14 Substrate scope of the system **(*S,S*)-19**/peptide **28**

Table 7.5 Control experiments performed in the epoxidation of α-methylstyrene

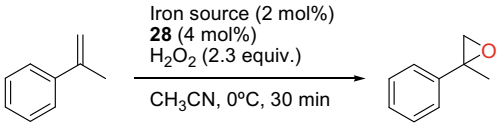

Entry	Iron source	Peptide	Conv. (Yield) (%)	ee (%)
1	(*S,S*)-**19**	**28**	92 (81)	58
2	–	**28**	–	–
3	(*S,S*)-**19**	–	Traces	nd[a]
4	$Fe(OTf)_2(CH_3CN)$	**28**	–	–
5	(*S,S*)-**19**	**28-OMe**[b]	23 (12)	21

[a]Non-determined
[b]The peptide contains a terminal methyl ester instead of a carboxylic acid

fore, the system shows an orthogonal selectivity with organocatalytic methods based in nucleophilic peroxides (Scheme 7.17).

These works by Cussó et al. evidenced that the reactivity and the stereoselectivity of an iron catalyst can be improved by enhancing the electron-donating properties of the ligand and by introducing steric encumbrance. Taking these elements into consideration, Sun and coworkers reported in 2017 a new iron catalyst that contains a bulky and strong electron-donating morpholine group on the pyridines of the ligand, (*R,R*)-[$Fe^{II}(OTf)_2(^{MP}mcp)$] **(21)** [78]. This catalyst, in combination with catalytic

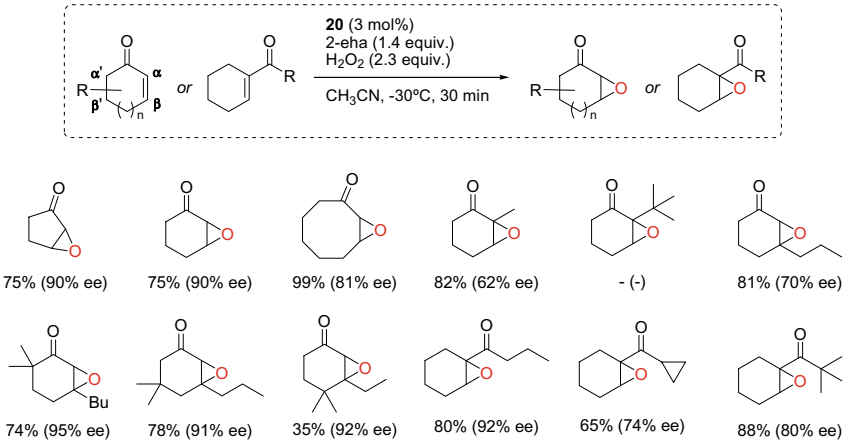

Scheme 7.15 Representative substrate scope of catalyst **20**

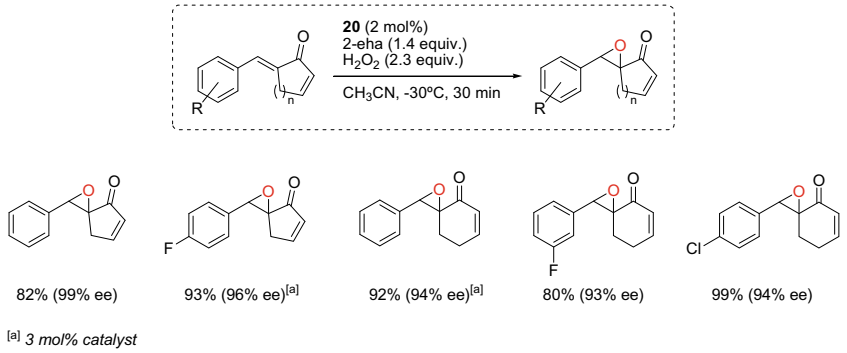

Scheme 7.16 Representative substrate scope of the regioselective epoxidation of dienones using **20**

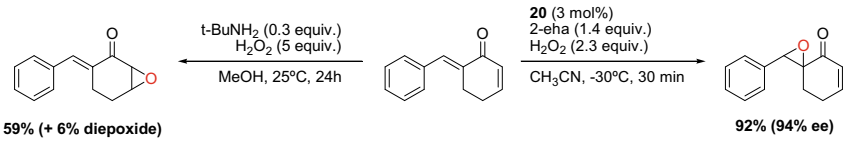

Scheme 7.17 Comparison of the products obtained using nucleophilic peroxides (left) and catalyst **20** (right)

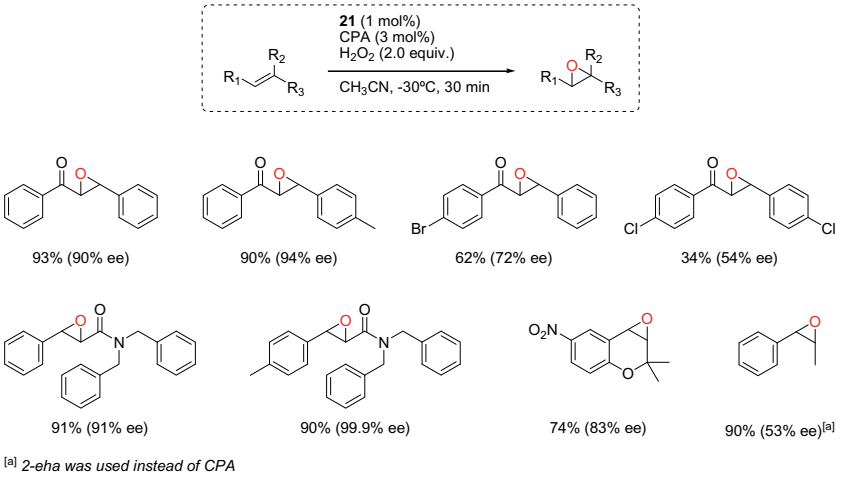

Scheme 7.18 Representative substrate scope of catalyst **21** in combination with CPA

amounts of camphoric acid (CPA), exhibit excellent yields and enantioselectivities in the asymmetric epoxidation of chalcones (up to 93% yield and 94% ee) and alkenyl amides (up to 91% yield and 99.9% ee) (Scheme 7.18).

7.3 Mechanistic Considerations

7.3.1 Mechanistic Considerations from Product Analysis

The reaction mechanisms of olefin oxidation with iron catalysts bearing tetradentate ligands that enforce two *cis*-labile sites and hydrogen peroxide, in the absence of carboxylic acids, were first explored by Que and coworkers [49, 79]. It was proposed that catalysts can be grouped in Class A and Class B. Class A catalysts contain strong field ligands and operate via a reactive $Fe^{V}(O)(OH)$ species, formed via a water-assisted O–O lysis of a ferric hydroperoxide precursor $Fe^{III}(OOH)(H_2O)$ (Scheme 7.19) [49].

Computational analyses indicate that reaction of the $Fe^{V}(O)(OH)$ intermediate with olefins can occur via two different paths; epoxidation results from the attack of the oxo ligand to the olefin. Instead, *syn*-dihydroxylation results if the hydroxyl moiety first attacks the olefin (Scheme 7.19) [80, 81]. Class B catalysts are proposed instead to operate via a side-on peroxide species, which mainly undergoes *syn*-dihydroxylation of olefins [79, 82–84]. So far, only Class A catalysts have found use as enantioselective epoxidation catalysts and the mechanistic discussion that follows is only based on these.

Addition of alkyl carboxylic acids (usually acetic acid) changes the chemoselectivity of the reactions, favoring epoxidation and inhibiting the *syn*-dihydroxylation

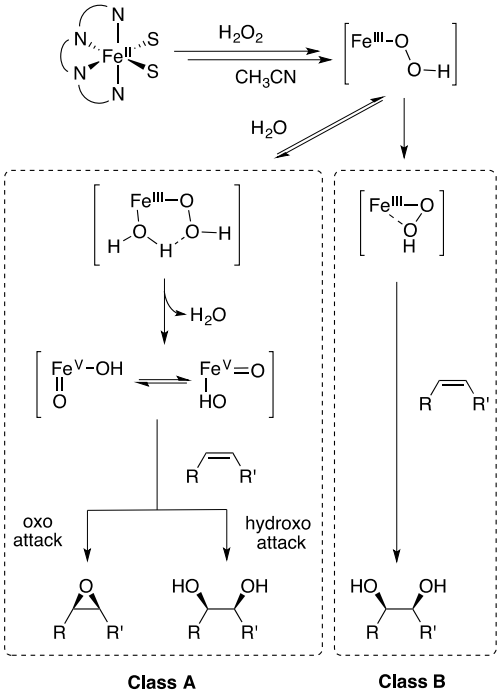

Scheme 7.19 Reaction mechanism proposed for the oxidation of olefins with iron catalysts containing tetradentate ligands. Tetradentate ligand is omitted for clarity. S stands for solvent molecules

reaction. In addition, product yields were substantially improved [60]. Que and coworkers proposed that carboxylic acids play a similar role as water molecules, helping in the heterolytic cleavage of the O–O bond of a ferric hydroperoxide species ($Fe^{III}(OOH)(HO_2CR)$). O–O cleavage is proposed to form a $Fe^{V}(O)(O_2CR)$ reactive intermediate and a water molecule [85]. This mechanistic picture was instrumental to explain the reaction mechanism of the pdp series of catalysts (Scheme 7.20) [68].

Of notice, the carboxylate moiety that results from O–O cleavage and water formation becomes a ligand in the active species $Fe^{V}(O)(O_2CR)$, which explains the influence of the carboxylic acid on the enantioselectivity of the reactions. In addition, it was proposed that the electron-donating character of the electron-rich pyridines exert a push effect that facilitates the O–O cleavage. Finally, the electron-donating ability of the ligand stabilizes the resulting high-valent iron-oxo species. This stabilization is proposed to enforce a closer approximation of the olefin to the metal-oxo, which implies the existence of a later transition state for the O-atom transfer to the olefin, which is translated into the improvement in enantioselectivity observed as the ligand becomes more electron rich [68]. More recent, computational studies by Wang and coworkers suggested that **Ic** is best described as a $Fe^{IV}(O)$ species with an unpaired electron delocalized over one of the pyridine rings and the Me_2N substituent in the ligand [86].

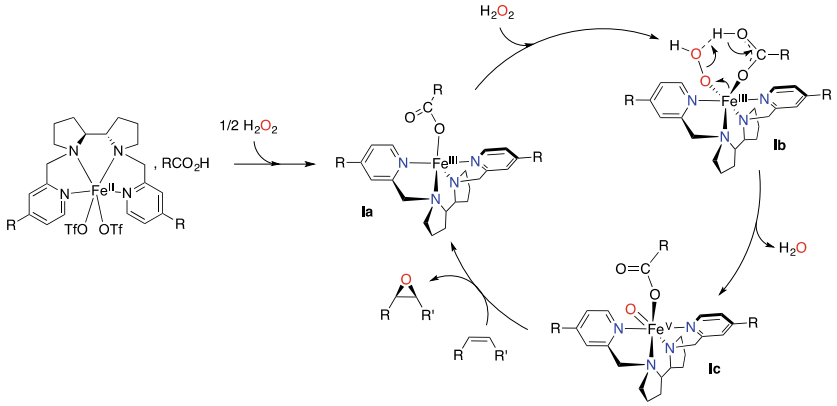

Scheme 7.20 Mechanistic scheme initially proposed for the pdp series of catalysts [68]

Computational analysis by Shaik, Que, and coworkers on the Fe(pdp)/H_2O_2/AcOH system (**14**) suggested that the $Fe^{V}(O)(OAc)$ species may be very close in energy to a ferric peracetate complex $Fe^{III}(OOC(O)CH_3)$, and a $Fe^{IV}(O)(\cdot OAc)$ electromer [87]. A logical consequence of this proposal is that analogous reactive species should be formed in reactions performed with either H_2O_2/AcOH or peracetic acid (AcOOH) as oxidant. On the other hand, Bryliakov, Talsi, and coworkers proposed that the active species depend on the oxidant; a high-valent $Fe^{V}(O)(OAc)$ is formed when H_2O_2/AcOH is used as oxidant, while the use of peracids is proposed to form a ferric peracetate (acylperoxide) $Fe^{III}(OOC(O)CH_3)$ oxidant, exhibiting different selectivity properties [88]. This can be exemplified in the asymmetric epoxidation of chalcone with catalyst **14** (Scheme 7.21). When H_2O_2/2-eha is used as oxidant, the epoxide is obtained with 82% ee. Instead, if peracetic acid is used instead of H_2O_2, the ee is reduced to 67% suggesting the implication of a less enantiodiscriminating oxidant.

In contrast, experiments by Cussó et al. showed that the epoxide resulting from the asymmetric epoxidation of *cis*-β-methyl styrene with catalyst **18** produced the same

Scheme 7.21 Enantioselective epoxidation of chalcone using **14** and different oxidants

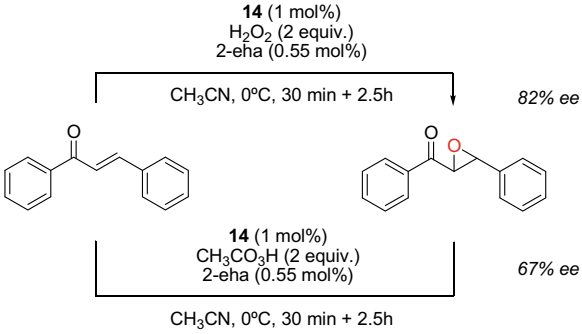

enantioselectivity (61% ee) irrespective of the oxidant; H_2O_2/AcOH, TBHP (*tert*-butyl hydroperoxide)/AcOH, or AcOOH [68]. This comparison could be extended to pairs of reactions performed with (a) H_2O_2/RCO_2H, (RCO_2H = acetic acid, nonanoic acid, cyclohexyl carboxylic acid, and 2-ethyl butanoic acid) and (b) the corresponding alkyl peracid (RCO_3H) are used as the oxidant [89]. For three different substrates (*cis*-*β*-methyl styrene, 1-cyclohexenone, and benzalacetone) and pdp type of catalysts (**14**, **19** and **29**; Fig. 7.4), enantioselectivities of the reactions were the same for each pair of conditions (see Scheme 7.22 for the results in the epoxidation of *cis*-*β*-methyl styrene with catalyst **18**). This suggested that both conditions resulted in the formation of a common oxidant.

The interpretation of the overall results is that carboxylic acids assist the cleavage of the O–O bond when peroxides are used as oxidants. In this process, they become

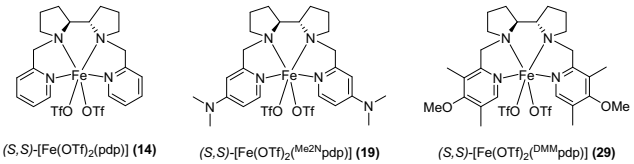

(S,S)-[Fe(OTf)$_2$(pdp)] **(14)** *(S,S)*-[Fe(OTf)$_2$(^{Me2N}pdp)] **(19)** *(S,S)*-[Fe(OTf)$_2$(^{DMM}pdp)] **(29)**

Fig. 7.4 Catalysts used in the study by Cussó et al. [87]

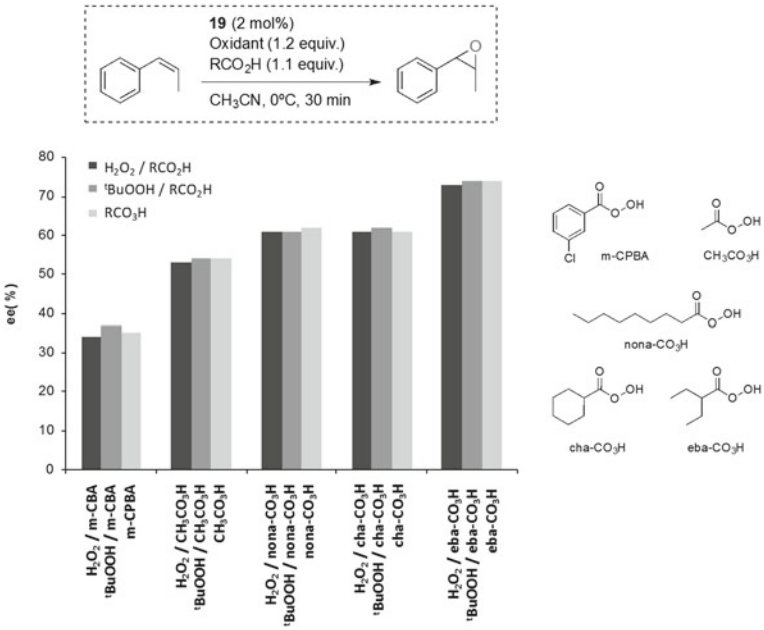

Scheme 7.22 Comparison between the enantioselectivity in the asymmetric epoxidation of *cis*-*β*-methylstyrene when using (i) H_2O_2/RCO_2H, (ii) $^tBuOOH/RCO_2H$, and (iii) RCO_3H (bottom)

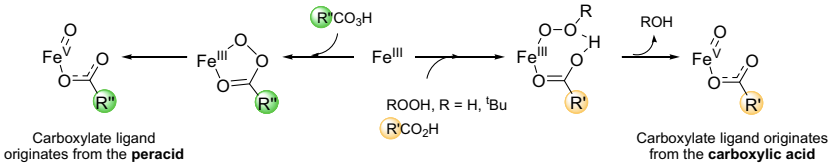

Scheme 7.23 Proposed mechanism for the formation of the $Fe^{V}(O)(RCO_2)$ species when peracids (left) and peroxides (right) are used as oxidants

a ligand in the final $Fe^{V}(O)(RCO_2)$ oxidizing species. Instead, peracids ($R'CO_3H$) do not require carboxylic acid assistance. Intramolecular cleavage of the O–O bond, presumably via a cyclic ferric peracetate complex, generates the $Fe^{V}(O)(R'CO_2)$ species without the incorporation of the external carboxylic acid (Scheme 7.23).

7.3.2 Mechanistic Considerations from Spectroscopic Analysis of Reaction Intermediates

More recent work by Que and coworkers identified reaction conditions that permit accumulation of a transient species with high anisotropy g values ($g_x = 1.72$, $g_y = 2.38$ and $g_z = 2.58$) in approximately 50% yield when electron-rich $[Fe(OTf)_2(tpa^*)]$ **(30)** reacts with H_2O_2 in the presence of acetic acid (Fig. 7.5). These species were spectroscopically and computationally characterized as a low-spin acylperoxoiron(III) intermediate and proved to be kinetically not competent for reacting

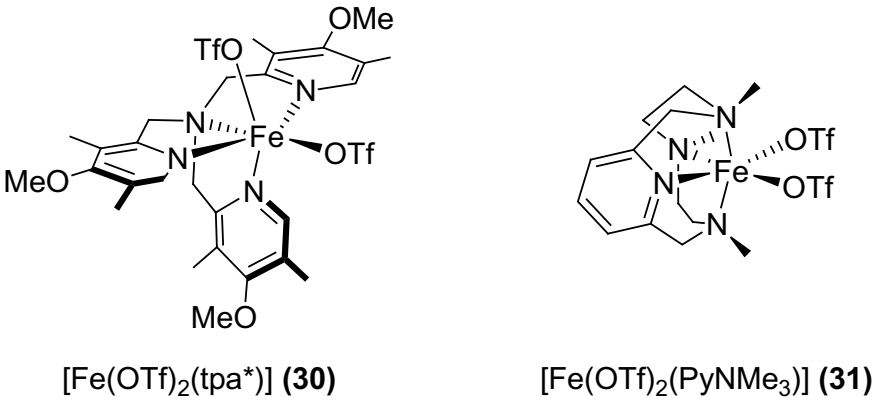

Fig. 7.5 Structure of catalysts used to stabilize reaction intermediates

with an olefin. Instead, rate-determining O–O cleavage was presumed to generate the active oxidant [90].

Identification of the $Fe^{V}(O)(OAc)$ species in catalytic mixtures of Fe(pdp) systems was first reported by Bryliakov and Talsi using EPR on catalytic mixtures at −70 °C [91]. A transient species with low anisotropy in the g values ($g_1 = 2.07$, $g_2 = 2.01$ and $g_3 = 1.96$) was observed besides a series of signal characteristics of low-spin ferric species. The unusual spectroscopic features were proposed to arise from a high-valent iron-oxo species, responsible for the epoxidation reaction. Furthermore, in subsequent work, the authors suggested that the electronic structure of the high-valent iron-oxo species was dependent on the nature of the carboxylic acid [92]. For carboxylic acids with primary and secondary α-carbon atoms (acetic acid, butyric acid, caproic acid), the active species exhibit electron paramagnetic resonance (EPR) spectra with large g-factor anisotropy ($g_1 = 2.7$, $g_2 = 2.4$, and $g_3 = 1.7$), whereas for those with tertiary α-carbon atoms (2-ethylhexanoic acid, valproic acid, and 2-ethylbutyric acid), the active species display EPR spectra with small g-factor anisotropy ($g_1 = 2.07$, $g_2 = 2.01$, and $g_3 = 1.96$). The former was assigned to $Fe^{V}(O)(RCO_2)$ species. On the other hand, the low anisotropy values are assigned to $Fe^{IV}(O)(RCO_2\cdot)$ species, where the carboxylate ligand has a radical character. Unfortunately, the compounds accumulated <2% of the total iron content of the sample, preventing further spectroscopic characterization.

Iron species with very similar EPR spectroscopic features were observed when a different iron complex $[Fe(OTf)_2(PyNMe_3)]$ **(31)** reacts with peracids at low temperature [93]. In this case, an intermediate with low anisotropy g values ($g_1 = 2.07$, $g_2 = 2.01$, and $g_3 = 1.95$) accumulates in 35–50% amounts and spectroscopic characterization could be pursued [94]. A combination of Mössbauer, EPR, X-ray absorption spectroscopy, resonance Raman, mass-spectrometry, and DFT analyses led to the conclusion that the intermediate was best formulated as a $Fe^{V}(O)(O_2CR)$ species. Interestingly, close analysis of the EPR spectra of catalytic mixtures reveal that these species appear to be in fast equilibrium with a ferric component, presumed to be its $Fe^{III}(OO(O)CR)$ precursor, displaying EPR parameters characteristic of low-spin mononuclear ferric complexes ($g_1 = 2.20$, $g_2 = 2.19$, and $g_3 = 1.99$) (Scheme 7.24) [93]. Interestingly, an analogous equilibrium was later observed in catalytic reactions with Fe(tpa) type of catalysts [95].

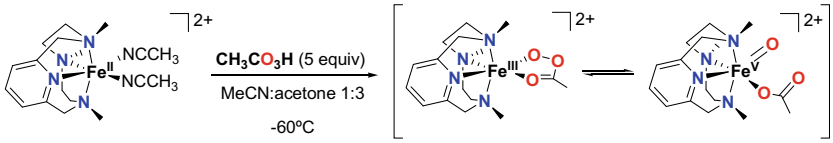

Scheme 7.24 Proposed mechanism for the formation of the $Fe^{V}(O)(RCO_2)$ species with the $Fe(PyNMe_3)$ system

In subsequent work, it was showed that the $[Fe^{V}(O)(O_2CR)(PyNMe_3)]$ intermediate is very reactive against olefins [96]. Reactions were extraordinarily fast and needed to be measured by stopped-flow at −60 °C in acetone:acetonitrile solvent mixtures. The catalytic relevance of the intermediate was evaluated in competition experiments in which two different olefins were reacted at the same time under catalytic conditions in a $[Fe^{II}(PyNMe_3)(CH_3CN)_2]^{2+}$/AcOOH system. The relative amounts of the two epoxide products produced from the catalytic oxidation were compared with the rate constants (k_2) obtained for the reaction of the intermediate with the individual alkenes (previously determined by the stopped-flow method at −60 °C). Reactions occurred with stereoretention and the relative amount of the two epoxides formed after each competition reaction matched the ratio of the corresponding k_2 values measured individually for the reaction of the intermediate with each olefin (k_2^A/k_2^B). This result provided strong evidence that the trapped $[Fe^{V}(O)(O_2CR)(PyNMe_3)]$ species was a relevant intermediate in catalytic epoxidation reactions. Furthermore, the EPR characteristics of this compound compare well with the transient species observed for Fe(pdp) and Fe(tpa) catalysts [89, 93], suggesting that it represents a good model for the key oxidizing species operating in the reactions of these catalysts.

Interestingly, a recent computational study by Ye and coworkers based in high-level multiconfigurational calculations suggests that the $[Fe^{V}(O)(O_2CR)(PyNMe_3)]$ intermediate is best described as a $[Fe^{IV}\text{-}O{\cdot}O_2CR)(PyNMe_3)]$ complex where the oxo ligand and an oxygen atom from the carboxylate form a weak single electron bond, and the iron center is in the Fe^{IV} state [97], suggesting that this structure is close to $[Fe^{IV}(O)(RCO_2{\cdot})(pdp)]$ proposed by Talsi and coworkers for the intermediate with similar g values ($g_1 = 2.07$, $g_2 = 2.01$, and $g_3 = 1.96$) [92]. The computations also explain the unusually high reactivity of the complex in C–H and C=C oxygenation reactions. Thus, despite the spectroscopic characterization of the complex being quite exhaustive, the precise description of the electronic structure of this magnificent reagent is still a matter of debate.

7.4 Concluding Remarks

Notable examples of efficient and highly enantioselective iron-catalyzed epoxidation reactions with hydrogen peroxide have been described during the last decade (Table 7.6). The identification of iron coordination complexes that activate this peroxide in a controlled and efficient manner, without significant production of hydroxyl radicals has been key for enabling this reaction. Mechanistic understanding has been key for successful catalyst design, and also for devising reaction conditions where epoxidation occurs in a stereoretentive, highly enantioselective manner. So far, the substrate scope for the reaction is rather limited. However, the coordination complexes described so far as catalysts have a very versatile structure and therefore, it is envisioned that the substrate scope of the reaction will be extended in the near future. From a mechanistic perspective, our current understanding is very much advanced, and there is little doubt nowadays that reactions are performed by high-valent iron-oxo species. However, the extraordinary reactivity of these species makes their identification and characterization a major challenge for the near future.

Table 7.6 Summary of non-heme iron complexes reported as catalysts for asymmetric epoxidation of olefins using H_2O_2

Entry	Catalyst	RCOOH	Olefins	Yield (%)	ee (%)	Ref.
1	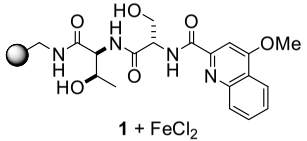 **1** + $FeCl_2$	–	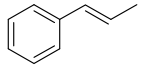	78	20	[50]
2	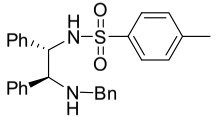 **4** + $FeCl_3{\cdot}6H_2O$	H_2pydic	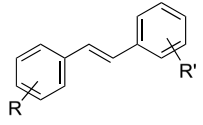	57–94	10–81	[51]
			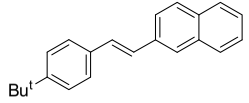	40	97	
			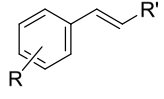	33–91	8–53	[52]
3	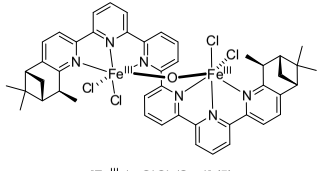 $[Fe^{III}_2(\mu\text{-}O)Cl_4(Spp)]$ **(5)**	AcOH	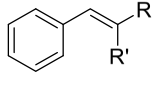	50–100	17–43	[53]

(continued)

Table 7.6 (continued)

Entry	Catalyst	RCOOH	Olefins	Yield (%)	ee (%)	Ref.
4	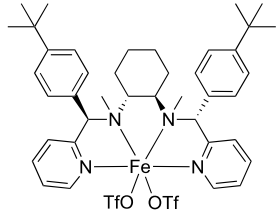 *(R,R,R′,R′)*-[Fe(OTf)$_2$(bpmcp)] **(8)**	AcOH	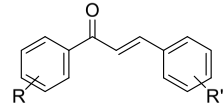	40–90	69–84	[62]
5	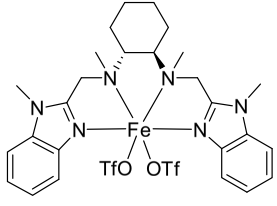 *(R,R)*-[Fe(OTf)$_2$(mcmb)] **(9)**	AcOH	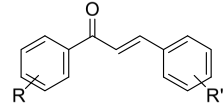	40–94	75–95	[63]
6	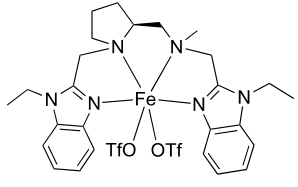 (*S*)-[Fe(OTf)$_2$(peb)] **(12)**	AcOH	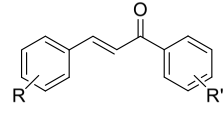	78–99	80–97	[64]

(continued)

Table 7.6 (continued)

Entry	Catalyst	RCOOH	Olefins	Yield (%)	ee (%)	Ref.
			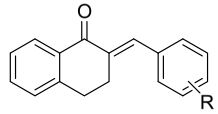	72–99	87–97	
			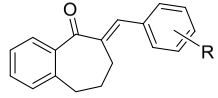	78–86	83–93	
			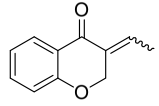	67	89	
7	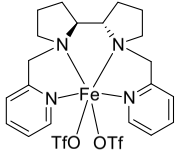 *(S,S)*-[Fe(OTf)$_2$(pdp)] **(14)**	AcOH	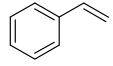	26	16	[65]
			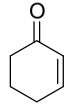	99	33	
			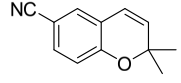	48	27	

(continued)

Table 7.6 (continued)

Entry	Catalyst	RCOOH	Olefins	Yield (%)	ee (%)	Ref.
		2-eha	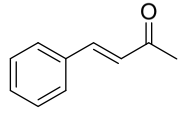	51	62	
			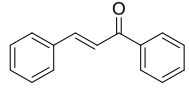	98	86	
8	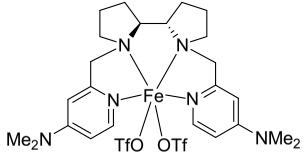 (*S,S*)-[Fe(OTf)$_2$(^{Me2N}pdp)] **(19)**	S-Ibp	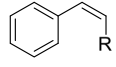	84–97	86–97	[68]
			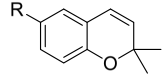	85–90	98–99	
		2-eha	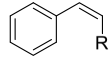	78–81	95	
			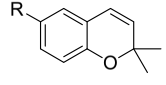	95–97	99	
			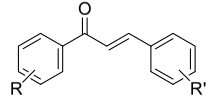	94–99	97–98	

(continued)

Table 7.6 (continued)

Entry	Catalyst	RCOOH	Olefins	Yield (%)	ee (%)	Ref.
			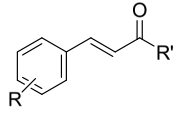	60–95	91–99	
			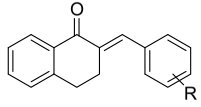	94–97	90–97	
		23	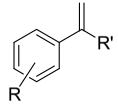	52–94	50–97	[69]
		28	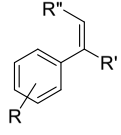	61–99	84–91	[70]
9	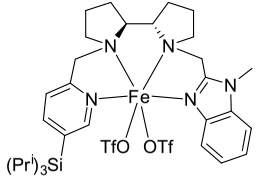 *(S,S)*-[Fe(OTf)$_2$(^{bz,tips}pdp)] **(20)**	2-eha	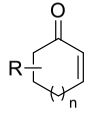	30–99	62–95	[73]

(continued)

Table 7.6 (continued)

Entry	Catalyst	RCOOH	Olefins	Yield (%)	ee (%)	Ref.
			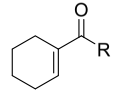	65–98	71–91	
10	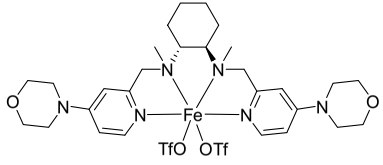 *(R,R)*-[Fe(OTf)$_2$(^{MP}mcp)] **(21)**	CPA	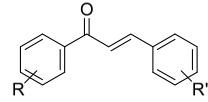	34–93	54–94	[78]
			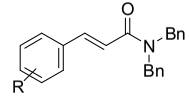	51–91	85–99.9	
			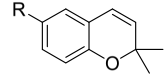	42–74	83–84	

References

1. Sheldon RA, Kochi J (1981) Metal-catalyzed oxidations of organic compounds. Academic Press, New York
2. Choi WJ, Choi CY (2005) Production of chiral epoxides: epoxide hydrolase-catalyzed enantioselective hydrolysis. Biotechnol Bioprocess Eng 10(3):167–179. https://doi.org/10.1007/BF02932009
3. Partridge JJ, Bray BL (1999) enantioselective synthesis: the optimum process. In: Gadamasetti KG (ed) Process chemistry in the pharmaceutical industry, vol 1. CRC Press, United States of America, pp 301–326
4. Hughes DL (2016) Patent review of manufacturing routes to oncology drugs: carfilzomib, osimertinib, and venetoclax. Org Process Res Dev 20(12):2028–2042. https://doi.org/10.1021/acs.oprd.6b00374
5. Bäckvall J-E (2004) Modern oxidation methods. Wiley-VCH, Weinheim
6. Bryliakov KP (2014) Environmentally sustainable catalytic asymmetric oxidations. CRC Press, Boca Raton
7. Wong OA, Shi Y (2008) Organocatalytic oxidation. Asymmetric epoxidation of olefins catalyzed by chiral ketones and iminium salts. Chem Rev 108(9):3958–3987. https://doi.org/10.1021/cr068367v
8. Davis RL, Stiller J, Naicker T, Jiang H, Jørgensen KA (2014) Asymmetric organocatalytic epoxidations: reactions, scope, mechanisms, and applications. Angew Chem Int Ed 53(29):7406–7426. https://doi.org/10.1002/anie.201400241
9. Zhu Y, Wang Q, Cornwall RG, Shi Y (2014) Organocatalytic asymmetric epoxidation and aziridination of olefins and their synthetic applications. Chem Rev 114(16):8199–8256. https://doi.org/10.1021/cr500064w
10. Krishnan KK, Thomas AM, Sindhu KS, Anilkumar G (2016) Recent advances and perspectives in the manganese-catalysed epoxidation reactions. Tetrahedron 72(1):1–16. https://doi.org/10.1016/j.tet.2015.11.003
11. De Faveri G, Ilyashenko G, Watkinson M (2011) Recent advances in catalytic asymmetric epoxidation using the environmentally benign oxidant hydrogen peroxide and its derivatives. Chem Soc Rev 40(3):1722–1760. https://doi.org/10.1039/c0cs00077a
12. Irie R, Uchida T, Matsumoto K (2015) Katsuki catalysts for asymmetric oxidation: design concepts, serendipities for breakthroughs, and applications. Chem Lett 44(10):1268–1283. https://doi.org/10.1246/cl.150747
13. Correa A, García Mancheño O, Bolm C (2008) Iron-catalysed carbon–heteroatom and heteroatom–heteroatom bond forming processes. Chem Soc Rev 37(6):1108–1117. https://doi.org/10.1039/B801794H
14. Enthaler S, Junge K, Beller M (2008) Sustainable metal catalysis with iron: from rust to a rising star? Angew Chem Int Ed 47(18):3317–3321. https://doi.org/10.1002/anie.200800012
15. Darwish M, Wills M (2012) Asymmetric catalysis using iron complexes—'ruthenium lite'? Catal Sci Technol 2(2):243–255. https://doi.org/10.1039/C1CY00390A
16. Gopalaiah K (2013) Chiral iron catalysts for asymmetric synthesis. Chem Rev 113(5):3248–3296. https://doi.org/10.1021/cr300236r
17. Fingerhut A, Serdyuk OV, Tsogoeva SB (2015) Non-heme iron catalysts for epoxidation and aziridination reactions of challenging terminal alkenes: towards sustainability. Green Chem 17(4):2042–2058. https://doi.org/10.1039/C4GC02413C
18. Olivo G, Cussó O, Borrell M, Costas M (2017) Oxidation of alkane and alkene moieties with biologically inspired nonheme iron catalysts and hydrogen peroxide: from free radicals to stereoselective transformations. J Biol Inorg Chem 22(2):425–452. https://doi.org/10.1007/s00775-016-1434-z
19. Talsi EP, Bryliakov KP (2012) Chemo- and stereoselective CH oxidations and epoxidations/cis-dihydroxylations with H_2O_2, catalyzed by non-heme iron and manganese complexes. Coord Chem Rev 256(13):1418–1434. https://doi.org/10.1016/j.ccr.2012.04.005

20. Carroll MA, Schwartzman M, Capdevila J, Falck JR, McGiff JC (1987) Vasoactivity of arachidonic acid epoxides. Eur J Pharmacol 138(2):281–283. https://doi.org/10.1016/0014-2999(87)90445-6
21. Guengerich FP (1991) Reactions and Significance of Cytochrome P-450 enzymes. J Biol Chem 266(16):10019–100222
22. Hashimoto T, Hayashi A, Amano Y, Kohno J, Iwanari H, Usuda S, Yamada Y (1991) Hyoscyamine 6 beta-hydroxylase, an enzyme involved in tropane alkaloid biosynthesis, is localized at the pericycle of the root. J Biol Chem 266(7):4648–4653
23. Hollenhorst MA, Bumpus SB, Matthews ML, Bollinger JM, Kelleher NL, Walsh CT (2010) The nonribosomal peptide synthetase enzyme DdaD tethers Nβ-Fumaramoyl-l-2,3-diaminopropionate for Fe(II)/α-ketoglutarate-dependent epoxidation by DdaC during dapdiamide antibiotic biosynthesis. J Am Chem Soc 132(44):15773–15781. https://doi.org/10.1021/ja1072367
24. Seo M-J, Zhu D, Endo S, Ikeda H, Cane DE (2011) Genome mining in streptomyces. Elucidation of the role of Baeyer−Villiger monooxygenases and non-heme iron-dependent dehydrogenase/oxygenases in the final steps of the biosynthesis of pentalenolactone and neopentalenolactone. Biochemistry 50(10):1739–1754. https://doi.org/10.1021/bi1019786
25. Ishikawa N, Tanaka H, Koyama F, Noguchi H, Wang CCC, Hotta K, Watanabe K (2014) Non-heme dioxygenase catalyzes atypical oxidations of 6,7-bicyclic systems to form the 6,6-quinolone core of viridicatin-type fungal alkaloids. Angew Chem Int Ed 53(47):12880–12884. https://doi.org/10.1002/anie.201407920
26. Que L, Tolman WB (2008) Biologically inspired oxidation catalysis. Nature 455(7211):333–340. https://doi.org/10.1038/nature07371
27. Gelalcha FG (2014) biomimetic iron-catalyzed asymmetric epoxidations: fundamental concepts, challenges and opportunities. Adv Synth Catal 356(2–3):261–299. https://doi.org/10.1002/adsc.201300716
28. Cussó O, Ribas X, Costas M (2015) Biologically inspired non-heme iron-catalysts for asymmetric epoxidation; design principles and perspectives. Chem Commun 51(76):14285–14298. https://doi.org/10.1039/C5CC05576H
29. Bryliakov KP (2017) Catalytic asymmetric oxygenations with the environmentally benign oxidants H_2O_2 and O_2. Chem Rev 117(17):11406–11459. https://doi.org/10.1021/acs.chemrev.7b00167
30. Groves JT, Nemo TE, Myers RS (1979) Hydroxylation and epoxidation catalyzed by iron-porphine complexes. Oxygen transfer from iodosylbenzene. J Am Chem Soc 101(4):1032–1033. https://doi.org/10.1021/ja00498a040
31. Groves JT, Myers RS (1983) Catalytic asymmetric epoxidations with chiral iron porphyrins. J Am Chem Soc 105(18):5791–5796. https://doi.org/10.1021/ja00356a016
32. Collman JP, Zhang X, Lee VJ, Uffelman ES, Brauman JI (1993) Regioselective and enantioselective epoxidation catalyzed by metalloporphyrins. Science 261(5127):1404. https://doi.org/10.1126/science.8367724
33. Collman JP, Wang Z, Straumanis A, Quelquejeu M, Rose E (1999) An efficient catalyst for asymmetric epoxidation of terminal olefins. J Am Chem Soc 121(2):460–461. https://doi.org/10.1021/ja9818699
34. Lindsay Smith JR, Reginato G (2003) Asymmetric alkene epoxidation catalysed by a novel family of chiral metalloporphyrins: effect of structure on catalyst activity, stability and enantioselectivity. Org Biomol Chem 1(14):2543–2549. https://doi.org/10.1039/B304212J
35. Rose E, Ren Q-Z, Andrioletti B (2003) A unique binaphthyl strapped iron-porphyrin catalyst for the enantioselective epoxidation of terminal olefins. Chem Eur J 10(1):224–230. https://doi.org/10.1002/chem.200305222
36. Nakagawa H, Sei Y, Yamaguchi K, Nagano T, Higuchi T (2004) Catalytic and asymmetric epoxidation by novel D4-symmetric chiral porphyrin derived from C_2-symmetric diol. J Molec Catal A Chem 219(2):221–226. https://doi.org/10.1016/j.molcata.2004.05.026
37. Ren Q, Hou Z, Zhang H, Wang A, Liu S (2009) Catalytic enantioselective epoxidation of olefins by chiral mono-faced strapped porphyrin with nitrogen blocking ligand. J Porphyr Phthalocyanines 13(12):1214–1220. https://doi.org/10.1142/S1088424609001583

38. Maux PL, Srour HF, Simonneaux G (2012) Enantioselective water-soluble iron–porphyrin-catalyzed epoxidation with aqueous hydrogen peroxide and hydroxylation with iodobenzene diacetate. Tetrahedron 68(29):5824–5828. https://doi.org/10.1016/j.tet.2012.05.014
39. Calvete MJF, Piñeiro M, Dias LD, Pereira MM (2018) Hydrogen peroxide and metalloporphyrins in oxidation catalysis: old dogs with some new tricks. ChemCatChem 10(17):3615–3635. https://doi.org/10.1002/cctc.201800587
40. Beller M (2004) The current status and future trends in oxidation chemistry. Adv Synth Catal 346(2–3):107–108. https://doi.org/10.1002/adsc.200404008
41. Noyori R, Aoki M, Sato K (2003) Green oxidation with aqueous hydrogen peroxide. Chem Commun 16:1977. https://doi.org/10.1039/b303160h
42. Bertini I (2007) Biological inorganic chemistry: structure and reactivity. University Science Books, California
43. Kovaleva EG, Lipscomb JD (2008) Versatility of biological non-heme Fe(II) centers in oxygen activation reactions. Nat Chem Biol 4(3):186–193. https://doi.org/10.1038/nchembio.71
44. Perry C, de los Santos Emmanuel LC, Alkhalaf LM, Challis GL (2018) Rieske non-heme iron-dependent oxygenases catalyse diverse reactions in natural product biosynthesis. Nat Prod Rep 35(7):622–632. https://doi.org/10.1039/c8np00004b
45. Kal S, Que L (2017) Dioxygen activation by nonheme iron enzymes with the 2-His-1-carboxylate facial triad that generate high-valent oxoiron oxidants. J Biol Inorg Chem 22(2):339–365. https://doi.org/10.1007/s00775-016-1431-2
46. Krebs C, Galonić Fujimori D, Walsh CT, Bollinger JM (2007) Non-heme Fe(IV)–oxo intermediates. Acc Chem Res 40(7):484–492. https://doi.org/10.1021/ar700066p
47. Oloo WN, Que L (2015) Bioinspired nonheme iron catalysts for C–H and C=C bond oxidation: insights into the nature of the metal-based oxidants. Acc Chem Res 48(9):2612–2621. https://doi.org/10.1021/acs.accounts.5b00053
48. Ray K, Pfaff FF, Wang B, Nam W (2014) Status of reactive non-heme metal-oxygen intermediates in chemical and enzymatic reactions. J Am Chem Soc 136(40):13942–13958. https://doi.org/10.1021/ja507807v
49. Chen K, Costas M, Kim J, Tipton AK, Que L (2002) Olefin Cis-dihydroxylation versus epoxidation by non-heme iron catalysts: two faces of an FeIII−OOH coin. J Am Chem Soc 124(12):3026–3035. https://doi.org/10.1021/ja0120025
50. Francis MB, Jacobsen EN (1999) Discovery of novel catalysts for alkene epoxidation from metal-binding combinatorial libraries. Angew Chem Int Ed 38(7):937–941. https://doi.org/10.1002/(SICI)1521-3773(19990401)38:7%3c937:AID-ANIE937%3e3.0.CO;2-O
51. Gelalcha FG, Bitterlich B, Anilkumar G, Tse MK, Beller M (2007) Iron-catalyzed asymmetric epoxidation of aromatic alkenes using hydrogen peroxide. Angew Chem Int Ed 46(38):7293–7296. https://doi.org/10.1002/anie.200701235
52. Gelalcha FG, Anilkumar G, Tse MK, Brückner A, Beller M (2008) Biomimetic Iron-catalyzed asymmetric epoxidation of aromatic alkenes by using hydrogen peroxide. Chem Eur J 14(25):7687–7698. https://doi.org/10.1002/chem.200800595
53. Yeung H-L, Sham K-C, Tsang C-S, Lau T-C, Kwong H-L (2008) A chiral iron-sexipyridine complex as a catalyst for alkene epoxidation with hydrogen peroxide. Chem Commun(32):3801–3803. https://doi.org/10.1039/b804281k
54. Codolà Z, Lloret-Fillol J, Costas M (2014) Aminopyridine iron and manganese complexes as molecular catalysts for challenging oxidative transformations. In: Progress in inorganic chemistry, vol 59. Wiley, pp 447–532. https://doi.org/10.1002/9781118869994.ch07
55. Costas M, Que L Jr (2002) Ligand topology tuning of iron-catalyzed hydrocarbon oxidations. Angew Chem Int Ed 114(12):2283–2285
56. Knof U, von Zelewsky A (1999) Predetermined chirality at metal centers. Angew Chem Int Ed 38(3):302–322. https://doi.org/10.1002/(SICI)1521-3773(19990201)38:3%3c302:AID-ANIE302%3e3.0.CO;2-G
57. Mas-Balleste R, Costas M, van den Berg T, Que L Jr (2006) Ligand topology effects on olefin oxidations by bio-inspired [FeII(N2Py2)] catalysts. Chem Eur J 12(28):7489–7500. https://doi.org/10.1002/chem.200600453

58. Cruchter T, Larionov VA (2018) Asymmetric catalysis with octahedral stereogenic-at-metal complexes featuring chiral ligands. Coord Chem Rev 376:95–113. https://doi.org/10.1016/j.ccr.2018.08.002
59. Zhang L, Meggers E (2017) Stereogenic-only-at-metal asymmetric catalysts. Chem Asian J 12(18):2335–2342. https://doi.org/10.1002/asia.201700739
60. White MC, Doyle AG, Jacobsen EN (2001) A synthetically useful, self-assembling MMO mimic system for catalytic alkene epoxidation with aqueous H_2O_2. J Am Chem Soc 123(29):7194–7195
61. Costas M, Tipton AK, Chen K, Jo D-H, Que L (2001) Modeling rieske dioxygenases: the first example of iron-catalyzed asymmetric cis-dihydroxylation of olefins. J Am Chem Soc 123(27):6722–6723
62. Wu M, Miao C-X, Wang S, Hu X, Xia C, Kühn FE, Sun W (2011) Chiral bioinspired non-heme iron complexes for enantioselective epoxidation of α, β-unsaturated ketones. Adv Synth Catal 353(16):3014–3022. https://doi.org/10.1002/adsc.201100267
63. Wang X, Miao C, Wang S, Xia C, Sun W (2013) Bioinspired manganese and iron complexes with tetradentate N ligands for the asymmetric epoxidation of olefins. ChemCatChem 5(8):2489–2494. https://doi.org/10.1002/cctc.201300102
64. Wang B, Wang S, Xia C, Sun W (2012) Highly enantioselective epoxidation of multisubstituted enones catalyzed by non-heme iron catalysts. Chem Eur J 18(24):7332–7335. https://doi.org/10.1002/chem.201200992
65. Lyakin OY, Ottenbacher RV, Bryliakov KP, Talsi EP (2012) Asymmetric epoxidations with H_2O_2 on Fe and Mn aminopyridine catalysts: probing the nature of active species by combined electron paramagnetic resonance and enantioselectivity study. ACS Catal 2(6):1196–1202. https://doi.org/10.1021/cs300205n
66. Suzuki K, Oldenburg PD, Que L (2008) Iron-catalyzed asymmetric olefin cis-dihydroxylation with 97% enantiomeric excess. Angew Chem Int Ed 47(10):1887–1889. https://doi.org/10.1002/anie.200705061
67. Chen MS, White MC (2007) A predictably selective aliphatic C-H oxidation reaction for complex molecule synthesis. Science 318(5851):783–787. https://doi.org/10.1126/science.1148597
68. Cussó O, Garcia-Bosch I, Ribas X, Lloret-Fillol J, Costas M (2013) Asymmetric epoxidation with H_2O_2 by manipulating the electronic properties of non-heme iron catalysts. J Am Chem Soc 135(39):14871–14878. https://doi.org/10.1021/ja4078446
69. Cussó O, Ribas X, Lloret-Fillol J, Costas M (2015) Synergistic interplay of a non-heme iron catalyst and amino acid coligands in H_2O_2 activation for asymmetric epoxidation of α-alkyl-substituted styrenes. Angew Chem Int Ed 54(9):2729–2733. https://doi.org/10.1002/anie.201410557
70. Cussó O, Giuliano MW, Ribas X, Miller SJ, Costas M (2017) A bottom up approach towards artificial oxygenases by combining iron coordination complexes and peptides. Chem Sci 8(5):3660–3667. https://doi.org/10.1039/C7SC00099E
71. Lichtor PA, Miller SJ (2012) Combinatorial evolution of site-and enantioselective catalysts for polyene epoxidation. Nat Chem 4(12):990–995. https://doi.org/10.1038/nchem.1469
72. Lichtor PA, Miller SJ (2014) Experimental lineage and functional analysis of a remotely directed peptide epoxidation catalyst. J Am Chem Soc 136(14):5301–5308. https://doi.org/10.1021/ja410567a
73. Cussó O, Cianfanelli M, Ribas X, Klein Gebbink RJ, Costas M (2016) Iron catalyzed highly enantioselective epoxidation of cyclic aliphatic enones with aqueous H_2O_2. J Am Chem Soc 138(8):2732–2738. https://doi.org/10.1021/jacs.5b12681
74. Wang X, Reisinger CM, List B (2008) Catalytic asymmetric epoxidation of cyclic enones. J Am Chem Soc 130(19):6070–6071. https://doi.org/10.1021/ja801181u
75. Lee A, Reisinger CM, List B (2012) Catalytic asymmetric epoxidation of 2-cyclopentenones. Adv Synth Catal 354(9):1701–1706. https://doi.org/10.1002/adsc.201200072
76. Aoki M, Seebach D (2001) Preparation of TADOOH, a hydroperoxide from TADDOL, and use in highly enantioface-and enantiomer-differentiating oxidations. Helv Chim Acta

84(1):187–207. https://doi.org/10.1002/1522-2675(20010131)84:1%3c187:AID-HLCA187%3e3.0.CO;2-O
77. Nomura K, Matsubara S (2009) Stereospecific construction of chiral tertiary and quaternary carbon by nucleophilic cyclopropanation with Bis(iodozincio)methane. Chem Asian J 5(1):147–152. https://doi.org/10.1002/asia.200900289
78. Wang W, Sun Q, Xu D, Xia C, Sun W (2017) Asymmetric epoxidation of olefins with H_2O_2 catalyzed by a bioinspired aminopyridine N_4 iron complex. ChemCatChem 9(3):420–424. https://doi.org/10.1002/cctc.201601293
79. Chen K, Costas M, Que L (2002) Spin state tuning of non-heme iron-catalyzed hydrocarbon oxidations: participation of FeIII–OOH and FeV=O intermediates. J Chem Soc Dalton Trans 5:672–679. https://doi.org/10.1039/b108629d
80. Bassan A, Blomberg MRA, Siegbahn PEM, Que L (2005) Two faces of a biomimetic non-heme HO-FeV=O oxidant: olefin epoxidation versus cis-dihydroxylation. Angew Chem Int Ed 44(19):2939–2941. https://doi.org/10.1002/anie.200463072
81. Prat I, Mathieson JS, Güell M, Ribas X, Luis JM, Cronin L, Costas M (2011) Observation of Fe(V)=O using variable-temperature mass spectrometry and its enzyme-like C-H and C=C oxidation reactions. Nat Chem 3(10):788–793. https://doi.org/10.1038/nchem.1132
82. Zang C, Liu Y, Xu ZJ, Tse CW, Guan X, Wei J, Huang JS, Che CM (2016) Highly enantioselective iron-catalyzed cis-dihydroxylation of alkenes with hydrogen peroxide oxidant via an Fe(III) −OOH reactive intermediate. Angew Chem Int Ed 55(35):10253–10257. https://doi.org/10.1002/anie.201603410
83. Fujita M, Costas M, Que L (2003) Iron-catalyzed olefin cis-dihydroxylation by H_2O_2: electrophilic versus nucleophilic mechanisms. J Am Chem Soc 125(33):9912–9913. https://doi.org/10.1021/ja029863d
84. Company A, Gómez L, Fontrodona X, Ribas X, Costas M (2008) A novel platform for modeling oxidative catalysis in non-heme iron oxygenases with unprecedented efficiency. Chem Eur J 14(19):5727–5731. https://doi.org/10.1002/chem.200800724
85. Mas-Ballesté R, Que L (2007) Iron-catalyzed olefin epoxidation in the presence of acetic acid: insights into the nature of the metal-based oxidant. J Am Chem Soc 129(51):15964–15972. https://doi.org/10.1021/ja075115i
86. Wang F, Sun W, Xia C, Wang Y (2017) DFT studies of the substituent effects of dimethylamino on non-heme active oxidizing species: iron(V)-oxo species or iron(IV)-oxo acetate aminopyridine cation radical species? J Biol Inorg Chem 22(7):987–998. https://doi.org/10.1007/s00775-017-1477-9
87. Wang Y, Janardanan D, Usharani D, Han K, Que L, Shaik S (2013) Nonheme iron oxidant formed in the presence of H_2O_2 and acetic acid is the cyclic ferric peracetate complex, not a perferryloxo complex. ACS Catal 3(6):1334–1341. https://doi.org/10.1021/cs400134g
88. Zima AM, Lyakin OY, Ottenbacher RV, Bryliakov KP, Talsi EP (2017) Iron-catalyzed enantioselective epoxidations with various oxidants: evidence for different active species and epoxidation mechanisms. ACS Catal 7(1):60–69. https://doi.org/10.1021/acscatal.6b02851
89. Cussó O, Serrano-Plana J, Costas M (2017) Evidence of a sole oxygen atom transfer agent in asymmetric epoxidations with Fe-pdp catalysts. ACS Catal 7(8):5046–5053. https://doi.org/10.1021/acscatal.7b01184
90. Oloo WN, Meier KK, Wang Y, Shaik S, Münck E, Que L (2014) Identification of a low-spin acylperoxoiron(III) intermediate in bio-inspired non-heme iron-catalysed oxidations. Nat Commun 5:3046–3055. https://doi.org/10.1038/ncomms4046
91. Lyakin OY, Zima AM, Samsonenko DG, Bryliakov KP, Talsi EP (2015) EPR spectroscopic detection of the elusive FeV=O intermediates in selective catalytic oxofunctionalizations of hydrocarbons mediated by biomimetic ferric complexes. ACS Catal 5(5):2702–2707. https://doi.org/10.1021/acscatal.5b00169
92. Zima AM, Lyakin OY, Ottenbacher RV, Bryliakov KP, Talsi EP (2016) Dramatic effect of carboxylic acid on the electronic structure of the active species in Fe(PDP)-catalyzed asymmetric epoxidation. ACS Catal 6(8):5399–5404. https://doi.org/10.1021/acscatal.6b01473

93. Serrano-Plana J, Oloo WN, Acosta-Rueda L, Meier KK, Verdejo B, García-España E, Basallote MG, Münck E, Que L, Company A, Costas M (2015) Trapping a highly reactive nonheme iron intermediate that oxygenates strong C–H bonds with stereoretention. J Am Chem Soc 137(50):15833–15842. https://doi.org/10.1021/jacs.5b09904
94. Fan R, Serrano-Plana J, Oloo WN, Draksharapu A, Delgado-Pinar E, Company A, Martin-Diaconescu V, Borrell M, Lloret-Fillol J, García-España E, Guo Y, Bominaar EL, Que L, Costas M, Münck E (2018) Spectroscopic and DFT characterization of a highly reactive non-heme Fe^{V}–Oxo intermediate. J Am Chem Soc 140(11):3916–3928. https://doi.org/10.1021/jacs.7b11400
95. Oloo WN, Banerjee R, Lipscomb JD, Que L (2017) Equilibrating (L)FeIII–OOAc and (L)FeV(O) species in hydrocarbon oxidations by bio-inspired nonheme iron catalysts using H_2O_2 and AcOH. J Am Chem Soc 139(48):17313–17326. https://doi.org/10.1021/jacs.7b06246
96. Serrano-Plana J, Aguinaco A, Belda R, García-España E, Basallote MG, Company A, Costas M (2016) Exceedingly fast oxygen atom transfer to olefins via a catalytically competent nonheme iron species. Angew Chem Int Ed 55(21):6310–6314. https://doi.org/10.1002/anie.201601396
97. Mondal B, Neese F, Bill E, Ye S (2018) Electronic structure contributions of non-heme oxo-iron(V) complexes to the reactivity. J Am Chem Soc 140(30):9531–9544. https://doi.org/10.1021/jacs.8b04275

Chapter 8
Recent Advances in Bioinspired Asymmetric Epoxidations with Hydrogen Peroxide

Roman V. Ottenbacher

Abstract Bioinspired asymmetric epoxidation of olefins with green oxidant hydrogen peroxide attracted much research interest in recent years. A variety of catalyst systems based on transition metal complexes has emerged, providing useful techniques to obtain chiral epoxides from different classes of olefins. In this chapter, we discuss the major advances in the field, with focus on ligands design, catalyst activity, enantioselectivity, and substrate scope of asymmetric epoxidations, as well as some mechanistic aspects of these reactions.

Keywords Epoxidation · Enantioselective · Asymmetric catalysis · Hydrogen peroxide · Titanium · Manganese

8.1 Introduction

Asymmetric epoxidation of olefins is one of the most beneficial and widely applicable reactions in asymmetric syntheses [1–4], because the resultant chiral epoxides, containing one or two stereogenic centers (Fig. 8.1), serve as proper precursors to optically pure drug molecules or other valuable compounds of fine chemical industry [5–7]. The first discoveries in the field of catalytic asymmetric epoxidations in the presence of vanadium [8] and molybdenum [9] chiral complexes were reported more than 40 years ago. The next decade brought the milestone achievements by

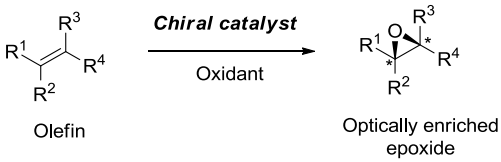

Fig. 8.1 A general scheme for the catalyzed asymmetric epoxidation reaction

R. V. Ottenbacher (✉)
Novosibirsk State University, Pirogova 2, Novosibirsk 630090, Russia
e-mail: ottenbacher@catalysis.ru

Boreskov Institute of Catalysis, Pr. Lavrentieva 5, Novosibirsk 630090, Russia

K. P. Bryliakov (ed.), *Frontiers of Green Catalytic Selective Oxidations*,
Green Chemistry and Sustainable Technology,
https://doi.org/10.1007/978-981-32-9751-7_8

Sharpless, who introduced titanium catalyzed asymmetric epoxidation of allylic alcohols [10] and by Jacobsen [11] and Katsuki [12] who independently presented the asymmetric epoxidation of unfunctionalized olefins catalyzed by manganese-salen complexes. All the above catalyst systems employed such oxidants as alkylhydroperoxides, sodium hypochlorite, and iodosylbenzene, which are not the best choice from the environmental viewpoint, and besides, have low active oxygen content. Hydrogen peroxide had attracted significant attention as a "greener" and cheaper alternative, having high (47%) active oxygen content, and producing water as the only by-product. The use of this oxidant falls into the paradigm of *biomimetic oxidation catalysis* [13], aimed at modeling catalytic functions of metalloenzymes by synthetic catalysts, conducting oxidation processes in a highly selective fashion with nontoxic reagents in mild conditions. Historically, iron complexes catalyzed oxidations held the central position as they were considered as models of both heme (cytochrome P450) and nonheme type (Rieske oxygenase, methane monooxygenase) enzymes [14]. However, in the last 15 years, other transition metal-based catalysts were also successfully developed and applied in bioinspired oxidations realm, particularly in the asymmetric epoxidations of various olefins with hydrogen peroxide [15–17]. This chapter is devoted to the suchlike catalyst systems excluding iron ones, considered in the previous chapter. Manganese, titanium, and some other metal-based systems will be overviewed with attention to ligands design, catalyst activity and enantioselectivity, substrate scope of asymmetric epoxidations, and mechanistic aspects of those reactions. The time span of this review is from 2005 up to 2018.

8.2 Manganese-Based Catalyst Systems

In 2009, Sun and coworkers reported [18] a family of manganese(II) complexes (**1a-c**) which were designed on a basis of the original Stack's complex **1d** (**Mn-mcp**) [19], with the ligand bearing two additional centers of chirality (Fig. 8.2). Sun's complexes efficiently catalyzed the asymmetric epoxidation of various olefins using 1 mol% catalyst loading and performing up to 100 turnovers (TN) with hydrogen peroxide added in excess (6 equivalents relative to the substrate). The catalyst system showed high enantioselectivity in the epoxidation of α,β-unsaturated ketones (up to 89% *ee*), and moderate enantioselectivity in the epoxidation of unfunctionalized alkenes (up to 46% *ee*) in the presence of acetic acid as an additive (5 equiv. vs. substrate). More recently, Abdi with coworkers reported structurally related complex **1e** (Fig. 8.2), which was tested in epoxidations of different olefins with hydrogen peroxide and showed high efficiencies (800–1000 TN) and moderate to good enantioselectivities (43–88% *ee*) [20]. Again, acetic acid additive was employed to ensure high catalytic activity and efficiency. In 2016, Nam and Sun with coworkers developed [21] a related manganese(II) complex **1f** (Fig. 8.2), which was able to catalyze asymmetric epoxidation with hydrogen peroxide using sulfuric acid as co-catalytic additive. The molecule of sulfuric acid was shown to be important for the catalytic reaction, the SO_4^{2-} anions and H^+ cations both being necessary. The catalyst per-

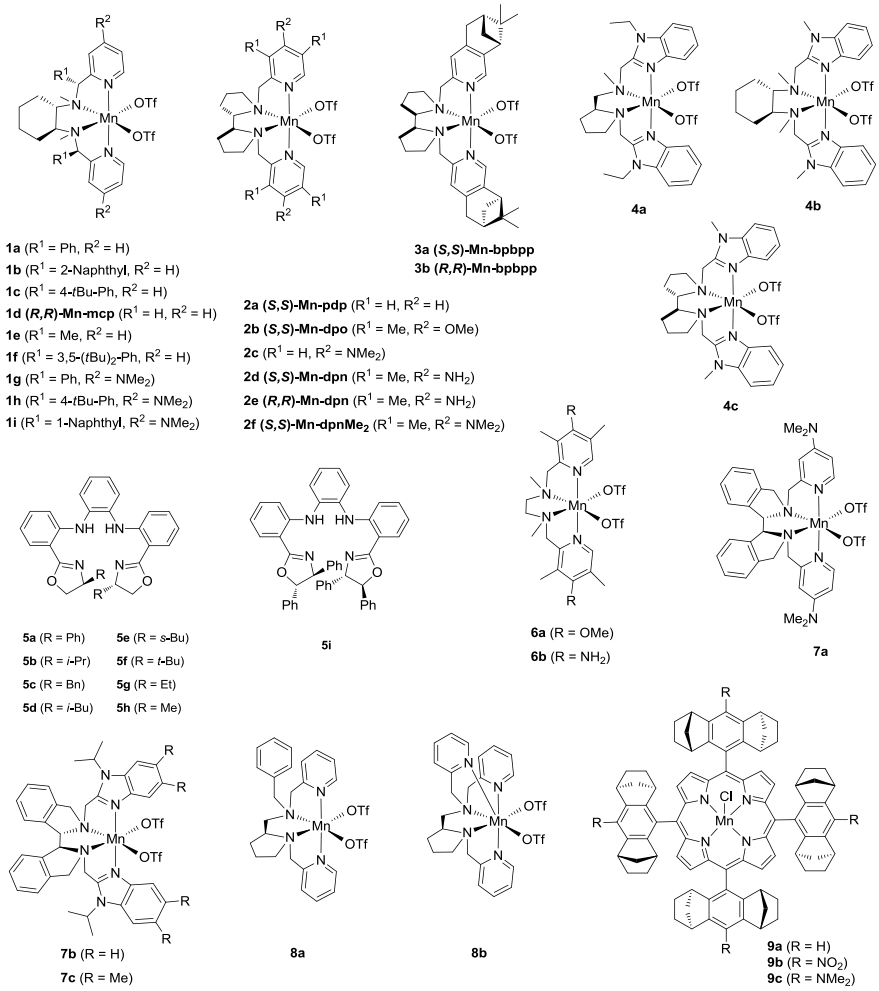

Fig. 8.2 Ligands and manganese complexes for asymmetric epoxidations

formed 100–500 TN in the epoxidation of various olefins (unfunctionalized alkenes, α,β-unsaturated esters and ketones) with moderate to excellent enantioselectivities (60–98% *ee*, Table 8.2, entries 1, 18). Very recently, Sun with coworkers reported [22] the catalyst system based on complex **1f** and graphene oxide (GO). GO was employed as an additive (in reduced amounts: 14 mg of GO per 1 mmol of substrate). The authors explained its co-catalytic activity by the presence of surface carboxylic groups in the GO, presumably playing the same role as "traditional" acetic acid (vide infra). The complex was used at 0.5% loadings, mediating the asymmetric epoxidation of chromenes (90–92% *ee*), substituted chalcones (82–99% *ee*), cinnamic esters (84–93% *ee*), and styrenes (41–49% *ee*).

Originally, Stack's chiral complex **1d** was applied [19] in non-stereoselective epoxidations of alkenes with peracetic acid, however, its C_2-symmetrical *N*-donor tetradentate ligand had provided a good platform for structural modifications at both the diamine backbone and the pyridyl units. The first alternative in the chiral diamine backbone architecture was suggested by Talsi and coworkers who contributed [23] 2,2′-bipyrrolidine based manganese(II) complex **2a** (Fig. 8.2, **Mn-pdp**) as an efficient catalyst for the asymmetric epoxidations with peracetic acid and hydrogen peroxide. Complex **2a** was capable of producing epoxides, performing typically 1000 TN, and demonstrating moderate to good enantioselection (up to 89% *ee*). In reactions with H_2O_2, the oxidant was used in only slight excess relative to a substrate (1.3 equiv.), which is attractive from the practical point of view; this protocol was adopted from the report of Costas and coworkers who applied [24] it in epoxidations with achiral Mn complex. The group of Costas described [25] further modifications in **Mn-pdp** catalyst as novel complexes **3a** and **3b** (Fig. 8.2) were synthesized. In contrast to the parent complex, the latter ones' ligands contained 4,5-pinene-appended pyridine rings. Such alteration did not turn out to be notably effective: the catalysts furnished good to excellent yields (80–100%, TN up to 1000) in the asymmetric epoxidation of various olefins by H_2O_2 (1.2 equiv.) in the presence of acetic acid additive (14 equiv. vs. substrate), demonstrating moderate enantioselectivities (66–73% *ee*) for a few substrates and low (4–54% *ee*) for others.

Sun and coworkers synthesized a family of manganese(II) complexes (**4a** [26], **4b** [27] and **4c** [28]) with N_4-donor ligands, bearing benzimidazole units instead of pyridine ones (Fig. 8.2), featuring various chiral backbones. Catalyst **4a** exhibited good enantioselectivity in the epoxidation of substituted chromenes (72–79% *ee*) and isopropyl cinnamate (74% *ee*) and high enantioselectivity in the epoxidation of substituted chalcones (up to 95% *ee*, Table 8.2, entries 5, 14) with H_2O_2, performing typically 300–500 TN [26].

All of the abovementioned Mn-catalyzed asymmetric epoxidations with H_2O_2 required externally added acetic acid to promote the catalytic reaction. Talsi and coworkers revealed [29] that the use of more sterically demanding carboxylic acid instead of acetic acid resulted in remarkable improvement of enantioselectivity of **Mn-pdp** catalyzed epoxidations (Table 8.1). In particular, the enantioselectivity increased with rising steric demand of the carboxylic acid, branched at the α-carbon; 2-ethylhexanoic acid (EHA) had demonstrated the best performance. These observations indicated that the active oxidizing species incorporated the carboxylic acid moiety, providing simple and efficient approach to tuning the catalyst's enantioselectivity.

Another approach for effective catalyst tuning was reported [30] by Costas and coworkers who constructed a series of Mn complexes (including **2b** and **2c**, Fig. 8.2) with electron-donating substituents at pyridine moieties of the ligand. Catalyst **2c** bearing –NMe_2 group (at 0.5 mol% cat. loading) mediated the epoxidation of olefins with excellent enantioselectivity (up to 98% *ee*, Table 8.2, entries 3, 8, 11, 15, 19) by H_2O_2 (2 equiv.) and EHA as the additive. Besides, catalyst **2b** (**Mn-dpo**) was shown to be active toward diastereoselective β-epoxidation of unsaturated steroids affording products which are considered as valuable biologically active compounds

Table 8.1 Asymmetric epoxidation of chalcone in the presence of different carboxylic acids catalyzed by **Mn-pdp**

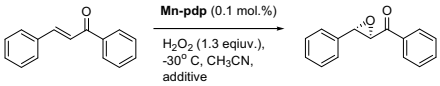

Entry	Additive	Epoxide yield, %	ee, % (config.)
1	–	0	–
2	AcOH[a]	98	78 (2*R*, 3*S*)
3	BA[b]	69	80 (2*R*, 3*S*)
4	VA[c]	48	80 (2*R*, 3*S*)
5	CA[d]	40	80 (2*R*, 3*S*)
6	IBA[e]	100	82 (2*R*, 3*S*)
7	PA[f]	47	86 (2*R*, 3*S*)
8	EHA[g]	97	93 (2*R*, 3*S*)

[a]AcOH = acetic acid. [b]BA = *n*-butyric acid. [c]VA = *n*-valeric acid. [d]CA = *n*-caproic acid. [e]IBA = *i*-butyric acid. [f]PA = pivalic acid. [g]EHA = 2-ethyl-hexanoic acid

[30]. Bryliakov and coworkers developed manganese complexes **2d** [31] (and its enantiomer **2e** [32]) and **2f** (Fig. 8.2). Complex **2d** comprised $–NH_2$ substituents at *para*-positions and—Me groups at *meta*-positions of the pyridine units. It was documented that the complex efficiently catalyzed the enantioselective epoxidation of various electron-deficient olefins with up to 99% *ee* (Table 8.2, entries 4, 16, 20, 21), performing 200–1000 TN. Moreover, a series of conjugated *cis*-olefins was successfully epoxidized in the presence of **2e** with good to excellent enantioselectivities (74–97% *ee*, Table 8.2, entries 9, 12). EHA was used as a necessary additive.

Subsequently, attempts to apply other sterically demanding carboxylic acids were also made. Sun with coworkers examined a family of manganese complexes (**1g–i**, Fig. 8.2) bearing two additional aromatic groups (as in **1a–c**) and with electron-donating $–NMe_2$ substituents at the pyridyl units [33]. Complex **1g** was capable of catalyzing the enantioselective epoxidation of different unfunctionalized olefins with H_2O_2 in the presence of 2,2-dimethylbutanoic acid additive with good yields (70–95%). As for enantioselectivity, *cis*-alkenes, substituted styrenes and *trans*-stilbenes were oxidized to the corresponding epoxides with up to 98% *ee* (Table 8.2, entries 7, 13), 80% *ee*, and 90% *ee*, respectively, while trisubstituted and aliphatic alkenes appeared to be challenging substrates, producing epoxides with only 31–64% *ee*.

Gao with coworkers synthesized [34, 35] a family of novel non-aminopyridine "porphyrin-inspired" ligands (**5a–i**, Fig. 8.2), and documented that the corresponding complexes with $Mn(OTf)_2$, prepared in situ, catalyzed the asymmetric epoxidation of olefins with H_2O_2 in a highly enantioselective fashion (up to 99% *ee*). The catalyst system exhibited superior results in the epoxidations of *cis*-alkenes (93% *ee* for indene and 96% *ee* for 1,2-dihydronaphthalene, Table 8.2, entry 10), 2,2-dimethylchromene derivatives (up to 99% *ee*, Table 8.2, entry 17), *trans*-stilbene

Table 8.2 Highly enantioselective epoxidations of olefins with H_2O_2 in the presence of Mn complexes

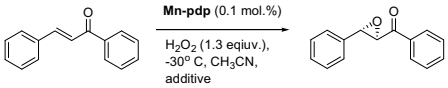

Entry	Substrate	Catalyst (mol.%)	Epoxide yield, %	ee, % (config.)	Ref.
1	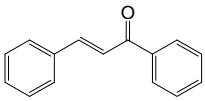	**1f** (0.2)	94	97	[21]
2		**2a** (0.1)	97	93 (*2R, 3S*)	[29]
3		**2c** (0.5)	95	96 (*2R, 3S*)	[30]
4		**2d** (0.2)	100	98 (*2R, 3S*)	[31]
5		**4a** (0.1)	93	92	[26]
6		**7b** (0.2)	85	96	[37]
7	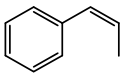	**1g** (0.1)	75	93	[33]
8		**2c** (0.1)	86	92	[30]
9		**2e** (0.1)	98	91	[32]
10	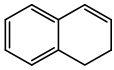	$Mn(OTf)_2$ + **5b**	99	96	[34]
11	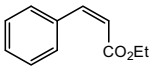	**2c** (0.1)	77	98	[30]
12		**2e** (0.1)	98	94	[32]
13	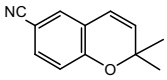	**1g** (0.1)	95	98	[33]
14		**2a** (0.1)	100	93 (*3R, 4R*)	[29]
15		**2c** (0.1)	95	97	[30]
16		**2d** (0.1)	100	99 (*3R, 4R*)	[31]
17		$Mn(OTf)_2$ + **5b**	90	98	[35]
18[a]	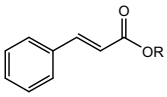	**1f** (0.2)	55	95	[21]
19[a]		**2c** (0.5)	93	92	[30]
20[b]		**2d** (0.2)	88	96 (*2R, 3S*)	[31]
21	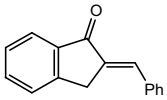	**2d** (0.2)	90	93 (*2R, 3S*)	[31]
22		**7b** (0.2)	82	99	[37]
23	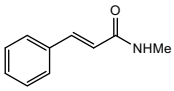	**7b** (0.05)	91	96	[37]

[a]R = Et. [b]R = *t*-Bu

(97% *ee*). At the same time, other tri-substituted and *trans*- olefins were converted to corresponding epoxides with much lower enantio-induction (51–67% *ee*). The catalyst loadings were in the range of 0.5–1.0 mol%; the system also required carboxylic acid additive, in particular acetic [34] and 1-adamantanoic or cyclohexanoic [35]), and as high as 2–4 equivalents of H_2O_2 relative to the substrate.

Bryliakov with coworkers established that *achiral* catalysts **6a** and **6b** (Fig. 8.2) can also mediate olefin epoxidation with well discernible enantioselectivity when used with additive of optically active *N-Boc*-(*L*)-proline, yielding chalcone epoxide with 32% and 50% *ee*, respectively. This phenomenon was documented as a rare case of *chiral environment amplification* [36].

There is also a recently reported [37] precedent of successful replacement of 2,2′-bipyrrolidine backbone with its phenyl-fused analog 1,1′-biisoindoline. Huang with coworkers synthesized complexes **7a–c** (Fig. 8.2), that exhibited excellent enantioselectivities (94.9–99.6% *ee*, Table 8.2, entry 23) in the epoxidation of a series of *trans*-cinnamic acid amide derivatives and of α,β-unsaturated ketoamides with H_2O_2 in the presence of acetic acid. Also, α,β-unsaturated ketones (chalcone and its analogs and derivatives) were epoxidized with high stereoselectivity (82–99% *ee*, Table 8.2, entries 6, 22). The catalysts carried out 400–500 TN with consumption of almost stoichiometric amount of hydrogen peroxide (1.2 equiv.).

The mechanism of the enantioselective epoxidation with hydrogen peroxide, catalyzed by manganese(II) aminopyridine, and related complexes, captured significant research attention [29, 31, 36, 38–40]. Although to date no direct spectroscopic data on the nature of the active epoxidizing species has been reported, a series of documented indirect experimental data has allowed proposing the nature of active centers in the catalytic system and the mechanism of epoxidation (vide infra).

It has been shown [29] that the additive of a carboxylic acid played a dual role in manganese aminopyridine catalyzed epoxidations: on the one hand, the presence of a carboxylic was necessary for the catalytic reaction to proceed with nonzero conversion, thus, it was suggested that a carboxylic acid participates in the generation of active species; on the other hand, the enantioselectivity of epoxidation correlated with the steric bulk of a carboxylic acid (vide supra), pointing to the presence of the latter (or its part) in the structure of active centers.

Manganese complex **2b** was found to catalyze the epoxidation of styrene in the presence of ^{18}O-isotopically labeled water [31] *without* added carboxylic acid, affording ^{18}O-labeled epoxide (35% enrichment) along with mono-labeled diol. These data were interpreted in favor of the formation of $Mn^{V}(O)(OH)$ active species. It was suggested that in the presence of carboxylic acid, the reaction pathway is similar, but with participation of the acid molecule in promoting the O–O bond heterolysis (Fig. 8.3) to form $Mn^{V}(O)(OC(O)R)$ active species [31]. It was also demonstrated that the active species were electrophilic, with Brown–Okamoto constant ρ^{+} of −1.51 observed in oxidations of *p*-substituted chalcones. Partial epimerization (5–7%) in **2a** and **2b** catalyzed epoxidations of *cis*-stilbene implied that the active species interaction with a substrate likely generated short-lived acyclic carbocationic intermediates [31].

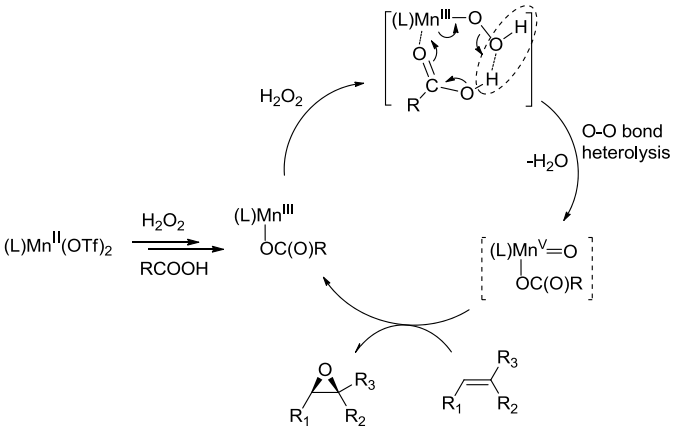

Fig. 8.3 Proposed "carboxylic acid-assisted" asymmetric epoxidation mechanism in the presence of Mn aminopyridine catalysts

The formation of manganese(V)-oxo species required two labile *cis*-coordination sites in octahedral complex structure. Indeed, all catalytically active manganese aminopyridine complexes with reported X-ray characterization featured *cis*-α ligand coordination topology, while the only reported *trans*-complex was shown to be catalytically inactive [31]. Very recently, Nam and Sun with coworkers confirmed [40] the importance of the availability of two out of six coordination sites. They elaborated two manganese complexes (**8a** and **8b**, Fig. 8.2) containing ligands with very similar steric demand but with different amount of *N*-donor units. Complex **8a** bearing tetradentate N_4-ligand did catalyze asymmetric epoxidation of olefins in anticipated fashion, while complex **8b** with pentadentate N_5-ligand was not able to mediate the reaction with H_2O_2 even in the presence of carboxylic acid.

Manganese complexes with chiral ligands of other types were also studied as catalysts of asymmetric epoxidation by H_2O_2. A number of papers focusing on Mn(III)-salen complexes with macrocyclic type ligands were reported by Abdi and coworkers [41–43]. As a rule, the catalyst systems required 2.5–5 mol% loadings, which is quite high as far as each catalyst molecule contained two manganese centers. The reactions were conducted with urea-hydrogen peroxide adduct (1.5–2 equiv. vs. substrate) as oxidant and pyridine-*N*-oxide as co-catalytic additive. The substrate scope was restricted to styrene, indene, and substituted chromenes, which showed good epoxidation yields and good to high enantioselectivity (up to 93% *ee*). Sfrazetto and coworkers studied [44] epoxidations with H_2O_2 (excess of 8 equiv. vs. alkene) using Jacobsen's catalyst [11] in aqueous media. The reaction was promoted by dimethyltetradecylamine-*N*-oxide that acted as both surfactant and co-catalyst. Simonneaux and coworkers explored [45] asymmetric epoxidation of styrenes in the presence of manganese(III)-porphyrin complexes **9a–c** (Fig. 8.2). It was demonstrated that the highest asymmetric induction (13–55% *ee*) was provided by catalyst

9b (2.5 mol%) bearing electron-deficient nitro-group. The catalyst system consumed 5 mol of hydrogen peroxide per mole of alkene.

8.3 Titanium-Based Catalyst Systems

Katsuki and coworkers were the first to explore titanium(IV) complexes with chiral salan (tetrahydrosalen) and salalen (dihydrosalen) ligands as catalysts in asymmetric epoxidation reactions. In 2005, the pioneering work was published [46], in which the authors reported the synthesis of homochiral dimeric di-μ-oxo Ti(IV)-salalen complex **10** (Fig. 8.4). The complex was studied in asymmetric epoxidation catalysis with stoichiometric amount of hydrogen peroxide, furnishing epoxides of conjugated alkenes with high yields and high enantioselectivity (88–99% *ee*, Table 8.3, entries 1, 11, 17, 22) and excellent efficiency (up to 4600 TN). The latter value was attained under slow oxidant addition (during 8 h) protocol, whereas, typically, the oxidant was added in one portion to the mixture containing 1 mol% of catalyst. Also, Katsuki with coworkers employed *ent*-**10** at 0.5–2.0 mol% loadings in the highly enantioselective (>99% *ee*, Table 8.3, entry 37) epoxidation of *cis*-alkenylsilanes. The resulting epoxysilanes can be easily converted to optically pure styrene oxides and geminally disubstituted epoxides. Simultaneously, complex **10** was tested [48] in the asymmetric epoxidations of aliphatic terminal and *cis*-alkenes. It was shown that the enantio- and regioselectivity in the epoxidation were mainly dictated by steric factors and the olefinic substitution pattern, the highest *ee* value was documented in reaction with vinylcyclohexane (95%, Table 8.3, entry 34). Other substrates in most cases afforded satisfactory yields (50–90% using 2–3 mol% of the catalyst), along with good *ee*'s (70–82%, Table 8.3, entry 31).

In original work, Katsuki described [46] the construction of **10** by in situ intramolecular Meerwein–Ponndorf–Verley reduction of the corresponding Ti(salen) complex. This synthesis was not universal, possibly applicable to this complex only; this problem was solved by Berkessel and coworkers who developed a general approach to the synthesis of unsymmetrical salalen ligands, and screened 13 correspondings in situ generated Ti(salalen) catalysts (ligands **11a–m**, Fig. 8.4) in the asymmetric epoxidations of alkenes with hydrogen peroxide [49]. The best catalyst **11m** performed only 10 TN; the most suitable substrates were indene and 1,2-dihydronaphthalene, yielding the epoxides in about 90% yields with 95–97% *ee* (Table 8.3, entries 12, 18), while aliphatic alkenes, as well as *trans*-β-methyl-styrene, showed poor conversions (<20%) with 30–81% *ee*. Further, Berkessel et al. studied [50] the mechanism and degradation pathways in the catalyst system by means of ESI-MS and kinetic data (monodeuteration of the salalen ligand). It was proposed that mononuclear titanium salalen is the catalytically active species, which degrades during reaction to the inactive Ti(salen) by the oxidation of N–H unit of the ligand. Earlier, Katsuki speculated [46] that the presence of N–H group was vital for epoxidation activity due to intramolecular hydrogen bonding with the peroxo moiety. The latter process is responsible for the activation of the peroxide bond and facilitates

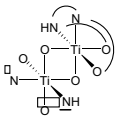

10

O-N-NH-O =

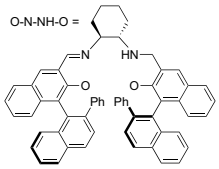

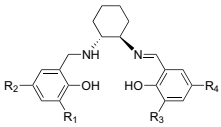

11a (R_1 = F, R_2 = F, R_3 = H, R_4 = H)
11b (R_1 = Cl, R_2 = Cl, R_3 = H, R_4 = H)
11c (R_1 = I, R_2 = I, R_3 = H, R_4 = H)
11d (R_1 = OMe, R_2 = H, R_3 = H, R_4 = H)
11e (R_1 = *t*-Bu, R_2 = *t*-Bu, R_3 = H, R_4 = H)
11f (R_1 = Ph, R_2 = H, R_3 = H, R_4 = H)
11g (R_1 = Ph, R_2 = H, R_3 = F, R_4 = F)
11h (R_1 = Ph, R_2 = H, R_3 = Cl, R_4 = Cl)
11i (R_1 = Ph, R_2 = H, R_3 = I, R_4 = I)
11j (R_1 = Ph, R_2 = H, R_3 = NO_2, R_4 = NO_2)
11k (R_1 = Ph, R_2 = H, R_3 = OMe, R_4 = H)
11l (R_1 = Ph, R_2 = H, R_3 = *t*-Bu, R_4 = *t*-Bu)
11m (R_1 = Ph, R_2 = H, R_3 = Ph, R_4 = H)

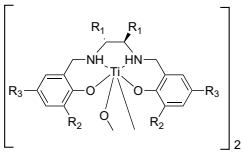

12a (R_1 = Ph, R_2 = *t*-Bu, R_3 = *t*-Bu)
12b (R_1 = Ph, R_2 = Ph, R_3 = H)
12c (R_1 = -$(CH_2)_4$-, R_2 = *t*-Bu, R_3 = *t*-Bu)
12d (R_1 = -$(CH_2)_4$-, R_2 = Ph, R_3 = H)

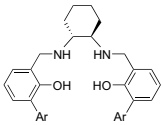

13a Ar = Ph
13c Ar = *m*-$MeOC_6H_4$
13e Ar = 2,6-$(MeO)_2C_6H_4$
13g Ar = *o*-$CF_3C_6H_4$
13i Ar = *o*-$EtOC_6H_4$
13k Ar = *o*-Biphenyl
13m Ar = 2-Naphthyl
13o Ar = 2,6-$Ph_2C_6H_3$
13b Ar = *o*-$MeOC_6H_4$
13d Ar = *p*-$MeOC_6H_4$
13f Ar = *o*-MeC_6H_4
13h Ar = *o*-EtC_6H_4
13j Ar = *o*-$BnOC_6H_4$
13l Ar = 1-Naphthyl
13n Ar = 9-Anthracenyl

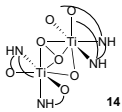

14

O-NH-NH-O = enantiomer of **13b**

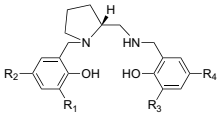

15a (R_1 = R_2 = R_3 = R_4 = *t*-Bu)
15b (R_1 = R_2 = *t*-Bu, R_3 = Ph, R_4 = H)
15c (R_1 = Ph, R_2 = H, R_3 = R_4 = *t*-Bu)
15d (R_1 = Ph, R_2 = H, R_3 = Ph, R_4 = H)

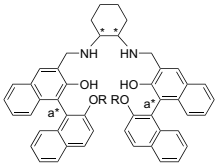

16a (*, a*, R) = (*R*,*S*), Me
16b (*, a*, R) = (*R*,*S*), Bn
16c (*, a*, R) = (*R*,*R*), Me
16d (*, a*, R) = (*S*,*S*), Me

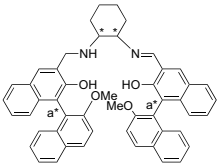

16e (*, a*, R) = (*R*,*S*)
16f (*, a*, R) = (*R*,*R*)

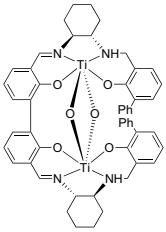

17

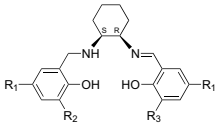

18a (R_1 = H, R_2 = R_3 = Ph)
18b (R_1 = H, R_2 = Ph, R_3 = 2-MeOPh)
18c (R_1 = H, R_2 = R_3 = 2-MeOPh)
18d (R_1 = H, R_2 = 2-MeOPh, R_3 = Ph)
18e (R_1 = Me, R_2 = R_3 = Me-*c*-hexyl)
18f (R_1 = H, R_2 = R_3 = *c*-hexyl)
18g (R_1 = H, R_2 = R_3 = C_6F_5)

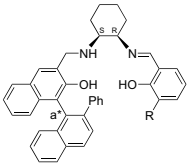

19a a*= (*S*), R = Ph
19b a*= (*R*), R = Ph
19c a*= (*S*), R = *c*-hexyl
19d a*= (*R*), R = *c*-hexyl

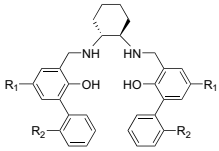

20a (R_1 = Ac, R_2 = H)
20b (R_1 = Br, R_2 = H)
20c (R_1 = NO, R_2 = H)
20d (R_1 = Me, R_2 = H)
20e (R_1 = OMe, R_2 = H)
20f (R_1 = H, R_2 = Cl)
20g (R_1 = H, R_2 = Me)
20h (R_1 = H, R_2 = OMe)
20i (R_1 = H, R_2 = Ph)
20j (R_1 = OMe, R_2 = OMe)

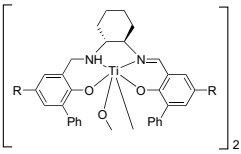

21a R = H
21b R = Br

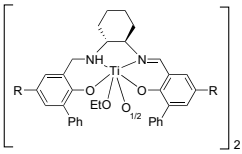

21c R = OMe

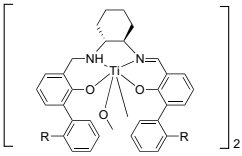

21d R = Et
21e R = OMe

Fig. 8.4 Salan and salalen ligands and Ti complexes employed asymmetric epoxidations

Table 8.3 Highly enantioselective epoxidations of olefins with H_2O_2 in the presence of Ti complexes

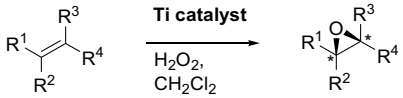

Entry	Substrate	Catalyst	Epoxide yield, %	ee, %	Ref.
1	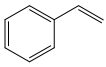	**10**	90	93	[46]
2		**12d**	47	82	[51]
3		**Ti(O*i*Pr)$_4$ + 13b**	68	89	[52]
4		**Ti(O*i*Pr)$_4$ + 15d**	71	98	[57]
5		**17**	70	90	[59]
6		**21d**	76	86	[65]
7	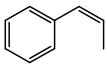	**Ti(O*i*Pr)$_4$ + 16f**	95	80	[58]
8		**17**	90	96	[59]
9		**Ti(O*i*Pr)$_4$ + 20h**	90	90	[63]
10		**21e**	85	82	[65]
11	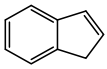	**10**	87	99	[46]
12		**Ti(O*i*Pr)$_4$ + 11m**	88	97	[49]
13		**12d**	72	95	[51]
14		**Ti(O*i*Pr)$_4$ + 13b**	86	98	[52]
15		**17**	89	97	[59]
16		**21e**	96	97	[65]
17	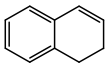	**10**	99	>99	[46]
18		**Ti(O*i*Pr)$_4$ + 11m**	91	96	[49]
19		**12d**	87	96	[51]
20		**Ti(O*i*Pr)$_4$ + 13g**	93	98	[52]
21		**21e**	94	98	[65]
22	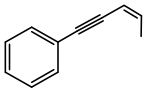	**10**	64	88	[46]
23		**12d**	69	90	[51]
24		**Ti(O*i*Pr)$_4$ + 13g**	92	96	[52]
25		**17**	92	92	[59]
26	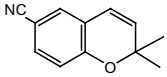	**12d**	77	99	[51]
27		**Ti(O*i*Pr)$_4$ + 13b**	75	>99	[52]

(continued)

Table 8.3 (continued)

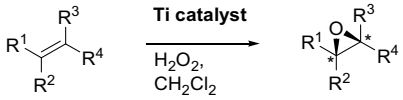

Entry	Substrate	Catalyst	Epoxide yield, %	ee, %	Ref.
28		**Ti(O*i*Pr)$_4$ + 16f**	92	99	[58]
29		**17**	90	99	[59]
30		**21e**	93	>99	[65]
31	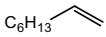	**10**	85	82	[48]
32		**Ti(O*i*Pr)$_4$ + 18f**	88	94	[60]
33		**Ti(O*i*Pr)$_4$ + 19d**	80	94	[61]
34	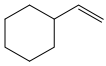	**10**	72	95	[48]
35		**Ti(O*i*Pr)$_4$ + 18f**	88	94	[60]
36		**Ti(O*i*Pr)$_4$ + 18g**	>99	94	[62]
37	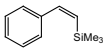	*ent*-**10**	87	>99	[47]
38	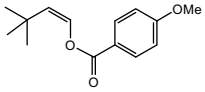	*ent*-**10**	90	>99	[55]
39	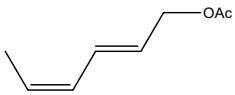	**Ti(O*i*Pr)$_4$ + 13b**	93[a]	96	[56]

[a]4,5-monoepoxide

the enatioselective oxygen transfer step. It was noted that the lifetime of Ti(salalen) catalyst in the presence of hydrogen peroxide is long enough for the epoxidation of electron-rich conjugated olefins, and at the same time is too short for effective oxygen transfer to electron-poor non-conjugated ones.

In parallel, titanium(IV) salan complexes emerged as easier prepared analogs of Ti-salalens. Katsuki and coworkers prepared four di-μ-oxo Ti(IV)-salan complexes (**12a–d**, Fig. 8.4) and probed them as catalysts in the asymmetric epoxidation of 1,2-dihydronaphthalene [51]. Complex **12d** exhibited the best performance in terms of activity and enantioselectivity. Other conjugated alkenes (6 examples) were also epoxidized with 1.5 equivalents of H_2O_2 in the reaction catalyzed by **12d** (5 mol% loadings), furnishing epoxides in high *ee*'s (82–99%, Table 8.3, entries 2, 13, 19, 23, 26) and acceptable yields (44–77%). The only tested aliphatic substrate, 1-octene, turned out to be a poor substrate for this catalyst system, with only 25% yield and 55% *ee*. In a subsequent paper, the authors modified [52] the 3,3′-positions of the salan ligand of **12d** and screened overall 14 Ti(salan) complexes (prepared in situ from Ti(O*i*Pr)$_4$ and ligands **13a–n**, Fig. 8.4). It was demonstrated that catalysts Ti(**13b**) and

Ti(**13g**) ensured enhanced yields and asymmetric induction, as compared with the parent Ti(**13a**). The catalyst system comprised 5 mol% of Ti(O*i*Pr)$_4$ and 6 mol% of chiral salan ligand and required nearly stoichiometric amount of hydrogen peroxide (1.1 equiv.). For 8 tested conjugated alkenes, excellent enantioselectivities (87–99% *ee*, Table 8.3, entries 3, 14, 20, 24, 27) and good yields were achieved. The above catalyst system was improved by the addition of phosphate buffer (pH 7.4–8.0) [53]. It was observed that the reaction media became more acidic in the course of the reaction, causing significant by-product formation, thus it was necessary to maintain the pH at neutral levels. As a side effect of such conditions modification, reaction rate deceleration was observed, that forced the authors to raise the temperature of asymmetric epoxidation to 40 °C. In this optimized condition the catalyst Ti(**13b**) required much lower loadings (1.3 mol%) to afford the epoxides of conjugated alkenes in high yields (65–99%) without significant loss in asymmetric induction (88–99% *ee*). Subsequently, the synthesis of peroxide-containing intermediate in Ti(salan) catalyzed epoxidations was reported by Katsuki and coworkers who obtained X-ray quality crystals of the μ-oxo-μ-η^2:η^2-peroxo titanium complex **14** (Fig. 8.4) by oxidizing dimeric complex [TiO(*ent*-**13b**)]$_2$ with 30% hydrogen peroxide [54]. It was shown that complex **14** was not an active oxidizing species itself but rather served as a reservoir, slowly converting into the active species.

Katsuki and coworkers expanded the substrate scope, making use of complex *ent*-**10** in the asymmetric epoxidation of (*Z*)-enol esters with hydrogen peroxide [55]. The catalyst performed up to 50 TN in reactions with both aliphatic and aromatic enol esters at room temperature, furnishing epoxides with generally high enantioselectivity (86–99% *ee*, Table 8.3, entry 38). It was shown that the obtained epoxides could be transformed into the corresponding 1,2-diols without erosion of enantiomeric excess. Falck and coworkers applied the *in situ* prepared catalyst Ti(**13b**) in diastereo- and enantioselective monoepoxidation of conjugated dienes with hydrogen peroxide [56]. The values of *de*/*ee* were in the range 88–98% (Table 8.3, entry 39), along with generally good yields (>80%), using 5 mol% of Ti(O*i*Pr)$_4$ and 6 mol% of **13b**. The regioselectivity in some cases was complementary to that achieved using Sharpless and other directed epoxidations. A strong preference for *Z*- over *E*-olefins was observed.

Alternative structures of the chiral diamine backbone were also investigated. The group of Katsuki synthesized [57] a novel family of proline-derived C_1-symmetrical salan ligands (**15a–d**, Fig. 8.4) and examined the corresponding in situ prepared Ti(salan) complexes in the asymmetric epoxidation 2-vinylnaphthalene as a model substrate. Under optimized conditions, at −20 °C the catalyst Ti(**15d**) promoted the asymmetric epoxidation of a series of substituted styrenes with excellent enantioselectivity (96–98% *ee*, Table 8.3, entry 4) and good yields (66–84%), albeit high catalyst loadings required (10 mol%).

Sun and coworkers designed and prepared [58] a series of salan and salalen ligands (**16a–f**, Fig. 8.4) derived from chiral binaphthol. The corresponding titanium complexes catalyzed the asymmetric epoxidation of conjugated alkenes with hydrogen peroxide in 71–99% *ee* (Table 8.3, entries 7, 28) performing up to 10 TN; however, aliphatic terminal alkenes were somewhat less suitable substrates for this

catalytic system, giving only 44–67% *ee*. In subsequent paper, the authors developed [59] a dinuclear μ-oxo titanium complex **17** (Fig. 8.4) with a single salalen ligand containing an intramolecular biaryl bridge. The complex **17** was examined in the asymmetric epoxidation of a few alkenes with H_2O_2, exhibiting enhanced robustness (up to 93 TN) and excellent enantioselectivity (90–99% *ee*, Table 8.3, entries 5, 8, 15, 25, 29) for aromatic terminal and *cis*-olefins. Aliphatic terminal substrates again demonstrated poorer results (10–56% yield and 61–78% *ee*). Also, comparative experiments with Berkessel's similar yet non-bridged complex $[TiO(\mathbf{11m})]_2$ were carried out showing better performance of Sun's novel catalyst **17**.

The challenging enantioselective epoxidation of aliphatic alkenes was investigated by Berkessel and coworkers who reported a series of titanium complexes with salalen ligands (**18a–g**, **19a–d**, Fig. 8.4) based on *cis*-1,2-diaminocyclohexane (*cis*-DACH) backbone rather than *trans*-one [60–62]. Initially, they studied *in situ* prepared Ti(**18a**) complex along with its *trans*-counterpart Ti(**11m**) in the asymmetric epoxidations of different alkenes with H_2O_2, and revealed that *cis*-DACH-based catalyst was more suitable for non-conjugated terminal olefins [60]. Further modifications of the parent ligand gave birth to the catalyst Ti(**18f**) which afforded excellent enantioselectivities (89–95% *ee*, Table 8.3, entries 32, 35) for substrates of this type. In the next paper, the authors examined the role of *ortho* substituents of phenolic moieties in more detail, presenting 14 novel *cis*-DACH ligands (selected examples are at Fig. 8.4) [61]. The catalyst screening resulted in complexes Ti(**19b**) and Ti(**19d**) which optimally combined high activity and enantioselectivity (82–94% *ee*, Table 8.3, entry 33) in the epoxidation of terminal aliphatic alkenes. The catalyst loadings could be reduced from regular 10 to 0.1 mol% when conducting the reaction in 1,2-dichloroethane. The next ligand structure optimization was the introduction of fluorinated substituents. In that manner, the catalyst Ti(**18g**) was explored in the asymmetric epoxidation of different aliphatic alkenes with H_2O_2 [62]. Terminal alkenes of various nature gave epoxides with excellent *ee*'s (up to 99%, Table 8.3, entry 36) and high yields, while *cis*-, *trans*- and 1,1-disubstituted alkenes demonstrated poorer results (84, 4 and 15% *ee*, respectively). The catalyst was used at relatively high loadings (10 mol%), with, typically, 1.5 equiv of oxidant relative to alkene.

Bryliakov with coworkers studied the influence of steric bulk and electronic properties of the chiral salan ligands on the enantioselectivity of epoxidation with H_2O_2 catalyzed by a series of titanium(IV) complexes (**20a–j**, Fig. 8.4) [63]. It was shown that the electronic properties influenced the catalytic activity without affecting the enantioselectivity, whereas the steric bulk (governed by variation of the *ortho*-aryl substituents) determined the enantioselectivity of epoxidation. A number of conjugated alkenes were epoxidized in presence of complexes Ti(**20e**), Ti(**20h**), and Ti(**20i**) with up to 99.7% *ee* (Table 8.3, entry 9), the catalysts performed up to 20 TN. The electrophilic nature of the active species was established by competitive oxidations of *para*-substituted styrenes, the enantioselectivity in these reactions was virtually constant irrespective of the substituent. On the basis of these findings and UV/Vis monitoring of the catalyst system, the reaction mechanism was suggested (Fig. 8.5). According to it, in the first (rate-limiting) step, an alkene coordinates to the active

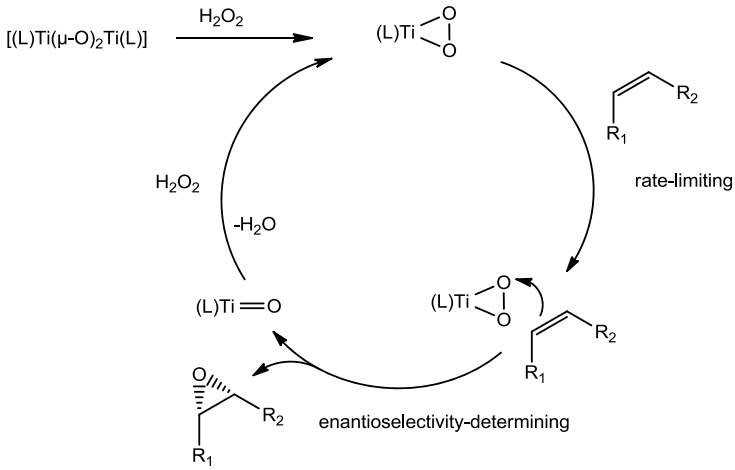

Fig. 8.5 Proposed mechanism of Ti(salan) catalyzed asymmetric epoxidations with H_2O_2 [63]

(presumably, titanium(η^2-peroxo)) species, followed by intramolecular enantioselective oxygen transfer. The authors also reported [64] more elaborated titanium salan catalyst with ligand **13o** (Fig. 8.4). The excess of steric bulk in the catalyst structure resulted in poor yield of styrene epoxidation and lower enantioselectivity compared with parent Ti(**20i**) complex. In the next paper, Bryliakov and coworkers explored the asymmetric epoxidation catalyzed by a number of titanium salalen complexes (**21a–e**, Fig. 8.4) [65]. The catalysts **21d** and **21e** exhibited good asymmetric induction in the epoxidations of conjugated alkenes and 1-decene (70–99% *ee*, Table 8.3, entries 6, 10, 16, 21, 30) with as low as 0.8 mol% catalyst loadings. Hammett correlation of the rate of epoxidation of *para*-substituted styrenes revealed electrophilic active species. Like for the Ti(salan)-based catalyst systems, the epoxidation enantioselectivity was independent of the *para*-substituents, implying a stepwise mechanism with separate rate-limiting and enantioselectivity determining steps. Thus, for Ti(salalen) catalyst systems, a mechanism analogous to that shown in Fig. 8.5, was proposed. A comparative catalytic and kinetic study of related salan and salalen complexes was undertaken; it was established that Ti(salalen) catalysts demonstrated higher activity and similar or slightly lower epoxidation enantioselectivity [65].

8.4 Catalyst Systems Based on Other Metals

Complexes of other metals were also examined as catalysts of asymmetric epoxidation with hydrogen peroxide. A few most recent examples will be overviewed below.

Katsuki and coworkers used chiral salan ligands as the chirality sources in niobium catalyzed asymmetric epoxidations of allylic alcohols [66]. The catalyst was prepared

in situ from Nb(O*i*-Pr)$_5$ (4 mol%) and salan ligand (5 mol%, **22a–c**, Fig. 8.6). Acceptable yields (40–82%) and high enantioselectivities (74–95% *ee*, Table 8.4, entries 1, 3) were documented in the epoxidation of *trans*-, *cis*-, trisubstituted, and geminally substituted allylic alcohols with aqueous hydrogen peroxide (1.5 equiv.). For the latter substrates, significant amount (10–20%) of overoxidation products (aldehydes) were observed. The catalyst system was found to be inactive toward epoxidation of unfunctionalized alkenes pointing that precoordination of allylic alcohol was essential for this epoxidation. It was suggested that monomeric peroxo heptacoordinated niobium species was the active intermediate.

Park with coworkers reported a heterogenized copper(II) complex immobilized on mesoporous silica containing chiral ligand **23** (Fig. 8.6) derived from *ortho*-phenylenediamine and (*L*)-proline [67]. The catalyst mediated the asymmetric epoxidation of α,β-unsaturated ketones with hydrogen peroxide under solvent-free conditions, showing good yields (88–92%) and enantioselectivities (82–83% *ee*, Table 8.4, entry 5) in the presence of triethylamine additive. The catalyst could be recycled several times without significant degradation.

Feng and coworkers developed a scandium(III)-based catalyst prepared *in situ* from Sc(OTf)$_3$ and chiral *N*,*N*′-dioxide ligand **24** (Fig. 8.6) [68]. The catalyst, used at 5 mol% loading, conducted the asymmetric epoxidation of α,β-unsaturated ketones with H_2O_2 (3 equiv.). The corresponding epoxides were obtained in high yields (70–99%) and extremely high *ee*'s (up to 99% in a few cases, Table 8.4, entry 6).

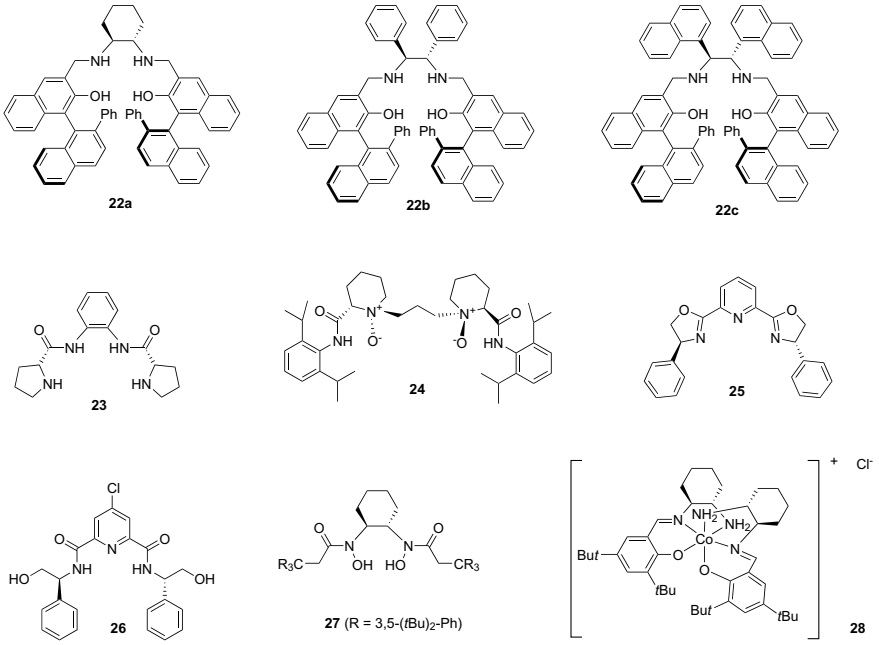

Fig. 8.6 Chiral ligands and metal complexes employed in asymmetric epoxidations

Table 8.4 Enantioselective epoxidations of olefins with H_2O_2 in the presence of various metals complexes

Entry	Substrate	Catalyst	Epoxide yield, %	ee, %	Ref.
1	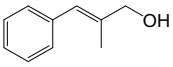	**Nb(O*i*Pr)$_5$ + 22b**	40	83	[66]
2		**WO_2(acac)$_2$ + 27**	87	84	[72]
3	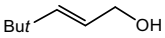	**Nb(O*i*Pr)$_5$ + 22c**	52	95	[66]
4		**WO_2(acac)$_2$ + 27**	88	98	[72]
5	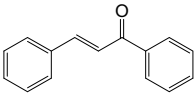	**Cu(23) on INC-2[a]**	88[b]	83	[67]
6		**Sc(OTf)$_3$ + 24**	99	98	[68]
7		**28**	85[b]	55	[73]
8	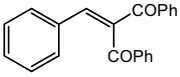	**Sc(OTf)$_3$ + 24**	74	98	[69]
9	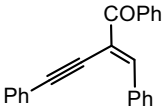	**Sc(OTf)$_3$ + 24**	95	99	[70]
10	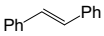	**MTO[c] + 26**	99	19	[71]

[a]The amino functionalized mesoporous silica. [b]Conversion. [c]Methyltrioxorhenium

The catalyst system was also explored in the asymmetric epoxidation of a series of 2-arylidene-1,3-diketones with hydrogen peroxide, affording chiral epoxides of good to excellent optical purity (82–99% *ee*, Table 8.4, entry 8) [69]. Very recently, Feng and coworkers expanded the substrate scope of this scandium(III)-based catalyst at the expense of 2-arylidene-1,3-diketones with electron-deficient groups [70]. The catalyst loadings of 0.5–2.0 mol% were sufficient to mediate the asymmetric epoxidation by hydrogen peroxide with high yields (90–97%) and enantioselectivities (95–99% *ee*, Table 8.4, entry 9).

Beller with coworkers reported the *in situ* generated complexes of methyltrioxorhenium (MTO) with ligands **25** and **26** (Fig. 8.6), that catalyzed the epoxidation of unfunctionalized alkenes with 53–99% conversion and modest enantioselectivity (not exceeding 19% *ee*, Table 8.4, entry 10) [71]. The loadings of the ligand were four times higher (12 mol%) than the amount of MTO (3 mol%). The system required twofold excess (vs. substrate) of hydrogen peroxide.

Wang and Yamamoto studied a tungsten-based catalyst in the asymmetric epoxidations of allylic and homoallylic alcohols with hydrogen peroxide [72]. The catalyst was prepared in situ by mixing WO_2(acac)$_2$ (2 mol%) with chiral bishydroxamic acid ligand **27** (2.4 mol%, Fig. 8.6). The corresponding chiral epoxides were obtained in high yields, demonstrating generally high asymmetric induction (80–98% *ee*, Table 8.4, entries 2, 4).

Belokon with coworkers examined [73] cobalt(III) catalyst **28** (Fig. 8.6) in the asymmetric epoxidation of chalcones with hydrogen peroxide under phase-transfer conditions. The oxidant was used in high excess relative to olefin (5 equiv.), the catalyst performing up to 10 TN. Moderate asymmetric induction was documented (35–55% *ee*, Table 8.4, entry 7).

8.5 Summary and Outlook

This chapter summarizes recent advances in the asymmetric olefin epoxidations with hydrogen peroxide, mediated by bioinspired transition metal complexes, excluding iron. The last 15 years have been the time of milestone discoveries in the field, bringing the new families of chiral aminopyridine manganese(II) and salan/salalen titanium(IV) catalysts. Systems of these two classes have complementary catalytic properties: manganese catalysts demonstrate excellent efficiencies and enantioselectivities (typically 1000 TN, up to 99% *ee*) in the epoxidation of electron-deficient olefins (e.g., various α,β-unsaturated carbonyl compounds), while titanium catalysts demonstrate perfect results with electron-rich olefins (typically 20–100 TN, up to 99% *ee*). Other transition metal complexes were also employed: scandium, niobium, and tungsten stand out among others. Scandium complexes were successfully used in the epoxidations of α,β-unsaturated ketones, while niobium and tungsten complexes were studied in reactions with allylic and homoallylic alcohols. Today, the available choice of catalysts is reaching enough to carry out the epoxidation with H_2O_2 of a wide range of olefinic substrates in a highly enantioselective fashion. Nonetheless, certain future developments are needed for the catalyst systems to meet practical (industrial) requirements. In particular, catalysts containing elaborate chiral ligands are awaiting improvements of catalytic activity and efficiency. The other shortcoming, specific for some of the systems, is low oxidant efficiency, resulting in overconsumption of hydrogen peroxide (in some cases up to 5–6 equiv. of H_2O_2 vs. substrate). Overall, further discoveries and improvements are anticipated in this booming area of biomimetic asymmetric epoxidations.

Acknowledgements This work was supported by the Russian Foundation for Basic Research project 17-03-00991.

References

1. McGarrigle EM, Gilheany DG (2005) Chromium− and Manganese−salen promoted epoxidation of alkenes. Chem Rev 105:1563–1602. https://doi.org/10.1021/cr0306945
2. Xia QH, Ge HQ, Ye CP, Liu ZM, Su KX (2005) Advances in homogeneous and heterogeneous catalytic asymmetric epoxidation. Chem Rev 105:1603–1662. https://doi.org/10.1021/cr0406458

3. Adam W, Zhang A (2005) Chiral-auxiliary-controlled diastereoselective epoxidations. Synlett 2005:1047–1072. https://doi.org/10.1055/s-2005-865214
4. Wong OA, Shi Y (2008) Organocatalytic oxidation. Asymmetric epoxidation of olefins catalyzed by chiral ketones and iminium salts. ChemRev 108:3958–3987. https://doi.org/10.1021/cr068367v
5. Weinstock LM, Mulvey DM, Tull RJ (1976) Synthesis of the β-adrenergic blocking agent timolol from optically active precursors. Org Chem 41:3121–3124. https://doi.org/10.1021/jo00881a011
6. Sundermeier U, Döbler C, Beller M (2004) Recent developments in the osmium-catalyzed dihydroxylation of olefins. In: Bäckvall JE (ed) Modern oxidation methods. Wiley, New York, p 1. https://doi.org/10.1002/3527603689.ch1
7. Bevinakatti H, Banerji AJ (1991) Practical chemoenzymic synthesis of both enantiomers of propranolol. J Org Chem 56:5372–5375. https://doi.org/10.1021/jo00018a032
8. Michaelson RC, Palermo RE, Sharpless KB (1977) Chiral hydroxamic acids as ligands in the vanadium catalyzed asymmetric epoxidation of allylic alcohols by *tert*-butyl hydroperoxide. J Am Chem Soc 99:1990–1992. https://doi.org/10.1021/ja00448a059
9. Yamada S, Mashiko T, Terashima S (1977) (Acetylacetonato)[(-)-N-alkylephedrinato]dioxomolybdenum, a new class of chiral chelate complexes which catalyze asymmetric epoxidation of allylic alcohol. J Am Chem Soc 99:1988–1990. https://doi.org/10.1021/ja00448a058
10. Katsuki T, Sharpless KB (1980) The first practical method for asymmetric epoxidation. J Am Chem Soc 102:5974–5976. https://doi.org/10.1021/ja00538a077
11. Zhang W, Loebach JL, Wilson SR, Jacobsen EN (1990) Enantioselective epoxidation of unfunctionalized olefins catalyzed by salen manganese complexes. J Am Chem Soc 112:2801–2803. https://doi.org/10.1021/ja00163a052
12. Irie R, Noda K, Ito Y, Matsumoto N, Katsuki T (1990) Catalytic asymmetric epoxidation of unfunctionalized olefins. Tetrahedron Lett 31:7345–7348. https://doi.org/10.1016/S0040-4039(00)88562-7
13. Que L Jr, Tolman WB (2008) Biologically inspired oxidation catalysis. Nature 455:333–340. https://doi.org/10.1038/nature07371
14. Meunier B (ed) (2000) Biomimetic oxidations catalyzed by transition metal complexes. Imperial College Press, London
15. De Faveri G, Ilyashenko G, Watkinson M (2011) Recent advances in catalytic asymmetric epoxidation using the environmentally benign oxidant hydrogen peroxide and its derivatives. Chem Soc Rev 40:1722–1760. https://doi.org/10.1039/c0cs00077a
16. Wang C, Yamamoto H (2015) Asymmetric epoxidation using hydrogen peroxide as oxidant. Chem Asian J 10:2056–2068. https://doi.org/10.1002/asia.201500293
17. Bryliakov KP (2017) Catalytic asymmetric oxygenations with the environmentally benign oxidants H_2O_2 and O_2. Chem Rev 117:11406–11459. https://doi.org/10.1021/acs.chemrev.7b00167
18. Wu M, Wang B, Wang S, Xia C, Sun W (2009) Asymmetric epoxidation of olefins with chiral bioinspired manganese complexes. Org Lett 11:3622–3625. https://doi.org/10.1021/ol901400m
19. Murphy A, Dubois G, Stack TDP (2003) Efficient epoxidation of electron-deficient olefins with a cationic manganese complex. J Am Chem Soc 125:5250–5251. https://doi.org/10.1021/ja029962r
20. Maity NC, Bera PK, Ghosh D, Abdi SHR, Kureshy RI, Khan NH, Bajaj HC, Suresh E (2014) Manganese complexes with non-porphyrin N4 ligands as recyclable catalyst for the asymmetric epoxidation of olefins. Catal Sci Technol 4:208–217. https://doi.org/10.1039/c3cy00528c
21. Miao C, Wang B, Wang Y, Xia C, Lee YM, Nam W, Sun W (2016) Proton-promoted and anion-enhanced epoxidation of olefins by hydrogen peroxide in the presence of nonheme manganese catalysts. J Am Chem Soc 138:936–943. https://doi.org/10.1021/jacs.5b11579
22. Miao C, Yan X, Xu D, Xia C, Sun W (2017) Bioinspired manganese complexes and graphene oxide synergistically catalyzed asymmetric epoxidation of olefins with aqueous hydrogen peroxide. Adv Synth Catal 359:476–484. https://doi.org/10.1002/adsc.201600848

23. Ottenbacher RV, Bryliakov KP, Talsi EP (2011) Non-heme manganese complexes catalyzed asymmetric epoxidation of olefins by peracetic acid and hydrogen peroxide. Adv Synth Catal 353:885–889. https://doi.org/10.1002/adsc.201100030
24. Garcia-Bosch I, Ribas X, Costas M (2009) A broad substrate-scope method for fast, efficient and selective hydrogen peroxide-epoxidation. Adv Synth Catal 351:348–352. https://doi.org/10.1002/adsc.200800650
25. Garcia-Bosch I, Gómez L, Polo A, Ribas X, Costas M (2012) Stereoselective epoxidation of alkenes with hydrogen peroxide using a bipyrrolidine-based family of manganese complexes. Adv Synth Catal 354:65–70. https://doi.org/10.1002/adsc.201100409
26. Wang B, Miao C, Wang S, Xia C, Sun W (2012) Manganese catalysts with C_1-symmetric N_4 ligand for enantioselective epoxidation of olefins. Chem Eur J 18:6750–6753. https://doi.org/10.1002/chem.201103802
27. Wang X, Miao C, Wang S, Xia C, Sun W (2013) Bioinspired manganese and iron complexes with tetradentate N ligands for the asymmetric epoxidation of olefins. ChemCatChem 5:2489–2494. https://doi.org/10.1002/cctc.201300102
28. Shen D, Miao C, Wang S, Xia C, Sun W (2014) A mononuclear manganese complex of a tetradentate nitrogen ligand—synthesis, characterizations, and application in the asymmetric epoxidation of olefins. Eur J Inorg Chem 2014:5777–5782. https://doi.org/10.1002/ejic.201402663
29. Lyakin OY, Ottenbacher RV, Bryliakov KP, Talsi EP (2012) Asymmetric epoxidations with H_2O_2 on Fe and Mn aminopyridine catalysts: probing the nature of active species by combined electron paramagnetic resonance and enantioselectivity study. ACS Catal 2:1196–1202. https://doi.org/10.1021/cs300205n
30. Cussó O, Garcia-Bosch I, Font D, Ribas X, Lloret-Fillol J, Costas M (2013) Highly stereoselective epoxidation with H_2O_2 catalyzed by electron-rich aminopyridine manganese catalysts. Org Lett 15:6158–6161. https://doi.org/10.1021/ol403018x
31. Ottenbacher RV, Samsonenko DG, Talsi EP, Bryliakov KP (2014) Highly enantioselective bioinspired epoxidation of electron—deficient olefins with H_2O_2 on aminopyridine Mn catalysts. ACS Catal 4:1599–1606. https://doi.org/10.1021/cs500333c
32. Ottenbacher RV, Talsi EP, Bryliakov KP (2018) Chiral manganese aminopyridine complexes: the versatile catalysts of chemo- and stereoselective oxidations with H_2O_2. Chem Rec 18:78–90. https://doi.org/10.1002/tcr.201700032
33. Shen D, Qiu B, Xu D, Miao C, Xia C, Sun W (2016) Enantioselective epoxidation of olefins with H_2O_2 catalyzed by bioinspired aminopyridine manganese complexes. Org Lett 18:372–375. https://doi.org/10.1021/acs.orglett.5b03309
34. Dai W, Li J, Li G, Yang H, Wang L, Gao S (2013) Asymmetric epoxidation of alkenes catalyzed by a porphyrin-inspired manganese complex. Org Lett 15:4138–4141. https://doi.org/10.1021/ol401812h
35. Dai W, Shang S, Chen B, Li G, Wang L, Ren L, Gao S (2014) Asymmetric epoxidation of olefins with hydrogen peroxide by an in situ-formed manganese complex. J Org Chem 79:6688–6694. https://doi.org/10.1021/jo501178k
36. Ottenbacher RV, Samsonenko DG, Talsi EP, Bryliakov KP (2016) Enantioselective epoxidations of olefins with various oxidants on bioinspired Mn complexes: evidence for different mechanisms and chiral additive amplification. ACS Catal 6:979–988. https://doi.org/10.1021/acscatal.5b02299
37. Chen X, Gao B, Su Y, Huang H (2017) Enantioselective epoxidation of electron-deficient alkenes catalyzed by manganese complexes with chiral N_4 ligands derived from rigid chiral diamines. Adv Synth Catal 359:2535–2541. https://doi.org/10.1002/adsc.201700541
38. Lyakin OY, Ottenbacher RV, Bryliakov KP, Talsi EP (2013) Active species of nonheme iron and manganese-catalyzed oxidations. Top Catal 56:939–949. https://doi.org/10.1007/s11244-013-0058-6
39. Ottenbacher RV, Talsi EP, Bryliakov KP (2016) Bioinspired Mn-aminopyridine catalyzed epoxidations of olefins with various oxidants: enantioselectivity and mechanism. Catal Today 278:30–39. https://doi.org/10.1016/j.cattod.2016.04.033

40. Du J, Miao C, Xia C, Lee YM, Nam W, Sun W (2018) Mechanistic insights into the enantioselective epoxidation of olefins by bioinspired manganese complexes: role of carboxylic acid and nature of active oxidant. ACS Catal 8:4528–4538. https://doi.org/10.1021/acscatal.8b00874
41. Maity NC, Abdi SHR, Kureshy RI, Khan NH, Suresh E, Dangi GP, Bajaj HC (2011) Chiral macrocyclic salen Mn(III) complexes catalyzed enantioselective epoxidation of non-functionalized alkenes using NaOCl and urea H_2O_2 as oxidants. J Catal 277:123–127. https://doi.org/10.1016/j.jcat.2010.10.002
42. Maity NC, Rao GVS, Prathap KJ, Abdi SHR, Kureshy RI, Khan NH, Bajaj HC (2013) Organic carbonates as solvents in macrocyclic Mn(III) salen catalyzed asymmetric epoxidation of non-functionalized olefins. J Mol Catal A Chem 366:380–389. https://doi.org/10.1016/j.molcata.2012.10.021
43. Maity NC, Bera PK, Saravanan S, Abdi SHR, Kureshy RI, Khan NH, Bajaj HC (2014) Diethyl tartrate linked chiral macrocyclic manganese(III)−salen complex for enantioselective epoxidation of olefins and oxidative kinetic resolution of racemic secondary alcohols. ChemPlusChem 79:1426–1433. https://doi.org/10.1002/cplu.201402131
44. Ballistreri FP, Gangemi CMA, Pappalardo A, Tomaselli GA, Toscano RM, Sfrazzetto GT (2016) (Salen)Mn(III) catalyzed asymmetric epoxidation reactions by hydrogen peroxide in water: a green protocol. Int J Mol Sci 17:1112. https://doi.org/10.3390/ijms17071112
45. Amiri N, Le Maux P, Srour H, Nasri H, Simonneaux G (2014) Nitration of Halterman porphyrin: a new route for fine tuning chiral iron and manganese porphyrins with application in epoxidation and hydroxylation reactions using hydrogen peroxide as oxidant. Tetrahedron 70:8836–8842. https://doi.org/10.1016/j.tet.2014.10.001
46. Matsumoto K, Sawada Y, Saito B, Sakai K, Katsuki T (2005) Construction of pseudo-heterochiral and homochiral Di-μ-oxotitanium (Schiff base) dimers and enantioselective epoxidation using aqueous hydrogen peroxide. Angew Chem Int Ed 44:4935–4939. https://doi.org/10.1002/anie.200501318
47. Matsumoto K, Kubo T, Katsuki T (2009) Highly enantioselective epoxidation of *cis*-alkenylsilanes. Chem Eur J 15:6573–6575. https://doi.org/10.1002/chem.200901048
48. Sawada Y, Matsumoto K, Katsuki T (2007) Titanium-catalyzed asymmetric epoxidation of non-activated olefins with hydrogen peroxide. Angew Chem Int Ed 46:4559–4561. https://doi.org/10.1002/anie.200700949
49. Berkessel A, Brandenburg M, Leitterstorf E, Frey J, Lex J, Schäfer M (2007) A practical and versatile access to dihydrosalen (salalen) ligands: highly enantioselective titanium in situ catalysts for asymmetric epoxidation with aqueous hydrogen peroxide. Adv Synth Catal 349:2385–2391. https://doi.org/10.1002/adsc.200700221
50. Berkessel A, Brandenburg M, Schäfer M (2008) Mass-spectrometric and kinetic studies on the mechanism and degradation pathways of titanium salalen catalysts for asymmetric epoxidation with aqueous hydrogen peroxide. Adv Synth Catal 350:1287–1294. https://doi.org/10.1002/adsc.200700601
51. Sawada Y, Matsumoto K, Kondo S, Watanabe H, Ozawa T, Suzuki K, Saito B, Katsuki T (2006) Titanium-salan-catalyzed asymmetric epoxidation with aqueous hydrogen peroxide as the oxidant. Angew Chem Int Ed 45:3478–3480. https://doi.org/10.1002/anie.200600636
52. Matsumoto K, Sawada Y, Katsuki T (2006) Catalytic enantioselective epoxidation of unfunctionalized olefins: utility of a $Ti(O\mathit{i}\text{-}Pr)_4$-salan-$H_2O_2$ system. Synlett 2006:3545–3547. https://doi.org/10.1055/s-2006-956496
53. Shimada Y, Kondo S, Ohara Y, Matsumoto K, Katsuki T (2007) Titanium-catalyzed asymmetric epoxidation of olefins with aqueous hydrogen peroxide: remarkable effect of phosphate buffer on epoxide yield. Synlett 2007:2445–2447. https://doi.org/10.1055/s-2007-985605
54. Kondo S, Saruhashi K, Seki K, Matsubara K, Miyaji K, Kubo T, Matsumoto K, Katsuki T (2008) A μ-Oxo-μ-η^2:η^2-peroxo titanium complex as a reservoir of active species in asymmetric epoxidation using hydrogen peroxide. Angew Chem Int Ed 47:10195–10198. https://doi.org/10.1002/anie.200804685
55. Matsumoto K, Feng C, Handa S, Oguma T, Katsuki T (2011) Asymmetric epoxidation of (*Z*)-enol esters catalyzed by titanium-(salalen) complex with aqueous hydrogen peroxide. Tetrahedron 67:6474–6478. https://doi.org/10.1016/j.tet.2011.06.022

56. Jat JL, De SR, Kumar G, Adebesin AM, Gandham SK, Falck JR (2015) Regio- and enantioselective catalytic monoepoxidation of conjugated dienes: synthesis of chiral allylic *cis*-epoxides. Org Lett 17:1058–1061. https://doi.org/10.1021/acs.orglett.5b00281
57. Matsumoto K, Oguma T, Katsuki T (2009) Highly enantioselective epoxidation of styrenes catalyzed by proline-derived C_1-symmetric titanium(salan) complexes. Angew Chem Int Ed 48:7432–7435. https://doi.org/10.1002/anie.200903567
58. Xiong D, Wu M, Wang S, Li F, Xia C, Sun W (2010) Synthesis of salan (salalen) ligands derived from binaphthol for titanium-catalyzed asymmetric epoxidation of olefins with aqueous H_2O_2. Tetrahedron Asymmetry 21:374−378. https://doi.org/10.1016/j.tetasy.2010.01.023
59. Xiong D, Hu X, Wang S, Miao CX, Xia C, Sun W (2011) Biaryl-bridged salalen ligands and their application in titanium-catalyzed asymmetric epoxidation of olefins with aqueous H_2O_2. Eur J Org Chem 2011:4289–4292. https://doi.org/10.1002/ejoc.201100512
60. Berkessel A, Günther T, Wang Q, Neudörfl JM (2013) Titanium salalen catalysts based on *cis*-1,2-diaminocyclohexane: enantioselective epoxidation of terminal non-conjugated olefins with H_2O_2. Angew Chem Int Ed 52:8467–8471. https://doi.org/10.1002/anie.201210198
61. Wang Q, Neudörfl JM, Berkessel A (2015) Titanium *cis*-1,2-diaminocyclohexane (*cis*-DACH) salalen catalysts for the asymmetric epoxidation of terminal non-conjugated olefins with hydrogen peroxide. Chem Eur J 21:247–254. https://doi.org/10.1002/chem.201404639
62. Lansing M, Engler H, Leuther TM, Neudörfl JM, Berkessel A (2016) Titanium *cis*-1,2-diaminocyclohexane (*cis*-DACH) salalen catalysts of outstanding activity and enantioselectivity for the asymmetric epoxidation of non-conjugated terminal olefins with H_2O_2. ChemCatChem 8:3706–3709. https://doi.org/10.1002/cctc.201601154
63. Talsi EP, Samsonenko DG, Bryliakov KP (2014) Titanium salan catalysts for the asymmetric epoxidation of alkenes: steric and electronic factors governing the activity and enantioselectivity. Chem Eur J 20:14329–14335. https://doi.org/10.1002/chem.201404157
64. Talsi EP, Bryliakova AA, Bryliakov KP (2016) Titanium salan/salalen complexes: the twofaced janus of asymmetric oxidation catalysis. Chem Rec 16:924–939. https://doi.org/10.1002/tcr.201500273
65. Talsi EP, Rybalova TV, Bryliakov KP (2016) Ti-salalen mediated asymmetric epoxidation of olefins with H_2O_2: effect of ligand on the catalytic performance, and insight into the oxidation mechanism. J Mol Catal A: Chem 421:131–137. https://doi.org/10.1016/j.molcata.2016.05.019
66. Egami H, Oguma T, Katsuki T (2010) Oxidation catalysis of Nb(salan) complexes: asymmetric epoxidation of allylic alcohols using aqueous hydrogen peroxide as an oxidant. J Am Chem Soc 132:5886–5895. https://doi.org/10.1021/ja100795k
67. Prasetyanto EA, Khan NH, Seo HU, Park SE (2010) Asymmetric epoxidation of α, β-unsaturated ketones over heterogenized chiral proline diamide complex catalyst in the solvent-free condition. Top Catal 53:1381–1386. https://doi.org/10.1007/s11244-010-9597-2
68. Chu Y, Liu X, Li W, Hu X, Lin L, Feng X (2012) Asymmetric catalytic epoxidation of α, β-unsaturated carbonyl compounds with hydrogen peroxide: additive-free and wide substrate scope. Chem Sci 3:1996–2000. https://doi.org/10.1039/c2sc20218b
69. Chu Y, Hao X, Lin L, Chen W, Li W, Tan F, Liu X, Feng X (2014) Chiral N, N′-dioxide−scandium (III)-catalyzed asymmetric epoxidation of 2-arylidene-1,3-diketones with hydrogen peroxide. Adv Synth Catal 356:2214–2218. https://doi.org/10.1002/adsc.201400341
70. Zhang H, Yao Q, Lin L, Xu C, Liu X, Feng X (2017) Catalytic asymmetric epoxidation of electron-deficient enynes promoted by chiral N, N′-dioxide-scandium(III) complex. Adv Synth Catal 359:3454–3459. https://doi.org/10.1002/adsc.201700555
71. Kiersch K, Li Y, Junge K, Szesni N, Fischer R, Kühn FE, Beller M (2012) Catalytic epoxidations with pyridinebis(oxazoline)−methyltrioxorhenium complexes and nitrogen-containing catalyst systems. Eur J Inorg Chem 2012:5972–5978. https://doi.org/10.1002/ejic.201200736

72. Wang C, Yamamoto H (2014) Tungsten-catalyzed asymmetric epoxidation of allylic and homoallylic alcohols with hydrogen peroxide. J Am Chem Soc 136:1222–1225. https://doi.org/10.1021/ja411379e
73. Larionov VA, Markelova EP, Smol'yakov AF, Savel'yeva TF, Maleev VI, Belokon YN (2015) Chiral octahedral complexes of Co(III) as catalysts for asymmetric epoxidation of chalcones under phase transfer conditions. RSC Adv 5:72764−72771. https://doi.org/10.1039/c5ra11760g

Chapter 9
Organometallic C–H Oxidation with O_2 Mediated by Soluble Group 10 Metal Complexes

Andrei N. Vedernikov

Abstract Selective catalytic C–H functionalization of organic compounds with O_2 as the terminal oxidant is an important and challenging practical goal justified from both economic and environmental perspective. Recent advances in organometallic palladium-catalyzed aerobic C–H functionalization chemistry are reviewed with an emphasis on the mechanism of the reaction basic steps. These steps include activation of alkenes, arenes, and alkanes at a palladium(II) center to form organopalladium intermediates with new Pd–C bonds, C–X bond-forming reactions at palladium(II) or palladium(IV) center, O_2 activation by palladium(II) hydrocarbyls, palladium(II) hydrides, and palladium(0) complexes. Some limitations of the current palladium-based systems and directions toward their possible future development are discussed. Considering organometallic aerobic C–H functionalization catalysis by other group 10 metals, a brief review is provided of a few existing platinum-based systems. Although no such catalytic systems based on nickel complexes have been reported yet, some relevant stoichiometric reactions at a nickel center have already been discovered which promises possible future development of organometallic aerobic C–H functionalization catalysis by this metal.

Keywords Selective aerobic C–H functionalization · Dioxygen activation · Mechanism · Organometallic catalysis · Palladium complexes · Platinum complexes · Nickel complexes

9.1 Introduction

Selective oxidative functionalization of hydrocarbons with O_2 as the terminal oxidant is an attractive goal. From an economic standpoint, atmospheric oxygen is one of the least expensive and abundant oxidizing agents. From an environmental perspective, the development of selective aerobic oxidation processes could minimize or even

A. N. Vedernikov (✉)
Department of Chemistry and Biochemistry, University of Maryland, College Park, MD 20742, USA
e-mail: avederni@umd.edu

K. P. Bryliakov (ed.), *Frontiers of Green Catalytic Selective Oxidations*,
Green Chemistry and Sustainable Technology,
https://doi.org/10.1007/978-981-32-9751-7_9

eliminate chemical waste. Organotransition metal catalysis is a viable approach to achieve these goals. In this Chapter, catalytic transformations of hydrocarbon C–H bonds will be considered that involve the use of O_2 as terminal oxidant and soluble organometallic group 10 metal complexes as catalysts or catalytic intermediates. As it will be shown in this Chapter, the involvement of organometallic species may allow for diverse transformations of their metal–carbon bonds [1] leading toward various value-added hydrocarbon functionalization products. Along with an overview of representative examples of major reaction types, a discussion of the mechanisms of the reactions will be provided.

Among the transition metals, and the group 10 metals, in particular, palladium has played a prominent role in the development of selective organic oxidation reactions with O_2 ("aerobic oxidation reactions"). A classic example of such processes is the oxidation of ethylene with O_2 to acetaldehyde in the presence of aqueous $[Pd^{II}Cl_4]^{2-}$ and $Cu^{II}Cl_2$ cocatalysts (the Wacker process) developed in the 1950s (Eq. 9.1) [2–4]:

$$2CH_2{=}CH_2 + O_2 \rightarrow 2CH_3CH{=}O \tag{9.1}$$

The Wacker process is an organometallic oxidation involving reactive alkylpalladium(II) species as key intermediates. The $[Pd^{II}Cl_4]^{2-}$complex is responsible for ethylene oxidation to acetaldehyde with palladium(0) as another reaction product, which is a known stoichiometric reaction. In turn, the role of the copper cocatalyst is twofold. In its oxidized form, $Cu^{II}Cl_2$, it can convert palladium(0) back to palladium(II) producing copper(I) species as another product. In its reduced form, $[Cu^{I}Cl_2]^{-}$, it activates O_2 with concomitant conversion of copper(I) species back to copper(II). Reaction (9.1) has been used on an industrial scale since the 1960s.

The use of soluble platinum complexes in aerobic oxidation of organic substrates has been known since the 1980s. An early example of such transformations utilizing O_2 as the oxidant is the Shilov reaction, conversion of methane to CH_3X products (X=OH, Cl) catalyzed by aqueous $[Pt^{II}Cl_4]^{2-}$ and a heteropolyacid redox cocatalyst (Eqs. 9.2, 9.3) [5]:

$$2CH_4 + O_2 \rightarrow 2CH_3OH \tag{9.2}$$

$$2CH_4 + O_2 + 2HCl \rightarrow 2CH_3Cl + 2H_2O \tag{9.3}$$

The original version of the reaction reported about 10 years earlier [6] utilized expensive H_2PtCl_6 as the oxidant. It was then discovered that H_2PtCl_6 could be used in a catalytic fashion with O_2 as the terminal oxidant when a heteropolyacid redox cocatalyst is employed [5]. The Shilov reaction, similar to Wacker process, is also an organometallic oxidation process which involves methylplatinum(II) intermediates resulting from methane activation by platinum(II), as well as their methylplatinum(IV) derivatives resulting from oxidation of the former [7, 8]. The Shilov reaction's main limitations are low catalyst turnover numbers (TON) resulting from gradual conversion of platinum(II) catalyst to inactive platinum(IV) and platinum(0)

species, as well as poor (≤50%) selectivity in CH_3X-type products due to "overoxidation" of methane leading to formaldehyde, formic acid, and CO_2. Aerobic C–H functionalization reactions mediated by soluble platinum complexes have gained, so far, no practical applications although they remain in the focus of academic research [9, 10].

Finally, organometallic functionalization reactions of organic substrates mediated by nickel complexes are under development [11, 12] and the use of O_2 as the terminal oxidant in such reaction has not yet been reported.

This quick introduction suggests that the most part of this chapter will be dedicated to organopalladium catalysis with much less attention paid to reactions of the other two group 10 metals.

9.2 Homogeneous Organometallic Palladium-Catalyzed Aerobic C–H Functionalization

Various types of organometallic palladium-catalyzed C–H oxidation (Eq. 9.4) and aerobic oxidative coupling of C–H (R–H) and X–H fragments (Eq. 9.5) leading to products with new C–X (R–X) bonds have been reported:

$$2R{-}H + O_2 \rightarrow 2ROH \tag{9.4}$$

$$2R{-}H + 2X{-}H + O_2 \rightarrow 2R{-}X + 2H_2O \tag{9.5}$$

In an ideal case of a 100% selective transformation, reactions of the first type would produce no chemical waste. In the second case, ideally, the only by-product would be water. An extensive recent review covering aerobic functionalization of olefinic substrates is available [13]. Some representative examples of reactions of both types, (Eq. 9.4) and (Eq. 9.5), are listed in Table 9.1 and structures of the specific ligands **1–11** used in these reactions are given in Fig. 9.1. A literature analysis shows that oxidative aerobic transformations of olefinic substrates and arenes are explored better than those of alkanes. While compiling representative organometallic palladium-catalyzed aerobic C–H functionalization reactions, preference was given to more challenging processes involving arene, olefin, or alkane C–H activation (all entries except 9–12). The assignment of the type of a C–H bond involved in oxidative functionalization is purely formal for some reactions involving olefins serving either as hydrocarbon substrates (entries 9–12) or as coupling partners (entries 20–26). In these specific examples, the relevant organopalladium intermediates result from the addition of palladium(II) species across an olefin C=C bond (olefin insertion into Pd^{II}-ligand bond) and not from the olefin C–H bond activation. As an alternative to the olefin insertion, activation of olefins at a Pd^{II} center may involve direct allylic C–H bond cleavage leading to allylpalladium(II) intermediates (entry 5).

Table 9.1 Some representative examples of C–H oxidation and oxidative aerobic coupling of C–H bonds of organic substrates and X–H bonds of their coupling partners mediated by Pd complexes. The structures of specific ligands **1–11** used in these reactions are given in Fig. 9.1

	C–H bond type/substrate	X–H bond type/coupling partner	Resulting bond/coupling product	Catalyst, loading in mol%	References
Arene hydroxylation					
1	$C(sp^2)$–H/benzoic acids 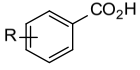		$C(sp^2)$–O/2-hydroxybenzoic acids 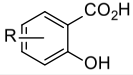	$Pd(OAc)_2$, 10	[14]
Arene and alkane acetoxylation and chlorination					
2	$C(sp^2)$–H/benzene	O–H/AcOH	$C(sp^2)$–O/phenylacetate	$Pd(OAc)_2$, 0.1/HNO_3 (conc.), 30	[15]
3	$C(sp^3)$–H/8-methylquinolines 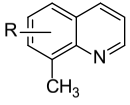	O–H/AcOH	$C(sp^3)$–O/8-(acetoxymethyl) quinolines 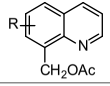	$Pd(OAc)_2$, 5/4-hydroxy-2,6-pyridinedicarboxylic acid **1**, 5	[16, 17]
4	$C(sp^3)$–H/2-alkylpyridines, oxime ethers 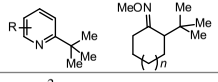	O–H/AcOH or HCl	$C(sp^3)$–O or $C(sp^3)$–Cl/acetates or chlorides 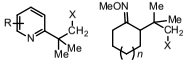	$Pd(OAc)_2$, 5/$NaNO_3$, 100	[18]
5	$C(sp^3)$–H (allylic)/ olefins 	O–H/AcOH	$C(sp^3)$–O/allylacetates 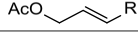	$Pd(OAc)_2$, 5/4,5-diazafluoren-9-one **2**, 5	[19]

(continued)

Table 9.1 (continued)

	C–H bond type/substrate	X–H bond type/coupling partner	Resulting bond/coupling product	Catalyst, loading in mol%	References
Arene and alkene amidation/amination					
6	C(sp^2)–H/2-(N-acetylamino)cinnamate esters 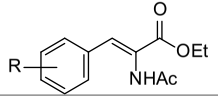	(Ac)N–H/(intramolecular)	C(sp^2)–N(Ac)/N-acetylindoles 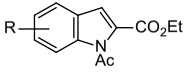	$Pd(OAc)_2$, 10/DMSO (solvent)	[20]
7	C(sp^2)–H/3,3-diarylacrylamides 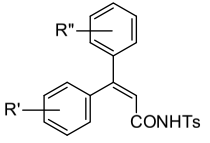	N–H/(intramolecular)	C(sp^2)–N/4-aryl-2-quinolinones 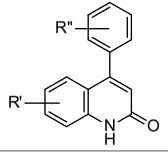	$PdCl_2$, 10/$Cu(OAc)_2$, 50	[21]
8	C(sp^2)–H/N-(biphenyl-2-yl)acetamides 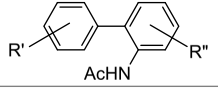	(Ac)N–H/(intramolecular)	C(sp^2)–N(Ac)/N-acetylcarbazoles 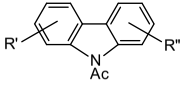	$Pd(OAc)_2$, 5/$Cu(OAc)_2$, 100	[22]
9	C–H/olefins 	(R)(R′)N–H/e.g., phthalimide	C(sp^2)–N(R)(R′)/N-vinylphthalimides 	$Pd(OAc)_2$, 10/PhCN (solvent)	[23, 24]
10	C–H/N-(hex-4-enyl)tosylamide 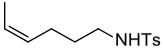	(Ts)N–H (intramolecular)	C(sp^3)–N(Ts)/racemic 2-vinylpyrrolidine 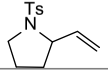	$Pd(OAc)_2$, 5/4,5-diazafluoren-9-one **2**, 5	[25]

(continued)

Table 9.1 (continued)

	C–H bond type/substrate	X–H bond type/coupling partner	Resulting bond/coupling product	Catalyst, loading in mol%	References
11	C–H/N-hex-4-enyltosylamide 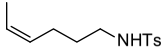	(Ts)N–H (intramolecular)	C(sp^3)–N(Ts)/(*R*)-2-vinylpyrrolidine 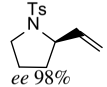 *ee* 98%	$Pd(O_2CCF_3)_2$, 5/(*R*)-pyrox **3**, 7.5	[26]
12	C–H/N-allylsulfonediamide 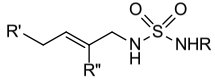	(SO_2)N–H (intramolecular)	C(sp^3)–N/N,N'-alkylidenesulfonediamide 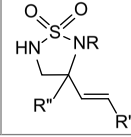	$Pd(O_2CCF_3)_2$, 5/DMSO, 10	[27]
(Hetero)arene imidoylation					
13	C(sp^2)–H/N-methoxy pyrrolohetarenecarboxamides 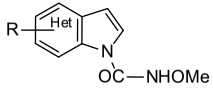	- /*t*-BuNC	C(sp^2)–C(sp^2)/hetarene-fused imidazopyrroles 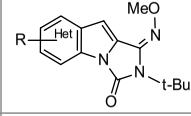	$Pd_2(dba)_3$, 5	[28]
14	C(sp^2)–H/N-methoxyhetarenecarboxamides 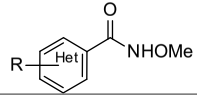	- /*t*-BuNC	C(sp^2)–C(sp^2)/pyrrolohetarenes 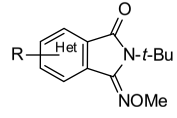	$Pd_2(dba)_3$, 2.5	[29]

(continued)

Table 9.1 (continued)

	C–H bond type/substrate	X–H bond type/coupling partner	Resulting bond/coupling product	Catalyst, loading in mol%	References
15	C(sp^2)–H/N-methoxy-hetarylbenzamides 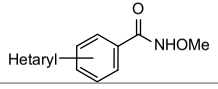	- /*t*-BuNC	C(sp^2)–C(sp^2)/hetarylisoindolines 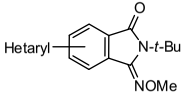	$Pd_2(dba)_3$, 5	[30]
Arene homocoupling					
16	C(sp^2)–H/*o*-xylene 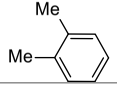	C(sp^2)–H/*o*-xylene	C(sp^2)–C(sp^2)/ 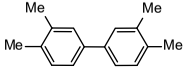	$Pd(OAc)_2$, 0.1/$Cu(OTf)_2$, 0.1/2-fluoropyridine **4**, 0.2	[31, 32]
Arene arylation					
17	C(sp^2)–H/N-acylanilines 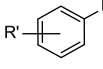	C(sp^2)–H/arenes 	C(sp^2)–C(sp^2)/N-acyl-2-aminobiphenyls 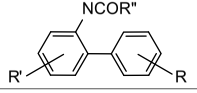	$Pd(OAc)_2$, 5–10/DMSO, 10–20/TFA, 500–1000	[33]
18	C(sp^2)–H/anilines 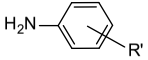	C(sp^2)–H/aryltriflates 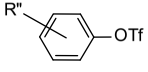	C(sp^2)–C(sp^2)/carbazoles 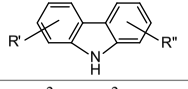	$Pd(OAc)_2$, 10/phosphine **5**, 15	[34]
19	C(sp^2)–H/arylacetic acids 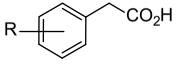	C(sp^2)–B/aryltrifluoroborates $[ArBF_3]^-$	C(sp^2)–C(sp^2)/(2-arylphenyl)acetic acids 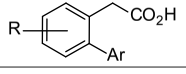	$Pd(OAc)_2$, 5/N-acetylisoleucine **6**, 10/benzoquinone, 5	[35]

(continued)

Table 9.1 (continued)

	C–H bond type/substrate	X–H bond type/coupling partner	Resulting bond/coupling product	Catalyst, loading in mol%	References
Arene and alkane alkenylation					
20	C(sp^2)–H/arylacetic acids 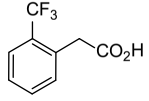 acids	C–H/*n*-hexylacrylate 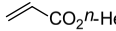	C(sp^2)–C(sp^2)/2-vinylarylacetates 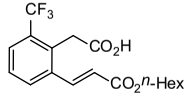	Pd(OAc)$_2$, 5/N-acetylisoleucine **6**, 10	[36]
21	C(sp^2)–H/N-sulfonylbenzamides 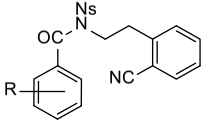	C–H/olefin 	C(sp^2)–C(sp^2)/N-sulfonyl-3-vinylbenzamides 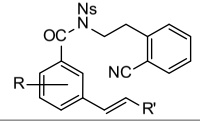	Pd(OAc)$_2$, 10/N-acetylglycine **7**, 60–100	[37]
22	C(sp^2)–H/N-protected pyrroles 	C–H/olefin 	C(sp^2)–C(sp^2)/2- or 3-vinylpyrroles 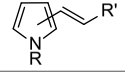	Pd(OAc)$_2$, 10/DMSO (solvent)	[38]
23	C(sp^2)–H/N-(perfluoro-*p*-tolyl)arylacetamides 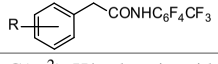	C–H/alkene	C(sp^2)–C(sp^2)/N-(perfluoro-*p*-tolyl)-2-vinylarylacetamides 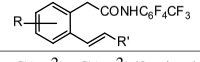	Pd(OAc)$_2$, 5/quinoline **8**, 10/Cu(OAc)$_2$, 20	[39]
24	C(sp^2)–H/arylacetic acids 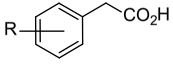	C–H/ethylacrylate 	C(sp^2)–C(sp^2)/2-vinylarylacetic acids 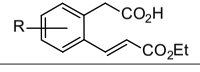	Pd(OAc)$_2$, 5/N-acetylisoleucine **6**, 10	[40]

(continued)

Table 9.1 (continued)

	C–H bond type/substrate	X–H bond type/coupling partner	Resulting bond/coupling product	Catalyst, loading in mol%	References
25	$C(sp^3)$–H/2-alkylpyridines 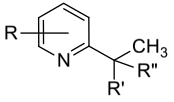	C–H/ 	$C(sp^3)$–$C(sp^2)$/2-homoallylpyridines 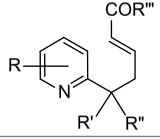	$Pd(MeCN)_4(BF_4)_2$, 10/NaOAc, 10/$H_4[PMo_{11}VO_{40}]$, 3	[41]
Alkylation					
26	$C(sp^2)$–H/3-alkenylindoles 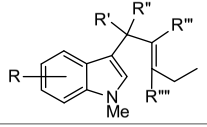	C–H/olefin (intramolecular)	$C(sp^2)$–$C(sp^3)$/cyclopenta[b]indoles 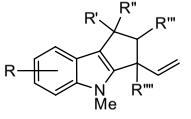	$Pd(OAc)_2$, 10/ethylnicotinate **9**, 40	[42]
Dehydrogenation					
27	$C(sp^3)$–H/cyclohexene	$C(sp^3)$–H (intramolecular)	$C(sp^2)$=$C(sp^2)$/benzene	$Pd(O_2CCF_3)_2$, 5	[43]
28	$C(sp^3)$–H/cyclohexanones 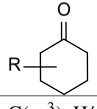	$C(sp^3)$–H (intramolecular)	$C(sp^2)$=$C(sp^2)$/phenols 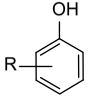	$Pd(O_2CCF_3)_2$, 5/2-dimethylaminopyridine **10**, 10/TsOH, 20	[44]
29	$C(sp^3)$–H/cyclohexenes 	$C(sp^3)$–H (intramolecular)	$C(sp^2)$=$C(sp^2)$/arenes 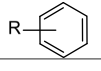	$Pd(O_2CCF_3)_2$, 5/anthraquinone **11**, 20	[45]

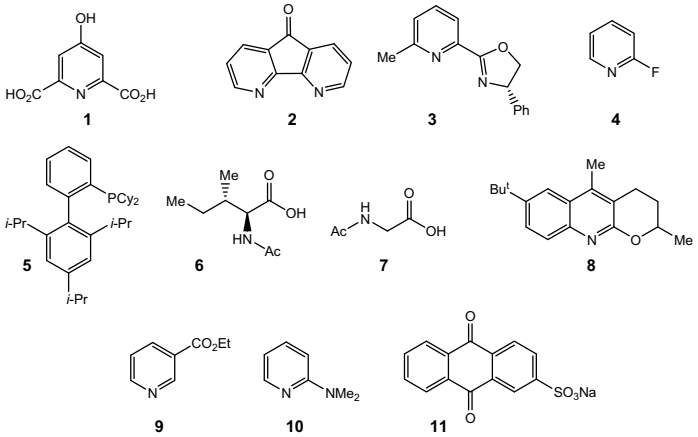

Fig. 9.1 Ligands **1–11** used in reactions in Table 9.1

The reactions in Table 9.1 are organized according to the type of the functional group introduced and new C–X bond formed, the type of the substrate C–H bonds involved, and the type of the X–H coupling partner, when applicable. Reactions leading to functionalization of substrate C(sp^2)–H bonds include hydroxylation (entry 1), acetoxylation (entry 2), amidation/amination (entries 6–9), imidoylation (entries 13–15), homocoupling (entry 16), arylation (entries 17–19), alkenylation (entries 20–24), and alkylation (entry 26). Transformations of substrate C(sp^3)–H bond include acetoxylation (entries 3–5), chlorination (entry 4), amidation/amination (entries 10–12), alkenylation (entry 25), and oxidative dehydrogenation of cyclohexane derivatives (entries 27–29). Besides X–H type coupling partners, boronic acid derivatives were also used in some cases (entry 19). Notably, the use of chiral supporting ligands may lead to a highly enantioselective product formation with the product enantiomeric excess up to 98% (entry 11).

The key to understanding and overcoming challenges associated with the development of aerobic C–H functionalization reactions and, in particular, most difficult aerobic functionalization of alkanes, lies in the understanding of their mechanisms. Notably, in the past two decades, the rapid development of Pd-catalyzed aerobic oxidative C–H functionalization has become possible thanks to close attention paid to mechanisms of palladium-mediated C–H bond activation [46] and O_2 activation reactions [47]. Accordingly, in the subsequent discussion, some key mechanistic details of these reactions will be considered.

9.2.1 General Mechanisms of Palladium-Mediated Aerobic C–H Functionalization

Three plausible catalytic cycles showing major steps of palladium-catalyzed aerobic C–H functionalization are given in Scheme 9.1. In the "non-redox" Pd^{II}—only catalytic cycle **A**, the metal oxidation state remains the same during three major steps, the substrate activation step *a*, the O_2 activation step *b*, and the product-releasing step *c* leading to the substrate functionalization product (hydrocarbyl-OH).

In mechanism **B**, a Pd^{II}/Pd^0 redox couple is involved. The +2 metal oxidation state is not changed at the substrate activation step *a*. The step *b* leading to substrate functionalization product (hydrocarbyl-X) involves elimination of C–X bond from a

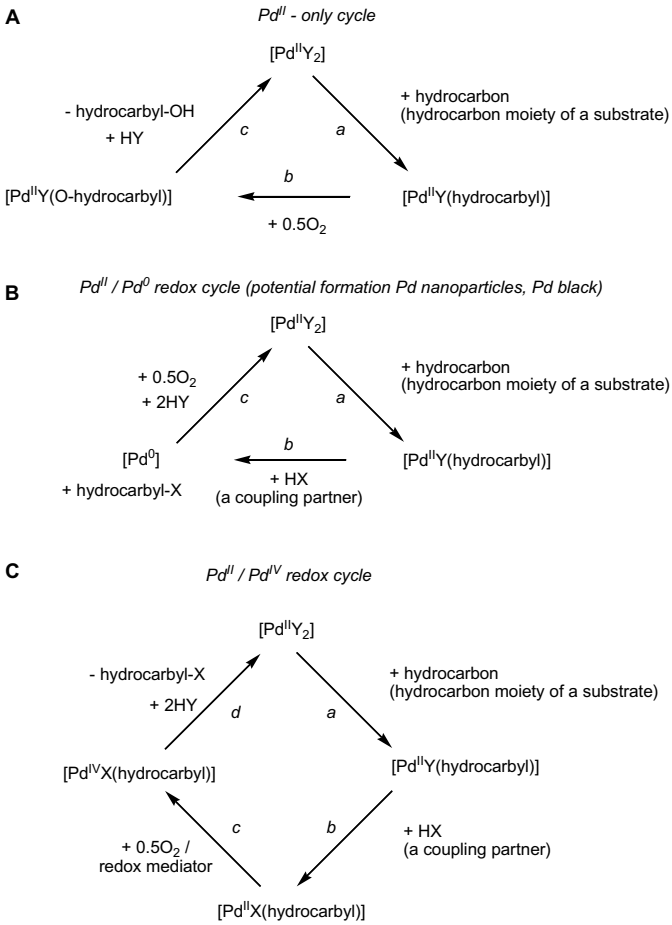

Scheme 9.1 Plausible simplified catalytic cycles for palladium-mediated aerobic C–H bond functionalization

palladium(II) center with concomitant reduction of Pd^{II} to Pd^{0}, and the O_2 activation step *c* leads to reoxidation of Pd^{0} to Pd^{II}.

Finally, the mechanism **C** is also palladium redox-based and involves Pd^{II}/Pd^{IV} redox couple. The Pd^{II} center does not change its oxidation state during the substrate activation step *a* and subsequent reaction with a coupling partner HX, step *b*. Two other steps, *c* and *d*, involve oxidation of Pd^{II} hydrocarbyls to their Pd^{IV} derivatives and C–X elimination of the product (hydrocarbyl-X) from the palladium(IV) center with concomitant reduction of Pd^{IV} to Pd^{II}, respectively.

9.2.1.1 Substrate Activation Step

All the basic mechanisms **A–C** in Scheme 9.1 imply that substrate activation leading to hydrocarbylpalladium(II) species (step *a*) occurs without change of the metal oxidation state +2.

Even in the cases where palladium(0) complexes are used as pre-catalysts (examples in entries 13–15 in Table 9.1), the authors argue that the actual catalytically active species are palladium(II) complexes. The latter result from oxidation of palladium(0) species with O_2 involving N–H acidic substrates, O-methyl hydroxamic acids, which serve as a source of anionic amido ligands for the resulting Pd^{II} center (see step *b*, mechanism **B**) [29], see, e.g. Eq. 9.6:

$$2\left[Pd^{0}\right] + O_2 + 4H{-}N(OMe)(COR) \rightarrow 2\left[Pd^{II}(N(OMe)COR)_2\right] + 2H_2O \quad (9.6)$$

Similar may be the role in Pd^{0} recycling of protected aminoacids **6** and **7** (Fig. 9.1) used as ligands in some aerobic C–H functionalization reactions (examples in entries 19–21, 24, Table 9.1).

Importantly, all the mechanisms of substrate activation by palladium(II) complexes discussed below require prior substrate coordination to the metal. Hence, the slow rates of ligand substitution in catalytically active metal species and strong coordination to palladium(II) center of a supporting ligand or substrate may decrease dramatically the overall catalyst turnover frequency. As a result, the judicious choice of supporting ligand for a catalyst may be very important, which is, in particular, a reason for the success of catalytic systems utilizing weakly coordinating 2-fluoropyridine **4** [31, 32] or bidentate 4,5-diazafluoren-9-one **2** [25] ligands (Fig. 9.1).

Holding these considerations in mind, it is very remarkable that the $Pd_2^0(dba)_3$-based catalytic system in examples in entries 13–15, Table 9.1 is very tolerant of heterocyclic donor groups present in substrates. These donor groups can strongly bind to palladium(II) center and severely inhibit catalysis of C–H functionalization by palladium(II) complexes. A possible explanation to this tolerance is that the palladium(II) center which is generated in reaction (9.6) above is coordinated to basic amido ligands and as such can be involved in substrate C–H bond activation/deprotonation (vide infra), experiencing minimal inhibiting effect of coordinating heterocyclic donor groups of the substrates [29].

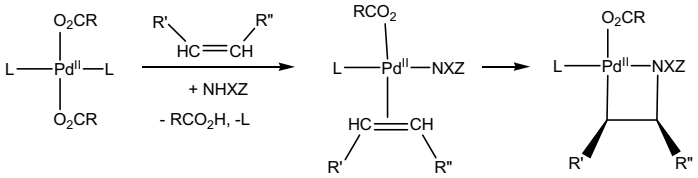

Scheme 9.2 Formation of alkylpalladium(II) intermediates as a result of *cis*-aminopalladation of olefinic substrates

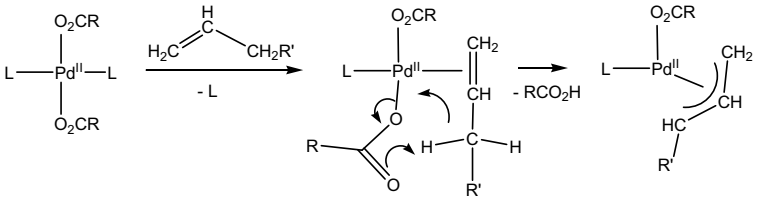

Scheme 9.3 Formation of allylpalladium(II) intermediates as a result of deprotonation of allylic C–H bonds of olefinic substrates involving coordinated carboxylate ligand

Olefin Insertion into Pd^{II}-Ligand Bond

Following substrate coordination to a palladium(II) center, its activation by the metal leading to hydrocarbylpalladium(II) species may proceed either as the substrate C–H bond cleavage or, for unsaturated substrates, as an addition (insertion) reaction. For olefinic substrates, even with available relatively acidic allylic C–H bonds, step *a* may not involve the substrate C–H activation, as it is the case in oxidative amination of olefins in the examples in entries 9–12, Table 9.1. Instead, based on available mechanistic tests, authors of these catalytic systems propose that formation of alkylpalladium(II) intermediates in step *a* occurs as *cis*-aminopalladation of the olefinic C=C bonds (Scheme 9.2), and not as allylic C–H bond cleavage [27].

Deprotonation of Pd^{II}–Coordinated C–H Bonds

Allylic C–H Deprotonation of Olefins

In turn, in the absence of strong nucleophilic ligands such as amides in examples given in entries 9–12, Table 9.1, olefinic substrates with available allylic C–H bonds can undergo allylic C–H deprotonation by the action of a metal-coordinated carboxylate (Scheme 9.3) [19] or a similar basic ligand [29], or even a free carboxylate serving as a base, as it was found computationally [48]. Some representative reactions involving activation of olefinic substrates via allylic C–H bond cleavage are given in entries 5, 27–29, Table 9.1.

Directed C–H Activation. Concerted Metallation–Deprotonation Mechanism

Considering non-olefinic substrates in Table 9.1, their quick inspection shows that many of them have metal-coordinating heteroatoms, e.g., carboxylate oxygens, examples in entries 1, 19–20, 24, a quinoline nitrogen, entry 3, an oxime or pyridine nitrogen in entries 4, 25, an anionic amide nitrogen resulting from N–H bond deprotonation in entries 6–8, 13–15, 17, 23, in a close proximity to C–H bonds involved in subsequent oxidative functionalization reaction. It was shown that functionalized hydrocarbon substrates containing suitable donor groups undergo C–H bond activation only after prior coordination of the donor group to the metal [49]. As a result, only those C–H bonds of the substrate that are accessible for the donor group-coordinated metal can be involved in subsequent transformations. Hence, the position of the donor groups relative to the substrate's various C–H bonds determines the regioselectivity of the C–H activation step *a*. Formation of five-membered palladacyclic intermediates is usually kinetically favored over six-membered metallacycles. Notably, metallacyclic intermediates with both smaller and larger rings can form. As a result, for arene derivatives with donor groups (DG) attached to one of the arene carbon atoms, such as CO_2^-, $CH_2CO_2^-$, $CONR_2$, NHCOR, CH_2NR_2, 2-pyridyl, 2-oxazolyl, 2-imidazolyl, N=NAr, CH_2SR, or CH_2OH selective metallation and subsequent functionalization is most facile for the arene C–H bonds that are positioned *ortho*- to the donor group [49, 50] (examples in entries 1, 6–8, 13–15, 17–20, 23–24, Table 9.1). Similar rules apply for alkane C–H bond functionalization when dealing with functionalized alkane substrates bearing directing groups [49, 51] (examples in entries 3, 4, 25, Table 9.1). Importantly, by changing the length and configuration of a tether between an arene carbon to which the tether is attached and the donor group, one can achieve a rare selective *meta*-C–H bond functionalization of the arene, as it is the case in an example in entry 21 in Table 9.1 [37].

The considerations above also imply that for substrates having several types of chemically nonequivalent C–H bonds, selective functionalization of some of them may be a daunting problem in palladium catalysis. At the same time, this is one of the points of growth and development of this area [37, 47], where joint experimental and computational modeling efforts are especially promising [52].

The mechanism of C–H activation most common for substrates with donor groups and substrates not having directing groups such as non-functionalized arenes or alkanes (entries 2, 16, Table 9.1) is the concerted metallation–deprotonation (Scheme 9.4) [46], which was also studied computationally [53, 54]. In either case, before the deprotonation step can occur, a substrate C–H bond has to be coordinated to the metal center. Such coordination can enhance dramatically the C–H bond acidity and facilitate subsequent C–H deprotonation. Expectedly, C–H bonds of nonactivated alkane fragments are the least acidic and, as such, are most difficult to activate and functionalize.

A substrate C–H bond coordination to the metal is greatly facilitated when the substrate has a donor group that can coordinate to the metal, thanks to the absence of the entropic penalty for the C–H bond coordination step (Scheme 9.4, top). Since hydrocarbon C–H bonds are very poor electron donors, the latter effect is of immense

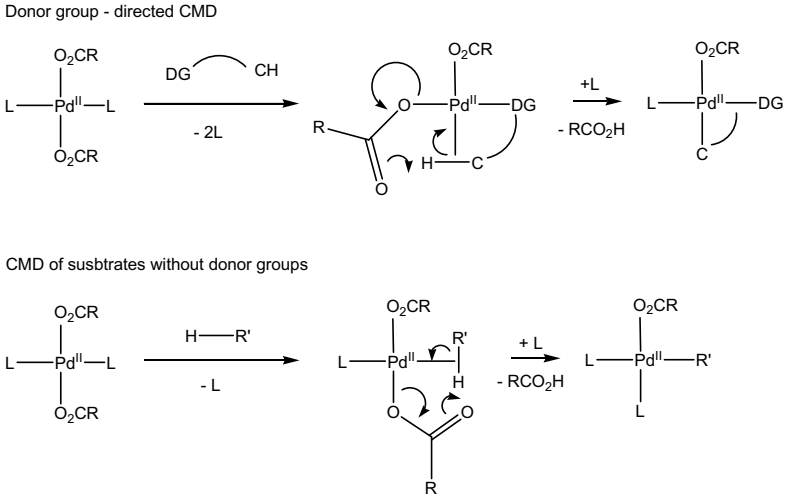

Scheme 9.4 Formation of palladium(II) hydrocarbyls as a result of a concerted metallation-deprotonation (CMD)

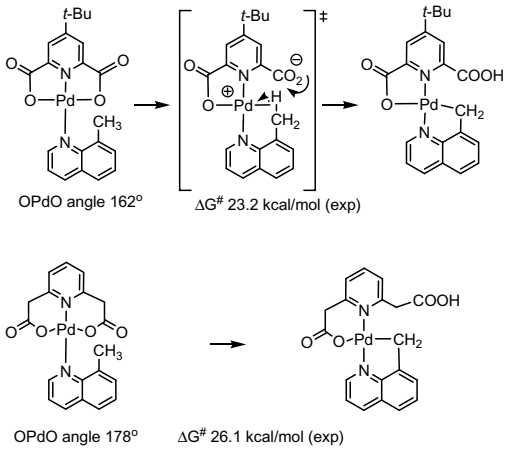

Scheme 9.5 C–H bond activation by palladium(II) pyridine-2,6-dicarboxylate complexes [16]

importance for metal-mediated C–H activation and functionalization. Interestingly, coordination of a substrate C–H bond to the metal center can be facilitated when a palladium(II) carboxylate is a strained chelate, such as palladium(II) pyridine-2,6-dicarboxylate (Scheme 9.5, top) [16, 17]. Dissociation of a carboxylate arm from the metal relives the chelate ring strain and is, therefore, facilitated, which accelerates coordination of the substrate C–H bond to be functionalized. Non-strained analogs with larger chelate size are less reactive (Scheme 9.5, bottom).

9.2.1.2 C–X Bond Formation Step

This step is the most critical for achieving a desirable type of C–H bond functionalization. Since the key reaction intermediates produced at the step *a* are organopalladium(II) species, knowledge of their reactivity [1] is very important when designing new catalytic reactions. This step can be viewed as functionalization of transient organopalladium species.

In any of the mechanisms **A–C** (Scheme 9.1), the C–X bond formation may result already at the step *a* when the substrate is an olefin involved in an insertion reaction (see, e.g., Scheme 9.2).

If step *a* involves a substrate C–H bond cleavage which results in a hydrocarbylpalladium(II) intermediate, then the C–X bond formation occurs typically at the step *b* (mechanisms **A**, **B**) or *d* (mechanism **C**).

O_2 Insertion into Pd^{II}–C Bond

According to mechanism **A** in Scheme 9.1, the Pd^{II}–C bond functionalization (step *b*) may be as "simple" as O_2 insertion into Pd^{II}–C bond which does not involve the metal redox change, (see an example in entry 1 in Table 9.1 as well as a discussion in the next section, "O_2 activation step"). The expected O_2 insertion product is a hydrocarbylperoxo complex. A few such well-defined stoichiometric reactions are known. They involve methylpalladium(II) complexes [55–59]. One of the first reported O_2 insertion reactions (Scheme 9.6, top) involves a dimethylpalladium(II) species and is a radical chain process [55], similar to a reported later analogous O_2 insertion involving a neutral monomethylpalladium(II) compound [56]. Another reaction in Scheme 9.6 is photochemical and involves cationic monomethylpalladium(II) species (Scheme 9.6, bottom) [57–59]. All of these reactions occur in aprotic media and the resulting methylperoxo palladium(II) species are formed in high yields.

Protonolysis of the products of O_2 insertion into Pd^{II}–CH_3 bond in Scheme 9.6 can lead to free methylhydroperoxide, an unstable and explosive chemical. Hence, the practical value of such products may be low. In this regard, an in situ conversion of hydrocarbylperoxo metal species into palladium(II) alkoxo complexes or free alcohols would be more desirable. In fact, both MeO_2H and MeOH form in a photocatalytic reaction of O_2 with a water-soluble anionic methyl palladium complex $[(dpms)Pd^{II}Me(OH)]^-$, besides ethane which is a major reaction product (Scheme 9.7, top) [60]. Importantly, the formation of MeO_2H can be fully suppressed by a slight modification of the reaction conditions with a concomitant increase of the MeOH yield up to 50% with the rest of the balance being ethane. It was shown that various hydroperoxides RO_2H (R=H, Me, *t*-Bu) react cleanly and rapidly with the methylpalladium(II) reagent, $[(dpms)Pd^{II}Me(OH)]^-$, to form the corresponding ROH in high yields. A proposed reaction sequence shown in Scheme 9.7 (center and bottom) involves formation of a hypothesized highly electrophilic methylpalladium(IV) species responsible for the production of various Me–X products detected in the

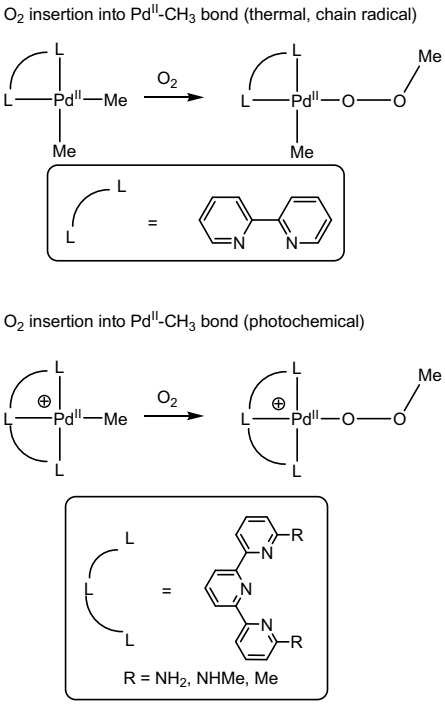

Scheme 9.6 Some reported examples of direct thermal [55] or photochemical [57–59] O_2 insertion into Pd^{II}–CH_3 bond of methylpalladium(II) species

mixtures with various nucleophiles and resulting from their attack at the CH_3–Pd^{IV} fragment of the proposed methylpalladium(IV) transient.

Reductive Elimination of C–X Bond from a Pd^{II} or a Pd^{IV} Center

According to mechanisms **B** and **C** (Scheme 9.1), C–X bond formation occurs as a result of reductive elimination from Pd^{II}(X) hydrocarbyls (mechanism **B**, step *b*) or Pd^{IV}(X) hydrocarbyls (mechanism **C**, step *d*) species. The ligands X necessary for such reductive coupling are introduced into palladium(II) coordination sphere prior to the C–X bond elimination (mechanism **B**) and, typically, but not always, prior to the Pd^{II} to Pd^{IV} oxidation step *c* (mechanism **C**) as a result of a ligand exchange, olefin insertion into palladium(II)-ligand bond (examples in entries 20–26) or, rarely, C–H bond activation at the electrophilic Pd^{IV} center [61].

Mechanism **C** involving a Pd^{II}/Pd^{IV} redox couple is rare in aerobic C–H functionalization chemistry. In particular, the authors of the catalytic system in entry 2 [15], Table 9.1, proposed involvement of a Pd^{II}/Pd^{IV} redox couple with a C(sp^2)–O reductive elimination from a Pd^{IV} hydrocarbyl resulting from the oxidation of its Pd^{II} precursor with HNO_3. Similarly, possible involvement of the Pd^{II}/Pd^{IV} redox couple was discussed for reactions in entries 3 [16] and 4 [18] leading to C(sp^3)–X (X=O, Cl) reductive elimination from Pd^{IV} species which, in fact, occurs as an S_N2 process. In the latter system, the oxidant responsible for the generation of Pd^{IV} hydrocarbyls

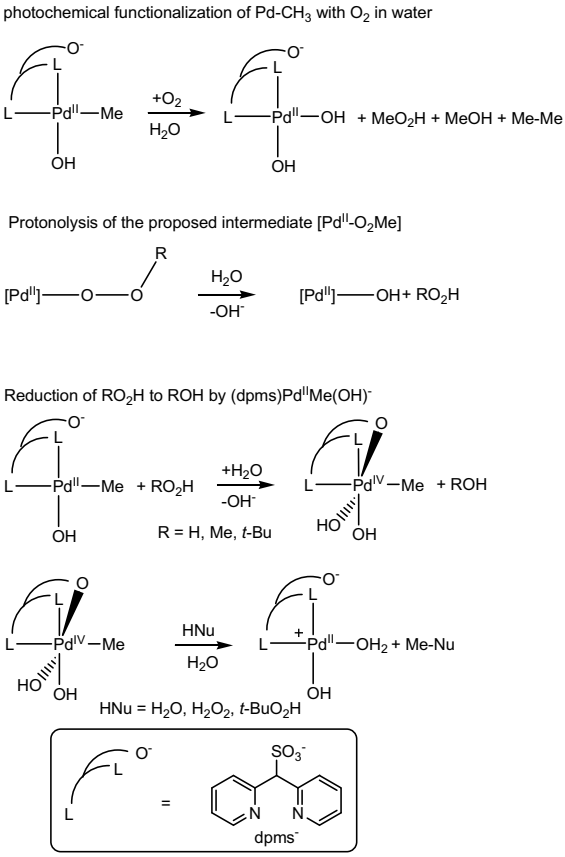

Scheme 9.7 Photochemical dioxygen activation by a water-soluble methylpalladium(II) complex and conversion of RO_2H to ROH [60]

is HNO_3, similar to the reaction in entry 2. In turn, for the catalytic system in entry 3, the Pd^{IV} hydrocarbyls were speculated to be produced aerobically from their Pd^{II} precursors [16]. It was shown computationally that the formation of Pd^{IV} transients is thermodynamically viable thanks to the ability of the tripod ligand **1** (Fig. 9.1) to adapt a facial coordination mode. At the same time, a mechanism involving an O_2 insertion into Pd^{II}–C bond also could not be excluded [17]. Notably, there are precedents of reactions between O_2 and dimethylpalladium(II) complexes supported by facially chelating ligands that lead to palladium(IV) derivatives [62, 63].

The involvement of Pd^{II}/Pd^0 redox catalysis (mechanism **B**) is most commonly proposed in various aerobic C–H functionalization reactions. The relevant examples in Table 9.1 are the reactions leading to $C(sp^3)$–O bond formation, such as in the catalytic system in entry 5, $C(sp^2)$–N bond formation, such as in arene and alkene amination reactions in entries 6–12, and C–C bond formation, such as in the arene imidoylation reactions (entries 13–15), arene homocoupling (entry 16), arene arylation (entries 17–19), arene and alkane alkenylation (entries 20–25) and alkylation (entry 26).

Finally, a special case of the product forming step associated with the mechanism **B** which does not require the presence of an actual coupling partner is dehydrogenation of various cyclohexane derivatives in reactions in entries 27–29. In this case, the new C=C bonds result from β-hydrogen atom elimination of palladium(II) hydrocarbyl intermediates.

O_2 Activation Step

Another step which is critical for any catalytic aerobic C–H functionalization process is O_2 activation. Direct O_2 insertion into Pd^{II}–C bond is one of the possibilities which has been already characterized in section "O_2 Insertion into Pd^{II}–C Bond".

O_2 Activation by Redox Cocatalysts

O_2 activation carried out by a redox cocatalyst is very common in aerobic Pd-catalyzed C–H functionalization, especially in its older versions. Some redox cocatalysts that were proven efficient are copper(II) complexes, heteropolyacids, and lower nitrogen oxides NO_x ($x = 1, 1.5, 2$). These cocatalysts in their reduced form, e.g., copper(I) or NO, react rapidly with O_2 to form species capable of oxidizing palladium center from lower to higher oxidation states, Pd^0 to Pd^{II} (mechanism **B**, Scheme 9.1) or, in some cases, converting Pd^{II} hydrocarbyls to Pd^{IV} hydrocarbyls (mechanism **C**). Some of the catalytic systems in Table 9.1 utilize these cocatalysts, CuX_2 (entries 7, 8, 23), NO_x (entries 2, 4), and a heteropolyacid $H_4[PMo_{11}VO_{40}]$ (entry 25). While copper(II) cocatalysts are traditionally assumed to support recycling of Pd^0 to Pd^{II} species (mechanism **B**), the systems utilizing NO_x as redox mediators (entries 2, 4) are proposed to support reactions involving a Pd^{II}/Pd^{IV} redox couple (mechanism **C**, Scheme 9.1).

The presence of a redox-active cocatalyst in a catalytic system, such as those mentioned above, does not exclude the option that O_2 activation will actually be carried out by palladium species. In particular, the authors of the reaction in entry 16 have observed only negligible effect of $Cu(OTf)_2$ additive on Pd^0 reoxidation. They have concluded that the major role of $Cu(OTf)_2$ cocatalyst in the palladium-catalyzed oxidative homocoupling of *o*-xylene is not O_2 activation but rather that of a Lewis acid enhancing reactivity of $Pd(OAc)_2$ [31].

O_2 Activation by Pd^0 Species

The catalytic systems where O_2 activation is carried out by Pd^0 species are becoming increasingly important practically and are interesting mechanistically. These reactions convert Pd^0 complexes to Pd^{II} peroxo species (Eq. 9.7), e.g., $Pd(PPh_3)_4$ is oxidized to $Pd(\kappa^2\text{-}O_2)(PPh_3)_2$ [64]. Notably, triphenylphosphine liberated in the latter reaction can reduce palladium peroxide and form corresponding phosphine oxide. This fact suggests that the practical value of phosphine ligands in aerobic palladium catalysis may be limited.

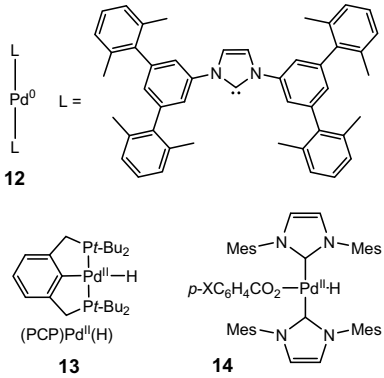

Fig. 9.2 Some palladium complexes characterized in O_2 activation

O_2 activation by Pd^0 species can be most efficient when suitable ligands are present. For instance, a PdL_2 complex **12** with very bulky N-heterocyclic carbene (NHC) ligands L=N,N'-bis(2,2",6,6"-tetramethyl-*m*-terphen-5'-yl)imidazole-2-ylidene) (Fig. 9.2) reacts with O_2 at room temperature even in a solid state [65].

$$L_nPd^0 + O_2 \rightarrow \text{cis-}L_2Pd^{II}(O_2) + (n-2)L \tag{9.7}$$

The resulting palladium(II) peroxo complexes are relatively basic and can react stepwise with acids to form first palladium(II) hydroperoxo complexes (Eq. 9.8) and, eventually, H_2O_2 (Eq. 9.9):

$$\text{cis-}L_2Pd^{II}(O_2) + HX \rightarrow Pd^{II}X(OOH)L_2 \tag{9.8}$$

$$Pd^{II}X(OOH)L_2 + HX \rightarrow Pd^{II}X_2L_2 + H_2O_2 \tag{9.9}$$

In turn, H_2O_2 released in the last reaction may act as an oxidant with respect to Pd^0 and/or reactive hydrocarbyl Pd^{II} species (e.g., Scheme 9.7, bottom) [60] or decompose into O_2 and H_2O.

In the absence of suitable ligands, the rate of the oxidation reaction in Eq. 9.7 may be too slow and/or the stability of Pd^0 complexes may be too low, so that a catalyst deactivation leading to the formation of catalytically inactive Pd black may become highly competitive with the reaction (9.7). Such catalyst deactivation is the major reason why many palladium-based catalytic systems involving Pd^{II}/Pd^0 couple (mechanism **B**, Scheme 9.1) require high catalyst loading, 10–20% and even higher (see Table 9.1 for examples). Notably, at some intermediate stages leading to the formation of palladium black, palladium(I) species [25, 66] and, ultimately, soluble palladium clusters/nanoparticles may be produced which often are also catalytically active in aerobic oxidation reactions [67, 68].

Interestingly, until recently, the utilization of organic ligands in aerobic functionalization catalysis by palladium compounds was not practiced, although some polar solvents such as DMSO that can coordinate to palladium(II) center were used successfully in a number of aerobic palladium-catalyzed C–H functionalization reactions (examples in entries 6, 22, Table 9.1). This situation is, in part, a reflection of a formerly poor understanding of the underlying aerobic chemistry of Pd^0 species [47]. One of the important reasons for this lag is related to the fact that rates of aerobic C–H functionalization by soluble palladium complexes are often zero order in $[O_2]$, and their turnover-limiting step is the substrate C–H activation, so making the characterization of the O_2 activation step difficult in such systems.

O_2 Activation by Pd^{II} Hydrides Versus Pd^0 Species

Catalytically competent palladium(0) species are expected to result from C–X reductive elimination of Pd^{II}(hydrocarbyl)X complexes in mechanism **B**, Scheme 9.1. Alternatively, palladium(0) species may be produced as a result of H–Y elimination of palladium(II) hydrides (Eq. 9.10) which, in turn, are formed as a result of β-hydrogen atom elimination of suitable palladium(II) alkyl, alkoxo, or similar species.

$$L_nPd^{II}(H)Y \rightarrow L_nPd^0 + HY \tag{9.10}$$

Importantly, palladium(II) hydrides are also able to react with O_2. The reaction proceeds via O_2 hydrogen atom abstraction/radical recombination pathway leading to O_2 insertion into Pd–H bond and formation of palladium(II) hydroperoxides [69] (Eq. 9.11), so allowing to return Pd^{II} back to the catalytic cycle.

$$L_nPd^{II}(H)Y + O_2 \rightarrow L_nPd^{II}(OOH)Y \tag{9.11}$$

The reaction between O_2 and a (PCP)Pd^{II}(H) complex **13** (Fig. 9.2) was characterized kinetically to reveal a first-order dependence of its rate on pO_2 and a large deuterium kinetic isotope effect, $k_{PdH}/k_{PdD} = 5.8$, all consistent with an H-atom abstraction mechanism. The mechanism was also analyzed computationally [70].

More extensive studies of reactions between various palladium(II) hydride complexes and O_2 (Eq. 9.11) have led to a conclusion that an alternative reaction sequence (9.10)–(9.7)–(9.8), that is HY reductive elimination—oxidation, leading to palladium(II) hydroperoxo complexes can be faster than the direct route (9.11) [71], although, in general, both pathways may be very competitive kinetically [72, 73]. In some cases, just a minor variation in the electronic properties of the anionic ligand Y, e.g., a *p*-substituted benzoate in *bis*-NHC palladium(II) hydride complexes *trans*-$L_2Pd^{II}(H)(O_2CC_6H_4$-*p*-X) **14** (Fig. 9.2), can lead to a change in the reaction mechanism from the direct O_2 insertion (Eq. 9.11), with a large deuterium kinetic isotope effect, $k_{PdH}/k_{PdD} = 3.1$ for X = OMe [73], to a stepwise transformation (9.10)–(9.7)–(9.8), with a very small $k_{PdH}/k_{PdD} = 1.3$ for X = H [71]. Interestingly, benzoquinone additives which are often present as a cocatalyst in palladium-

catalyzed aerobic C–H functionalization reactions (see, e.g., an example in entry 19 in Table 9.1) were found to accelerate the reaction sequence (9.10)–(9.7)–(9.8) [74].

Notably, the HY reductive elimination—oxidation reaction sequence (9.10)–(9.7)–(9.8) and, in particular, its first step (9.10), is strongly favored in palladium(II) complexes bearing labile monodentate L-type ligands since three-coordinate $LPd^{II}(H)Y$ species resulting from a ligand L dissociation eliminate H–Y at faster rates (Eq. 9.10, $n = 1$ vs. $n = 2$). The use of bidentate ligands appears to also favor the HY reductive elimination—oxidation reaction sequence, as compared to the direct pathway (Eq. 9.11), when one of the ligand's donor atoms is basic enough to deprotonate the Pd^{II}–H bond. That is usually the case for N-donor ligands. The deprotonation can occur upon this donor atom dissociation from the metal. As a result, the authors of [47] conclude that the O_2 activation in most aerobic catalytic systems used till date is carried out, most typically, by Pd^0 species and not by palladium(II) hydrides.

9.3 Homogeneous Organometallic Platinum—Catalyzed Aerobic CH Oxidation

As it was mentioned in the introduction, the first-ever developed platinum-based catalytic system for aerobic C–H functionalization allowed to carry out an overall very challenging transformation, the conversion of gaseous methane to CH_3X products (Eqs. 9.2, 9.3), albeit with low $[PtCl_4]^{2-}$ catalyst turnover ($\leq$6) and poor selectivity in CH_3X products ($\leq$50%) [5]. The reaction mechanism [7, 8] is similar to mechanism C shown in Scheme 9.1 for aerobic palladium catalysis. Notably, the heteropolyacid used in these experiments as a redox mediator was also shown by the authors to oxidize methanol, so contributing to the overall low reaction selectivity in CH_3X products. Subsequent attempts to develop more efficient variants of the reaction were made. In 2001, some modifications to the aerobic system were undertaken by introducing aqueous $CuCl_2$ as a redox mediator instead of a heteropolyacid and using water-soluble alkanesulfonic acids as substrates which are much easier to handle than gaseous methane. Water was used as the reaction medium [75]. These changes allowed to achieve the catalyst turnover numbers up to 43–52 after 4 h of reaction at 160 °C for ethanesulfonic acid as a substrate (Eq. 9.12):

$$2C_2H_5SO_3Na + O_2 \rightarrow 2HOCH_2CH_2SO_3Na \tag{9.12}$$

The reaction was ~50–76% selective with respect to the methyl group oxidation product, 2-hydroxyethanesulfonic acid shown in Eq. 9.12, with the rest of the balance being mostly the corresponding aldehyde and carboxylic acid.

A more recent reinvestigation of the Shilov reaction was undertaken in 2010 [9]. The authors used microfluidics technique and screened a number of redox mediators for the reaction of CH_4 with O_2 in water at 180 °C. They observed up to 49 catalyst

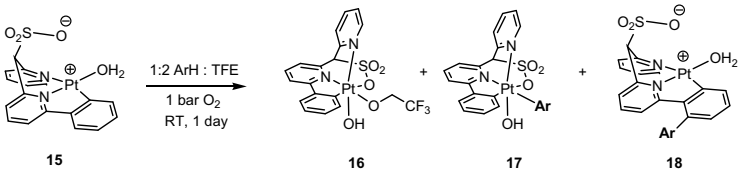

ArH		Me, Me	Me, Me, Me	F, F	F, F
Conversion, 1 day	68%	73%	69%	23%	16%
16 : 17 : 18	1 / 1 / 0.1	1 / 1 / 0.1	1 / 1 / 0.1	1 / 0.5 / -	1 / 0.5 / -

Scheme 9.8 Aerobic stoichiometric C–H functionalization of arenes mediated by platinum(II) complex **15** [10]

turnovers after 6 h with the selectivity in CH_3OH ~50% using either $Fe_2(SO_4)_3$ or a heteropolyacid as a redox mediator. Formic acid accounted for the rest of the balance.

Although the catalyst turnover numbers in both cases are much better than in the original Shilov publication [5] and, in fact, in many palladium-based systems listed in Table 9.1, the resulting oxidation products, 2-hydroxyethanesulfonic acid and methanol, may, most likely, be readily available at a lower cost using traditional methods of their preparation. Further reaction developments are in order.

Notably, learning from recent progress in aerobic catalytic C–H functionalization by palladium complexes, a possible direction for future research in catalytic platinum chemistry may target a better understanding of the underlying C–H activation, aerobic oxidation, and C–X reductive elimination chemistry of platinum species involved and rational design of ligands for these transformations [76]. As an example of such efforts, platinum(II) complex **15** supported by a newly designed sulfonated pincer ligand in Scheme 9.8 supports facile aerobic stoichiometric C–H functionalization of a series of arenes leading to derived arylplatinum(IV) complexes **17** [10]. The reaction is more efficient for electron-rich arenes. The minor products of the arenes functionalization are oxidatively C–C coupled complexes **18**. The fraction of the undesirable product **16** forming along with **18** can be significantly reduced in the presence of *p*-hydroquinone.

9.4 Development of Homogeneous Organometallic Nickel-Catalyzed Aerobic CH Oxidation

Nickel-based catalytic systems for organometallic aerobic C–H functionalization are still at an early stage of development. In fact, no such systems have been reported so far. At the same time, some basic step of a plausible catalytic cycle incorpo-

rating nickel complexes can be envisioned. A recent publication [77] discloses a possible approach toward donor group/auxiliary **19**-directed C(sp^3)–H activation at a nickel(II) center to produce metallacyclic nickel(II) alkyls **20** (Scheme 9.9). The behavior of the reported system resembles that of similar palladium(II) systems, although at somewhat higher temperatures for the nickel-based one. The kinetics of the reaction in Scheme 9.9 has been characterized in detail, including a large deuterium kinetic isotope effect, $k_H/k_D \sim 7$, and the reaction was proposed to operate a concerted metallation—deprotonation mechanism also common in palladium chemistry.

Notably, although not shown to involve organonickel intermediates, hydrogen atom transfer (HAT) chemistry involving C–H bonds of a series of alkylarenes such as 9,10-dihydroanthracene, toluene, and ethylbenzene has also been demonstrated in their reactions with a few isolated nickel(III) complexes [78].

In turn, stoichiometric aerobic Ni–C bond functionalization reactions have been known for a long time. Examples of aerobic oxidative C(sp^2)–O [79] and C(sp^3)–N [80] coupling reactions are given in Scheme 9.9, bottom.

Finally, there is a substantial body of recent work detailing the intimate chemistry of dioxygen activation at a nickel(I) center supported by various chelating ligands which can lead to nickel(II) superoxo or peroxo complexes and even nickel(III) peroxo species [81].

Overall, the fact that the key steps of a potential catalytic cycle of aerobic C–H functionalization by nickel are established, may be viewed as a promise of possible future development of the related catalytic chemistry.

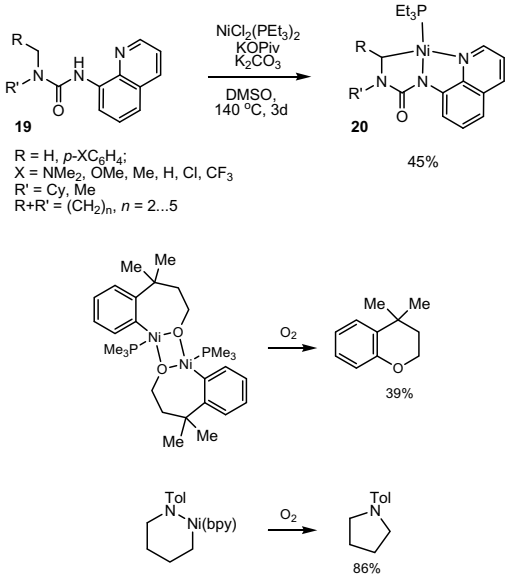

Scheme 9.9 Auxiliary-directed C(sp^3)–H activation at a nickel(II) center (top) [77] and aerobic oxidative functionalization of Ni^{II}-C(sp^3) bonds (bottom) [78, 79]

9.5 Conclusions

Aerobic organometallic C–H functionalization catalysis by palladium complexes has shown a significant development over the past two decades. The major driving force behind this success was an increased attention to and an improved understanding of the reaction mechanisms and the role that the ligand environment at the metal plays in such reactions. Numerous challenges remain on the way toward making hydrocarbon C–H bonds a "functional group" that can be readily and selectively transformed to another "classic" functional group by using the right catalytic system. Understanding the mechanism of C–H activation and the factors that control its selectivity in substrates with chemically non-equivalent C–H bonds can drive the progress in this area. A collaboration of experimentalists and computational chemists in such a challenging area of research may become fruitful. While organometallic palladium aerobic oxidation catalysis has already been an established and has a solid reputation among synthetic chemists, analogous platinum-based systems for aerobic C–H functionalization are scarce. Slower reaction rates of reactions involving platinum species, as compared to analogous palladium chemistry, maybe a reason behind such poor performance in aerobic platinum catalysis. But as in the case of the recent development in aerobic palladium catalysis, greater attention to reaction mechanisms and ligand design might help improve the situation. Finally, organometallic nickel aerobic oxidation catalysis is not established yet but there are some promising reports that suggest possible future development of this field. Overall, selective catalytic aerobic C–H functionalization reactions are poised to grow in their importance in the coming years and the group 10 metals can continue contributing to this development.

Acknowledgements The author is grateful to the National Science Foundation for the continuing support of his work in the field of aerobic C–H functionalization by late transition metal complexes (grants CHE-1464772, CHE-1800089).

References

1. Hartwig JF (2010) The organotransition metal chemistry: from bonding to catalysis. University Science Books, Sausalito
2. Smidt J, Hafner W, Jira R et al (1959) Catalytic reactions of olefins on compounds of the platinum group. Angew Chem 71(5):176–182. https://doi.org/10.1002/ange.19590710503
3. Moiseev II, Vargaftik MN, Syrkin YK (1960) Mechanism of the reaction of palladium salts with olefins in hydroxyl-containing solvents. Dokl Akad Nauk SSSR 133:377–380
4. Smidt J, Hafner W, Jira R et al (1962) The oxidation of olefins with palladium chloride catalysts. Angew Chem Int Ed 1(2):80–88. https://doi.org/10.1002/anie.196200801
5. Geletii YV, Shilov AE (1983) Catalytic oxidation of alkanes by molecular oxygen - oxidation of methane in the presence of platinum salts and heteropoly acids. Kinet Catal 24:413–416
6. Goldshleger NF, Shteinman AA, Shilov AE et al (1972) Reactions of alkanes in solutions of chloride complexes of platinum. Russ J Phys Chem 46:785–786
7. Shilov AE, Shulpin GB (1997) Activation of C–H bonds by metal complexes. Chem Rev 97:2879–2932. https://doi.org/10.1021/cr9411886

8. Shteinman A (2017) Activation and selective oxy-functionalization of alkanes with metal complexes: Shilov reaction and some new aspects. J Mol Catal A Chem 426:305–315. https://doi.org/10.1016/j.molcata.2016.08.020
9. Lin MR, Shen CY, Garcia-Zayas EA et al (2001) Catalytic Shilov chemistry: platinum chloride-catalyzed oxidation of terminal methyl groups by dioxygen. J Am Chem Soc 123(5):1000–1001. https://doi.org/10.1021/ja001926+
10. Watts D, Zavalij PY, Vedernikov AN (2018) Consecutive C–H and O_2 activation at a Pt(II) center to produce Pt(IV) aryls. Organometallics 37(22):4177–4180. https://doi.org/10.1021/acs.organomet.8b00662
11. Chong E, Kampf JW, Ariafard A, Canty AJ et al (2017) Oxidatively induced C–H activation at high valent nickel. J Am Chem Soc 139(17):6058–6061. https://doi.org/10.1021/jacs.7b02387
12. Camasso NM, Sanford MS (2015) Design, synthesis, and carbon-heteroatom coupling reactions of organometallic nickel(IV) complexes. Science 347(6227):1218–1220. https://doi.org/10.1126/science.aaa4526
13. McDonald RI, Liu G, Stahl SS (2011) Palladium-catalyzed alkene functionalization via nucleopalladation: stereochemical pathways and enantioselective catalytic applications. Chem Rev 111(4):2981–3019. https://doi.org/10.1021/cr100371y
14. Zhang Y-H, Yu J-Q (2009) Pd(II)-catalyzed hydroxylation of arenes with 1 atm of O_2 or air. J Am Chem Soc 131(41):14654–14655. https://doi.org/10.1021/ja907198n
15. Zultanski SL, Stahl SS (2015) Palladium-catalyzed aerobic acetoxylation of benzene using NOx-based redox mediators. J Organomet Chem 793:263–268. https://doi.org/10.1016/j.jorganchem.2015.03.003
16. Zhang J, Khaskin E, Anderson NP et al (2008) Catalytic aerobic oxidation of substituted 8-methylquinolines in pd^{ii} – 2,6-pyridinedicarboxylic acids systems. Chem Commun 31:3625–3627. https://doi.org/10.1039/B803156H
17. Wang D, Zavalij PY, Vedernikov AN (2013) Aerobic C–H acetoxylation of 8-methylquinoline in PdII – pyridinecarboxylic acids systems: some structure – reactivity relationships. Organometallics 32(17):4882–4891. https://doi.org/10.1021/om400618n
18. Stowers KJ, Kubota A, Sanford MS (2012) Nitrate as a redox co-catalyst for the aerobic Pd-catalyzed oxidation of unactivated sp^3-C–H bonds. Chem Sci 3(11):3192–3195. https://doi.org/10.1039/c2sc20800h
19. Campbell AN, White PB, Guzei IA et al (2010) Allylic C−H acetoxylation with a 4,5-diazafluorenone-ligated palladium catalyst: a ligand-based strategy to achieve aerobic catalytic turnover. J Am Chem Soc 132(43):15116–15119. https://doi.org/10.1021/ja105829t
20. Clagg K, Hou H, Weinstein AB et al (2016) Synthesis of indole-2-carboxylate derivatives via palladium-catalyzed aerobic amination of aryl C–H bonds. Org Lett 18(15):3586–3589. https://doi.org/10.1021/acs.orglett.6b01592
21. Inamoto K, Saito T, Hiroya K et al (2010) Palladium-catalyzed intramolecular amidation of C(sp^2)-H bonds: synthesis of 4-aryl-2-quinolinones. J Org Chem 75(11):3900–3903. https://doi.org/10.1021/jo100557s
22. Tsang WCP, Zheng N, Buchwald SL (2005) Combined C–H functionalization/C–N bond formation route to carbazoles. J Am Chem Soc 127(42):14560–14561. https://doi.org/10.1021/ja055353i
23. Rogers MM, Kotov V, Chatwichien J et al (2007) Palladium-catalyzed oxidative amination of alkenes: improved catalyst reoxidation enables the use of alkene as the limiting reagent. Org Lett 9(21):4331–4334. https://doi.org/10.1021/ol701903r
24. Brice JL, Harang JE, Timokhin VI et al (2005) Aerobic oxidative amination of unactivated alkenes catalyzed by palladium. J Am Chem Soc 127(9):2868–2869. https://doi.org/10.1021/ja0433020
25. White PB, Jaworski JN, Zhu GH et al (2016) Diazafluorenone-promoted oxidation catalysis: insights into the role of bidentate ligands in Pd-catalyzed aerobic aza-wacker reactions. ACS Catal 6(5):3340–3348. https://doi.org/10.1021/acscatal.6b00953
26. McDonald RI, White PB, Weinstein AB et al (2011) Enantioselective Pd(II)-catalyzed aerobic oxidative amidation of alkenes and insights into the role of electronic asymmetry in pyridine-oxazoline ligands. Org Lett 13(11):2830–2833. https://doi.org/10.1021/ol200784y

27. McDonald RI, Stahl SS (2010) Modular synthesis of 1,2-diamine derivatives by palladium-catalyzed aerobic oxidative cyclization of allylic sulfamides. Angew Chem Int Ed 49(32):5529–5532. https://doi.org/10.1002/anie.200906342
28. Kong W-J, Chen X, Wang M et al (2018) Rapid syntheses of heteroaryl-substituted imidazo[1,5-a]indole and pyrrolo[1,2-c]imidazole via aerobic C2-H functionalizations. Org Lett 20(1):284–287. https://doi.org/10.1021/acs.orglett.7b03596
29. Liu Y-J, Xu H, Kong W-J et al (2014) Overcoming the limitations of directed C–H functionalizations of heterocycles. Nature 515(7527):389–393. https://doi.org/10.1038/nature13885
30. Tereniak SJ, Stahl SS (2017) Mechanistic basis for efficient, site-selective, aerobic catalytic turnover in Pd-catalyzed C–H imidoylation of heterocycle-containing molecules. J Am Chem Soc 139(41):14533–14541. https://doi.org/10.1021/jacs.7b07359
31. Wang D, Stahl SS (2017) Pd-Catalyzed aerobic oxidative biaryl coupling: non-redox cocatalysis by $Cu(OTf)_2$ and discovery of $Fe(OTf)_3$ as a highly effective cocatalyst. J Am Chem Soc 139(16):5704–5707. https://doi.org/10.1021/jacs.7b01970
32. Izawa Y, Stahl SS (2010) Aerobic oxidative coupling of o-xylene: discovery of 2-fluoropyridine as a ligand to support selective Pd-catalyzed C–H functionalization. Adv Synth Catal 352(18):3223–3229. https://doi.org/10.1002/adsc.201000771
33. Brasche G, Garcia-Fortanet J, Buchwald SL (2008) Twofold C–H functionalization: palladium-catalyzed ortho arylation of anilides. Org Lett 10(11):2207–2210. https://doi.org/10.1021/ol800619c
34. Watanabe T, Ueda S, Inuki S et al (2007) One-pot synthesis of carbazoles by palladium-catalyzed N-arylation and oxidative coupling. Chem Commun 43:4516–4518. https://doi.org/10.1039/B707899D
35. Engle KM, Thuy-Boun PS, Dang M et al (2011) Ligand-accelerated cross-coupling of $C(sp^2)$-H bonds with arylboron reagents. J Am Chem Soc 133(45):18183–18193. https://doi.org/10.1021/ja203978r
36. Baxter RD, Sale D, Engle KM et al (2012) Mechanistic rationalization of unusual kinetics in Pd-catalyzed C–H olefination. J Am Chem Soc 134(10):4600–4606. https://doi.org/10.1021/ja207634t
37. Li S, Cai L, Ji H et al (2016) Pd(II)-catalyzed *meta*-C–H functionalizations of benzoic acid derivatives. Nat Commun 7:10443. https://doi.org/10.1038/ncomms10443
38. Beck EM, Grimster NP, Hatley R et al (2006) Mild aerobic oxidative palladium (II) catalyzed C–H bond functionalization: regioselective and switchable C–H alkenylation and annulation of pyrroles. J Am Chem Soc 128(8):2528–2529. https://doi.org/10.1021/ja058141u
39. Lu M-Z, Chen X-R, Xu H et al (2018) Ligand-enabled ortho-C–H olefination of phenylacetic amides with unactivated alkenes. Chem Sci 9(5):1311–1316. https://doi.org/10.1039/C7SC04827K
40. Engle KM, Wang D-H, Yu J-Q (2010) Ligand-accelerated C–H activation reactions: evidence for a switch of mechanism. J Am Chem Soc 132(40):14137–14151. https://doi.org/10.1021/ja105044s
41. Stowers KJ, Fortner KC, Sanford MS (2011) Aerobic Pd-catalyzed sp^3 C–H olefination: a route to both N-heterocyclic scaffolds and alkenes. J Am Chem Soc 133(17):6541–6544. https://doi.org/10.1021/ja2015586
42. Ferreira EM, Stoltz BM (2003) Catalytic C–H bond functionalization with palladium(II): aerobic oxidative annulations of indoles. J Am Chem Soc 125(32):9578–9579. https://doi.org/10.1021/ja035054y
43. Bercaw JE, Hazari N, Labinger JA (2008) oxidative aromatization of olefins with dioxygen catalyzed by palladium trifluoroacetate. J Org Chem 73(21):8654–8657. https://doi.org/10.1021/jo8016296
44. Izawa Y, Pun D, Stahl SS (2011) Palladium-catalyzed aerobic dehydrogenation of substituted cyclohexanones to phenols. Science 333(6039):209–213. https://doi.org/10.1126/science.1204183
45. Iosub AV, Stahl SS (2015) Palladium-catalyzed aerobic oxidative dehydrogenation of cyclohexenes to substituted arene derivatives. J Am Chem Soc 137(10):3454–3457. https://doi.org/10.1021/ja512770u

46. Gorelsky SI, Lapointe D, Fagnou KJ (2012) Analysis of the palladium-catalyzed (aromatic) C−H bond metalation − deprotonation mechanism spanning the entire spectrum of arenes. J Org Chem 77(1):658–668. https://doi.org/10.1021/jo202342q
47. Wang D, Weinstein AB, White PB et al (2018) Ligand-promoted palladium-catalyzed aerobic oxidation reactions. Chem Rev 118(5):2636–2679. https://doi.org/10.1021/acs.chemrev.7b00334
48. Engelin C, Jensen T, Rodriguez- Rodriguez S et al (2013) Mechanistic investigation of palladium-catalyzed allylic C–H activation. ACS Catal 3(3):294–302. https://doi.org/10.1021/cs3007878
49. Ryabov AD (1990) Mechanisms of intramolecular activation of C−H bonds in transition-metal complexes. Chem Rev 90(2):403–424. https://doi.org/10.1021/cr00100a004
50. Engle KM, Mei T-S, Wasa M et al (2012) Weak coordination as a powerful means for developing broadly useful C–H functionalization reactions. Acc Chem Res 45(6):788–802. https://doi.org/10.1021/ar200185g
51. He J, Wasa M, Chan KSL et al (2017) Palladium-catalyzed transformations of alkyl C−H bonds. Chem Rev 117(13):8754–8786. https://doi.org/10.1021/acs.chemrev.6b00622
52. Yang Y-F, Houk KN, Hong X et al (2017) Experimental-computational synergy for selective Pd(II)-catalyzed C–H activation of aryl and alkyl groups. Acc Chem Res 50(11):2853–2860. https://doi.org/10.1021/acs.accounts.7b00440
53. Davies DL, Donald SMA, Macgregor SA (2005) Computational study of the mechanism of cyclometalation by palladium acetate. J Am Chem Soc 127(4):13754–13755. https://doi.org/10.1021/ja052047w
54. García-Cuadrado D, Braga AAC, Maseras F et al (2006) Proton abstraction mechanism for the palladium-catalyzed intramolecular arylation. J Am Chem Soc 128(4):1066–1067. https://doi.org/10.1021/ja056165v
55. Boisvert L, Denney MC, Hanson SK et al (2009) Insertion of molecular oxygen into a palladium(II) methyl bond: a radical chain mechanism involving palladium(III) intermediates. J Am Chem Soc 131(43):15802–15814. https://doi.org/10.1021/ja9061932
56. Zeitler HE, Kaminsky WA, Goldberg KI (2018) Insertion of molecular oxygen into the metal − methyl bonds of platinum(II) and palladium(II) 1,3-bis(2-pyridylimino)isoindolate complexes. Organometallics 37(21):3644–3648. https://doi.org/10.1021/acs.organomet.8b00573
57. Taylor RA, Law DJ, Sunley GJ et al (2009) Towards photocatalytic alkane oxidation: the insertion of dioxygen into a platinum(II) − methyl bond. Angew Chem Int Ed 48(32):5900–5903. https://doi.org/10.1002/anie.200806187
58. Petersen AR, Taylor RA, Vicente-Hernández I et al (2014) Oxygen insertion into metal carbon bonds: formation of methylperoxo Pd(II) and Pt(II) Complexes via photogenerated dinuclear intermediates. J Am Chem Soc 136(40):14089–14099. https://doi.org/10.1021/ja5055143
59. Fernández-Alvarez VM, Ho SKY, Britovsek GJP et al (2018) A DFT-based mechanistic proposal for the light-driven insertion of dioxygen into Pt(II) − C bonds. Chem Sci 9(22):5039–5046. https://doi.org/10.1039/c8sc01161c
60. Sberegaeva AV, Zavalij PY, Vedernikov AN (2016) Oxidation of a monomethylpalladium(II) complex with O_2 in water: tuning reaction selectivity to form ethane, methanol or methylhydroperoxide. J Am Chem Soc 138(4):1446–1455. https://doi.org/10.1021/jacs.5b12832
61. Maleskis A, Sanford MS (2011) Facial tridentate ligands for stabilizing palladium(IV) complexes. Organometallics 30(24):6617–6627. https://doi.org/10.1021/om200779j
62. Khusnutdinova JR, Qu F, Zhang Y et al (2012) Formation of the palladium(IV) complex [(Me3tacn)PdIVMe3] + through aerobic oxidation of (Me3tacn)PdIIMe2 (Me3tacn = N, N′, N″- Trimethyl-1,4,7-triazacyclononane). Organometallics 31(13):4627–4630. https://doi.org/10.1021/om300426r
63. Tang F, Zhang Y, Rath NP et al (2012) Detection of Pd(III) and Pd(IV) intermediates during the aerobic oxidative C–C bond formation from a Pd(II) dimethyl complex. Organometallics 31(18):6690–6696. https://doi.org/10.1021/om300752w
64. Wilke G, Schott H, Heimbach P (1967) Oxygen complexes of zerovalent nickel, palladium, and platinum. Angew Chem Int Ed 6(1):92–93. https://doi.org/10.1002/anie.196700921

65. Yamashita M, Goto K, Kawashima T (2005) Fixation of both O_2 and CO_2 from air by a crystalline palladium complex bearing heterocyclic carbene ligands. J Am Chem Soc 127(20):7294–7295. https://doi.org/10.1021/ja051054h
66. Jaworski JN, McCann SD, Guzei IA et al (2017) Detection of palladium(I) in aerobic oxidation catalysis. Angew Chem Int Ed 56(13):3605–3610. https://doi.org/10.1002/anie.201700345
67. Vargaftik MN, Zagorodnikov VP, Stolarov IP et al (1989) Giant palladium clusters as catalysts of oxidative reactions of olefins and alcohols. J Mol Catal 53(3):315–348. https://doi.org/10.1016/0304-5102(89)80066-5
68. Pun D, Diao T, Stahl SS (2013) Aerobic dehydrogenation of cyclohexanone to phenol catalyzed by $Pd(TFA)_2$/2-dimethylaminopyridine: evidence for the role of Pd nanoparticles. J Am Chem Soc 135(22):8213–8221. https://doi.org/10.1021/ja403165u
69. Denney MC, Smythe NA, Cetto KL et al (2006) Insertion of molecular oxygen into a palladium(II) hydride bond. J Am Chem Soc 128(8):2508–2509. https://doi.org/10.1021/ja0562292
70. Keith JM, Muller RP, Kemp RA et al (2006) Mechanism of direct molecular oxygen insertion in a palladium(II) − hydride bond. Inorg Chem 45(24):9631–9633. https://doi.org/10.1021/ic061392z
71. Konnick MM, Stahl SS (2008) Reaction of molecular oxygen with a Pd^{II}-hydride to produce a Pd^{II}-hydroperoxide: experimental evidence for an HX-reductive-elimination pathway. J Am Chem Soc 130(17):5753–5762. https://doi.org/10.1021/ja7112504
72. Popp BV, Stahl SS (2007) Insertion of molecular oxygen into a palladium-hydride bond: computational evidence for two nearly isoenergetic pathways. J Am Chem Soc 129(14):4410–4422. https://doi.org/10.1021/ja069037v
73. Konnick MM, Decharin N, Popp BV et al (2011) O_2 insertion into a palladium(II)-hydride bond: Observation of mechanistic crossover between HX-reductive-elimination and hydrogen-atom-abstraction pathways. Chem Sci 2(2):326–330. https://doi.org/10.1039/C0SC00392A
74. Decharin N, Stahl SS (2011) Benzoquinone-promoted reaction of O_2 with a Pd^{II}-hydride. J Am Chem Soc 133(15):5732–5735. https://doi.org/10.1021/ja200957n
75. Kreutz JE, Shukhaev A, Du W et al (2010) Evolution of catalysts directed by genetic algorithms in a plug-based microfluidic device tested with oxidation of methane by oxygen. J Am Chem Soc 132(9):3128–3132. https://doi.org/10.1021/ja909853x
76. Vedernikov AN (2012) Direct functionalization of M-C (M=PtII, PdII) bonds using environmentally benign oxidants, O_2 and H_2O_2. Acc Chem Res 45(6):803–813. https://doi.org/10.1021/ar200191k
77. Beattie DD, Grunwald AC, Perse T et al (2018) Understanding Ni(II)-mediated $C(sp^3) - H$ activation: tertiary ureas as model substrates. J Am Chem Soc 140(39):12602–12610. https://doi.org/10.1021/jacs.8b07708
78. Pirovano P, Farquhar ER, Swart M et al (2016) Tuning the reactivity of terminal nickel(III) − oxygen adducts for C−H bond activation. J Am Chem Soc 138(43):14362–14370. https://doi.org/10.1021/jacs.6b08406
79. Han R, Hillhouse GL (1997) Carbon–oxygen reductive-elimination from nickel(II) oxametallacycles and factors that control formation of ether, aldehyde, alcohol, or ester products. J Am Chem Soc 119(34):8135–8136. https://doi.org/10.1021/ja9714999
80. Koo K, Hillhouse GL (1995) Carbon-nitrogen bond formation by reductive elimination from nickel(II) amido alkyl complexes. Organometallics 14(9):4421–4423. https://doi.org/10.1021/om00009a054
81. Kieber-Emmons MT, Riordan CG (2007) Dioxygen activation at monovalent nickel. Acc Chem Res 40(7):618–625. https://doi.org/10.1021/ar700043n

Chapter 10
Direct C–H Oxidation of Aromatic Substrates in the Presence of Biomimetic Iron Complexes

Oleg Y. Lyakin and Evgenii P. Talsi

Abstract This chapter is dedicated to one of the most challenging areas of oxidation catalysis—direct oxidation of aromatic C–H groups. The development of environmentally friendly catalyst systems for the direct hydroxylation of aromatic hydrocarbons is an important task of modern catalysis. Biomimetic approach, based on the functional modeling of enzymes by iron complexes of a relatively simple structure, is considered as a promising approach for designing catalyst systems for direct aromatic hydroxylation, relying on nontoxic hydrogen peroxide used as the oxidant. The mechanism of catalytic performance of biomimetic systems is a question of primary importance; deep insight into this issue can both substantially rationalize the development of novel practical catalyst systems for the direct oxidation of aromatic hydrocarbons and enrich our knowledge on the mechanisms of natural metalloenzyme-mediated oxidations. In this chapter, the state-of-the-art in this area is provided, with the mechanistic part based mostly on the authors' own works.

Keywords Aromatic hydrocarbons · Bioinspired catalysis · Biomimetics · Electrophilic substitution · Enzyme models · EPR spectroscopy · Hydroxylation · Homogeneous catalysis · Hydrogen peroxide · Intermediates · Iron · Oxidation · Oxoiron species · Reaction mechanism · Selectivity

Abbreviations

CHP	Cumene hydroperoxide
EHA	2-Ethylhexanoic acid
DFT	Density functional theory
EPR	Electron paramagnetic resonance
GC	Gas chromatography

O. Y. Lyakin (✉) · E. P. Talsi
Boreskov Institute of Catalysis, Pr. Lavrentieva 5, Novosibirsk 630090, Russia
e-mail: lyakin@catalysis.ru

Novosibirsk State University, Pirogova 2, Novosibirsk 630090, Russia

K. P. Bryliakov (ed.), *Frontiers of Green Catalytic Selective Oxidations*,
Green Chemistry and Sustainable Technology,
https://doi.org/10.1007/978-981-32-9751-7_10

IBA	Isobutyric acid
IVA	Isovaleric acid
Me_3HQ	2,3,5-Trimethylhydroquinone
NHC	N-heterocyclic carbene(s) ligand
PDP	N,N′-bis(2-pyridylmethyl)-(*S*,*S*)-2,2′-bipyrrolidine ligand
PhSH	Thioanisole
TPA	Tris(2-pyridylmethyl)amine ligand
TOF	Turnover frequency of the catalyst
TN	Turnover number of the catalyst
UV-Vis	Ultraviolet-visible spectroscopy

10.1 Introduction

The search for new, highly efficient catalyst systems for the selective oxidation of hydrocarbons, relying on complexes of cheap and nontoxic iron and hydrogen peroxide as "green" oxidant, is a highly challenging task, due to the growing demands of fine chemical and pharmaceutical industry, as well as toughening environmental constraints in general [1–3]. Remarkable selectivity and versatility of the reactions mediated by iron oxygenases encourage researchers to mimic their catalytic properties by relatively simple synthetic iron complexes (a so-called biomimetic or bioinspired approach) [4–6].

Phenols are important intermediates in the production of drugs, agrochemicals, and plastics such as polycarbonates, phenolic, and epoxide resins [7, 8]. At present, the annual world demand for phenol exceeds 10 million tons. Phenol is mostly (>95%) produced from petroleum-derived benzene, via three-step cumene process, involving (1) benzene alkylation with propylene to form cumene, which is typically catalyzed by acidic compounds or zeolites; (2) oxidation of cumene with O_2 to form cumene hydroperoxide, CHP; (3) CHP cleavage to phenol and acetone, catalyzed by sulfuric acid [7].

Cumene process, affording relatively cheap phenol, is not ecologically sustainable. Rather low overall efficiency (5%), as well as the formation of toxic and explosive intermediates, inspires the search for greener and more atom-economical alternatives of the cumene process of phenol production [7]. Apparently, the most tempting route to phenols is the direct hydroxylation of aromatic hydrocarbons. However, the high stability of the aromatic motif toward oxidation so far limits the success of such one-stage processes. The catalytic systems to be developed should be highly reactive, capable of hydroxylating very strong aromatic C–H bonds (BDE for C_6H_6 112 kcal/mol) [9], and at the same time, highly selective—to avoid subsequent phenol oxidation. That is why the oxidation of benzene by molecular oxygen is defined as one of the "top-10 challenges in catalysis" [10]. Several synthetically useful direct aromatic hydroxylation protocols have been reported so far [11–18]. All of them

have serious drawbacks, e.g., the use of catalysts based on toxic metals (V, Ni, Ru, Pd), high reaction temperature, or low substrate conversion.

In nature, the catalytic aromatic hydroxylations are mediated mainly by iron-containing oxygenases [19], such as cytochrome P450 [20–22] and nonheme diiron hydroxylases, such as methane monooxygenase [23, 24] and toluene-4-monooxygenase [25–27]. All aforementioned metalloenzymes exhibit remarkable catalytic activity toward the aromatic C–H hydroxylation, thus inspiring the search for their synthetic mimics [28]. A number of synthetic iron-based catalyst systems for the direct hydroxylation of arenes has been developed in the last two decades. This chapter surveys such systems based on bioinspired nonheme iron complexes and hydrogen peroxide, with a focus on oxidation efficiency and selectivity, and their correlation with the structure of the Fe complex. Available mechanistic details of aromatic C–H oxidation by nonheme iron-based systems are discussed.

10.2 Oxidation of Arenes with Bioinspired Iron Catalyst Systems

10.2.1 Under Biomimetic Conditions

In 2002, Mansuy with coworkers designed the nonheme ferrous complex $Fe(TPAA)(ClO_4)_2$ (**1**) bearing the ligand of the 2-aminopyridine family (Fig. 10.1) [29]. Unexpectedly, **1** demonstrated much better performance in the catalytic hydroxylation of aromatic C–H groups with H_2O_2 than in the epoxidation of alkenes, that are much more prone to oxidation. Benzene was transformed into phenol, catalyst **1** performing 22 turnovers (TN), which corresponds to 22% yield (based on oxidant) under substrate-excess ("biomimetic") conditions (Table 10.1, entry 1). A CH_3CN/H_2O (v/v 9:1) mixture was used as a solvent. No other benzene oxidation products were reported by the authors. Unexpectedly, high chemoselectivity (89%) toward aromatic ring (rather than benzylic) oxidation was observed in the case of toluene, *o*- and *p*-cresol being the major reaction products (Table 10.2, entry 1). Similarly, catalytic oxidation of chlorobenzene and anisole led to equimolar mixtures of

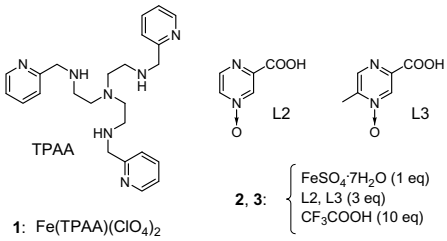

Fig. 10.1 Ligands and corresponding iron-based catalysts applied for the aromatic C−H hydroxylation

Table 10.1 Iron-catalyzed oxidation of benzene with H_2O_2 under substrate-excess conditions

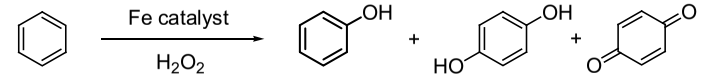

No.	Catalyst (mol% Fe)[a]	[Fe]:[H_2O_2]:[C_6H_6]	T, °C (t, h)[b]	Conversion of H_2O_2, TN[c]	Phenol yield, TN[c]	Selectivity toward phenol (%)	Solvent	References
1	**1** (1)	1:100:3000	20 (2)	22	22		CH_3CN/H_2O[d]	[29]
2	**2** (2.3)	1:44:440	37 (4)	35.8	35.5	99	CH_3CN/H_2O[e]	[30]
3	**3** (2.3)	1:44:440	37 (4)	36.6	35.5	97	CH_3CN/H_2O[e]	[31]
4	**4** (5)	1:20:3000	20 (2)	9.2	9.2		CH_3CN/CH_2Cl_2[f]	[32]
5[g]	**4** (5)	1:20:3000	20 (2)	11.8	11.8		CH_3CN/CH_2Cl_2[f]	[32]
6[h]	**4** (5)	1:20:3000	20 (2)	7.4	7.4		CH_3CN/CH_2Cl_2[f]	[32]
7[i]	**4** (5)	1:20:3000	20 (2)	6	6		CH_3CN/CH_2Cl_2[f]	[32]
8	**5** (5)	1:20:3000	20 (2)	5	5		CH_3CN/CH_2Cl_2[f]	[32]
9[g]	**5** (5)	1:20:3000	20 (2)	5.2	5.2		CH_3CN/CH_2Cl_2[f]	[32]
10[h]	**5** (5)	1:20:3000	20 (2)	3	3		CH_3CN/CH_2Cl_2[f]	[32]
11[i]	**5** (5)	1:20:3000	20 (2)	6.2	6.2		CH_3CN/CH_2Cl_2[f]	[32]
12	**6** (10)	1:10:300	25 (1/4)	1.4	1.4	>99	CH_3CN	[28]
13[j]	**6** (10)	1:10:300	25 (1/4)	2.0	2.0	>99	CH_3CN	[28]

[a]Relative to H_2O_2. [b]Conditions: reaction temperature and time. [c]TN, turnover number of the catalyst = moles of product(s)/mol Fe. [d]v/v 9:1. [e]v/v 1:1. [f]v/v 1:1. [g]In the presence of 50 mol% of 1-naphthol (relative to H_2O_2). [h]In the presence of 50 mol% of Me_3HQ. [i]In the presence of 50 mol% of PhSH. [j]In the presence of 10 mol% of acetic acid (relative to H_2O_2)

Table 10.2 Iron-catalyzed oxidation of toluene with H_2O_2 under substrate-excess conditions

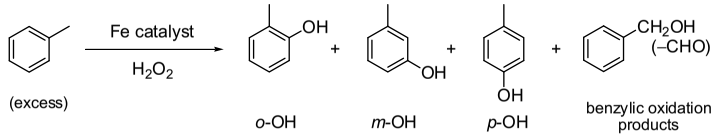

No.	Catalyst (mol% Fe)[a]	[Fe]:[H_2O_2]:[C_7H_8]	T, °C (t, h)[b]	Conv. of H_2O_2, TN[c]	*o*-OH, TN:*m*-OH, TN:*p*-OH, TN[d]	Aromatic oxidation selectivity (%)[e]	References
1	**1** (5)	1:20:3000	20 (2)	3.8	1.6:0.4:1.4	89	[29]
2	**2** (2.3)	1:44:440	37 (4)	12.1	3.2:0.1:4.4	64	[30]
3	**3** (2.3)	1:44:440	37 (4)	8.3	1.9:0.1:2.7	57	[31]
4	**6** (10)	1:10:300	25 (1/4)	1.2	0.4:0.3:0.3	83	[28]
5	**6** (10)[f]	1:10:300	25 (1/4)	2.6	1.2:0.4:0.8	92	[28]

[a]Relative to H_2O_2. [b]Conditions: reaction temperature and time. For solvents used, see entries with the same catalysts in Table 10.1. [c]TN, turnover number of the catalyst = moles of product(s)/mol Fe. [d]Yields of cresols expressed in TN. [e]Selectivity toward oxidation of the aromatic ring. [f]In the presence of acetic acid, [Fe]:[CH_3COOH] = 1:1

o- and *p*-hydroxylated products with 10.6 and 2.6 TN, respectively (53% and 13% yields based on H_2O_2).

It should be noted that the data obtained under substrate-excess conditions should be interpreted with care. Indeed, under such conditions, extensively used in the model and mechanistic studies (see below), the arene conversions remain low, rarely exceeding several percents. Extending the reaction to higher conversions, the reported high oxidation selectivities may become unachievable, owing to pronounced further oxidative transformations of the primary oxidation products. So, the use of substrate-excess conditions may mask the synthetic limitations of the corresponding catalyst systems.

Bianchi and coworkers developed [30, 31] a catalytic protocol for hydroxylation of aromatic hydrocarbons with H_2O_2, using the three-component system $FeSO_4 \cdot 7H_2O$/pyrazine-3-carboxylic acid *N*-oxide ligand/trifluoroacetic acid (molar ratio 1:3:10) in a biphasic reaction medium, containing water, acetonitrile, and aromatic substrate (for ligand structure, see Fig. 10.1). The use of biphasic mixtures allowed a convenient recovery and recycling of the catalyst by phase separation techniques. Again, catalytic experiments were performed under substrate-excess conditions (10:1 substrate:oxidant molar ratio). Oxidation of benzene in the presence of in situ generated catalysts **2** and **3** (Fig. 10.1, Table 10.1, entries 2 and 3) demonstrated good oxygenation efficiencies (35.8–36.6 TN) and very high selectivity toward phenol (97–99%). At higher temperatures, the turnover frequency (TOF) of catalyst **2** in benzene oxidation substantially increased (from 37 h^{-1} at 37 °C to >230 h^{-1} at 70 °C), while the oxidation efficiency sharply decreased (from 84% to 55%). The only detected by-product was 1,4-benzoquinone. When toluene was used as a substrate, much lower oxidation efficiency was documented (8.3–12.1 TN; Table 10.2, entries 2 and 3). Moreover, significant amounts of benzylic oxidation products were detected, which deteriorated the selectivity toward aromatic oxidation (57 and 64% for **2** and **3**, respectively). Benzaldehyde was the main by-product. For ethylbenzene, the side-chain oxidation was even more pronounced, resulting in only 21% selectivity toward cresols for catalyst **2**. Conversely, the oxidation of *tert*-butylbenzene yielded *para-tert*-butylphenol as virtually the only product with 97% selectivity, resulting from the low reactivity toward oxidation and strong directing effect of the bulky *tert*-butyl moiety. For all alkylbenzenes studied, the formation of over-oxidation products was negligible. At the same time, anisole was oxidized into a complex mixture of high-molecular-weight oligomers with polyoxygenated aromatic rings.

Banse and coworkers reported the use of aminopyridine iron complexes **4** and **5** with hexadentate N_6-donor ligands (Fig. 10.2) in the catalytic aromatic hydroxylation of benzene, ethylbenzene, chlorobenzene, and anisole [32]. To improve the yields of phenols, a number of reducing agents, such as 2,3,5-trimethylhydroquinone (Me_3HQ), thioanisole (PhSH), and 1-naphthol, was added to the catalyst systems. The oxidation of aromatic substrates with hydrogen peroxide was conducted under biomimetic conditions ([Fe]:[H_2O_2]:[C_6H_6] = 1:20:3000, T = 20 °C, t = 2 h). Benzene oxidation, catalyzed by complexes **4** and **5**, afforded low phenol yields (9.2 and 5 TN, Table 10.1, entries 4 and 8). Similarly, for complex **1** [29], no phenol over-

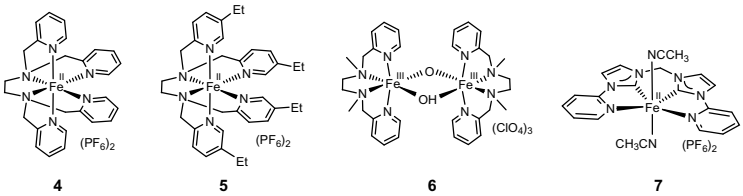

Fig. 10.2 Iron complexes for catalytic aromatic hydroxylation

oxidation products were reported for catalyst systems based on **4** and **5**. The addition of the reducing agents did not noticeably improve the phenol yield (Table 10.1, entries 5–7 and 9–11). Similarly, the low effect of additives was documented for the oxidation of chlorobenzene. On the contrary, the addition of 1-naphthol to complex **4** and PhSH to complex **5** substantially enhanced the efficiency of anisole hydroxylation from 8.2 to 18.8 TN and from 3.6 to 8.2 TN, respectively. 2-Methoxyphenol was the major hydroxylation product, phenol and 4-methoxyphenol being the only detected by-products. Without additives, **4** and **5** are poor catalysts for the aromatic hydroxylation of ethylbenzene, producing predominantly benzylic oxidation products 1-phenylethanol and acetophenone, and performing 3.4 and 0.6 TN toward ethylphenols with 26 and 8% selectivity toward aromatic hydroxylation. The addition of 1-naphthol substantially improved both the yield of ethylphenols (7.7 and 3.1 TN) and the aromatic hydroxylation selectivity of catalysts **4** and **5** (55 and 49%). For all studied substrates, **4** was shown to be a better aromatic hydroxylation catalyst than **5** [32].

In 2015, Biswas with coauthors reported the aromatic hydroxylation catalyzed by an oxo-bridged diiron(III) complex **6** (Fig. 10.2), mimicking dinuclear iron core of toluene-4-monooxygenase [28]. Benzene oxidation with H_2O_2 in the presence of **6** under substrate-excess conditions exhibited very poor phenol yield (1.4 TN, Table 10.1, entry 12), yet with >99% selectivity (*p*-quinone was the only minor side product). The addition of acetic acid did not substantially improve the phenol yield (Table 10.1, entry 13). In toluene oxidation, catalyst **6** performed 1.2 TN with 83% selectivity toward cresols (Table 10.2, entry 4); these values increased to 2.6 TN and 92% upon the addition of acetic acid (Table 10.2, entry 5).

10.2.2 Under Catalytic Conditions

Kühn and coworkers have designed iron complex **7** (Fig. 10.2) with *N*-heterocyclic carbene (NHC) ligand that is excellent σ-donor compared to other ligands [33]; moreover, NHC-based complexes are very stable toward oxidative ligand destruction, which is crucial for designing metal-based catalysts for hydrocarbon oxygenation [33–35]. Unlike in papers discussed so far, where the high substrate excess was used, the remarkable stability of the Fe(NHC) complex allowed the use of "real catalytic

conditions", with the equimolar substrate/H_2O_2 ratio or excess of the oxidant. In the former case, the benzene conversion was 7.4% (7.4 TN) with the selectivity of 94% for phenol (Table 10.3, entry 2), whereas 1,4-benzoquinone was identified as the major by-product [33]. Although stoichiometric reactants were used, with only 1 mol% of Fe, high selectivity toward phenol was achieved. The influence of the oxidant/substrate ratio on the catalytic benzene oxidation in the presence of **7** was examined. Similarly, high selectivities were documented when the molar ratio of H_2O_2/C_6H_6 was changed from 0.5 to 5 (Table 10.3, entries 1–4). Only when a 10-fold excess of H_2O_2 was applied, the phenol selectivity dropped from 94% to 87% (Table 10.3, entries 2 versus 5). Upon a 20-fold increase of the H_2O_2 loading, the phenol yield has only doubled (5.6 versus 11.2 TN, entries 1 versus 5), implying a pronounced decomposition of hydrogen peroxide at high concentrations. Moreover, the catalyst suffers deactivation over time as proven by the second addition of H_2O_2, which caused no significant change in the phenol yield. The reaction temperature was probed as a factor influencing the catalytic performance. The following tendency was revealed: at elevated temperature, the selectivity toward phenol decreased drastically (from 94% at 25 °C to 36% at 60 °C, Table 10.3, entries 2 and 6–9). At the same time, a two-fold rise of the benzene conversion (from 7.4% to 15.1%) was accompanied by a slight decrease of the phenol yield (from 6.9 to 5.5 TN), which means that over-oxidation predominates at elevated temperature.

Complex **7** catalyzed the oxidation of toluene ([Fe]:[H_2O_2]:[C_7H_8] = 1:100:100) with 15.2% conversion to *o*-/*m*-/*p*-cresols as main products and benzyl alcohol and benzaldehyde as minor products (Table 10.4, entry 2), demonstrating rather high selectivity toward ring oxidation (78%). In addition, 17% of consumed toluene was converted to benzylic oxidation products and residual 5% was over-oxidized to 2-methyl-*p*-quinone. *Ortho*- and *para*-positions of toluene were clearly preferred upon oxidation. The ratio of *o*-/*p*-cresol was about 1.6, which is close to the expected stochastic value of 2. The higher conversions of toluene (Table 10.4) compared to benzene (Table 10.3) were explained by the more electron-rich aromatic system in toluene. Only a slight increase in toluene conversion was observed when going from 50 to 1000 equiv. of H_2O_2 (Table 10.4, entries 1–5). The side-chain oxidation was more pronounced at higher H_2O_2 concentration. However, the selectivity of aromatic ring hydroxylation was still 75% with 1000 equiv. of hydrogen peroxide. Interestingly, the formation of *m*-cresol was accelerated at higher amounts of H_2O_2. Furthermore, the hydroxylation of the aromatic ring was clearly preferred at a lower temperature (Table 10.4, entries 6–8). At higher temperature, benzylic oxidation became as likely as aromatic ring hydroxylation (Table 10.4, entries 9–11).

In 2016, Silva and Carneiro reported the direct benzene hydroxylation with hydrogen peroxide in the presence of a number of iron complexes with acetylacetonate and N_2O_2-, N_4-donor Schiff base ligands (complexes **8–13**, Fig. 10.3) that can be easily prepared in high yields from readily available precursors [36]. Iron complex **8** with the N_4-donor Schiff base ligand was found to be the most active and selective catalyst for the hydroxylation of benzene under substrate-limited conditions ([Fe]:[H_2O_2]:[C_6H_6] = 1:300:100), affording 65% conversion of benzene and 98% selectivity toward phenol in 3 h at 50 °C (Table 10.3, entry 10). The major by-product

Table 10.3 Iron-catalyzed oxidation of benzene with H_2O_2 under substrate-limited conditions

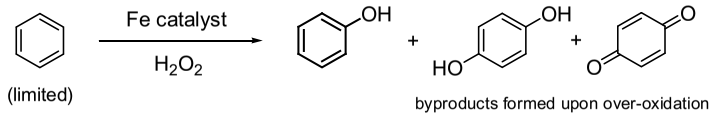

No.	Catalyst (mol% Fe)[a]	[Fe]:[H_2O_2]:[C_6H_6]	T, °C (t, h)[b]	Benzene conv. (%)	Phenol yield, TN[c]	Selectivity toward phenol (%)	Solvent	References
1	**7** (1)	1:100:50	25 (1)	6.0	5.6	94	CH_3CN	[33]
2	**7** (1)	1:100:100	25 (1)	7.4	6.9	94	CH_3CN	[33]
3	**7** (1)	1:100:200	25 (1)	8.5	7.9	93	CH_3CN	[33]
4	**7** (1)	1:100:500	25 (1)	8.8	8.0	91	CH_3CN	[33]
5	**7** (1)	1:100:1000	25 (1)	13.0	11.2	87	CH_3CN	[33]
6	**7** (1)	1:100:100	30 (1)	10.0	6.8	84	CH_3CN	[33]
7	**7** (1)	1:100:100	40 (1)	10.7	6.3	59	CH_3CN	[33]
8	**7** (1)	1:100:100	50 (1)	13.6	5.9	43	CH_3CN	[33]
9	**7** (1)	1:100:100	60 (1)	15.1	5.5	36	CH_3CN	[33]
10	**8** (1)	1:300:100	50 (3)	65	64	98	CH_3CN	[36]
11	**8** (2)	1:150:50	50 (3)	51	25	99	CH_3CN	[36]
12	**8** (1)	1:600:100	50 (3)	77	77	100	CH_3CN	[36]
13	**9** (1)	1:300:100	50 (3)	55	49	90	CH_3CN	[36]
14	**10** (1)	1:300:100	50 (3)	47	43	91	CH_3CN	[36]
15	**11** (1)	1:300:100	50 (3)	32	26	81	CH_3CN	[36]
16	**12** (1)	1:300:100	50 (3)	22	21	96	CH_3CN	[36]
17	**13** (1)	1:300:100	50 (3)	20	19	96	CH_3CN	[36]

(continued)

Table 10.3 (continued)

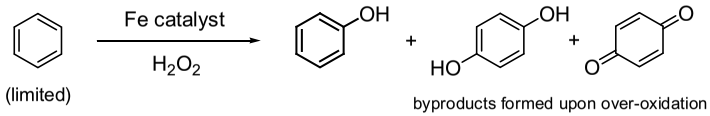

18	**14** (1)	1:100:100	25 (1.5)	18	15	83	CH_3CN	[37]
19	**14** (1)	1:150:100	25 (1.5)	28	21	75	CH_3CN	[37]
20	**14** (1)	1:250:100	25 (1.5)	31	24	77	CH_3CN	[37]
21	**14** (1)	1:350:100	25 (1.5)	25	20	80	CH_3CN	[37]
22	**14** (3)	1:83:33	25 (1.5)	28	6.0	64	CH_3CN	[37]
23	**14** (5)	1:50:20	25 (1.5)	24	3.2	67	CH_3CN	[37]
24	**14** (1)	1:250:100	25 (0.5)	12	12	99	CH_3CN	[37]
25	**14** (1)	1:250:100	25 (1)	22	17	77	CH_3CN	[37]
26	**14** (1)	1:250:100	25 (3)	28	20	71	CH_3CN	[37]
27	**14** (1)	1:250:100	25 (6)	24	17	71	CH_3CN	[37]
28	**15** (1)[d]	1:200:100	−30 (3)	2.6	2.3	88	CH_3CN	[38]
29	**15** (1)[d]	1:200:100	0 (3)	2.4	1.5	63	CH_3CN	[38]
30	**15** (1)[d]	1:200:100	25 (3)	4.0	1.0	25	CH_3CN	[38]
31	**15** (1.24)[e]	1:323:81	0 (2.5)	15.6	1.2	10	CH_3CN	[38]
32	**25** (1.24)[e]	1:323:81	0 (2.5)	14.5	2.2	19	CH_3CN	[42]

[a]Relative to C_6H_6. [b]Conditions: reaction temperature and time. [c]TN, turnover number of the catalyst = moles of the product/mol Fe. [d]Acetic acid (1 equiv with respect to benzene) was added before the reaction onset. [e]Acetic acid (10 equiv with respect to benzene) was added before the reaction onset

Table 10.4 Iron-catalyzed oxidation of toluene with H_2O_2 under substrate-limited conditions

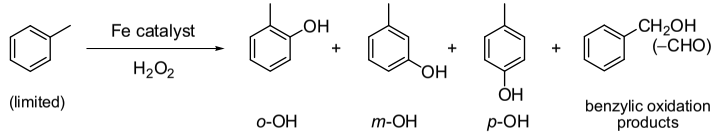

No.	Catalyst (mol% Fe)[a]	[Fe]:[H_2O_2]:[C_7H_8]	T, °C (t, h)[b]	Conv. of C_7H_8 (%)	*o*-OH, TN:*m*-OH, TN:*p*-OH, TN[c]	Aromatic oxidation selectivity (%)[d]	References
1	**7** (1)	1:100:50	25 (1)	14.7	6.4:1.1:4.1	79	[33]
2	**7** (1)	1:100:100	25 (1)	15.2	6.6:1.2:4.1	78	[33]
3	**7** (1)	1:100:200	25 (1)	15.9	7.1:1.3:4.0	78	[33]
4	**7** (1)	1:100:500	25 (1)	16.2	6.9:1.7:3.8	76	[33]
5	**7** (1)	1:100:1000	25 (1)	19.7	7.7:2.4:4.6	75	[33]
6	**7** (1)	1:100:100	0 (1)	11.8	5.5:0.6:3.4	81	[33]
7	**7** (1)	1:100:100	10 (1)	12.0	5.3:0.8:3.3	79	[33]
8	**7** (1)	1:100:100	30 (1)	15.7	6.2:1.4:4.1	74	[33]
9	**7** (1)	1:100:100	40 (1)	11.7	3.5:1.1:2.6	61	[33]
10	**7** (1)	1:100:100	50 (1)	12.4	2.8:1.0:2.3	49	[33]
11	**7** (1)	1:100:100	60 (1)	12.8	2.4:0.8:2.0	42	[33]
12	**14** (1)	1:250:100	25 (1.5)	25	10:2.5:7.5	92	[37]
13	**15** (1.24)[e]	1:323:81	0 (2.5)	20.3	0.8:–:1.1	91	[38]
14	**25** (1.24)[e]	1:323:81	0 (2.5)	26	0.8:0.4:1.7	93	[42]

[a]Relative to H_2O_2. [b]Conditions: reaction temperature and time. For solvents used, see entries with the same catalysts in Table 10.3. [c]Yields of cresols expressed in TN, turnover number of the catalyst = moles of the product/mol Fe. [d]Selectivity toward oxidation of the aromatic ring. [e]10 equiv of acetic acid (with respect to benzene) was added before the reaction onset

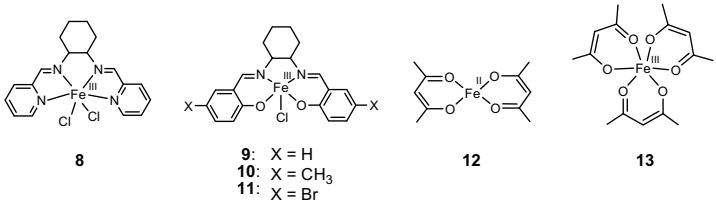

Fig. 10.3 Iron complexes with acetylacetonate and Schiff base ligands

was 1,4-benzoquinone. Extending the reaction time did not improve the phenol yield. Increasing the catalyst loading to 2 mol% did not improve the phenol yield in TN or percent (Table 10.3, entry 11), the higher catalyst load probably facilitating H_2O_2 decomposition and thus deteriorating the phenol yield. The increase in H_2O_2 amount improved the phenol yield, i.e., doubling its quantity resulted in 77 TN phenol yield (entry 12) versus 64 TN (entry 10). Iron complex **9** with the N_2O_2-donor Schiff base ligand also demonstrated good catalytic performance (55% conversion of benzene and 90% selectivity toward phenol, Table 10.3, entry 13). The introduction of electron-donating (CH_3) or electron-withdrawing (Br) groups to the iron complex **9** with the N_2O_2-donor Schiff base ligand did not improve the benzene conversion, 43 and 26 TN phenol formation being observed for catalysts **10** and **11**, respectively (Table 10.3, entries 14 and 15). The ferrous and ferric acetylacetonate complexes **12** and **13** catalyzed benzene oxidation with 96% selectivity toward phenol but showed lower efficiency (21 and 19 TN to phenol, Table 10.3, entries 16 and 17). Hence, the incorporation of nitrogen atoms into the ligand structure substantially increases the catalytic efficiency of the corresponding iron complexes (Fig. 10.3) in benzene oxidation.

Very recently, Di Stefano with coworkers designed iminopyridine ferrous complex **14** (Fig. 10.4) that can be easily prepared in situ by self-assembly of commercially available starting materials (2-picolylamine, 2-picolylaldehyde, and iron(II) triflate) [37]. Complex **14** was found to mediate catalytic benzene hydroxylation with hydrogen peroxide under mild conditions (room temperature, 1 mol% of the catalyst). At 1:1 H_2O_2/C_6H_6 ratio, benzene was oxidized with 18% conversion and 83% selectivity for phenol (Table 10.3, entry 18), *p*-benzoqinone being the only by-product. Remarkably, no products of radical coupling, such as biphenyl, were detected, suggesting that radical-driven oxygenation mechanism is not the case. The increase of the hydrogen peroxide amount up to $[H_2O_2]:[C_6H_6] = 3.5$ enhanced the phenol yield up to 24% but also increased over-oxidation to *p*-benzoqinone, slightly deteriorating phenol selectivity to 75–80% (Table 10.3, entries 19–21). The authors concluded that the best H_2O_2 amount for the catalytic benzene hydroxylation was 2.5 equiv. with respect to benzene. Increasing the catalyst loading to 3–5 mol% caused a significant loss in the phenol yield and selectivity (Table 10.3, entries 22 and 23), thus indicating that 1 mol% of Fe is the optimal catalyst loading. At higher catalyst loading, oxidative degradation of **14** may take place, reducing the catalytic efficiency and/or triggering side reactions.

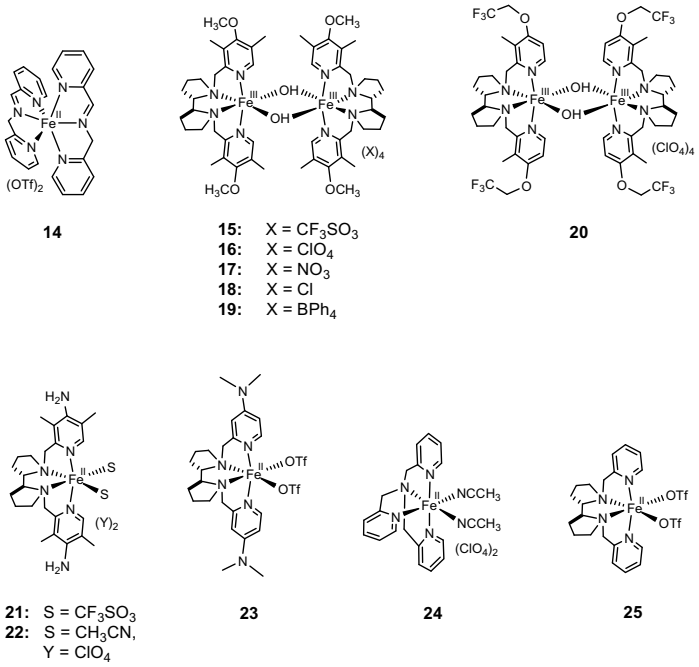

Fig. 10.4 Iron complexes that catalyze aromatic hydroxylation

The effect of the reaction time on the catalytic performance was examined. While the increase from 30 to 90 min was necessary to improve the benzene conversion (Table 10.3, entries 24, 25 and 20), further increase to 180 min or longer decreased the substrate conversion and the selectivity toward phenol (Table 10.3, entries 26 and 27). The yield of *p*-benzoquinone increased with time that is consistent with phenol over-oxidation. The obtained catalytic data outlined the following optimized conditions for the benzene hydroxylation: catalyst **14** loading 1 mol% Fe, 250 mol% H_2O_2, reaction time 90 min (conditions of entry 20 in Table 10.3). Using catalyst **14**, benzene oxidation was scaled up without loss in catalytic efficiency. The catalytic reaction was performed on a 0.5 g scale affording 26% phenol yield.

Next, the catalytic oxidation of other aromatic substrates was studied under the optimized conditions described above. Oxidation of toluene afforded a mixture of cresols as the main products with 20% yield (o:m:p = 10:2.5:7.5), along with benzaldehyde (2%) and 2-methyl-1,4-benzoquinone (3%), indicating high selectivity (92%) of catalyst **14** for aromatic over aliphatic oxidation (Table 10.4, entry 12). Achieving high chemoselectivity in the oxidation of substituted benzenes is challenging, since aliphatic chain can compete with the aromatic ring for the oxidation. The propensity for benzylic oxidation usually correlates with the energy of aliphatic C–H bonds, that is, C–H groups with lower BDE are more prone to oxidation. When ethylbenzene was used as a substrate possessing secondary aliphatic C–H bonds,

the selectivity toward the aromatic ring oxidation was, however, maintained (92%), providing 15% yield of ethylphenols with the *o*:*m*:*p* ratio of 3:1:2, 3% of 2-ethyl-1,4-benzoquinone, 1% of acetophenone, and 0.5% of 1-phenylethanol. Cumene was converted mainly to isopropylphenols (21% yield, $o:p = 1:2$). Also, the formation of 2-phenyl-2-propanol (6% yield) and 2-isopropyl-1,4-benzoquinone (3% yield) was detected, leading to 80% aromatic oxidation selectivity, which is somewhat smaller than for toluene and ethylbenzene. This is consistent with a much weaker tertiary benzylic C–H bond in cumene.

The oxidation of *tert*-butylbenzene with H_2O_2 catalyzed by complex **14** provided the best results in the series (28% yield of phenols, 3% of *tert*-butyl-1,4-benzoquinone), demonstrating 100% selectivity toward aromatic C–H oxidation. Note that in all these cases, hydroxylation on the *o*- and *p*-positions of the alkylbenzenes was favored, exhibiting a selectivity pattern resembling that for electrophilic aromatic substitutions. Fluoro-, chloro-, and bromobenzenes were smoothly oxidized with H_2O_2 to the corresponding halogenated phenols (with 9%, 17%, and 29% yield, respectively), along with some 1,4-benzoquinones (2, 3 and 4%). Halogens are *o*-/*p*-directing substituents in aromatic substitution reactions. In line with this, only *o*- and *p*-halogenophenols were observed.

Electron-withdrawing groups (such as trifluoromethyl and cyano group), deactivating the aromatic rings toward electrophiles, completely prevented the aromatic oxidation. On the contrary, anisole was oxidized with 21% yield (10% of 2-methoxyphenol, 8% of 4-methoxyphenol, and 3% of *p*-benzoquinone), since electron-donating groups increase the electron density of the aromatic ring and thus favor its oxidation. A preference for the oxidation of electron-rich aromatic rings may allow selective hydroxylation of only one aromatic ring in substrates with different aromatic rings. For example, catalyst system **14**/H_2O_2 preferentially hydroxylated the more electron-rich phenolic ring over the benzoylic moiety of phenyl benzoate, providing mainly *o*- and *p*-phenols (20, 2, and 24% yields of *o*-, *m*-, *p*-phenols) with the total conversion of 52% and the selectivity toward phenolic ring oxidation of 92%. The most electron-donating substituent was found to determine the regioselectivity in the oxidation of disubstituted benzene derivatives, 5-bromo-2-methoxyphenol being the only phenolic product obtained upon the oxidation of *p*-bromoanisole. So, the chemoselectivity of the catalytic reaction can be finely tuned by just modifying the electronic properties of substituents at the aromatic ring.

In 2018, Talsi with coworkers reported [38] the aromatic hydroxylation catalyzed by the aminopyridine diferric complex **15** that previously demonstrated high efficiency and enantioselectivity in the asymmetric alkene epoxidations [39, 40]. It is of note that a carboxylic acid (generally, acetic acid) should be present in the catalyst systems based on aminopyridine diferric complexes in order to enable catalytic oxygenation [41]. Applying catalyst **15** (1 mol% Fe) in the presence of acetic acid at the $[C_6H_6]:[H_2O_2]:[CH_3COOH]$ ratio of 1:2:1 provided only a few percent conversion of benzene. Increasing the reaction temperature from −30 to 25 °C increased benzene conversion from 2.6 TN to 4 TN, but drastically reduced the selectivity toward phenol (from 88 to 25%, Table 10.3, entries 28–30), hydroquinone being the only detected by-product. This indicates that catalyst systems based on **15** favor phenol

over-oxidation at ambient temperature, demonstrating very low substrate conversion. Thus, the reaction condition tuning is needed to improve the benzene conversion.

The increase of the oxidant and acetic acid amounts has proved useful for this purpose. When 4 equiv of H_2O_2 and 10 equiv of CH_3COOH (with respect to benzene) were applied, much higher benzene conversion was observed (15.6% with 1.24 mol% Fe). However, over-oxidation of phenol to hydroquinone became the predominant process, demonstrating 90% selectivity toward hydroquinone (Table 10.3, entry 31). Under the same conditions, 20.3% of toluene was converted into the oxidized products, 1.9 TN cresols (o:p = 3:4), 8.2 TN methylhydroquinone, and 4.9 TN 4-(hydroxymethyl)phenol being formed, giving as high as 91% selectivity toward aromatic oxidation (Table 10.4, entry 13).

Conversions and aromatic oxidation selectivities for the oxidations of different alkyl-substituted benzenes in the presence of **15** are provided in Table 10.5, left data columns. Catalyst **15** performed 10.8–13.5 TN and 23.1–30.8 TN toward the aromatic oxidation of mono- and dialkyl-substituted benzenes, respectively (the only

Table 10.5 Oxidation of substituted benzenes with H_2O_2 catalyzed by biomimetic aminopyridine iron complexes **15** and **25**[a]

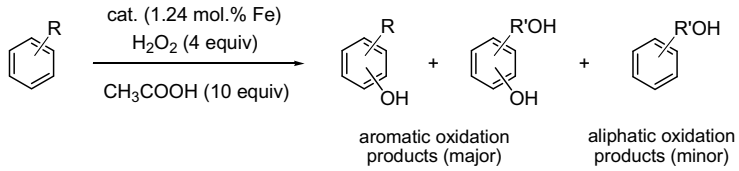

No.	Substrate	Catalyst **15**			Catalyst **25**		
		Conv. (%)	Aromatic oxidation yield, TN[b]	Aromatic oxidation selec. (%)[c]	Conv. (%)	Aromatic oxidation yield, TN[b]	Aromatic oxidation selec. (%)[c]
1	ethylbenzene	20.5	13.5	82	27	18.9	86
2	cumene	17.0	10.9	80	15.5	10.4	83
3	isobutylbenzene	16.9	10.8	79	25.5	18.2	89
4	*o*-xylene	32.2	23.1	88	34.5	25.3	91
5	*m*-xylene				57.5	42.5	91
6	*p*-xylene	36.5	30.8	84	51.5	38.3	92
7	2-ethyltoluene	21.7	14.4	66	32	17.4	68
8	3-ethyltoluene	33.8	28.4	84	41	27.0	76
9	4-ethyltoluene	29.4	25.1	85	33	19.9	74

[a]Reaction conditions: 100 μmol of substrate, 400 μmol of H_2O_2, 1000 μmol of CH_3COOH, catalyst loading 1.24 μmol Fe (1.24 mol%), 0 °C, reaction time 2.5 h, solvent CH_3CN [38]. [b]Yield expressed in TN, turnover number of the catalyst = moles of products/mol Fe. [c]Selectivity toward oxidation of the aromatic ring, including products simultaneously oxygenated at aromatic and aliphatic positions

exception was 2-ethyltoluene which demonstrated only 14.4 TN yield of aromatic oxidation products). In the latter case, the yields were higher, since dialkylbenzenes are more electron-rich than monoalkylbenzenes. Again, for dialkylbenzenes, higher selectivities toward aromatic oxidation were documented (84–88%), compared with those for monoalkylbenzenes (79–82%), except the 66% selectivity for 2-ethyltoluene (Table 10.5).

Soon after, Bryliakov with coworkers undertook a systematic study of iron complexes with aminopyridine ligands, bearing different substituents at pyridine rings, and different counteranions, in the aromatic oxidation of a variety of substituted benzenes [42]. The effect of counteranion on the catalytic properties of aminopyridine diiron complexes in the oxidation of *o*-xylene has been studied (**15**–**19**, Fig. 10.4).

Triflate complex **15** demonstrated the best catalytic performance in the series, yielding 32.2% conversion of *o*-xylene with 88% selectivity toward aromatic oxidation (Table 10.6, entry 1). Perchlorate complex **16** exhibited slightly lower catalytic activity (22.5% conversion) and selectivity (77%, Table 10.6, entry 2). Complexes with NO_3, Cl, and BPh_4 counteranions proved to be much less efficient and selective (Table 10.6, entries 3–5). A similar counteranion effect was observed for complexes **21** and **22** (Table 10.6, entries 7 and 8). Interestingly, in the presence of an amino group instead of a methoxy group, virtually the same efficiency and selectivity were observed (compare complexes **21**, **22** and **15**, **16** in Table 10.6). Diferric complex **20** (Fig. 10.4), bearing 3-methyl and 4-trifluoroethoxy substituents at the pyridine ring of the common PDP core, demonstrated results similar to those of the parent complex **15** with 3,5-dimethyl and 4-methoxy groups (Table 10.6, entries 1 versus 6). Complex **23** of the Fe-PDP series, possessing NMe_2 groups, appeared to be less efficient (Table 10.6, entry 9), as well as the Fe(TPA) complex **24** (Table 10.6, entry 10). The parent complex **25** appeared to be the most active and selective catalyst in the series of Fe-PDP type complexes, affording 34.5% conversion of *o*-xylene and 91% selectivity toward oxidation of the aromatic ring (Table 10.6, entry 11).

Further, complex **25** was studied in the catalytic oxidation of benzene, toluene, and different alkyl-substituted benzenes under the previously identified optimized catalytic conditions (1.24 mol% Fe, [arene]:[H_2O_2]:[CH_3COOH] = 1:4:10, 0 °C). The oxidation of benzene, catalyzed by complex **25** afforded predominantly hydroquinone (9.6 TN), with only 19% phenol selectivity (Table 10.3, entry 32). Hence, Fe-PDP complexes **15** and **25** (Fig. 10.4) demonstrate very close activities in the benzene oxidation (entries 31 and 32). The same is true for toluene, the latter complex exhibiting higher conversion (26% versus 20.3%, Table 10.4, entries 13 and 14). For both complexes, similar toluene aromatic oxidations selectivities were documented (91% and 93%, respectively). For some alkyl-substituted benzenes, much higher conversions were observed (up to 57.5% for *m*-xylene), along with high selectivity toward aromatic oxidation (up to 91–92% for *o*-, *m*-, *p*-xylenes, Table 10.5, right data columns). As a general trend, the conversions of dialkylbenzenes were higher than those of monoalkylbenzenes, that is consistent with the increasing electrophilicity of the aromatic ring bearing electron-donating alkyl substituents.

Previously, the structure of carboxylic acid was reported to have a dramatic effect on the catalytic performance of iron aminopyridine complexes in the asymmetric

Table 10.6 Catalytic oxidation of *o*-xylene with H_2O_2 in the presence of biomimetic aminopyridine iron complexes[a]

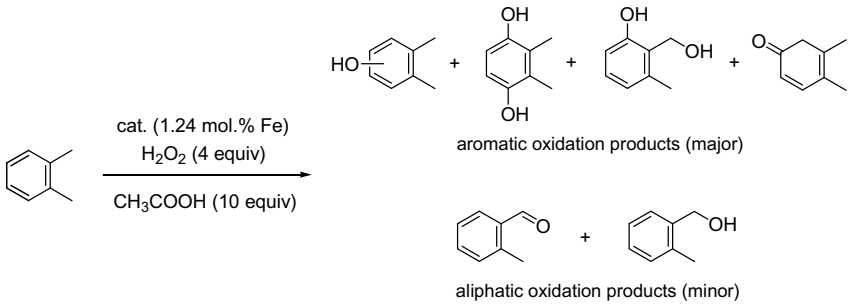

No.	Catalyst	Conversion of *o*-xylene (%)	Aromatic oxidation product yields, TN[b]	Selectivity for aromatic oxidation (%)[c]
1	**15**	32.2	23.1	88
2	**16**	22.5	14.0	77
3	**17**	5.7	3.0	65
4	**18**	2.8	1.2	52
5	**19**	3.8	1.7	55
6	**20**	22	13.8	78
7	**21**	32.5	20.4	78
8	**22**	21	12.9	75
9	**23**	13.5	8.1	72
10	**24**	10	5.3	67
11	**25**	34.5	25.3	91

[a]Reaction conditions: 100 μmol of *o*-xylene, 400 μmol of H_2O_2, 1000 μmol of CH_3COOH, catalyst loading 1.24 μmol Fe (1.24 mol%), 0 °C, reaction time 2.5 h, solvent CH_3CN. [b]Yield expressed in TN, turnover number of the catalyst = moles of products/mol Fe. [c]Selectivity toward oxidation of the aromatic ring, including products simultaneously oxygenated at aromatic and aliphatic positions [42]

olefin epoxidation reactions [39, 43]. Bryliakov with coworkers studied the effect of different carboxylic acid additives on the efficiency and selectivity of aromatic hydrocarbon oxidations, mediated by Fe-PDP complexes [44]. First, different carboxylic acids (Fig. 10.5) were tested in the oxidation of *m*-xylene, catalyzed by complex **25**,

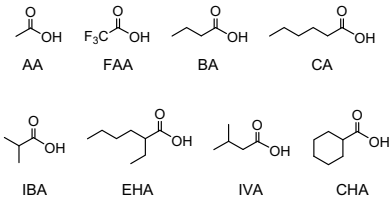

Fig. 10.5 Carboxylic acids used as the catalytic additives in the iron-catalyzed aromatic hydrocarbon oxidation

since this substrate/catalyst combination provided the highest conversion and aromatic oxidation selectivity among the aminopyridine iron-catalyzed aromatic oxidations (Table 10.5). In the presence of the strongest trifluoroacetic acid, *m*-xylene demonstrated negligible conversion (1.6%, Table 10.7, entry 1)—even lower than without added carboxylic acid (8%, entry 9). The use of branched carboxylic acids (IBA, IVA, and EHA) resulted in a higher *m*-xylene conversion (up to 75–98%, Table 10.7, entries 6–8), compared with linear acids and cyclohexanecarboxylic acid (17.5–67%, entries 2–5). Similarly, the selectivity for aromatic ring oxidation was higher with the use of branched acids. In the case of isovaleric and 2-ethylhexanoic acids, the aromatic oxidation selectivity exceeded 99% (entries 7 and 8). Thus, 2-ethylhexanoic acid proved to be the best carboxylic acid additive, ensuring the highest conversion of *m*-xylene (98.3%) and selectivity (>99%) at the same time.

Table 10.7 Oxidation of *m*-xylene with H_2O_2 catalyzed by complex **25** in the presence of different carboxylic acids[a]

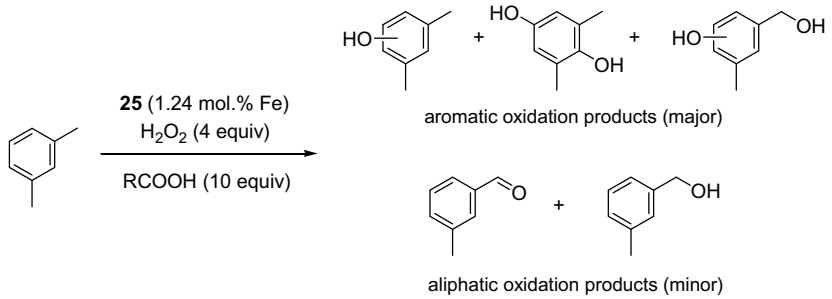

No.	Carboxylic acid additive	Conversion of *m*-xylene (%)	Aromatic oxidation product yields, TN[b]	Selectivity for aromatic oxidation (%)[c]
1	FAA	1.6	0.8	62
2	AA	67	49.4	98
3	CA	17.5	13.0	96
4	BA	46.4	34.8	99
5	CHA	31	22.5	99
6	IBA	75.1	56.0	99
7	IVA	83.3	61.9	>99
8	EHA	98.3	77.8	>99
9	– [d]	8.0	5.3	55

[a]Reaction conditions: 100 μmol of *m*-xylene, 400 μmol of H_2O_2, 1000 μmol of CH_3COOH, catalyst loading 1.24 μmol Fe (1.24 mol%), 0 °C, reaction time 3 h, solvent CH_3CN. [b]Yield expressed in TN, turnover number of the catalyst = moles of products/mol Fe. [c]Selectivity toward oxidation of the aromatic ring, including products simultaneously oxygenated at aromatic and aliphatic positions [44]. [d] Carboxylic acid was not added; 3 mmol of exogenous H_2O was present in the reaction mixture from the beginning of the reaction.

In conclusion, to date, the highest conversion (77% or 77 TN) and phenol selectivity (almost 100%, Table 10.3, entry 12) in the iron-catalyzed benzene oxidation with H_2O_2 has been obtained with the complex **8** bearing N_4-donor Schiff base ligand (Fig. 10.3) studied by Silva and Carneiro [36]. The highest efficiency and selectivity toward aromatic oxidation of alkyl-substituted benzenes have been reported by Brylaikov and coworkers: *m*-xylene was oxidized with H_2O_2 in the presence of aminopyridine iron complex **25** (Fig. 10.4) and 2-ethylhexanoic acid, demonstrating 98.3% conversion and virtually 100% selectivity toward the aromatic ring oxidation (Table 10.7, entry 8) [44].

10.3 Active Species of Iron-Catalyzed Oxidation of Aromatic C–H Groups

The search for novel perspective catalyst systems requires a deep understanding of catalytic reaction mechanisms. Getting deep insight into the nature of active sites and the overall oxidation mechanism is crucial for the rational design of efficient and chemoselective iron-based catalyst systems for the aromatic hydroxylation. However, in situ investigation of active species of this catalytic process is a very difficult task, due to very low concentration and extremely high reactivity of active species.

A number of studies have been undertaken in order to shed light on the mechanism of the aromatic hydroxylation catalyzed by biomimetic iron complexes under substrate-limited conditions. In the majority of studies, the authors were unable to directly observe active species of the aromatic hydroxylation and utilized indirect methods such as isotopic labeling studies (using fully or particularly deuterated substrates and $H_2^{18}O$), addition of radical scavengers, comparison of chemo- and regioselectivity patterns in the oxidation of different arenes, and DFT calculations [32, 33, 37, 45]. In some cases, ferric precursors of putative active species were monitored by UV-Vis and EPR spectroscopy [28, 46].

Gratifyingly, Talsi with coworkers managed to trap the iron(V)-oxo reactive intermediate **15a**, formed upon the interaction of aminopyridine diferric complex **15**, hydrogen peroxide, and acetic acid (molar ratio of 1:6:20) at very low temperature (−75 … −85 °C) by EPR spectroscopy [41]. On the basis of the characteristic EPR parameters ($g_1 = 2.07$, $g_2 = 2.01$, $g_3 = 1.96$) of **15a** and its high reactivity toward olefin epoxidation, virtually identical to those for previously characterized oxoiron(V) complexes [47, 48], **15a** has been assigned to the low-spin ($S = 1/2$) iron(V)-oxo species (Fig. 10.6) [41].

In 2018, Talsi and coworkers observed structurally similar intermediates **15a** and **15b** at −70 °C in the systems **15**/peracetic acid/acetic acid and **15**/peracetic acid/2-ethylhexanoic acid, respectively [38]. These species were found to be very unstable even at −70 °C, demonstrating half-life time of 5–7 min. The application of peracetic acid proved to produce iron(V)-oxo species in 10-fold higher concentration compared with H_2O_2-containing systems (the maximum observed concentration of

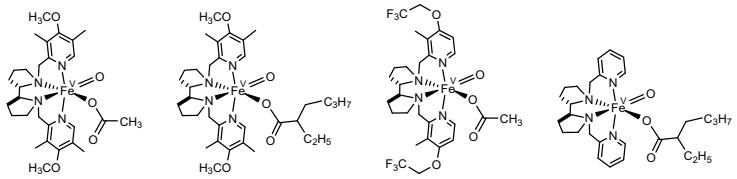

Fig. 10.6 Proposed structures of the active perferryl intermediates of aromatic hydroxylations [38, 42, 44]

ca. 10% versus 1% with respect to the total iron concentration). This allowed direct evaluation of the reactivity of nonheme iron(V)-oxo intermediates toward aromatic C−H oxidation at −70 °C. The second-order rate constants k_2 for the reaction of the number of substituted benzenes with **15a** and **15b** were determined. For more electron-rich arenes, much higher k_2 values have been observed, increasing in the order nitrobenzene < acetophenone < chlorobenzene < benzene < toluene. For the last two substrates, very rapid oxidation by oxoiron species occurred, thus allowing only rough estimation of the second-order rate constant ($k_2 > 10\ M^{-1}\ s^{-1}$). For nitrobenzene, acetophenone, and chlorobenzene, the rates of the interaction with **15a** and **15b** were determined more precisely (3.4×10^{-3} and $1 \times 10^{-3}\ M^{-1}s^{-1}$, 0.25 and $0.16\ M^{-1}s^{-1}$, 6 and $2\ M^{-1}s^{-1}$, respectively). A somewhat lower reactivity of **15b** may be caused by the more sterically hindered 2-ethylhexanoate moiety, in comparison with the acetate moiety of **15a**. Close values of the phenol yield, predicted from the kinetic data and the experimental phenol yield measured by GC at −70 °C, supported the key role of the iron(V)-oxo species in the aromatic hydroxylation catalyzed by aminopyridine iron complex **15**. The above data, as well as an inverse kinetic isotope effect ($k_H/k_D = 0.9$), is consistent with the electrophilic aromatic substitution mechanism of arene hydroxylation by the catalyst system **15**/H_2O_2 [38].

Shortly after, Bryliakov and coworkers trapped a similar oxoiron(V) active species **20a** (Fig. 10.6) [42]. The observed pseudo-first-order rate constant of the decay of intermediate **20a** at −85 °C dramatically increased in the presence of benzene (0.02 M), thus providing the opportunity to evaluate the second-order rate constant for the direct reaction of **20a** with benzene ($k_2 \sim 5\ M^{-1}\ s^{-1}$).

Finally, the active species of the best aromatic oxidation catalyst system based on complex **25** and EHA was probed by in situ EPR spectroscopy. It has been clearly established that the iron(V)-oxo intermediate **25b** (Fig. 10.6) with characteristic EPR parameters ($g_1 = 2.07$, $g_2 = 2.01$, $g_3 = 1.96$) is the active species responsible for the oxidation of aromatic C−H groups catalyzed by Fe-PDP complex **25** [44]. Species **25b** directly reacted with benzene at −80 °C ($k_2 = 0.6\ M^{-1}\ s^{-1}$) and with toluene ($k_2 > 1\ M^{-1}\ s^{-1}$), thus giving strong evidence for its key role in the selective oxygenation of aromatic substrates.

10.4 Summary and Outlook

Direct selective hydroxylation of aromatic C–H groups is a particularly challenging task of synthetic chemistry. This process requires catalyst systems, at the same time exhibiting high reactivity toward very strong aromatic C–H bonds and tolerating aliphatic side chains of alkylarenes; high resistance to self-oxidation is needed, too. Biomimetic philosophy, based on modeling the functional properties of natural oxygenases using relatively simple iron complexes, is considered as a promissory approach for designing catalyst systems for the direct aromatic hydroxylation.

To date, there have been no reports on catalyst systems for the aerobic selective C–H oxidation of arenes (aside from phenols). The most likely reason for this is the absence of catalysts, capable of activating dioxygen molecule via a heterolytic pathway, which is a prerequisite for achieving high C–H oxidation selectivity. Designing such catalysts, desirably requiring no sacrificial co-reductants, has been a longstanding target of biomimetic catalysis, which so far has no general solution.

At the same time, iron-catalyzed biomimetic aromatic C–H oxidations with hydrogen peroxide have demonstrated appreciable progress in the last 10–15 years. A number of synthetic iron complexes have been synthesized and studied in the oxidation of benzene and alkylarenes with the environmentally friendly oxidant H_2O_2. The vast majority of the reported catalyst systems demonstrated moderate catalytic efficiency in the C–H oxidation of arenes ($\leq$25 TN), although high aromatic oxidation selectivities (up to 99%) have been occasionally observed.

Gratifyingly, in 2018, novel iron aminopyridine-based catalyst systems were reported, capable of conducting the oxidation of alkyl-substituted benzenes with H_2O_2 with >98% substrate conversion (150 TN) and virtually 100% aromatic oxidation selectivity. The active species of aromatic C–H hydroxylation in these systems have been trapped using in situ EPR spectroscopy, and their reactivities toward aromatic substrates have been evaluated. On the basis of the EPR and reactivity data, the active species were identified as perferryl complexes of the type $[(L)Fe^{V} = O(OC(O)R)]^{2+}$ (L = aminopyridine N_4-donor ligand, RCOOH = acetic or 2-ethylhexanoic acid).

Further studies, focused on designing more efficient catalyst systems with improved productivity, oxidant efficiency, and selectivity toward particular oxygenated products, as well as on detailed mechanisms of C–H oxidation, are foreseen.

Acknowledgements Lyakin O.Y. thanks the Russian Foundation for Basic Research, project 18-33-20078, for financial support.

References

1. Sheldon RA, Arends IWCE, Hanefeld U (2007) Green chemistry and catalysis. Wiley-VCH, Weinheim
2. Bryliakov KP (2017) Catalytic asymmetric oxygenations with the environmentally benign oxidants H_2O_2 and O_2. Chem Rev 117(17):11406–11459. https://doi.org/10.1021/acs.chemrev.7b00167
3. Sun CL, Li BJ, Shi ZJ (2011) Direct C–H transformation via iron catalysis. Chem Rev 111(3):1293–1314. https://doi.org/10.1021/cr100198w
4. Talsi EP, Bryliakov KP (2012) Chemo- and stereoselective C–H oxidations and epoxidations/cis-dihydroxylations with H_2O_2, catalyzed by non-heme iron and manganese complexes. Chem Soc Rev 256(13–14):1418–1434. https://doi.org/10.1016/j.ccr.2012.04.005
5. Cussó O, Ribas X, Costas M (2015) Biologically inspired non-heme iron-catalysts for asymmetric epoxidation; design principles and perspectives. Chem Commun 51:14285–14298. https://doi.org/10.1039/c5cc05576h
6. Olivo G, Cussó O, Costas M (2016) Biologically inspired C–H and C=C oxidations with hydrogen peroxide catalyzed by iron coordination complexes. Chem Asian J 11(22):3148–3158. https://doi.org/10.1002/asia.201601170
7. Weber M, Weber M, Kleine-Boymann M (2004) Phenol. In: Ullmann's encyclopedia of industrial chemistry, vol. 26. Wiley-VCH, Weinheim, pp 503–519. https://doi.org/10.1002/14356007.a19_299.pub2
8. Fiege H (2000) Cresols and xylenols. In: Ullmann's encyclopedia of industrial chemistry, vol. 10. Wiley-VCH, Weinheim, pp 419–461. https://doi.org/10.1002/14356007.a08_025
9. Davico GE, Bierbaum VM, DePuy CH, Barney Ellison G, Squires RR (1995) The C–H bond energy of benzene. J Am Chem Soc 117(9):2590–2599. https://doi.org/10.1021/ja00114a023
10. Cornils B, Herrmann WA (2003) Concepts in homogeneous catalysis: the industrial view. J Catal 216(1–2):23–31. https://doi.org/10.1016/S0021-9517(02)00128-8
11. Si Niwa, Eswaramoorthy M, Nair J, Raj A, Itoh N, Shoji H, Namba Y, Mizukami F (2002) A one-step conversion of benzene to phenol with a palladium membrane. Science 295(5552):105–107. https://doi.org/10.1126/science.1066527
12. Enthaler S, Company A (2011) Palladium-catalysed hydroxylation and alkoxylation. Chem Soc Rev 40(10):4912–4924. https://doi.org/10.1039/c1cs15085e
13. Tanev PT, Chlbwe M, Pinnavaia TJ (1994) Titanium-containing mesoporous molecular sieves for catalytic oxidation of aromatic compounds. Nature 368:321–323. https://doi.org/10.1038/368321a0
14. Lücke B, Narayana KV, Martin A, Jähnisch K (2004) Oxidation and ammoxidation of aromatics. Adv Synth Catal 346(12):1407–1424. https://doi.org/10.1002/adsc.200404027
15. Kamata K, Yamaura Y, Mizuno N (2012) Chemo- and regioselective direct hydroxylation of arenes with hydrogen peroxide catalyzed by a divanadium-substituted phosphotungstate. Angew Chem Int Ed 51(29):7275–7278. https://doi.org/10.1002/anie.201201605
16. Morimoto Y, Bunno S, Fujieda N, Sugimoto H, Itoh S (2015) Direct hydroxylation of benzene to phenol using hydrogen peroxide catalyzed by nickel complexes supported by pyridylalkylamine ligands. J Am Chem Soc 137(18):5867–5870. https://doi.org/10.1021/jacs.5b01814
17. Wienhöfer G, Schröder K, Möller K, Junge K, Beller M (2010) A novel process for selective ruthenium-catalyzed oxidation of naphthalenes and phenols. Adv Synth Catal 352(10):1615–1620. https://doi.org/10.1002/adsc.201000137
18. Roslan N, Endud S, Ramli Z, Lintang HO (2016) Copper(II) porphyrin as biomimetic catalyst for oxidation of trimethylphenol. Mater Sci Forum 846:706–711. https://doi.org/10.4028/www.scientific.net/MSF.846.706
19. Ullrich R, Hofrichter M (2007) Enzymatic hydroxylation of aromatic compounds. Cell Mol Life Sci 64(3):271–293. https://doi.org/10.1007/s00018-007-6362-1
20. Mansuy D, Battioni P (1999) Dioxygen activation at heme centers in enzymes and synthetic analogs. In: Reedijk J, Bouwman E (eds) Bioinorganic catalysis, 2nd edn. Marcel Dekker, New York, pp 323–354. https://doi.org/10.1201/9780203908457

21. Denisov IG, Makris TM, Sligar SG, Schlichting I (2005) Structure and chemistry of cytochrome P450. Chem Rev 105(6):2253–2277. https://doi.org/10.1021/cr0307143
22. Ortiz de Montellano PR (2015) Substrate oxidation by cytochrome P450 enzymes. In: Ortiz de Montellano PR (ed) Cytochrome P450 structure, mechanism and biochemistry, 4th edn. Springer, Heidelberg, pp 111–176. https://doi.org/10.1007/978-3-319-12108-6
23. Green J, Dalton H (1989) Substrate specificity of soluble methane monooxygenase. Mechanistic implications. J Biol Chem 264(30):17698–17703
24. Lipscomb JD (1994) Biochemistry of the soluble methane monooxygenase. Annu Rev Microbiol 48:371–399
25. Whited GM, Gibson DT (1991) Toluene-4-monooxygenase, a three-component enzyme system that catalyzes the oxidation of toluene to p-cresol in Pseudomonas mendocina KR1. J Bacteriol 173(9):3010–3016. https://doi.org/10.1128/jb.173.9.3010-3016.1991
26. Tao Y, Fishman A, Bentley WE, Wood TK (2004) Altering toluene 4-monooxygenase by active-site engineering for the synthesis of 3-methoxycatechol, methoxyhydroquinone, and methylhydroquinone. J Bacteriol 186(14):4705–4713. https://doi.org/10.1128/JB.186.14.4705-4713.2004
27. Mitchell KH, Rogge CE, Gierahn T, Fox BG (2003) Insight into the mechanism of aromatic hydroxylation by toluene 4-monooxygenase by use of specifically deuterated toluene and p-xylene. Proc Natl Acad Sci 100(7):3784–3789. https://doi.org/10.1073/pnas.0636619100
28. Kejriwal A, Bandyopadhyay P, Biswas AN (2015) Aromatic hydroxylation using an oxo-bridged diiron(III) complex: a bio-inspired functional model of toluene monooxygenases. Dalton Trans 44(39):17261–17267. https://doi.org/10.1039/c5dt01773d
29. Bartoli JF, Lambert F, Morgenstern-Badarau I, Battioni P, Mansuy D (2002) Unusual efficiency of a non-heme iron complex as catalyst for the hydroxylation of aromatic compounds by hydrogen peroxide: comparison with iron porphyrins. C R Chimie 5(4):263–266. https://doi.org/10.1016/S1631-0748(02)01375-9
30. Bianchi D, Bertoli M, Tassinari R, Ricci M, Vignola R (2003) Direct synthesis of phenols by iron-catalyzed biphasic oxidation of aromatic hydrocarbons with hydrogen peroxide. J Mol Catal A: Chem 200(1–2):111–116. https://doi.org/10.1016/S1381-1169(03)00041-4
31. Bianchi D, Bertoli M, Tassinari R, Ricci M, Vignola R (2003) Ligand effect on the iron-catalysed biphasic oxidation of aromatic hydrocarbons by hydrogen peroxide. J Mol Catal A: Chem 204–205:419–424. https://doi.org/10.1016/S1381-1169(03)00323-6
32. Thibon A, Bartoli JF, Guillot R, Sainton J, Martinho M, Mansuy D, Banse F (2008) Non-heme iron polyazadentate complexes as catalysts for aromatic hydroxylation by H_2O_2: particular efficiency of tetrakis(2-pyridylmethyl) ethylenediamine–iron(II) complexes. J Mol Catal A: Chem 287(1–2):115–120. https://doi.org/10.1016/j.molcata.2008.03.006
33. Raba A, Cokoja M, Herrmann WA, Kühn FE (2014) Catalytic hydroxylation of benzene and toluene by an iron complex bearing a chelating di-pyridyl-di-NHC ligand. Chem Commun 50:11454–11457. https://doi.org/10.1039/c4cc02178a
34. Rogers MM, Stahl SS (2007) N-Heterocyclic carbenes as ligands for high-oxidation-state metal complexes and oxidation catalysis. Top Organomet Chem 21:21–46. https://doi.org/10.1007/3418_025
35. Strassner T (2007) The role of NHC ligands in oxidation catalysis. Top Organomet Chem 22:125–148. https://doi.org/10.1007/3418_040
36. Carneiro L, Silva AR (2016) Selective direct hydroxylation of benzene to phenol with hydrogen peroxide by iron and vanadyl based homogeneous and heterogeneous catalysts. Catal Sci Technol 6(22):8166–8176. https://doi.org/10.1039/c6cy00970k
37. Capocasa G, Olivo G, Barbieri A, Lanzalunga O, Di Stefano S (2017) Direct hydroxylation of benzene and aromatics with H_2O_2 catalyzed by a self-assembled iron complex: evidence for a metal-based mechanism. Catal Sci Technol 7(23):5677–5686. https://doi.org/10.1039/c7cy01895a
38. Lyakin OY, Zima AM, Tkachenko NV, Bryliakov KP, Talsi EP (2018) Direct evaluation of the reactivity of nonheme iron(V)−pxo intermediates toward arenes. ACS Catal 8(6):5255–5260. https://doi.org/10.1021/acscatal.8b00661

39. Zima AM, Lyakin OY, Ottenbacher RV, Bryliakov KP, Talsi EP (2016) Dramatic effect of carboxylic acid on the electronic structure of the active species in Fe(PDP)-catalyzed asymmetric epoxidation. ACS Catal 6(8):5399–5404. https://doi.org/10.1021/acscatal.6b01473
40. Zima AM, Lyakin OY, Ottenbacher RV, Bryliakov KP, Talsi EP (2017) Iron-catalyzed enantioselective epoxidations with various oxidants: evidence for different active species and epoxidation mechanisms. ACS Catal 7(1):60–69. https://doi.org/10.1021/acscatal.6b02851
41. Lyakin OY, Zima AM, Samsonenko DG, Bryliakov KP, Talsi EP (2015) EPR spectroscopic detection of the elusive Fe^{V}=O intermediates in selective catalytic oxofunctionalizations of hydrocarbons mediated by biomimetic ferric complexes. ACS Catal 5(5):2702–2707. https://doi.org/10.1021/acscatal.5b00169
42. Tkachenko NV, Ottenbacher RV, Lyakin OY, Zima AM, Samsonenko DG, Talsi EP, Bryliakov KP (2018) Highly efficient aromatic C–H oxidation with H_2O_2 in the presence of iron complexes of the PDP family. ChemCatChem 10(18):4052–4057. https://doi.org/10.1002/cctc.201800832
43. Lyakin OY, Ottenbacher RV, Bryliakov KP, Talsi EP (2012) Asymmetric epoxidations with H_2O_2 on Fe and Mn aminopyridine catalysts: Probing the nature of active species by combined electron paramagnetic resonance and enantioselectivity study. ACS Catal 2(6):1196–1202. https://doi.org/10.1021/10.1021/cs300205n
44. Tkachenko NV, Lyakin OY, Zima AM, Talsi EP, Bryliakov KP (2018) Effect of different carboxylic acids on the aromatic hydroxylation with H_2O_2 in the presence of an iron aminopyridine complex. J Organomet Chem 871:130–134. https://doi.org/10.1016/j.jorganchem.2018.07.016
45. Lindhorst AC, Drees M, Bonrath W, Schütz J, Netscher T, Kühn FE (2017) Mechanistic insights into the biomimetic catalytic hydroxylation of arenes by a molecular Fe(NHC) complex. J Catal 352:599–605. https://doi.org/10.1016/j.jcat.2017.06.018
46. Makhlynets OV, Rybak-Akimova EV (2010) Aromatic hydroxylation at a non-heme iron center: Observed intermediates and insights into the nature of the active species. Chen Eur J 16(47):13995–14006. https://doi.org/10.1002/chem.201002577
47. Van Heuvelen KM, Fiedler AT, Shan X, De Font RF, Meier KK, Bominaar EL, Münck E, Que L Jr (2012) One-electron oxidation of an oxoiron(IV) complex to form an $[O{=}Fe^{V}{=}NR]^{+}$ center. Proc Natl Acad Sci USA 109(30):11933–11938. https://doi.org/10.1073/pnas.1206457109
48. Serrano-Plana J, Oloo WN, Acosta-Rueda L, Meier KK, Verdejo B, García-España E, Basallote MG, Münck E, Que L Jr, Company A, Costas M (2015) Trapping a highly reactive nonheme iron intermediate that oxygenates strong C–H bonds with stereoretention. J Am Chem Soc 137(50):15833–15842. https://doi.org/10.1021/jacs.5b09904

Chapter 11
Catalytic Asymmetric C–H Oxidation with H_2O_2 and O_2

Konstantin P. Bryliakov

Abstract This chapter surveys the existing catalyst systems, either organocatalytic or metal-based, for the chemo- and stereoselective oxidation of C–H groups with the environmentally benign oxidants H_2O_2 and O_2, reported in the last 30 years. Both the approaches relying on "classical" asymmetric oxidation and oxidative desymmetrization of complex substrates are considered, with focus on the catalytic properties of the catalysts, such as chemo- and stereoselectivity, activity, efficiency, and substrate scope. Currently available data on the nature of the catalytically active sites, the mechanisms of oxidant activation and C–H activation, and of oxygen transfer, are presented.

Keywords Asymmetric oxidation · C–H oxidation · Dioxygen · Homogeneous catalysis · Hydrogen peroxide · Mechanism

11.1 Introduction

In the last decades, predictably selective catalytic oxidation of C–H groups of complex organic molecules has been regarded as one of the most urgent topics of synthetic chemistry [1–4], which encouraged active search for designing novel catalyst systems, both organocatalytic and metal-based, for these challenging transformations. Direct C–H oxidations, occurring without intermediate formation of C-metal bonds, have attracted great interest in the oxidation of challenging substrates like alkanes that contain no π-electrons and thus are not prone to coordinating to the catalyst (which stage is indispensable for subsequent formation of organometallic intermediate) [5, 6]. Catalyzed C–H oxidations of various substrates by environmentally benign oxidants H_2O_2 and O_2 are considered in Chaps. 1, 2, 9 and 10. Herewith, we

K. P. Bryliakov (✉)
Novosibirsk State University, Pirogova 2, Novosibirsk 630090, Russian Federation
e-mail: bryliako@catalysis.ru

Boreskov Institute of Catalysis, Pr. Lavrentieva 5, Novosibirsk 630090, Russian Federation

K. P. Bryliakov (ed.), *Frontiers of Green Catalytic Selective Oxidations*,
Green Chemistry and Sustainable Technology,
https://doi.org/10.1007/978-981-32-9751-7_11

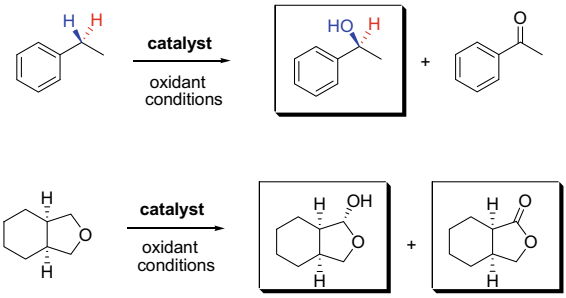

Fig. 11.1 Examples of catalyzed asymmetric oxidation of CH_2 groups with enantiotopic hydrogen atoms (top) and oxidative desymmetrization (bottom) of prochiral substrates. Bottom sketch: both the lactol and lactone products are chiral

overview direct C–H oxidations in the presence of chiral catalysts, occurring with generation of asymmetric induction in the course of the oxidative transformation.

In this chapter, we survey in detail only those asymmetric catalytic C–H oxidations that comply with the Henry Kagan's definition (i.e., those occurring with control of the enantioselective reaction by a chiral catalyst [7]). Both the approaches relying on asymmetric oxidation of CH_2 groups with enantiotopic hydrogens and catalyzed oxidative desymmetrization are considered; in the latter case new C*–O asymmetric centers are not necessarily created, the asymmetric induction being generated as a result of loss of symmetry elements of prochiral substrates (Fig. 11.1). Enantio- and diastereospecific catalytic reactions, occurring without creation of new centers of chirality, and diastereoselective reactions on chiral substrates involving a chiral catalyst are not covered. Biocatalytic asymmetric oxidations are excluded from consideration, too.

In the last three decades, various transition metal-based catalyst systems, capable of oxidizing prochiral substrates with different oxidants (typically 2,6-dichloropyridine *N*-oxide, iodosylarenes, or iodobenzene diacetate) in a stereoselective fashion, have been reported [8–19]. However, it is only in the last few years that transition metal-based catalyst systems emerged, capable of mediating enantioselective C–H oxidations with the environmentally benign oxidant hydrogen peroxide. Within similar timeframe, the asymmetric organocatalytic α-hydroxylation of carbonyl compounds with dioxygen was developing. The latter area is also overviewed in this chapter.

Catalytic properties, i.e., activity, chemo- and stereoselectivity, efficiency, and substrate scope, are the major focus of this contribution. At the same time, given the importance of establishing the mechanisms of stereoselective C–H activation and oxygen transfer, as well as the mechanisms of activation of the oxidants, H_2O_2 or O_2, available mechanistic details of these transformations are discussed briefly.

11.2 Organocatalytic α-Hydroxylation of Carbonyl Compounds

In 1988, Shiori with coworkers pioneered the enantioselective α-hydroxylation of carbonyl compounds with molecular oxygen in the presence of chiral phase-transfer catalysts (CPTC)—quaternary ammonium salts, derived from either cinchona alkaloids (cinchonine and cinchonidine) or from ephedrine and cyclohexanediamine [20]. Cinchonine derived compounds of type **1** (Fig. 11.2) were identified as the best catalysts in the series (**1a**–**1d**) for the asymmetric hydroxylation of 2-alkyltetralones and

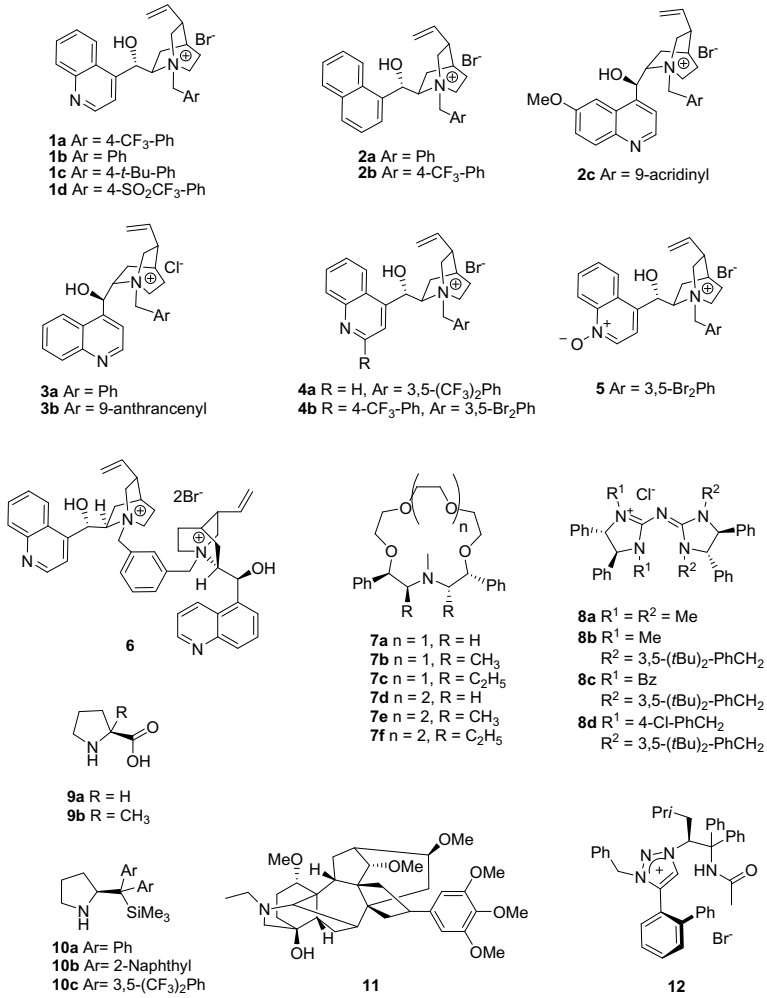

Fig. 11.2 Phase-transfer catalysts for the aerobic α-hydroxylation of carbonyl compounds

2-alkylindanones (up to 98% yield and up to 79% *ee*); some examples are presented in Fig. 11.3. The reaction required 5 mol% catalyst loading and 50% aqueous NaOH solution (the alkali served to deprotonate the substrate and so initiate molecular oxygen capture), and typically proceeded within 5–48 h.

The reaction proceeded via oxidation of the tertiary C–H group with oxygen to the corresponding hydroperoxide; the latter was in situ reduced with excess of triethylphosphite $(EtO)_3P$ to the target α-hydroxy carbonyl compound. It was proposed that the asymmetric induction originated from ion pairing between the CPTC and the substrate (Fig. 11.4) [20].

Dehmlow with coworkers studied several structural analogs of Shiori's catalysts of type **2** (Fig. 11.2) in the oxidation of 2-ethyltetralone [21]. As compared with complexes of type **1**, catalysts of type **2** exhibited lower enantioselectivities, not exceeding 66% *ee* (Fig. 11.3) [21].

Much later, Itoh with coworkers screened a series of quaternary ammonium salts and identified cinchonidine derived compounds of type **3** (Fig. 11.2) as highly enantioselective catalysts for the oxidation of 3-substituted-2-oxindoles to the corresponding 3-hydroxy-products (Fig. 11.3) [22]. The reaction proceeded in toluene at −20 °C under ambient atmosphere, in the presence of 50% KOH_{aq}, and required 4 equiv. of $(EtO)_3P$. The oxygenated products were obtained in high yields (>90%) and good to high enantioselectivities (67–93% *ee*). At 20 mol% catalyst loadings, excellent yields (91–98%) were reported within 4 h. Reducing the catalyst loading to 5–10 mol% resulted in a dramatic drop of the enantioselectivity.

More recently, Meng with coworkers screened several cinchonine derivatives as catalysts of the aerobic C–H hydroxylation of various indane-based adamantyl β-keto esters [23]. The authors used K_2HPO_4 solution as the deprotonating agent, and conducted the reaction under visible light irradiation, with tetraphenylporphine (TPP) serving as sensitizer. With **4a**, the best catalyst (5 mol%) in the series, moderate to good enantioselectivities (up to 75% *ee*) and good yields were achieved at −18 °C (81–98%). The authors postulated the involvement of singlet oxygen $^1O_2$ in the reaction. Subsequently, the authors developed catalyst **4b** with aryl substituent at the quinoline C2 [24], which demonstrated superior efficiency and enantioselectivity (up to 90% *ee*) in the aerobic oxidation of various indanone- and tetralone-derived β-keto esters (Fig. 11.3). Under irradiation with 3W LED yellow lamp (or sunlight) in a 8:2 toluene:chloroform mixed solvent, the oxidation was complete within 30–60 min at 2.5 mol% catalyst loading; in the dark, the reaction did not occur [24]. Later, the authors explored a series of cinchona-derived *N*-oxides (with **5** being the best in the series) as asymmetric phase-transfer catalysts of various β-keto esters and β-keto amides [25]. Under 3W LED irradiation, high yields (>90%) and good to high enantioselectivities (up to 83% *ee*) were reported; the reaction required 0.5 up to 4 h at room temperature in the presence of 5 mol% catalyst loadings. It was reported that the *N*-oxide catalysts of this type can be separated and reused with only a minor loss of reactivity and enantioselectivity.

Zhao with coworkers constructed the more elaborate phase-transfer catalyst **6** (Fig. 11.2), which demonstrated moderate to high yields (34–98%) and good enantioselectivities (62–98% *ee*) in the oxidations of various cyclic ketones (mostly 2-

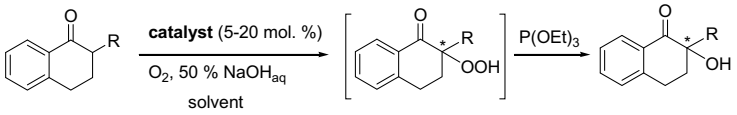

Hydroxylation of tetralones and indanones

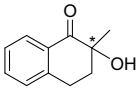

Catalyst	Yield	*ee*
1a	95 %	70 %
6	98 %	98 %
7a	89 %	66 %

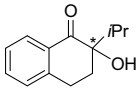

Catalyst	Yield	*ee*
1a	59 %	77 %
6	78 %	86 %

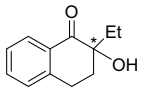

Catalyst	Yield	*ee*
1a	98 %	72 %
1b	98 %	59 %
2a	60 %	50 %
2b	71 %	43 %
6	78 %	86 %

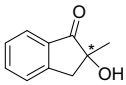

Catalyst	Yield	*ee*
1a	94 %	73 %
6	98 %	94 %
7a	93%	52%

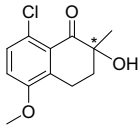

Catalyst	Yield	*ee*
1a	95 %	79 %

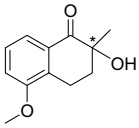

Catalyst	Yield	*ee*
1a	98 %	0 %

Hydroxylation of oxindoles

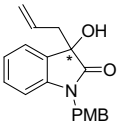

Catalyst	Yield	*ee*
3b	98 %	85 %
8d	91 %	91 %

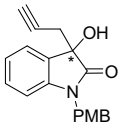

Catalyst	Yield	*ee*
3b	92 %	93 %
8d	83 %	94 %

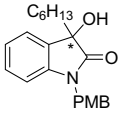

Catalyst	Yield	*ee*
3b	100 %	92 %

Hydroxylation of *β*-keto esters

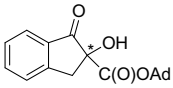

Catalyst	Yield	*ee*
4a	87 %	75 %
4b	98 %	90 %
5	>99 %	81 %

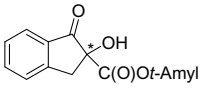

Catalyst	Yield	*ee*
4b	96 %	78 %
5	95 %	66 %

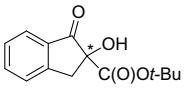

Catalyst	Yield	*ee*
4b	97 %	76 %
5	95 %	67 %

Hydroxylation of acyclic ketones

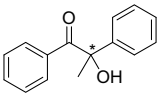

Catalyst	Yield	*ee*
6	75 %	88 %

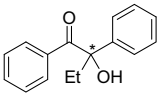

Catalyst	Yield	*ee*
6	85 %	68 %

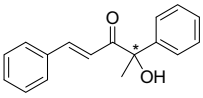

Catalyst	Yield	*ee*
6	62 %	82 %

Fig. 11.3 Organocatalyzed α-hydroxylation of carbonyl compounds

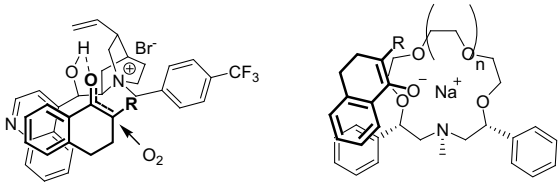

ref. 20 ref. 27

Fig. 11.4 Proposed transition states for the oxidation of cyclic ketones with dioxygen in the presence of CPTC

alkyltetralones and 2-alkylindanones) (Fig. 11.3) [26]. At 5 mol% catalyst loadings, the reaction proceeded in benzene within 18–72 h at 10 °C. In some cases, essentially for the oxidation of 2-substituted tetralones, catalyst **6** demonstrated the highest ever enantioselectivities (up to 98% *ee*). Moreover, it was successfully applied to the oxidation of various acyclic ketones, with moderate to high enantioselectivities (up to 88% *ee*, Fig. 11.3). Plausible oxidation mechanism was proposed, explaining the distinctions between the catalytic reactivity of **6** toward cyclic and acyclic ketones.

Chiral phase-transfer catalysts of other types have also been reported. Brussee with coworkers synthesized several crown ethers of type **7** (Fig. 11.2) and tested them in the aerobic oxidation of several 2-substituted tetralones and indanones in toluene at 10 mol% catalyst loadings [27]. For **7a**, the best catalyst of the series, moderate to good enantioselectivities (43–72%) were reported, along with generally high yields (80–95%); at the same time, unsubstituted 1-indanone, as well as a tetralone-derived β-keto ester, was inert under the reaction conditions. The authors proposed a model of the transition state, assuming the oxidation of the enolate form of the ketone (Fig. 11.4) [27].

Tan with coworkers examined a series of pentanidium catalysts of type **8** (Fig. 11.2) in the enantioselective α-hydroxylation of 3-substituted-2-oxindoles with molecular oxygen [28]. Without co-reductant, the catalyst system gave a mixture of the alcohol (major product) and the hydroperoxide (minor product), having opposite absolute configurations. Under optimized conditions (5 mol% of **8d**, toluene, −60 °C, 72–96 h), the system afforded the desired alcohols in high yields (84–92%) and enantioselectivities (86–98% *ee*). The catalytic reaction apparently occurred in two steps: the initially formed non-racemic hydroperoxide oxindole further underwent kinetic resolution, yielding the target alcohol.

UV-light assisted oxidation of aldehydes [29] and ketones [30] in the presence of chiral amino acids of type **9** (Fig. 11.2) was reported by Córdoba with coworkers. The oxidation of aldehydes was conducted in DMF at 0 °C, with TPP as sensitizer; the initially formed α-carbonyl hydroperoxides were in situ reduced by $NaBH_4$ to afford optically active diols (Fig. 11.5). The oxidation of ketones was performed at room temperature in DMSO [30]. For the oxidation of aldehydes, α-methyl-proline **9b** showed the highest enantioselectivity (up to 66% *ee*), while for the oxidation of ketones, alanine and valine were most stereoselective (28–72% *ee*). Subsequently, a family of protected diaryl prolinol based catalysts of type **10** (Fig. 11.2) was reported [31]. Oxidation of aldehydes in chloroform in the presence of catalyst **10a**, followed

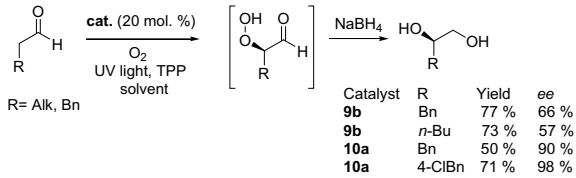

Fig. 11.5 Synthesis of optically active 1,2-diols from aldehydes

by reduction with $NaBH_4$, yielded chiral 1,2-diols with up to 98% *ee* (Fig. 11.5). The main drawback of this catalyst system is the high loading (20 mol%) of the aminoacid catalyst [29–31].

In addition to the above aerobic asymmetric catalytic α-hydroxylations of carbonyl compounds, there have been two reports on the use of hydrogen peroxide as oxidant for this purpose. In 2014, Meng with coworkers examined several analogs of lappaconitine as catalysts in the enantioselective α-hydroxylation of β-keto esters with commercially available hydrogen peroxide [32]. At 10 mol% loadings, catalyst **11** (Fig. 11.2) ensured the highest yields (73–98%) and enantioselectivities (82–92% *ee*) in the oxidation of a series of indanone-derived β-keto esters (Fig. 11.6). The

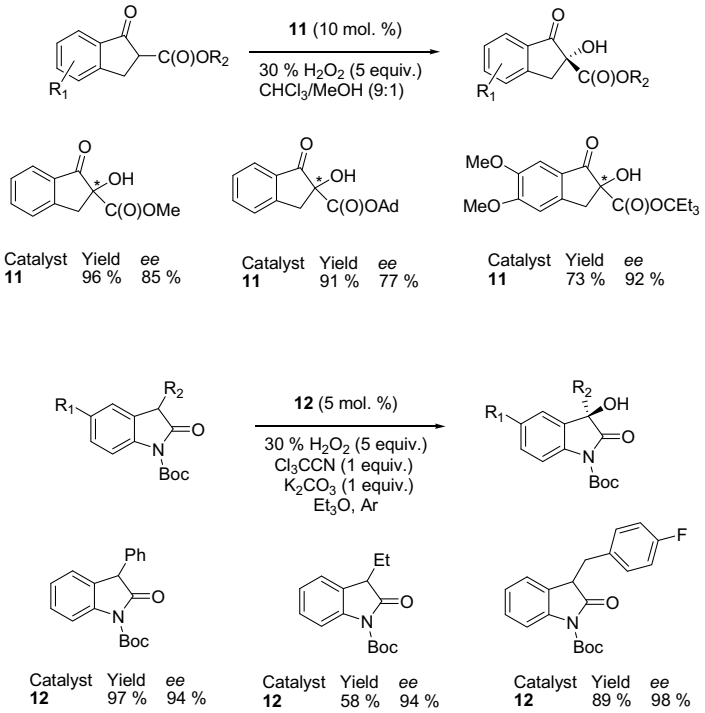

Fig. 11.6 Asymmetric α-hydroxylation of β-keto esters and 3-substituted oxindoles with hydrogen peroxide

reaction proceeded within 6–48 h at 15 °C, and required neither aqueous base nor co-reductant. The authors postulated the oxidation of the enolate form of the substrates [32].

More recently, Ooi with coworkers applied a series of chiral 1,2,3-triazolium salts in the oxidation of 3-substituted oxindoles with H_2O_2 [33]. Salt **12** (5 mol%) demonstrated the highest enantioselectivities in the series (90–98% *ee*), along with good to high yields (58–96% within 24 h) at −10 °C. To activate hydrogen peroxide, the authors used trichloroacetonitrile: the latter reacted with H_2O_2, affording peroxy trichloroacetimidic acid, which was believed to play the role of the actual electrophilic oxygenating agent. The reaction was shown to occur in the absence of the triazolium salt, too, yet in non-enantioselective fashion.

11.3 Transition Metal Catalyzed Asymmetric C–H Hydroxylations

Direct asymmetric C–H oxidation of prochiral substrates with the environmentally benign oxidants H_2O_2 and O_2 has been extremely challenging; to the best of our knowledge, there have been no reported asymmetric C–H oxidations using dioxygen as the terminal oxidant. At the same time, several transition metal-mediated oxidations relying on H_2O_2 as oxidant appeared in the last few years; existing catalysts either mediate the enantiotopic hydroxylation of CH_2 groups or desymmetrization of prochiral substrates; in the latter case, the reaction center and the chirality center(s) may be different.

The first report on the direct asymmetric hydroxylation of the CH_2 groups was contributed by Simonneaux with coworkers. The authors synthesized several chiral manganese porphyrins [34, 35] and tested them as catalysts in the oxidation of several arylalkanes with 5 equiv. of H_2O_2 [34, 35]. The water-soluble, sulfonated Halterman porphyrin **13** (Fig. 11.7) showed the best results. In water–methanol solutions, at 2.5 mol% catalyst loadings (and 10 mol% of catalytic additive, imidazole), the reaction took 1 h at room temperature. Good conversions (88–100%) were reported, along with moderate enantioselectivities (32–57% *ee*) (Fig. 11.8). Importantly, the system ensured good to very high alcohol selectivities, the alcohol/ketone ratios varying from 1.3 (for ethylbenzene) to 13 (for 4-ethyltoluene), which apparently rules out significant contribution of kinetic resolution (if any); the asymmetric induction appears at the C–H oxidation step itself. Modified Halterman porphyrins, with the SO_3^- groups substituted with H, NO_2, or NMe_2, exhibited lower alcohol selectivities and enantioselectivities.

Bryliakov with coworkers studied the oxidation of arylalkanes with H_2O_2 in the presence of chiral manganese aminopyridine complex **14** (Fig. 11.7) and its enantiomer [36]. Very low catalyst loadings (only 0.05–0.1 mol%) were sufficient to perform the oxidation within 3 h in acetonitrile at 0 °C in the presence of catalytic additives—carboxylic acids (preferentially 2-ethylhexanoic acid). Enantioenriched

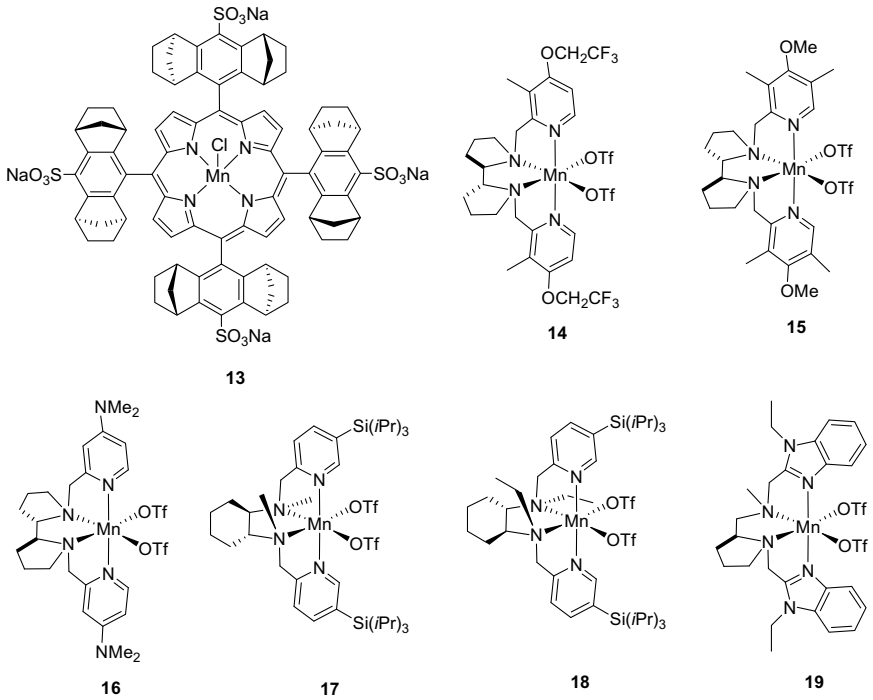

Fig. 11.7 Transition-metal-based catalysts for the asymmetric C–H oxidations with H_2O_2

1-arylethanols having up to 50% *ee* were obtained. However, the resulting alcohols were very prone to further oxidation to ketones under the reaction conditions, which required high excess of substrate to obtain alcohol as the major product. Subsequently, N-Boc-*L*-Proline (15–50 mol%) was used as the chiral additive, which, in combination with *ent*-**14**, afforded chiral 1-arylethanols with up to 86% *ee* [37]. The optical purity of 1-phenylethanol slightly increased over the reaction course (from 71 to 83% *ee*), which is an indication of minor contribution of oxidative kinetic resolution to the observed enantioselectivity.

The mechanism of manganese catalyzed asymmetric C–H oxidation has so far remained debatable. Apparently, the overall reaction rate is limited by the C–H bond-breaking step, i.e., either a hydrogen atom transfer or hydride transfer at the benzylic position (reflected by the primary k_H/k_D of 3.5–3.6 in CH_3CN [37] and 3.2 in trifluoroethanol [38]), followed by O-rebound affording the target product (Fig. 11.9).

Company, Bietti, and Costas with coworkers suggested that acetonitrile be replaced with 2,2,2-trifluoroethanol, which resulted in significantly improved alcohol/ketone ratios in the presence of 1 mol% of manganese complexes **15** and **16**, and 2-ethylhexanoic acid, with moderate to good enantioselectivities (up to 66% *ee*, Fig. 11.8) [39]. Complex **16** demonstrated higher alcohol yields but somewhat

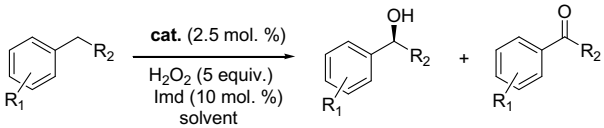

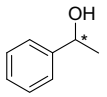

Catalyst	Yield	A/K	*ee*
13	50 %	1.3	38 %

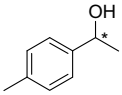

Catalyst	Yield	A/K	*ee*
13	90 %	13.3	57 %

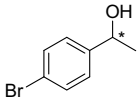

Catalyst	Yield	A/K	*ee*
13	80 %	4.0	49 %

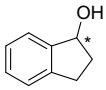

Catalyst	Yield	A/K	*ee*
13	68 %	3.3	32 %

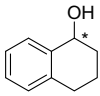

Catalyst	Yield	A/K	*ee*
13	56 %	1.6	43 %

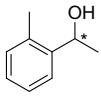

Catalyst	Yield	A/K	*ee*
13	76 %	6.7	52 %

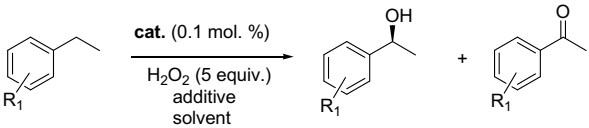

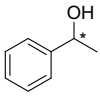

Catalyst	Yield	A/K	*ee*
14	130	1.0	86 %
15	16	8.0	55 %

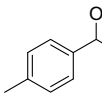

Catalyst	Yield	A/K	*ee*
14	130	2.2	80 %
15	21	85	56 %

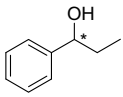

Catalyst	Yield	A/K	*ee*
15	12	12	66 %
16	22	6.3	60 %

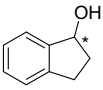

Catalyst	Yield	A/K	*ee*
14	100	1.0	44 %

Catalyst	Yield	A/K	*ee*
14	170	3.4	19 %

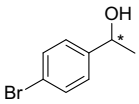

Catalyst	Yield	A/K	*ee*
14	50	0.5	78 %

Fig. 11.8 Asymmetric oxidation of 1-arylalkanes with H_2O_2 in the presence of manganese complexes. A/K is alcohol/ketone ratio. For oxidations in the presence of **14–16**, alcohol yield is given in mol alcohol/mol of catalyst

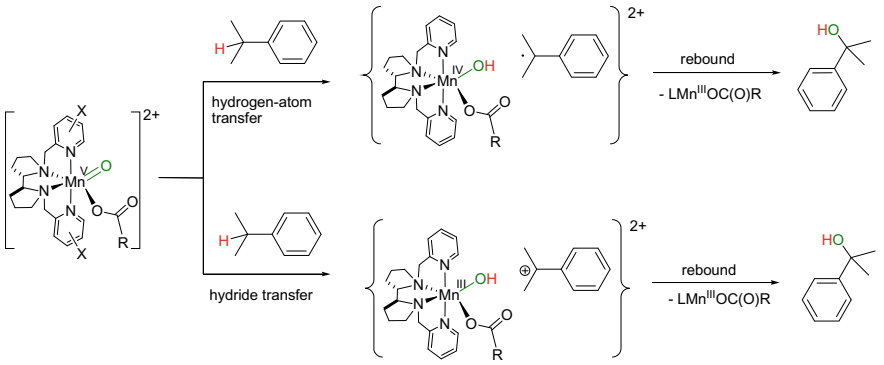

Fig. 11.9 Alternative mechanisms of benzylic C–H oxidation with H_2O_2 in the presence of Mn aminopyridine complexes (reproduced with permission from Ref. [37]. Copyright 2017 John Wiley and Sons)

lower enantioselectivities than catalyst **15**. The origin of the observed increase of the alcohol formation selectivity in trifluoroethanol was not entirely clear. Presumably, this effect could be ascribed to the formation of hydrogen bonds between this solvent and the alcohol hydroxyl group, which resulted in relative deactivation of the α-H toward hydrogen abstraction (Fig. 11.10) [39].

Bryliakov with coworkers monitored the kinetics of ethylbenzene oxidation with H_2O_2 in the presence of 0.1 mol% **14** and 2-ethylhexanoic acid in different solvents at −30 °C (Fig. 11.11) [38]. The alcohol selectivity increased in the following order: acetonitrile < 2-fluoroethanol < 2,2-difluoroethanol (DFE) < 2,2,2-trifluoroethanol (TFE); in the latter case, maximum alcohol yield (47%) was achieved (at 75% ethylbenzene conversion), acetophenone being the major reaction byproduct. Evidently, the alcohol selectivity is governed by the relative rates of the first oxidation step (the oxidation of ethylbenzene to 1-phenylethanol) and the second step (the oxidation of 1-phenylethanol to acetophenone). The ratios of the apparent rate constants for the first and second steps, k_1/k_2, were evaluated in different solvents, and were

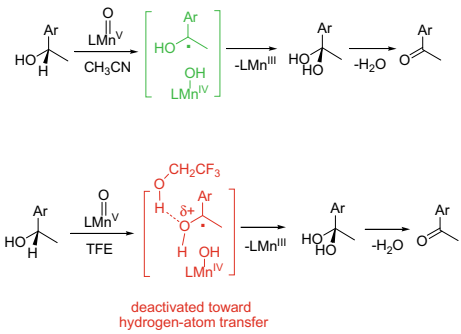

Fig. 11.10 Proposed model of the effect of trifluoroethanol on the observed electronic nature of the transition state

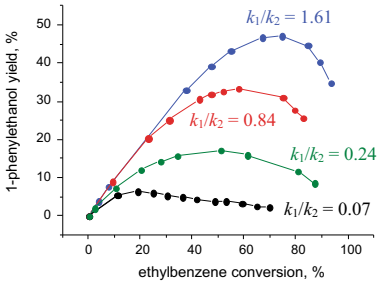

Fig. 11.11 1-Phenylethanol yield versus conversion for the oxidation of ethylbenzene in the presence of **14** at −30 °C in acetonitrile (black), 2-fluoroethanol (olive), 2,2-difluoroethanol (red) and 2,2,2-trifluoroethanol (blue) (reproduced with permission from Ref. [38]. Copyright 2018 John Wiley and Sons)

found to increase in the order: CH_3CN < monofluoroethanol < difluoroethanol < trifluoroethanol (Fig. 11.11).

At the same time, difluoroethanol solvent ensured higher enantioselectivity with 2-ethylhexanoic acid (61% *ee*) than trifluoroethanol (59% *ee*). Replacing 2-ethylhexanoic acid with chiral additive N-Boc-*L*-Proline in DFE afforded 1-phenyl ethanol having 77% enantiomeric excess in 32% chemical yield, which corresponds to 320 mol of alcohol per mol **14** [38]. Oxidation of several alkylarenes in 2,2-difluoroethanol afforded the corresponding alcohols with 56–89% *ee* (Fig. 11.12) [38].

It has been shown that the nature of the transition state of benzylic C–H oxidation apparently changes when passing from CH_3CN to trifluoroethanol media. In the former case, competitive oxidation of *p*-substituted ethylbenzenes witnessed linear correlation between the $\mathrm{Log}(k_X/k_H)$ and the polar σ^+ substituent parameters ($\rho^+ = -1.4$). In the latter case, correlation with the non-polar substituent parameter σ ($\rho = -2.7$) has been observed [38], reflecting formally non-electron-deficient transition state. The origin of this apparent difference is unclear at the moment.

11.4 Desymmetrization of Prochiral Substrates, Occurring via Catalyzed C–H Oxidation

In 2016, Hua with coworkers reported the preparation of a new class of chiral poly-*N*-vinylpyrrolidinones, containing asymmetric center at pyrrolidinone C5 [40]. The chiral polymers were used to stabilize Cu/Au nanoparticles, serving as the active components of oxidation catalysts. The resulting materials were used to oxidize prochiral cycloalkanes with H_2O_2. The oxidation preferentially occurred at the C3 position, affording the corresponding C3-ketone with a new center of chirality at the tertiary or quaternary C1 position (Fig. 11.13). The unprecedented high selectivity toward the C3 methylenic sites was remarkable, resulting in high yield of ketones

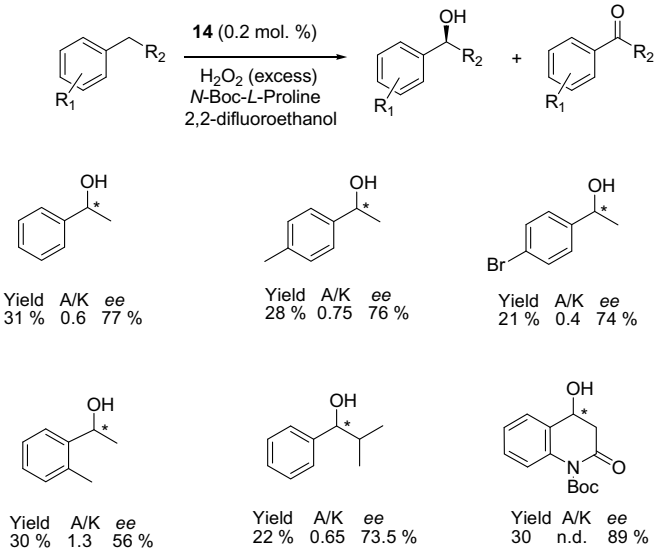

Fig. 11.12 Asymmetric oxidation of 1-arylalkanes with H_2O_2 in the presence of manganese complexes. A/K is alcohol/ketone ratio. n.d.—not determined

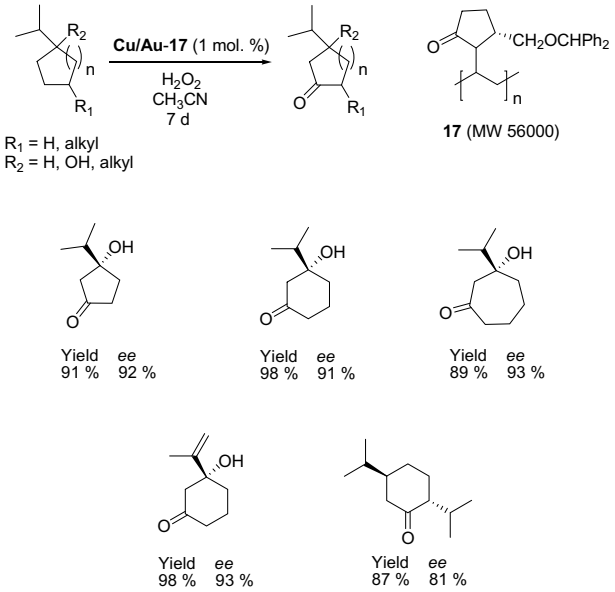

Fig. 11.13 Oxidative desymmetrization of cycloalkanes with H_2O_2 in the presence of chiral polymer-supported bimetallic nanoparticles

(87–98% within 7 days at 1 mol% catalyst loading and at 50 °C), having high optical purities (81–93% *ee*, Fig. 11.13). Despite the restricted substrate scope, a severe limitation of the reported system is the high oxidant consumption, which required adding 30 equivalents of H_2O_2 (vs. substrate).

A complementary approach, relying on homogeneous catalysts based on chiral manganese complexes was proposed by Milan, Bietti, and Costas [41]. The authors synthesized aminopyridine complexes **17** and **18** (Fig. 11.7) and tested them in the oxidation of monosubstituted cyclohexanes with H_2O_2 in the presence of carboxylic acid additives at −40 °C (Fig. 11.14). In most cases, the catalyst system showed good to very high selectivity for the oxidation at the C3 position ($K_3/K_4 = 2$ to >99). With cyclopropanecarboxylic acid, the best catalytic additive, enantioselectivities up to 96% *ee* were achieved. The highest K_3/K_4 and enantioselectivities were achieved with a series of amide substituted cyclohexanes (Fig. 11.14).

The authors hypothesized that the enantioselectivity originated at the first, presumably hydrogen atom transfer (HAT), step. The key role of the basic amine moiety in dictating regio- and enantioselectivity has remained not well understood [41].

Nam and Sun with coworkers developed a similar approach for the oxidative desymmetrization of spirocyclic β-ketones in the presence of several benzimidazole derived manganese aminopyridine complexes at −30 °C [42]. C1-Symmetric catalyst **19** (Fig. 11.7) was the most stereoselective in the series, affording spirocyclic β,β'-diketones in reasonably good yields and good to excellent enantioselectivities (Fig. 11.15). The authors demonstrated scalability of the oxidation protocol to gram quantities, and proposed further ketone reduction protocol (to alcohols), retaining the enantiomeric purity [42]. Subsequently, the authors reported the similarly high enantioselectivities for the oxidation of Boc-protected spirocyclic oxindoles and dihydroquinolines in the presence of 2 mol% of the same catalyst **19** (Fig. 11.15) [43].

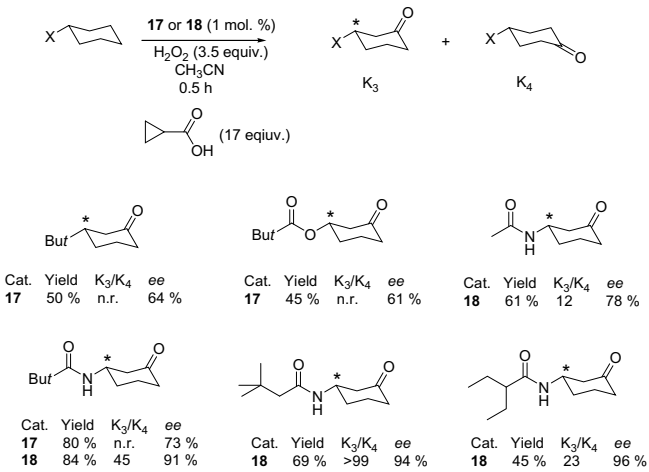

Fig. 11.14 Oxidative desymmetrization of substituted cyclohexanes in the presence of manganese aminopyridine complexes. Yield corresponds to the sum of K_3 and K_4 products; n.r. = not reported

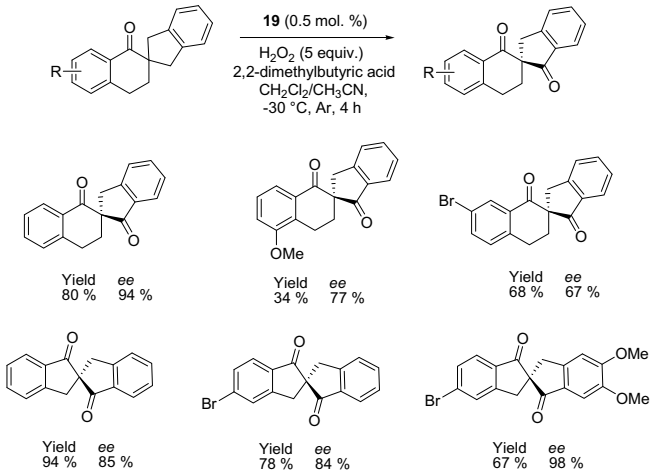

Fig. 11.15 Oxidative desymmetrization of spirocyclic β-ketones in the presence of manganese aminopyridine complex **19**

Giving credit to the proposed system for the high stereoselectivity, the substrate scope of the system, so far restricted to the spirocyclic compounds shown in Figs. 11.15 and 11.16, maybe a practical limitation of the proposed catalytic oxidation protocol.

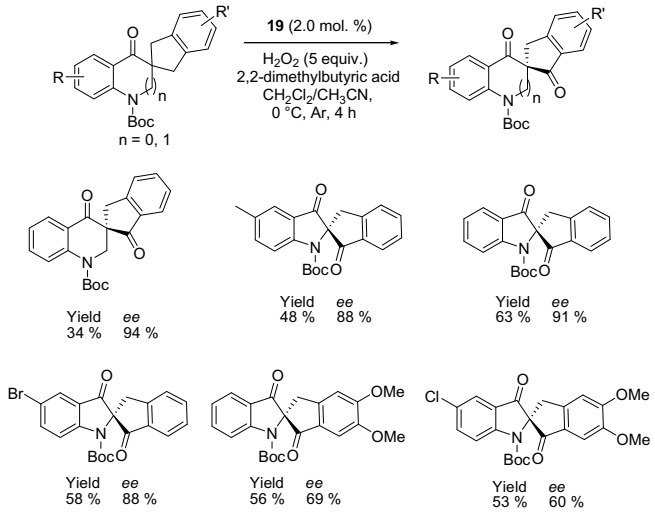

Fig. 11.16 Oxidative desymmetrization of spirocyclic oxindoles and dihydroquinolines in the presence of manganese aminopyridine complex **19**

11.5 Conclusions

This chapter surveys the existing catalyst systems, capable of conducting enantioselective oxidation of C–H groups in organic molecules with the environmentally benign oxidants O_2 and H_2O_2. The systems for the enantioselective α-hydroxylation of carbonyl compounds with O_2 and H_2O_2, relying on chiral phase-transfer organocatalysts, are not numerous. The substrate scope of the reported catalyst systems has so far been restricted to cyclic aromatic ketones (mostly substituted tetralones and indanones), some acyclic ketones, cyclic β-keto esters, 3-substituted oxindoles, and a few aldehydes. In several cases, perfect enantioselectivities were documented (up to 98% *ee*). The aerobic oxidation protocols typically require external co-reductant (for in situ reduction of the hydroperoxide intermediate); in some cases, the reaction can be appreciably accelerated by UV or visible light irradiation. Common drawback of all systems is the low efficiency, the existing oxidation techniques requiring 5 up to 20 mol% chiral catalyst loadings.

So far, examples of enantioselective hydroxylation of prochiral CH_2 groups with H_2O_2 have been restricted to the systems of Simonneaux [34, 35] and Bryliakov [36–38]. To date, the reported enantioselectivities do not exceed 89% *ee* [38]. The major drawbacks of those catalyst systems are the narrow substrate scope (limited with substrates bearing benzylic CH_2 moieties), moderate enantioselectivities, and significant overoxidation to ketone, deteriorating the yield of the target chiral alcohol. However, replacing acetonitrile solvent with polyfluorinated alcohols significantly improves the selectivity for the target reaction product, the chiral alcohol yield exceeding 40%.

Recently reported catalyst systems for the oxidative desymmetrization of prochiral substrates with H_2O_2 [41–43] in several cases demonstrate excellent enantioselectivities (up to 98% *ee*), but have so far been applied to specific substrates only, which also leaves much room for further developments. Gratifyingly, the overwhelming majority of stereoselective catalyst systems rely on manganese-based C–H oxidation catalysts, which success initially could not be foreseen [44]. The author expects that the current success of manganese will predetermine its dominance in medium-term perspective.

Overall, both the organocatalytic and transition metal-based systems are very far from maturity; the development of highly efficient and at the same time highly chemo- and enantioselective oxidation methods with broad applicability remains a challenging goal, which inspires rapid progress in this area. The author would be particularly eager to witness the emergence of so far unprecedented direct aerobic enantiotopic hydroxylation of non-activated CH_2 groups. However, at present, virtually any amendment of the existing catalyst systems surveyed above is welcome and may be potentially highly rewarding.

Acknowledgements The author acknowledges financial support from the Russian Foundation for Basic Research (#16-29-10666 and # 18-33-20078).

References

1. Chen MS, White MC (2007) A predictably selective aliphatic C–H oxidation reaction for complex molecule synthesis. Science 318:783–787. https://doi.org/10.1126/science.1148597
2. Chen MS, White MC (2010) Combined effects on selectivity in Fe-catalyzed methylene oxidation. Science 327:566–571. https://doi.org/10.1126/science.1183602
3. Shul'pin GB (2010) Selectivity enhancement in functionalization of C–H bonds: a review. Org Biomol Chem 8:4217–4228. https://doi.org/10.1039/c004223d
4. Shul'pin GB (2016) New trends in oxidative functionalization of carbon-hydrogen bonds: a review. Catalysts 6:4. https://doi.org/10.3390/catal6040050
5. Hartwig JF, Larsen MA (2016) Undirected, homogeneous C–H bond functionalization: challenges and opportunities. ACS Cent Sci 2:281–292. https://doi.org/10.1021/acscentsci.6b00032
6. Ottenbacher RV, Talsi EP, Bryliakov KP (2016) Direct selective oxidative functionalization of C–H bonds with H_2O_2: Mn-aminopyridine complexes challenge the dominance of non-heme Fe catalysts. Molecules 21:1454. https://doi.org/10.3390/molecules21111454
7. Kagan H (1999) Historical perspective. In: Jacobsen EN, Pfalz A, Yamamoto H (eds) Comprehensive asymmetric catalysis. Springer, Berlin, p 1999
8. Groves JT, Viski P (1989) Asymmetric hydroxylation by a chiral iron porphyrin. J Am Chem Soc 111:8537–8538. https://doi.org/10.1021/ja00204a047
9. Groves JT, Viski P (1990) Asymmetric hydroxylation, epoxidation, and sulfoxidation catalyzed by vaulted binaphthyl metalloporphyrins. J Org Chem 55:3628–3634. https://doi.org/10.1021/jo00298a046
10. Hamachi K, Irie R, Katsuki T (1996) Asymmetric benzylic oxidation using a Mn-salen complex as catalyst. Tetrahedron Lett 37:4979–4982. https://doi.org/10.1016/0040-4039(96)00984-7
11. Hamada T, Irie R, Mihara J, Hamachi K, Katsuki T (1998) Highly enantioselective benzylic hydroxylation with concave type of (salen)manganese(III) complex. Tetrahedron 54:10017–10028. https://doi.org/10.1016/S0040-4020(98)00603-6
12. Zhang R, Yu WY, Lai TS, Che CM (1999) Enantioselective hydroxylation of benzylic C–H bonds by D_4-symmetric chiral oxoruthenium porphyrins. Chem Commun 1791–1792. https://doi.org/10.1039/a904100a
13. Murahashi SI, Noji S, Komiya N (2004) Catalytic enantioselective oxidation of alkanes and alkenes using (salen)manganese complexes bearing a chiral binaphthyl strapping unit. Adv Synth Catal 346:195–198. https://doi.org/10.1002/adsc.200303190
14. Zhang R, Yu WY, Che CM (2005) Catalytic enantioselective oxidation of aromatic hydrocarbons with D_4-symmetric chiral ruthenium porphyrin catalysts. Tetrahedron Asymmetry 16:3520–3526. https://doi.org/10.1016/j.tetasy.2005.08.059
15. Le Maux P, Srour HF, Simonneaux G (2012) Enantioselective water-soluble iron–porphyrin-catalyzed epoxidation with aqueous hydrogen peroxide and hydroxylation with iodobenzene diacetate. Tetrahedron 68:5824–5828. https://doi.org/10.1016/j.tet.2012.05.014
16. Miyafuji A, Katsuki T (1998) Asymmetric desymmetrization of meso-tetrahydrofuran derivatives by highly enantiotopic selective C–H oxidation. Tetrahedron 54:10339–10438. https://doi.org/10.1016/S0040-4020(98)00489-X
17. Komiya N, Noji S, Murahashi SI (1998) Manganese catalyzed asymmetric oxidation of alkanes to optically active ketones bearing asymmetric center at the α-position. Tetrahedron Lett 39:7921–7924. https://doi.org/10.1016/S0040-4039(98)01757-2
18. Murahashi SI, Noji S, Hirabayashi T, Komiya N (2005) Manganese-catalyzed enantioselective oxidation of C–H bonds of alkanes and silyl ethers to optically active ketones. Tetrahedron Asymmetry 16:3527–3535. https://doi.org/10.1016/j.tetasy.2005.08.056
19. Frost JR, Huber SM, Breitenlechner S, Bannwarth C, Bach T (2015) Enantiotopos-selective C–H oxygenation catalyzed by a supramolecular ruthenium complex. Angew Chem Int Ed 54:691–695. https://doi.org/10.1002/anie.201409224

20. Masui M, Ando A, Shioiri T (1988) New methods and reagents in organic synthesis. 75. asymmetric synthesis of α-hydroxy ketones using chiral phase transfer catalysts. Tetrahedron Lett 29:2835–2838. https://doi.org/10.1016/0040-4039(88)85224-9
21. Dehmlow EV, Düttmann D, Neumann B, Stammler HG (2002) Monodeazacinchona alkaloid derivatives: synthesis and preliminary applications as phase-transfer catalysts. Eur J Org Chem 2087–2093. https://doi.org/10.1002/1099-0690(200207)2002:13%3c2087::aid-ejoc2087%3e3.0.co;2-z
22. Sano D, Nagata K, Itoh T (2008) Catalytic asymmetric hydroxylation of oxindoles by molecular oxygen using a phase-transfer catalyst. Org Lett 10:1593–1595. https://doi.org/10.1021/ol800260r
23. Lian M, Li Z, Cai Y, Meng Q, Gao Z (2012) Enantioselective photooxygenation of β-keto esters by chiral phase-transfer catalysis using molecular oxygen. Chem Asian J 7:2019–2023. https://doi.org/10.1002/asia.201200358
24. Wang Y, Zheng Z, Lian M, Yin H, Zhao J, Meng Q, Gao Z (2016) Photo-organocatalytic enantioselective α-hydroxylation of β-keto esters and β-keto amides with oxygen under phase transfer catalysis. Green Chem 18:5493–5499. https://doi.org/10.1039/C6GC01245K
25. Wang H, Yin H, Tang X, Wu Y, Meng Q, Gao Z (2016) A series of cinchona-derived *N*-oxide phase-transfer catalysts: application to the photo-organocatalytic enantioselective α-hydroxylation of β-dicarbonyl compounds. J Org Chem 81:7042–7050. https://doi.org/10.1021/acs.joc.6b00856
26. Sim SBD, Wang M, Zhao Y (2015) Phase-transfer-catalyzed enantioselective α–hydroxylation of acyclic and cyclic ketones with oxygen. ACS Catal 5:3609–3612. https://doi.org/10.1021/acscatal.5b00583
27. de Vries EFJ, Ploeg L, Colao M, Brussee J, van der Jen A (1995) Enantioselective oxidation of aromatic ketones by molecular oxygen, catalyzed by chiral monoaza-crown ethers. Tetrahedron Asymmetry 6:1123–1132. https://doi.org/10.1016/0957-4166(95)00138-f
28. Yang Y, Moinodeen F, Chin W, Ma T, Jiang Z, Tan CH (2012) Pentanidium-catalyzed enantioselective α-hydroxylation of oxindoles using molecular oxygen. Org Lett 14:4762–4765. https://doi.org/10.1021/ol302030v
29. Córdova A, Sundén H, Engqvist M, Ibrahem I, Casas J (2004) The direct amino acid-catalyzed asymmetric incorporation of molecular oxygen to organic compounds. J Am Chem Soc 126:8914–8915. https://doi.org/10.1021/ja047930t
30. Sundén H, Engqvist M, Casas J, Ibrahem I, Córdova A (2004) Direct amino acid catalyzed asymmetric α-oxidation of ketones with molecular oxygen. Angew Chem Int Ed 43:6532–6535. https://doi.org/10.1002/anie.200460295
31. Ibrahem I, Zhao GL, Sundén H, Córdova A (2006) A route to 1,2-diols by enantioselective organocatalytic α-oxidation with molecular oxygen. Tetrahedron Lett 47:4659–4663. https://doi.org/10.1016/j.tetlet.2006.04.133
32. Li Z, Lian M, Yang F, Meng Q, Gao Z (2014) Diterpenoid alkaloid lappaconine derivative catalyzed asymmetric α-hydroxylation of β-dicarbonyl compounds with hydrogen peroxide. Eur J Org Chem 3491–3495. https://doi.org/10.1002/ejoc.201402019
33. Ohmatsu K, Ando Y, Ooi T (2017) In situ electrophilic activation of hydrogen peroxide for catalytic asymmetric α-hydroxylation of 3-substituted oxindoles. Synlett 28:1291–1294. https://doi.org/10.1055/s-0036-1558958
34. Srour H, Le Maux P, Simonneaux G (2012) Enantioselective manganese-porphyrin-catalyzed epoxidation and C–H hydroxylation with hydrogen peroxide in water/methanol solutions. Inorg Chem 51:5850–5856. https://doi.org/10.1021/ic300457z
35. Amiri N, Le Maux P, Srour H, Nasri H, Simonneaux G (2014) Nitration of Halterman porphyrin: a new route for fine tuning chiral iron and manganese porphyrins with application in epoxidation and hydroxylation reactions using hydrogen peroxide as oxidant. Tetrahedron 70:8836–8842. https://doi.org/10.1016/j.tet.2014.10.001
36. Talsi EP, Samsonenko DG, Bryliakov KP (2017) Asymmetric autoamplification in the oxidative kinetic resolution of secondary benzylic alcohols catalyzed by manganese complexes. ChemCatChem 9:2599–2607. https://doi.org/10.1002/cctc.201700438

37. Talsi EP, Samsonenko DG, Ottenbacher RV, Bryliakov KP (2017) Highly enantioselective C–H oxidation of arylalkanes with H_2O_2 in the presence of chiral Mn aminopyridine complexes. ChemCatChem 9:4580–4586. https://doi.org/10.1002/cctc.201701169
38. Ottenbacher RV, Talsi EP, Rybalova TV, Bryliakov KP (2018) Enantioselective benzylic hydroxylation of arylalkanes with H_2O_2 in fluorinated alcohols in the presence of chiral Mn aminopyridine complexes. ChemCatChem 10:5323–5330. https://doi.org/10.1002/cctc.201801476
39. Dantignana V, Milan M, Cussó O, Company A, Bietti M Costas M (2018) Chemoselective aliphatic C–H bond oxidation enabled by polarity reversal. ACS Cent Sci 3:1350–1358. https://doi.org/10.1021/acscentsci.7b00532
40. Hao B, Gunaratna MJ, Zhang M, Weerasekara S, Seiwald SN, Nguyen VT, Meier A, Hua DH (2016) Chiral-substituted Poly-*N*-vinylpyrrolidinones and bimetallic nanoclusters in catalytic asymmetric oxidation reactions. J Am Chem Soc 138:16839–16848. https://doi.org/10.1021/jacs.6b12113
41. Milan M, Bietti M, Costas M (2017) Highly enantioselective oxidation of nonactivated aliphatic C–H bonds with hydrogen peroxide catalyzed by manganese complexes. ACS Cent Sci 3:196–204. https://doi.org/10.1021/acscentsci.6b00368
42. Qiu B, Xu D. Sun, Q, Miao C, Lee YM, Li XX, Nam W, Sun W (2018) Highly enantioselective oxidation of spirocyclic hydrocarbons by bioinspired manganese catalysts and hydrogen peroxide. ACS Catal 8:479–487. https://doi.org/10.1021/acscatal.7b03601
43. Qiu B, Xu D, Sun Q, Lin J, Sun W (2019) Manganese-catalyzed asymmetric oxidation of methylene C–H of spirocyclic oxindoles and dihydroquinolinones with hydrogen peroxide. Org Lett 21:618–622. https://doi.org/10.1021/acs.orglett.8b03652
44. Ottenbacher RV, Samsonenko DG, Talsi EP, Bryliakov KP (2012) Highly efficient, regioselective, and stereospecific oxidation of aliphatic C–H groups with H_2O_2, catalyzed by aminopyridine manganese complexes. Org Lett 14:4310–4313. https://doi.org/10.1021/ol3015122